(De)hydrogenation reactions catalyzed by manganese(I) complexes

Antoine Bruneau-Voisine

UNIVERSITE MATIERE BRETAGNE MOLECULES LOIRE ET MATERIAUX

UNIVERSITÉ DE RENNES 1

THESE DE DOCTORAT DE

L'UNIVERSITE DE RENNES 1
COMUE UNIVERSITE BRETAGNE LOIRE

ECOLE DOCTORALE N° 596
Matière Molécules et Matériaux
Spécialité : Chimie Moléculaire et Macromoléculaire

Par

Antoine BRUNEAU-VOISINE

Réactions de (dé)hydrogénation catalysées par des complexes de manganèse(I)

Thèse présentée et soutenue à Rennes, le 17 Octobre 2018

Unité de recherche : UMR 6226, CNRS, Université de Rennes 1, Institut des Sciences Chimiques de Rennes

Rapporteurs avant soutenance :

Estelle METAY
Chargée de recherche, CNRS,
Université Claude Bernard Lyon 1

Thibault CANTAT
Ingénieur chercheur, CEA, Saclay

Composition du Jury :

Muriel HISSLER
Professeure, Université de Rennes 1

Estelle METAY
Chargée de recherche, CNRS,
Université Claude Bernard Lyon 1

Thibault CANTAT
Ingénieur chercheur, CEA, Saclay

Philippe MARION
Advanced Organic Chemistry Manager, Solvay R&I, Lyon

Jean-Baptiste SORTAIS
Professeur, Université Paul Sabatier Toulouse 3
Directeur de thèse

Christophe DARCEL
Professeur, Université de Rennes 1
Co-directeur de thèse

Remerciements

L'aboutissement de ce projet doctoral est évidemment un travail d'équipe et le fruit de nombreuses discussions et collaborations réalisées dans l'équipe Organométallique : Matériaux et Catalyse, à Rennes et dans l'équipe A, au Laboratoire de Chimie de Coordination à Toulouse.

Tout d'abord, j'exprime ma sincère gratitude aux membres du jury : Pr. Muriel Hissler, Dr. Thibault Cantat, Dr. Estelle Métay et Dr. Philippe Marion, qui ont accepté d'évaluer ce travail. Merci pour le temps passé à lire et corriger ce manuscrit, et encore plus aux rapporteurs : Dr. T. Cantat, Dr. E. Métay.

Je tiens à chaleureusement remercier mes directeurs de thèse, Pr. Jean-Baptiste Sortais et Pr. Christophe Darcel, pour leurs nombreux soutiens, conseils et avis critiques prodigués tout au long de cette thèse. Je leur suis également reconnaissant pour la confiance, la liberté, leur disponibilité et leurs encouragements apportés pendant ces trois ans.
Plus particulièrement, j'ai pu apprendre quotidiennement aux côtés de Jean-Baptiste qui a été, plus qu'un directeur de thèse, un ami avec lequel j'ai pu partager mes idées, mes découvertes mais aussi mes doutes et mes rêveries. Réciproquement, sa pédagogie dans la transmission de ses connaissances, son optimisme, son expérience et sa vision critique ont eu un rôle décisif dans ce travail.
Christophe a également été très important pour moi durant cette thèse, et même avant... Il a été mon premier professeur de chimie organométallique et catalyse et a su me transmettre son enthousiasme pour ce domaine. Grâce à son partage de connaissances, il m'a énormément appris et je lui dois, en grande partie, ma vision et ma passion pour cette chimie. Son influence s'étend à mes stages en entreprises (Hoffman-La Roche et Firmenich) réalisés en master et pour lesquels il m'a fortement soutenu. De plus, son sens du travail et sa rigueur ont été exemplaires pour moi.

Ayant passé mes deux premières années de thèse à Rennes, je voudrais également remercier, pour leurs aides, enseignements, discussions, tous les membres permanents de la partie catalyse de l'équipe OMC que j'ai pu côtoyer quotidiennement : Dr. C. Bruneau, Pr. P. H. Dixneuf, Dr. C. Fischmeister, Dr. J.-F. Soulé, Dr. R. Gramage-Doria, Dr. M. Achard, Dr. H. Doucet, Dr. S. Derien. Cette liste peut également être élargie à tous les membres de l'équipe OMC participant aux réunions mensuelles inter-équipes.

Pendant une année à Toulouse, j'ai aussi rencontré des chercheurs : Dr. N. Lugan, Dr. V. César, Dr. Y. Canac, Dr. S. Bastin et Dr. D. Valyaev, spécialisés dans la chimie organométallique qui m'ont accueilli chaleureusement et m'ont apporté une autre vision sur mes travaux. Merci à eux pour leur soutien, leurs précisions et leurs débats ainsi qu'aux voisins de l'équipe G, dont Pr. R. Poli et Dr. E. Manoury, avec qui nous avons eu régulièrement des réunions inter-équipes.

Un support financier est indispensable pour réaliser une thèse dans de bonnes conditions : merci à l'Agence Nationale de la Recherche ainsi qu'au réseau public/privé INCREASE, piloté par Dr. François Jérôme, qui m'a permis de prendre part à des colloques stimulants entre académiques et industriels.

J'ai eu la chance de profiter de services d'analyses bien organisés et efficaces. Je suis reconnaissant envers Clément Orionne, Dr. Elsa Caytan (service RMN à Rennes) ; Francis Lacassin, David Paryl (service RMN au LCC) ; Drs. Thierry Roisnel, Vincent Dorcet (service D-RX, Rennes) ; Laure Vendier, Carine Duhayon (service D-RX, Toulouse) ; Dr. Murielle Escadeillas (service d'analyse élémentaire, Rennes) ; Philippe Jéhan (service de spectrométrie de masse, Rennes) pour leurs aides techniques.

Ayant passé une grande partie de mon temps au laboratoire à la paillasse, je tiens donc à remercier tous les collègues que j'ai côtoyés pendant ces trois années pour leur convivialité et l'excellente ambiance qui a régné aux laboratoires, indispensable pour travailler dans de bonnes conditions:
- à Rennes : Duo Wei, Ding Wang, Haoran Li, Chang-Sheng Wang, Hortense Lauwick, Apurba Sahoo, Shendong Wang, Xinzhe Shi, Haiyun Huang, Arpan Sasmal, Imane Idris, Meriem Abderrezak, Salekh Masoud, Paolo Zardi, Yuchao Yuan, Aymen Skhiri.
- à Toulouse : Lenka Pallova, Idir Benaissa, Alina Grineva, Rachid Taakili, Karim Azouzi, Cécile Barthès, Ruqaya Buhaibeh, Katarzyna Gajda.
J'ai adoré travailler dans un environnement international et je vous remercie tous pour votre aide au labo mais aussi pour tous les bons moments en dehors du labo où nous avons pu échanger sur beaucoup plus que la chimie.

Pour finir je tiens à remercier mes parents, ma famille, mes amis et Lucille pour m'avoir accompagné et supporté tout au long de ces trois années.

Contents

Chapter 1 - General Introduction

A – Chemistry and sustainability

In the context of the socio-ecological transition to build up a sustainable society, chemistry will have to play a significant role. New chemical processes that minimize the environmental and societal impact of chemistry are key concepts to develop a sustainable chemistry. These concepts have been formalized and rationalized by P. Anastas and J. Warner introducing the twelve principles of Green Chemistry in 1998.[1] The overarching goals of Green Chemistry are principles based on common sense, which aim to guide scientific innovation towards safer and more environmentally friendly chemical reactions. Some metrics such as atom economy or environmental factor (E-factor) introduced by B. M. Trost[2] and R. Sheldon[3] appeared in the 1990's to measure the efficiency of a reaction through the chemical yield and waste production. Atom economy is defined as: atom economy = (molecular mass of desired product / molecular mass of all reactants) x 100. This definition implies that the maximum of atom from the starting material should be present in the product but it does not take into account other wastes such as solvents or work up procedures. In contrast, the E-factor, defined as E-factor = total waste mass / product mass, lists all the involved chemicals.

Among the twelve principles of Green Chemistry, the use of renewable raw materials is primordial. Biomass resources, especially inedible resources currently considered as waste and burned to provide heat, have the potential to replace fossil resources in order to produce targeted platform molecules. Biomass is inexpensive and accessible at a scale that can fulfil the requirements of chemical industry. A major challenge to face for chemists is the change of paradigm coming from the nature of the raw materials. In fact, while petroleum derivatives, compounded mostly of carbon and

hydrogen, need to be oxidized and functionalized, the use of highly oxygenated and functionalized biomass requires the development of chemistry involving selective reduction, depolymerization, defunctionalization reactions (**Figure A[1].1**). Two main approaches have been envisioned for the valorization of biomass resources.[4] In the medium term, the "drop-in strategy" converts the biomass into the current bulk chemicals. Long-term "emerging strategies" will create new bio-based platform materials that are more in line with the intrinsic high degree of functionalities of biopolymers.

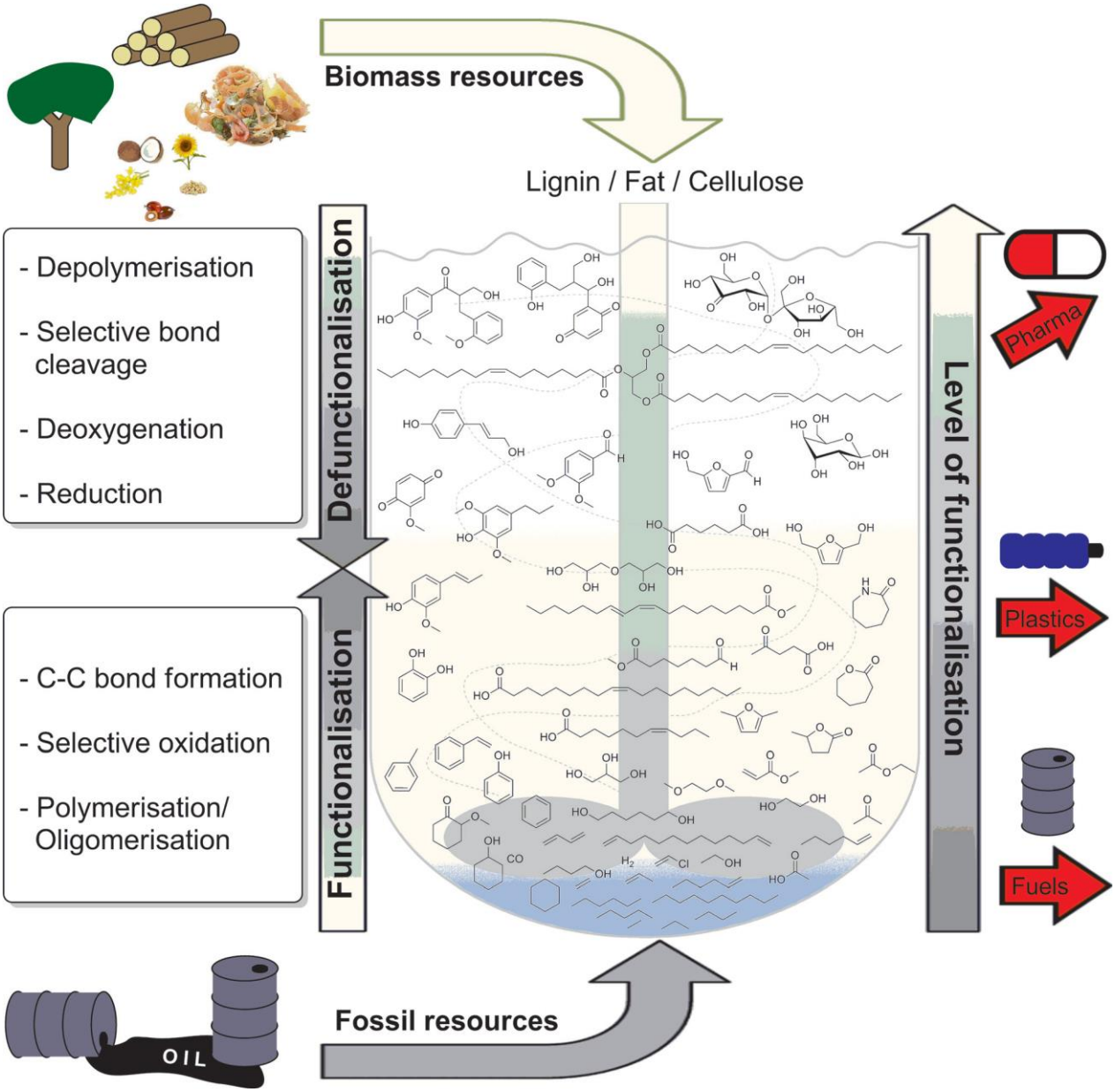

Figure A[1].1 Comparison between the valorization of biomass and fossil resources, taken from P. J. Deuss, K. Barta, J. G. de Vries, *Catal. Sci. Technol.*, **2014**, *4*, 1174.

Among the twelve principles of Green Chemistry, catalysis plays also a pivotal role: catalytic reactions allow a dramatic reduction of wastes by avoiding stoichiometric reagents and enhancing selectivity of the process, while reducing the overall energy consumed. Therefore, catalysis has received enormous considerations for more than a century, leading to several Nobel Laureates, including Knowles, Noyori and Sharpless for enantioselective catalytic reactions in 2001; Chauvin, Grubbs and Schrock for metathesis in 2005; Ertl for chemical processes on heterogeneous catalysts in 2007; Heck, Negishi and Suzuki for cross-coupling reactions in 2010. Like in other fields of the ecological transition such as digital transition (magnets) or energy (batteries),[5] the key technology of these outstanding advances is to take advantage of the properties of specific metals. Due to their high activity and reactivity, late noble transition metals have been the metals of choice in homogeneous catalysis for decades. However, their scarcity and low natural occurrence make them precious and thus expensive. In fact the natural occurrence in the Earth's crust of late noble transition metals (Ru, Pd, Ir, Rh, Os) is about 0.001 ppm (mass percentage) while iron, titanium, manganese are present at 50 000 ppm, 5 000 ppm and 1 000 ppm respectively (for abundance of elements in the Earth's crust, see **Figure A^{1}.2**). Behind these figures, upstream of the use of such rare metals, laborious extractions requiring a lot of energy and chemicals are needed. In term of geopolitics, production of all the rare metals from the platinum group is concentrated in few countries, South Africa being the major supplier (83 % of the worldwide production). As result, most of noble metals are listed as critical raw materials for European Union.[6] On the contrary, production of abundant metals is better distributed.[7]

In addition, base metals have higher contamination limits in pharmaceuticals, *i.e.* for iron: 1300 ppm and for manganese: 250 ppm while for ruthenium, iridium, rhodium: 10 ppm, so their separations require less efforts for the fine chemical industry.[8]

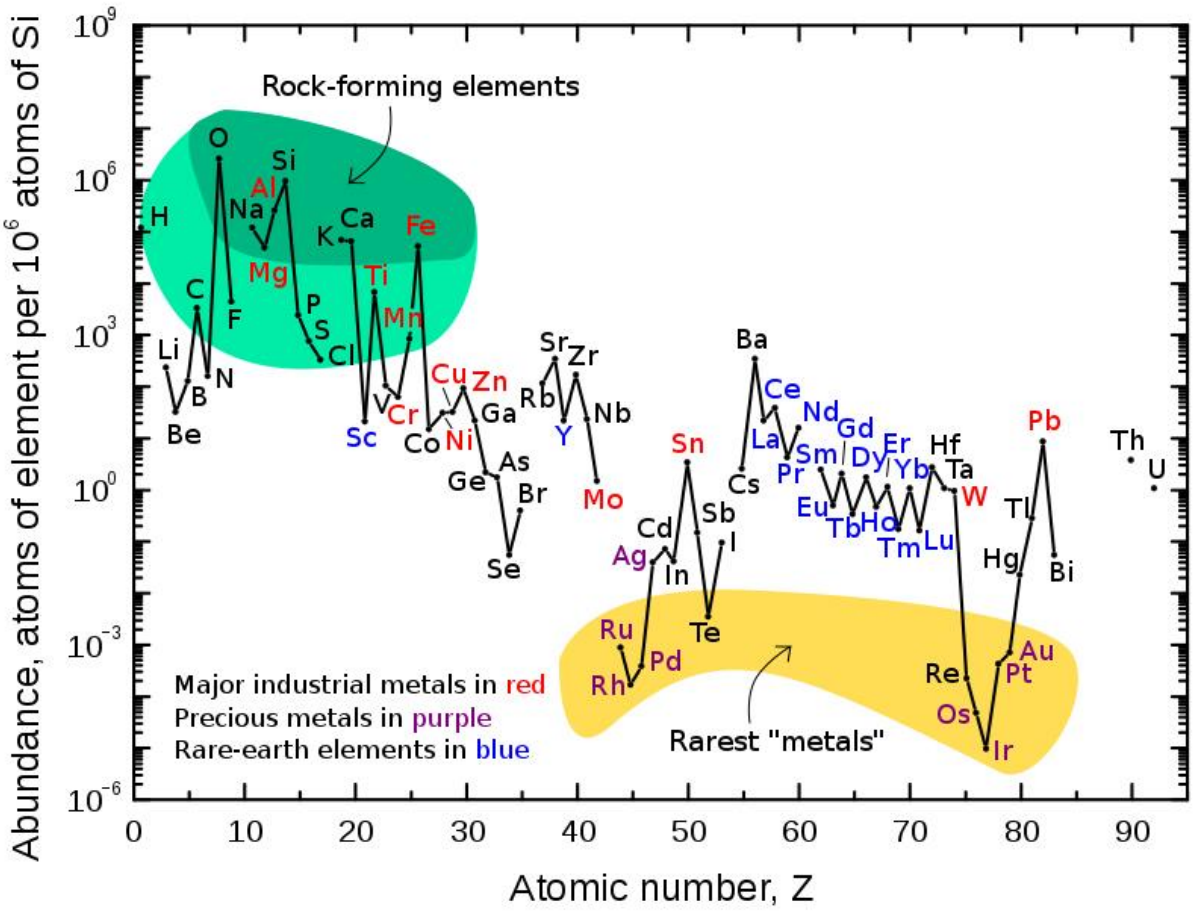

Figure A[1].2 Abundance of atoms in Earth's crust correlated with atomic number highlighting rarest elements. Source: http://pubs.usgs.gov/fs/2002/fs087-02/

For all these reasons, base metals, disregarded for decades, are now reconsidered as surrogates to precious metals in many catalytic transformations. Iron, being the most abundant and cheapest base metal, has been studied in the field of reduction since decades. On the opposite manganese is mainly popular for its high oxidation state complexes that are able to perform oxidation reactions ($KMnO_4$, MnO_2) or catalyze oxidation reactions (Jacobsen's catalysts[9]), and it was not known to catalyze either hydrogenation reactions or the reverse dehydrogenation reactions before the beginning of this PhD thesis.

B – Landmarks in catalytic (de)hydrogenation reactions

In the second part of the introduction, a personal account of the development of hydrogenation reaction with dihydrogen as reductant, then the transfer hydrogenation with various hydrogen donors and finally the hydrogen borrowing reactions, or hydrogen auto-transfer, is presented.

I- Hydrogenation

Hydrogenation with molecular dihydrogen (H_2) is a clean, atom-economic and efficient reaction that has drawn a huge interest for more than a century since the Nobel Prize of Sabatier in 1912 for heterogeneous hydrogenation catalyzed by nickel powder.[10]

a) Hydrogenation with precious transition metals

A good way to show the importance of homogeneous hydrogenation is to take examples from the industry where homogeneous hydrogenation, in particular asymmetric hydrogenation, is a well-established methodology. In comparison with heterogeneous hydrogenation, the fine-tuning of the properties of the molecularly defined catalyst is often the key to reach high degree of chemo-, regio- and enantioselectivity. An in deep control of the parameters of the reaction is often needed to obtain a high level in selectivity starting from prochiral substrates. Moreover, in comparison with other approaches such as crystallization of diastereomeric adducts, HPLC separations, uses of stoichiometric chiral auxiliaries or bio-catalysis with specific enzymes, the asymmetric homogeneous catalysis is an elegant way to obtain enantio-pur products without the need for huge volumes of solvents or production of large amount of wastes.

In general, for asymmetric hydrogenation, high turnover numbers are mandatory to make the process economically viable, *i.e.* over 1000 for high value products and over 50000 for large-scale or less expensive products. In term of selectivity, enantiomeric excess (e.e., %) over 99% are expected for pharmaceuticals but in most cases e.e.'s over 90% are acceptable, as often a crystallization allows to gain highest e.e.'s.[11] The most common metals to achieve this level of activity are rhodium, iridium and ruthenium. The chemoselectivity is also very important especially when multifunctional substrates are involved.

Several reviews report the achievements made in hydrogenation reaction and its asymmetric version including in industrial applications.[11–14]

Even if the first homogeneous hydrogenation reactions were developed with copper in the 1930's,[15] a breakthrough was made by Wilkinson in the 1960's using a homogenous catalyst $RhCl(PPh_3)_3$ to hydrogenate alkenes with an activity comparable to heterogeneous catalysts (**Figure B^{1l}.1**).[16]

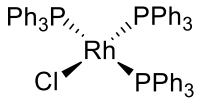

Rh-1 Wilkinson

Figure B^{1l}.1 First efficient homogeneous catalyst for hydrogenation developed by Wilkinson.

Monodentate phosphine ligands have been privileged for many years in order to stabilize catalysts and modulate the hydricity of hydrides. In order to solve the classical issue of stability of the complexes related to ligand dissociation, and to increase the spatial control around the metallic center, polydentates ligands have emerged as powerful ligands in the eighties.

With this respect, chiral bidentate phosphine ligands were introduced by Noyori, Knowles and Kagan who have demonstrated an unprecedented level of control for asymmetric hydrogenation. In 1987, the group of Noyori described the asymmetric hydrogenation of β-ketoesters using a ruthenium catalyst **Ru-1** bearing a chiral BINAP ligand in its coordination sphere (**Scheme B^{1l}.1**).[17] These catalysts are now widely used in the production of several drugs, such as the antibacterial Levofloxin, the antibiotic Carbapenem, and the antipsychotic agent BMS181100.

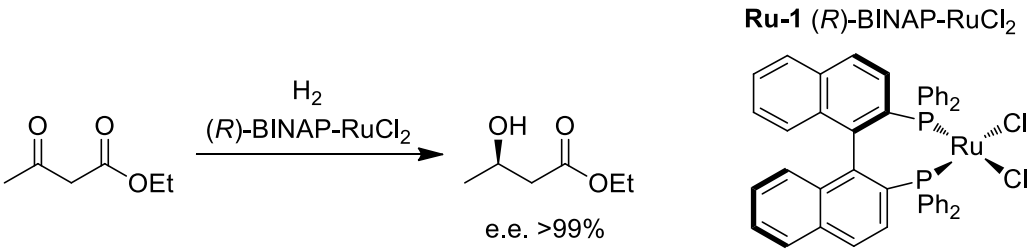

Scheme B[1l].1 Asymmetric hydrogenation of β-ketoesters by Noyori.

The first large-scale plant was developed by Knowles at Monsanto for the synthesis of *L*-Dopa, a drug to treat the Parkinson disease. In the overall synthesis, the key step was the enantioselective hydrogenation of an enamide intermediate (**Scheme B[1l].2**).[18] The reaction conditions were very mild: 25 °C and 10 bar of H_2. To avoid the slow racemization of the free ligand, isolated $[Rh(dipamp)(diene)]^+BF_4^-$ complex was used as catalyst, showing a very good performance (unusual at this time): 95% e.e., TON 10000-20000, TOF 1000 h^{-1}.

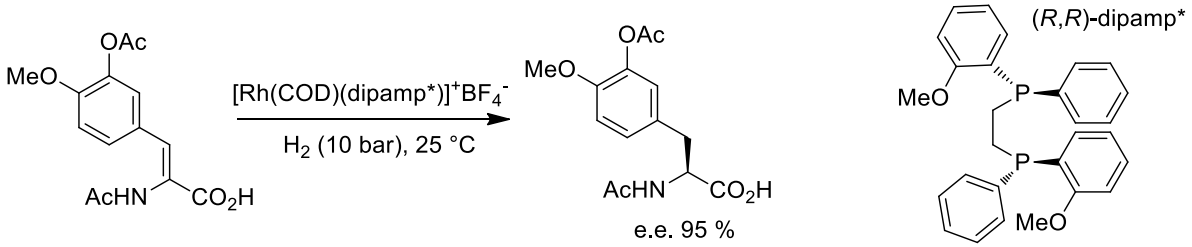

Scheme B[1l].2 Industrial application of hydrogenation by Monsanto.

In the same vein, researchers at BASF developed a very atom-economic synthesis of *L*-menthol (**Scheme B[1l].3**).[12] The key step in the procedure was the catalytic asymmetric hydrogenation of C=C bond of neral to *D*-citronellal using $Rh_4(CO)_{12}$/Chiraphos as catalytic system which could be recovered after the reaction.

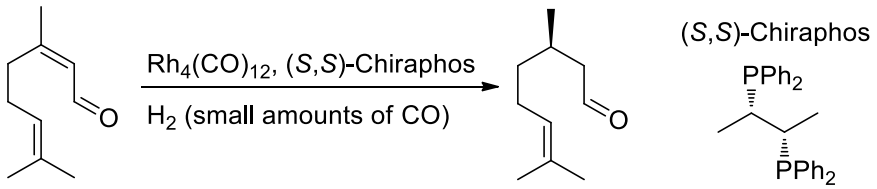

Scheme B[1l].3 Industrial application of hydrogenation by BASF.

More than just affecting electronic and steric properties of catalysts, some ligands, inspired by the nature and the active sites of enzymes, can actively participate in the activation of substrates: the so-called cooperative metal-ligand catalysts or non-innocent ligands. Usually the metal-ligand cooperativity is driven by the ability of the

ligand to act as proton shuttle (*via* protonation/deprotonation) or electron shuttle (*via* electron transfer to or from the metal). Hydrogen bonding or electrostatic interactions can be described as cooperative interactions as well.

In 1995, Noyori published the use of BINAP-Ru-diamine **Ru-2** to reduce acetophenone with a TOF of 6700 h^{-1} while without the diamine ligand, the parent pre-catalyst has almost no activity (TOF less than 5 h^{-1}).[19,20] Noyori rationalized the use of diamine ligands to promote fast hydrogenation reactions through the "N-H effect": due to the basicity the NH_2 moieties, the protic hydrogen can be deprotonate by the reduced substrate (alkoxide in this particular case) and also subsequently actively participate to the heterolytic cleavage of H_2 (**Figure B^{1l}.2**). This cooperation helped to reduce simple ketones that do not have a functional group able to coordinate on the metal which were the substrates of choice with **Ru-1** to reach high level of selectivity. In addition, these catalysts were also able to reduce selectively the polar C=O bonds in the presence of non-polar C=C bonds, usually easier to reduce with previous catalysts.

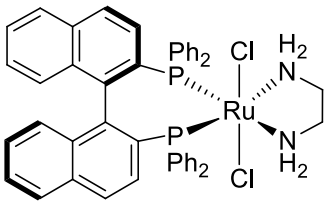

Ru-2 Noyori

Figure B^{1l}.2 First efficient homogeneous catalyst for asymmetric hydrogenation of simple ketones

This first example led to intensive mechanistic studies to fully understand the role of the "NH moieties" in hydrogenation. Noyori and Morris described a new mechanism, called outer-sphere mechanism by opposition to the inner-sphere one, in which the participation of non-innocent ligand containing N-H bond help to reduce the substrate.[21] For diphosphine-diamine-ruthenium catalysts, the active species is a dihydride ruthenium complex which reduces the substrate delivering, in a concerted manner, one hydride from the metal and one proton from the ligand to the C=O bond. Depending on the presence of a base or not, the reaction pathway can involve cationic or neutral species for the heterolytic cleavage the dihydrogen, as described below (**Scheme B^{1l}.4**).

Some revisions have been made recently to mention that the Ru-H bond is cleaved to produce the C-H bond of the product but the η^2-H_2 ligand within the cationic Ru complex serves as an acid to neutralize the alkoxide anion stepwise (**Scheme B[1l].4** d) step). A solvent-assisted mechanism to cleave the dihydrogen is also possible.[22]

Other mechanisms are also described when a large excess of base, such as *t*BuOK, is needed to run the reaction. A proton from the amine moiety on the ligand is replaced by the cation K^+ and this more basic NHK scaffold accelerates the hydride transfer and the H_2 splitting (d) step).[23,24]

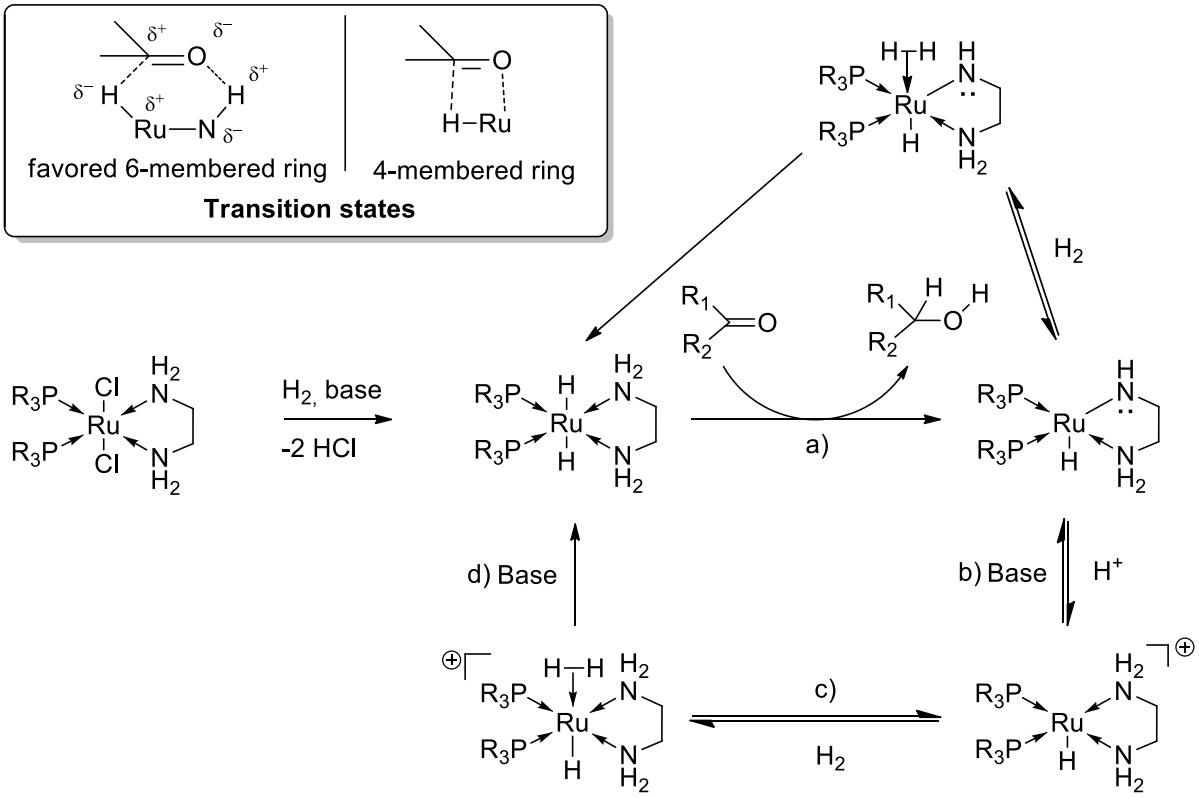

Scheme B[1l].4 Mechanism proposed by Noyori.

Shvo, with the ruthenium complex **Ru-3**, highlighted the participation of the cyclopentadienone ligand in the hydrogenation of polar bond also *via* an outer-sphere mechanism.[25]

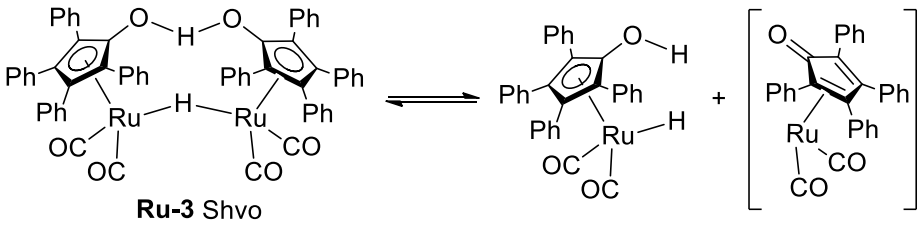

Ru-3 Shvo

Figure B[1I].3 Catalyst developed by Shvo for hydrogenation.

Since these early achievements, a plethora of bifunctional catalysts has been developed. In particular, selective reduction of carbonyl group in the presence of other functionalities such as olefins is also perform at industrial scale by Firmenich for the synthesis of Polysantol®, Firsantol® and Dartanol® which are analogues to the precious and rare East Indian sandalwood natural oil widely used in perfumery. In these cases catalytic loadings as low as 0.00125 mol% of **Ru-4** complex could be used: it is worth noting that this catalyst proceeds without the addition of an external base which avoids side-reactions.[26]

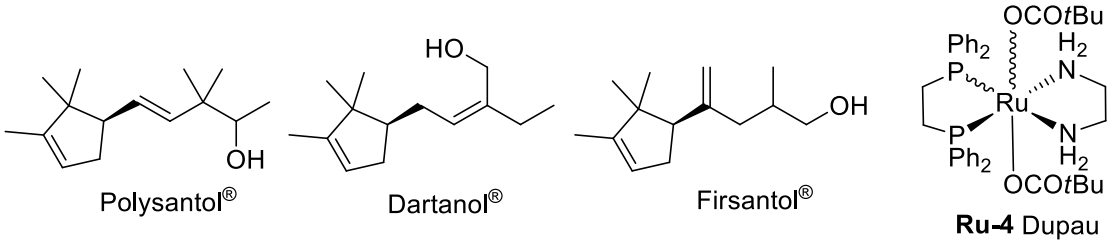

Polysantol® Dartanol® Firsantol®

Ru-4 Dupau

Figure B[1I].4 Catalyst for base-free hydrogenation of aldehydes developed at Firmenich.

In terms of substrates, the scope of the hydrogenation reaction is large and can be described according to the difficulty to reduce unsaturated bonds: alkene, alkyne < aldehyde, aldimine < ketones, ketimine, nitro < anhydride, imide < ester, cyano, carboxylic acids < amides < CO_2. Behind these general features, the presence of other functionalities or heteroatoms, bulky substituents, can make the substrate more challenging to reduce. In addition, the possibility to perform side reactions can make the reduction more complicated. For example, aldehydes are sensitive to basic conditions under which competitive aldolisation, Claisen-Tishchenko or Cannizaro reactions can occurred.

In the context of conversion of biomass to fuel, the hydrogenation of esters to alcohols has encountered a renewal of interest in the last decades. First approached by Elsevier in 1998,[27] the hydrogenation of esters was efficiently tackled by the

group of Saudan at Firmenich, changing the bisphosphine and diamine ligands by two amino phosphine ligands or the corresponding tetradentate ligand (**Figure B^{1l}.5**) to perform this reaction with a high activity (TON 2000, TOF 800-2000 h^{-1}).[28]

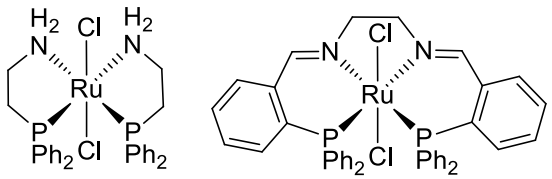

Ru-5 Saudan **Ru-6**

Figure B^{1l}.5 Catalysts for hydrogenation of esters developed at Firmenich.

Another breakthrough in this field was made in 2011 by Kuriyama[29] from Takasago, as an alternative strategy to the one of Firmenich using tridentate ligand instead of bidentate ligands (**Figure B^{1l}.6**). They mentioned that with this new type of ligand, bisphosphinoamine called MACHO, the ruthenium complex **Ru-7** was less subject to ligand dissociation and to carbonylation/decarbonylation reactions. Therefore the hydrogenation of esters on large scale was applied with a high efficiently (TON up to 4000).

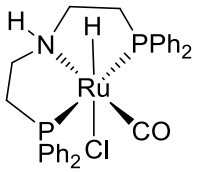

Ru-7
MACHO-Ru
Kuriyama

Figure B^{1l}.6 Catalyst for hydrogenation of esters developed at Takasago.

Despite the success of phosphines in catalysis, they have well-known drawbacks: their preparation is often complicated, requires inert atmosphere and is costly on large scale. Efforts have been made to replace phosphine moieties on the ligand, for example by oxazolidine or carbene groups.[30–32] Remarkably, Gusev published very active catalysts **Ru-8** and **Ru-10** for the hydrogenation of esters by replacing one phosphorus wingtip by a pyridine one or the two phosphorus atoms by sulfur ones (TON up to 18000-40000) (**Figure B^{1l}.7**).[33,34] Interestingly, reacting **Ru-8** with one equivalent of base, an unusual new dimeric complex **Ru-9** was isolated and fully characterized. Furthermore, this complex was efficient for the base-free hydrogenation of esters.

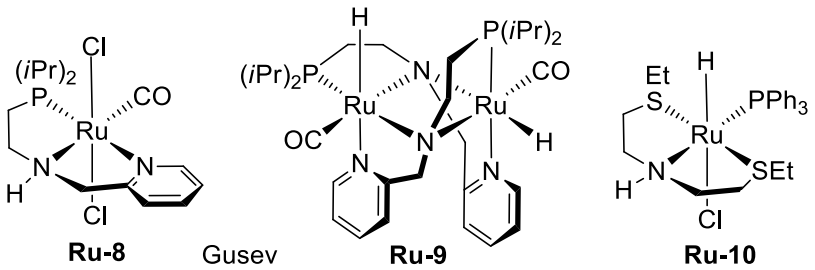

Figure B[1l].7 Catalysts developed by Gusev for ester hydrogenation.

To go further in the entire control of the coordination sphere, Lv and Zhang increased the denticity of the ligand. They published in 2015 one of the most efficient tetradentate complex **Ru-11** for hydrogenation of esters (TON up to 80000), combining Gusev and Saudan strategies (**Figure B[1l].8**).[35] They also performed hydrogenation of cellulose to hexitols with **Ru-12**.[36]

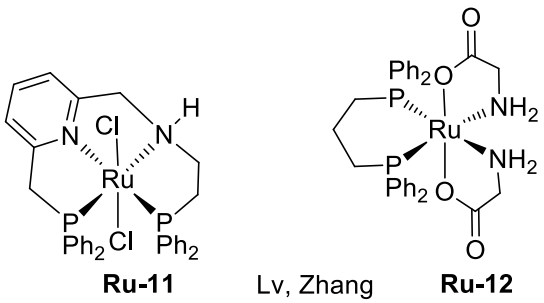

Figure B[1l].8 Catalysts developed by Lv and Zhang.

b) Hydrogenation with base transition metals

For more than a century, catalytic hydrogenation has been performed with the help of transition metals belonging to groups 8-10, mainly with noble late transition metals. A decade ago, iron emerged as an alternative to ruthenium for the hydrogenation of carbonyl derivatives (**Figure B[1l].9**),[37] when Casey and Guan described the first well-defined iron catalyst for the hydrogenation of ketones using a Knölker's type catalyst **Fe-1** efficient at room temperature under low hydrogen pressure with high chemoselectivity. Since then, tremendous progress has been accomplished with this type of catalysts especially in hydrogenation, by the groups of Berkessel, Beller, Renaud, Piarulli, Wills and others. [38–40]

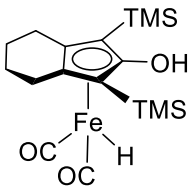

Fe-1 Casey, Guan
2007

Figure B^{1l}.9 First iron catalyst developed by Casey and Guan for hydrogenation.

Casey's work paved the way for the development of various types of hydrogenation catalysts based on iron and non-innocent ligands. Among that, Chirik has demonstrated that ligands able to act as single-electron donor or acceptor (such as bis(imino)pyridine ligands which exist in several oxidation states), are highly relevant to activate substrates (**Figure B^{1l}.10**).[41] Redox non-innocent ligands are of growing interest in the field of first raw metal catalysis, as base metals often tend to undergo one-electron oxidation state changes while noble metals are more familiar with two-electron oxidation changes matching with the classical organometallic elementary steps.

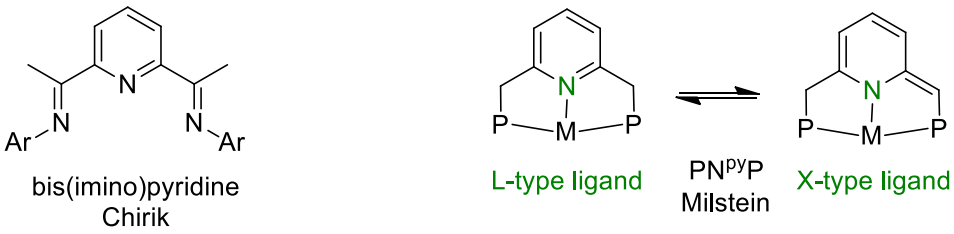

Figure B^{1l}.10 Example of red-ox non-innocent ligands.

Interesting metal-ligand cooperation was described by Milstein with pincer PN^{py}P ligand. In the presence of a base, the deprotonation of one CH_2 on a wingtip of the ligand occurred leading to a new mode of coordination of the pyridine group, changing from L-type to X-type ligand *via* de-aromatization (**Figure B^{1l}.10**).

The group of Milstein associated their PN^{py}P ligand with iron creating an efficient pre-catalyst **Fe-2** for hydrogenation of various carbonyl derivatives (**Figure B^{1l}.11**).[42,43] Ketones, and even esters, could be hydrogenated at room temperature while amides needed 140 °C to be reduced. An asymmetric version was also developed by Mezzetti later.[44] In parallel, the group of Kirchner showed that switching from CH_2 linker on the wingtip to an NH could lead to an efficient catalyst **Fe-3** for the hydrogenation of ketones or CO_2.[45]

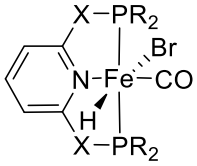

Fe-2 Milstein **2011** X=CH_2
Fe-3 Kirchner **2014** X=NH
Fe-4 Mezzetti **2018** X=CH_2

Figure B^{1I}.11 Iron complexes developed by Milstein and others.

Using MACHO-type ligand on iron **Fe-5**, Guan *et al.* were able to reduce fatty esters into fatty alcohols (**Figure B^{1I}.12**).[46] Other derivatives from this PNP-Fe system were published to hydrogenate different substrates such as esters (at 60 °C), nitriles,[47] amides (at 70 °C) and even CO_2[48,49] including asymmetric hydrogenation.[50]

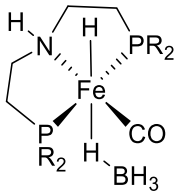

Fe-5
Guan **2014**
Jones, Schneider **2014**
Beller **2014**
Morris **2014**

Figure B^{1I}.12 MACHO-Iron complexes developed in 2014.

The group of Morris used similar complexes **Fe-8/9** for the asymmetric hydrogenation of ketones (**Figure B^{1I}.13**). They also studied the use of tetradentate ligands in this field, the activity of these pre-catalysts **Fe-6/7** is similar than their tridentate counterparts while the enantioselectivity is lower for hydrogenation.[51] However, **Fe-7** was very efficient in transfer hydrogenation.

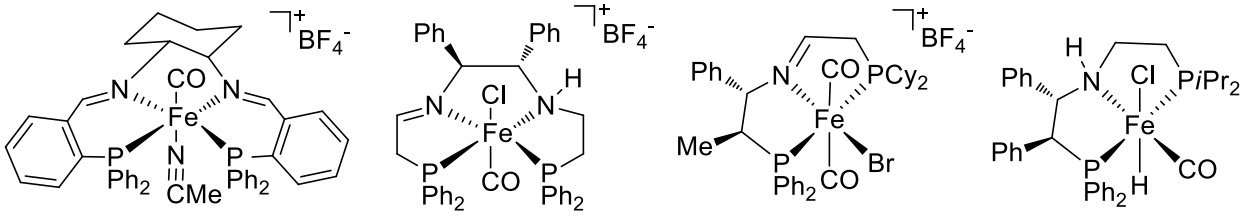

Fe-6 Morris 2008 **Fe-7** 2014 **Fe-8** 2014 **Fe-9** 2016

Figure B^{1I}.13 Iron complexes developed by Morris.

Among the base late transition metals, cobalt complexes are also known since 2014 to catalyze the hydrogenation reactions but will not be discussed herein.[52]

Finally, manganese was applied for the first time by the group of Beller in 2016 for the hydrogenation of various substrates. This field is growing extremely rapidly and the use of manganese in hydrogenation will be discussed in the conclusion of my thesis.

II- Transfer hydrogenation

An alternative methodology for reduction, transfer hydrogenation is also a well-established methodology using a hydrogen donor as hydride source (typically isopropanol or formic acid). Compared to direct hydrogenation, the transfer hydrogenation methodology is more convenient at laboratory scale as it does not require pressurized H_2 gas and dedicated equipment such as autoclaves. The hydrogen donors are often readily available, inexpensive, easy-to-handle and the major by product can be recycled.

a) With noble transition metals

The first example of transfer hydrogenation type reaction was reported by Knoevenagel in 1903 using Pd black as catalyst.[53]

The first transfer hydrogenation of carbonyl compounds was published independently by Verley and Meerwein in 1925 [54,55] using stoichiometric amount of aluminum alkoxide, now called Meerwein-Ponndorf-Verley (MPV) reduction (**Scheme B^{II}.1**). This reaction suffered from slow kinetics but Ponndorf increased significantly the rate of the reduction using aluminum isopropoxide in isopropanol. The reverse reaction, *i.e.* oxidation of secondary alcohol, is also possible in similar conditions, well known as the Oppenauer oxidation.

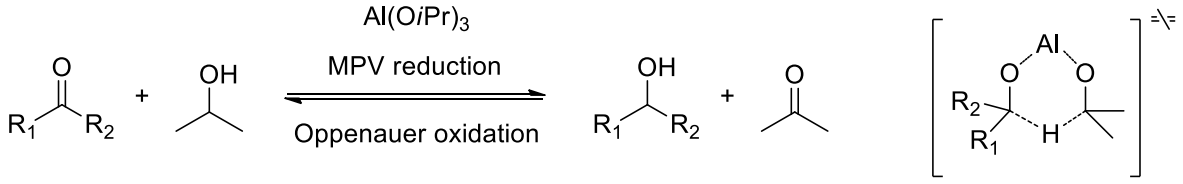

Scheme B^{II}.1 Equilibrium between MPV reduction and Oppenauer oxidation.

At this point it has to be noted that a simple base containing alkali metal such as Li, Na, K can catalyzed itself the transfer hydrogenation of ketones with isopropanol

(**Scheme B^{1II}.2**).[56] For example, sodium hydroxide (10 mol%) could catalyze the reduction of acetophenone derivatives in isopropanol at reflux during 24 hours. As bases are often used to activate pre-catalysts, long reaction times or refluxing conditions should be avoided.

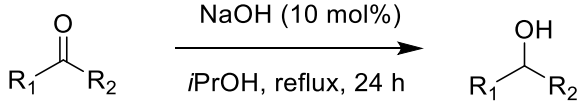

Scheme B^{1II}.2 Base catalyzed reduction of ketones.

In the 60's, the introduction of metal hydrides to catalyze transfer hydrogenation constituted a milestone.[57] The main key advances were the use of diamines as ligands with ruthenium introduced by Noyori,[58,59] and the use of catalytic excess of base to accelerate the reaction by Bäckvall.[60]

Since then, tremendous improvements have been accomplished especially using first-, second-, and third-row transition metals of groups 8, 9, 10, and 11. This topic has been reviewed intensively and only selected examples are discussed hereafter.[61,62]

As with hydrogenation, asymmetric transfer hydrogenation was intensively studied due to the importance of optically active alcohols and has found applications in the industry. Piano-stool ruthenium *p*-cymene diamine complexes, introduced by Noyori (**Ru-13**) are the archetypal widely applied catalysts in this field. Numerous derivatives from this catalyst have been published.[61,63]

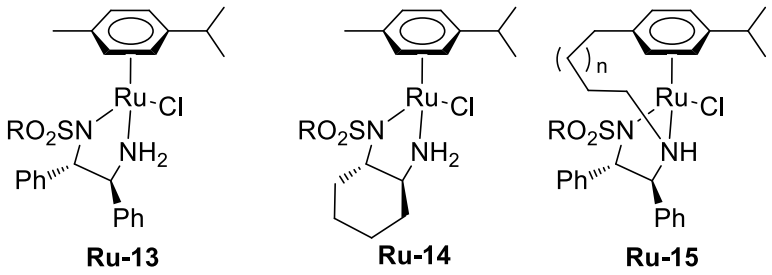

Figure B^{1II}.1 Noyori type catalysts for transfer hydrogenation.

For industrial relevant examples (**Scheme B^{1II}.3**), the synthesis of (+)-erythro Mefloquine relies on synthesis the intermediate **int-1** obtained with a very high enantioselectivity by transfer hydrogenation using 0.001 mol% of **Ru-13** and a 1:1 HCO_2H/Et_3N mixture as reductant in DMF at 20 °C during 20 h.[64] The original Noyori's catalyst was also applied for the reduction of 3-trifluoromethylacetophenone

which is an intermediate **int-2** of a fungicide, and in the course (**int-3**) of the synthesis of Dorzolamide.

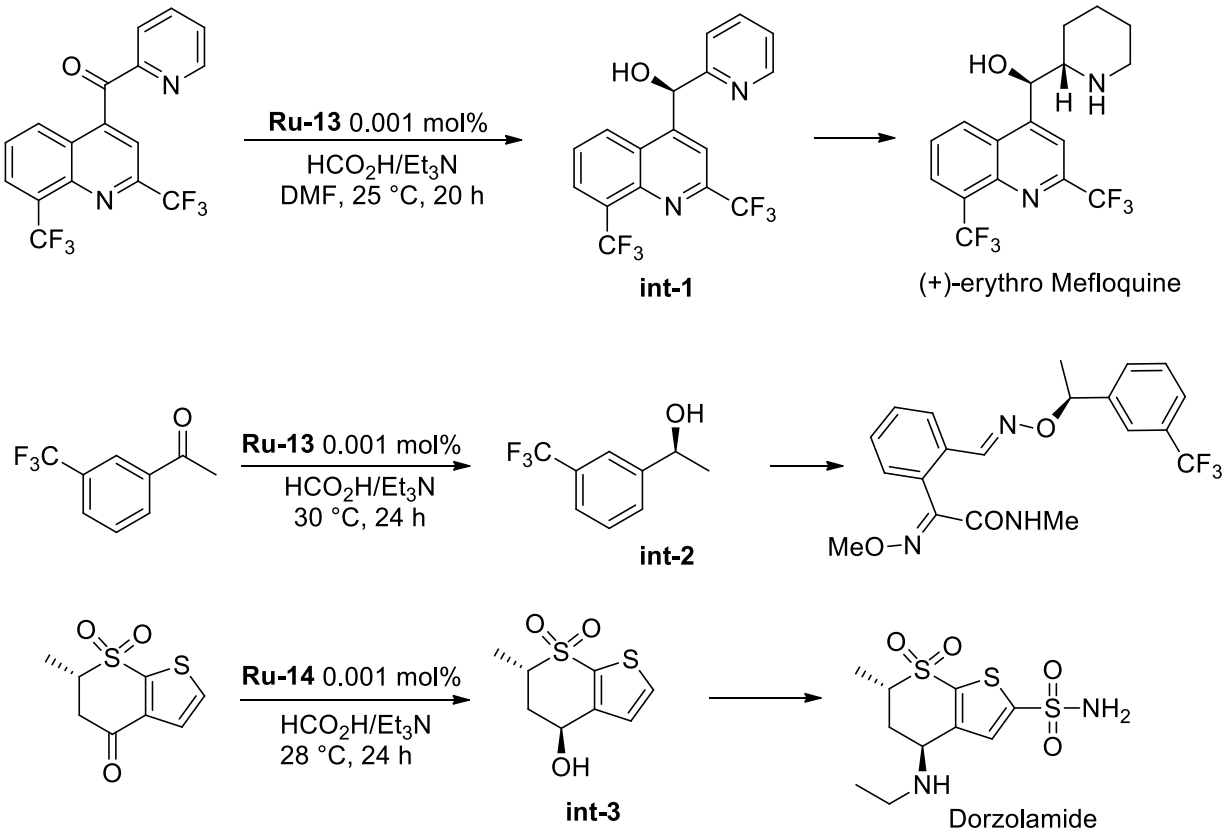

Scheme B^{III}.3 Industrial applications of Noyori's type catalysts for transfer hydrogenation of ketones.

Among the significant modifications, the use of tethered catalysts such as **Ru-15**, introduced by Wills and Ikariya, allowed the decrease of the catalytic loading by avoiding ligand dissociation (**Figure B^{III}.1**).[65]

The development of "superlative" ruthenium catalysts has been realized by Baratta: they demonstrated the beneficial effect of the aminomethylpyridine ligand in Noyori's type catalyst (associated with bisphosphine, **Ru-16**) for this reaction (**Figure B^{III}.2**). While the classical Noyori's catalyst containing ethylenediamine is poorly active in transfer hydrogenation,[19] the similar complex with aminomethylpyridine is very active (TOF up to 3.10^5 h^{-1}).[66] They further developed their catalyst using cyclometalation to avoid ligand dissociation. In fact, the tridentate cyclometalated CNN complex **Ru-17** reached TOF up to $2.5.10^6$ h^{-1} for the transfer hydrogenation of ketones.[67]

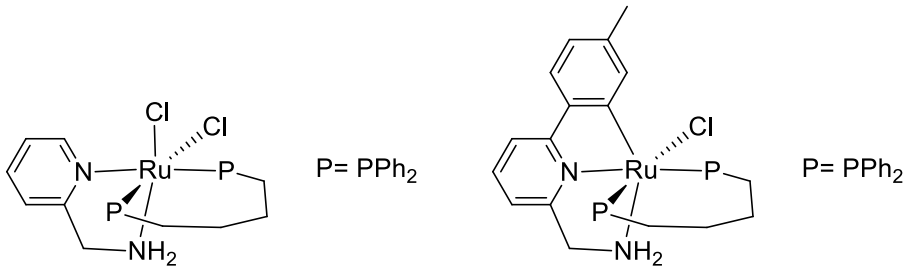

Ru-16 0.005 mol%, 2 mol% NaOH, *i*PrOH, 82 °C, 1 min. TOF: 3 10^5 h^{-1}

Ru-17 0.005 mol%, 2 mol% NaOH, *i*PrOH, 82 °C, 5 min. TOF: 2.5 10^6 h^{-1}

Figure B^{1II}.2 Complexes developed by Baratta

Aside from chemical modifications of catalysts, an emerging field relies on the modification of the nature of the reaction media. It is now established that transition metal complexes can be useful drugs for cancer treatment, such as *cis*-platin. Combining their experience in ruthenium complexes for cancer treatment and transfer hydrogenation, Sadler and Wills have studied, recently, the possibility to promote hydrogen transfer reaction in cancer cells, by killing them through a disruption of their redox balance. They found that osmium catalysts (**Os-1**, analogue to Noyori's catalyst) are efficient for the asymmetric reduction of pyruvate and are less prawn to degradation than ruthenium catalysts (**Scheme B^{1II}.4**).[68]

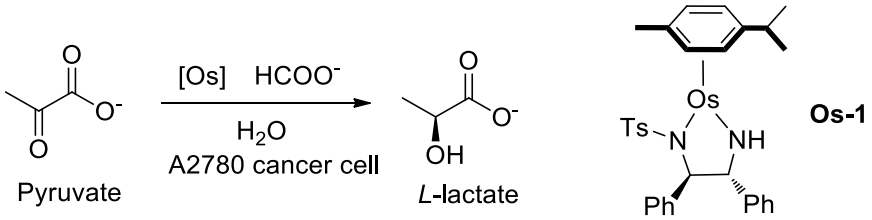

Scheme B^{1II}.4 Asymmetric transfer hydrogenation in cells developed by Wills and Sadler

b) <u>With non-noble transition metals.</u>

First raw transition metals have also been applied for transfer hydrogenation: iron and cobalt complexes represent the mostly used catalysts. An overview of the progress made in this field will be done starting with cobalt catalysts, then with iron catalysts. The very new field of manganese catalysts will be discussed in conclusion of this PhD manuscript.

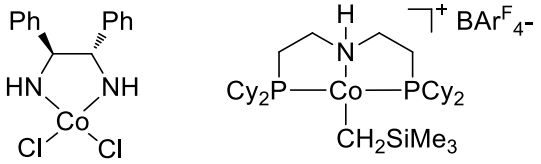

Lemaire **1997**
Co-1 5 mol%,
20 mol% *t*BuOK,
*i*PrOH 25 °C, 6 days,
conv. 8%,
e.e. up to 58%.

Hanson **2013**
Co-2 2 mol%,

*i*PrOH/THF,
25 °C, 24 h.

Figure B^{1II}.3 Cobalt complexes for transfer hydrogenation of carbonyl derivatives

The first pre-catalyst for the transfer hydrogenation of ketones with cobalt was described by Lemaire in 1997 using a simple **Co-1** complex bearing one chiral diamine, achieving a modest conversion (8%) after 6 days at 25 °C in *i*PrOH (**Figure B^{1II}.3**).[69] The second catalytic system appeared only sixteen years later: in 2013, Hanson reported the transfer hydrogenation of ketones, aldehydes and aldimines catalyzed by **Co-2**, bearing a MACHO-type ligand, at room temperature in *i*PrOH/THF.[70]

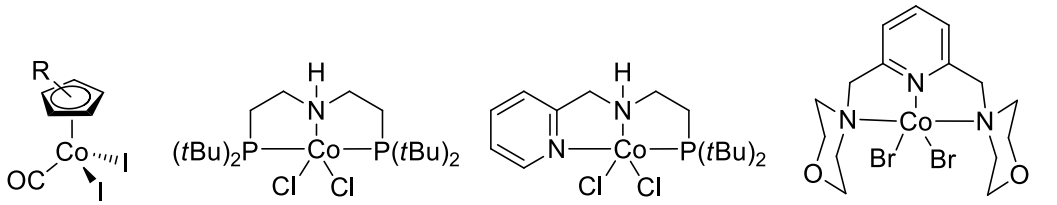

Waterman **2015**
Co-3 1.2 mol%,
NH_3BH_3 in THF,
65 °C, 6 h.

Zhou, Liu **2016**
Co-4 1 mol%,
NH_3BH_3 in MeOH,
50 °C, 16 h.

Co-5 1 mol%,
NH_3BH_3 in hexane,
50 °C, 16 h.

Madhu, Balaraman **2016**
Co-6 2 mol%,
NH_3BH_3 in MeOH,
50 °C, 16 h.

Figure B^{1II}.4 Cobalt complexes for transfer hydrogenation of alkenes and alkynes.

With the same catalytic system, Zhang *et al.* were able to reduce alkene at 100 °C in *i*PrOH (**Figure B^{1II}.4**). In 2015, Waterman introduced the use of ammonia-borane as hydrogen source to reduce alkenes with a simple **Co-3** catalyst at 65 °C in THF. In 2016, the group of Zhou and Liu succeeded to reduce alkynes to alkenes with a *Z*-selectivity using PNP **Co-4** and a *E*-selectivity using less sterically hindered N^{py}NP **Co-5** in MeOH at 50 °C. Nitriles could also be chemoselectively reduced to amines at only 50 °C in *n*-hexane. In both cases, the reductant was NH_3BH_3, the major issue with this reductant is the generation of unrecovered by-products. The same year, Madhu and Balaraman developed a phosphine-free catalytic system **Co-6** for the *Z*-selective semi-hydrogenation of alkynes under similar conditions.

It is worth noting that in most of the examples described here above, in order to stabilize the cobalt complexes, and to get activity, tridentate ligands (MACHO or Gusev's types) have been used. Similar feature will be found in the case of iron, and later manganese.

The first iron catalytic system able to reduce C=O bond of benzylideneacetone derivatives was published by the group of Peruzzini, Graziani and Bianchini in 1993 (**Figure B^{1II}.5**).[71] Unfortunately, the catalyst **Fe-10** (1 mol%), made of tetraphosphine ligand, was extremely substrate-dependent as only the reduction benzylideneacetone derivatives gave the corresponding unsaturated alcohols in high yields in a mixture dioxane/*i*PrOH at 80 °C for 7 h without additives.

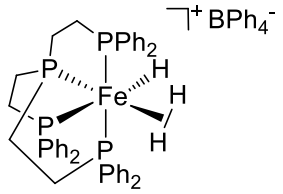

Bianchini, Graziani **1993**
Fe-10 1 mol%,
dioxane/*i*PrOH,
80 °C, 7 h.

Figure B^{1II}.5 First iron catalyst for transfer hydrogenation of ketones

The group of Beller in 2006 generated *in situ* a catalytic system from [Fe]/terpy/PPh_3 (1 mol%) in the presence of *i*PrONa (5 mol%) in *i*PrOH at 100 °C for 7 h to reduce various ketones.[72] The role of the metal under such conditions has been investigated and parallel base promoted transfer hydrogenation could not be ruled out.[73]

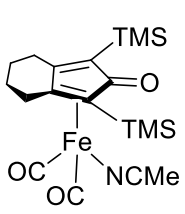

Funk **2012**
Fe-11 5 mol%,
*i*PrOH, 80 °C, 18 h.

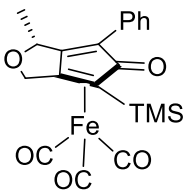

Wills **2012**
Fe-12 10 mol%,
10 mol% Me_3NO,
HCO_2H/Et_3N, 28 °C, 48 h,
e.e. up to 25%.

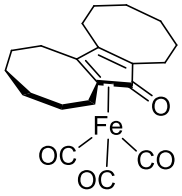

Genari **2017**
Fe-11b 2 mol%,
4 mol% Me_3NO,
*i*PrOH,100 °C, 17 h.

Figure B^{1II}.6 Knölker's type iron catalysts for (asymmetric) transfer hydrogenation

Knölker's type iron complexes, introduced by Casey and Guan in 2007, were applied in transfer hydrogenation of aldehydes and ketones (**Fe-11**) in 2012 by Funk[74] and

even in asymmetric transfer hydrogenation of ketones (**Fe-12**) by Wills, although moderate e.e.'s were reached (**Figure B^{1II}.6**).[75] The scope has been extended to imines by the group of Genari using **Fe-11b** catalyst at 100 °C in *i*PrOH.

Morris synthesized in 2009 iron tetradentate PNNP complex **Fe-13**, analogue to the previously described ruthenium complexes (**Figure B^{1II}.7**). After few years of an elegant rational design of the ligand thanks to studies of the mechanism shedding light on the active species in catalysis, they developed the most active catalyst known to date for the asymmetric transfer hydrogenation of ketones and imines. TON up to 6000 and TOF up to 160 s^{-1} were achieved for reduction of ketones with the help of 0,016 mol% of catalyst **Fe-7** and 0,033 mol% of *t*BuOK in *i*PrOH at 28 °C in just a few minutes. During the optimization of the catalyst design, they discovered that the presence of a carbonyl ligand and a tetradentate partially oxidized ligand, bearing one imine and one amine moieties, were important, as well as a 5-membered metallacycle.[51,76] They also highlighted that iron nanoparticules could be the active species.[77] This work is one of the rare examples where a base metal (Fe) can surpass noble late transition metals (Ru, Ir, Rh, Pd) in terms of activity (TOF up to 242 s^{-1}).[78]

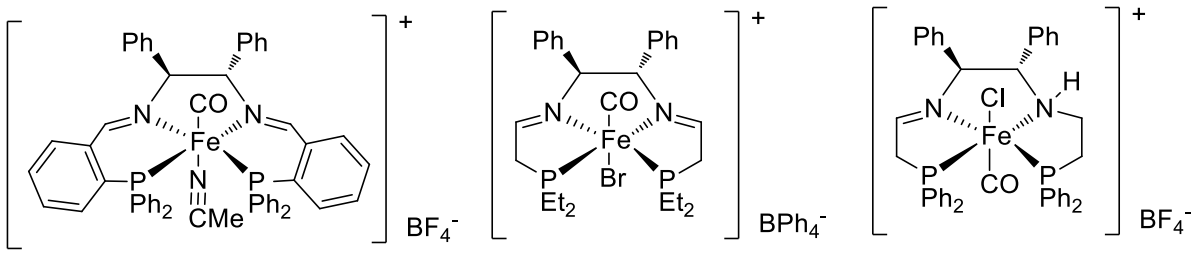

Morris **2009**
Fe-13 0.17 mol%,
1.33 mol% *t*BuOK, *i*PrOH,
24 °C, 15 min, e.e. up to 96%.

2010
Fe-14 0.1 mol%,
0.8 mol% *t*BuOK, *i*PrOH,
50 °C, 10 min, e.e. up to 60%.

2013
Fe-7 0.016 mol%,
0.033 mol% *t*BuOK, *i*PrOH,
28 °C, 3 min, e.e. up to 98%.

Figure B^{1II}.7 Iron complexes developed by Morris.

Inspired by the work of Morris in hydrogenation, the group of Le Floch developed an iron complex **Fe-15** based on tetradentate iminophosphorane ligand that was able to reduce acetophenone with a low catalytic loading (0.1 mol%) in *i*PrOH at reflux with 4 mol% of *i*PrONa.[79]

Finally, Mezzetti succeeded to attain the highest level of enantioselectivity (up to 99%) using 0.1 mol% of macrocylclic PNNP **Fe-16** at 50 °C in *i*PrOH during 15 min

without any additives thanks to the use of a very labile ligand (CN*t*Bu) instead of Cl.[80,81]

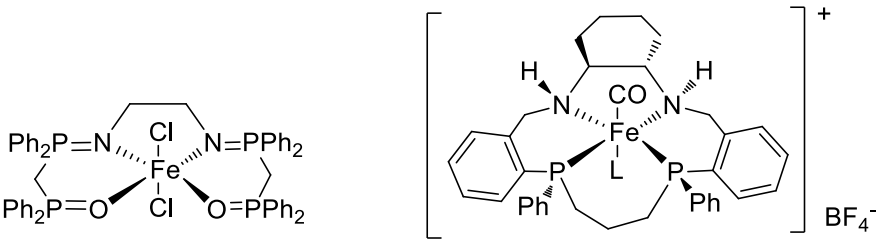

Le Floch **2009**
Fe-15 0.1 mol%,
4 mol% *i*PrONa, *i*PrOH,
82 °C, 24 h.

Mezzetti **2017**
Fe-16 0.1 mol% (L=CN*t*Bu),
50 °C, *i*PrOH,15 min,
e.e. up to 99%.

Figure B^{1II}.8 Other tetradentate iron complexes.

This brief overview of the development of iron based catalysts for reduction demonstrates that the activity of iron catalysts in reduction have reached new heights within a decade, owing to the design of adapted ligands, mostly bearing a non-innocent NH functional group in a polydentate mode.

III- Hydrogen borrowing (hydrogen auto-transfer) reactions

New strategies to produce C-C, C-N bonds under catalytic conditions starting from renewable resources are highly desirable to develop sustainable chemistry.[1,82] Hydrogen borrowing, or hydrogen auto-transfer strategy is a powerful tool to reach this goal starting from alcohols. The general concept is described in **Scheme B^{1III}.1**. First an alcohol is dehydrogenated by the catalyst to produce the corresponding carbonyl derivative (step i) and formally a di-hydride metal complex. Subsequently the electrophilic C=O moiety reacts with a nucleophile (step ii) through for example condensation reactions. The *in situ* produced unsaturated compound is then reduced by the *in situ* produced metal hydride (step iii) to recover the initial catalyst and produce the targeted saturated product. Hence, the catalyst should be able to perform sequentially an oxidation (step i) and a reduction (step iii) in the same batch.

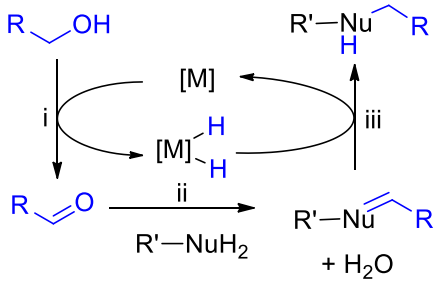

Scheme B^{III}.1 Principle of hydrogen borrowing methodology.

This redox-neutral method has an interesting environmental impact, as water is the sole stoichiometric by-product. This safe methodology is in agreement with the principles of Green Chemistry. In addition, alcohol is used as environmentally benign, inexpensive and abundant alkylating agent. The availability of alcohols is due to the fact that several industrial processes such as hydroformylation/reduction of olefins, hydration of olefins, fermentation of sugars and fractionation of lignocellulosic biomass are producing alcohols at large-scales.

The very beginning of this chemistry was reported by Adkins and Winans back to 1932 using heterogeneous nickel catalysts.[83] The first examples of homogenous catalytic complexes were published in the 1980's by Grigg for alkylation and methylation of arylacetonitriles with alcohols under the catalysis of $RhH(PPh_3)_4$, $IrCl(PPh_3)_3$ and $RuH_2(PPh_3)_4$ (5 mol %) heating at 65 °C.[84]

Tremendous progress was accomplished with homogeneous catalysts mainly based on precious metals such as rhodium, ruthenium and iridium thanks to the works of Grigg, Watanabe, Williams, Yus, Cho, Ishii, Fujita, Yamaguchi, Milstein and Beller. Several reviews give a general overview of the topic.[85–91]

In the majority of reactions, alcohols are involved as coupling partners and react with a nucleophile to make new C-C or C-N bonds.

Before discussing metal catalyzed reactions, it should be noted that a base can promote the alkylation of alcohols, or ketones, with alcohols as proved by Crabtree[92] and Xu[93] (**Scheme B^{III}.2**). Similarly, the synthesis of quinolines from (2-aminophenyl)methanol and ketones has also been achieved by Xu in metal-free system (**Scheme B^{III}.3**).[94]

In fact, the alcohols can be oxidized *via* the Oppenauer oxidation mechanism in the presence of a stoichiometric amount of specific bases and can be reduced *via*

Meerwein–Ponndorf–Verley reduction. Even if the substrate scope is quite limited in both cases and the selectivity is moderate, these results suggest that the use of stoichiometric amount of base at elevated temperature should not be applied without careful blank experiments.

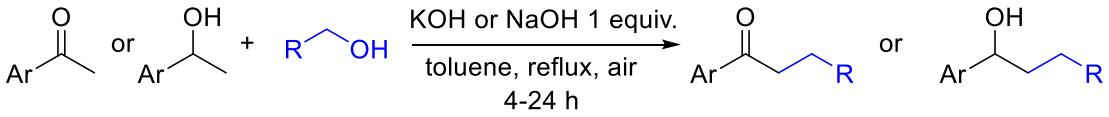

Scheme B^{1III}.2 Metal-free alkylation of ketones or alcohols.

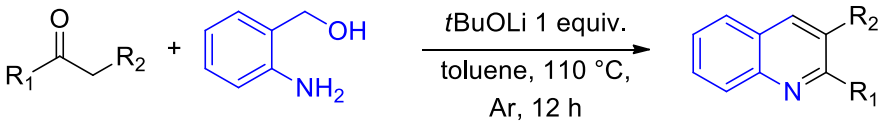

Scheme B^{1III}.3 Base-promoted synthesis of quinolines.

The coupling of alcohols with many types of nucleophiles (**Scheme B^{1III}.6**) allows the buildup of a large diversity of organic molecules. The nature of the metal is also large as Ru, Ir, Rh, Pd, Os, Fe, Cu based catalysts can be employed. The catalytic loadings are often high 1-5 mol % and a temperature over 100 °C (typically reflux of toluene) is commonly used. The most popular catalysts are dimers such as $[Cp^*MCl_2]_2$ with M=Ru, Ir or $RuCl_2(PPh_3)_3$.

a) For C-C bond formation

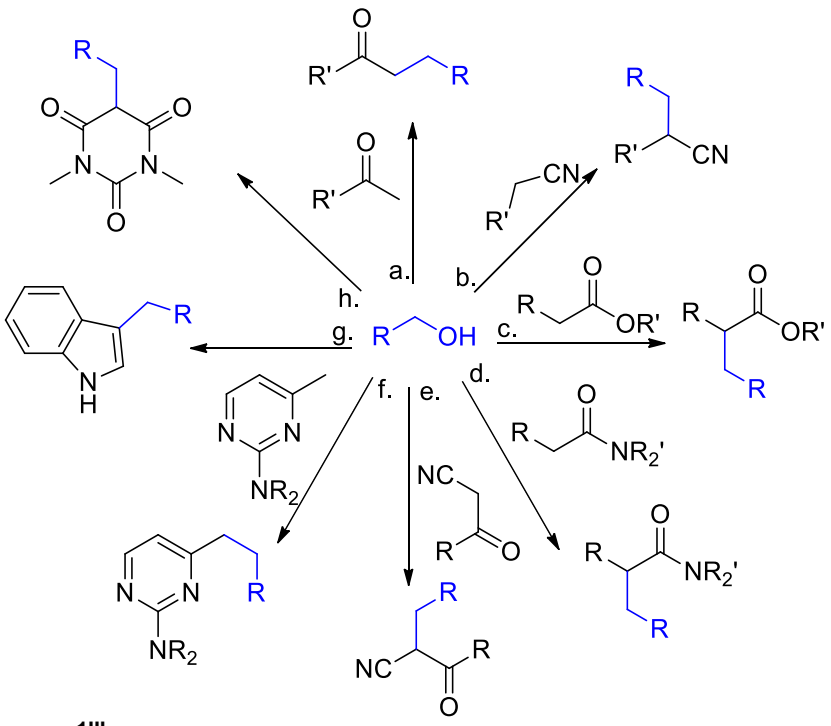

Scheme B^{1III}.4 Substrate scope for C-C bond formation with alcohols.

α-Alkylation of various substrates with alcohols can be accomplished. For example, ketones[93,94] (**Scheme B^{1III}.4**, a.) or nitriles, including acetonitrile,[97] (**Scheme B^{1III}.4**, b.) were also α-alkylated by primary alcohols with various iridium or ruthenium catalysts.

Acetates, esters and even lactones (**Scheme B^{1III}.4**, c.) were, as well, efficiently alkylated: notably, Huang showed that NCP **Ir-1** complex allowed to work under low catalytic load (0.5 mol%) and at unusual low temperature (60 °C) for this kind of reaction, even if a stoichiometric amount of base was utilized (**Figure B^{1III}.1**).[98]

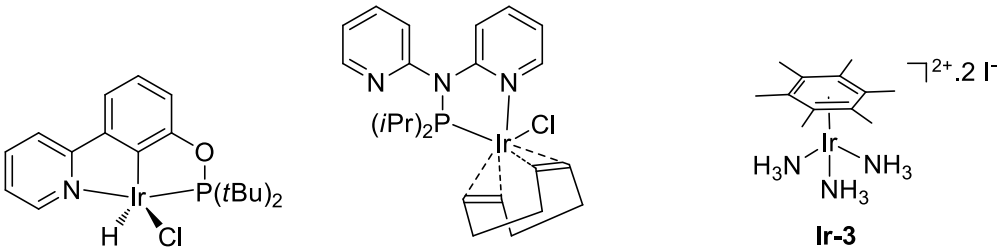

Ir-1 Huang **2015** **Ir-2** Kempe **2010** **Ir-3** Fujita, Yamaguchi **2011**

Figure B^{1III}.1 Iridium complexes used for hydrogen borrowing reactions.

1,3-Di-carbonyl nucleophiles, which can undergo a Knoevenagel reaction (step ii), have also been successfully studied: for example ketonitriles (**Scheme B^{1III}.4**, e.) were alkylated using 0.5 mol% of a ruthenium precursor in association with Xantphos diphosphine ligand and 5 mol% of piperidinium acetate as sole additive.[99] Barbiturate derivatives (**Scheme B^{1III}.4**, h.) could also be alkylated with good to excellent yields.[100]

Heterocycles could also be employed as coupling partners. Alkylation at the *C*-3 position of indole derivatives (**Scheme B^{1III}.4**, g.), proceeding *via* an indole anion, was published by Grigg using $[Cp^*IrCl_2]_2$/KOH system: interestingly no *N*-alkylation was observed in this case.[101]

Catalytic alkylation of activated methyl group from methyl-*N*-heteroaromatics (**Scheme B^{1III}.4**, f.) with alcohols has been achieved by Kempe using well-defined PN^3 **Ir-2** complex (1 mol%) with stoichiometric amount of *t*BuOK in diglyme at 110 °C (**Figure B^{1III}.1**).[102]

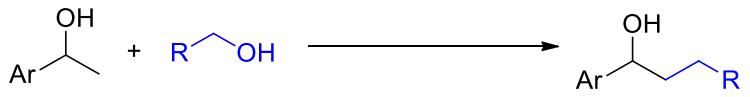

Scheme B^{III}.5 Formal β-alkylation of alcohols.

The reaction of two alcohols in the presence of $[Cp^*IrCl_2]_2$ and *t*BuONa (1 equiv.) using the same methodology (**Scheme B^{III}.5**), *via* a double (de)hydrogenation, led to the formal β-alkylation of alcohols.[103] .

b) For C-N bond formation

Amines are one of the most important chemicals for the industry. So converting alcohols into amines, *via* hydrogen borrowing, has been intensively studied. From a global view, the catalysts and conditions of reaction are similar except that the amount of base is relatively lowered (even can be avoided) in comparison to C-C bond formation due to the intrinsic basicity of the coupling partner.

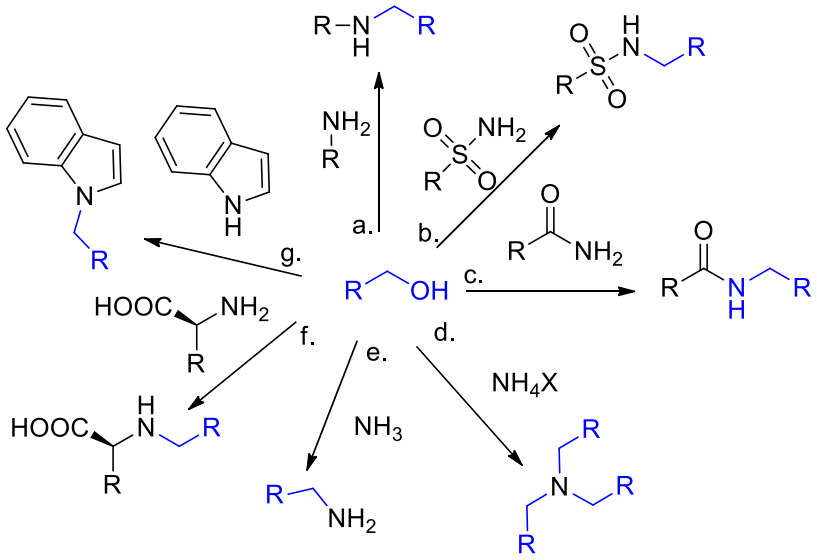

Scheme B^{III}.6 Substrate scope for C-N bond formation with alcohol.

In 1981, Watanabe was the first one to catalyze the *N*-alkylation of anilines using $RuCl_2(PPh_3)_3$ at 180 °C (**Scheme B^{III}.6**, a.).[104] Milder reaction conditions are operating nowadays including the use of aqueous media under air with, for example, water soluble **Ir-3**, reported by Fujita and Yamaguchi (**Figure B^{III}.1**).[105] This powerful methodology was applied for the production at kilogram-scale of a precursor of a GlyT1 inhibitor using the classical $[Cp^*IrCl_2]_2$ complex under base-free conditions (**Scheme B^{III}.7**).[106] Interestingly the use of bio-based alcohols such as glycerol[107]

or carbohydrates[108] for amino-sugar synthesis has been studied with the same $[Cp^*IrCl_2]_2$ catalyst.

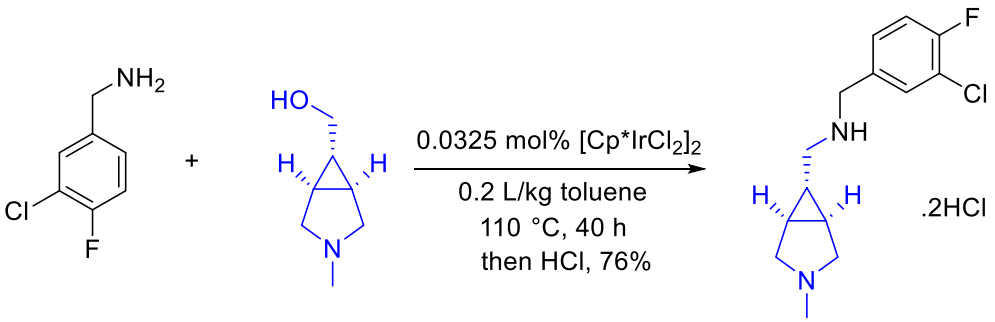

Scheme B^{III}.7 Industrial application of hydrogen borrowing methodology.

The scope of the C-N coupling with alcohols could be extended to others nitrogen containing nucleophiles such as sulfonamide or amide, as reported by Williams under solvent-free microwave conditions (**Scheme B^{III}.6**, b. and c.).[109]

Indoles (**Scheme B^{III}.6**, g.) which are poor nucleophiles and known to undergo *C*-3 alkylation in the presence of a base, could be alkylated at the nitrogen position using Shvo catalyst **Ru-3** and *p*-toluenesulfonic acid as additive as reported by Beller in 2010.[110] This work is one of the rare examples where acidic conditions can be used. With the same catalyst in 2017, Barta and Feringa were able to alkylate unprotected amino acids, leading in one step to detergents from bio-based reactants (**Scheme B^{III}.6**, f.).[111]

Ammonia surrogates (NH_4X **Scheme B^{III}.6**, d.) gave generally secondary or tertiary amines.[112] Using excess of NH_3 gas (**Scheme B^{III}.6**, e.), primary amines could be produced directly from the corresponding alcohols under the catalysis of **Ru-18** (0.1 mol%) under base-free conditions at 135 °C.[113]

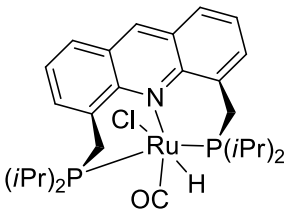

Ru-18 Milstein **2008**

Combining C-C and C-N bond formation is also possible. One elegant example is the work of Bruneau and Achard for the dialkylation of cyclic amines at both the *N* and the *C*-3 positions (**Scheme B^{III}.8**) catalyzed by **Ru-19** using camphorsulfonic acid (CSA) as additive.[114]

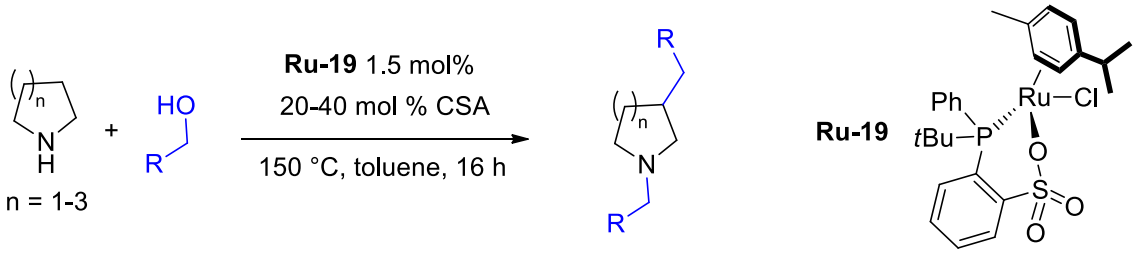

Scheme B^{III}.8 Combined C-C and C-N bond formations

In last few years, in line with the development of earth abundant catalysts for hydrogenation type reactions, first row metal complexes (Fe[115], Co[116], Mn[117]) were developed for hydrogen borrowing reactions, as the elementary steps are the same as in hydrogenation. Iron, cobalt and lately manganese, mainly supported by PNP ligands, were able to promote the alkylation of amines with alcohols, but with relatively high catalytic loadings (2-5 mol%) at temperatures between 80 °C and 140 °C (**Figure B^{III}.2**). Knölker's iron complex (or derivatives) could also be employed for this reaction.[118–120]

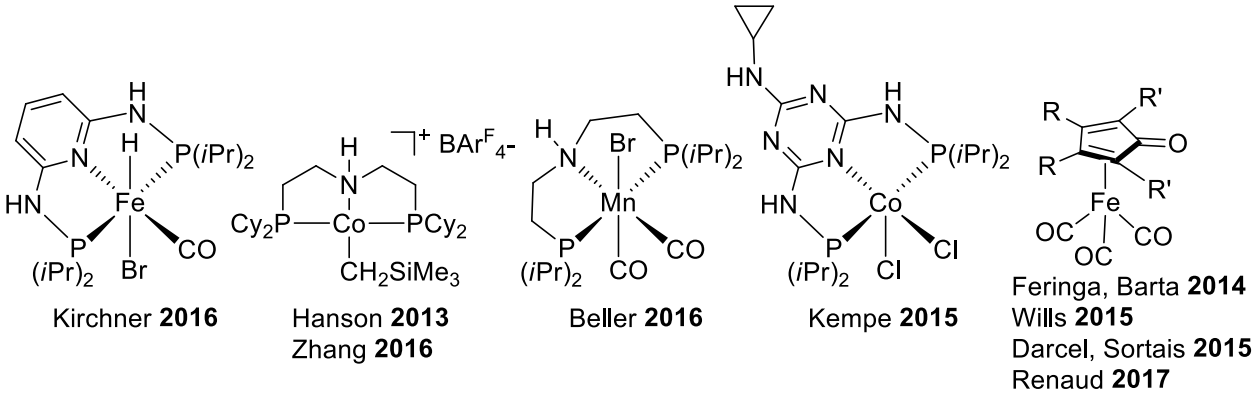

Figure B^{III}.2 Selected base metals published for hydrogen borrowing methodology.

c) (Acceptorless) dehydrogenative coupling

In all the reactions presented here above, both the dehydrogenation (step i) and hydrogenation (step iii) occurred in the same cycle, leading to an overall redox neutral reaction. Interestingly, depending on the catalyst (which can release H_2), or in the presence of hydrogen acceptor, the oxidized coupling product can be obtained.

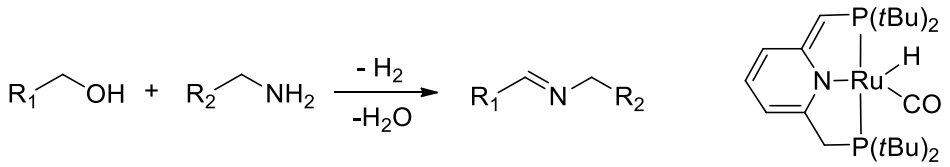

Ru-20 Milstein **2010**

Scheme B^{1III}.9 Acceptorless dehydrogenative coupling to produce imines.

A representative example of acceptorless dehydrogenative coupling is the synthesis of imines. The most common method for preparing imines is the original reaction discovered by Schiff consisting in the reaction of an aldehyde (respectively a ketone) with a primary amine.[121] One main drawback on this reaction is the stability or availability of aldehydes, especially aliphatic ones. Using an acceptorless dehydrogenative coupling, imines are readily obtained starting from stable alcohols and amines (**Scheme B^{1III}.9**). The aldehyde, generated *in situ*, is consumed before any degradation. Interestingly, H_2 is produced as the sole by-product. One of the first example was reported by Milstein using PNP **Ru-20** complexes (0.2 mol%) at 110 °C without any additive (**Scheme B^{1III}.9**).[122]

As for hydrogen auto-transfer reactions, the acceptorless dehydrogenative coupling allows the formation of a large variety of compounds with the help of different metals (Ir, Pd, Fe, Co) but will not be discussed in more details.[123]

IV- Objectives

According to these overviews, noble metals are widely used for (de)hydrogenation reactions, which are of importance for the production of valuable chemicals. As explained in the general introduction, for sustainability reasons, noble metals need to be replaced more and more by abundant metals in catalysis. Furthermore, exploring the integrity of the first row transition metals, *i.e.* not only late ones, would also be a durable approach.

In the recent years the use of base metals in reductive homogeneous catalysis has been popularized,[124] especially with the use of iron(II) catalysts, yet other metals were still underexplored such as manganese. To keep the same environment around the metal, *i.e.* d^6 transition metal complexes, we would like to develop manganese(I)

catalysts. As described in the introduction the necessity of an appropriate ligand is now recognized for base metal catalysts.

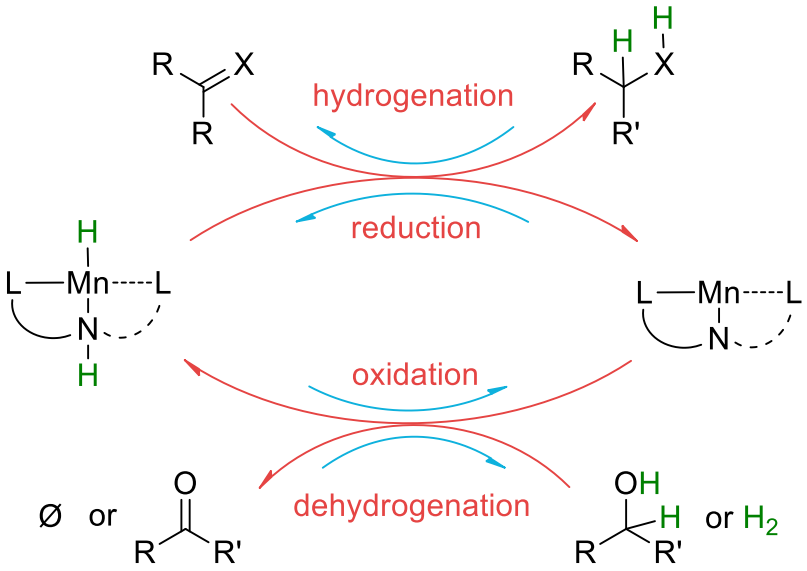

Scheme B^{1IV}.1 Principle of (de)hydrogenation with manganese thanks to the assistance of an appropriate ligand.

The overall purpose of this thesis was to develop manganese catalysts and to play with the ligand-assisted hydrogenation mechanism depicted on **Scheme B^{1IV}.1**. In the reductive cycle (**Scheme B^{1IV}.1**, red cycle), the manganese catalyst can deliver a hydride and the ligand a proton, thanks to well-established “NH-effect”, to perform the reduction, the source of hydrogen being either H_2 or hydrogen donors. Our interest also concerns the possibility of reversing the selectivity of this mechanism, *i.e.* to perform the oxidative cycle (**Scheme B^{1IV}.1**, blue cycle), by changing the nature of the ligand or the reaction conditions.

As the ultimate idea of this work is to valorize renewable raw materials, we focused on coupling or reduction of oxygenated substrates. In a long-term perspective, the dehydrogenative cycle of the mechanism (**Scheme B^{1IV}.1**, blue cycle) can produce both dihydrogen, as fuel, and chemical platforms from bio-sourced molecules.

In the second chapter, a first approach using tridentate manganese complexes allowed us to validate this concept. We initially focused our attention on the redox neutral coupling of methanol with nitrogen or oxygen containing molecules, *via* hydrogen borrowing. Then we studied the reduction of ketones with dihydrogen with the same catalyst.

In the third chapter we explored the possibility to obtain active catalysts for hydrogenation reactions with non-pincer ligands, which are usually not recommended for base metal catalysts (Fe, Co, Ni). [125–127]

The fourth chapter is devoted to the conclusion of this work, beginning with the recent advancements made in this field by manganese catalysts.

V- References

[1] P. T. Anastas, J. C. Warner, *Green Chemistry: Theory and Practice*, Oxford University Press, New York, **1998**.
[2] B. M. Trost, *Angew. Chem. Int. Ed.* **1995**, *34*, 259–281.
[3] R. A. Sheldon, *Green Chem.* **2017**, *19*, 18–43.
[4] J. G. de Vries, P. J. Deuss, K. Barta, *Catal. Sci. Technol.* **2014**, *4*, 1174–1196.
[5] G. Pitron, *La Guerre Des Métaux Rare, La Face Cachée de La Transition Énergétique et Numérique*, Edition Les Liens Qui Libèrent, **2018**.
[6] EU publications, *Study on the Review of the List of Critical Raw Materials, DOI: 10.2873/876644*, **2017**.
[7] W. F. Cannon, B. E. Kimball, L. A. Corathers, *Manganese, DOI: 10.3133/Pp1802L*, Reston, VA, **2017**.
[8] European Medicines Agency, *Guideline on the Specification Limits for Residues of Metal Catalysts or Metal Reagents*, **2008**.
[9] W. Zhang, J. L. Loebach, S. R. Wilson, E. N. Jacobsen, *J. Am. Chem. Soc.* **1990**, *112*, 2801–2803.
[10] P. Sabatier, *Ind. Eng. Chem* **1926**, *18*, 1005–1008.
[11] H. U. Blaser, E. Schmidt, *Asymmetric Catalysis on Industrial Scale*, Wiley-VCH, Weinheim, **2004**.
[12] D. J. Ager, A. H. M. de Vries, J. G. de Vries, *Chem. Soc. Rev.* **2012**, *41*, 3340–3380.
[13] J.-P. Genet, *Acc. Chem. Res.* **2003**, *36*, 908–918.
[14] L. A. Saudan, *Acc. Chem. Res.* **2007**, *40*, 1309–1319.
[15] M. Calvin, *J. Am. Chem. Soc.* **1939**, *61*, 2230–2234.
[16] J. A. Osborn, F. H. Jardine, J. F. Young, G. Wilkinson, *J. Chem. Soc. A* **1966**, 1711–1732.
[17] R. Noyori, T. Ohkuma, M. Kitamura, H. Takaya, N. Sayo, H. Kumobayashi, S. Akutagawa, *J. Am. Chem. Soc.* **1987**, *109*, 5856–5858.
[18] W. S. Knowles, *Acc. Chem. Res.* **1983**, *16*, 106–112.
[19] T. Ohkuma, H. Ooka, S. Hashiguchi, T. Ikariya, R. Noyori, *J. Am. Chem. Soc.* **1995**, *117*, 2675–2676.
[20] H. Doucet, T. Ohkuma, K. Murata, T. Yokozawa, M. Kozawa, E. Katayama, A. F. England, T. Ikariya, R. Noyori, *Angew. Chem. Int. Ed.* **1998**, *37*, 1703–1707.
[21] R. Noyori, T. Ohkuma, *Angew. Chem. Int. Ed.* **2001**, *40*, 40–73.
[22] P. A. Dub, N. J. Henson, R. L. Martin, J. C. Gordon, *J. Am. Chem. Soc.* **2014**, *136*, 3505–3521.
[23] R. Hartmann, P. Chen, *Angew. Chem. Int. Ed.* **2001**, *40*, 3581–3585.
[24] P. A. Dub, B. L. Scott, J. C. Gordon, *J. Am. Chem. Soc.* **2017**, *139*, 1245–1260.
[25] Y. Blum, D. Czarkie, Y. Rahamim, Y. Shvo, *Organometallics* **1985**, *4*, 1459–1461.
[26] P. Dupau, L. Bonomo, L. Kermorvan, *Angew. Chem. Int. Ed.* **2013**, *52*, 11347–11350.
[27] H. T. Teunissen, C. J. Elsevier, *Chem. Commun.* **1998**, 1367–1368.
[28] L. A. Saudan, C. Saudan, C. Becieux, P. Wyss, *Angew. Chem. Int. Ed.* **2007**, *46*, 7473–7476.
[29] W. Kuriyama, T. Matsumoto, O. Ogata, Y. Ino, K. Aoki, S. Tanaka, K. Ishida, T. Kobayashi, N. Sayo, T. Saito, *Org. Process Res. Dev.* **2012**, *16*, 166–171.
[30] G. A. Filonenko, E. Cosimi, L. Lefort, M. P. Conley, C. Copéret, M. Lutz, E. J. M. Hensen, E. A. Pidko, *ACS Catal.* **2014**, *4*, 2667–2671.
[31] K. Källström, I. J. Munslow, C. Hedberg, P. G. Andersson, *Adv. Synth. Catal.* **2006**, *348*, 2575–2578.
[32] W. Li, G. Hou, C. Wang, Y. Jiang, X. Zhang, *Chem. Commun.* **2010**, *46*, 3979–3981.
[33] D. Spasyuk, S. Smith, D. G. Gusev, *Angew. Chem. Int. Ed.* **2012**, *51*, 2772–2775.
[34] D. Spasyuk, S. Smith, D. G. Gusev, *Angew. Chem. Int. Ed.* **2013**, *52*, 2538–2542.
[35] X. Tan, Y. Wang, Y. Liu, F. Wang, L. Shi, K.-H. Lee, Z. Lin, H. Lv, X. Zhang, *Org. Lett.* **2015**, *17*, 454–457.
[36] G. Wang, X. Tan, H. Lv, M. Zhao, M. Wu, J. Zhou, X. Zhang, L. Zhang, *Ind. Eng. Chem. Res.* **2016**, *55*, 5263–5270.
[37] C. P. Casey, H. Guan, *J. Am. Chem. Soc.* **2007**, *129*, 5816–5817.
[38] I. Bauer, H.-J. Knölker, *Chem. Rev.* **2015**, *115*, 3170–3387.
[39] A. Lator, S. Gaillard, A. Poater, J.-L. Renaud, *Chem. Eur. J.* **2018**, *24*, 5770–5774.
[40] F. Kallmeier, R. Kempe, *Angew. Chem. Int. Ed.* **2018**, *57*, 46–60.

[41] R. P. Yu, J. M. Darmon, J. M. Hoyt, G. W. Margulieux, Z. R. Turner, P. J. Chirik, *ACS Catal.* **2012**, *2*, 1760–1764.
[42] R. Langer, G. Leitus, Y. Ben-David, D. Milstein, *Angew. Chem. Int. Ed.* **2011**, *50*, 2120–2124.
[43] T. Zell, Y. Ben-David, D. Milstein, *Angew. Chem., Int. Ed.* **2014**, *53*, 4685–4689.
[44] R. Huber, A. Passera, A. Mezzetti, *Organometallics* **2018**, *37*, 396–405.
[45] G. Bauer, K. A. Kirchner, *Angew. Chem. Int. Ed.* **2011**, *50*, 5798–5800.
[46] S. Chakraborty, H. Dai, P. Bhattacharya, N. T. Fairweather, M. S. Gibson, J. A. Krause, H. Guan, *J. Am. Chem. Soc.* **2014**, *136*, 7869–7872.
[47] C. Bornschein, S. Werkmeister, B. Wendt, H. Jiao, E. Alberico, W. Baumann, H. Junge, K. Junge, M. Beller, *Nat. Commun.* **2014**, *5*, 4111.
[48] N. M. Rezayee, D. C. Samblanet, M. S. Sanford, *ACS Catal.* **2016**, *6*, 6377–6383.
[49] R. Xu, S. Chakraborty, S. M. Bellows, H. Yuan, T. R. Cundari, W. D. Jones, *ACS Catal.* **2016**, *6*, 2127–2135.
[50] P. O. Lagaditis, P. E. Sues, J. F. Sonnenberg, K. Y. Wan, A. J. Lough, R. H. Morris, *J. Am. Chem. Soc.* **2014**, *136*, 1367–1380.
[51] R. H. Morris, *Acc. Chem. Res.* **2015**, *48*, 1494–1502.
[52] J.-L. Renaud, S. Gaillard, *Synthesis* **2016**, *48*, 3659–3683.
[53] E. Knoevenagel, B. Bergdolt, *Ber. Dtsch. Chem. Ges.* **1903**, *36*, 2857–2860.
[54] Verley, A., *Bull. Soc. Chim. Fr.* **1925**, *37*, 537–542.
[55] H. Meerwein, R. Schmidt, *Justus Liebigs Ann. Chem.* **1925**, *444*, 221–238.
[56] A. Ouali, J.-P. Majoral, A.-M. Caminade, M. Taillefer, *ChemCatChem* **2009**, *1*, 504–509.
[57] J. Trocha-Grimshaw, H. B. Henbest, *Chem. Commun.* **1967**, 544–544.
[58] A. Fujii, S. Hashiguchi, N. Uematsu, T. Ikariya, R. Noyori, *J. Am. Chem. Soc.* **1996**, *118*, 2521–2522.
[59] J.-X. Gao, T. Ikariya, R. Noyori, *Organometallics* **1996**, *15*, 1087–9.
[60] R. L. Chowdhury, J.-E. Backvall, *J. Chem. Soc., Chem. Commun.* **1991**, 1063–1064.
[61] D. Wang, D. Astruc, *Chem. Rev.* **2015**, *115*, 6621–6686.
[62] G. Brieger, T. J. Nestrick, *Chem. Rev.* **1974**, *74*, 567–580.
[63] B. Zhao, Z. Han, K. Ding, *Angew. Chem. Int. Ed.* **2013**, *52*, 4744–4788.
[64] W. P. Hems, W. P. Jackson, P. Nightingale, R. Bryant, *Org. Process Res. Dev.* **2012**, *16*, 461–463.
[65] M. Komiyama, T. Itoh, T. Takeyasu, *Org. Process Res. Dev.* **2015**, *19*, 315–319.
[66] W. Baratta, E. Herdtweck, K. Siega, M. Toniutti, P. Rigo, *Organometallics* **2005**, *24*, 1660–1669.
[67] W. Baratta, M. Bosco, G. Chelucci, A. Del Zotto, K. Siega, M. Toniutti, E. Zangrando, P. Rigo, *Organometallics* **2006**, *25*, 4611–4620.
[68] J. P. C. Coverdale, I. Romero-Canelón, C. Sanchez-Cano, G. J. Clarkson, A. Habtemariam, M. Wills, P. J. Sadler, *Nat. Chem.* **2018**, *10*, 347.
[69] R. ter Halle, A. Bréhéret, E. Schulz, C. Pinel, M. Lemaire, *Tetrahedron: Asymmetry* **1997**, *8*, 2101–2108.
[70] G. Zhang, S. K. Hanson, *Chem. Commun.* **2013**, *49*, 10151–10153.
[71] C. Bianchini, E. Farnetti, M. Graziani, M. Peruzzini, A. Polo, *Organometallics* **1993**, *12*, 3753–3761.
[72] S. Enthaler, B. Hagemann, G. Erre, K. Junge, M. Beller, *Chem. Asian J.* **2006**, *1*, 598–604.
[73] J. Ekström, J. Wettergren, H. Adolfsson, *Adv. Synth. Catal.* **2007**, *349*, 1609–1613.
[74] T. N. Plank, J. L. Drake, D. K. Kim, T. W. Funk, *Adv. Synth. Catal.* **2012**, *354*, 597–601.
[75] M. Darwish, M. Wills, *Catal. Sci. Technol.* **2012**, *2*, 243–255.
[76] W. Zuo, A. J. Lough, Y. F. Li, R. H. Morris, *Science* **2013**, *342*, 1080–1083.
[77] J. F. Sonnenberg, N. Coombs, P. A. Dube, R. H. Morris, *J. Am. Chem. Soc.* **2012**, *134*, 5893–5899.
[78] W. Zuo, A. J. Lough, Y. F. Li, R. H. Morris, *Science* **2013**, *342*, 1080–1083.
[79] A. Buchard, H. Heuclin, A. Auffrant, X. F. Le Goff, P. Le Floch, *Dalton Trans.* **2009**, 1659–1667.
[80] R. Bigler, R. Huber, A. Mezzetti, *Synlett* **2016**, 831–847.
[81] L. De Luca, A. Mezzetti, *Angew. Chem. Int. Ed.* **2017**, *56*, 11949–11953.
[82] C. S. Yeung, V. M. Dong, *Chem. Rev.* **2011**, *111*, 1215–1292.
[83] C. F. Winans, H. Adkins, *J. Am. Chem. Soc.* **1932**, *54*, 306–312.
[84] R. Grigg, T. R. B. Mitchell, S. Sutthivaiyakit, N. Tongpenyai, *J. Chem. Soc., Chem. Commun.* **1981**, 611–612.
[85] M. H. S. A. Hamid, P. A. Slatford, J. M. J. Williams, *Adv. Synth. Catal.* **2007**, *349*, 1555–1575.
[86] T. D. Nixon, M. K. Whittlesey, J. M. J. Williams, *Dalton Trans.* **2009**, 753–762.

[87] G. Guillena, D. J. Ramón, M. Yus, *Chem. Rev.* **2010**, *110*, 1611–1641.
[88] S. Bähn, S. Imm, L. Neubert, M. Zhang, H. Neumann, M. Beller, *ChemCatChem* **2011**, *3*, 1853–1864.
[89] C. Gunanathan, D. Milstein, *Science* **2013**, *341*, 1229712.
[90] Q. Yang, Q. Wang, Z. Yu, *Chem. Soc. Rev.* **2015**, *44*, 2305–2329.
[91] A. Corma, J. Navas, M. J. Sabater, *Chem. Rev.* **2018**, *118*, 1410–1459.
[92] L. J. Allen, R. H. Crabtree, *Green Chem.* **2010**, *12*, 1362–1364.
[93] X. Qing, C. Jianhui, T. Haiwen, Y. Xueqin, L. Shuangyan, Z. Chongkuan, J. Liu, *Angew. Chem. Int. Ed.* **2013**, *53*, 225–229.
[94] Y.-F. Liang, X.-F. Zhou, S.-Y. Tang, Y.-B. Huang, Y.-S. Feng, H.-J. Xu, *RSC Adv.* **2013**, *3*, 7739–7742.
[95] K. Taguchi, H. Nakagawa, T. Hirabayashi, S. Sakaguchi, Y. Ishii, *J. Am. Chem. Soc.* **2004**, *126*, 72–73.
[96] G. Guillena, J. Ramón Diego, M. Yus, *Angew. Chem. Int. Ed.* **2007**, *46*, 2358–2364.
[97] T. Sawaguchi, Y. Obora, *Chem. Lett.* **2011**, *40*, 1055–1057.
[98] L. Guo, X. Ma, H. Fang, X. Jia, Z. Huang, *Angew. Chem. Int. Ed.* **2015**, *54*, 4023–4027.
[99] A. E. W. Ledger, P. A. Slatford, J. P. Lowe, M. F. Mahon, M. K. Whittlesey, J. M. J. Williams, *Dalton Trans.* **2009**, 716–722.
[100] C. Lofberg, R. Grigg, A. Keep, A. Derrick, V. Sridharan, C. Kilner, *Chem. Commun.* **2006**, 5000–5002.
[101] S. Whitney, R. Grigg, A. Derrick, A. Keep, *Org. Lett.* **2007**, *9*, 3299–3302.
[102] B. Blank, R. Kempe, *J. Am. Chem. Soc.* **2010**, *132*, 924–925.
[103] K. Fujita, C. Asai, T. Yamaguchi, F. Hanasaka, R. Yamaguchi, *Org. Lett.* **2005**, *7*, 4017–4019.
[104] Y. Watanabe, Y. Tsuji, Y. Ohsugi, *Tetrahedron Lett.* **1981**, *22*, 2667–2670.
[105] R. Kawahara, K. Fujita, R. Yamaguchi, *Adv. Synth. Catal.* **2011**, *353*, 1161–1168.
[106] M. A. Berliner, S. P. A. Dubant, T. Makowski, K. Ng, B. Sitter, C. Wager, Y. Zhang, *Org. Process Res. Dev.* **2011**, *15*, 1052–1062.
[107] C. Crotti, E. Farnetti, S. Licen, P. Barbieri, G. Pitacco, *J. Mol. Catal. A.* **2014**, *382*, 64–70.
[108] I. Cumpstey, S. Agrawal, K. E. Borbas, B. Martin-Matute, *Chem. Commun.* **2011**, *47*, 7827–7829.
[109] A. J. A. Watson, A. C. Maxwell, J. M. J. Williams, *J. Org. Chem.* **2011**, *76*, 2328–2331.
[110] S. Bähn, S. Imm, K. Mevius, L. Neubert, A. Tillack, J. M. J. Williams, M. Beller, *Chem. Eur. J.* **2010**, *16*, 3590–3593.
[111] T. Yan, B. L. Feringa, K. Barta, *Sci. Adv.* **2017**, *3*, eaao6494.
[112] R. Yamaguchi, S. Kawagoe, C. Asai, K. Fujita, *Org. Lett.* **2008**, *10*, 181–184.
[113] C. Gunanathan, D. Milstein, *Angew. Chem. Int. Ed.* **2008**, *47*, 8661–8664.
[114] B. Sundararaju, Z. Tang, M. Achard, G. V. M. Sharma, L. Toupet, C. Bruneau, *Adv. Synth. Catal.* **2010**, *352*, 3141–3146.
[115] M. Mastalir, M. Glatz, N. Gorgas, B. Stöger, E. Pittenauer, G. Allmaier, L. F. Veiros, K. Kirchner, *Chem. Eur. J.* **2016**, *22*, 12316–12320.
[116] G. Zhang, Z. Yin, S. Zheng, *Org. Lett.* **2016**, *18*, 300–303.
[117] S. Elangovan, J. Neumann, J.-B. Sortais, K. Junge, C. Darcel, M. Beller, *Nat. Commun.* **2016**, *7*, 12641.
[118] T. Yan, B. L. Feringa, K. Barta, *Nat. Commun.* **2014**, *5*, 5602.
[119] C. Seck, M. D. Mbaye, S. Coufourier, A. Lator, J.-F. Lohier, A. Poater, T. R. Ward, S. Gaillard, J.-L. Renaud, *ChemCatChem* **2017**, *9*, 4410–4416.
[120] S. Elangovan, J.-B. Sortais, M. Beller, C. Darcel, *Angew. Chem. Int. Ed.* **2015**, *54*, 14483–14486.
[121] H. Schiff, *Justus Liebigs Ann. Chem.* **1866**, *140*, 92–137.
[122] B. Gnanaprakasam, J. Zhang, D. Milstein, *Angew. Chem. Int. Ed.* **2010**, *49*, 1468–1471.
[123] S. Werkmeister, J. Neumann, K. Junge, M. Beller, *Chem. Eur. J.* **2015**, *21*, 12226–12250.
[124] R. M. Bullock, *Science* **2013**, *342*, 1054–1055.
[125] R. Langer, F. Bönisch, L. Maser, C. Pietzonka, L. Vondung, T. P. Zimmermann, *Eur. J. Inorg. Chem.* **2015**, 141–148.
[126] J. F. Sonnenberg, A. J. Lough, R. H. Morris, *Organometallics* **2014**, *33*, 6452–6465.
[127] T. M. A. Jazzazi, H. Görls, G. Gessner, S. H. Heinemann, M. Westerhausen, *J. Organomet. Chem.* **2013**, *733*, 63–70.

Chapter 2 - Study of tridentate manganese complexes

A – Hydrogen borrowing reactions with methanol catalyzed by a PN^3P manganese complex

Methanol is a central molecule for the chemical industry, offering an alternative to depleted sources of fossil fuels. The concept of “methanol economy” was introduced by Friedrich Asinger and George Olah,[1] who demonstrated the potential of the simplest alcohol as chemical platform for the chemical industry. As for example, methanol is a convenient liquid fuel finding application, and a raw material for synthetic hydrocarbons.

Nowadays, the worldwide production of methanol is about 5,000 metric tons per day (2.3 billion liters per year). The state of the art for methanol production is based on synthesis gas but methanol can be obtained from a large variety of carbon feedstock.[2,3] The most sustainable approach relies on the production of methanol from CO_2, captured from industrial effluents or the atmosphere (which can be good regarding global-warming concerns). Indeed, the George Olah plant in Iceland

produces methanol from CO_2 collected from industrial emissions and hydrogen produced by the electrolysis of water, powered by geothermal energy, with a capacity of 5 million liters per year.[4]

The main utilization of methanol is the production of formaldehyde, mainly using heterogeneous iron-molybdenum-vanadium oxide catalyst at 250–400 °C (Formox process). Other important chemicals produced from methanol are methyl *tert*-butyl ether (MTBE) and *tert*-amyl methyl ether (TAME), as well as acetic acid, dimethyl ether (DME), olefins (MTO and MTP processes), methylamines, methyl methacrylate, and chloromethane. Moreover, methanol can be converted into conventional fuels by the methanol-to-gasoline process (MTG).[4]

The purpose of this part is to use methanol as methylating agent for the synthesis of high adding-value molecules under relatively mild conditions in agreement with the principles of green chemistry.

In 2017, Beller and Jagadeesh reviewed the utilization of methanol as C1 source in organic synthesis.[5] In addition, Fraga highlighted the importance of the methylation effect in the design of biological active compounds and drugs.[6]

I- Mono-*N*-methylation of anilines and sulfonamides

Contributions in the part: Synthesis of the complexes: A.B.-V., D.W., Optimization: D.W., Scope: A. B.-V., D.W. (minor), Mechanistic studies: A.B.-V.

Publication: A. Bruneau-Voisine, D. Wang, V. Dorcet, T. Roisnel, C. Darcel, J.-B. Sortais, *J . Catal.* **2017**, *347*, 57-62.

Amines are important building blocks that have found widespread applications in agrochemicals, pharmaceuticals, natural products, dyes and polymers.[7,8] In particular, *N*-methylamines are key intermediates and building blocks in organic synthesis.[9]

Classical methylation reagents, such as methyl iodide, methyl triflate or dimethyl sulfate, as well as formaldehyde, are usually toxic and hazardous reagents which suffer from selectivity issues, especially for selective mono-*N*-methylation.

New greener sources of "CH_3" have recently drawn the attention of chemists.[10,11] Among them, CO_2 was used as C1 source for the methylation of amines under reductive conditions with hydrosilanes or H_2,[12–15] including, for example, a metal-free catalytic system reported by the group of Cantat.[16] Formic acid[17,18] and dialkyl carbonates[19,20] are other renewable resources, derived from carbon dioxide, that are able to undergo methylation reaction. A major limitation for these greener sources is that an additional reductant is needed such as silanes or boranes involving the production of wastes affecting the E-factor of such transformations. Although the use of dihydrogen can overcome this limitation, high pressure apparatus is required in this case.

As an alternative approach, our goal is to use methanol, *via* hydrogen borrowing strategy, to produce methylamines with a low environmental impact, as the sole stoichiometric by-product is one molecule of water. In addition, this method do not required high-pressure devices although methanol can be heated at elevated temperature (*vide infra*) so a specific heavy-wall borosilicate glass tube is employed. It is important to note that compared to alkylation of amines with heavier alcohols, this reaction remain challenging using methanol due to the higher activation barrier for the dehydrogenation of methanol into formaldehyde compared to heavier alcohols, such as ethanol into ethanal (ΔH = +84 *vs* +68 kJ.mol^{-1}, respectively).[21]

Few catalytic systems, based on noble transition metals are known to promote the methylation of amines with methanol.[5] A detailed comparative study will be presented in the conclusion of this section.

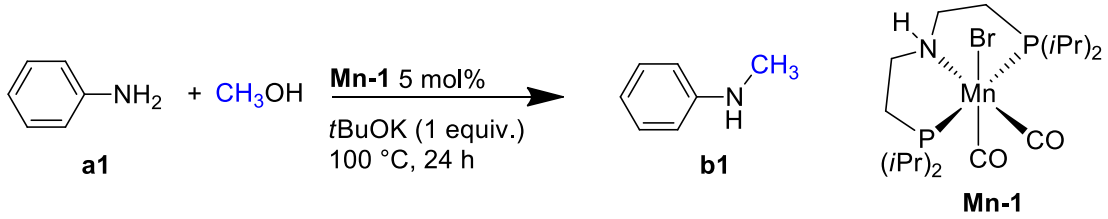

a1 **b1** **Mn-1**

Scheme A^{2l}.1 First mono-*N*-methylation of anilines catalyzed by the manganese complex **Mn-1** published by our group and Beller in 2016.

With earth abundant transition metals, when we started our study, only one single example had been reported in the literature, resulting from collaboration between our group and the group of Matthias Beller. The first manganese-catalyzed alkylation of amines with alcohols was achieved under the catalysis of **Mn-1**, supported by a MACHO-type ligand.[22] Interestingly, the methylation of anilines with methanol proceeded well, albeit it required stoichiometric amount of base (**Scheme A^{2I}.1**).

Intrigued by this result, we wanted to explore further methylation reactions with methanol catalysed by manganese complexes. Our main objective was to study if the reactivity observed was an intrinsic property of **Mn-1** or if it is a more general property of manganese catalysts, having in mind that iron catalysts were not reported to promote the dehydrogenation of methanol at this time. Regarding the choice of the ligand, we turned our attention towards PN^{3}P ligands which are as powerful ligand as MACHO ones in the case of iron.[23,24] It should be noted that in parallel to our work, Saravanakumar Elangovan, co-PhD student between our group and the one of Beller, explored another classical PNP ligand, namely diphosphinopyridine, for the same transformation (**Figure A^{2I}.1**).[25]

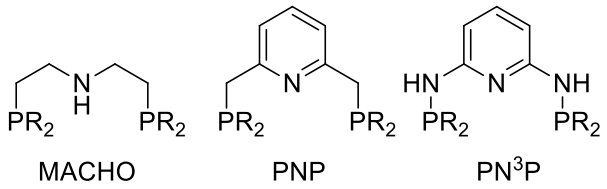

Figure A^{2I}.1 Variations of the ligands for mono-*N*-methylation of anilines catalyzed by manganese complexes.

a) Synthesis of the manganese complex

The straightforward synthesis of the desired PN^{3}P ligand has been previously described.[24,26] The ligand could be obtained in very high yield (96%), in one step starting from 2,6-diaminopyridine and chlorodiisopropylphosphine in THF in the presence of triethylamine (**Scheme A^{2I}.2**).

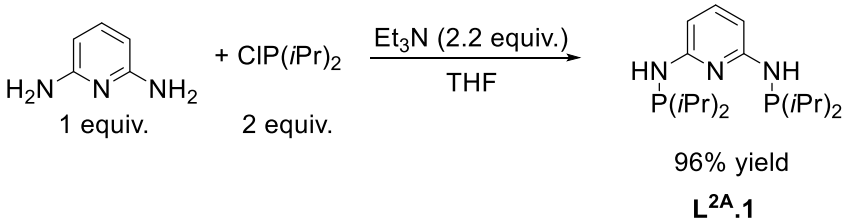

Scheme A^{2I}.2 Synthesis of the PN^{3}P ligand **L^{2A}.1**.

The synthesis of the manganese complex was achieved, on gram scale, by reacting 1 equivalent of PN^3P ligand **L^{2A}.1** with $Mn(CO)_5Br$ in toluene at 110 °C (**Scheme A^{2I}.3**). After one night, the cationic complex **C^{2A}.1** precipitated as a white solid from an orange solution. The difference of solubility in THF between the neutral **C^{2A}.2** (orange) and the cationic **C^{2A}.1** (white) complexes allowed us to isolate the complex **C^{2A}.1** in a pure form by washing the crude solid with cold distilled THF and distilled *n*-pentane (68% yield). Complex **C^{2A}.1** was fully characterized by NMR spectroscopies, mass spectrometry and elemental analysis. In particular, $^{31}P\{^1H\}$ NMR spectrum displayed a single signal at 133.8 ppm in DMSO-d_6.

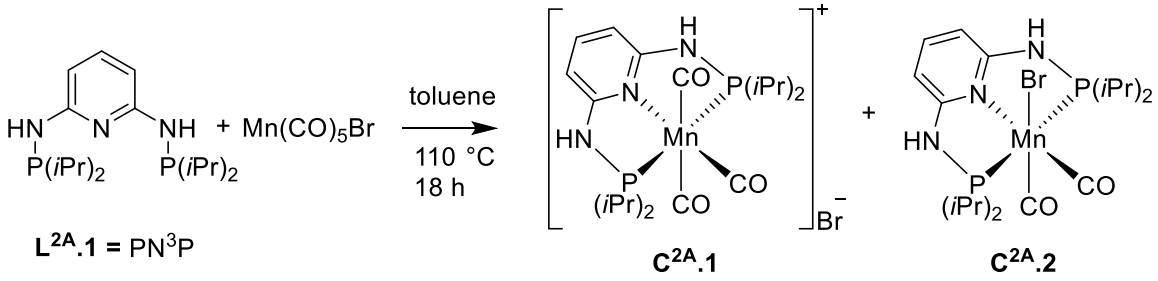

L^{2A}.1 = PN^3P **C^{2A}.1** **C^{2A}.2**

Scheme A^{2I}.3 Synthesis of the manganese PN^3P complex **C^{2A}.1**.

The molecular structure was also confirmed by X-ray diffraction analysis and showed a typical octahedral environment around the manganese(I) center (**Figure A^{2I}.2**). On the contrary, complex **C^{2A}.2** could not be isolated in a pure form but always in mixture with complex **C^{2A}.1**.

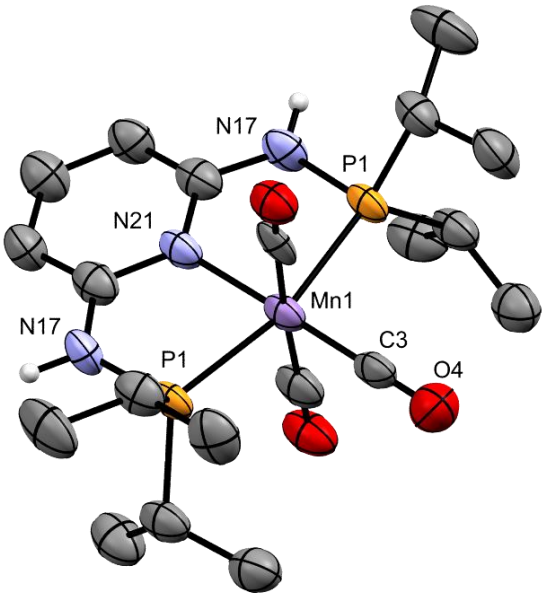

Figure A^{2I}.2 Perspective view of the molecular structure of the complex **C^{2A}.1** drawn at 50%. Br and H atoms, except the NH, and one molecule of MeOH were omitted for clarity. Only one of the two molecules of the asymmetric unit is depicted.

During our investigation, the group of Boncella published an alternative method to synthesize the complex **C^{2A}.1** (**Scheme A^{2I}.4**).[27] It is noteworthy that the choice of the solvent of the reaction (*i.e.* toluene) was crucial to get the cationic complex **C^{2A}.1** selectively: THF or fluorobenzene leaded to the formation of a mixture of **C^{2A}.1** and the new complex **C^{2A}.3**. The formation of **C^{2A}.3** resulted from the insertion of a carbonyl into P-N bond to form the metal-formamide moiety associated with a formal loss of (iPr)$_2$PBr, even if this latter species was not observed in ^{31}P NMR.

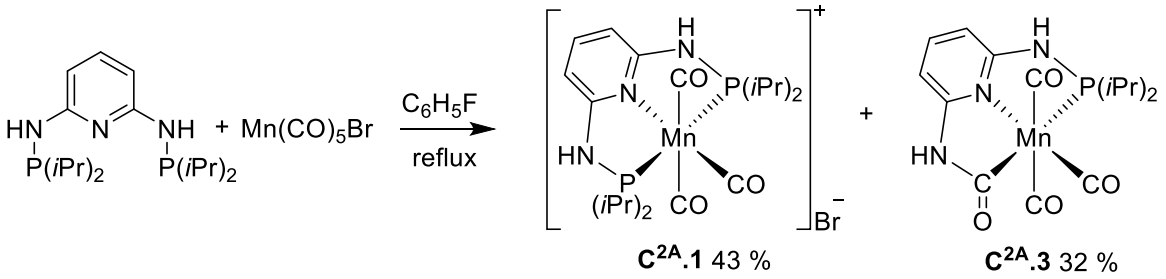

Scheme A^{2I}.4 Synthesis of the complex **C^{2A}.1** published by Boncella.[27]

Interestingly, the neutral complex **C^{2A}.2** was synthetized *in situ* upon heating a solution of complex **C^{2A}.1** in DMSO at 100 °C under vacuum for 5 h (**Scheme A^{2I}.5**). Even if the neutral complex cannot be isolated properly, ^{1}H NMR spectrum clearly showed a new and distinct set of signals in ^{1}H NMR (400 MHz, DMSO-d_6): δ (ppm) = 7.48 (t, **C^{2A}.1** H$_{para}$) *vs* 7.23 (t, **C^{2A}.2** H$_{para}$). More importantly, the chemical shift of the neutral complex **C^{2A}.2** in ^{31}P{^{1}H} NMR was very closed to the one of **C^{2A}.1** in DMSO-d_6 (133.8 ppm for **C^{2A}.1** *vs* 133.6 ppm for **C^{2A}.2**).

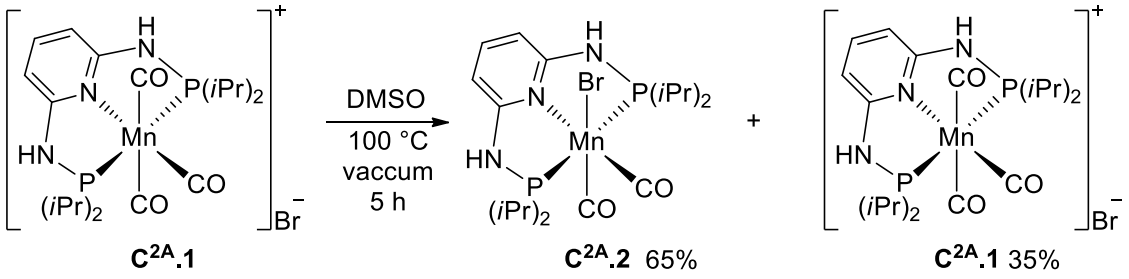

Scheme A^{2I}.5 Partial conversion of the complex **C^{2A}.1** into the complex **C^{2A}.2** published by Boncella.[27]

In addition, it must be noted that Kirchner had also described the synthesis of related [(iPrPN^{3}PiPr)MnCl$_2$] and [(iPrPN^{3}PiPr)Mn(CO)$_2$H] **C^{2A}.1d** complexes. In particular, for the preparation of the hydrido-manganese complex **C^{2A}.1d**, the crude mixture obtained by the reaction of PN^{3}P ligand with Mn(CO)$_5$Cl in dioxane at 70 °C was treated, without purification, with NaEt$_3$BH (**Scheme A^{2I}.6**). The catalyst **C^{2A}.1d** was

initially applied as catalyst in oxidative homocoupling of aryl Grignard reagents and oxidative coupling of amines with alcohols.[28]

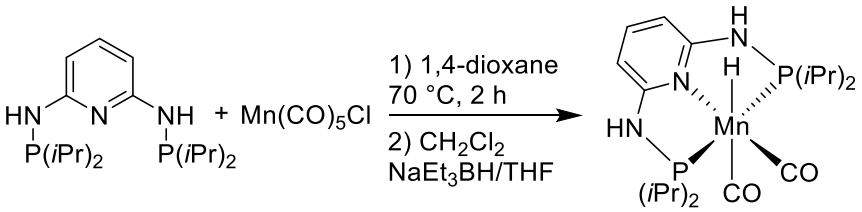

C^{2A}.1d 91 % yield

Scheme A^{2I}.6 Synthesis of the hydride complex **C^{2A}.1d** published by Kirchner.

b) <u>Methylation of anilines and sulfonamides</u>

To start our study, we selected the methylation of aniline **a1** with methanol as a model reaction to optimize the parameters of the reaction (**Table A^{2I}.1**). To our delight, at 120 °C, in the presence of a stoichiometric amount of *t*BuOK, the mono-methylation of aniline proceeded in the presence of 5 mol% of **C^{2A}.1**, showing the potential of this catalyst compared to **Mn-1** (entry 1). It is worth noting that in all the reactions, the mono-methylated product was obtained nearly exclusively and that the *N*,*N*-dimethylaniline was barely detected by GC and NMR spectroscopies. Interestingly, the reaction still occurred with good conversion when the amount of base was decreased to 10 mol% (entries 2-3). Then, the influence of the temperature was evaluated: increasing the temperature to 130 °C did not improve the conversion, whereas lowering it to 110 °C had a deleterious effect (entries 2, 4, 5). Several bases were tested (entries 6-9), *t*BuOK being the most efficient one. The presence of the ligand was found to be crucial to promote the reaction, as $Mn(CO)_5Br$ alone led to no conversion (entry 10). Finally, the optimal conditions selected to probe the substrate scope of the reaction were **C^{2A}.1** (5 mol%), *t*BuOK (20 mol%), toluene, 120 °C, 24 h (entry 11).

Table A[2I].1 Optimization of the conditions of the methylation of aniline **a1** under the catalysis of **C[2A].1**. [a]

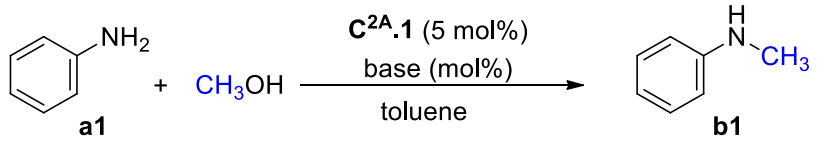

Entry	Base (mol%)	Time (h)	Temp. (°C)	Conv.[b] (Yield[c]) (%)
1	*t*BuOK (100)	62	120	98 (98)
2	*t*BuOK (10)	22	120	83 (83)
3	*t*BuOK (5)	22	120	37 (37)
4	*t*BuOK (10)	22	110	73 (73)
5	*t*BuOK (10)	22	130	84 (84)
6	Cs_2CO_3 (10)	22	120	81 (81)
7	K_2CO_3 (10)	22	120	78 (78)
8	NaOH (10)	22	120	38 (38)
9	KOH (10)	22	120	33 (33)
10[d]	*t*BuOK (20)	24	120	0 (0)
11	*t*BuOK (20)	24	120	96 (94)

[a] General conditions: aniline **a1** (0.5 mmol), MeOH (1 mL), toluene (1 mL), catalyst **C[2A].1** (5 mol%), and the base were mixed in this order and heated in a closed ACE® pressure tube in an oil bath; [b] Conversion of **a1** was determined by GC and ^{1}H NMR on the crude reaction mixture; [c] Yield in **b1** was determined by GC and ^{1}H NMR on the crude reaction mixture; [d] $Mn(CO)_5Br$ as catalyst.

Several substrates have been submitted to this reaction (**Scheme A[2I].7**). In general, electron-donating substituents, such as 4-methyl and 3,4-dimethyl- (**b2**, **b3**), 4-methoxy- (**b5**), naphthyl- (**b6**) or 4-benzyloxy- (**b15**) groups were well tolerated. However, this catalytic system was sensitive to steric hindrance as 2-phenylaniline (**a4**) and 2 methylaniline were methylated with only 35% and 10% conversion, respectively, and 2,6-dimethylaniline did not react. The presence of halide substituents allowing further functionalization of the formed products (4-iodo- **b7**, 3-bromo- **b8**, 4-chloro- **b9** and 2,4-difluoro- **b10**) did not alter the reactivity.

Scheme A[2I].7 Scope of the methylation of anilines to give *N*-methyl-anilines under the catalysis of **C[2A].1**.[a]

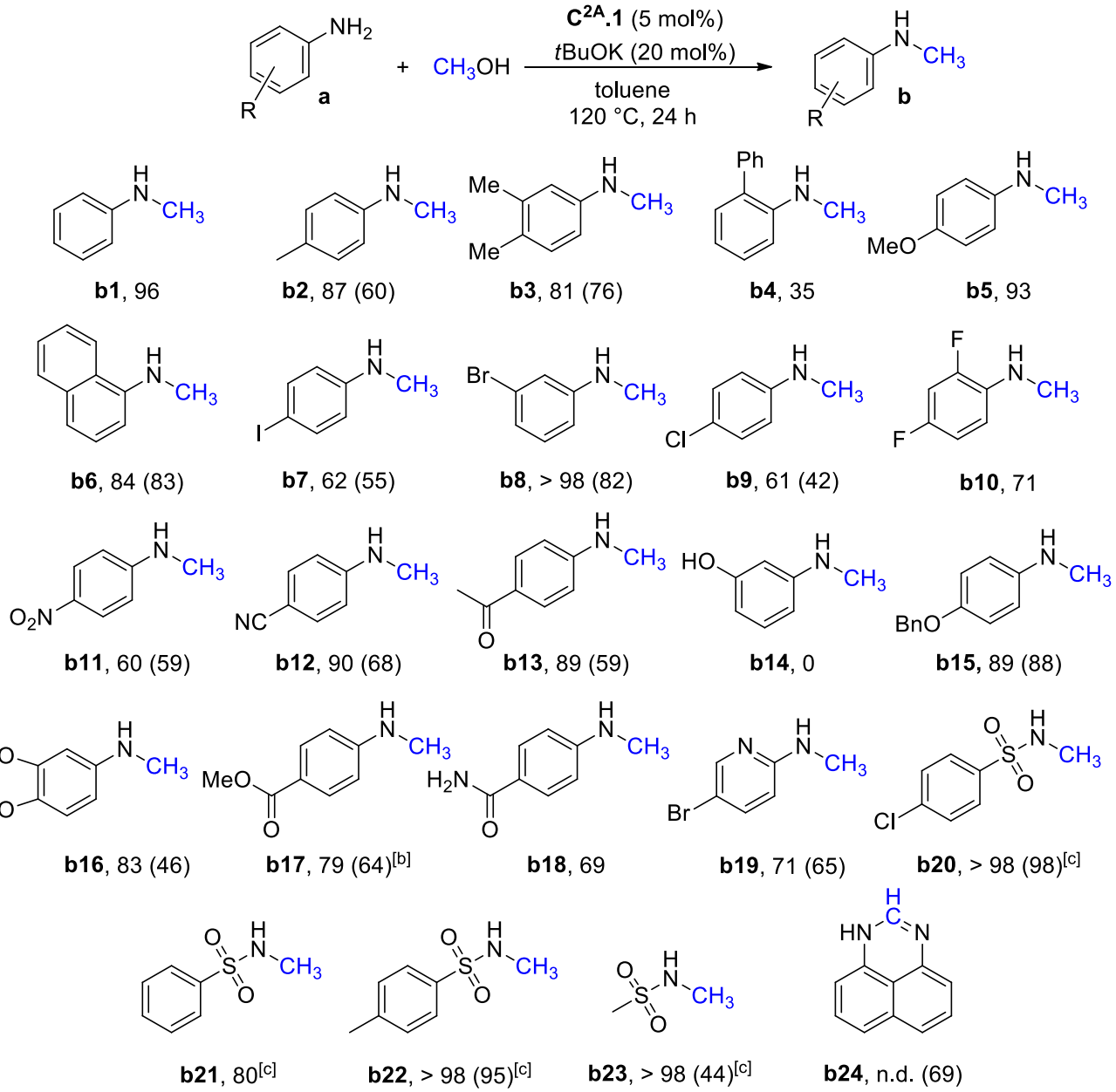

[a] General conditions: aniline (0.5 mmol), MeOH (1 mL), toluene (1 mL), catalyst **C[2A].1** (5 mol%), and *t*BuOK (20 mol%) were mixed in this order and heated in a closed ACE® pressure tube in an oil bath; [b] Starting from ethyl 4-aminobenzoate **a17**, methyl 4-*N*-methylaminobenzoate **b17** was obtained; [c] 1.2 equiv. *t*BuOK, 60 h.

Interestingly, this catalytic system was tolerant to several reducible or reactive functional groups such as nitro (**b11**), cyano (**b12**), acetyl (**b13**), acetal (**b16**), ester (**b17**) and primary amide (**b18**). 4-Bromo-2-amino-pyridine (**a19**) could also be methylated in satisfactory yield. It must be noted that an acidic phenol substituent inhibited the reaction (**b14**).

Furthermore, sulfonamides (**a20-23**), which are common moieties in biologically active compounds,[29] could also be methylated with this methodology with excellent yields, although under harsher conditions (1.2 equiv. of base for 60 h).[30]

Starting from 1,8-diaminonaphthalene, 1*H*-perimidine (**b24**) was obtained as the major product, resulting from the cyclization of the imine intermediate to the aminal derivative which undergoes dehydrogenation to yield the cyclic formamidine.[31]

c) Mechanistic insights

Next, we performed a series of experiments to get mechanistic insights. Based on the results obtained by Huang on parent ruthenium and iridium complexes,[32–34] on DFT calculations performed by Veiros on complex **C^{2A}.1d**[28] and on calculations on rhenium PNP complex from our group,[35] we assumed that, in the presence of a base, the N-H of pre-catalyst **C^{2A}.1** should be deprotonated, inducing the de-aromatization of the pyridine ring and facilitating the decoordination of one CO ligand to produce the active catalyst as a neutral dicarbonyl 16 electron manganese complex, which would dehydrogenate methanol to form the manganese hydride complex **C^{2A}.1d**. Indeed, upon the addition of *t*BuOK, the solution of **C^{2A}.1** in toluene turned to blue, leading after addition of pentane to a very sensitive blue solid that we were not able to characterize further due to its possible paramagnetic nature. By analogy with the work of Milstein,[36] we postulated that this compound was the de-aromatized di-carbonyl 16 electron complex. Upon the addition of methanol to this powder, the solution immediately turned to yellow. After slow evaporation of the solvent in a glovebox, single crystals suitable for X-Ray diffraction studies were grown. Surprisingly, we did not obtain the manganese hydride **C^{2A}.1d**, but a neutral, 18 electrons, de-aromatized manganese complex **C^{2A}.1b** bearing three carbonyl ligands (**Figure A^{2I}.3**). The deprotonated complex is stabilized in the solid state by a network of hydrogen bonding though molecules of methanol that have co-crystallized. The length of the bonds were significantly modified in **C^{2A}.1b** compared to **C^{2A}.1** (**Scheme A^{2I}.8**), showing the de-aromatization of the pyridine-ring. Complex **C^{2A}.1b** was also generated quantitatively at r.t., by reaction of **C^{2A}.1** with 1 equiv. of *t*BuOK, in a mixture of toluene and methanol (1:1, v:v). The $^{31}P\{^{1}H\}$ NMR in DMSO-d_6

displayed a single signal at 130.18 ppm ($\delta(^{31}P\{^{1}H\}$, tol-d_8) = 129.7 ppm), probably due to a fast scrambling of the N-H protons. In the ^{1}H NMR, the aromatic protons of **C^{2A}.1b** appeared as two sets of signals (δ (ppm) = 6.75 (t, H_{para}), 5.59 (d, $2H_{meta}$)), shielding compared to the cationic complex **C^{2A}.1** (δ (ppm) = 7.48 (t, H_{para}), 6.39 (d, $2H_{meta}$)), which is in line with the increased electron density of the pyridinyl ring.

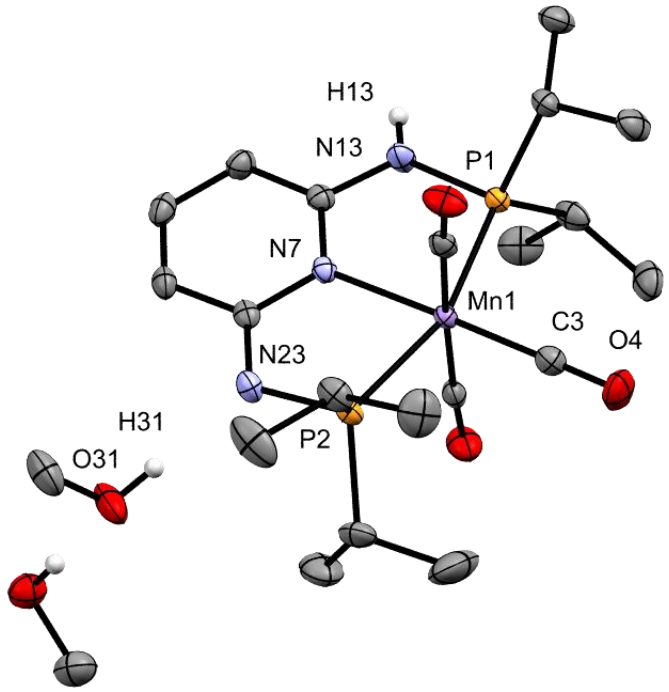

Figure A^{2I}.3 Perspective view of the molecular structure of the complex **C^{2A}.1b** drawn at 50%. H atoms, except on the heteroatoms, were omitted for clarity.

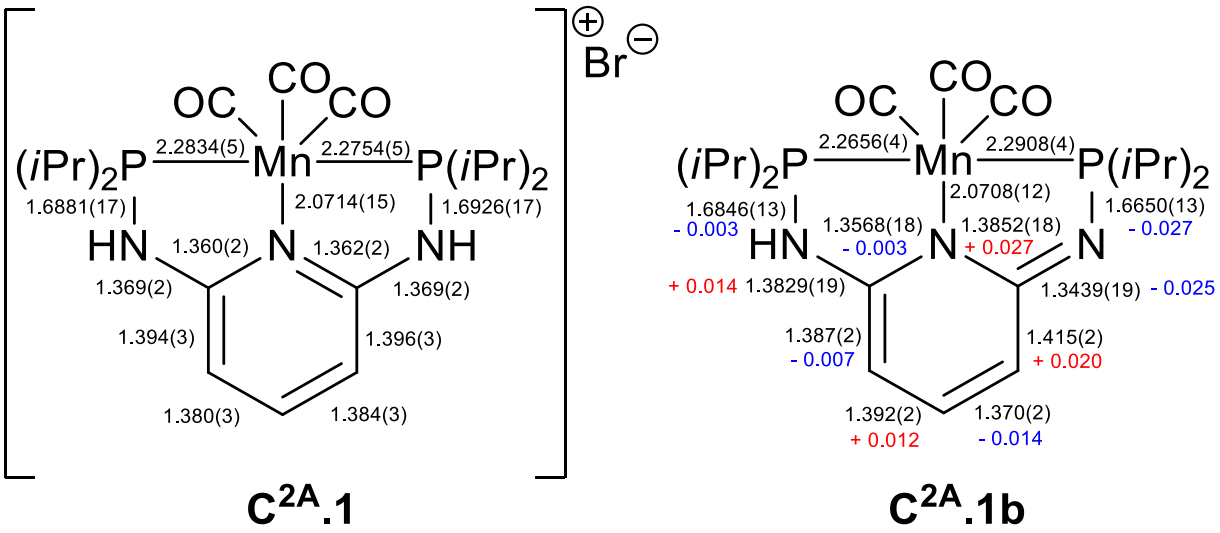

C^{2A}.1 **C^{2A}.1b**

Scheme A^{2I}.8 Principal bond lengths (Å) of complexes **C^{2A}.1** and **C^{2A}.1b** (in blue and red the difference in between the bond lengths of **C^{2A}.1** and **C^{2A}.1b**).

Finally, in a Young type NMR tube, a mixture of **C^{2A}.1**, *t*BuOK (2 equiv.) and methanol (5 equiv.) in toluene-d_8 was heated at 120 °C for 18 h. The $^{31}P\{^1H\}$ NMR (**Figure A^{2I}.4**) displayed three broad singlets, at 164.2 ppm, 132.9 ppm and 129.5 ppm, matching with the ^{31}P chemical shift of hydride **C^{2A}.1d** described by Kirchner,[28] complex **C^{2A}.1** (or the neutral bromo-dicarbonyl manganese complex[27]) and **C^{2A}.1b**, respectively.

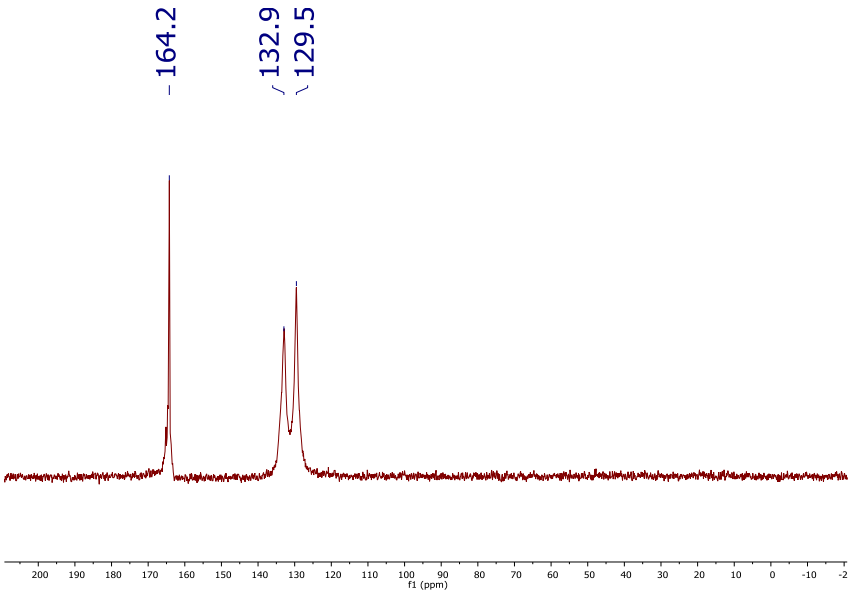

Figure A^{2I}.4 Crude $^{31}P\{^1H\}$ NMR spectrum after heating at 120 °C overnight a mixture of **C^{2A}.1** + *t*BuOK in toluene-d_8 /MeOH recorded at 162 MHz.

The presence of the hydride was also ascertained by the presence of the characteristic triplet at –5.70 ppm in the ^1H NMR spectrum (**Figure A^{2I}.5**). The same signals were also observed by $^{31}P\{^1H\}$ NMR when a catalytic reaction, *i.e.* in the presence of aniline, was performed in a NMR tube.

These experiments showed that upon heating, in the presence of methanol and base, the manganese hydride **C^{2A}.1d** was formed.

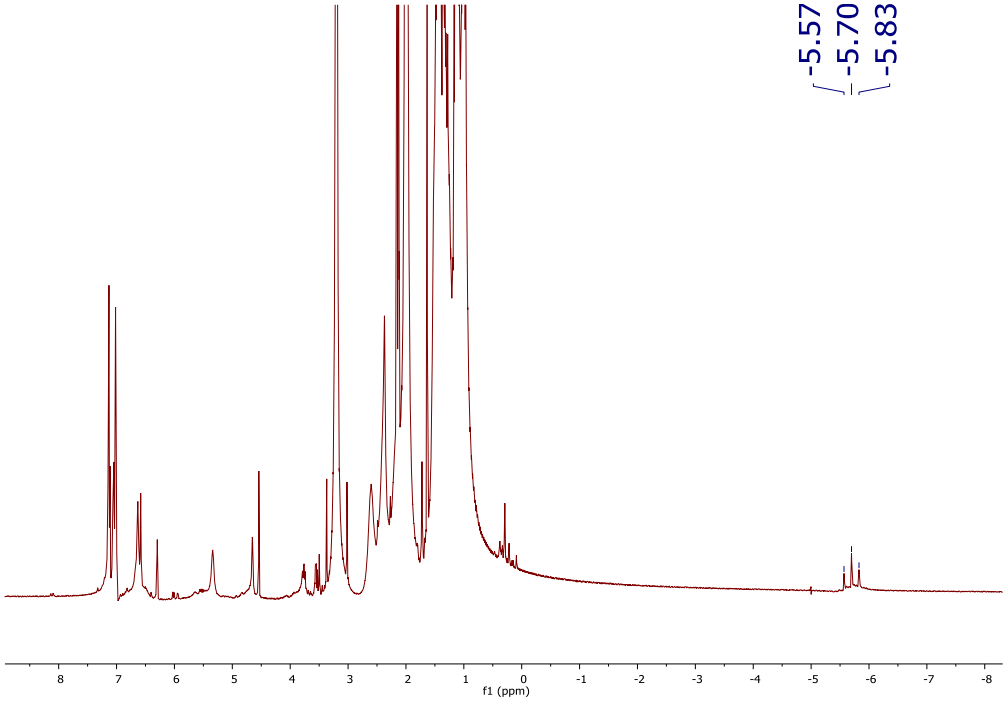

Figure A^{2I}.5 Crude ^{1}H NMR spectrum of after heating at 120 °C overnight a mixture of **C^{2A}.1** + *t*BuOK in toluene-d_8/MeOH recorded at 400 MHz showing the presence of the Mn-H signal.

Finally, the deprotonated complex **C^{2A}.1b** was tested as catalyst without the addition of an external base under standard conditions: with 10 mol% of **C^{2A}.1b**, the *N*-methylaniline was obtained in 31% yield, showing that an excess of base is needed after the deprotonation of the pre-catalyst to run the reaction (**Scheme A^{2I}.9**). In the presence of molecular sieves, the yield raised up to 46%, showing that the water produced *in situ* could alter the reaction. The yield could even be increased to 92% by adding Me_3NO (20 mol%) which is known as decarbonylative agent and molecular sieves as additives. Under the same conditions, *i.e.* using Me_3NO and molecular sieves, the cationic pre-catalyst **C^{2A}.1** gave no conversion even after 3 days. Hence, the role of the base might be to help the decarbonylation, *via* Hieber type mechanism, as well as recovering the active catalyst after undesired reaction at the metal centre. For example, water (or formic acid potentially produced *in situ* in small quantities by reaction of formaldehyde with water) could react with the 16 electron species **C^{2A}.1c** to produce a hydroxyl complex as published by Boncella.[37,38]

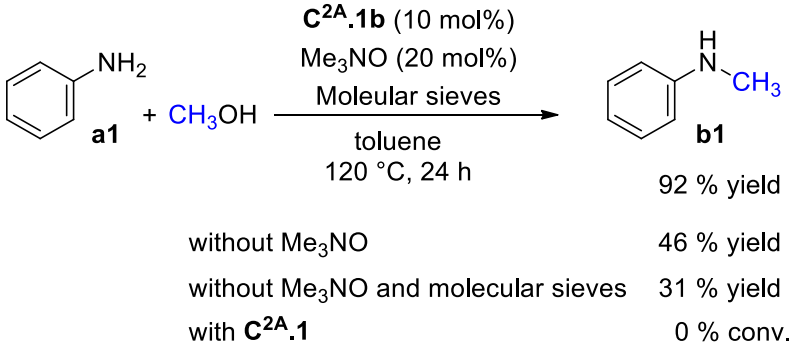

Scheme A^{2I}.9 Base-free experiments. Yields were determined by ^{1}H NMR and GC analysis.

d) Proposed mechanism

With this information in mind, we proposed the following mechanism (**Scheme A^{2I}.10**): the pre-catalyst **C^{2A}.1** is firstly deprotonated to give the 18 electron intermediate complex **C^{2A}.1b** bearing a de-aromatized ligand. This complex is then decarbonylated, *via* heating or *via* Hieber type reaction with the help of the base, to produce the 16 electron species **C^{2A}.1c**. This unstable species then dehydrogenates methanol to form formaldehyde and the hydride complex **C^{2A}.1d**. This molecule of formaldehyde reacts, *via* a condensation mechanism, with the aniline to produce the imine intermediate which is reduced by the manganese mono-hydride complex **C^{2A}.1d**. The active species **C^{2A}.1c** and the targeted amine are finally formed.

The exact mechanism of the dehydrogenation of methanol is not known. According to our work on base-free experiments and to DFT calculations performed by Kirchner and Veiros, the participation of the ligand with an outer-sphere mechanism is preferred even if an inner sphere mechanism with β-hydride elimination of a coordinated methoxy group cannot be totally excluded (**Scheme A^{2I}.11**).

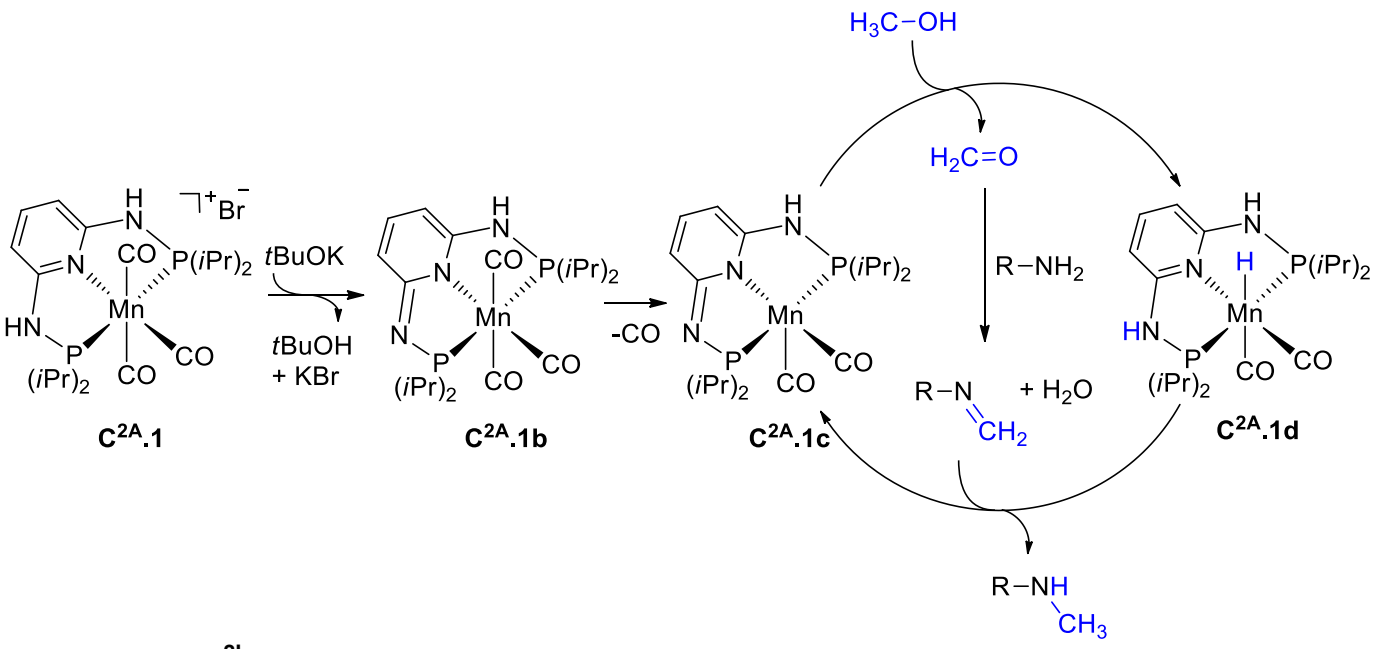

Scheme A^{2I}.10 Proposed global mechanism.

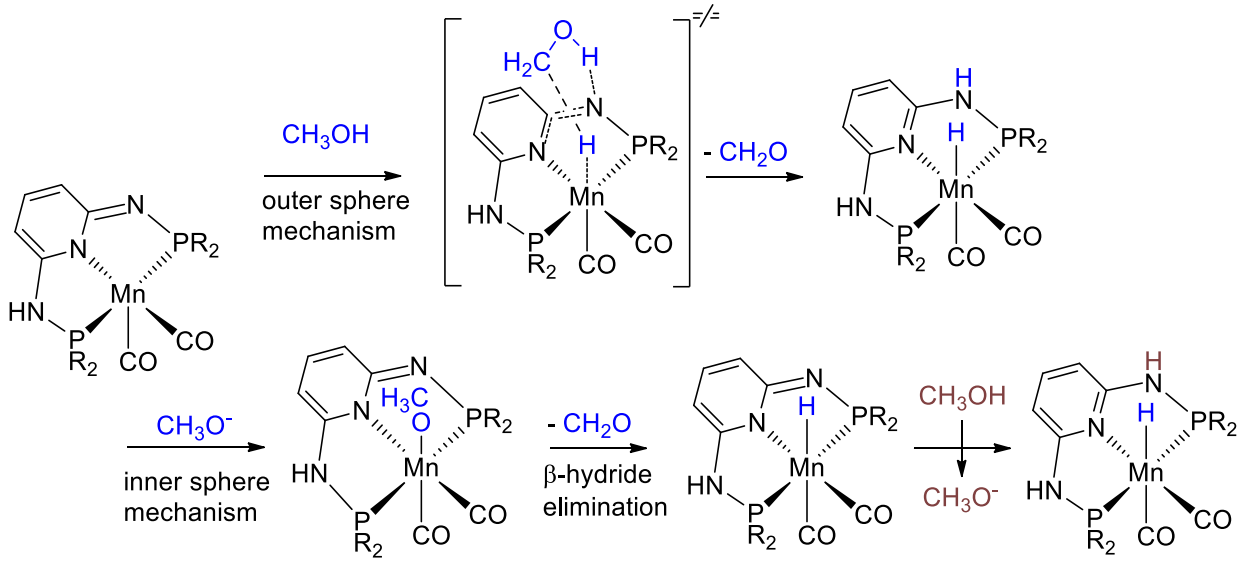

Scheme A^{2I}.11 Differences between inner sphere or outer sphere mechanisms for dehydrogenation of MeOH with **C^{2A}.1**.

To conclude this part, we successfully developed a catalytic system based on bis-(diaminopyridine)phosphine manganese(I) complex **C^{2A}.1** which is able to perform hydrogen borrowing with methanol to produce a variety of *N*-methylanilines and sulfonamides.

e) Comparison between manganese and other metal based catalysts

As mentioned in the introduction, three catalytic systems, based on manganese, including **C^{2A}.1**, are now known to promote the methylation of amines with similar scopes (**Scheme A^{2l}.12**). Our system required a lower base loading than **Mn-1** and **Mn-17** (20 mol% *vs* 1 equiv. for **Mn-1** and 50 mol% for **Mn-17**). Our initial goal was to use the lowest amount of base as possible, at the expense of the catalytic charge (5 mol% with **C^{2A}.1** vs 2 mol% for **Mn-17**) and the temperature (20 °C higher than the other catalysts).[20,22]

In the last two years, two catalytic systems based on other base metals, respectively cobalt and iron, were found to activate methanol by dehydrogenation. The system based on cobalt, stabilized with a tetradentate phosphine ligand operated at 140°C.[39] With iron, suitable conditions to promote the methylation of various substrates (in particular 2 equivalent of K_2CO_3, **Fe-20**, 80 °C) were found this year with Knölker's catalyst, already known to catalyze the alkylation of amines with heavier alcohols.[40,41]

Using noble metals, Grigg mentioned in 1981, in one of the first reports on hydrogen borrowing, that methanol could be activated by a rhodium catalytic system for the methylation of arylacetonitrile but the yield was very low.[42] Cyclopentadienyl ruthenium complexes were reported by Baratta in 2004 to catalytically methylate aliphatic amines, although the reaction failed with aniline derivatives.[43] A decade later, Seayad showed that 0.5 mol% of $[Cp^*RuCl_2]_2$ and only 5 mol% of *t*BuOLi could catalyze the reaction at 100 °C.[44] The use of micro-wave irradiations allowed to lower the reaction time as proved by Crabtree with **Ir-4**.[45] Very recently, Hong reported that using Ru-MACHO-BH **Ru-22** permitted to selectively mono-methylate challenging aliphatic amines: the use of hydrogen pressure was crucial to avoided undesired over-methylation.[46]

In summary, we can conclude that, for this reaction, the activity of base metals such as manganese and, very recently, iron can compete with the activity of catalysts based on noble metals.

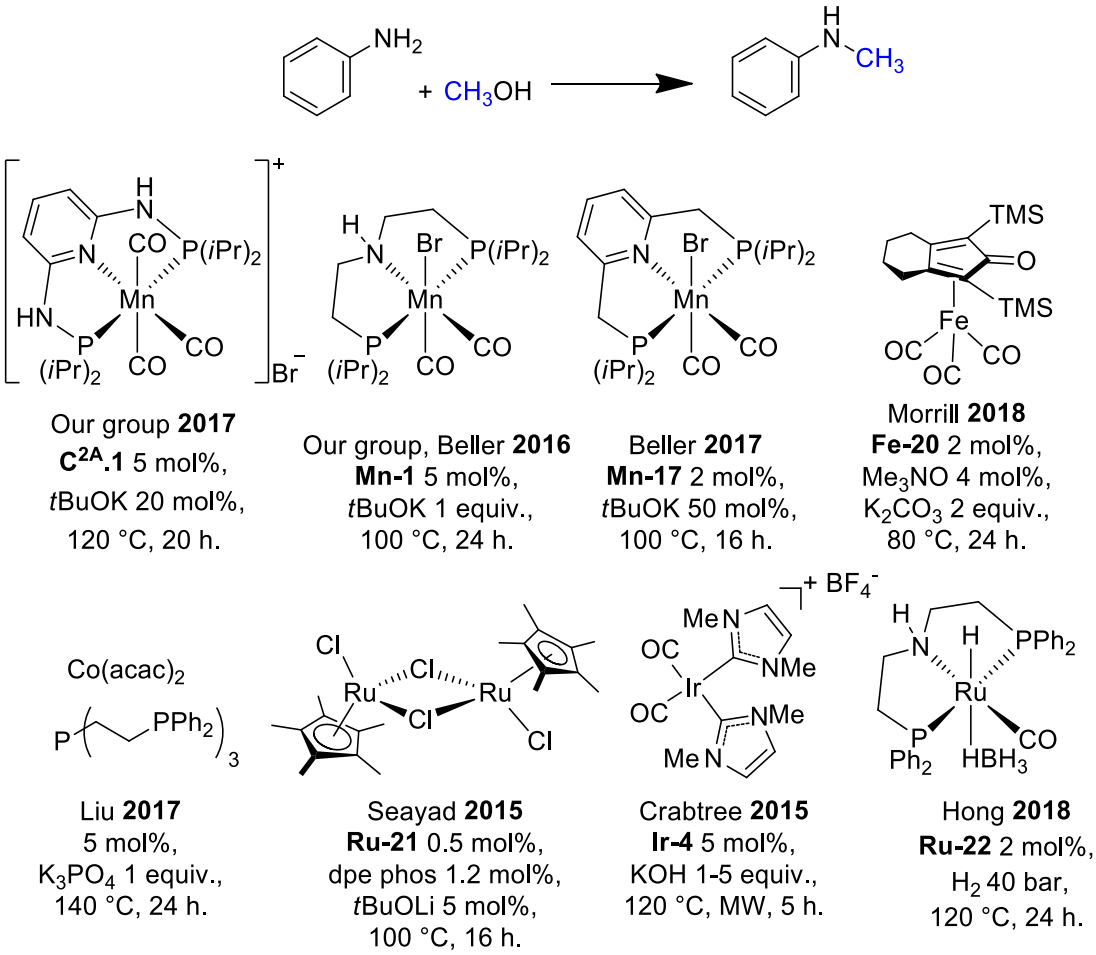

Scheme A[2I].12 Comparison of the experimental conditions for the methylation of anilines with MeOH catalyzed by base and noble metals.

These promising results encouraged us to study further the scope of substrates that can be methylated with methanol, notably carbonyl compounds.

II- α-Methylation of carbonyl derivatives

Contributions in the part: A. B.-V.

α-Methylated carbonyl functions are often encountered in biological active molecules.[6] Classically, α-alkylation of ketones is achieved by reaction of the corresponding enolate with an alkyl halide, thus generating as stoichiometric amount of wastes. In the prospect of sustainable chemistry, new strategies to introduce a methyl group under catalytic conditions starting from renewable resources and in an atom economical manner are indeed highly desirable. In this respect, alkylation at the α–position of carbonyl derivatives with alcohols *via* hydrogen borrowing strategy is a powerful tool to develop new synthetic routes.

Yet, although alkylation of ketones with alcohols in the presence of homogeneous catalysts based on precious metals[47] is well established, α-methylation using methanol still remains challenging. In 2014, the first reports for the α-methylation of ketones were published by Donohoe[48] and Obora[49], using respectively $[Cp^*RhCl_2]_2$ (5 mol%) and $[Cp^*IrCl_2]_2$ (5 mol%), as catalysts. A year later, Donohoe demonstrated that $[Cp^*IrCl_2]_2$ (1 mol%) and PPh_3 as ligand (4 mol%) was also efficient for this transformation.[50] The same year, Andersson developed a well-defined iridium catalyst based on *N*-heterocyclic carbene-phosphino ligand (1 mol%).[51] In 2016, Seayad reported the first ruthenium based system ($[Cp^*RuCl_2]_2$ (0.5 mol%) and dpePhos (1.2 mol%) for the methylation of ketones with methanol.[52]

In this context, the implementation of efficient systems based on inexpensive and abundant base metals constitutes an additional challenge, some successes being recently reported by Liu[53] then Morrill[41] using cobalt or iron-based systems, respectively.

The potential of manganese in (de)hydrogenation reactions has been demonstrated in the previous section showing that methanol can be efficiently use as C1 source *via* a partial oxidation.[54–57]

So, following our promising results on mono-*N*-methylation of anilines and sulfonamides, we wanted to use **C^{2A}.1** to catalytically promote the α-*C*-methylation of

ketones, which are known to undergo more side reactions under these conditions (**Scheme A^{2II}.1**).

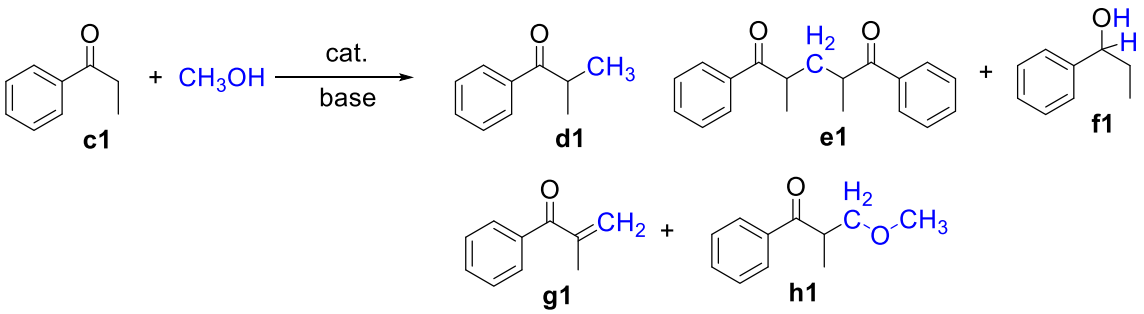

Scheme A^{2II}.1 Possible products obtained during the methylation of propiophenone **c1** with MeOH.

a) Optimization

Table A^{2II}.1. Optimization of the parameters for the α-methylation of **c1** catalyzed by **C^{2A}.1**.

Entry	base (mol%)	CH_3OH (mL)	Toluene (mL)	Conv. (%)	Yield [c]	
					d1	**e1**
1[a]	*t*BuONa (20)	1	1	94	55(55)	39(14)
2[a]	*t*BuONa (50)	2	4	98	90	10
3	*t*BuONa (50)	2	4	99	87(64)	13
4	*t*BuOK (50)	2	4	99	86	14
5	KHMDS (50)	2	4	99	77	23
6	K_3PO_4 (50)	2	4	99	82	18
7[b]	*t*BuONa (50)	6	12	50	44	6
8	*t*BuONa (50)	6	0	99	84	16
9[d]	*t*BuONa (50)	2	4	29	11	18
10[d]	*t*BuONa (100)	0.5	0.5	99	33	66 (63)
11[e]	*t*BuONa (100)	2	4	2	0	2

Conditions: In a glovebox, an ACE® pressure tube was charged with propiophenone **c1** (0.5 mmol, 66 µL), MeOH, toluene, **C^{2A}.1** (3 mol%, 8.4 mg) and, base, in that order. The closed pressure tube was then heated at 120 °C for 20 h. [a] 5 mol% of **C^{2A}.1** (14 mg), 20 mol% *t*BuONa [b] propiophenone **c1** (1.5 mmol, 198 µL), **C^{2A}.1** (1.5 mol%, 16 mg) [c] NMR yield was determined by ^{1}H NMR spectroscopy, and compared with GC/MS, on the crude mixture, isolated yield in parantheses [d]: 100 °C. [e] no Mn catalyst.

The optimization of the reaction parameters was performed for the methylation of propiophenone **c1** with methanol (**Scheme A^{2II}.1**) as model reaction (**Table A^{2II}.1**).

Initial assessment was carried out in a sealed ACE® pressure tube, at 120 °C for 20 h. In the presence of catalyst **C^{2A}.1** (5 mol%) and *t*BuONa (20 mol%), the ketone was converted (93%), the major product being the desired isobutyrophenone **d1** (55%).

Interestingly, no alcohol **f1** resulting from transfer hydrogenation, no enone **g1**, and no methyl ether **h1** were detected by ^{1}H NMR or GC-MS in the crude mixture. 1,5-diphenyl-2,4-dimethylpenta-1,5-dione **e1**, resulting from the Michael addition of the enolate on to the transient enone **g1**, is the only by-product. It indicates that the hydrogenation step is relatively slow compared to the Michael addition. To lower this side reaction, the reaction mixture was diluted, and the amount of base was increased to 0.5 equivalent: a full conversion was then obtained with a good selectivity toward the desired methylated ketone (90%, entry 2).

The catalytic loading could be decreased to 3 mol% (99%, entry 3) but with 1.5 mol% of **C^{2A}.1**, the conversion dropped (50%, entry 7). Different alternative bases (*t*BuOK, KHMDS, K_3PO_4) were tried, leading to similar conversions and selectivities (entries 3-6). When the reaction was carried out in pure methanol, the product was obtained in good yield (84%, entry 8) but toluene greatly improved the solubility of most substrates (see **Scheme A^{2II}.3** for the scope). If the temperature is lower to 100 °C, the conversion decreased to 29% (**Table A^{2II}.1**, entry 9). Finally, as 1,5-diketones are valuable products as starting materials for the synthesis of pyridines[58] or cyclic alkenes,[59] the formation of **e1** was optimized. Under concentrated conditions, in the presence of a stoichiometric amount of base, and at 100 °C, to disfavor the reduction of the enone, 1,5-diphenyl-2,4-dimethyl-penta-1,5-dione **e1** was obtained in 66% yield (entry 10). Under the same conditions, 2,2'-Methyleneditetralone **e3** was obtained starting from α-tetralone **c3** in 38% isolated yield. The blank reaction, in absence of any manganese catalyst (entry 11) led to 2% conversion and a total selectivity for the formation of 1,5 diketone **e1**.

According to our idea of the mechanism (**Scheme A^{2II}.2**), the kinetic of the reduction of the enone **g1** into ketone **d1** is the crucial step to avoid the formation of the 1,5 diketone **e1**. Inspired by the work of Métay and Lemaire,[60] calcium hydride (0.5 equiv.) was used to convert the molecule of water produced *in situ* into dihydrogen to speed up the hydrogenation of the enone **g1**. Unfortunately, the yield decreased to 48 %. We also considered taking advantage of introducing another catalyst known to

reduce C=C bonds of α-β unsaturated ketones. As described in the chapter 3 (*vide infra*), we developed the only manganese catalyst **C^{3A}.2** able to reduce C=C bonds in the presence of conjugated C=O bonds. Unfortunately, the additional use of **C^{3A}.2** (2 mol%) led to 72 % yield (*versus* 87 % for optimized conditions **Table A^{2I}.1**, entry 3).

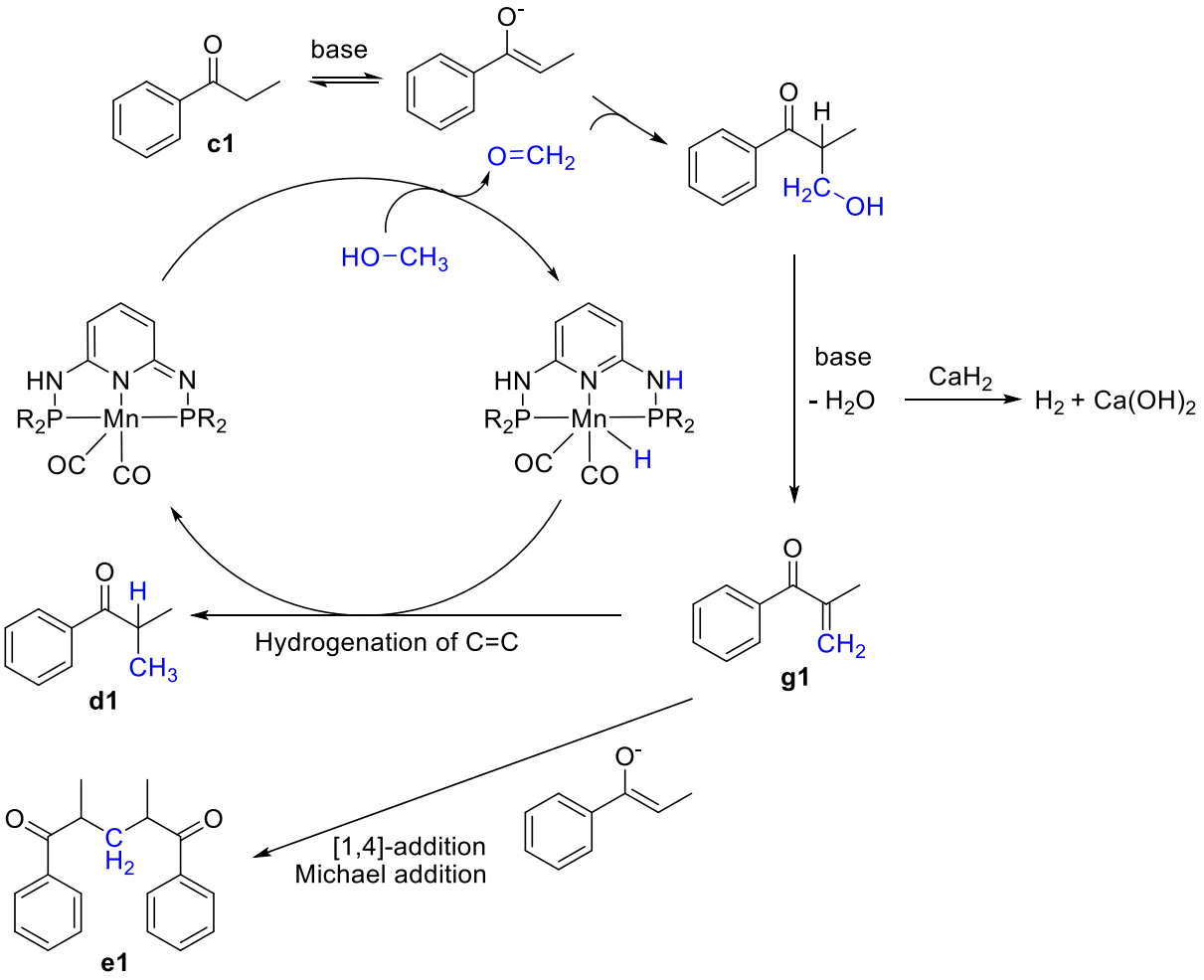

Scheme A^{2II}.2 Proposed mechanism for the reaction, highlighting the role of CaH_2 in the additional experiments.

b) Scope

With the optimized conditions in hand, a series of ketones were methylated with methanol (**Scheme A^{2II}.3**): propiophenone **c1** and acetophenone **c2** led to the same product, namely, isobutyrophenone **d1,** in 87% and 67% NMR yield, respectively. It is worth noting that in the case of acetophenone, which is less sterically hindered than **c1**, more 1,5-diketones was formed. Cyclic ketones such as α-tetralone **c3**, 1-indanone **c4** and 2-benzylidenecyclohexanone **c5** could be methylated with moderate to good yields (82%, 95% and 73% respectively). Steric hindrance disfavored the formation of undesired 1,5-diketones, therefore the double methylation of 2',4',6'-trimethylacetophenone **c6** and 2'-methylacetophenone **c7** gave high yields (92% and 80% respectively). This protocol is also tolerant toward chlorinated substrates **c8**, affording the corresponding 4-chloroisobutyrophenone **d8** (65%). In the case of 2'-aminoacetophenone **c9**, the methylation occurred at the α-position of the carbonyl, the isobutyrophenone derivative was obtained as the major product. This result contrasts with the *N*-methylation of 4'-aminoacetophenone, with the same catalyst under similar conditions, where methylation occurred at the nitrogen. It is likely that intramolecular hydrogen bonds N-H-O, favored the formation of the enolate and directed the selectivity. Furthermore, we have previously noticed that *ortho*-substituted anilines were more difficult to methylate.

Dihydrochalcone **c10** (**Scheme A^{2II}.3 (continued)**), in which the transient enolate and enone are stabilized by the phenyl ring, was methylated in very high yield (95%). A series of dihydrochalcone derivatives **c11**-**c15** have been methylated. The presence of a pyridinyl moiety in **c13** had a negative impact on the yield of the reaction (51 %). Interestingly, the catalytic system tolerated brominated substrate (**c14**), but dehalogenation (about 10%) was observed with iodo-derivative **c15**. Finally, deuterated methanol CD_3OD could be employed as alkylating agent to introduce deuterated CD_3 fragment, useful in molecular drug design.[61] For example, 2-(methyl-d_3)-2-*d*-1,3-diphenylpropan-1-one **d16** was formed in high yield from dihydrochalcone **c10**.

Scheme A^{2II}.3 Scope of the methylation of ketones with MeOH in the presence of **C^{2A}.1** as pre-catalyst.

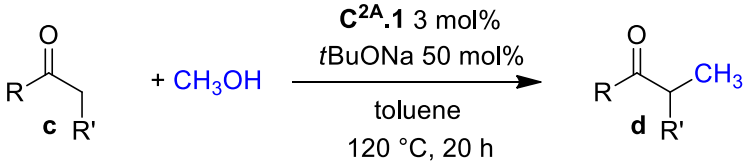

Entry	Substrate		Product		NMR yield (%) (isolated yield)
1	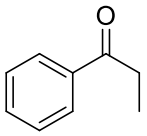	**c1**	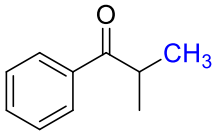	**d1**	87 (64)
2	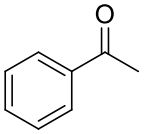	**c2**	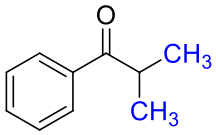	**d1**	67 (43)
3	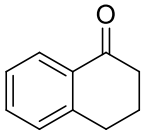	**c3**	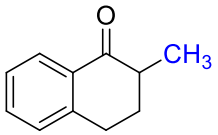	**d3**	82 (38)
4	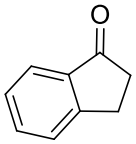	**c4**	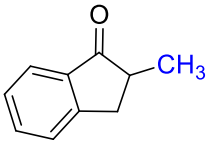	**d4**	95 (46)
5	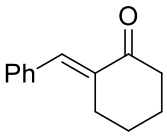	**c5**	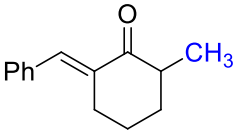	**d5**	73 (51)
6	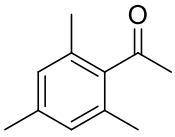	**c6**	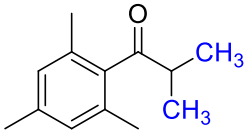	**d6**	92 (66)
7	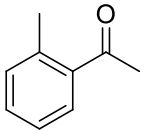	**c7**	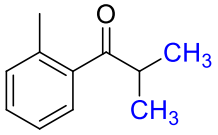	**d7**	80 (71)
8	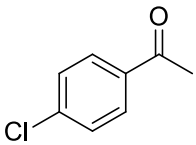	**c8**	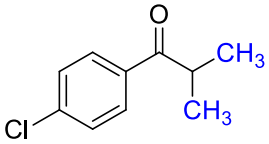	**d8**	65 (56)
9	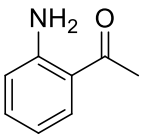	**c9**	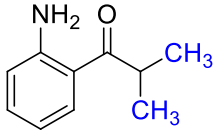	**d9**	45 (40)

Scheme A^{2II}.3 (continued) Scope of the methylation of ketones with MeOH in the presence of **C^{2A}.1** as pre-catalyst.

Entry	Substrate	Product	NMR yield (%) (isolated yield)
10	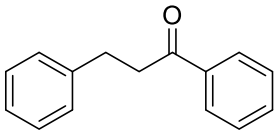 **c10**	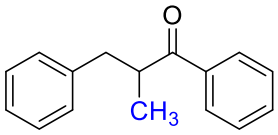 **d10**	95 (80)
11	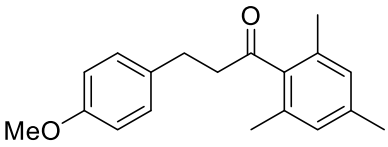 **c11**	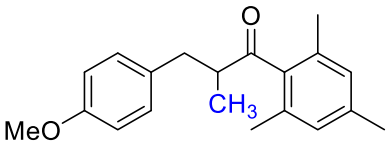 **d11**	99 (93)
12	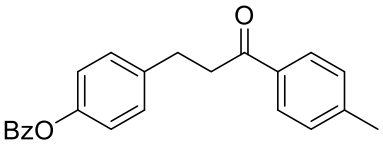 **c12**	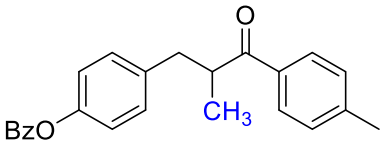 **d12**	93 (86)
13	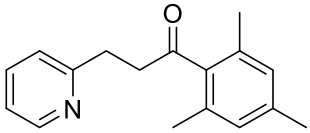 **c13**	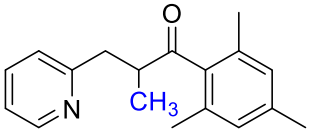 **d13**	60 (51)
14	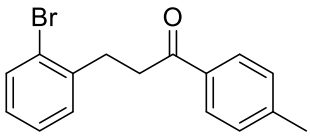 **c14**	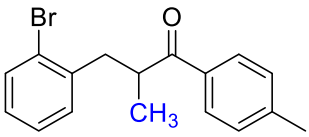 **d14**	82 (82)
15	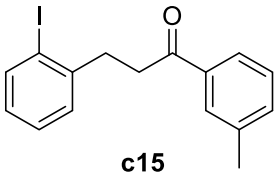 **c15**	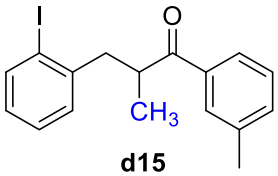 **d15**	67 (40[a])
16	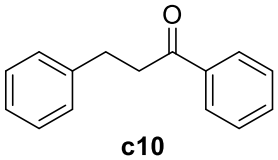 **c10**	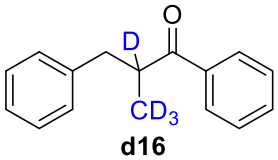 **d16**	84 (82)[b]

Conditions: In a glovebox, an ACE® pressure tube was charged with ketone (0.5 mmol), MeOH (2 mL), toluene (4 mL), **C^{2A}.1** (3 mol%, 8.4 mg) and *t*BuONa (50 mol%, 24.0 mg), in that order. The closed pressure tube was then heated at 120 °C for 20 h. Yields were determined by analysis of the ^{1}H NMR of the crude mixture and confirmed with GC-Mass analysis. [a] 10% of deiodination product was identified.

Scheme A^{2II}.4 Scope of the α-methylation of esters with MeOH in the presence of **C^{2A}.1** as pre-catalyst.

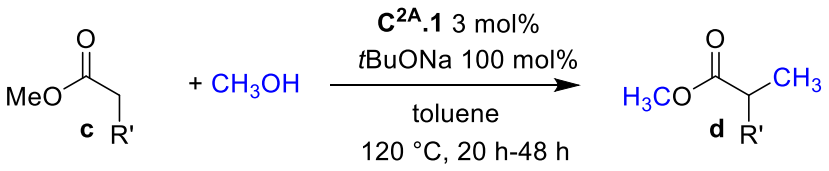

Entry	Substrate	Product	NMR yield (%) (isolated yield)
1	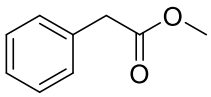 **c17**	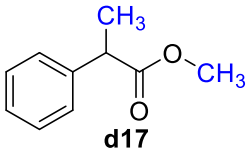 **d17**	95
2	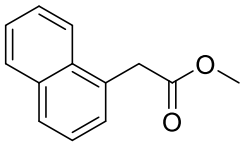 **c18**	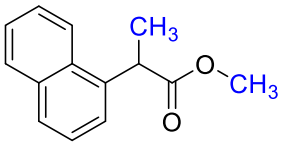 **d18**	95 (31)
3	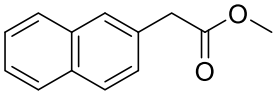 **c19**	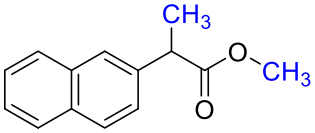 **d19**	50 (37)[a]
4	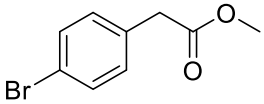 **c20**	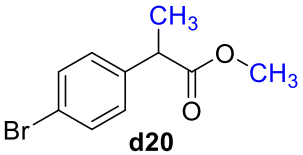 **d20**	68 (35)
5	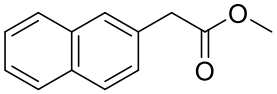 **c19**	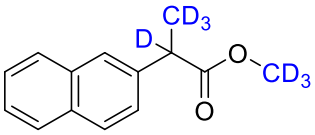 **d21**	n.d. (20)[b]

Conditions: In a glovebox, an ACE® pressure tube was charged with ester (0.5 mmol), MeOH (2 mL), toluene (4 mL), **C^{2A}.1** (3 mol%, 8.4 mg) and *t*BuONa (100 mol%, 48.1 mg), in that order. The closed pressure tube was then heated at 120 °C for 20 h. Yields were determined by analysis of ^{1}H NMR of the crude mixture and confirmed with GC-Mass analysis. [a] 50 mol % of *t*BuOK (24 mg) was used [b] CD_3OD instead of MeOH, 48 h.

The scope of the reaction was finally extended to the catalytic α-methylation of esters (**Scheme A^{2II}.4**), which has barely been achieved, even using noble metal pre-catalysts.[52] Under same reaction conditions as above yet in the presence of one equivalent of base, several esters **c16-c20** were methylated with methanol in moderate to good yields (**Scheme A^{2II}.4**), including brominated substrates (**c20**) or

deuterated product (**d21**). It is worth nothing that isolation of the methylated esters as pure product was difficult, thus leading to low yields.

In conclusion, the first manganese catalyzed α-alkylation of ketones and esters was achieved. In the presence of PN^3P manganese catalyst $\mathbf{C^{2A}.1}$ (3 mol%) at 120 °C, a series of ketones could be methylated using methanol as green alkylating reagent. This protocol has been expended to the more challenging esters derivatives with success, demonstrating further the great potential of manganese catalysis for (de)-hydrogenation reactions.

III- Conclusion, Part A

In conclusion, we have demonstrated in this part that the new manganese complex $\mathbf{C^{2A}.1}$ is an efficient catalyst to methylate anilines, sulfonamides, ketones and esters using methanol as C1 source, under hydrogen borrowing conditions. Overall, these methylations are red-ox neutral processes combining an oxidation and a reduction in the same catalytic cycle. In the next part, we will focus on reductive reactions using dihydrogen as reductant.

IV- References

[1] G. A. Olah, *Angew. Chem. Int. Ed.* **2005**, *44*, 2636–2639.
[2] P. H. Dixneuf, *Nat. Chem.* **2011**, *3*, 578.
[3] G. Bozzano, F. Manenti, *Prog. Energy Combust. Sci.* **2016**, *56*, 71–105.
[4] "Generalities about methanol", can be found under http://www.methanol.org, **2018**.
[5] K. Natte, H. Neumann, M. Beller, R. V. Jagadeesh, *Angew. Chem. Int. Ed.* **2017**, *56*, 6384–6394.
[6] E. J. Barreiro, A. E. Kümmerle, C. A. M. Fraga, *Chem. Rev.* **2011**, *111*, 5215–5246.
[7] A. Ricci (Ed.), *Amino Group Chemistry: From Synthesis to the Life Sciences*, Wiley-VCH Verlag GmbH & Co., Weinheim, Germany, **2007**.
[8] S. A. Lawrence, *Amines: Synthesis, Properties and Applications*, Cambridge University Press, Cambridge, **2004**.
[9] "Application of methylamines", can be found under https://www.chemours.com/Methylamines/en_US/uses_apps/index.html, **2018**.
[10] B. Li, J.-B. Sortais, C. Darcel, *RSC Adv.* **2016**, *6*, 57603–57625.
[11] G. Yan, A. J. Borah, L. Wang, M. Yang, *Adv. Synth. Catal.* **2015**, *357*, 1333–1350.
[12] O. Jacquet, X. Frogneux, C. Das Neves Gomes, T. Cantat, *Chem. Sci.* **2013**, *4*, 2127–2131.
[13] A. Tlili, X. Frogneux, E. Blondiaux, T. Cantat, *Angew. Chem. Int. Ed.* **2014**, *53*, 2543–2545.
[14] G. Jin, C. G. Werncke, Y. Escudié, S. Sabo-Etienne, S. Bontemps, *J. Am. Chem. Soc.* **2015**, *137*, 9563–9566.
[15] Q. Liu, L. Wu, R. Jackstell, M. Beller, *Nat. Commun.* **2015**, *6*, 5933.
[16] E. Blondiaux, J. Pouessel, T. Cantat, *Angew. Chem. Int. Ed.* **2014**, *53*, 12186–12190.
[17] S. Savourey, G. Lefevre, J.-C. Berthet, T. Cantat, *Chem. Commun.* **2014**, *50*, 14033–14036.
[18] I. Sorribes, K. Junge, M. Beller, *Chem. Eur. J.* **2014**, *20*, 7878–7883.
[19] J. Zheng, C. Darcel, J.-B. Sortais, *Chem. Commun.* **2014**, *50*, 14229–14232.
[20] J. R. Cabrero-Antonino, R. Adam, K. Junge, M. Beller, *Catal. Sci. Technol.* **2016**, *6*, 7956–7966.
[21] W.-H. Lin, H.-F. Chang, *Catal. Today* **2004**, *97*, 181–188.
[22] S. Elangovan, J. Neumann, J.-B. Sortais, K. Junge, C. Darcel, M. Beller, *Nat. Commun.* **2016**, *7*, 12641.
[23] D. Benito-Garagorri, K. Kirchner, *Acc. Chem. Res.* **2008**, *41*, 201–213.
[24] H. Li, B. Zheng, K.-W. Huang, *Coord. Chem. Rev.* **2015**, *293–294*, 116–138.
[25] J. Neumann, S. Elangovan, A. Spannenberg, K. Junge, M. Beller, *Chem. Eur. J.* **2017**, *23*, 5410–5413.
[26] D. Benito-Garagorri, K. Kirchner, *Acc. Chem. Res.* **2008**, *41*, 201–213.
[27] A. M. Tondreau, J. M. Boncella, *Polyhedron* **2016**, *116*, 96–104.
[28] M. Mastalir, M. Glatz, N. Gorgas, B. Stöger, E. Pittenauer, G. Allmaier, L. F. Veiros, K. Kirchner, *Chem. Eur. J.* **2016**, *22*, 12316–12320.
[29] E. Perspicace, A. Giorgio, A. Carotti, S. Marchais-Oberwinkler, R. W. Hartmann, *Eur. J. Med. Chem.* **2013**, *69*, 201–215.
[30] F. Li, J. Xie, H. Shan, C. Sun, L. Chen, *RSC Adv.* **2012**, *2*, 8645–8652.
[31] O. Jacquet, C. Das Neves Gomes, M. Ephritikhine, T. Cantat, *ChemCatChem* **2013**, *5*, 117–120.
[32] L.-P. He, T. Chen, D.-X. Xue, M. Eddaoudi, K.-W. Huang, *J. Organomet. Chem.* **2012**, *700*, 202–206.
[33] L.-P. He, T. Chen, D. Gong, Z. Lai, K.-W. Huang, *Organometallics* **2012**, *31*, 5208–5211.
[34] S. Qu, Y. Dang, C. Song, M. Wen, K.-W. Huang, Z.-X. Wang, *J. Am. Chem. Soc.* **2014**, *136*, 4974–4991.
[35] D. Wei, T. Roisnel, C. Darcel, E. Clot, J.-B. Sortais, *ChemCatChem* **2017**, *9*, 80–83.
[36] A. Mukherjee, A. Nerush, G. Leitus, L. J. W. Shimon, Y. Ben David, N. A. Espinosa Jalapa, D. Milstein, *J. Am. Chem. Soc.* **2016**, *138*, 4298–4301.
[37] A. M. Tondreau, R. Michalczyk, J. M. Boncella, *Organometallics* **2017**, *36*, 4179–4183.
[38] A. M. Tondreau, J. M. Boncella, *Organometallics* **2016**, *35*, 2049–2052.
[39] Z. Liu, Z. Yang, X. Yu, H. Zhang, B. Yu, Y. Zhao, Z. Liu, *Adv. Synth. Catal.* **2017**, *359*, 4278–4283.
[40] T. Yan, B. L. Feringa, K. Barta, *Nat. Commun.* **2014**, *5*, 5602.
[41] K. Polidano, B. D. W. Allen, J. M. J. Williams, L. C. Morrill, *ACS Catal.* **2018**, *8*, 6440–6445.

[42] R. Grigg, T. R. B. Mitchell, S. Sutthivaiyakit, N. Tongpenyai, *Tetrahedron Lett.* **1981**, *22*, 4107–4110.
[43] A. Del Zotto, W. Baratta, M. Sandri, G. Verardo, P. Rigo, *Eur. J. Inorg. Chem.* **2004**, *2004*, 524–529.
[44] T. T. Dang, B. Ramalingam, A. M. Seayad, *ACS Catal.* **2015**, *5*, 4082–4088.
[45] J. Campos, L. S. Sharninghausen, M. G. Manas, R. H. Crabtree, *Inorg. Chem.* **2015**, *54*, 5079–5084.
[46] G. Choi, S. H. Hong, *Angew. Chem. Int. Ed.* **2018**, *57*, 6166–6170.
[47] A. Corma, J. Navas, M. J. Sabater, *Chem. Rev.* **2018**, *118*, 1410–1459.
[48] L. K. M. Chan, D. L. Poole, D. Shen, M. P. Healy, T. J. Donohoe, *Angew. Chem. Int. Ed.* **2014**, *53*, 761–765.
[49] S. Ogawa, Y. Obora, *Chem. Commun.* **2014**, *50*, 2491–2493.
[50] D. Shen, D. L. Poole, C. C. Shotton, A. F. Kornahrens, M. P. Healy, T. J. Donohoe, *Angew. Chem. Int. Ed.* **2015**, *54*, 1642–1645.
[51] X. Quan, S. Kerdphon, P. G. Andersson, *Chem. Eur. J.* **2015**, *21*, 3576–3579.
[52] T. T. Dang, A. M. Seayad, *Adv. Synth. Catal.* **2016**, *358*, 3373–3380.
[53] Z. Liu, Z. Yang, X. Yu, H. Zhang, B. Yu, Y. Zhao, Z. Liu, *Org. Lett.* **2017**, *19*, 5228–5231.
[54] S. Chakraborty, U. Gellrich, Y. Diskin-Posner, G. Leitus, L. Avram, D. Milstein, *Angew. Chem. Int. Ed.* **2017**, *56*, 4229–4233.
[55] M. Andérez-Fernández, L. K. Vogt, S. Fischer, W. Zhou, H. Jiao, M. Garbe, S. Elangovan, K. Junge, H. Junge, R. Ludwig, et al., *Angew. Chem. Int. Ed.* **2017**, *56*, 559–562.
[56] M. Mastalir, E. Pittenauer, G. Allmaier, K. Kirchner, *J. Am. Chem. Soc.* **2017**, *139*, 8812–8815.
[57] A. Bruneau-Voisine, D. Wang, V. Dorcet, T. Roisnel, C. Darcel, J.-B. Sortais, *J. Catal.* **2017**, *347*, 57–62.
[58] T. W. Bell, S. D. Rothenberger, *Tetrahedron Lett.* **1987**, *28*, 4817–4820.
[59] A. Fürstner, B. Bogdanović, *Angew. Chem. Int. Ed., Engl.* **1996**, *35*, 2442–2469.
[60] C. Guyon, M.-C. Duclos, E. Métay, M. Lemaire, *Tetrahedron Lett.* **2016**, *57*, 3002–3005.
[61] B. Belleau, J. Burba, M. Pindell, J. Reiffenstein, *Science* **1961**, *133*, 102–104.

B - Hydrogenation catalyzed by tridentate manganese complexes

Homogeneous catalysts for hydrogenation reactions are mainly based on late transition metals (Ru, Rh, Ir, Fe).[1] Yet, few catalysts based on early transition metals[2] (especially Ti[3,4]), as well as few group 6 metals,[5] showed interesting activities for reduction of unpolarised bonds. Surprisingly, manganese was unknown before 2016 as catalyst for this type of reaction.[6,7]

I- Hydrogenation of ketones with PN^3P Mn C^{2A}.1

Contributions in the part: Synthesis of the complex: A.B.-V., D.W., Scope, Optimization, Mechanistic studies: A.B.-V.

Publication: A. Bruneau-Voisine, D. Wang, V. Dorcet, T. Roisnel, C. Darcel, J.-B. Sortais, *Catal. Commun*., **2017**, *92*, 1-4.

Using the same manganese complex **C^{2A}.1,** previously employed for methylation reactions, we wondered if the catalyst can cleave molecular dihydrogen and if hydrogenation reaction could proceed in a catalytic way.

a) Optimization

Our initial investigations to probe the hydrogenation catalytic activity of **C^{2A}.1** were carried out with acetophenone **a1** (**Table B^{2I}.1**). In the presence of 2.5 mol% of pre-catalyst **C^{2A}.1**, 5 mol% of *t*BuOK at 130 °C and under 50 bar of H_2, the ketone was converted in 68% to the corresponding alcohol **b1** (entry 1). The temperature was important, as almost no conversion was observed at 110 °C (entry 2). With 30 bar of H_2, the conversion dropped to 31% (entry 3). The hydrogenation proceeded with various bases, although with slightly lower conversion as compared to *t*BuOK (entries 3-6). Finally, the optimal conditions selected to probe the substrate scope of the reaction were 5 mol% of **C^{2A}.1**, 10 mol% of *t*BuOK, 50 bar of H_2 in toluene at 130 °C

for 20 h (entry 7). The decrease of the base load to 5 mol% resulted in a drop of the conversion to 47 % with the same other conditions (entry 8).

Table B^{2l}.1 Optimization of the parameters for the hydrogenation of acetophenone.

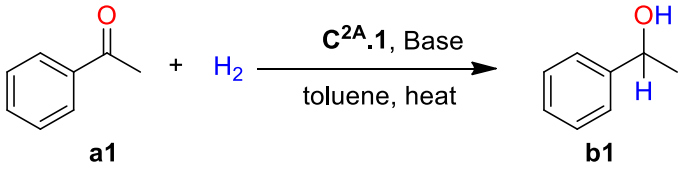

Entry	Catalyst **C^{2A}.1** (mol%)	Base (mol%)	Pressure (bar)	Temp. (°C)	Conv. (%)[a]
1	2.5	*t*BuOK (5)	50	130	68
2	2.5	*t*BuOK (5)	50	110	4
3	2.5	*t*BuOK (5)	30	130	31
4	2.5	NaOH (5)	50	130	54
5	2.5	KOH (5)	50	130	15
6	2.5	Cs_2CO_3 (5)	50	130	9
7	5	*t*BuOK (10)	50	130	>98
8	5	*t*BuOK (5)	50	130	47

Typical reaction conditions: In a glovebox, an autoclave is filled with 1) acetophenone a1 (0.5 mmol), 2) toluene (2 mL), 3) catalyst **C^{2A}.1** and 4) the base, in this order. The autoclave is then pressurized and heated in an oil bath with strong magnetic stirring for 20 h. [a] Conversion was determined by ^{1}H NMR and GC on the crude mixture.

b) Scope

Under optimized conditions (**Scheme B^{2l}.1**), various aromatic ketones bearing electron-donating, *p*-methoxy **a2**, *p*- or *o*-methyl **a3-a4**, were reduced to the corresponding alcohols in good yield. Interestingly, halogenated ketones with F, Cl and Br were well tolerated (**a5-a8**), but 4-iodoacetophenone **a8** led to low conversion even after 62 h. The presence of an electron withdrawing group such as CF_3 at the *para*-position of the aromatic ring **a9** or at the *alpha*-position to the ketone **a10** did not alter the catalytic activity. Primary amines were well tolerated, as 4-aminoacetophenone **a11** was reduced in high yield, whereas an acidic phenol group at the *para*-position totally inhibited the catalyst. Interestingly, even if the conversion was moderate, 4-cyanoacetophenone **a12** was selectively converted into the corresponding 1-(4'-cyanophenyl)ethanol **b12**, showing that this catalyst is tolerant to

nitrile group. Furthermore, aliphatic and cyclic ketones were converted to the corresponding alcohols **b14**-**b19**.

Scheme B^{2l}.1 Scope of the hydrogenation of ketones to give alcohols under the catalysis of **C^{2A}.1**.

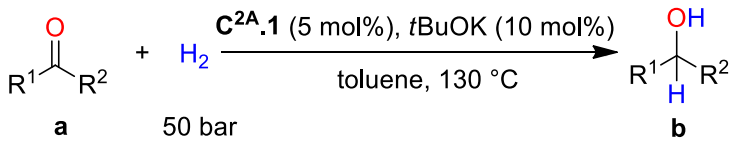

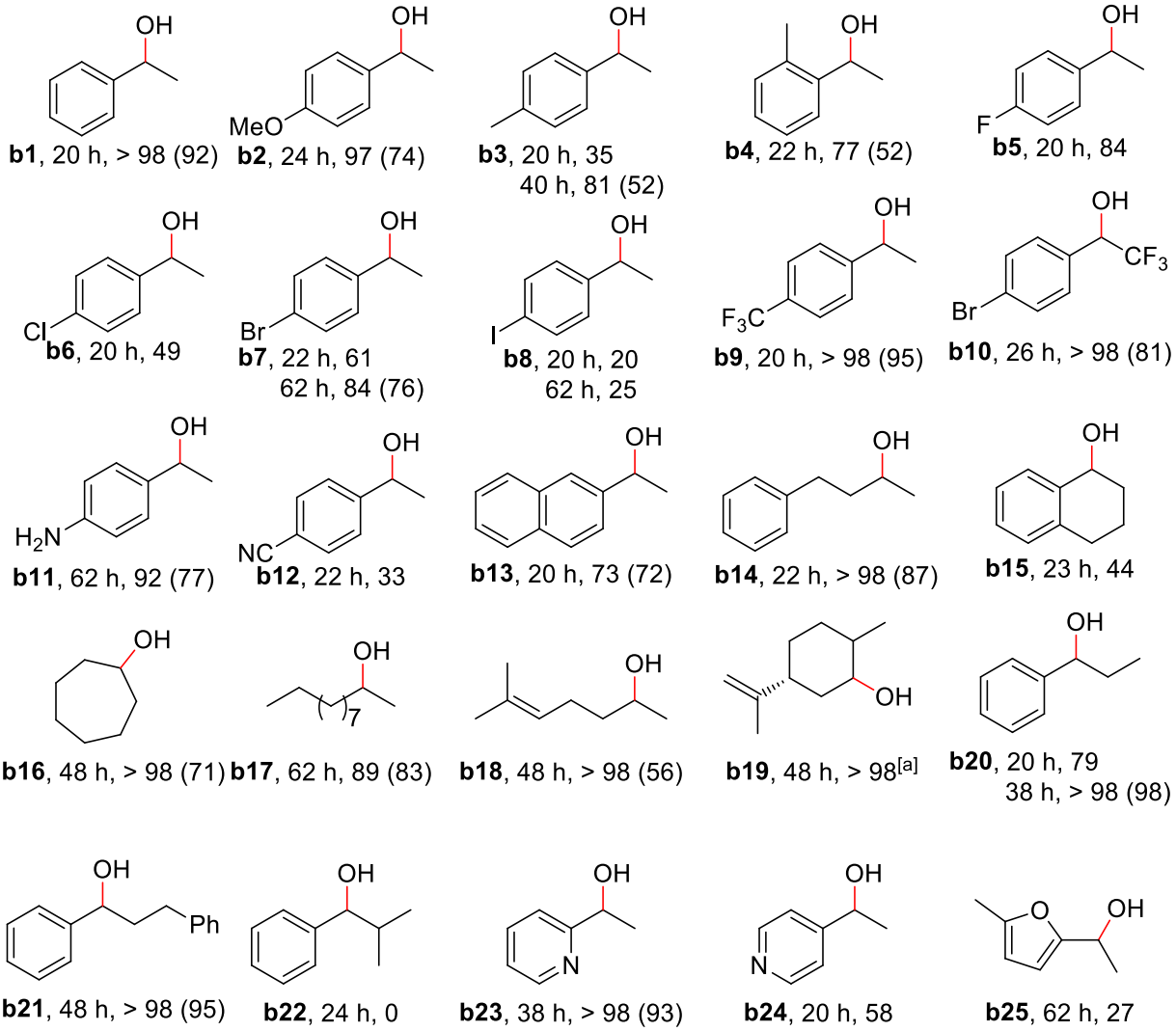

General conditions: ketone **a** (0.5mmol), toluene (2 mL), precatalyst **C^{2A}.1** (0.025 mmol, 5 mol%), *t*BuOK (0.05 mmol, 10 mol%), 130 °C. Conversion determined by ^{1}H NMR of the crude mixture. (Isolated yield in parentheses). [a] Obtained as a mixture of isomers of dihydrocarveol.

Satisfyingly, non-conjugated C=C bonds in 6-methylhept-5-en-2-one **a18** and (*R*)-(-)-carvone **a19** were not reduced, however the conjugated C=C in **a19** was fully reduced leading to a mixture of isomers of dihydrocarveol **b19**. It is noteworthy that

steric hindrance hampered the reduction of the carbonyl moieties: for example, propiophenone **a20** was fully converted to **b20**, while isobutyrophenone **a22**, or 2,4,6-trimethylacetophenone gave no conversion. Finally, hetero-aromatic ketones, such as pyridine **a23**-**a24**, and furan **a25**, were also reduced with our catalytic system.

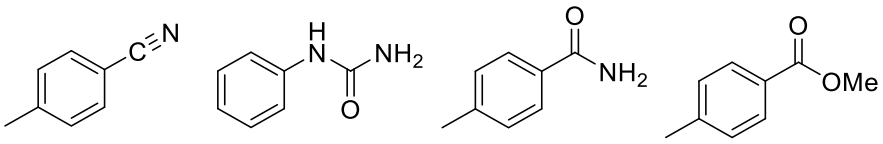

Scheme B^{2l}.2 Substrates that are not reduced with our system.

Other functionalities (**Scheme B^{2l}.2**) such as nitrile, urea, amide or ester were not reduced (or less than 10% for the ester) even with harsher conditions, upon heating until 160°C.

To explore further the catalytic activity of this manganese system, we have also investigated the reverse reaction, *i.e.* the dehydrogenation of 1-phenylethanol **b1**, in the absence of oxidant or hydrogen acceptor. When a solution of **b1**, the pre-catalyst **C^{2A}.1** (5 mol%) and *t*BuOK (10 mol%) was refluxed in toluene under a stream of argon for 22 h, the acetophenone **a1** was obtained in 84% yield (**Scheme B^{2l}.3**). These results are in line with the first step of the coupling of alcohol with amines to give imines recently described with **C^{2A}.1d** catalyst.[8]

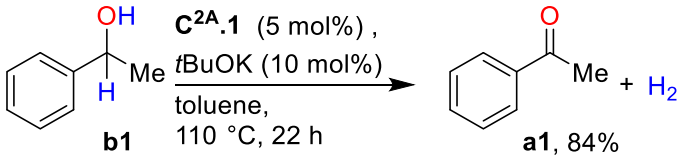

Scheme B^{2l}.3 Oxidation of alcohols. Conversion was determined by GC.

c) Mechanistic considerations

Finally, to gain insight into the nature of the catalytic active species, we performed stoichiometric experiments with the complex **C^{2A}.1**, under the catalytic conditions. In toluene, upon addition of base, the solution turns to dark blue, leading to a highly sensitive compound, that we were not able to isolate, nor to characterize by NMR spectroscopy due to its paramagnetic nature. However, when the deprotonation of complex **C^{2A}.1** was achieved in a Young NMR tube, in toluene-d_8 and then exposed

to H_2 (1.5 bar) at room temperature, the solution turned, within a few minutes, from blue to yellow.

The ^{1}H NMR spectrum of the crude mixture (**Figure B^{2I}.1**) exhibited the presence of the characteristic signal of a manganese hydride complex, as the main compound, which appeared as a triplet at -5.90 ppm (J_{HP} = 51.4 Hz).

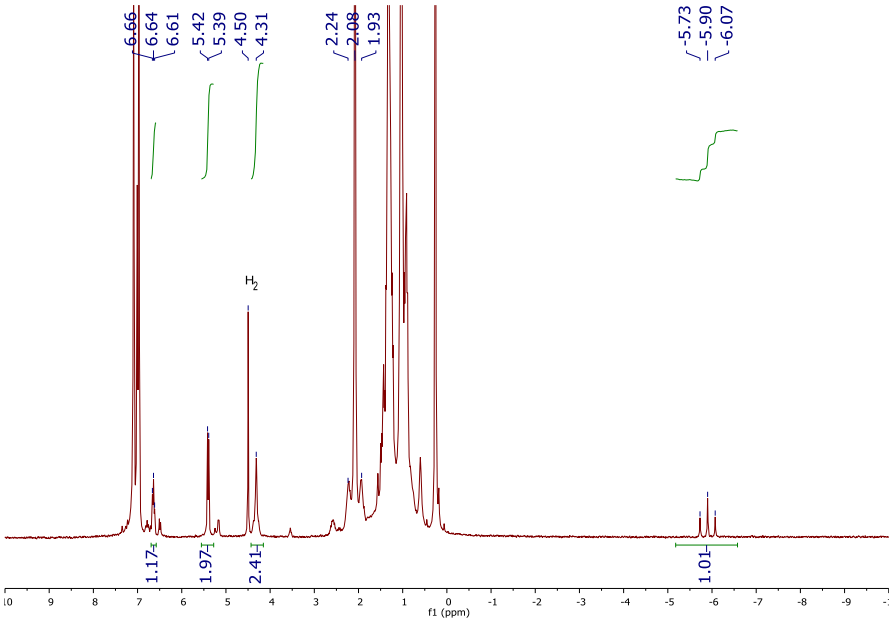

Figure B^{2I}.1 ^{1}H NMR spectrum of the crude mixture of complex **C^{2A}.1**, *t*BuOK and H_2 in toluene-d_8 recorded at 300 MHz.

The ^{31}P{^{1}H} NMR signal of the phosphorus atoms was also shifted significantly from 133.86 ppm to 164.7 ppm (**Figure B^{2I}.2**). These signals matched the reported data for **C^{2A}.1d** complex (^{1}H NMR $\delta_{(Mn\text{-}H)}$ = -5.72 ppm, t, J_{HP} = 51.4 Hz; ^{31}P{^{1}H} NMR δ = 164.8 ppm, in C_6D_6).[8] These preliminary results show that the active catalyst is likely the mono-hydride species, generated *in situ* in the presence of base and H_2, *via* N-H deprotonation/de-aromatization of the pre-catalyst.[8–10]

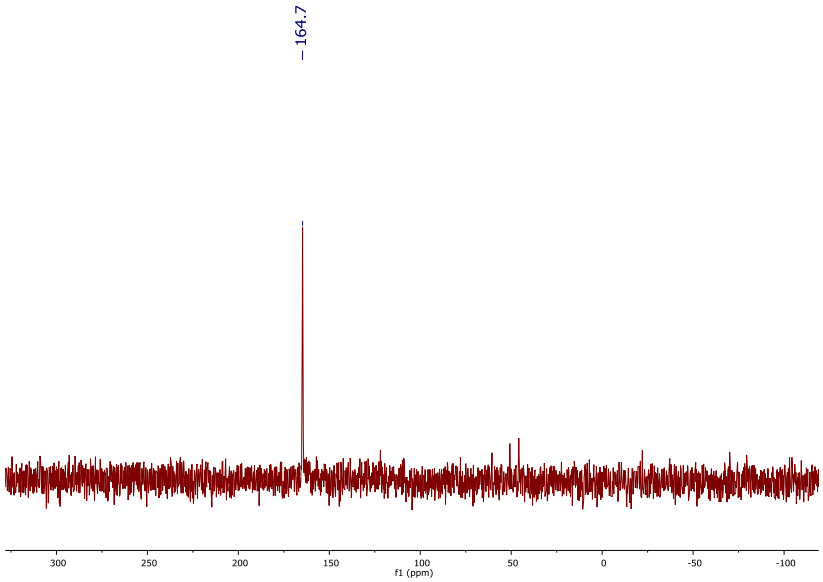

Figure B^{2I}.2 $^{31}P\{^{1}H\}$ NMR spectrum of the crude mixture of complex **C^{2A}.1**, *t*BuOK and H_2 in toluene-d_8 recorded at 121 MHz.

Since our work, the group of Kirchner recently published a manganese mono-hydride complex **C^{2A}.1d**, involved in our catalytic system, that performed the hydrogenation of carbon monoxide[11] and aldehydes[12]. Under their experimental conditions for the chemoselective hydrogenation of aldehydes (in EtOH, 0.1 mol% **C^{2A}.1d**, 25 °C), ketones were not reduced, due to higher activation barriers according to DFT calculations. Interestingly, in both papers, the complex bearing a methyl group on the nitrogen on the ligand instead of proton, to suppress the "NH" effect, was less active in catalysis (**Scheme B^{2I}.4**). These results showed that the assistance of the proton on the nitrogen was crucial to increase the activity of the catalytic system.

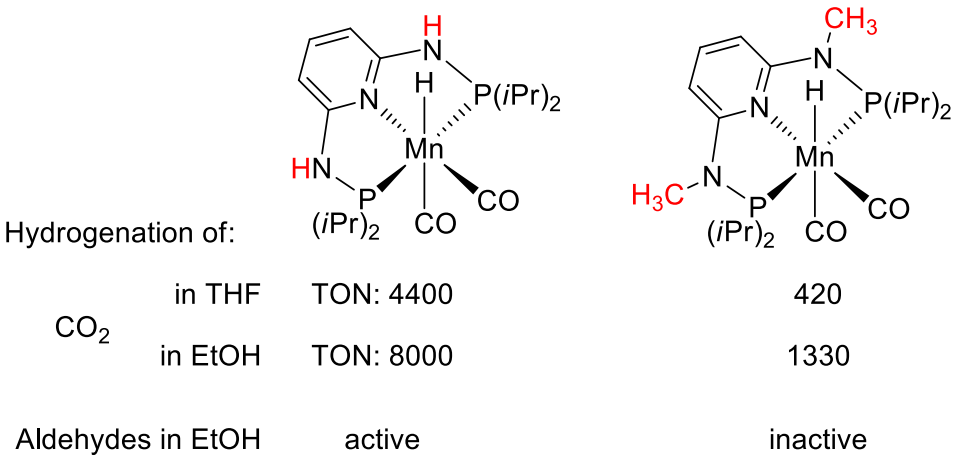

Scheme B^{2I}.4 Comparison of the activity for hydrogenation of aldehydes and CO_2 catalyzed by manganese complexes bearing a proton (complex on the left) or methyl group (complex on the right) on the nitrogen, published by Kirchner *et al.*[12,13]

In addition, both catalytic cycles (for hydrogenation of CO_2 and of aldehydes) were investigated by calculations. Depending on the substrates, an inner or an outer sphere mechanism seemed to be favored. In the case of aldehydes, the preferred pathway (lower free energy values of the intermediates) was found to be a bifunctional mechanism, with the participation of the N-H bond from the PN^3P ligand. In the case of hydrogenation of CO_2, the purely metal-centered mechanism was 2 $kcal.mol^{-1}$ more stable than the one with participation of the ligand, which can explain why the N-Me complex is an active catalyst. However, the cooperative mechanism cannot be ruled out to explain the higher activity of the NH-catalyst.

d) Conclusion

In conclusion, we have developed an efficient hydrogenation of carbonyl derivatives using a well-defined PN^3P manganese pre-catalyst **C^{2A}.1**. This catalyst system is also suitable for the reverse reaction, *i.e.* the oxidation of alcohol to the corresponding ketone. Even if this third manganese catalytic system (**Scheme B^{2I}.5**), based on classical 2,6-(diaminopyridinyl)diphosphine ligand, is less active than the first two recently reported examples based on aminodiphosphine[7] or 2,6-(diaminotriazinyl)-diphosphine,[13] further improvement of the design of the ligand will allow developing highly active manganese based hydrogenation catalysts (*vide infra*).

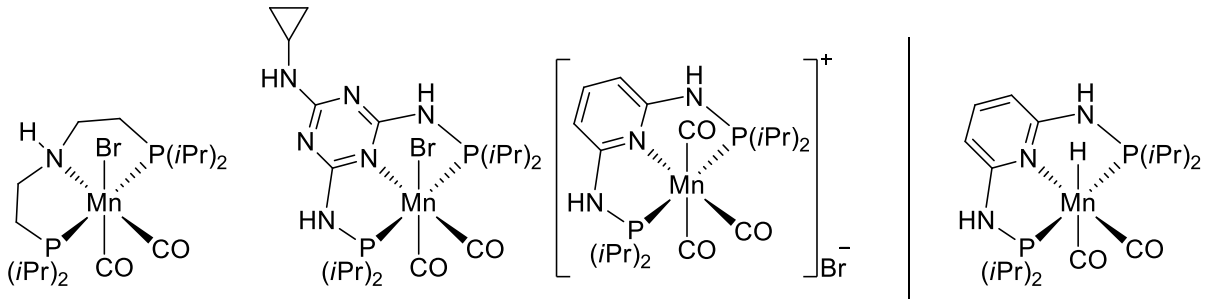

Scheme B^{2I}.5 Comparison of the experimental conditions for hydrogenation of ketones and aldehydes catalyzed by manganese complexes.

II- Study of aliphatic tridentate complexes for hydrogenation reactions

Contributions in the part: Synthesis of the ligands: M. D., A.B.-V., H. L.; Synthesis of the complexes: A.B.-V., M. D.; Hydrogenation: A.B.-V.

Publication: H. Li, D. Wei, A. Bruneau-Voisine, M. Ducamp, M. Henrion, T. Roisnel, V. Dorcet, C. Darcel, J.-F. Carpentier, J.-F. Soulé, J.-B. Sortais, *Organometallics* ***2018****, 37, 1271–1279.*

Among the various tridendate ligands developed[14,15], aliphatic PN(H)P ligands, also called "MACHO" type ligands,[16] have been demonstrating a broad versatility with a number of non-noble transition metals to promote hydrogenation reactions (Fe[17,18], Co[19], Ni[20,21], Mn[7]). Yet, one drawback of these ligands, which is also a drawback of PN^3P ligand, is their high price and relatively low modularity or difficulty of synthesis. So, we were looking for easily accessible ligands, with a higher degree of modularity.[22] Following our previous work, we focused on aminophosphine and phosphinite ligands, which are easily prepared from the corresponding alcohols or amines with readily available chlorophosphines.

a) Synthesis of complexes

Three amino-bis(phosphinite) ligands **L^{2B}.1** to **L^{2B}.3**, substituted at the nitrogen by H, Me and Bn, respectively, and on amino-bis-aminophosphine **L^{2B}.4** were prepared in high yields from the corresponding diethanolamine or bis(aminoethyl)amine and chlorodiisopropylphosphine in THF in the presence of Et_3N following literature procedures described by Stephan (**Scheme B^{2II}.1**).[23,24]

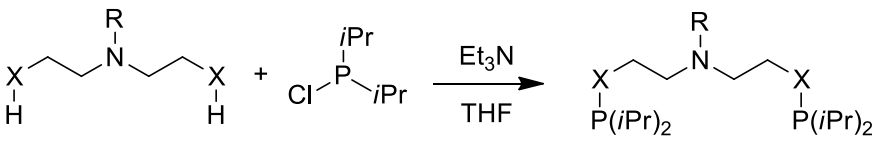

X = O R = H
= O = CH_3
= O = Bn
= NH = H

X = O, R = H, **L^{2B}.1**
= O, = CH_3, **L^{2B}.2**
= O, = Bn, **L^{2B}.3**
= NH, = H, **L^{2B}.4**

Scheme B^{2II}.1 Synthesis of PONOP ligands **L^{2B}.1-4**.

Manganese complexes **C^{2B}.1-2** were synthesized starting from $Mn(CO)_5Br$ and the corresponding ligand by heating at reflux of toluene overnight (**Scheme B^{2II}.2**). Manganese complexes were obtained as orange solids in excellent yields after one recrystallization step. Note that in the case of ligand **L^{2B}.3**, a black oily crude product was obtained and could not be purified. The complexes were fairly stable to air and moisture and could be handled without special precautions; yet, they were best stored under argon in the dark at room temperature.

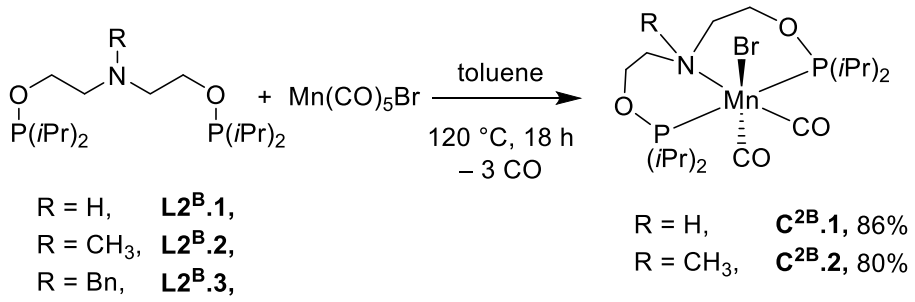

R = H, **L2^{B}.1,**
R = CH_3, **L2^{B}.2,**
R = Bn, **L2^{B}.3,**

R = H, **C^{2B}.1,** 86%
R = CH_3, **C^{2B}.2,** 80%

Scheme B^{2II}.2 Synthesis of PONOP manganese complexes **C^{2B}.1-2**.

The complexes were diamagnetic and were fully characterized by NMR (^{1}H, ^{13}C and ^{31}P) and IR spectroscopies, HR-mass spectrometry and elemental analysis. Coordination of the tridentate ligand was confirmed by the presence of a single signal in the $^{31}P\{^{1}H\}$ NMR spectra (δ 174.7 and 172.2 ppm for **C^{2B}.1** and **C^{2B}.2**, respectively). In contrast, with our previous synthesis of PN^{3}P-Mn complex **C^{2A}.1**, for which cationic tricarbonyl complexes were obtained as a mixture of neutral and cationic compounds, with this family of PONOP ligands, neutral dicarbonyl complexes were exclusively obtained, as confirmed by elemental analysis.

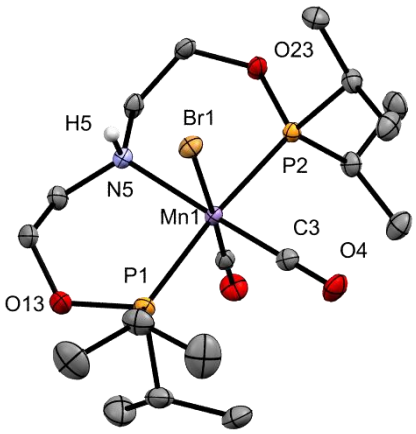

Figure B^{2II}.1 Perspective view of the molecular structure of complex **C^{2B}.1**, with thermal ellipsoids drawn at 50% probability. Hydrogen atoms, except N*H*, were omitted for clarity.

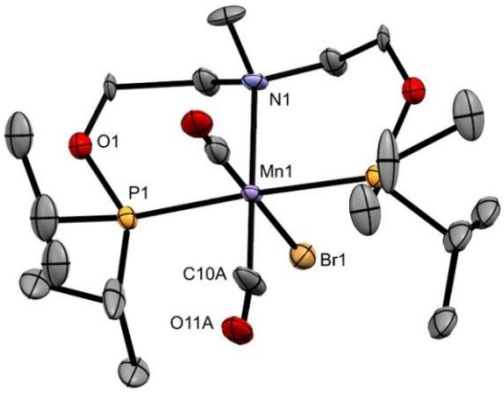

Figure B^{2II}.2 Perspective view of the molecular structure of complex **C^{2B}.2** with thermal ellipsoids drawn at 50% probability. Hydrogen atoms were omitted for clarity. Two configurations of the compound are superimposed in the crystal structure, only one is depicted.

The molecular solid-state structures of the complexes were also confirmed by single crystal X-ray diffraction studies. Representative perspective figures are disclosed in **Figures B^{2II}.1 -2** for **C^{2B}.1** and **C^{2B}.2** respectively. In all the cases, the metal lies in an octahedral environment, the tridentate ligand being in a meridional coordination mode, and the two carbonyl ligands in *cis*-position. The bromide atom was found randomly in *cis* or *trans* position with respect to the substituent on the nitrogen atom.

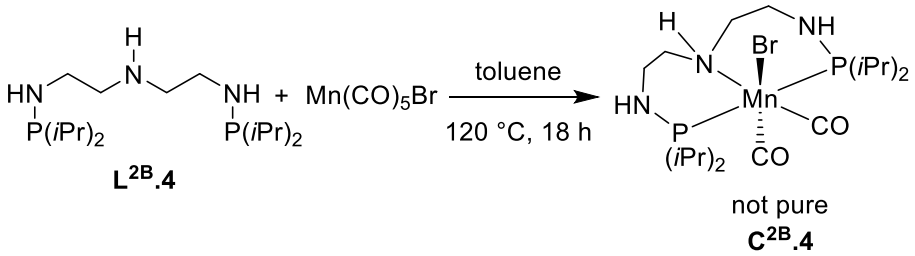

L^{2B}.4

C^{2B}.4

Scheme B^{2II}.3 Synthesis of PNNNP manganese complex **C^{2B}.4**.

The reaction of **L^{2B}.4** with the same manganese precursor under similar conditions led to a mixture of two compounds that we were not able to separate either by crystallization or washing with various solvents. The exact structure of the complexes remains unknown. The $^{31}P\{^{1}H\}$ NMR spectrum showed two signals (δ 174.6 and 107.4 ppm) with one major signal at 107.4 ppm. The ^{1}H NMR spectrum displayed only broad signals which hampered any assignments (see S.I. PartB-II Figure S19-20). This result was quickly disappointing as the same amino-bis(aminophosphine) ligand **L^{2B}.4** has been used in our team for the efficient reduction of esters with a ruthenium complex.[25]

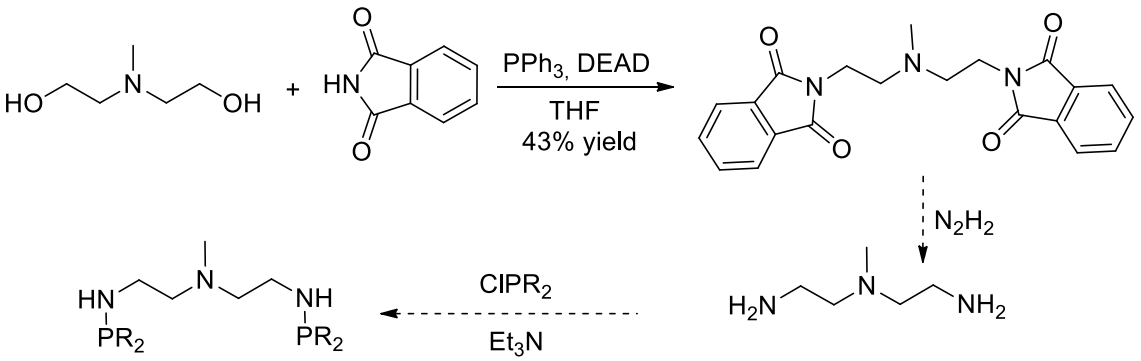

Scheme B^{2II}.4 Proposed synthesis of *N*-methyl analogue to **L^{2B}.4**.

We also wanted to prepare the *N*-methyl analogue **L^{2B}.4** in order to study the effect of the NH in catalysis. Combining a Mitsonobu reaction with a Gabriel synthesis, as described by Sienkiewicz,[26] we planned to substitute the hydroxyl group of commercially available *N*-methyldiethanolamine by a primary amine (**Scheme B^{2II}.4**). The first step has been successfully performed, but due to lack of time and difficulties to fully characterize **C^{2B}.4** we didn't pursue this synthesis.

b) Catalytic tests in hydrogenation

With these new complexes in hand, we explored their catalytic activities in the reduction of ketones with molecular hydrogen (**Table B^{2II}.1**). Initial experiments were performed on acetophenone as the model substrate at 120 °C under 50 bar of H_2, with 1 mol% of catalyst **C^{2B}.1** and 2 mol% of *t*BuOK leading to a conversion of 25% (entry 1). Surprisingly, the N-Me complex **C^{2B}.2** led to nearly the same conversion (*i.e.* 20%, entry 2) as the NH one **C^{2B}.1**, suggesting that the reaction with these manganese complexes may proceed *via* a different mechanism than participation of the N-H ligand.

The complex **C^{2B}.4**, yet not fully characterized and not pure, seemed to have a better activity, as a conversion of 67% (entry 4) was obtained using catalyst **C^{2B}.4** (2 mol%), *t*BuOK (4 mol%) at lower temperature and pressure (100 °C, 30 bar), than with **C^{2A}.1** (entry 3) and **C^{2B}.1-2**. Surprisingly, in a more diluted media, a full conversion was obtained maybe due to a better solubility of the catalyst (entry 5).

Table B^{2II}.1 Comparison of reaction parameters for the hydrogenation of acetophenone.

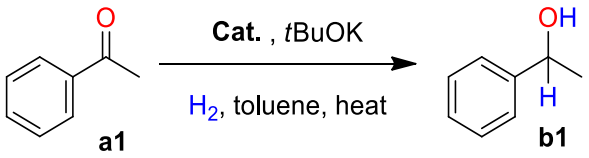

Entry	Cat. (mol%)	H_2 (bar)	*t*BuOK (mol%)	Temp. (°C)	Time (h)	Conv. (%)[b]
1	**C^{2B}.1** (1)	50	2	120	20	25
2	**C^{2B}.2** (1)	50	2	120	20	20
3	**C^{2A}.1** (5)	50	10	130	18	92
4	**C^{2B}.4** (2)	30	4	100	20	67
5[c]	**C^{2B}.4** (2)	30	4	100	20	99
6	**Re-1** (0.5)	30	1	120	20	98

General conditions: Under argon, an autoclave was charged with the (pre)catalyst, toluene (1.0 mL), followed by acetophenone **a1** (0.25 mmol, 29 μL) and *t*BuOK, in this order. The autoclave was then charged with H_2 and heated in an oil bath. [b] The conversion (%) was determined by ^{1}H NMR on the crude reaction mixture. [c] toluene (2 mL).

It should be pointed out that the parent complexes based on rhenium, such as **Re-1** (**Figure B^{2II}.3**), have been prepared and displayed significantly better activities for the hydrogenation of carbonyl compounds (entry 6). Therefore, due to their low activity compare to PN^{3}P **C^{2A}.1** and to the rhenium analogues, we did not study further this family of catalysts.

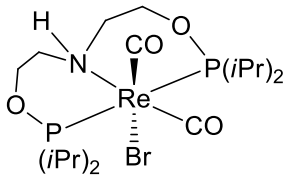

Re-1

Figure B^{2II}.3 Similar rhenium complex studied in our group for hydrogenation of ketones.

Preliminary tests for the hydrogenation of nitro group have been also studied (**Table C-III.2**). The first experiment was performed on 4-nitrotoluene **c1** as the model substrate at 130 °C, with 5 mol% of catalyst **C^{2A}.1** and 10 mol% of *t*BuOK under 50 bar of hydrogen. A conversion of 52% was obtained with a total selectivity for *p*-toluidine **d1** (entry 1). In comparison, the complex **C^{2B}.4**, which can hydrogenate ketones at lower temperature than **C^{2A}.1**, gave only 5% conversion under similar

conditions (Entry 2). The use of MeOH as co-solvent at elevated temperature (150 °C) allowed achieving a full conversion with **C^{2A}.1** (Entry 3). A mixture of *p*-toluidine **d1** (45%), *p*-azotoluene **e1** (21%) and *N*-methyltoluidine **f1** (34%) was identified as products, which indicates that MeOH can be dehydrogenated even in the presence of H_2 pressure. When EtOH was used as the solvent, a full conversion was obtained with a selectivity of 80% for *p*-toluidine **d1** after 4 days. Further optimizations are needed, in terms of conditions and catalysts, to bring these preliminary results to a broad and efficient hydrogenation of nitro-compounds.

Table B^{2II}.2 Optimisation of experimental parameters for the hydrogenation of 4-nitrotoluene **c1**.

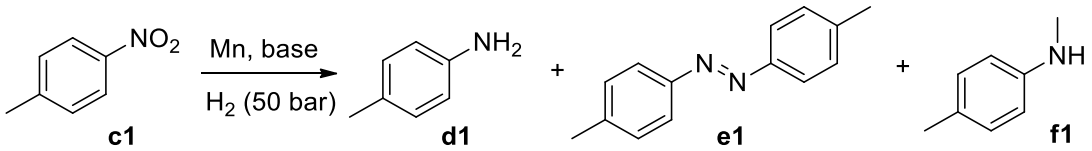

c1 **d1** **e1** **f1**

Entry	Cat. (5 mol%)	*t*BuOK (mol%)	Solvent (mL)	Temp. (°C)	Time (h)	Conv. (%)[b]	Selectivity (%) d	e	f
1	**C^{2A}.1**	10	Toluene (2)	130	21	52	100	-	-
2	**C^{2B}.4**	20	Toluene (2)	130	21	5	Maj	-	-
3	**C^{2A}.1**	20	Toluene (1) MeOH (1)	150	22	100	45	21	34
4	**C^{2A}.1**	20	EtOH (2)	130	96	100	80	15	-

General conditions: Under argon, an autoclave was charged with the (pre)catalyst, solvent, followed by 4-nitrotoluene **c1** (0.5 mmol, 58 µL) and *t*BuOK, in this order. The autoclave was then charged with H_2 and heated in an oil bath. [b] The conversion (%) was determined by ^{1}H NMR on the crude reaction mixture and compared with GC/MS.

III- Conclusion, Chapter 2

In conclusion, this chapter summarize our first achievements made with manganese catalysts bearing tridentate ligands for hydrogen borrowing reactions with methanol and hydrogenation with molecular dihydrogen.

We have first developed a highly active complex based on 2,6-diaminopyridine scaffold, *i.e.* PN^3P Mn **C^{2A}.1**, for methylation of aromatic amines, ketones and esters with methanol under hydrogen borrowing conditions. This catalytic system, based on an earth abundant metal, can even almost compete the best catalytic systems based on noble metals for the methylation of amines in term of activity.

Interestingly, the same complex **C^{2A}.1** was also active for the hydrogenation of ketones. First attempts proved that nitro-arenes could be reduced to anilines. Even if the catalytic activity may seem modest now, this catalytic system was only the third system based on manganese to promote the hydrogenation of ketones, confirming that manganese catalysts are promising in reduction reactions.

Finally, taking into account the relatively low modularity of the PN^3P or MACHO ligands, we have explored easily accessible and tunable ligands based on diethanolamine, namely the aliphatic PONOP ligands. Unfortunately, the complexes based on manganese displayed a modest activity in hydrogenation compared to their rhenium analogues.

Our initial design of catalyst was guided by a decade of development of iron catalysts, for which tridentate or tetradendate ligands were the privileged platforms to support the metal. In the next chapter, we will see that bidendante ligands can be suitable ligands to design very active manganese catalysts.

IV- References

[1] J. G. De Vries, C. J. Elsevier, *The Handbook of Homogeneous Hydrogenation*, Wiley-VCH, Weinhem, **2007**.
[2] C. Copéret, in *The Handbook of Homogeneous Hydrogenation*, Wiley-VCH, **2007**, pp. 111–151.
[3] C. A. Willoughby, S. L. Buchwald, *J. Am. Chem. Soc.* **1994**, *116*, 11703–11714.
[4] B. Demerseman, P. L. Coupanec, P. H. Dixneuf, *J. Organomet. Chem.* **1985**, *287*, C35–C38.
[5] P. A. Tooley, C. Ovalles, S. C. Kao, D. J. Darensbourg, M. Y. Darensbourg, *J. Am. Chem. Soc.* **1986**, *108*, 5465–5470.
[6] D. A. Valyaev, G. Lavigne, N. Lugan, *Coord. Chem. Rev.* **2016**, *308*, 191–235.
[7] S. Elangovan, C. Topf, S. Fischer, H. Jiao, A. Spannenberg, W. Baumann, R. Ludwig, K. Junge, M. Beller, *J. Am. Chem. Soc.* **2016**, *138*, 8809–8814.
[8] M. Mastalir, M. Glatz, N. Gorgas, B. Stöger, E. Pittenauer, G. Allmaier, L. F. Veiros, K. Kirchner, *Chem. Eur. J.* **2016**, *22*, 12316–12320.
[9] S. Qu, Y. Dang, C. Song, M. Wen, K.-W. Huang, Z.-X. Wang, *J. Am. Chem. Soc.* **2014**, *136*, 4974–4991.
[10] T. Chen, H. Li, S. Qu, B. Zheng, L. He, Z. Lai, Z.-X. Wang, K.-W. Huang, *Organometallics* **2014**, *33*, 4152–4155.
[11] F. Bertini, M. Glatz, N. Gorgas, B. Stoger, M. Peruzzini, L. F. Veiros, K. Kirchner, L. Gonsalvi, *Chem. Sci.* **2017**, *8*, 5024–5029.
[12] M. Glatz, B. Stöger, D. Himmelbauer, L. F. Veiros, K. Kirchner, *ACS Catal.* **2018**, 4009–4016.
[13] F. Kallmeier, T. Irrgang, T. Dietel, R. Kempe, *Angew. Chem. Int. Ed.* **2016**, *55*, 11806–9.
[14] H. Li, B. Zheng, K.-W. Huang, *Coord. Chem. Rev.* **2015**, *293–294*, 116–138.
[15] C. Gunanathan, D. Milstein, *Acc. Chem. Res.* **2011**, *44*, 588–602.
[16] W. Kuriyama, T. Matsumoto, O. Ogata, Y. Ino, K. Aoki, S. Tanaka, K. Ishida, T. Kobayashi, N. Sayo, T. Saito, *Org. Process Res. Dev.* **2012**, *16*, 166–171.
[17] S. Chakraborty, H. Dai, P. Bhattacharya, N. T. Fairweather, M. S. Gibson, J. A. Krause, H. Guan, *J. Am. Chem. Soc.* **2014**, *136*, 7869–7872.
[18] C. Bornschein, S. Werkmeister, B. Wendt, H. Jiao, E. Alberico, W. Baumann, H. Junge, K. Junge, M. Beller, *Nat. Commun.* **2014**, *5*, 4111.
[19] G. Zhang, B. L. Scott, S. K. Hanson, *Angew. Chem. Int. Ed.* **2012**, *51*, 12102–12106.
[20] K. V. Vasudevan, B. L. Scott, S. K. Hanson, *Eur. J. Inorg. Chem.* **2012**, 4898–4906.
[21] F. Schneck, M. Finger, M. Tromp, S. Schneider, *Chem. Eur. J.* **2017**, *23*, 33–37.
[22] A. A. Danopoulos, P. G. Edwards, *Polyhedron* **1989**, *8*, 1339–1344.
[23] M. J. Sgro, D. W. Stephan, *Organometallics* **2012**, *31*, 1584–1587.
[24] M. J. Sgro, D. W. Stephan, *Dalton Trans.* **2012**, *41*, 6791–6802.
[25] M. Henrion, T. Roisnel, J.-L. Couturier, J.-L. Dubois, J.-B. Sortais, C. Darcel, J.-F. Carpentier, *Mol. Catal.* **2017**, *432*, 15–22.
[26] J. Sienkiewicz, E. Goss, A. Stanczak, *Pol. J. Chem.* **1990**, *64*, 77–86.

Supporting Information Chapter 2

General Informations

All reactions were carried out with oven-dried glassware using standard Schlenk techniques under an inert atmosphere of dry argon or in an argon-filled glove-box. Toluene, THF, diethyl ether (Et_2O), and CH_2Cl_2 were dried over Braun MB-SPS-800 solvent purification system and degassed by thaw-freeze cycles. MeOH (Honeywell, Chromasolv for HPLC, gradient grade ≥ 99.9%) was degassed and stored on molecular sieves 4 Å. Technical grade petroleum ether and diethyl ether were used for chromatography column. Analytical TLC was performed on Merck $60F_{254}$ silica gel plates (0.25 mm thickness). Column chromatography was performed on Across Organics Ultrapure silica gel (mesh size 40-60µm, 60Å). All reagents were obtained from commercial sources and liquid reagents were dried on 4 Å molecular sieves and degassed prior to use. Manganese pentacarbonyl bromide, min. 98%, was purchased from Strem Chemicals.

^{1}H, ^{13}C and ^{31}P NMR spectra were recorded in $CDCl_3$, C_6D_6, C_7D_8 at 298 K unless otherwise stated, on Bruker, AVANCE 400 and AVANCE 300 spectrometers at 400 and 300 MHz, respectively. ^{1}H and ^{13}C NMR spectra were calibrated using the residual solvent signal as internal standard (^{1}H: $CDCl_3$ 7.26 ppm, C_6D_6 7.16 ppm, C_7H_8 2.08 ppm, DMSO-*d*$_6$ 2.50 ^{13}C: $CDCl_3$, central peak is 77.16 ppm, C_6D_6, central peak is 128.1 ppm, C_7D_8, central peak is 20.4 ppm, DMSO-*d*$_6$, central peak is 39.5 ppm). ^{31}P NMR spectra were calibrated against an external H_3PO_4 standard. Chemical shift (δ) and coupling constants (*J*) are given in ppm and in Hz, respectively. The peak patterns are indicated as follows: (s, singlet; d, doublet; t, triplet; q, quartet; quin, quintet; sex, sextuplet; sept, septuplet; oct, octuplet; m, multiplet, and br. for broad).

HR–MS spectra and microanalysis were carried out by the corresponding facilities at the CRMPO (Centre Régional de Mesures Physiques de l'Ouest), University of Rennes 1.

GC analyses were performed with GC-2014 (Shimadzu) 2010 equipped with a 30 m capillary column (Supelco, SPB^{TM}-20, fused silica capillary column, 30 m × 0.25 mm × 0.25 mm film thickness).

GC-MS were obtained on a QP2010 Ultra GC/MS apparatus from Shimadzu equipped with a 30 m capillary column (Phenomenex, Zebron, ZB-5ms, fused silica capillary column, 30 M × 0.25 mm × 0.25 mm film thickness).

A – I - Mono-*N*-methylation anilines and sulfonamides

ACE® pressure tube with front seal (15 mL) were used for the methylation reaction.

Synthesis of the manganese complex $C^{2A}.1$

To a solution of *N,N'*-Bis(diisopropylphosphino)-2,6-diaminopyridine $L^{2A}.1$ ligand[1] (3.297 g, 9.6 mmol) in distilled toluene (100 mL), was added 1.0 equivalent of pentacarbonyl manganese bromide ($Mn(CO)_5Br$) (2.64 g, 9.6 mmol). After stirring at 110 °C overnight, the reaction mixture was filtered and the solid was washed four times with cold distilled THF (4×40 mL) and five times with distilled *n*-pentane (5×30 mL). The product was dried under vacuum and a white solid was obtained (3.678 g, 68 % yield). Suitable single crystals for X-Ray diffraction studies were obtained by diffusion of *n*-pentane into a solution of $C^{2A}.1$ (CH_2Cl_2/MeOH, 4/1 ratio).

^{1}H NMR (300 MHz, DMSO-d_6) δ 8.99 (s, 2H), 7.48 (t, *J* = 8.0 Hz, 1H), 6.39 (d, *J* = 8.0 Hz, 2H), 2.90 – 2.64 (m, 4H), 1.40 (dd, *J* = 16.0, 6.8 Hz, 12H), 1.28 (dd, *J* = 16.9, 7.2 Hz, 12H).

The integration of the signals of THF (δ 3.60 (m, 4H), 1.75 (m, 4H)) can give the approximate ratio of complex and THF is 2:1.

^{13}C{^{1}H} NMR (101 MHz, DMSO-d_6) δ 220.9, 215.2, 160.6 (t, *J* = 7.4 Hz), 140.7, 99.0, 30.6 – 30.1 (m), 17.7 (d, *J* = 17 Hz).

^{31}P{^{1}H} NMR (162 MHz, DMSO-d_6): δ133.86.

Anal. Calc (%). for $(C_{20}H_{33}N_3O_3BrP_2Mn)(C_4H_8O)_{0.5}$: C, 44.31; H, 6.25; N, 7.05. Found: C, 44.49; H, 6.16; N, 6.93.
0.5 molecule of THF compare to complex $C^{2A}.1$ is present in ^{1}H and ^{13}C NMR spectra. Due to high affinity of the solvent to the complex, extensive drying did not allow to obtain solvent-free elemental analysis.[2]

HR MS (ESI): m/z $[M]^+$ calcd for ($C_{20}H_{33}N_3O_3P_2Mn$) 480.1372, found 480.1373 (0 ppm); m/z $[M-CO]^+$ calcd for ($C_{19}H_{33}N_3O_2P_2Mn$) 452.1423 m/z found 452.1429 (1 ppm); m/z $[2M^+, Br^-]^+$ calcd for ($C_{40}H_{66}N_6O_6{}^{79}BrP_4Mn_2$) 1039.1933 m/z found 1039.1936 (0 ppm).

General procedure for methylation reactions

In an argon filled glove box, a 15 mL Ace® pressure tube was charged with the desired amine (0.5 mmol), toluene (1 mL), MeOH (1 mL), Mn complex $C^{2A}.1$ (14 mg, 5 mol%) followed by *t*-BuOK (11.2 mg, 20 mol%), in this order. The mixture was stirred for 24 hours at 120 °C in an oil bath. The solution was then diluted with ethyl acetate and filtered through a short pad of silica (2 cm in a Pasteur pipette). The silica was washed with ethyl acetate. The filtrate was evaporated and the crude residue was purified by column chromatography (SiO_2, mixture of petroleum ether/ethyl acetate or diethyl ether as eluent).

Characterization of the methylated products

_N_-Methyl-4-methylaniline (b2)[3]

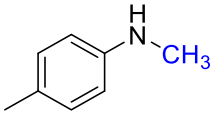

According to general procedure 4-methylaniline (53.6 mg, 0.5 mmol) gave the title compound **b2** as a yellow oil (34 mg, 60%).

^{1}H NMR (400 MHz, $CDCl_3$) δ 7.03 (d, *J* = 7.9 Hz, 2H), 6.57 (d, *J* = 7.9 Hz, 2H), 3.30 (br. s, 1H), 2.83 (s, 3H), 2.27 (s, 3H).
$^{13}C\{^{1}H\}$ NMR (101 MHz, $CDCl_3$) δ 147.3, 129.8, 126.6, 112.7, 31.2, 20.5.

_N_-Methyl-3,4-dimethylaniline (b3)[4]

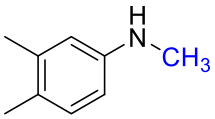

According to general procedure 3,4-dimethylaniline (60.6 mg, 0.5 mmol) gave the title compound **b3** as a yellow oil (52 mg, 76%).

^{1}H NMR (400 MHz, $CDCl_3$) δ 7.01 (d, *J* = 8.0 Hz, 1H), 6.50 (d, *J* = 2.3 Hz, 1H), 6.45 (dd, *J* = 8.0, 2.3 Hz, 1H), 3.36 (s, 1H), 2.85 (s, 3H), 2.26 (s, 3H), 2.22 (s, 3H).
$^{13}C\{^{1}H\}$ NMR (101 MHz,$CDCl_3$) δ 147.7, 137.3, 130.3, 125.3, 114.4, 110.0, 31.2, 20.1, 18.8.

_N_-Methyl-1-napthylamine (b6)[5]

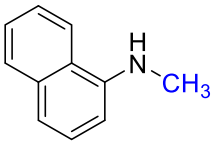

According to general procedure 1-naphthylamine (71.6 mg, 0.5 mmol) gave the title compound **b6** as a white solid (65 mg, 83%).

^{1}H NMR (400 MHz, $CDCl_3$) δ 7.86 (d, *J* = 7.6 Hz, 1H), 7.81 (d, *J* = 8.2 Hz, 1H), 7.59 – 7.39 (m, 3H), 7.32 (d, *J* = 8.2 Hz, 1H), 6.66 (d, *J* = 7.5 Hz, 1H), 4.44 (s, 1H), 3.04 (s, 3H).
$^{13}C\{^{1}H\}$ NMR (101 MHz, $CDCl_3$) δ 144.6, 134.3, 128.7, 126.8, 125.8, 124.7, 123.5, 119.9, 117.4, 103.8, 31.1.

4-Iodo-_N_-methyl-aniline (b7)[3]

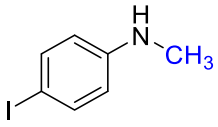

According to general procedure, 4-iodoaniline (109.5 mg, 0.5 mmol) gave the title compound **b7** as a colorless oil (64 mg, 55%).

^{1}H NMR (400 MHz, $CDCl_3$) δ 7.43 (d, *J* = 8.8 Hz, 2H), 6.39 (d, *J* = 8.8 Hz, 2H), 3.74 (br. s, 1H), 2.80 (s, 3H).
$^{13}C\{^{1}H\}$ NMR (101 MHz, $CDCl_3$) δ 148.9, 137.8, 114.7, 77.8, 30.6.

3-Bromo-*N*-methyl-aniline (b8)[6]

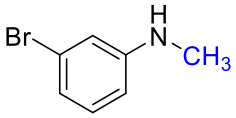

According to general procedure, 3-bromoaniline (54.5 µL, 0.5 mmol) gave the title compound **b8** as a colorless oil (76 mg, 82%).

^{1}H NMR (400 MHz, $CDCl_3$) δ 7.03 (t, *J* = 8.0 Hz, 1H), 6.87 – 6.78 (m, 1H), 6.74 (t, *J* = 2.0 Hz, 1H), 6.52 (dd, *J* = 8.2, 1.7 Hz, 1H), 3.78 (br. s, 1H), 2.81 (s, 3H).
$^{13}C\{^{1}H\}$ NMR (101 MHz, $CDCl_3$) δ 150.6, 130.5, 123.4, 119.9, 114.9, 111.3, 30.6.

4-Chloro-*N*-methyl-aniline (b9)[3]

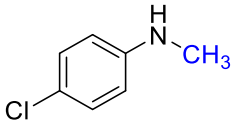

According to general procedure, 4-chloroaniline (63.8 mg, 0.5 mmol) gave the title compound **b9** as a colorless oil (30mg, 42%).

^{1}H NMR (400 MHz, $CDCl_3$) δ 7.13 (d, *J* = 8.9 Hz, 2H), 6.53 (d, *J* = 8.8 Hz, 2H), 3.71 (br. s, 1H), 2.81 (s, 3H).
$^{13}C\{^{1}H\}$ NMR (75 MHz, $CDCl_3$) δ 148.0, 129.1, 121.9, 113.5, 30.9.

***N*-Methyl-4-nitro-aniline (b11)**[7]

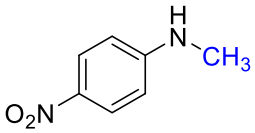

According to general procedure, 4-nitroaniline (68 mg, 0.5 mmol) gave the title compound **b11** as a colorless oil (44 mg, 59%).

^{1}H NMR (400 MHz, $CDCl_3$) δ 8.08 (d, *J* = 9.0 Hz, 2H), 6.52 (d, *J* = 9.1 Hz, 2H), 4.67 (br. s, 1H), 2.93 (d, *J* = 5.1 Hz, 3H).
$^{13}C\{^{1}H\}$ NMR (101 MHz $CDCl_3$) δ 154.4, 138.0, 126.5, 110.8, 30.2.

***N*-Methyl-4-cyano-aniline (b12)**[3]

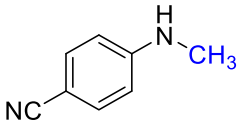

According to general procedure, 4-aminobenzonitrile (59.1 mg, 0.5 mmol) gave the title compound **b12** as a colorless oil (45 mg, 68%).

^{1}H NMR (400 MHz, $CDCl_3$) δ 7.42 (d, *J* = 8.7 Hz, 2H), 6.55 (d, *J* = 8.7 Hz, 2H), 4.33 (br. s, 1H), 2.87 (d, *J* = 4.9 Hz, 3H).
$^{13}C\{^{1}H\}$ NMR (101 MHz, $CDCl_3$) δ 152.3, 133.7, 120.7, 111.9, 98.5, 30.0.

4-Acetyl-*N*-methylaniline (b13)[3]

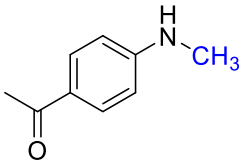

According to general procedure, 4-aminoacetophenone (67.6 mg, 0.5 mmol) gave the title compound **b13** as a colorless oil (40 mg, 59%).

^{1}H NMR (400 MHz, $CDCl_3$) δ 7.81 (d, *J* = 8.4 Hz, 2H), 6.53 (d, *J* = 8.4 Hz, 2H), 4.50 (br. s, 1H), 2.86 (d, *J* = 4.9 Hz, 3H), 2.48 (s, 3H).
^{13}C{^{1}H}, NMR (101 MHz, $CDCl_3$) δ 196.5, 153.3, 130.8, 126.4, 111.0, 30.1, 26.0.

***N*-Methyl-4-benzyloxyaniline (b15)**

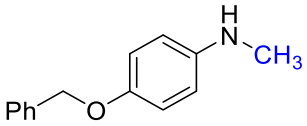

According to general procedure, 4-(benzyloxy)aniline hydrochloride* (117.9 mg , 0.5 mmol) gave the title compound **b15** as a brown oil (106 mg, 88%).

*= the amine.HCl salt was first deprotonated by *t*BuOK (1.1 equiv.) in the mixture of MeOH/toluene for 20 min, and then the catalyst and the base were added.

^{1}H NMR (400 MHz, $CDCl_3$) δ 7.55 – 7.47 (m, 2H), 7.47 – 7.40 (m, 2H), 7.37 (t, *J* = 7.2 Hz, 1H), 6.94 (d, *J* = 8.9 Hz, 2H), 6.63 (d, *J* = 8.9 Hz, 2H), 5.05 (s, 2H), 3.48 (br. s, 1H), 2.84 (s, 3H).
^{13}C{^{1}H} NMR (101 MHz, $CDCl_3$) δ 151.3, 144.0, 137.7, 128.5, 127.8, 127.5, 116.2, 113.6, 70.9, 31.5.

***N*-Methyl-3,4-methylenedioxyaniline (b16)**

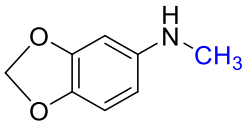

According to general procedure, 3,4-(methylenedioxy)aniline (70 mg, 0.51 mmol) gave the title compound **b16** as a brown oil (36 mg, 46%).

^{1}H NMR (400 MHz, $CDCl_3$) δ 6.68 (d, *J* = 8.3 Hz, 1H), 6.25 (d, *J* = 2.3 Hz, 1H), 6.05 (dd, *J* = 8.3, 2.3 Hz, 1H), 5.85 (s, 2H), 3.37 (br. s, 1H), 2.79 (s, 3H).
^{13}C{^{1}H} NMR (101 MHz$CDCl_3$) δ 148.5, 145.4, 139.7, 108.7, 103.9, 100. 7, 95.7, 31.8.

Methyl-4-(methylamino)benzoate (b17)[3]

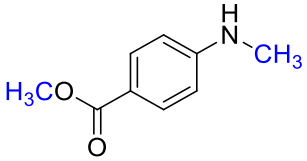

According to general procedure, ethyl 4-aminobenzoate (82.6 mg, 0.5 mmol) gave the title compound **b17** as a colorless oil (52 mg, 64%).

^{1}H NMR (400 MHz, $CDCl_3$) δ 7.87 (d, *J* = 8.6 Hz, 2H), 6.54 (d, *J* = 8.6 Hz, 2H), 4.26 (br. s, 1H), 3.84 (s, 3H), 2.86 (s, 3H).
^{13}C{^{1}H} NMR (101 MHz, $CDCl_3$) δ 167.5, 153.0, 131.6, 118.2, 111.1, 51.6, 30.2.

5-Bromo-2-methylamino-pyridine (b19)[8]

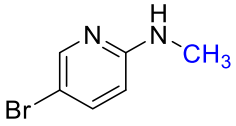

According to general procedure, 2-amino-5-bromo-pyridine (86.5 mg, 0.5 mmol) gave the title compound **b19** as a colorless oil (61 mg, 65%).

^{1}H NMR (400 MHz, $CDCl_3$) δ 8.14 – 8.01 (m, 1H), 7.48 (dd, *J* = 8.8, 2.3 Hz, 1H), 6.29 (d, *J* = 8.8 Hz, 1H), 4.67 (br. s, 1H), 2.88 (d, *J* = 5.1 Hz, 3H).
^{13}C{^{1}H} NMR (101 MHz, $CDCl_3$) δ 158.2, 148.7, 139.8, 107.7, 106.9, 29.3.

4-Chloro-*N*-methylbenzenesulfonamide (b20)

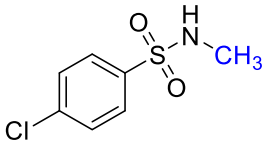

According to general procedure, 4-chlorobenzenesulfonamide (96 mg, 0.5 mmol) gave the title compound **b20** as a white solid (102 mg, 98%).

^{1}H NMR (400 MHz, $CDCl_3$) δ 7.80 (d, *J* = 8.0 Hz, 2H), 7.50 (d, *J* = 8.0 Hz, 2H), 4.53 (br. s, 1H), 2.67 (s, 3H).
^{13}C{^{1}H} NMR (101 MHz, $CDCl_3$) δ 139.3, 137.4, 129.5, 128.8, 29.3.

***N*-Methyl-*p*-toluenesulfonamide (b22)**[3]

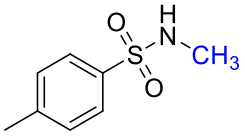

According to general procedure, *p*-toluenesulfonamide (85.6 mg, 0.5 mmol) gave the title compound **b22** as a white solid (88 mg, 95%).

^{1}H NMR (400 MHz, $CDCl_3$) δ 7.75 (d, *J* = 8.2 Hz, 2H), 7.31 (d, *J* = 8.2 Hz, 2H), 4.58 (br. s, 1H), 2.63 (d, *J* = 5.0 Hz, 3H), 2.43 (s, 3H).
^{13}C{^{1}H} NMR (101 MHz, $CDCl_3$) δ 143.6, 135.9, 129.8, 127.4, 29.4, 21.6.

***N*-Methylmethanesulfonamide (b23)**

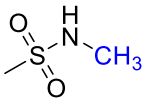

According to general procedure, methanesulfonamide (47.6 mg, 0.5 mmol) gave the title compound **b23** as a white solid (24 mg, 44%).

^{1}H NMR (400 MHz, $CDCl_3$) δ 4.24 (br. s, 1H), 2.95 (s, 3H), 2.84 (d, *J* = 4.4 Hz, 3H).
^{13}C{^{1}H} NMR (101 MHz, $CDCl_3$) δ 38.8, 29.4.

1*H*-Perimidine (b24)[9]

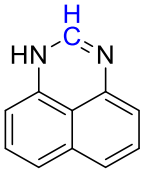

According to general procedure, 1,8-diaminonaphthalene (79 mg, 0.5 mmol) gave the title compound **b24** as a yellow solid (58 mg, 69%).

^{1}H NMR (400 MHz, $CDCl_2$) δ 7.21 (s, 1H), 7.15-7.05 (m, 4H), 6.45 (d, *J* = 5.2 Hz, 2H).
^{13}C{^{1}H} NMR (101 MHz, CD_2Cl_2) δ 145.3, 140.5, 136.0, 128.6, 123.7, 120.2, 108.7.

Mechanistic studies

Synthesis of manganese complex **C^{2A}.1b**

First method:

In an Ace tube, to a solution of complex **C^{2A}.1** (56 mg, 0.1 mmol) in toluene was added *t*BuOK (22.4 mg, 0.2 mmol). The solution turned to blue within one hour, and a precipitate appeared. The blue solution was transferred to a second Schlenk tube, and concentrated (note: without reaching dryness). After the addition of n-pentane, a thin blue powder precipitated after one night, and was isolated after the removal of the solvent with a syringe.

The solid was dissolved in methanol, leading to a yellow solution from which single crystals of **C^{2A}.1b** were grown by slow evaporation.

Second method:

In a Schlenk tube, to a solution of complex **C^{2A}.1** (30 mg, 0.053 mmol) in toluene/MeOH (2mL/2mL) was added *t*BuOK (1 equiv., 6 mg). The mixture was stirred at r.t. overnight. The crude mixture was evaporated to dryness and the complex **C^{2A}.1b** was directly characterized by NMR spectroscopies.

^{1}H NMR (400 MHz, DMSO-d_6) δ 6.76 (t, *J* = 7.8 Hz, 1H), 5.59 (d, *J* = 7.8 Hz, 2H), 2.47 – 2.35 (m, 4H), 1.31 (dd, *J* = 14.5, 6.9 Hz, 12H), 1.20 (dd, *J* = 15.6, 7.3 Hz, 12H).

^{13}C{^{1}H} NMR (101 MHz, DMSO-d_6) δ 136.97, 30.93 (d, *J* = 28.8 Hz), 18.06 (d, *J* = 22.5 Hz).
Note : the two carbon in *meta* position and CO were not observed.

^{31}P NMR (162 MHz, DMSO-d_6) δ 130.18.

Catalysis with the deprotonated complex

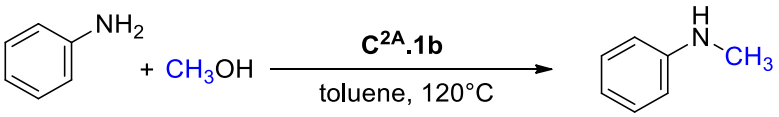

First condition: 10 mol% **C^{2A}.1b**, 31% yield.

In an argon filled glove box, a 15 mL Ace® pressure tube was charged with freshly distilled aniline (0.5 mmol, 53 µL), freshly distilled toluene (1 mL), freshly distilled MeOH (1 mL), **C^{2A}.1b** (23 mg, 10 mol%).

The mixture was stirred for 24 hours at 120 °C in an oil bath. The 31% yield was determined by the ^{1}H NMR of an aliquot after evaporation and confirmed by GC and GC/MS analysis.

Second condition: 10 mol% **C^{2A}.1b**, molecular sieves, 46 % yield.

In an argon filled glove box, a 15 mL Ace® pressure tube was charged with freshly distilled aniline (0.5 mmol, 53 µL), freshly distilled toluene (1 mL), freshly distilled MeOH (1 mL), **C^{2A}.1b** (23 mg, 10 mol%) and around 20 mg of molecular sieves (4 beads, 4 Å). The mixture was stirred for 24 hours at 120 °C in an oil bath. The 46 % yield was determined by the ^{1}H NMR of an aliquot after evaporation and confirmed by GC and GC/MS analysis.

Third condition: 10 mol% **C^{2A}.1b**, molecular sieves, 20 mol% Me_3NO, 92 % yield.

In an argon filled glove box, a 15 mL Ace® pressure tube was charged with freshly distilled aniline (0.5 mmol, 53 µL), freshly distilled toluene (1 mL), freshly distilled MeOH (1 mL), Me_3NO (20 mol%, 8 mg), **C^{2A}.1b** (23 mg, 10 mol%) and around 20 mg of molecular sieves (4 beads, 4 Å). The mixture was stirred for 24 hours at 120 °C in an oil bath. The 92 % yield was determined by the ^{1}H NMR of an aliquot after evaporation and confirmed by GC and GC/MS analysis.

NMR data

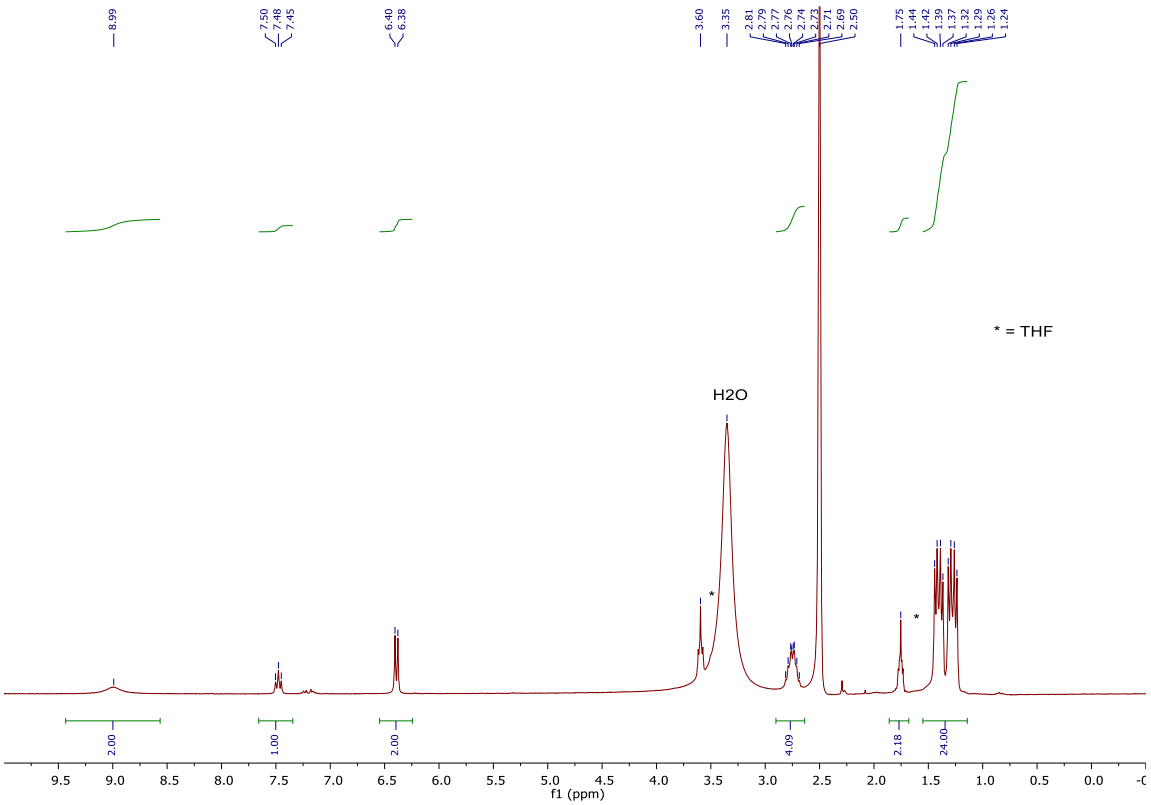

Figure S1: ^{1}H NMR spectrum of complex **C^{2A}.1** in DMSO-d_6 recorded at 300MHz.

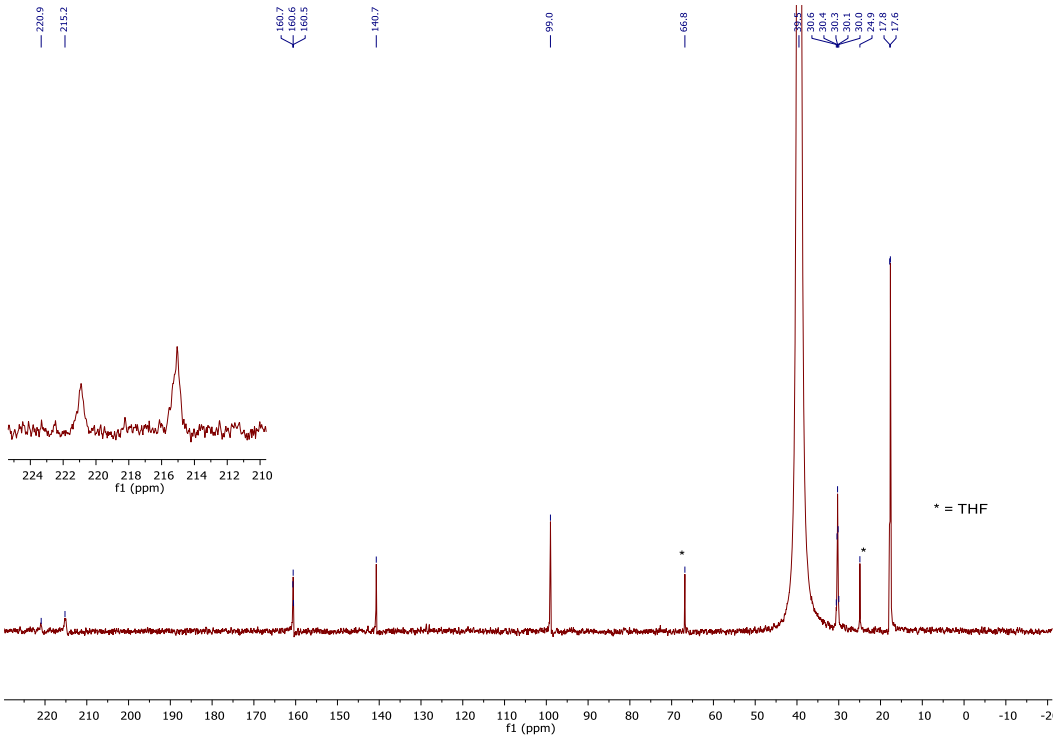

Figure S2: $^{13}C\{^{1}H\}$ NMR spectrum of complex **C^{2A}.1** in DMSO-d_6 recorded at 101 MHz.

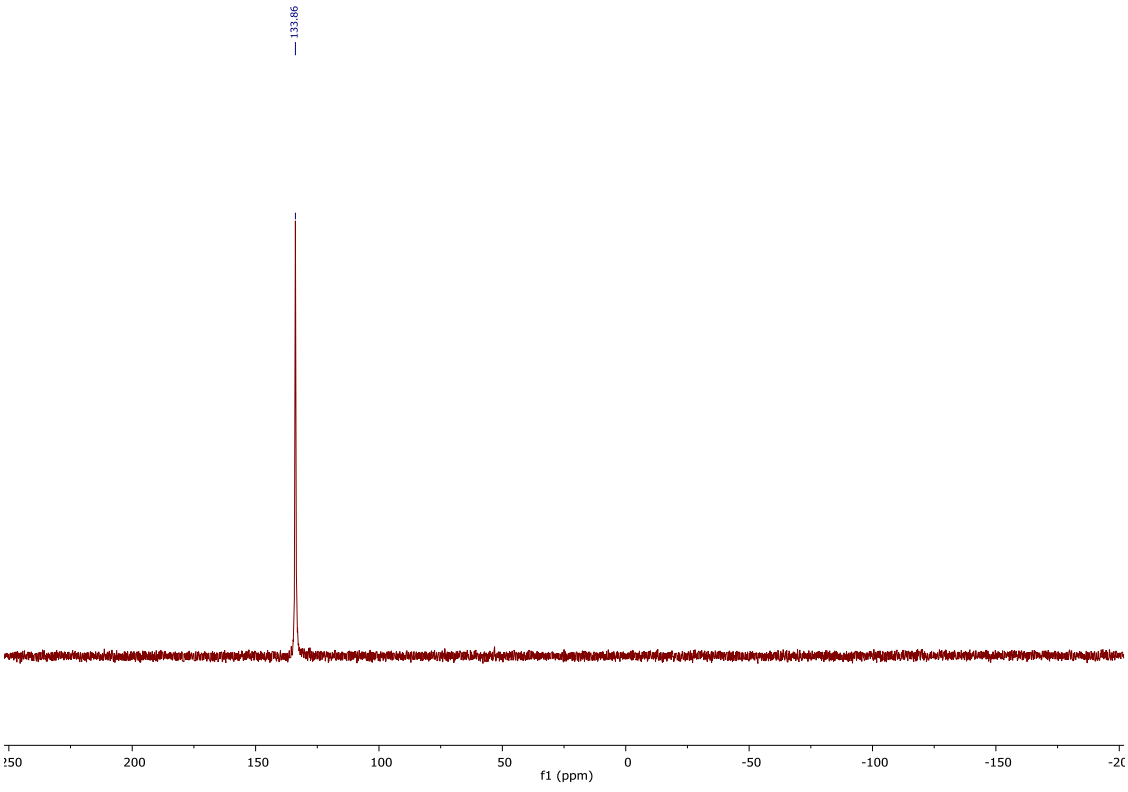

Figure S3: $^{31}P\{^{1}H\}$ NMR spectrum of complex **C^{2A}.1** in DMSO-d_6 recorded at 162 MHz.

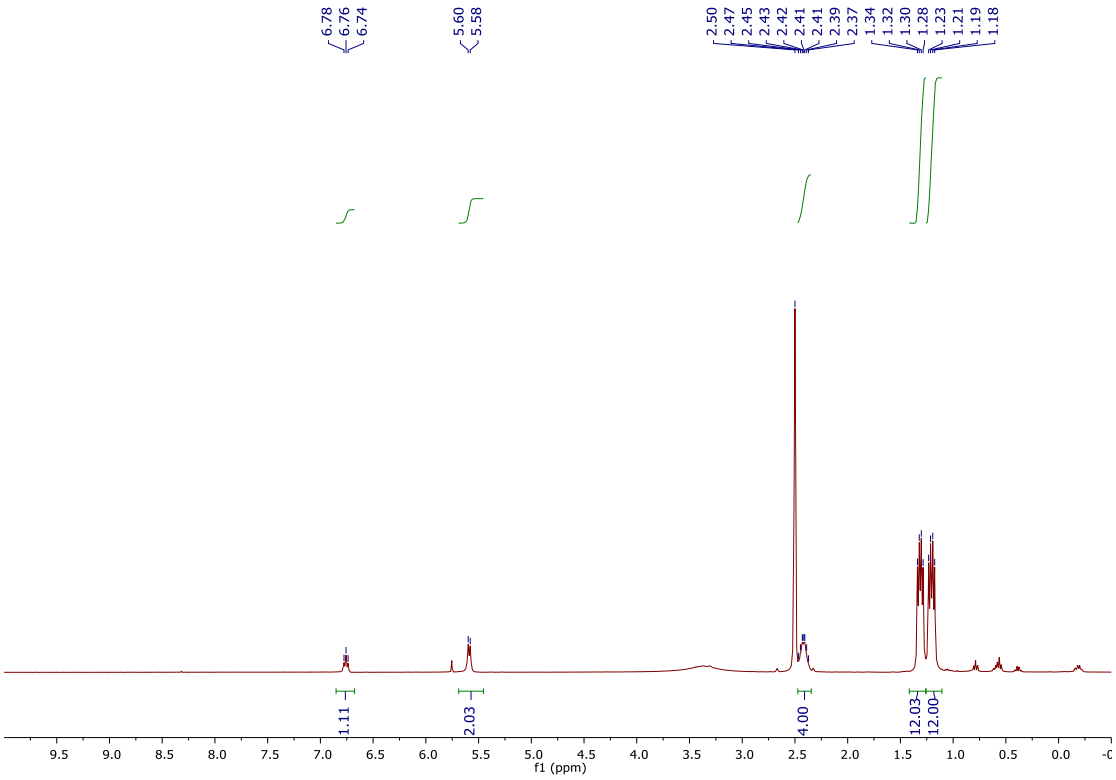

Figure S4: ^{1}H NMR spectrum of complex **C^{2A}.1b** in DMSO-d_6 recorded at 400 MHz.

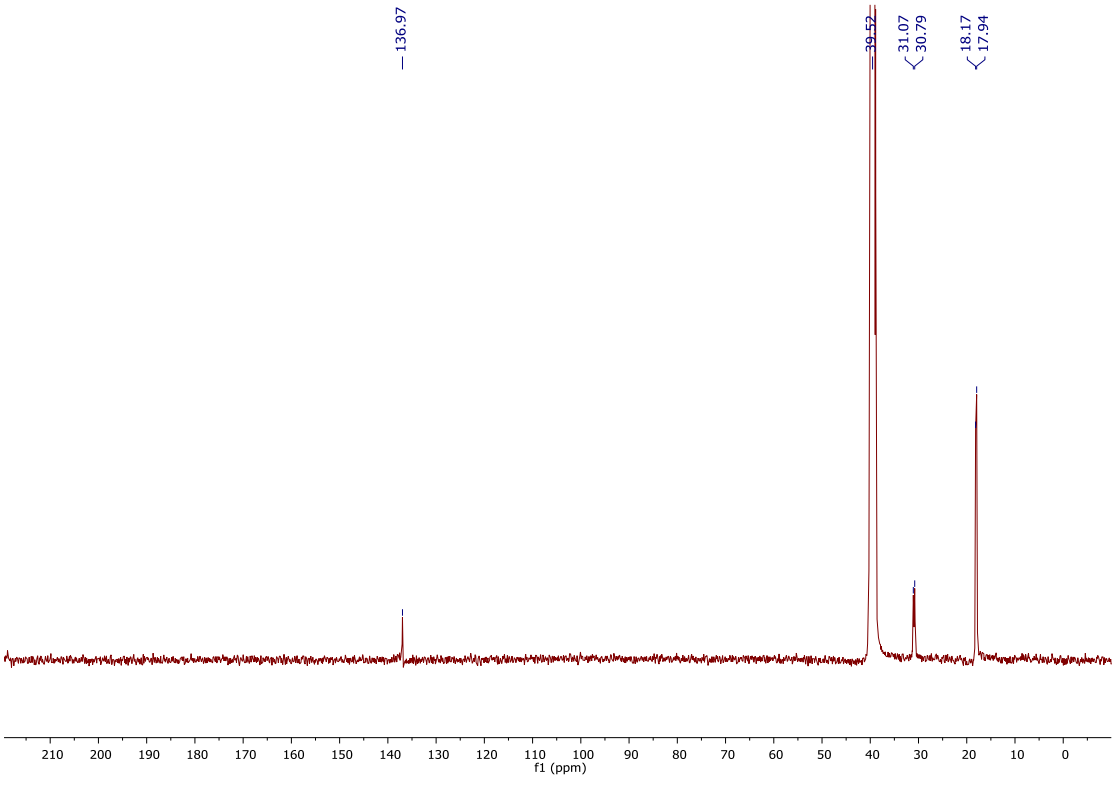

Figure S5: ^{13}C{^{1}H} NMR spectrum of complex **C^{2A}.1b** in DMSO-d_6 recorded at 101 MHz.

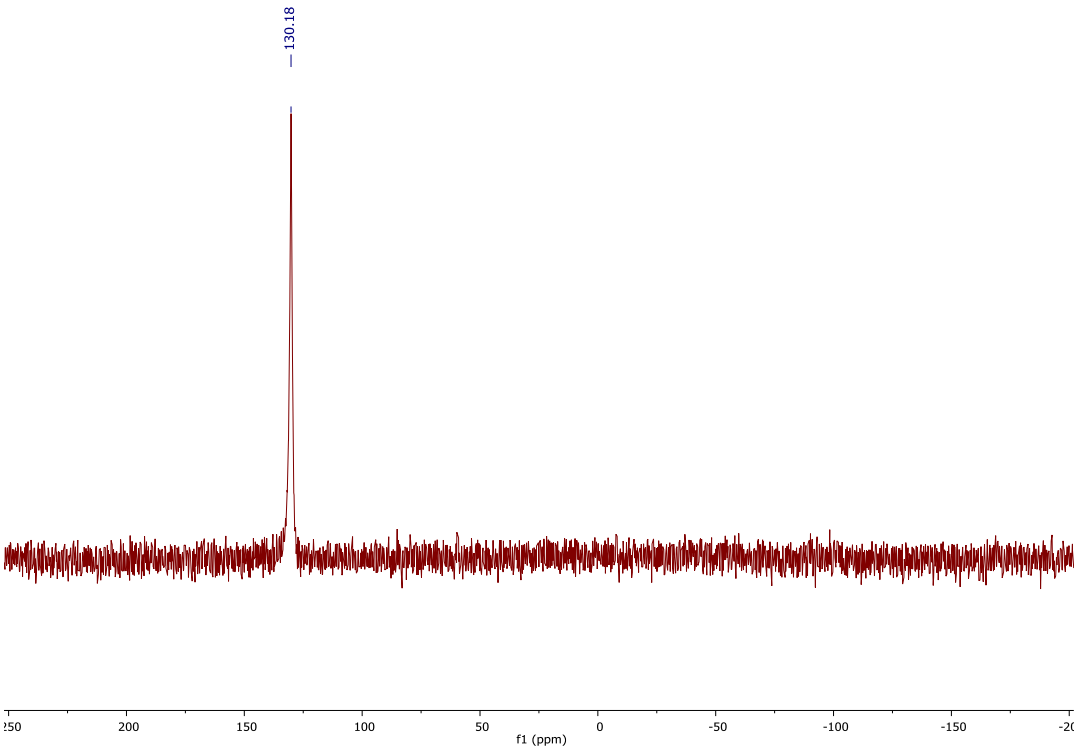

Figure S6: $^{31}P\{^{1}H\}$ NMR spectrum of complex **C^{2A}.1b** in DMSO-d_6 recorded at 162 MHz.

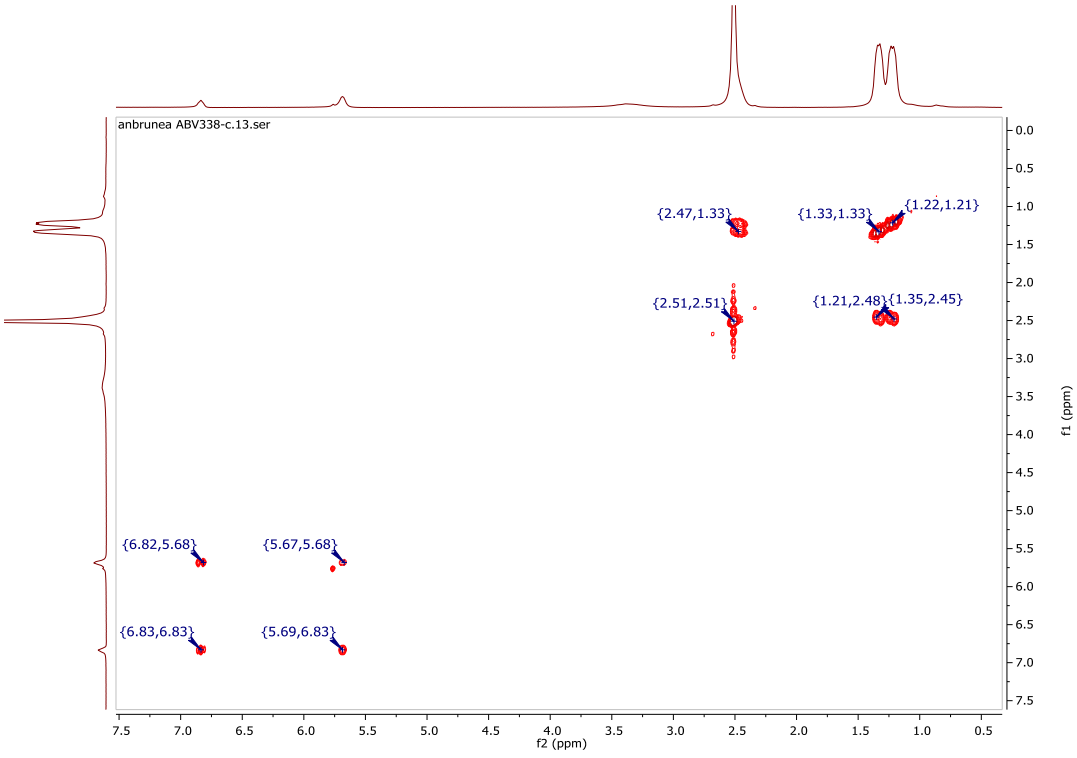

Figure S7: ^{1}H COSY NMR spectrum of complex **C^{2A}.1b** in DMSO-d_6 recorded at 400 MHz.

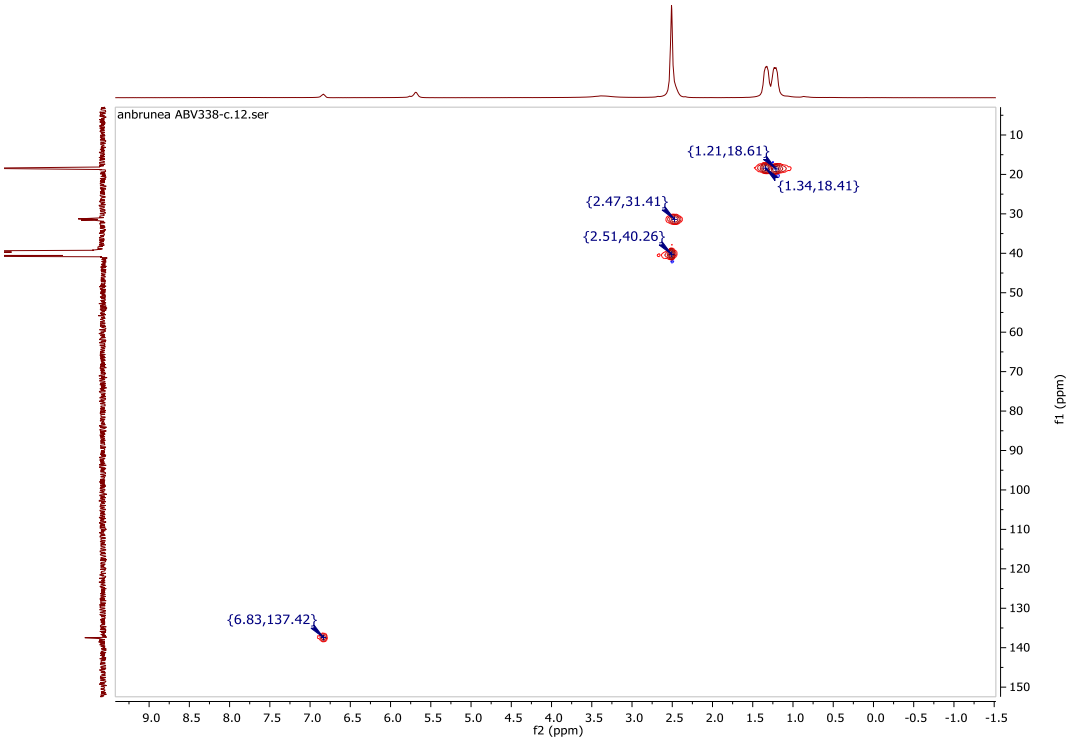

Figure S8: HSQC Edited NMR spectrum of complex **C^{2A}.1b** in DMSO-d_6 recorded at 400/101 MHz.

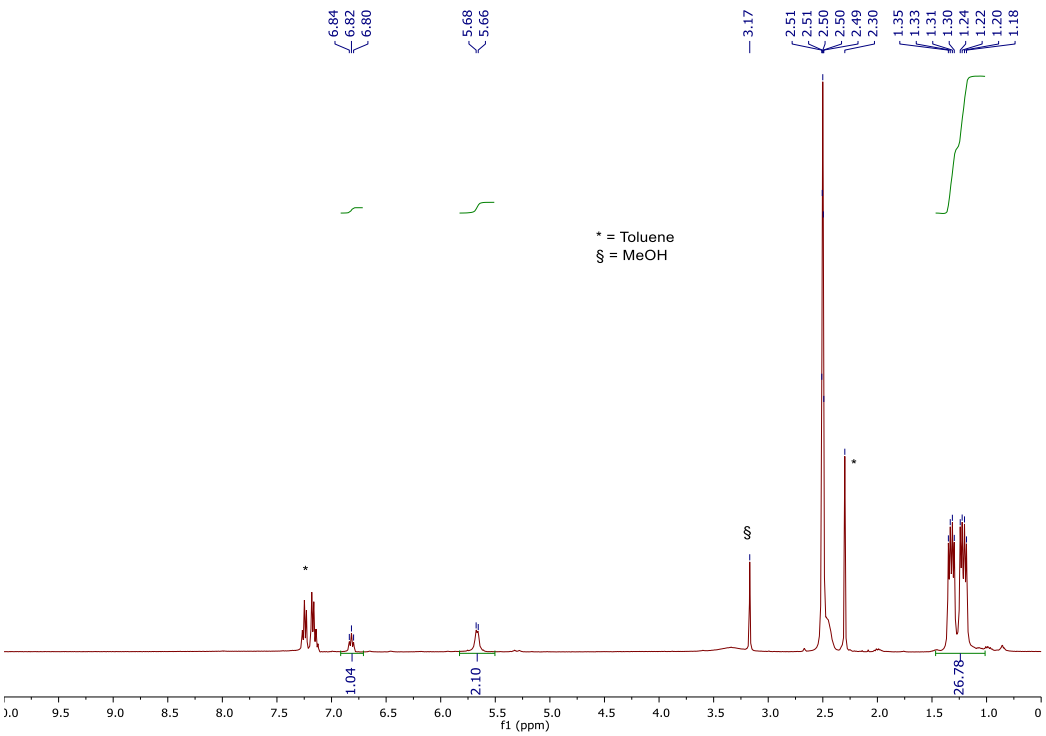

Figure S9: Crude ^{1}H NMR spectrum of the synthesis of complex **C^{2A}.1b** (**C^{2A}.1**+tBuOK in toluene/MeOH at r.t.) in DMSO-d_6 recorded at 400 MHz.

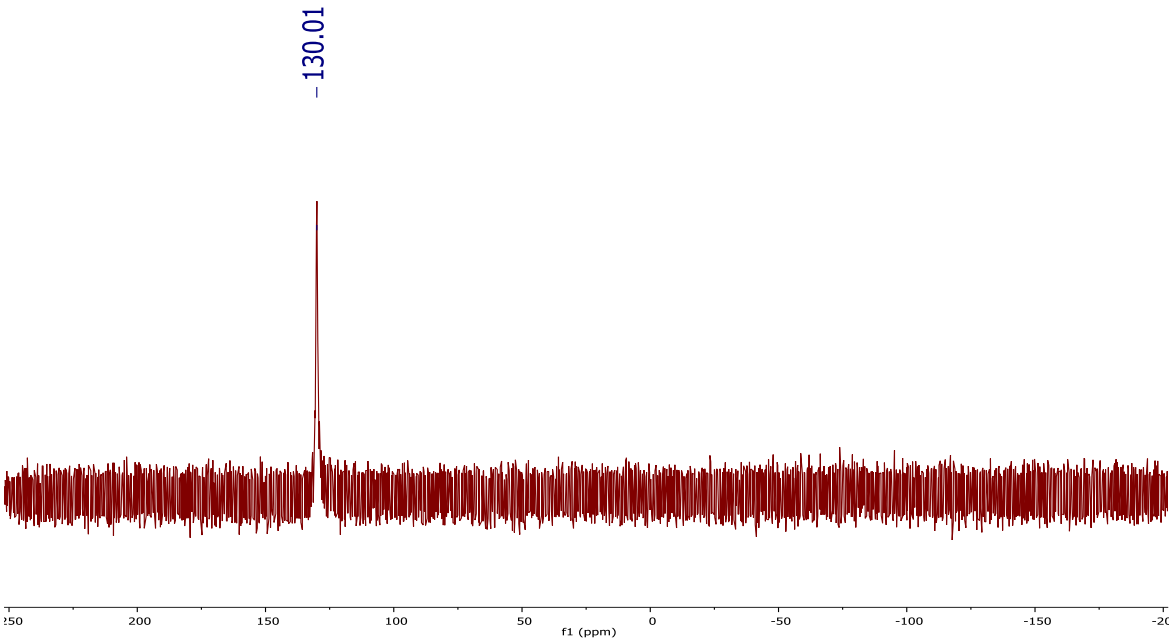

Figure S10: Crude $^{31}P\{^{1}H\}$ NMR spectrum of the synthesis of complex **C^{2A}.1b** (**C^{2A}.1**+tBuOK in toluene/MeOH at r.t.) in DMSO-d_6 recorded at 162 MHz.

X-ray data

Complex $\mathbf{C^{2A}.1}$

X-ray diffraction data were collected on a D8 VENTURE Bruker AXS diffractometer equipped with a PHOTON 100 CMOS detector, using multilayers monochromated Mo-Ka radiation (λ = 0.71073 Å) at T = 150(2) K. The structure was solved by direct methods using the *SHELXT* program,[10] and then refined with full-matrix least-square methods based on F^2 (*SHELXL-2014*).[11] All non-hydrogen atoms were refined with anisotropic atomic displacement parameters. Except nitrogen linked hydrogen atoms that were introduced in the structural model through Fourier difference maps analysis, H atoms were finally included in their calculated positions. A final refinement on F^2 with 12049 unique intensities and 609 parameters converged at $\omega R(F^2)$ = 0.0582 ($R(F)$ = 0.0274) for 10016 observed reflections with $I > 2\sigma(I)$.

Complete details of the X-ray analyses reported herein have been deposited at the Cambridge Crystallographic Data Center (CCDC 1503907).

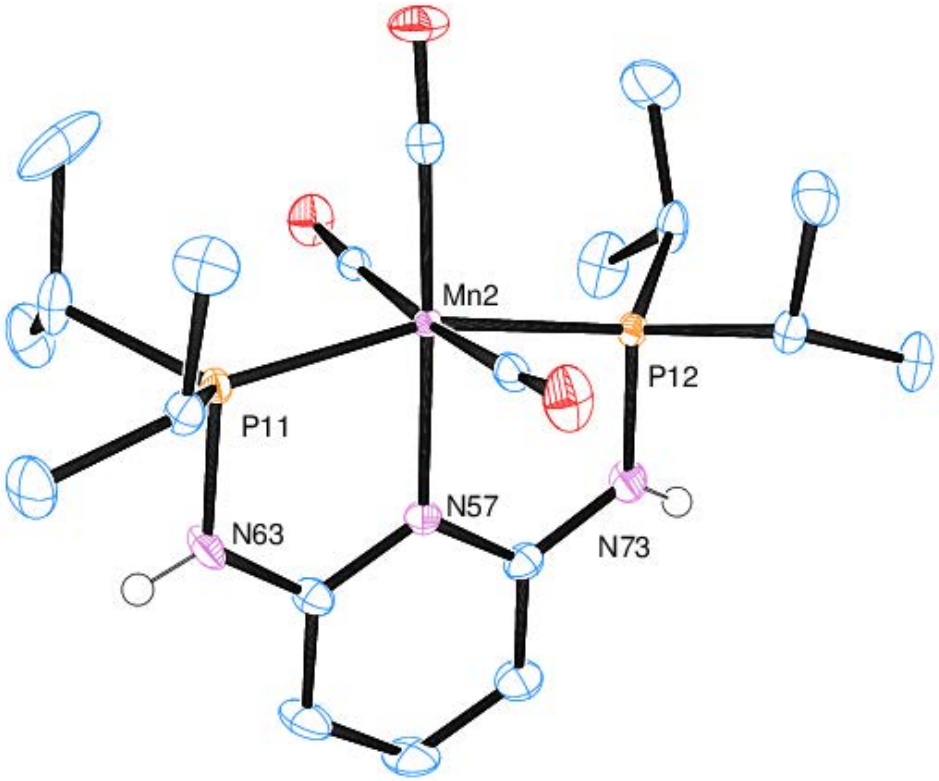

Figure S11: ORTEP view of the molecular structure of complex $\mathbf{C^{2A}.1}$ with thermal ellipsoids drawn at 50% probability. Hydrogens atoms, except the NH, bromide, and one molecule of MeOH were omitted for clarity. Only one of the two molecules of asymmetric unit is depicted.

Table S1. Crystal data and structure refinement for complex **C^{2A}.1**.

Empirical formula	$C_{42}\ H_{74}\ Br_2\ Mn_2\ N_6\ O_8\ P_4$
Extended formula	$2(C_{20}\ H_{33}\ Mn\ N_3\ O_3\ P_2)$, $2(C\ H_4\ O)$, 2(Br)
Formula weight	1184.65
Temperature	150 K
Wavelength	0.71073 Å
Crystal system, space group	Triclinic, P -1
Unit cell dimensions	a = 14.0483(10) Å, α = 90.219(2) °
	b = 14.1550(11) Å, β = 109.177(2) °
	c = 15.0726(9) Å, γ = 110.370(2) °
Volume	2630.1(3) $Å^3$
Z, Calculated density	2, 1.496 ($g.cm^{-3}$)
Absorption coefficient	2.174 mm-1
F(000)	1224
Crystal size	0.160 x 0.140 x 0.120 mm
Crystal color	colorless
Theta range for data collection	2.922 to 27.482 °
h_min, h_max	-17, 18
k_min, k_max	-18, 18
l_min, l_max	-19, 18
Reflections collected / unique	57617 / 12049 [R(int)[a] = 0.0488]
Reflections [I>2σ]	10016
Completeness to theta_max	0.999
Absorption correction type	multi-scan
Max. and min. transmission	0.770, 0.689
Refinement method	Full-matrix least-squares on F^2
Data / restraints / parameters	12049 / 0 / 609
[b]Goodness-of-fit	1.015
Final R indices [I>2σ]	R1[c] = 0.0274, wR2[d] = 0.0582
R indices (all data)	R1[c] = 0.0401, wR2[d] = 0.0629
Largest diff. peak and hole	0.630 and -0.463 e-.$Å^{-3}$

[a] $R_{int} = \sum |F_o^2 - \langle F_o^2 \rangle| / \sum [F_o^2]$

[b] $S = \{\sum [w(F_o^2 - F_c^2)^2] / (n - p)\}^{1/2}$

[c] $R1 = \sum ||F_o| - |F_c|| / \sum |F_o|$

[d] $wR2 = \{\sum [w(F_o^2 - F_c^2)^2] / \sum [w(F_o^2)^2]\}^{1/2}$

$w = 1 / [\sigma(F_o^2) + aP^2 + bP]$ where $P = [2F_c^2 + MAX(F_o^2, 0)] / 3$

Complex **C^{2A}.1b**

X-ray diffraction data were collected on an APEXII Bruker AXS diffractometer equipped with a PHOTON 100 CMOS detector, using multilayers monochromated Mo-Ka radiation (λ = 0.71073 Å) at T = 150K. The structure was solved by dual-space algorithm using the *SHELXT* program,[10] and then refined with full-matrix least-square methods based on F^2 (*SHELXL-2016*).[11] All non-hydrogen atoms were refined with anisotropic atomic displacement parameters. Except nitrogen hydrogen atom that was introduced in the structural model through Fourier difference maps analysis, H atoms were finally included in their calculated positions. A final refinement on F^2 with 6018 unique intensities and 313 parameters converged at $\omega R(F^2)$ = 0.0719 ($R(F)$ = 0.0287) for 5376 observed reflections with $I > 2\sigma(I)$.

Complete details of the X-ray analyses reported herein have been deposited at the Cambridge Crystallographic Data Center (CCDC 1522960).

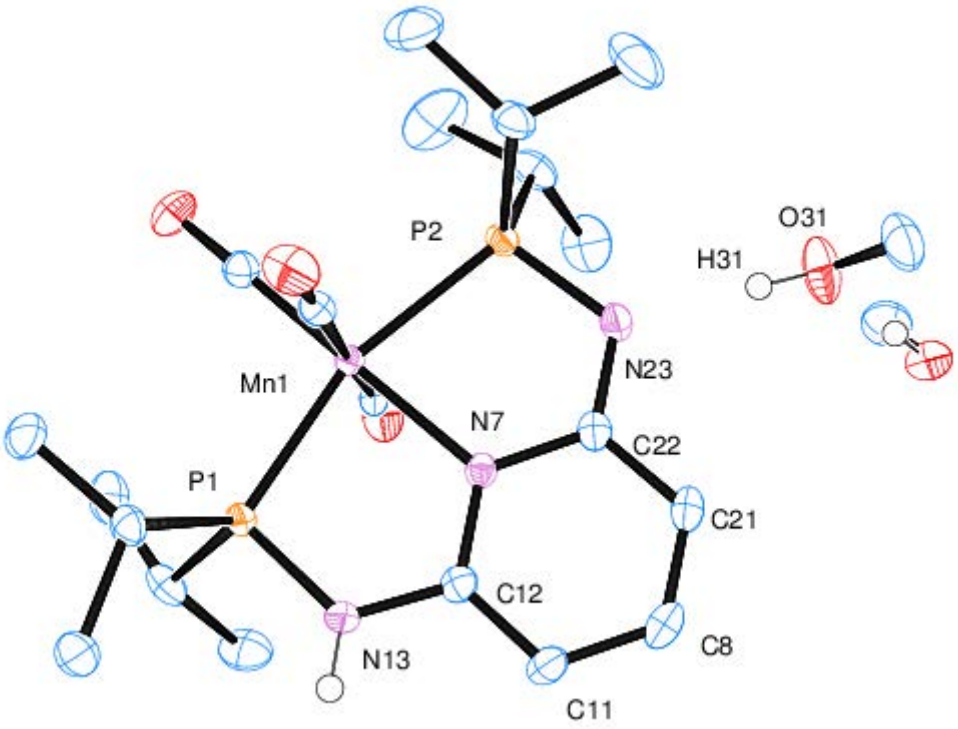

Figure S12: ORTEP view of the molecular structure of complex **C^{2A}.1b** with thermal ellipsoids drawn at 50% probability. Hydrogens atoms, except the NH, were omitted for clarity.

Table S2. Crystal data and structure refinement for complex **C^{2A}.1b**.

Empirical formula	C_{22} H_{40} Mn N_3 O_5 P_2
Extended formula	C_{20} H_{32} Mn N_3 O_3 P_2, 2(C H_4 O)
Formula weight	543.45
Temperature	150 K
Wavelength	0.71073 Å
Crystal system, space group	triclinic, P -1
Unit cell dimensions	a = 9.9276(8) Å, alpha = 105.414(3) °
	b = 10.0777(9) Å, beta = 103.210(3) °
	c = 14.3188(12) Å, gamma = 90.891(3) °
Volume	1340.0(2) $Å^3$
Z, Calculated density	2, 1.347 ($g.cm^{-3}$)
Absorption coefficient	0.648 mm^{-1}
F(000)	576
Crystal size	0.310 x 0.230 x 0.100 mm
Crystal color	colorless
Theta range for data collection	2.917 to 27.484 °
h_min, h_max	-12, 12
k_min, k_max	-8, 12
l_min, l_max	-18, 18
Reflections collected / unique	20311 / 6018 [R(int)[a] = 0.0219]
Reflections [I>2sigma(I)]	5376
Completeness to theta_max	0.981
Absorption correction type	multi-scan
Max. and min. transmission	0.937, 0.880
Refinement method	Full-matrix least-squares on F^2
Data / restraints / parameters	6018 / 0 / 313
[b]Goodness-of-fit	1.044
Final R indices [I>2sigma(I)]	$R1^c$ = 0.0287, $wR2^d$ = 0.0719
R indices (all data)	$R1^c$ = 0.0339, $wR2^d$ = 0.0752
Largest diff. peak and hole	0.422 and -0.269 $e^-.Å^{-3}$

$^a R_{int} = \sum |F_o^2 - \langle F_o^2 \rangle| / \sum [F_o^2]$

$^b S = \{\sum [w(F_o^2 - F_c^2)^2] / (n - p)\}^{1/2}$

$^c R1 = \sum ||F_o| - |F_c|| / \sum |F_o|$

$^d wR2 = \{\sum [w(F_o^2 - F_c^2)^2] / \sum [w(F_o^2)^2]\}^{1/2}$

$w = 1 / [\sigma(F_o^2) + aP^2 + bP]$ where $P = [2F_c^2 + MAX(F_o^2, 0)] /3$

References

[1] D. Benito-Garagorri, E. Becker, J. Wiedermann, W. Lackner, M. Pollak, K. Mereiter, J. Kisala, K. Kirchner, *Organometallics* **2006**, *25*, 1900-1913.
[2] A. M. Tondreau, J. M. Boncella, *Polyhedron* **2016**, *116*, 96-104.
[3] T. T. Dang, B. Ramalingam, A. M. Seayad, *ACS Catal.* **2015**, *5*, 4082-4088.
[4] Y. Imada, H. Iida, S. Ono, Y. Masui, S.-I. Murahashi *Chem. Asian J.* **2006**, *1*, 136-147.
[5] A. C. Kung, D. E. Falvey, *J. Org. Chem.* **2005**, *70*, 3127-3132.
[6] I. González, J. Mosquera, C. Guerrero, R. Rodríguez, J. Cruces, *Org. Lett.* **2009**, *11*, 1677-1680.
[7] A. R. Katritzky, K. S. Laurenzo, *J. Org. Chem.* **1988**, *53*, 3978-3982.
[8] V. Martínez-Barrasa, F. Delgado, C. Burgos, J. Luis García-Navío, M. Luisa Izquierdo, J. Alvarez-Builla, *Tetrahedron* **2000**, *56*, 2481-2490.
[9] O. Jacquet, C. Das Neves Gomes, M. Ephritikhine, T. Cantat, *ChemCatChem* **2013**, *5*, 117-120.
[10] G. M. Sheldrick, *Acta Cryst.* **2015**, *A71*, 3-8.
[11] G. M. Sheldrick, *Acta Cryst.* **2015**, *C71*, 3-8.

A – II- α-Methylation of carbonyl derivatives

Dihydrochalcones derivatives **c10-c15** were synthesized according to literature procedure.[1]

General procedure for α-methylation of ketones.

In an argon filled glove box, a 15 mL ACE® pressure tube was charged with ketone (0.5 mmol), MeOH (2 mL), toluene (4 mL), **C^{2A}.1** (3 mol%, 8.4 mg) and *t*BuONa (50 mol%, 24.0mg), in that order. The closed pressure tube was then heated at 120 °C for 20 h. After cooling to room temperature, the solution was diluted with ethyl acetate (2.0 mL) and filtered through a small pad of celite (2 cm in a Pasteur pipette). The celite was washed with ethyl acetate (2×2.0 mL). Yields were determined by analysis of ^{1}H NMR of the crude mixture and confirmed with GC/GC-Mass analysis. The crude residue was purified by column chromatography (SiO_2, mixture of petroleum ether/ethyl acetate as eluent, 90/10 for ketones, and 99/1 for esters).

Characterization of the products of the catalysis

Isobutyrophenone (d1) [2]

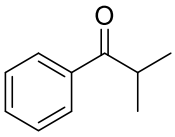

According to general procedure, propiophenone **c1** (66 µL, 0.5 mmol) gave the title compound **d1** as a colorless oil (47 mg, 64%).

Alternatively, according to general procedure, acetophenone **c2** (58 µL, 0.5 mmol) gave the title compound **d1** as a colorless oil (32 mg, 43%).

^{1}H NMR (400.1 MHz, $CDCl_3$) δ 7.99 – 7.91 (m, 2H), 7.61 – 7.51 (m, 1H), 7-48 - 7.46 (m, 2H), 3.56 (hept, *J* = 6.8 Hz, 1H), 1.22 (d, *J* = 6.8 Hz, 6H).

^{13}C {^{1}H} NMR (75.5 MHz, $CDCl_3$) δ 204.6, 136.3, 132.9, 128.7, 128.4, 35.4, 19.3.

2-Methyl-1-tetralone (d3) [2]

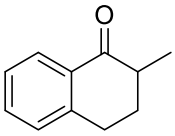

According to general procedure, 1-tetralone **a3** (67 µL, 0.5 mmol) gave the title compound **b3** as a colorless oil (30 mg, 38%).

^{1}H NMR (300.1 MHz, $CDCl_3$) δ 8.00 (d, *J* = 7.8 Hz, 1H), 7.42 (t, *J* = 7.2 Hz, 1H), 7.33 – 7.10 (m, 2H), 3.01-2.94 (m, 2H), 2.62-2.49 (m, 1H), 2.16 (dq, *J* = 13.2, 4.4 Hz, 1H), 2.00 – 1.67 (m, 1H), 1.24 (d, *J* = 6.7 Hz, 3H).

^{13}C {^{1}H} NMR (75.5 MHz, $CDCl_3$) δ 200.9, 144.3, 133.2, 132.5, 128.8, 127.5, 126.7, 42.8, 31.5, 29.0, 15.6.

2-Methyl-1-indanone (d4) [3]

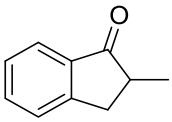

According to general procedure, 1-indanone **c4** (66 mg, 0.5 mmol) gave the title compound **d4** as a colorless oil (34 mg, 46%).

^{1}H NMR (300.1 MHz, $CDCl_3$) δ 7.74 (d, *J* = 7.4 Hz, 1H), 7.64 – 7.49 (m, 1H), 7.45 – 7.42 (m, 1H), 7.38 – 7.32 (m, 1H), 3.43 – 3.34 (m, 1H), 2.84 – 2.52 (m, 2H), 1.30 (d, *J* = 7.2 Hz, 3H).

^{13}C {^{1}H} NMR (75.5 MHz, $CDCl_3$) δ 209.5, 153.6, 136.5, 134.8, 127.4, 126.6, 124.1, 42.1, 35.1, 16.4.

2-Benzylidene-6-methylcyclohexanone (d5) [4]

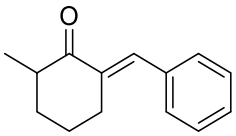

According to general procedure, 2-benzylidenecyclohexanone **c5** (93 mg, 0.5 mmol) gave the title compound **d5** as a white solid (51 mg, 51%).

^{1}H NMR (300.1 MHz, $CDCl_3$) δ 7.42 – 7.35 (m, 5H), 7.34 – 7.27 (m, 1H), 3.12 – 2.92 (m, 1H), 2.73-2.61 (m, 1H), 2.54 – 2.39 (m, 1H), 2.12-2.04 (m, 1H), 1.95-1.84 (m, 1H), 1.78 – 1.54 (m, 2H), 1.20 (d, *J* = 6.8 Hz, 3H).

^{13}C {^{1}H} NMR (101.6 MHz, $CDCl_3$) δ 204.9, 137.5, 136.0, 134.8, 130.2, 128.41, 128.41, 44.5, 32.1, 29.4, 23.1, 16.5.

2-Methyl-1-(2',4',6'-trimethylphenyl)- 1-propanone (d6)

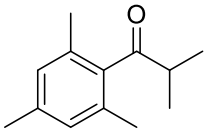

According to general procedure, 2'-4'-6' trimethylacetophenone **c6** (83 µL, 0.5 mmol) gave the title compound **d6** as a colorless oil (63 mg, 66%).

^{1}H NMR (400.1 MHz, $CDCl_3$) δ 6.84 (s, 2H), 2.98 (hept, *J* = 6.9 Hz, 1H), 2.28 (s, 3H), 2.19 (s, 6H), 1.17 (d, *J* = 6.9 Hz, 6H).

^{13}C {^{1}H} NMR (101.6 MHz, $CDCl_3$) δ 214.4, 139.2, 138.4, 133.4, 128.7, 42.4, 21.2, 19.8, 18.1.

LRMS (EI) m/z th for $C_{13}H_{18}O$ = 190. measured m/z (%) = 190 ([M]+, 3), 147 (100), 119 (30), 91 (9).

2-Methyl-1-(2'-methylphenyl)-1-propanone (d7) [5]

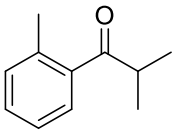

According to general procedure, 2'-methylacetophenone **c7** (65 µL, 0.5 mmol) gave the title compound **d7** as a colorless oil (57 mg, 71%).

^{1}H NMR (400.1 MHz, $CDCl_3$) δ 7.50 (dd, *J* = 7.9, 1.4 Hz, 1H), 7.34 (td, *J* = 7.5, 1.4 Hz, 1H), 7.28 – 7.10 (m, 2H), 3.34 (hept, *J* = 6.9 Hz, 1H), 2.42 (s, 3H), 1.17 (d, *J* = 6.9 Hz, 6H).

^{13}C {^{1}H} NMR (101.6 MHz, CDCl3) δ 209.4, 138.8, 137.5, 131.7, 130.7, 127.5, 125.6, 38.9, 20.9, 18.7.

1-(4'-Chlorophenyl)-2-methyl-1-propanone (d8) [3]

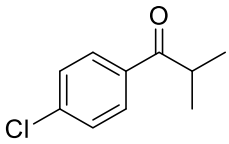

According to general procedure, 4'-chloroacetophenone **c8** (65 µL, 0.5 mmol) gave the title compound **d8** as a yellow oil (51 mg, 56%).

^{1}H NMR (400.1 MHz, $CDCl_3$) δ 7.89 (d, *J* = 8.4 Hz, 2H), 7.43 (d, *J* = 8.4 Hz, 2H), 3.49 (hept, *J* = 6.8 Hz, 1H), 1.21 (d, *J* = 6.8 Hz, 6H).

^{13}C {^{1}H} NMR (101.6 MHz, $CDCl_3$) δ 203.3, 139.3, 134.6, 129.9, 129.1, 35.6, 19.2.

1-(2'-Aminophenyl)-2-methyl-propan-1-one (d9) [6]

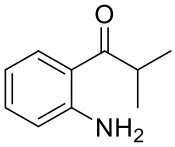

According to general procedure, 2'-aminoacetophenone **c9** (68 mg, 0.5 mmol) gave the title compound **d9** as a yellow oil (33 mg, 40%). The GC-MS of the crude mixture shows the presence of only **c9**, **d9** and the mono-methylated product 1-(2'-aminophenyl)-propan-1-oneb **d9'** (isolated in c.a. 15% yield).

^{1}H NMR (400.1 MHz, $CDCl_3$) δ 7.78-7.76 (m, 1H), 7.34 – 7.14 (m, 1H), 6.68-6.64 (m, 2H), 6.28 (br. s, 2H), 3.59 (hept, *J* = 6.8 Hz, 1H), 1.21 (d, *J* = 6.8 Hz, 6H).

^{13}C {^{1}H} NMR (101.6 MHz, $CDCl_3$) δ 207.2, 151.0, 134.2, 131.1, 117.7, 117.0, 115.9, 35.4, 19.8.

1-(2'-Aminophenyl)-propan-1-one (d9')

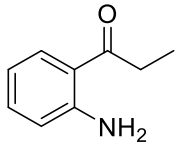

^{1}H NMR (300 MHz, $CDCl_3$) δ 7.86 – 7.70 (m, 1H), 7.36 – 7.12 (m, 1H), 6.70 – 6.59 (m, 2H), 6.26 (s, 2H), 2.97 (q, *J* = 7.3 Hz, 2H), 1.20 (t, *J* = 7.1 Hz 3H).

2-Methyl-1,3-diphenylpropan-1-one (d10) [3]

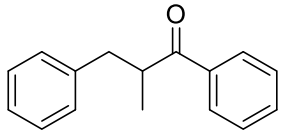

According to general procedure, 3-phenylpropiophenone **c10** (105 mg, 0.5 mmol) gave the title compound **d10** as a colorless oil (90 mg, 80%).

^{1}H NMR (400.1 MHz, $CDCl_3$) δ 7.94-7.91 (m, 2H), 7.60 – 7.49 (m, 1H), 7.48 – 7.40 (m, 2H), 7.29 – 7.23 (m, 2H), 7.22 – 7.13 (m, 3H), 3.84 – 3.71 (m, 1H), 3.17 (dd, *J* = 13.7, 6.3 Hz, 1H), 2.69 (dd, *J* = 13.7, 7.9 Hz, 1H), 1.20 (d, *J* = 6.9 Hz, 3H).

^{13}C {^{1}H} NMR (101.6 MHz, $CDCl_3$) δ 203.9, 140.1, 136.6, 133.1, 129.2, 128.8, 128.5, 128.4, 126.3, 42.9, 39.5, 17.5.

1-Mesityl-3-(4-methoxyphenyl)-2-methylpropan-1-one (d11)

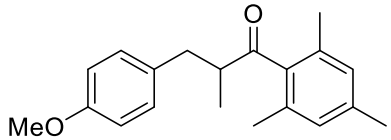

According to general procedure, 1-mesityl-3-(4-methoxyphenyl)propan-1-one **c11** (141 mg, 0.5 mmol) gave the title compound **d11** as a colorless oil (142 mg, 93%).

^{1}H NMR (400.1 MHz, $CDCl_3$) δ 7.10 (d, *J* = 8.6 Hz, 2H), 6.92 – 6.65 (m, 4H), 3.79 (s, 3H), 3.24 – 3.01 (m, 2H), 2.52 (dd, *J* = 13.3, 9.1 Hz, 1H), 2.28 (s, 3H), 2.17 (s, 6H), 1.08 (d, *J* = 6.9 Hz, 3H).

^{13}C {^{1}H} NMR (101.6 MHz, $CDCl_3$) δ 213.3, 158.2, 138.8, 138.6, 133.6, 132.1, 130.3, 128.9, 113.9, 55.4, 50.1, 37.2, 21.2, 19.8, 15.6.

LRMS (EI) m/z th for $C_{20}H_{24}O_2$ = 296. measured m/z (%) = 296 ([M]+, 23), 147 (100), 119 (36), 91 (18).

3-(4-(Benzyloxy)phenyl)-2-methyl-1-(4-methylphenyl)propan-1-one (d12)

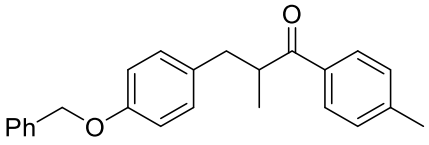

According to general procedure, 3-(4-(benzyloxy)phenyl)-1-(p-tolyl)propan-1-one **c12** (165 mg, 0.5 mmol) gave the title compound **d12** as a white solid (148 mg, 86%).

^{1}H NMR (400.1 MHz, $CDCl_3$) δ 7.88 (d, *J* = 8.2 Hz, 2H), 7.52 – 7.33 (m, 5H), 7.27 (d, *J* = 8.5 Hz, 2H), 7.15 (d, *J* = 8.6 Hz, 2H), 6.92 (d, *J* = 8.6 Hz, 2H), 5.05 (s, 2H), 3.95 – 3.47 (m, 1H), 3.15 (dd, *J* = 13.8, 6.3 Hz, 1H), 2.67 (dd, *J* = 13.8, 7.7 Hz, 1H), 2.43 (s, 3H), 1.23 (d, *J* = 6.9 Hz, 3H).

^{13}C {^{1}H} NMR (101.6 MHz, $CDCl_3$) δ 203.5, 157.3, 143.7, 137.2, 134.0, 132.5, 130.1, 129.4, 128.6, 128.5, 127.9, 127.5, 114.8, 70.1, 42.8, 38.7, 21.7, 17.5.

LRMS (EI) m/z th for $C_{24}H_{24}O_2$ = 344. measured m/z (%) = 344 ([M]+, 35), 119 (40), 91 (100), 65 (16).

1-Mesityl-2-methyl-3-(pyridin-2-yl)propan-1-one (d13)

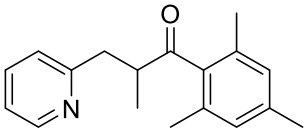

According to general procedure, 1-mesityl-3-(pyridin-2-yl)propan-1-one **c13** (125 mg, 0.5 mmol) gave the title compound **d13** as a colorless oil (68 mg, 51%).

^{1}H NMR (400.1 MHz, $CDCl_3$) δ 8.51 (d, *J* = 4.1 Hz, 1H), 7.56 (td, *J* = 7.7, 1.8 Hz, 1H), 7.20 (d, *J* = 7.8 Hz, 1H), 7.09 (ddd, *J* = 7.4, 4.9, 0.9 Hz, 1H), 6.79 (s, 2H), 3.61 – 3.46 (m, 1H), 3.35 (dd, *J* = 13.5, 6.0 Hz, 1H), 2.76 (dd, *J* = 13.5, 8.2 Hz, 1H), 2.25 (s, 3H), 2.13 (s, 6H), 1.12 (d, *J* = 7.1 Hz, 3H).

^{13}C {^{1}H} NMR (101.6 MHz, $CDCl_3$) δ 212.9, 160.0, 149.4, 138.50, 138.47, 136.3, 133.6, 128.8, 124.4, 121.3, 48.1, 40.2, 21.1, 19.7, 16.1.

LRMS (EI) m/z th for $C_{18}H_{21}NO$ = 267. measured m/z (%) = 267 ([M]+, 4), 147 (100), 120 (63), 93 (17).

3-(2-bromophenyl)-2-methyl-1-(p-tolyl)propan-1-one (d14)

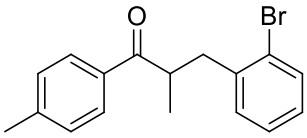

According to general procedure, 3-(2-bromophenyl)-1-(*p*-tolyl)propan-1-one **c14** (152 mg, 0.5 mmol) gave the title compound **d14** as a colorless oil (130 mg, 82%).

^{1}H NMR (400.1 MHz, $CDCl_3$) δ 7.89 – 7.81 (m, 2H), 7.52 (dd, *J* = 8.0, 1.3 Hz, 1H), 7.25 – 7.19 (m, 3H), 7.16 (td, *J* = 7.4, 1.3 Hz, 1H), 7.03 (ddd, *J* = 7.9, 7.2, 2.0 Hz, 1H), 3.93 (sex, *J* = 7.0 Hz, 1H), 3.24 (dd, *J* = 13.5, 6.9 Hz, 1H), 2.85 (dd, *J* = 13.6, 7.5 Hz, 1H), 2.39 (s, 3H), 1.20 (d, *J* = 7.0 Hz, 3H).

^{13}C {^{1}H} NMR (101.6 MHz, $CDCl_3$) δ 203.5, 143.9, 139.4, 134.1, 133.0, 132.1, 129.4, 128.6, 128.1, 127.4, 124.7, 40.3, 39.7, 21.7, 17.8.

LRMS (EI) m/z th for $C_{17}H_{17}BrO$ = 317. measured m/z (%) = 317 ([M]+, >1), 301 (3), 237 (55), 119 (100), 91 (46), 65 (12).

3-(2-Iodophenyl)-2-methyl-1-(*m*-tolyl)propan-1-one (d15)

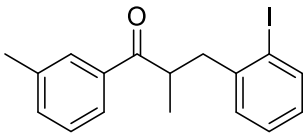

According to general procedure, 3-(2-iodophenyl)-1-(*m*-tolyl)propan-1-one **c15** (87 mg, 0.25 mmol) gave the title compound **d15** as a colorless oil (38 mg, 42%). The product is contaminated with 10% of the dehalogenated product according to ^{1}H NMR.

^{1}H NMR (400.1 MHz, $CDCl_3$) δ 7.81 (d, *J* = 7.7 Hz, 1H), 7.75 – 7.65 (m, 2H), 7.42 – 7.27 (m, 2H), 7.23 – 7.14 (m, 2H), 6.89-6.82 (m, 1H), 3.92 (h, *J* = 7.0 Hz, 1H), 3.25 (dd, *J* = 13.6, 7.2 Hz, 1H), 2.84 (dd, *J* = 13.6, 7.1 Hz, 1H), 2.38 (s, 3H), 1.22 (d, *J* = 6.9 Hz, 3H).

^{13}C {^{1}H} NMR (101.6 MHz, $CDCl_3$) δ 204.0, 142.7, 139.7, 138.5, 136.6, 133.9, 131.2, 129.1, 128.6, 128.3, 128.2, 125.7, 100.9, 43.8, 40.8, 21.5, 17.9.

LRMS (EI) m/z th for $C_{17}H_{17}IO$ = 364. measured m/z (%) = 364 ([M]+, >1), 349 (>1), 237 (39), 119 (100), 91 (46), 65 (9).

2-(Methyl-*d*$_3$)-2-*d*-1,3-diphenylpropan-1-one (d16)

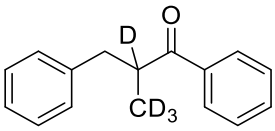

According to general procedure using CD_3OD instead of MeOH, 3-phenylpropiophenone **c10** (105 mg, 0.5 mmol) gave the title compound **d16** as a colorless oil (93 mg, 82%).

^{1}H NMR (400 MHz, $CDCl_3$) δ 7.92 (dd, *J* = 8.3, 1.4 Hz, 2H), 7.55 – 7.51 (m, 1H), 7.45 – 7.41 (m, 2H), 7.30 – 7.24 (m, 2H), 7.24 – 7.14 (m, 3H), 3.18 (d, *J* = 13.7 Hz, 1H), 2.71 (d, *J* = 13.7 Hz, 1H).

^{13}C {^{1}H} NMR (101 MHz, $CDCl_3$) δ 203.8, 140.0, 136.5, 133.0, 129.1, 128.7, 128.4, 128.3, 126.3, 42.2 (t, *J* = 19.2 Hz), 39.3, 16.6 (hept, *J* = 19.2 Hz). (One additional signal is present at 42.6 ppm belonging to the same compound with a proton at the carbon C*H*(CD_3)).

LRMS (EI) m/z th for $C_{16}H_{12}D_4O$ = 228. measured m/z (%) = 228 ([M]+, 33), 105 (100), 91 (12), 77 (32).

Methyl 2-phenylpropanoate (d17)

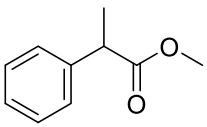

According to general procedure, methyl 2-phenylacetate **c17** (88 µL, 0.5 mmol) gave the title compound **d17** (95% conversion).

^{1}H NMR (400 MHz, $CDCl_3$) δ 7.38 – 7.21 (m, 5H), 3.73 (q, *J* = 7.2 Hz, 1H), 3.66 (s, 3H), 1.50 (d, *J* = 7.2 Hz, 3H).

Methyl 2-(naphthalen-1-yl)propanoate (d18) [7]

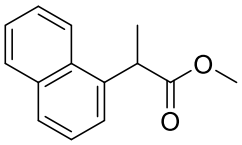

According to general procedure, methyl 2-(naphthalen-1-yl)acetate **c18** (88 µL, 0.5 mmol) gave the title compound **d18** as a colorless oil (33 mg, 31%).

^{1}H NMR (300.1 MHz, $CDCl_3$) δ 8.09 (d, = 8.3 Hz, 1H), 7.89-7.86 (m, 1H), 7.83 – 7.75 (m, 1H), 7.61 – 7.45 (m, 4H), 4.52 (q, *J* = 7.1 Hz, 1H), 3.66 (s, 3H), 1.67 (d, *J* = 7.1 Hz, 3H).

^{13}C {^{1}H} NMR (75.5 MHz, $CDCl_3$) δ 175.6, 136.9, 134.1, 131.4, 129.1, 127.9, 126.5, 125.8, 125.7, 124.6, 123.2, 52.3, 41.5, 18.4.

Methyl 2-(naphthalen-2-yl)propanoate (d19) [8]

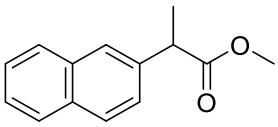

According to general procedure (using 50 mol% *t*BuONa), methyl 2-(naphthalen-2-yl)acetate **c19** (88 µL, 0.5 mmol) gave the title compound **d19** as a colorless oil (40 mg, 37%).

^{1}H NMR (400 MHz, $CDCl_3$) δ 7.89 – 7.78 (m, 3H), 7.77 – 7.72 (m, 1H), 7.49-7.43 (m, 3H), 3.91 (q, *J* = 7.1 Hz, 1H), 3.68 (s, 3H), 1.61 (d, *J* = 7.1 Hz, 3H).

^{13}C NMR (101 MHz, $CDCl_3$) δ 175.1, 138.1, 133.6, 132.7, 128.5, 127.9, 127.7, 126.29, 126.25, 125.9, 125.8, 52.2, 45.7, 18.7.

Methyl 2-(4-bromophenyl)propanoate (d20) [8]

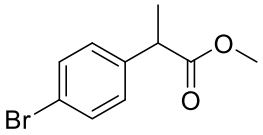

According to general procedure, methyl 2-(4-bromophenyl)acetate **c20** (114 mg, 0.5 mmol) gave the title compound **d20** as a colorless oil (43 mg, 35%).

^{1}H NMR (300.1 MHz, $CDCl_3$) δ 7.44 (d, *J* = 8.5 Hz, 2H), 7.18 (d, *J* = 8.5 Hz, 2H), 3.69 (q, *J* = 7.2 Hz, 1H), 3.66 (s, 3H), 1.48 (d, *J* = 7.2 Hz, 3H).

^{13}C {^{1}H} NMR (75.5 MHz, $CDCl_3$) δ 174.6, 139.6, 131.9, 129.4, 121.2, 52.3, 45.0, 18.6.

Methyl-*d_3* 2-(naphthalen-2-yl)-2,3,3,3-*d_4*-propanoate (d21)

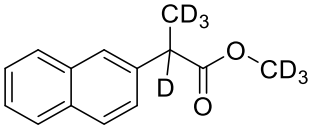

According to general procedure using CD_3OD, methyl 2-(naphthalen-2-yl)acetate **c19** (88 µL, 0.5 mmol) gave the title compound **d21** as a colorless oil (22 mg, 20%).

^{1}H NMR (400 MHz, $CDCl_3$) δ 7.87 – 7.77 (m, 3H), 7.79-7.74 (m, 1H), 7.48 – 7.33 (m, 3H).

^{13}C NMR (101 MHz, $CDCl_3$) δ 175.1, 138.0, 133.6, 132.7, 128.5, 127.9, 127.8, 126.3, 126.3, 126.0, 125.8.

LRMS (EI) m/z th for $C_{14}H_7D_7O_2$ = 221. measured m/z (%) = 221 ([M]+, 54), 159 (100), 129 (10).

2,4-dimethyl-1,5-diphenylpentane-1,5-dione (e1) [2]

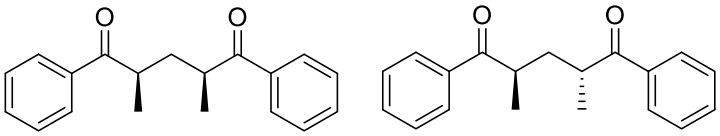

According to an alternative procedure, an ACE® pressure tube was charged with propiophenone **c1** (66 µL, 0.5 mmol), MeOH (0.5 mL), toluene (0.5 mL), Mn-complex **C^{2A}.1** (3 mol%, 8 mg) and, *t*BuONa (1 equiv., 48 mg), in that order. The same work up gave the title compound **e1**, obtained as a mixture of two diastereoisomers, as a colorless oil (44 mg, 63%).

^{1}H NMR (300 MHz, $CDCl_3$) δ 8.11 – 7.97 (m, 4H), 7.81 – 7.75 (m, 4H), 7.62 – 7.42 (m, 8H), 7.38 – 7.28 (m, 4H), 3.63 (h, *J* = 7.0 Hz, 2H), 3.50 (h, 7.0 Hz, 2H), 2.44 (dt, *J* = 13.7, 7.2 Hz, 1H), 2.01 (t, *J* = 7.1 Hz, 2H), 1.49 (dt, *J* = 13.9, 7.1 Hz, 1H), 1.21 (d, *J* = 7.0 Hz, 6H), 1.17 (d, *J* = 6.9 Hz, 6H).

^{13}C NMR (75 MHz, $CDCl_3$) δ 204.5, 203.9, 136.6, 136.4, 133.2, 133.1, 128.9, 128.7, 128.6, 128.3, 38.7, 38.2, 37.4, 37.1, 18.8, 17.7.

LRMS (EI) m/z th for $C_{19}H_{20}O_2$ = 280. m/z measured = 280 ([M]+, 10), 134 (73), 105 (100), 77 (54), 51 (7).

2,2'-Methyleneditetralone (e3)

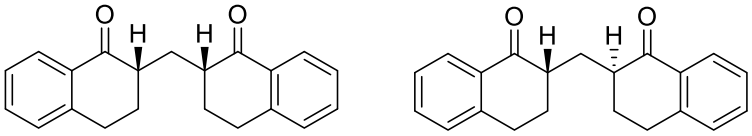

According to an alternative procedure, an ACE® pressure tube was charged with 1-tetralone **c3** (268 µL, 2 mmol), MeOH (1mL), toluene (1mL), Mn-complex **C^{2A}.1** (1.5 mol%, 16 mg) and, NaOH (1 equiv., 80 mg), in that order. The same work up gave the title compound **e3,** obtained as a mixture of the two diastereoisomers (ratio 1:1), as a colorless oil (116 mg, 38%).

^{1}H NMR (400.1 MHz, $CDCl_3$) δ 8.01 (dt, *J* = 7.9, 1.7 Hz, 4H), 7.46 (tt, *J* = 7.5, 1.5 Hz, 4H), 7.33 – 7.27 (m, 4H), 7.24 (m, 4H), 3.05 (m, 8H), 2.88 – 2.75 (m, 4H), 2.74-2.96 (m, 1H), 2.33 (m, 4H), 2.04 (t, *J* = 6.6 Hz, 2H), 1.94 (m, 4H), 1.63-1.56 (m, 1H).

^{13}C{^{1}H} NMR (101.6 MHz, $CDCl_3$) δ 201.0, 200. 5, 144.1, 144.0, 133.35, 133.34, 132.7, 132.6, 128.9 (2C), 127.6, 127.5, 126.7 (2C), 46.0 45.0, 31.0, 30.1, 29.5, 29.3, 28.7, 28.6.

LRMS (EI) m/z th for $C_{21}H_{20}O_2$ = 304. m/z measured = 304 ([M]+, 5), 286 (3), 159(10), 146 (100), 131 (20), 90 (12).

References

[1] Q. Xu, J. Chen, H. Tian, X. Yuan, S. Li, C. Zhou, J. Liu, *Angew. Chem. Int. Ed.*, **2014**, *53*, 225-229.
[2] C. B. Reddy, R. Bharti, S. Kumar, P. Das, *ACS Sustainable Chem. Eng.*, **2017**, *5*, 9683-9691.
[3] T. T. Dang, A. M. Seayad, *Adv. Synth. Catal.*, **2016**, *358*, 3373-3380.
[4] N. G. Kozlov, L. I. Basalaeva, *Russ. J. Org. Chem.*, **2009**, *45*, 587-590.
[5] M. Jean, J. Renault, P. van de Weghe, *Tetrahedron Lett.*, **2009**, *50*, 6546-6548.
[6] A. Boelke, L. D. Caspers and B. J. Nachtsheim, *Org. Lett.*, **2017**, *19*, 5344-5347.
[7] M. Noji, H. Sunahara, K.-i. Tsuchiya, T. Mukai, A. Komasaka, K. Ishii, *Synthesis*, **2008**, 3835-3845.
[8] D. B. Nielsen, B. A. Wahlqvist, D. U. Nielsen, K. Daasbjerg , T. Skrydstrup, *ACS Catal.*, **2017**, *7*, 6089-6093.

B- I- Hydrogenation of ketones with PN3P Mn C^{2A}.1

Non-stirred Parr autoclaves (22 mL) were used for the hydrogenation reactions.

General procedure for hydrogenation reactions

In an argon filled glove box, an autoclave was charged with the desired ketone (0.5 mmol), toluene (2 mL), Mn complex **C^{2A}.1** (14 mg, 5 mol%) followed by *t*BuOK (5.6 mg, 10 mol%), in this order. The autoclave is then closed and charged with H_2 (50 bar) out of the glovebox. The mixture was stirred for 20 hours at 130 °C in an oil bath. The solution was then diluted with ethyl acetate and filtered through a small pad of silica (2 cm in a Pasteur pipette). The silica was washed with ethyl acetate. The filtrate was evaporated and the crude residue was purified by column chromatography (SiO_2, mixture of petroleum ether/ethyl acetate or diethyl ether as eluent).

Characterization of the hydrogenated products

1-Phenylethanol (b1)

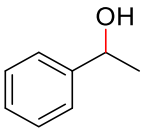

According to general procedure, acetophenone (58 µL, 0.5 mmol) gave the title compound **b1** as a colourless oil (56 mg, 92%).
^{1}H NMR (400 MHz, $CDCl_3$) δ 7.63 – 7.08 (m, 5H), 4.92 (q, *J* = 6.4 Hz, 1H), 2.02 (s, 1H), 1.52 (d, *J* = 6.4 Hz, 3H).
$^{13}C\{^1H\}$ NMR (101 MHz, $CDCl_3$) δ 145.9, 128.6, 127.6, 125.5, 70.5, 25.2.

1-(4-Methoxyphenyl)ethanol (b2)

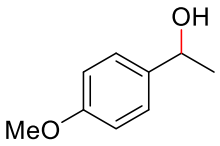

According to general procedure, 4-methoxyacetophenone (75 mg, 0.5 mmol) gave the title compound **b2** as a colourless oil (56 mg, 74%).
^{1}H NMR (400 MHz, $CDCl_3$) δ 7.28 (d, *J* = 8.6 Hz, 2H), 6.87 (d, *J* = 8.6 Hz, 2H), 4.82 (q, *J* = 6.4 Hz, 1H), 3.79 (s, 3H), 2.18 (s, 1H), 1.46 (d, *J* = 6.4 Hz, 3H).
^{13}C{^{1}H} NMR (101 MHz, $CDCl_3$) δ 159.0, 138.1, 126.7, 113.9, 70.0, 55.3, 25.1.

1-(4-Methylphenyl)ethanol (b3)

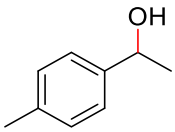

According to general procedure, 4-methylacetophenone (67 µL, 0.5 mmol) gave the title compound **b3** as a colourless oil (35 mg, 52%).
^{1}H NMR (400 MHz,$CDCl_3$) δ 7.27 (d, *J* = 7.9 Hz, 2H), 7.17 (d, *J* = 7.9 Hz, 2H), 4.86 (q, *J* = 6.5 Hz, 1H), 2.36 (s, 3H), 1.99 (s, 1H), 1.49 (d, *J* = 6.5 Hz, 3H).
^{13}C{^{1}H} NMR (101 MHz, $CDCl_3$) δ 143.0, 137.2, 129.3, 125.5, 70.3, 25.2, 21.2.

1-(2-Methylphenyl)ethanol (b4)

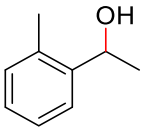

According to general procedure, 2-methylacetophenone (66 µL, 0.5 mmol) gave the title compound **b4** as a colourless oil (35 mg, 52%).
^{1}H NMR (400 MHz, $CDCl_3$) δ 7.52 (d, *J* = 7.6 Hz, 1H), 7.37 – 7.01 (m, 3H), 5.13 (q, *J* = 6.4 Hz, 1H), 2.35 (s, 3H), 1.90 (s, 1H), 1.47 (d, *J* = 6.4 Hz, 3H).
^{13}C{^{1}H} NMR (101 MHz, $CDCl_3$) δ 143.9, 134.3, 130.5, 127.3, 126.5, 124.6, 66.9, 24.0, 19.0.

1-(4-bromophenyl)ethanol (b7)

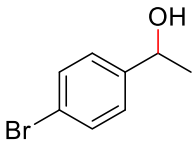

According to general procedure, 4-bromoacetophenone (99 mg, 0.5 mmol) gave the title compound **b7** as an oil (76 mg, 98%).
^{1}H NMR (400 MHz, $CDCl_3$) δ 7.46 (d, *J* = 8.4 Hz, 2H), 7.23 (d, *J* = 8.4 Hz, 2H), 4.84 (q, *J* = 6.5 Hz, 1H), 2.10 (s, 1H), 1.45 (d, *J* = 6.5 Hz, 3H).
^{13}C{^{1}H} NMR (101 MHz, $CDCl_3$) δ 144.9, 131.6, 127.2, 121.2, 69.8, 25.3.

1-(4-Trifluoromethylphenyl)ethanol (b9)

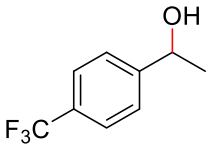

According to general procedure, 4-trifluoromethylacetophenone (103 µL, 0.5 mmol) gave the title compound **b9** as a colourless oil (91 mg, 95%).

^{1}H NMR (400 MHz, $CDCl_3$) δ 7.58 (d, *J* = 8.2 Hz, 2H), 7.45 (d, *J* = 8.2 Hz, 2H), 4.91 (q, *J* = 6.5 Hz, 1H), 2.52 (s, 1H), 1.47 (d, *J* = 6.5 Hz, 3H).
^{13}C{^{1}H} NMR (101 MHz, $CDCl_3$) δ 149.8, 129.7 (q, *J* = 32.4 Hz), 125.8, 125.5 (q, *J* = 3.7 Hz), 124.3 (q, *J* = 271.9 Hz), 69.9, 25.4.
^{19}F NMR (376 MHz, $CDCl_3$) δ -62.49.

1-(4-Bromophenyl)-2,2,2-trifluoroethanol (b10)

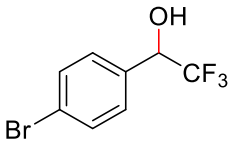

According to general procedure, 4-bromo-α,α,α-trifluoroacetophenone (126 mg, 0.5 mmol) gave the title compound **b10** as a colourless oil (104 mg, 81%).
^{1}H NMR (300 MHz, $CDCl_3$) δ 7.55 (d, *J* = 7.7 Hz, 2H), 7.36 (d, *J* = 7.7 Hz, 2H), 5.01 (s, 1H), 2.81 (s, 1H).
^{19}F NMR (376 MHz, $CDCl_3$) δ -78.51.
^{13}C{^{1}H} NMR (101 MHz, $CDCl_3$) δ 133.0, 131.9, 129.2, 124.1 (q, *J* = 282.1 Hz), 123.9, 72.4 (q, *J* = 32.5 Hz).

1-(4-Aminophenyl)ethanol (b11)

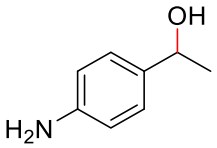

According to general procedure, 4-aminoacetophenone (68 mg, 0.5 mmol) gave the title compound **b11** as a brown oil (53 mg, 77%).

^{1}H NMR (400 MHz, $CDCl_3$) δ 7.16 (d, *J* = 8.0 Hz, 2H), 6.65 (d, *J* = 8.0 Hz, 2H), 4.79 (q, *J* = 6.1 Hz, 1H), 3.56 (br. s, 2H), 1.46 (d, *J* = 6.1 Hz, 3H).
^{13}C{^{1}H} NMR (101 MHz, $CDCl_3$) δ 145.9, 136.1, 126.7, 115.2, 70.2, 24.9.

1-(2-naphthyl)ethanol (b13)

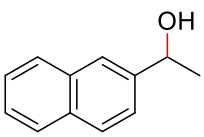

According to general procedure, 2'-acetonaphthone (85 mg, 0.5 mmol) gave the title compound **b13** as a white solid (64 mg, 72%).

^{1}H NMR (400 MHz, $CDCl_3$) δ 7.97 – 7.70 (m, 4H), 7.61 – 7.38 (m, 3H), 5.04 (q, *J* = 6.4 Hz, 1H), 2.23 (s, 1H), 1.58 (d, *J* = 6.4 Hz, 3H).
^{13}C{^{1}H} NMR (101 MHz, $CDCl_3$) δ 143.3, 133.4, 132.9, 128.3, 128.0, 127.7, 126.2, 125.8, 123.9, 123.8, 70.5, 25.2.

4-Phenyl-butan-2-ol (b14)

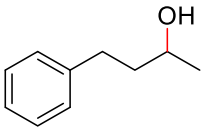

According to general procedure, 4-phenylbutan-2-one (75 µL, 0.5 mmol) gave the title compound **b14** as a colourless oil (65 mg, 87%).
^{1}H NMR (400 MHz, $CDCl_3$) δ 7.60 – 6.96 (m, 5H), 3.84 (m, 1H), 2.90 – 2.55 (m, 2H), 1.91 – 1.74 (m, 2H), 1.74 (s, 1H), 1.24 (d, *J* = 6.2 Hz, 3H).
^{13}C{^{1}H} NMR (101 MHz, $CDCl_3$) δ 142.2, 128.5, 125.9, 67.6, 40.9, 32.2, 23.7.

Cycloheptanol (b16)

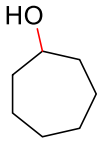

According to general procedure, cycloheptanone (59 µL, 0.5 mmol) gave the title compound **b16** as a colourless oil (41 mg, 71%).

^{1}H NMR (400 MHz, $CDCl_3$) δ 3.86-3.80 (m, 1H), 1.98 – 1.80 (m, 2H), 1.74 – 1.46 (m, 9H), 1.46 – 1.31 (m, 2H).
^{13}C{^{1}H} NMR (101 MHz, $CDCl_3$) δ 72.9, 37.7, 28.2, 22.7.

Undecan-2-ol (b17)

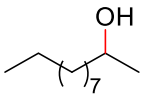

According to general procedure, undecan-2-one (103 µL, 0.5 mmol) gave the title compound **b17** as a yellow oil (72 mg, 83%).
^{1}H NMR (400 MHz, $CDCl_3$) δ 3.77 (m, 1H), 1.59 – 1.03 (m, 20H), 0.87 (t, *J* = 6.8 Hz, 3H).
^{13}C{^{1}H} NMR (101 MHz, $CDCl_3$) δ 68.3, 39.5, 32.0, 29.8, 29.8, 29.7, 29.5, 25.9, 23.6, 22.8, 14.2.

6-Methylhept-5-en-2-ol (b18)

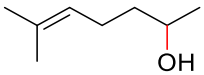

According to general procedure, 6-methylhept-5-en-2-one (74 µL, 0.5 mmol) gave the title compound **b18** as a colourless oil (36 mg, 56%).

^{1}H NMR (400 MHz, $CDCl_3$) δ 5.12 (t, *J* = 7.2 Hz, 1H), 3.82-3.75 (m, 1H), 2.21 – 1.89 (m, 2H), 1.68 (s, 3H), 1.68 (br. s, 1H, OH), 1.60 (s, 3H), 1.56 – 1.35 (m, 2H), 1.18 (d, *J* = 6.2 Hz, 3H).
^{13}C{^{1}H} NMR (101 MHz, $CDCl_3$) δ 132.1, 124.2, 68.1, 39.3, 25.8, 24.6, 23.5, 17.8.

1-Phenylpropan-1-ol (b20)

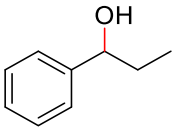

According to general procedure, propiophenone (132 µL, 1 mmol) gave the title compound **b20** as a colourless oil (136 mg, 98%).
^{1}H NMR (400 MHz, $CDCl_3$) δ 7.50 – 7.17 (m, 5H), 4.61 (t, *J* = 6.6 Hz, 1H), 2.11 (s, 1H), 1.97 – 1.63 (m, 2H), 0.95 (t, *J* = 7.4 Hz, 3H).
^{13}C{^{1}H} NMR (101 MHz, $CDCl_3$) δ 144.7, 128.3, 127.4, 126.0, 75.9, 31.8, 10.1.

1,3-Diphenylpropan-1ol (b21)

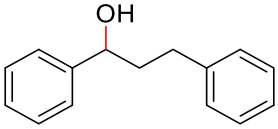

According to general procedure, 1,3-diphenylpropan-1-one (105 mg, 0.5 mmol) gave the title compound **b21** as a colourless oil (101 mg, 95%).

^{1}H NMR (400 MHz, $CDCl_3$) δ 7.44 – 7.36 (m, 4H), 7.36 – 7.28 (m, 3H), 7.28 – 7.17 (m, 3H), 4.70 (dd, *J* = 7.8, 5.4 Hz, 1H), 2.86 – 2.60 (m, 2H), 2.30 (s, 1H), 2.20 – 1.98 (m, 2H).
^{13}C{^{1}H} NMR (101 MHz, $CDCl_3$) δ 144.7, 141.9, 128.55, 128.52, 128.4, 127.6, 126.0, 125.9, 73.9, 40.5, 32.1.

1-(Pyridin-2-yl)ethanol (b23)

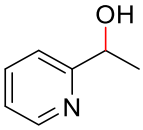

According to general procedure, 2-acetylpyridine (112 µL, 1 mmol) gave the title compound **b23** as a colourless oil (95 mg, 93%).
^{1}H NMR (400 MHz, $CDCl_3$) δ 8.52 (s, 1H), 7.66 (t, *J* = 7.2 Hz, 1H), 7.40 – 7.24 (m, 1H), 7.19 (s, 1H), 4.89 (s, 1H), 4.37 (s, 1H), 1.50 (d, *J* = 5.2 Hz, 3H).
^{13}C{^{1}H} NMR (75 MHz, $CDCl_3$) δ 163.3, 148.6, 137.0, 122.6, 120.1, 69.2, 24.5.

Experiment for Mn-H species

In a glovebox, in a Young NMR tube, a solution of *t*BuOK (1.12 mg, 0.01 mmol) in toluene-d_8 was added to a solution of the complex **C^{2A}.1** (5.6 mg, 0.01 mmol) in toluene-d_8. After shaking, the color of the solution turned to blue. The mixture was kept overnight at -30 °C, leading to a blue a solution with a dark blue precipitate. The ^{1}H and ^{31}P{^{1}H} NMR of the solution displayed no detectable signals. The NMR tube was then pressurized with H_2 (1.5 bar). The solution turned quickly to yellow. The ^{1}H and the ^{31}P{^{1}H} NMR displayed the characteristic signal of [(^{iPr}PN^{3}P$_{iPr}$)Mn(CO)$_2$H] **C^{2A}.1d** complex.

^{1}H NMR (300 MHz, toluene-d_8) δ 6.64 (t, *J* = 7.5 Hz, 1H), 5.40 (d, *J* = 7.9 Hz, 2H), 4.31 (s, 2H), -5.90 (t, *J* = 51.6 Hz, 1H) (Selected signals).
^{31}P{^{1}H} NMR (121 MHz, Toluene-d_8) δ 164.71.

See spectra in the main text **Figure B^{2I}.1-2**

B – II – Study of aliphatic tridentate complexes for hydrogenation reactions

Synthesis of complexes

Complex C^{2B}.1

Bis(2-((diisopropylphosphino)oxy)ethyl)amine L^{2B}.1 (100.0 mg, 0.296 mmol, 1.0 equiv.) was added to a solution of $Mn(CO)_5Br$ (81.4 mg, 0.296 mmol), in anhydrous toluene (2 mL). The mixture was stirred at 100 °C overnight. Toluene was then evaporated. The crude residue was then recrystallized from dichloromethane (1 mL) and pentane (5 mL) to afford orange solid. The orange solid was washed with pentane (2×2 mL) to afford the pure compound (129.5 mg, 82%). Single crystals suitable for X-Ray diffraction studies were grown by slow diffusion of pentane into a CH_2Cl_2 solution of C^{2B}.1 at r.t.

^{1}H NMR (400 MHz, CD_2Cl_2) δ 4.30 – 3.85 (m, 4H, *CH*$_2$), 3.66 – 3.32 (m, 2H, *CH*$_{i\text{Pr}}$), 3.24 – 2.92 (m, 3H, NH+ *CH*$_2$), 2.81 (dd, *J* = 10.4, 3.1 Hz, 2H, *CH*$_2$), 2.75 – 2.62 (m, 2H, *CH*$_{i\text{Pr}}$), 1.47 – 1.14 (m, 24H, *CH*$_{3i\text{Pr}}$).

^{13}C{^{1}H} NMR (101 MHz, CD_2Cl_2) δ 64.8 (*CH*$_2$), 57.4 (br., *CH*$_2$), 31.4-31.1 (m, 2C, *CH*$_{i\text{Pr}}$), 18.3 (br., *CH*$_{3i\text{Pr}}$), 17.9 (*CH*$_{3i\text{Pr}}$), 17.6 (br., *CH*$_{3i\text{Pr}}$), 16.5 (br., *CH*$_{3i\text{Pr}}$). (CO signals not detected)

^{31}P{^{1}H} NMR (162 MHz, CD_2Cl_2) δ 174.7.

Anal. Calc (%). for ($C_{18}H_{37}NO_4BrP_2Mn$): C, 40.92; H, 7.06; N, 2.65, Found: C, 40.82; H, 6.73; N, 2.42.

HR-MS (ESI): m/z $[M]^{+\cdot}$ calcd for $C_{18}H_{37}NO_4{}^{79}BrP_2Mn$ 527.0756, found 527.0754 (0 ppm); m/z $[M-.2CO]^{+\cdot}$ calcd for $C_{16}H_{37}NO_2{}^{79}BrP_2Mn$ 471.08579, found 471.0854 (1 ppm)

IR (ν, cm^{-1}, CH_2Cl_2): 1953, 1927, 1846. [1]

The presence of three absorption bands in IR probably results from the presence of two isomers, related to the relative *syn* or *anti* position of the bromide atom and the substituent on the nitrogen atom.

Complex C^{2B}.2.

Following the same procedure as for the synthesis of complex C^{2B}.1, starting from L^{2B}.2 (100.0 mg, 0.284 mmol) and $Mn(CO)_5Br$ (78.1 mg, 0.284 mmol), complex C^{2B}.2 was obtained as an orange solid (124.0 mg, 80%).

^{1}H NMR (400 MHz, CD_2Cl_2) δ 4.41-4.25 (br. s, 2H, *CH*$_2$), 4.11 – 3.80 (br., 4H, *CH*$_2$), 3.53-3.38 (br., 2H, *CH*$_{i\text{Pr}}$), 2.91-2.73 (br., 5H, *CH*$_{i\text{Pr}}$ + N-*CH*$_3$), 1.72-1.61 (br., 2H, *CH*$_2$), 1.50-1.19 (br. m, 24H, *CH*$_{3i\text{Pr}}$).

^{13}C{^{1}H} NMR (75 MHz, CD_2Cl_2) δ 61.4 (CH_2), 61.3 (CH_2), 46.9 (N-CH_3), 31.5-31.1 (m, 2C, *CH*$_{i\text{Pr}}$), 17.4 (*CH*$_{3i\text{Pr}}$), 16.8 (*CH*$_{3i\text{Pr}}$), 16.5 (*CH*$_{3i\text{Pr}}$), 16.4 (*CH*$_{3i\text{Pr}}$). (CO signals not detected)

^{31}P{^{1}H} NMR (162 MHz,CD_2Cl_2) δ 172.2.

Anal. Calc (%). for ($C_{19}H_{39}NO_4BrP_2Mn$).(CH_2Cl_2): C, 38.30; H, 6.59; N, 2.23, Found: C, 38.21; H, 6.48; N, 2.88.

HR-MS (ESI): m/z $[M-Br]^+$ calcd for $C_{19}H_{39}NO_4P_2Mn$ 462.1729, found 462.1737 (2 ppm);m/z $[M]^{+\cdot}$ calcd for $C_{19}H_{39}NO_4{}^{79}BrP_2Mn$ 541.09127, found 541.0912 (0 ppm); m/z $[M-.2CO]^{+\cdot}$ calcd for $C_{17}H_{39}NO_2{}^{79}Br$ P_2Mn 485.10144, found 485.1015 (0 ppm)

IR (ν, cm^{-1}, CH_2Cl_2): 1946, 1923, 1842. [1]

Mixture of complexes **C^{2B}.4.**

Amino-bis(aminophosphine) ligand **L^{2B}.4** (375.0 mg, 1.118 mmol, 1.0 equiv.) was added to a solution of $Mn(CO)_5Br$ (307.3 mg, 1.118 mmol), in anhydrous toluene (20 mL). The mixture was stirred at 100 °C overnight. Toluene was then evaporated. The orange solid was washed with pentane (2×10 mL).

^{31}P NMR (162 MHz, Acetone-d_6) δ 175.64 (minor), 107.44.

N,*N*'-(Methyliminodiethylene)bisphthalimide

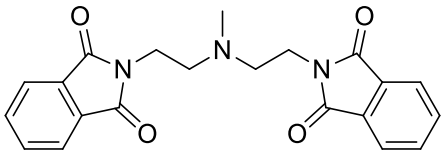

Phthalimide (1.47 g, 10 mmol) and diethanolmethylamine (1.26 mL, 11 mmol) and PPh_3 (3.6 g, 14 mmol) were dissolved in THF (10 mL). The mixture was cooled to 0 °C and diethyl azodicarboxylate (DEAD, 40% in toluene, 2.5 mL, 14 mmol) was added dropwise. The mixture was stirred at r.t. for 18 h. Under vigorous stirring, pentane was carefully added and a suspension formed. After 1 h, the solids were filtered off, and the filter cake was washed with 2:1 pentane/EtOAc . The filtrate was concentrated and the resulting material was purified by flash chromatography (EtOAc/ Petroleum Ether). The product was obtained as a white solid (1.6 g, 43%). [2]

^1H NMR (400 MHz, $CDCl_3$) δ 7.62 (m, 8H), 3.70 (t, *J* = 6.4 Hz, 4H), 2.67 (t, *J* = 6.4 Hz, 4H), 2.35 (s, 3H).

NMR data

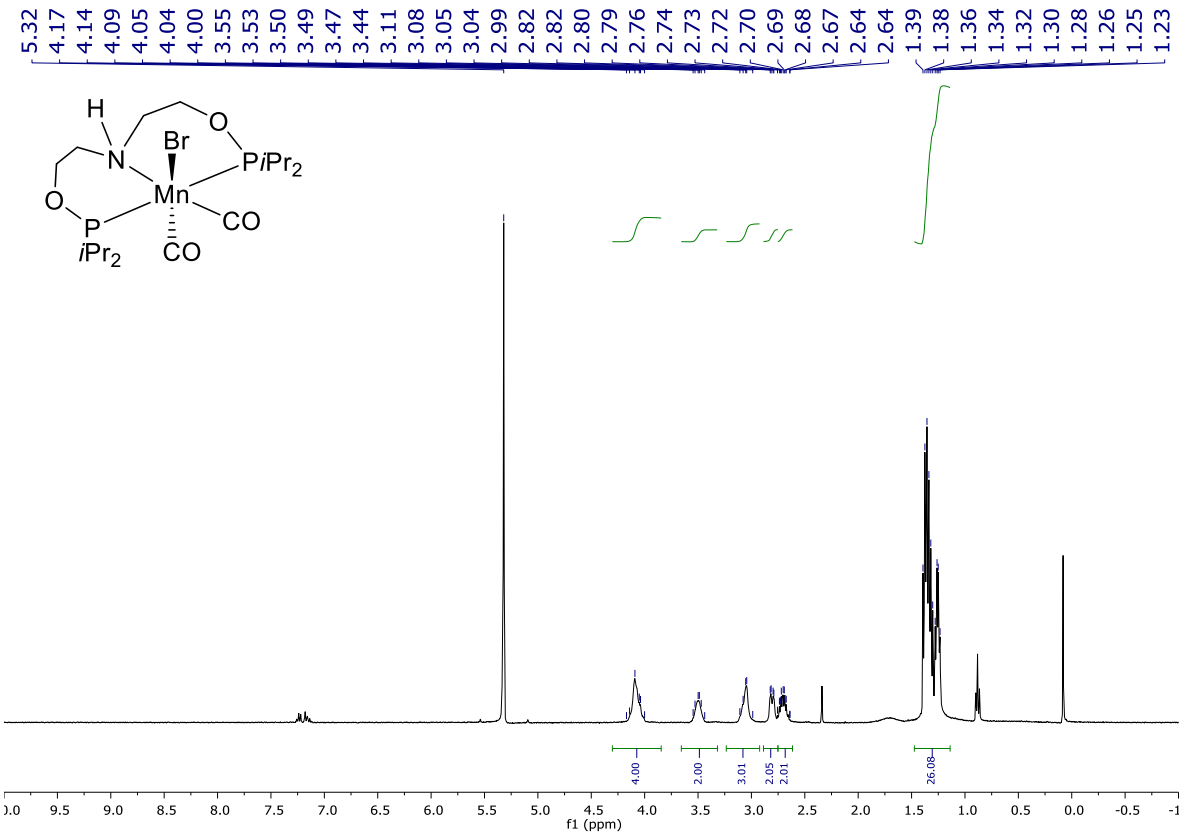

Figure S13: ^{1}H NMR spectrum of Complex **C^{2B}.1** in CD_2Cl_2 (400 MHz).

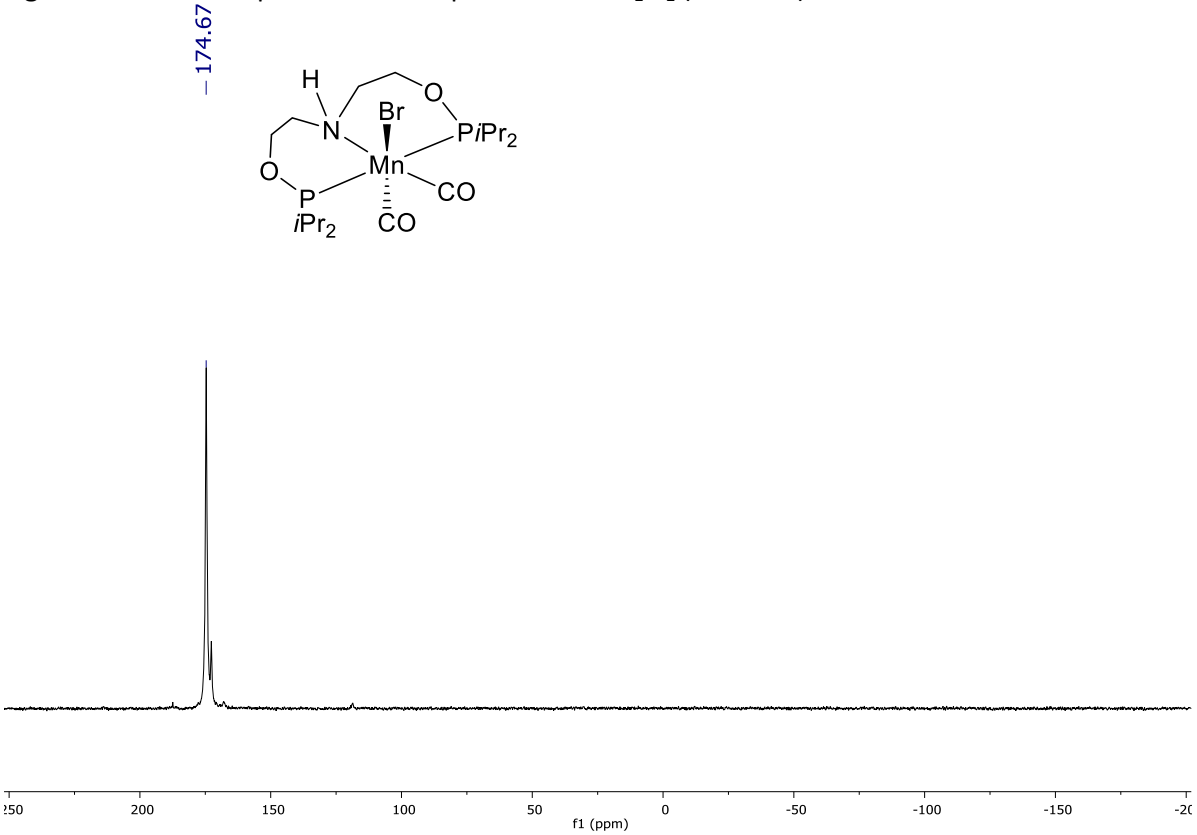

Figure S14: $^{31}P\{^{1}H\}$ NMR spectrum of Complex **C^{2B}.1** in CD_2Cl_2 (162 MHz)

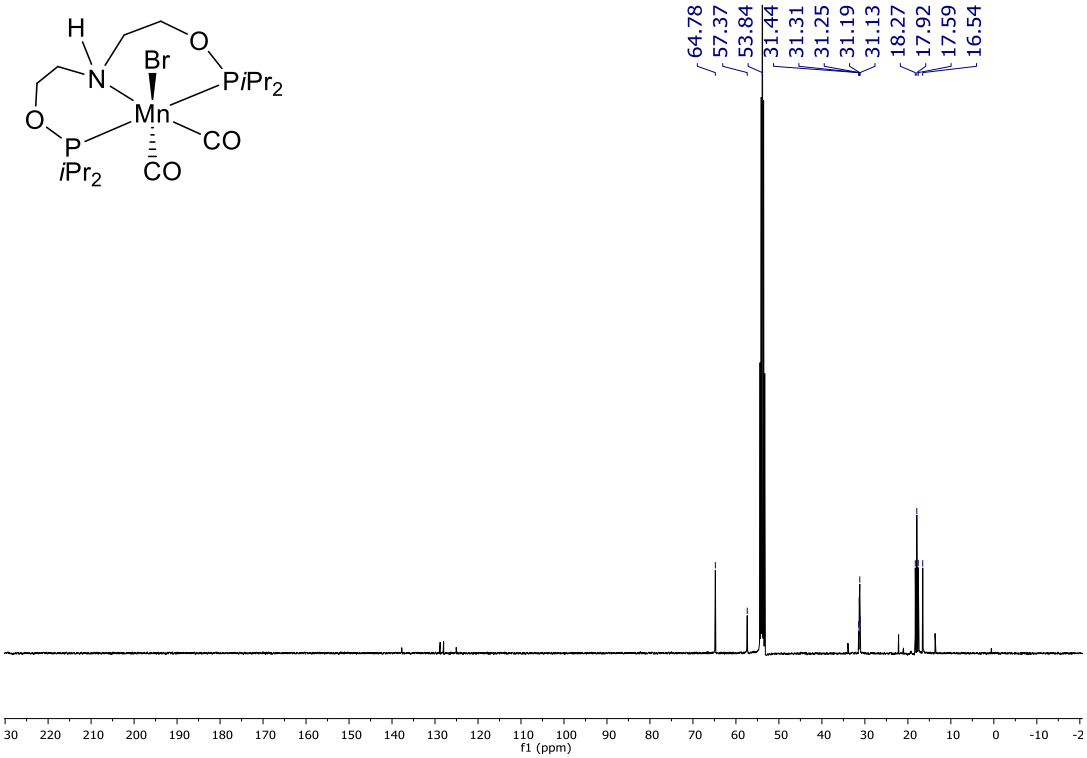

Figure S15: $^{13}C\{^{1}H\}$ NMR spectrum of Complex **C^{2B}.1** in CD_2Cl_2 (101 MHz).

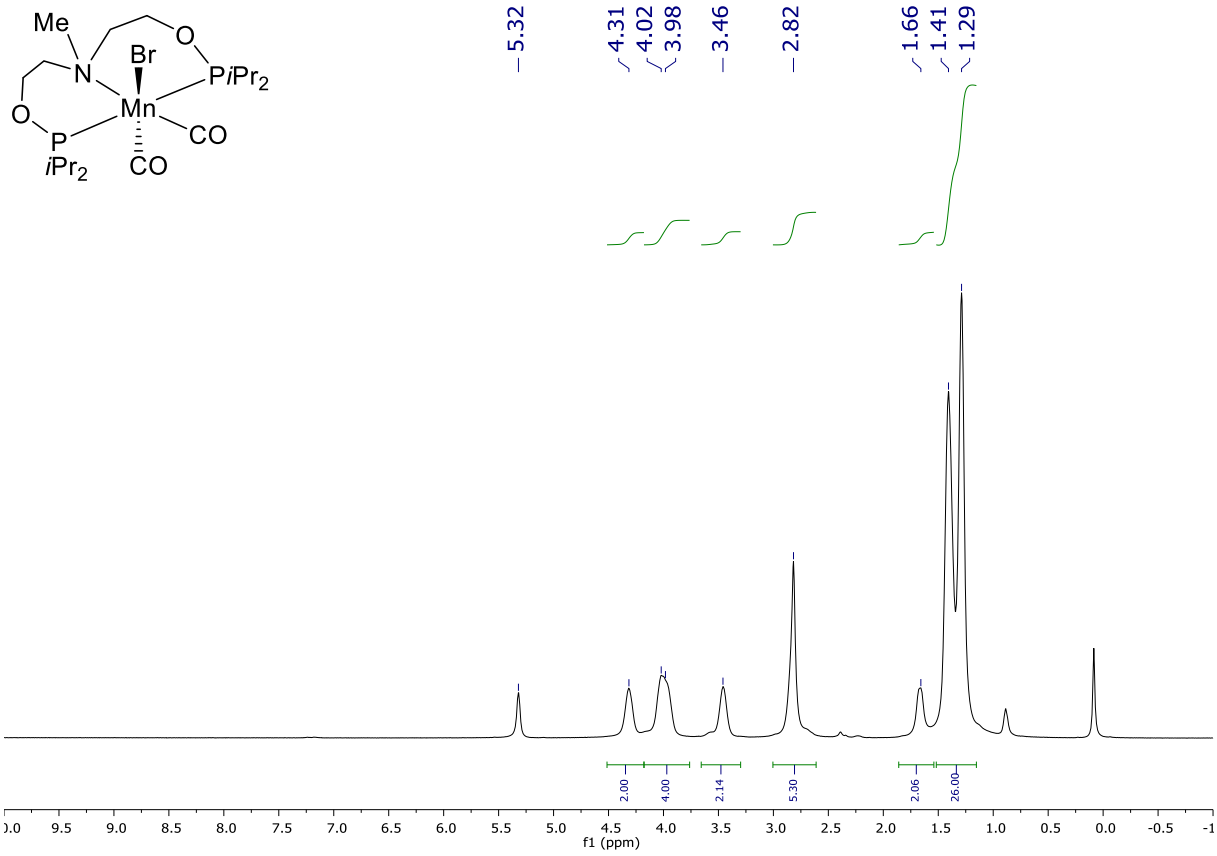

Figure S16: ^{1}H NMR spectrum of Complex **C^{2B}.2** in CD_2Cl_2 (400 MHz).

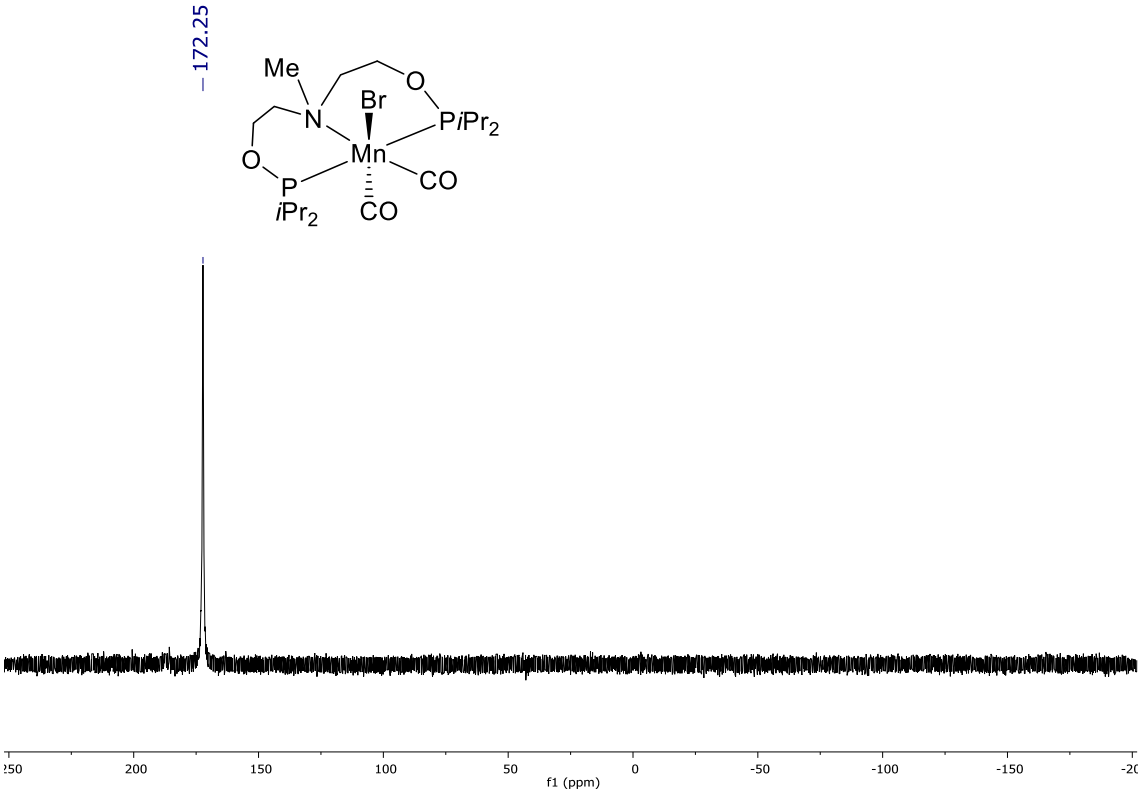

Figure S17: $^{31}P\{^{1}H\}$ NMR spectrum of Complex **C^{2B}.2** in CD_2Cl_2 (162 MHz)

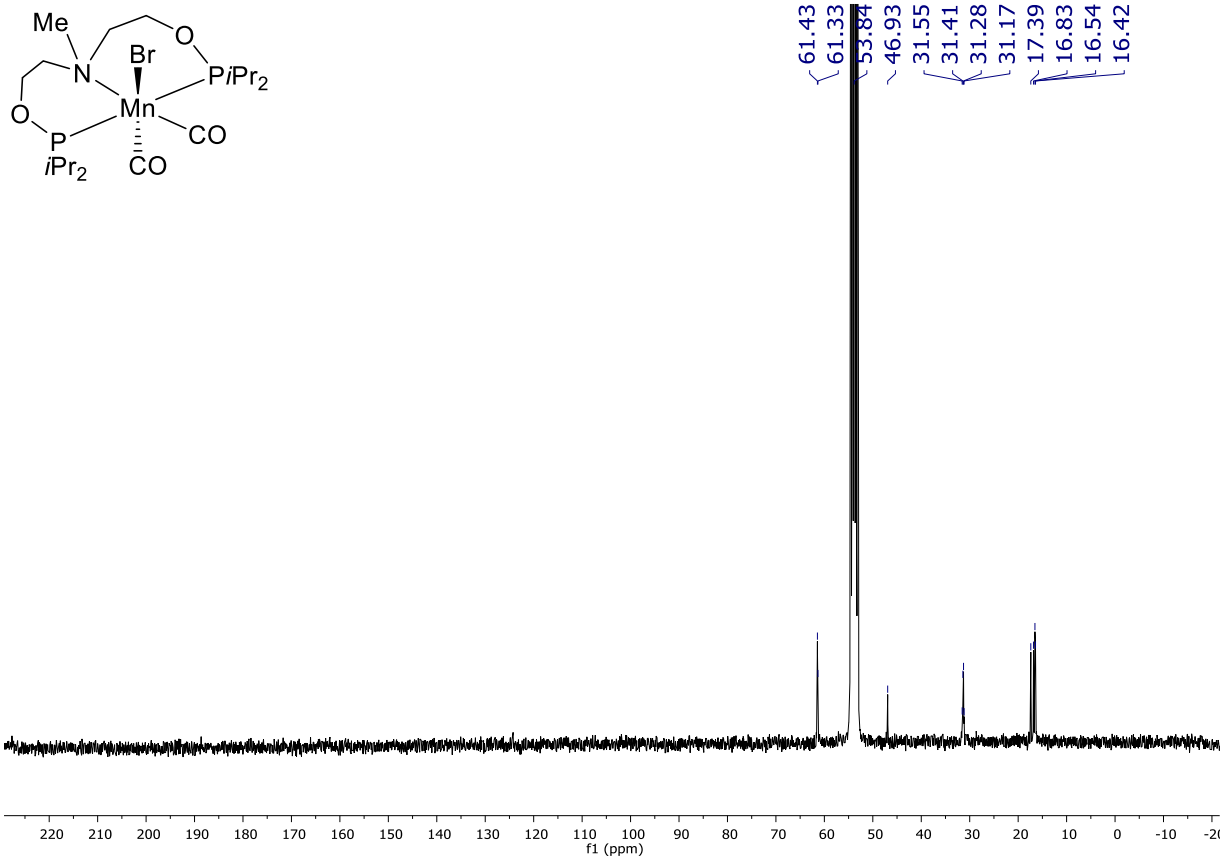

Figure S18: $^{13}C\{^{1}H\}$ NMR spectrum of Complex **C^{2B}.2** in CD_2Cl_2 (75 MHz).

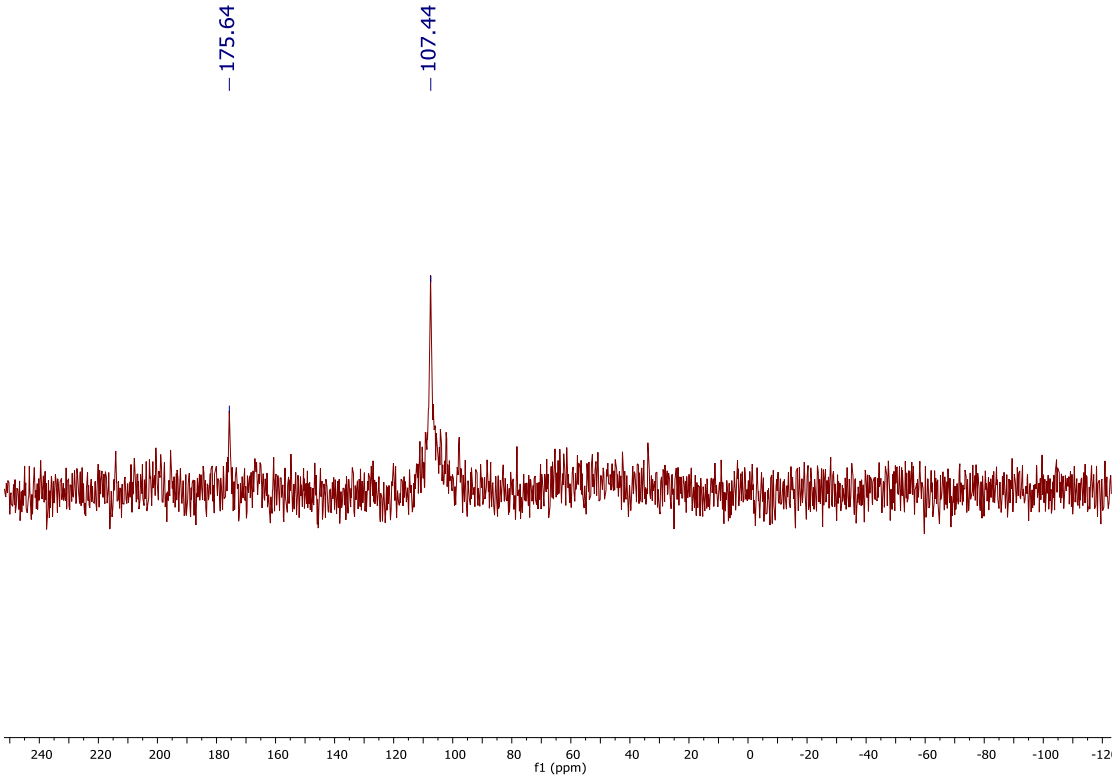

Figure S19: $^{31}P\{^{1}H\}$ NMR spectrum of complexes **C^{2B}.4** in Acetone-d_6 (162 MHz)

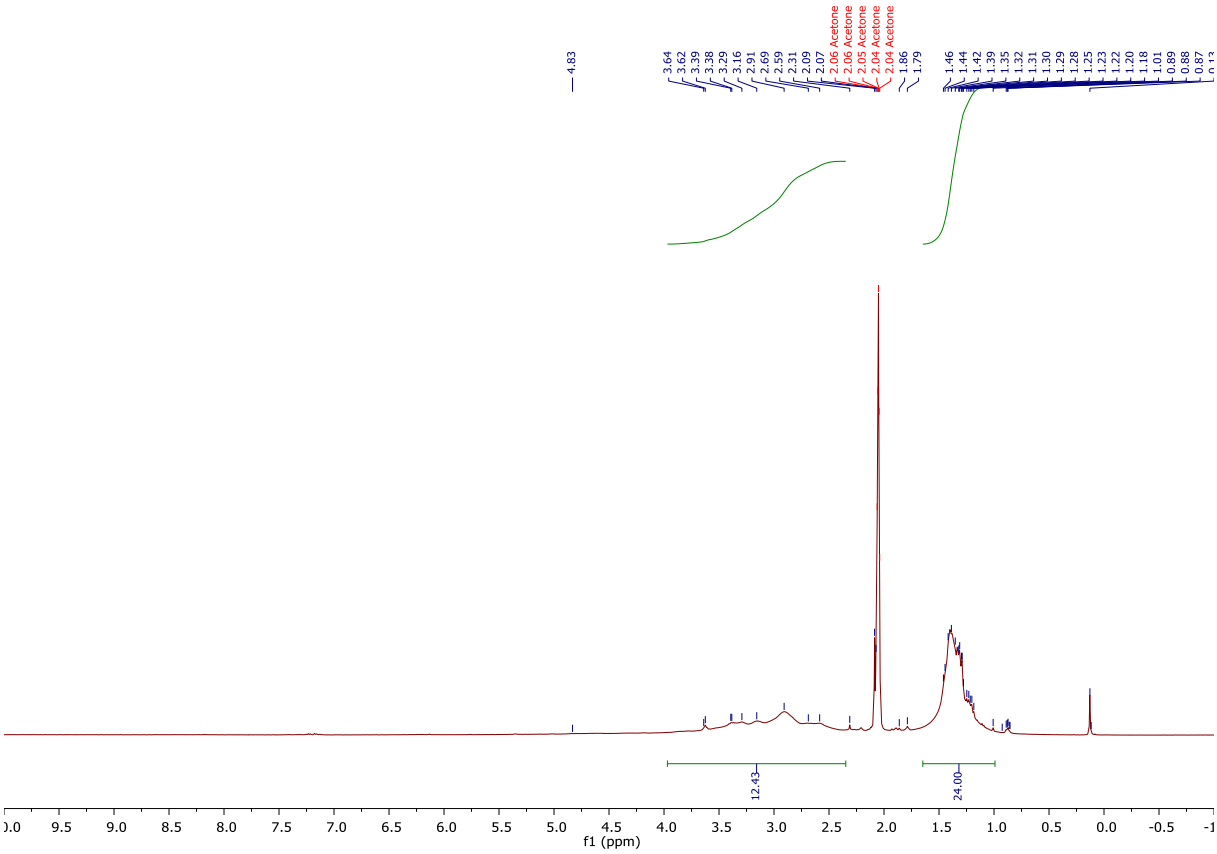

Figure S20: ^{1}H NMR spectrum of complexes **C^{2B}.4** in Acetone-d_6 (400 MHz).

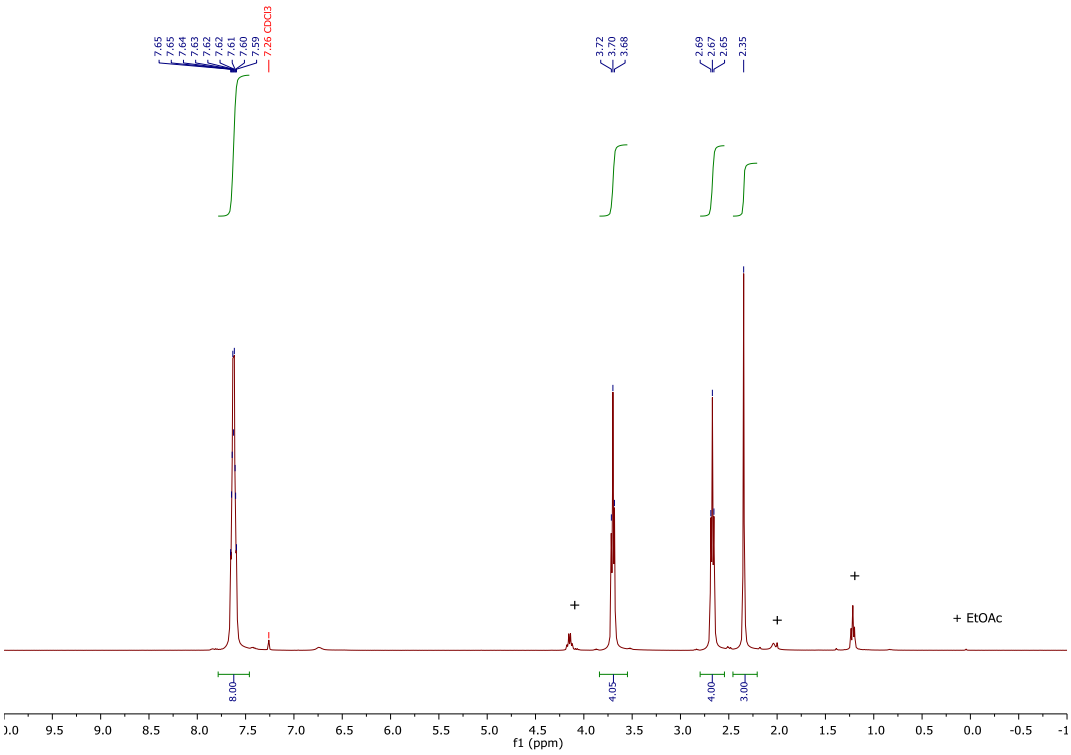

Figure S21: ^{1}H NMR spectrum of *N*,*N*'-(methyliminodiethylene)bisphthalimide in $CDCl_3$ (400 MHz).

Example of analysis of crude mixture for 4-nitrotoluene hydrogenation

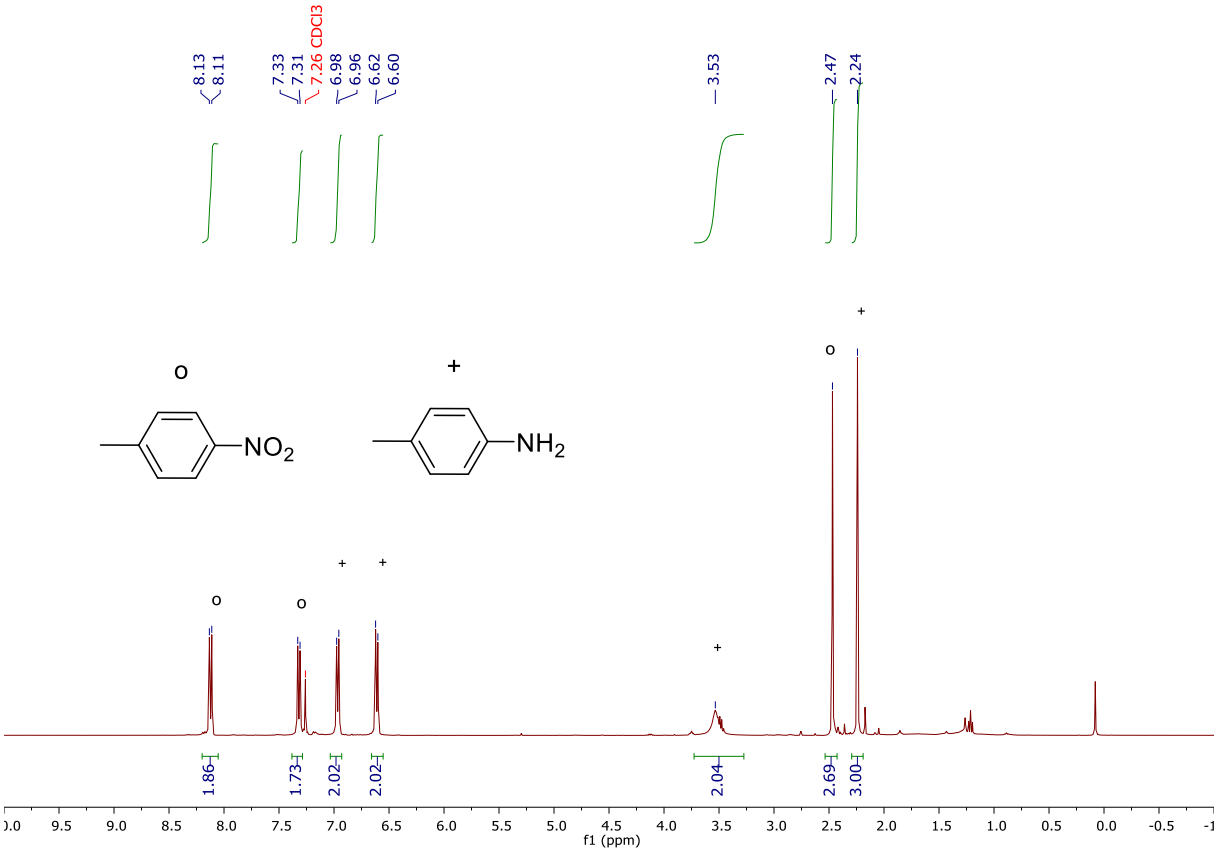

Figure S22: ^{1}H NMR spectrum of the crude mixture from **Table B^{2II}.2, entry 1** in $CDCl_3$ (400 MHz).

X-ray data

Complex $\mathbf{C^{2B}.1}$

CCDC 1815476

X-ray diffraction data were collected on a D8 VENTURE Bruker AXS diffractometer equipped with a PHOTON 100 CMOS detector, using multilayers monochromated Mo-Kα radiation (λ = 0.71073 Å) at T = 150(2) K. The structure was solved by direct methods using the *SIR97* program,[3] and then refined with full-matrix least-square methods based on F^2 (*SHELXL-97*).[4] All non-hydrogen atoms were refined with anisotropic atomic displacement parameters. H atoms were finally included in their calculated positions. A final refinement on F^2 with 5385 unique intensities and 252 parameters converged at $\omega R(F^2) = 0.1213$ ($R(F) = 0.0543$) for 3802 observed reflections with $I > 2\sigma(I)$.

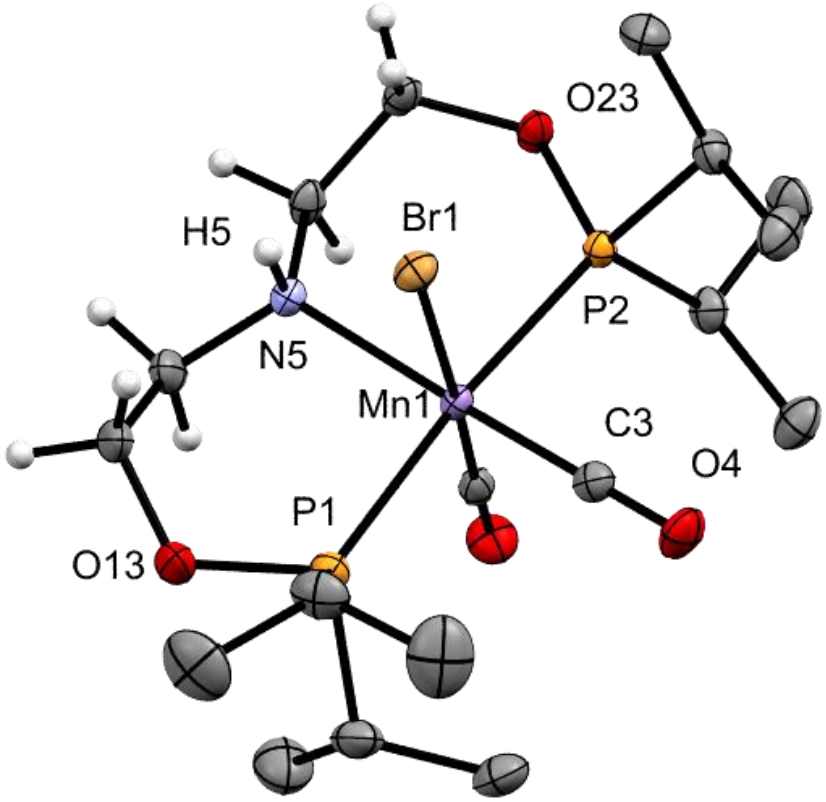

Figure S23: Perspective view of the molecular structure of complex $\mathbf{C^{2B}.1}$ with thermal ellipsoids drawn at 50% probability. Hydrogen atoms on isopropyl groups were omitted for clarity.

Table S3. Crystal data and structure refinement for complex **C^{2B}.1**.

Empirical formula	C_{18} H_{37} Br Mn N O_4 P_2
Formula weight	528.27
Temperature	150(2) *K*
Wavelength	0.71073 Å
Crystal system, space group	monoclinic, *P* $2_1/c$
Unit cell dimensions	a = 12.7762(11) Å, α = 90 °
	b = 11.0856(10) Å, β = 90.200(3) °
	c = 16.6191(13) Å, γ = 90 °
Volume	2353.8(3) $Å^3$
Z, Calculated density	4, 1.491 ($g.cm^{-3}$)
Absorption coefficient	2.416 mm^{-1}
F(000)	1096
Crystal size	0.340 x 0.250 x 0.020 mm
Crystal color	yellow
Theta range for data collection	2.920 to 27.483 °
h_min, h_max	-16, 16
k_min, k_max	-14, 14
l_min, l_max	-17, 21
Reflections collected / unique	27929 / 5385 [R(int)[a] = 0.0931]
Reflections [I>2σ]	3802
Completeness to theta_max	0.998
Absorption correction type	multi-scan
Max. and min. transmission	0.953 , 0.682
Refinement method	Full-matrix least-squares on F^2
Data / restraints / parameters	5385 / 0 / 252
[b]Goodness-of-fit	1.025
Final *R* indices [I>2σ]	$R1^c$ = 0.0543, $wR2^d$ = 0.1213
R indices (all data)	$R1^c$ = 0.0890, $wR2^d$ = 0.1397
Largest diff. peak and hole	1.508 and -0.835 $e^-.Å^{-3}$

$^a R_{int} = \sum |F_o^2 - < F_o^2>| / \sum [F_o^2]$

$^b S = \{\sum [w(F_o^2 - F_c^2)^2] / (n - p)\}^{1/2}$

$^c R1 = \sum | |F_o| - |F_c| | / \sum |F_o|$

$^d wR2 = \{\sum [w(F_o^2 - F_c^2)^2] / \sum [w(F_o^2)^2]\}^{1/2}$

$w = 1 / [\sigma(F_o^2) + aP^2 + bP]$ where $P = [2F_c^2 + MAX(F_o^2, 0)] /3$

Complex **C^{2B}.2**

CCDC 1815481

X-ray diffraction data were collected on a D8 VENTURE Bruker AXS diffractometer equipped with a PHOTON 100 CMOS detector, using multilayers monochromated Mo-Kα radiation (λ = 0.71073 Å) at T = 150 K. The structure was solved by dual-space algorithm using the *SHELXT* program,[5] and then refined with full-matrix least-squares methods based on F^2 (*SHELXL*).[6] All non-hydrogen atoms were refined with anisotropic atomic displacement parameters. H atoms were finally included in their calculated positions and treated as riding on their parent atom with constrained thermal parameters. A final refinement on F^2 with 2734 unique intensities and 152 parameters converged at $\omega R(F^2)$ = 0.1827 ($R(F)$ = 0.0707) for 2238 observed reflections with $I > 2\sigma(I)$.

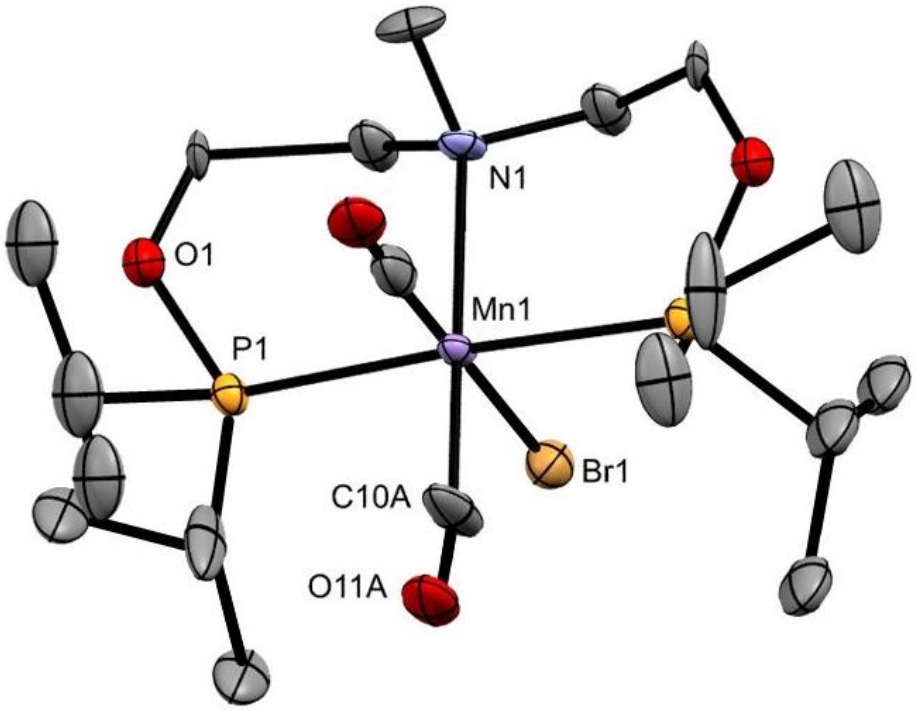

Figure S24: Perspective view of the molecular structure of complex **C^{2B}.2** with thermal ellipsoids drawn at 50% probability. Hydrogen atoms were omitted for clarity. Two configurations of the compound are superimposed in the crystal structure, only one is depicted.

Table S4. Crystal data and structure refinement for complex **C^{2B}.2**.

Empirical formula	C_{19} H_{39} Br Mn N O_4 P_2
Formula weight	542.30 g/mol
Temperature	150 *K*
Wavelength	0.71073 Å
Crystal system, space group	monoclinic, *C* 2/*c*
Unit cell dimensions	a = 19.541(3) Å, α = 90 °
	b = 8.9597(14) Å, β = 103.159(5) °
	c = 13.9901(19) Å, γ = 90 °
Volume	2385.1(6) $Å^3$
Z, Calculated density	4, 1.510 $g.cm^{-3}$
Absorption coefficient	2.387 mm^{-1}
F(000)	1128
Crystal size	0.600 x 0.120 x 0.020 mm
Crystal color	orange
Theta range for data collection	2.141 to 27.504 °
h_min, h_max	-25, 25
k_min, k_max	-11, 11
l_min, l_max	-18, 14
Reflections collected / unique	15852 / 2734 [R(int)[a] = 0.0733]
Reflections [I>2σ]	2238
Completeness to theta_max	0.998
Absorption correction type	multi-scan
Max. and min. transmission	0.953 , 0.771
Refinement method	Full-matrix least-squares on F^2
Data / restraints / parameters	2734 / 0 / 152
[b]S (Goodness-of-fit)	1.290
Final *R* indices [I>2σ]	$R1^c$ = 0.0707, $wR2^d$ = 0.1827
R indices (all data)	$R1^c$ = 0.0869, $wR2^d$ = 0.1891
Largest diff. peak and hole	0.839 and -1.448 $e^-.Å^{-3}$

$^a R_{int} = \sum |F_o^2 - < F_o^2 >| / \sum [F_o^2]$

$^b S = \{\sum [w(F_o^2 - F_c^2)^2] / (n - p)\}^{1/2}$

$^c R1 = \sum | |F_o| - |F_c| | / \sum |F_o|$

$^d wR2 = \{\sum [w(F_o^2 - F_c^2)^2] / \sum [w(F_o^2)^2]\}^{1/2}$

$w = 1 / [\sigma(F_o^2) + aP^2 + bP]$ where $P = [2F_c^2 + MAX(F_o^2, 0)] /3$

References

The references for the alcohol products are given in the chapter 3.

[1] A. M. Tondreau, J. M. Boncella, *Organometallics* **2016**, *35*, 2049–2052.

[2] S. H. Graeme, S. F. Lincoln, S. G. Teague, D. G. Rowe, *Aust. J. Chem.* **1979**, *32*, 519–36.

[3] A. Altomare, M. C. Burla, M. Camalli, G. L. Cascarano, C. Giacovazzo, A. Guagliardi, A. G. G. Moliterni, G. Polidori, R. Spagna, *J. Appl.Crystallogr.* **1999**, *32*, 115-119.

[4] G. M. Sheldrick , *Acta Crystallogr.* **2008**, *A64*, 112-122.

[5] G. M. Sheldrick, *Acta Cryst*. **2015**, *A71*, 3-8.

[6] G. M. Sheldrick , *Acta Cryst*. **2015**, *C71*, 3-8.

Chapter 3 - Study of bidentate manganese complexes

As explained at the end of the previous chapter, we envisioned that tridentate ligands might not be mandatory in the case of manganese catalysts to obtain efficient catalysts. In particular, such catalysts seemed to be accessible as complexes bearing a single bidentate ligands and carbonyl are stable in the case of manganese in contrast with the coordination chemistry of iron.[1,2] For example, bipyridinyl-tricarbonyl complexes are well established for the electrochemical reduction of CO_2 into CO, as published by Chardon-Noblat and co-workers (**Figure A^3.1**).[3]

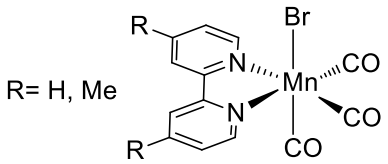

Figure A^3.1 Previous example of bidentate manganese complex used for the electrochemical reduction of CO_2.[3]

Following our study of PN^{3}P-Mn complexes, our initial goal was to prepare the parent complexes bearing only a bidentate phosphinopyridine PN^2 ligand (**Figure A^3.2**), and compare their catalytic activities in hydrogenation.

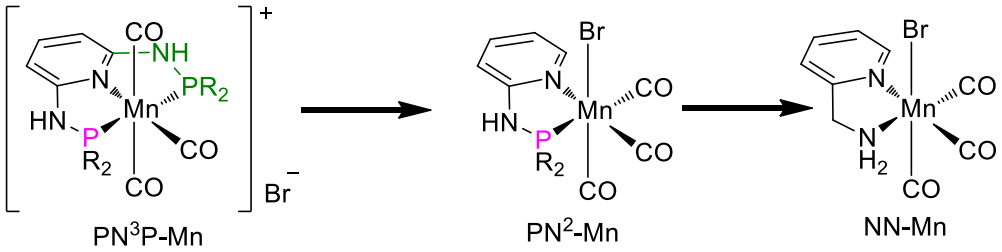

Figure A^3.2 Evolution of the well-defined pre-catalysts during this PhD.

In a second part, to simplify further the catalyst, a new family of phosphine-free NN-Mn pre-catalysts was developed for transfer hydrogenation reactions (**Figure A^3.2**).

A – Hydrogenation catalyzed by bidentate manganese complexes

I- Hydrogenation of ketones

Contributions in the part: Synthesis of the complexes: D. W., A.B.-V.; Optimization, Scope: D. W.; Mechanistic studies: A.B.-V.

Publication: D. Wei, A. Bruneau-Voisine, T. Chauvin, V. Dorcet, T. Roisnel, D. A. Valyaev, N. Lugan, J.-B. Sortais, *Adv. Synth. Catal*. **2018**, *360*, 676.

To start our study on bidentate manganese complexes, we decided to explore two families of ligands, namely phosphinopyridine and aminophosphinopyridine, as the corresponding tridentate ligands are both efficient ligands with manganese for (de)hydrogenation reactions (**Figure A^{3I}.1**).[4,5]

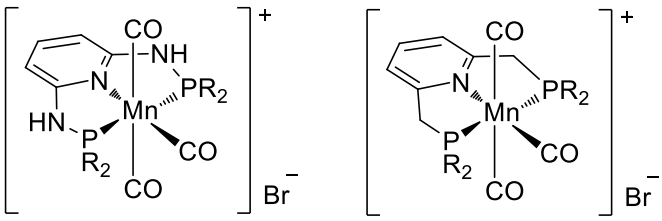

Our group **2017** Milstein **2016**

Figure A^{3I}.1 Previous efficient pre-catalysts for (de)hydrogenation reactions.[4,5]

a) Synthesis of the complexes

The ligands R_2P–X–Py (**L^{3A}.1**: R = *i*Pr, X = NH; **L^{3A}.2**: R = Ph, X = NH; **L^{3A}.3**: R = Ph, X = CH_2) and Ph_2P–CH_2–Qn (**L^{3A}.4**) were obtained in high yields starting from the appropriate chlorophosphines R_2PCl and 2-aminopyridine (for **L^{3A}.1**, **L^{3A}.2**),[6,7] 2-picoline (for **L^{3A}.3**),[8] or 2-methylquinoline (for **L^{3A}.4**),[9] respectively, according to literature procedures. The corresponding complexes $Mn(CO)_3Br(\kappa^2P,N$- **L^{3A}.1-4**) (**C^{3A}.1-4)** (**Fig. A^{3I}.2**) were readily obtained in excellent yields (87-91%) upon simple heating of an equimolar mixture of $Mn(CO)_5Br$ and the given ligand in toluene at 100 °C overnight. They were fully characterized by IR and NMR spectroscopies, high-

resolution mass spectrometry and elemental analysis, and their solid-state structures were determined by single-crystal X-ray diffraction. Perspective views of the complexes are displayed on **Figure A^{3I}.3** for complexes **C^{3A}.1-4**. All the complexes showed a typical octahedral environment for the Mn center, the **L^{3A}.1-4** ligands being coordinated in a κ^2*P*,*N* mode and the three carbonyl ligands being in facial position.

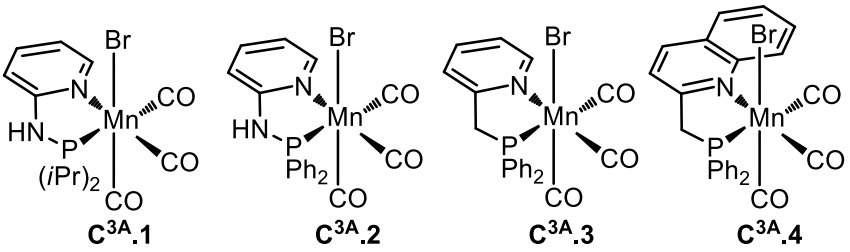

Figure A^{3I}.2 Manganese complexes synthesized for this study.

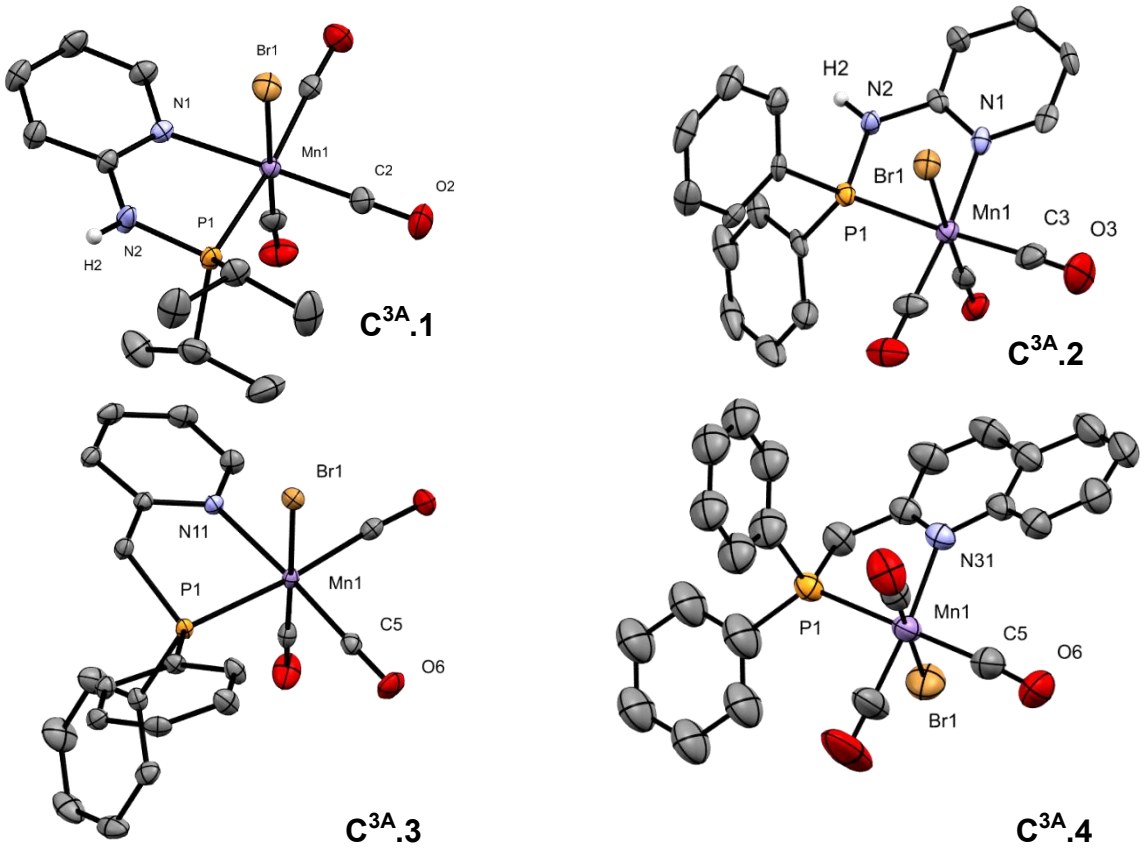

Figure A^{3I}.3 Perspective views of complex **C^{3A}.1-4** with thermal ellipsoids drawn at the 50% probability level. Hydrogen atoms, except N*H*, were omitted for clarity.

b) Optimization of experimental conditions

The catalytic activity of the new complexes **C^{3A}.1-4** was then evaluated for the reduction of ketones under hydrogenation conditions (**Table A^{3I}.1**). Under the previously optimized reaction conditions determined for the PN^3P catalyst **C^{2A}.1**, *i.e.* complex **C^{3A}.1** (5 mol%), *t*BuOK (10 mol%) as the base, toluene, 110 °C, H_2 (50 bar), 22 h, a full conversion of acetophenone **a1** to the corresponding alcohol **b1** was obtained (entry 1). The catalytic loading could be reduced to 1 mol% without any degradation of the activity (**Table A^{3I}.1**, entry 2). The performance of the four complexes was then compared at 80 °C (entries 3-6): complex **C^{3A}.1** bearing the amino-bridged diisopropylphosphino-pyridinyl bidentate ligand gave a moderate conversion (65%), whereas the diphenylphosphino derivative **C^{3A}.2** gave the alcohol in 90% yield. Disappointingly, complexes **C^{3A}.3** and **C^{3A}.4** featuring the methylene–bridged PN bidentate ligands **L^{3A}.3** and **L^{3A}.4** led to low conversions (15 and 16%, respectively, entries 5 and 6). The nature of the base was then optimized using **C^{3A}.2** as pre-catalyst. KHMDS (potassium bis(trimethylsilyl)amide) appeared to be the best one leading to a full conversion with 1 mol% of complex and 2 mol% of base at 80 °C in toluene (entry 7). With this base, the catalytic loading could be even decreased to 0.5 mol% (entries 8-10). With 0.1 mol% of catalyst, a TON of 430 was achieved (entry 11). The temperature could also be lowered to 50 °C without significant loss of efficiency (entries 12-13). At 30 °C, however, the conversion dropped to 44% (entry 14).

Table A^{3I}.1 Optimization of the reaction parameters.

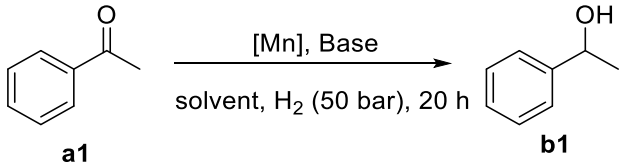

Entry	Catalyst (mol%)	Base (mol%)	Temp. (°C)	Solvent	Yield (%)[a]
1	**C^{3A}.1** (5)	*t*BuOK (10)	110	toluene	> 98
2	**C^{3A}.1** (1)	*t*BuOK (2)	110	toluene	> 98
3	**C^{3A}.1** (1)	*t*BuOK (2)	80	toluene	65
4	**C^{3A}.2** (1)	*t*BuOK (2)	80	toluene	90
5	**C^{3A}.3** (1)	*t*BuOK (2)	80	toluene	15
6	**C^{3A}.4** (1)	*t*BuOK (2)	80	toluene	16
7	**C^{3A}.2** (1)	KHMDS (2)	80	toluene	> 98
8	**C^{3A}.2** (0.5)	KHMDS (1)	80	toluene	81
9	**C^{3A}.2** (0.5)	KHMDS (1)	80	*t*-amyl alcohol	76
10	**C^{3A}.2** (0.5)	KHMDS (2)	80	toluene	95
11	**C^{3A}.2** (0.1)	KHMDS (1)	80	toluene	43
12	**C^{3A}.2** (0.5)	KHMDS (2)	50	toluene	93
13	**C^{3A}.2** (0.5)	KHMDS (2)	50	*t*-amyl alcohol	51
14	**C^{3A}.2** (0.5)	KHMDS (2)	30	toluene	44
15	**-**	KHMDS (2)	50	toluene	0
16	**C^{3A}.2** (0.5)	-	50	toluene	0
17[b]	**C^{3A}.2** (0.5)	KHMDS (2)	80	toluene	93

Typical conditions: in an autoclave, **C^{3A}.2** (0.5 mol%), toluene (4 mL), ketone (2 mmol), KHMDS (2 mol%), H_2 (50 bar) were added in this order. [a] Yields are determined by GC and ^{1}H NMR. [b] 300 equiv. of Hg (vs **C^{3A}.2**) were added before H_2 in the reaction mixture.

The influence of the solvent and of the pressure was also evaluated (**Table A^{3I}.2**). Notably, *tert*-amyl alcohol was found to be suitable for this reaction at 80 °C, as an alternative greener solvent (**Table A^{3I}.1**, entries 9 and 13).[10] Control experiment showed that the presence of Hg has no influence on the reaction meaning that heterogeneous nanoparticles are not the active species (entry 17 vs entry 10). Eventually, the optimal condition selected were catalyst **C^{3A}.2** (0.5 mol%), KHMDS (2 mol%), toluene, 50 bar of hydrogen, 20 h (entry 10).

Table A[3l].2 Optimization of the solvent and the pressure of H_2.

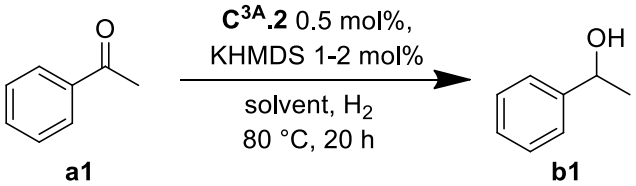

a1 b1

Entry	KHMDS (mol%)	Pressure H_2 (bar)	Solvent	Yield (%)[a]
1	1	50	toluene	81
2	1	50	*t*-amyl alcohol	76
3	1	50	THF	2
4	1	50	1,4-dioxane	11
5	2	50	toluene	95
6	2	30	toluene	87
7	2	10	toluene	7

Typical conditions: in an autoclave, **C[3A].2** (0.5 mol%), solvent (4 mL), acetophenone (2 mmol), KHMDS (1-2 mol%), H_2 were added in this order. [a] Yield determined by GC and ^{1}H NMR.

c) Scope of the reaction

Next, we explored the substrate scope amenable for the PN manganese pre-catalyst **C[3A].2** in hydrogenation (**Scheme A[3l].1**). In general, arylketones bearing both electron withdrawing and electron donating substituents were reduced in very good yields. In the case of halogenated ketones, fluoro- and bromo-derivatives (**a5**, **a7**) were well tolerated with low catalytic loading, whereas chloro- and iodo-substituted ketones (**a6**, **a8**) were not fully reduced, even under slightly forcing conditions. Steric hindrance had a noticeable influence as increasing the length and the branching of the alkyl chains from methyl (**a1**), ethyl (**a13**) to isopropyl (**a14**) induced a significant drop in the conversion (93% for **b1**, 97% for **b13** to 35% for **b14**). In line with these observations, 2',4',6'-trimethylacetophenone **a15** was not reduced with this system.

Among the various coordinating functional groups, primary amines **a12**, benzofurane **a16**, and pyridine **a17** were tolerated, but required a higher catalytic loading. Conversely, cyano-derivatives **a10** was reduced in very low yield, and nitro **b11**, even

in a competitive reaction in the presence of 4-nitrotoluene **z4** (**Table A^{3I}.3**, entry 4), and thiophene **b18** moieties completely inhibited the reaction. A series of aliphatic and cyclic ketones was reduced smoothly (**b19**-**b23**). Isolated tri-substituted C=C double bond in **a23** remained completely intact during the hydrogenation process. In order to confirm this selectivity, a series of competitive reduction of acetophenone, in the presence of 1-decene **z1**, 5-decene **z2** and 5-decyne **z3**, respectively, were conducted. In all the cases, the reduction of the ketone proceeded without the reduction of the insaturated C-C bond (**Table A^{3I}.3**, entries 1-3).

Table A^{3I}.3 Competitive reactions.

Entry	Competitive substrate	**C^{3A}.2** (mol%)	Base (mol%)	Temp. (°C)	Conv. (%)[a] **a1**/**z**
1	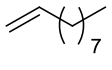 **z1**	5	*t*BuOK (10)	110	92/0
2	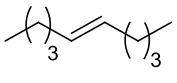 **z2**	5	*t*BuOK (10)	110	99/0
3	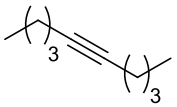 **z3**	0.5	KHMDS (2)	50	97/0
4	*p*-Me-C_6H_4-NO_2 **z4**	0.5	KHMDS (2)	80	0/0

Typical conditions: acetophenone **a1** (2 mmol), competitive substrate (2 mmol), toluene (0.5 M), **C^{3A}.2**, base, H_2 (50 bar), temp., 18 h. [a] Conversion by ^{1}H NMR.

Finally, *para*-substituted benzaldehydes (**a24**-**a26**) were also reduced to the corresponding benzylic alcohols in high yields showing the tolerance towards ester (**b25**) and amide (**b26**) groups.

Scheme A[3l].1 Scope of the hydrogenation of carbonyl derivatives under the catalysis of **C[3A].2**.[a]

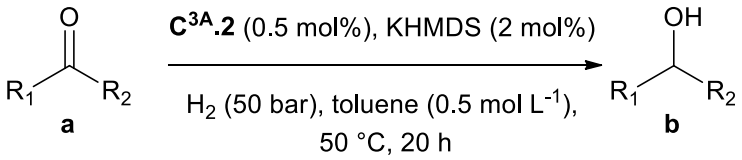

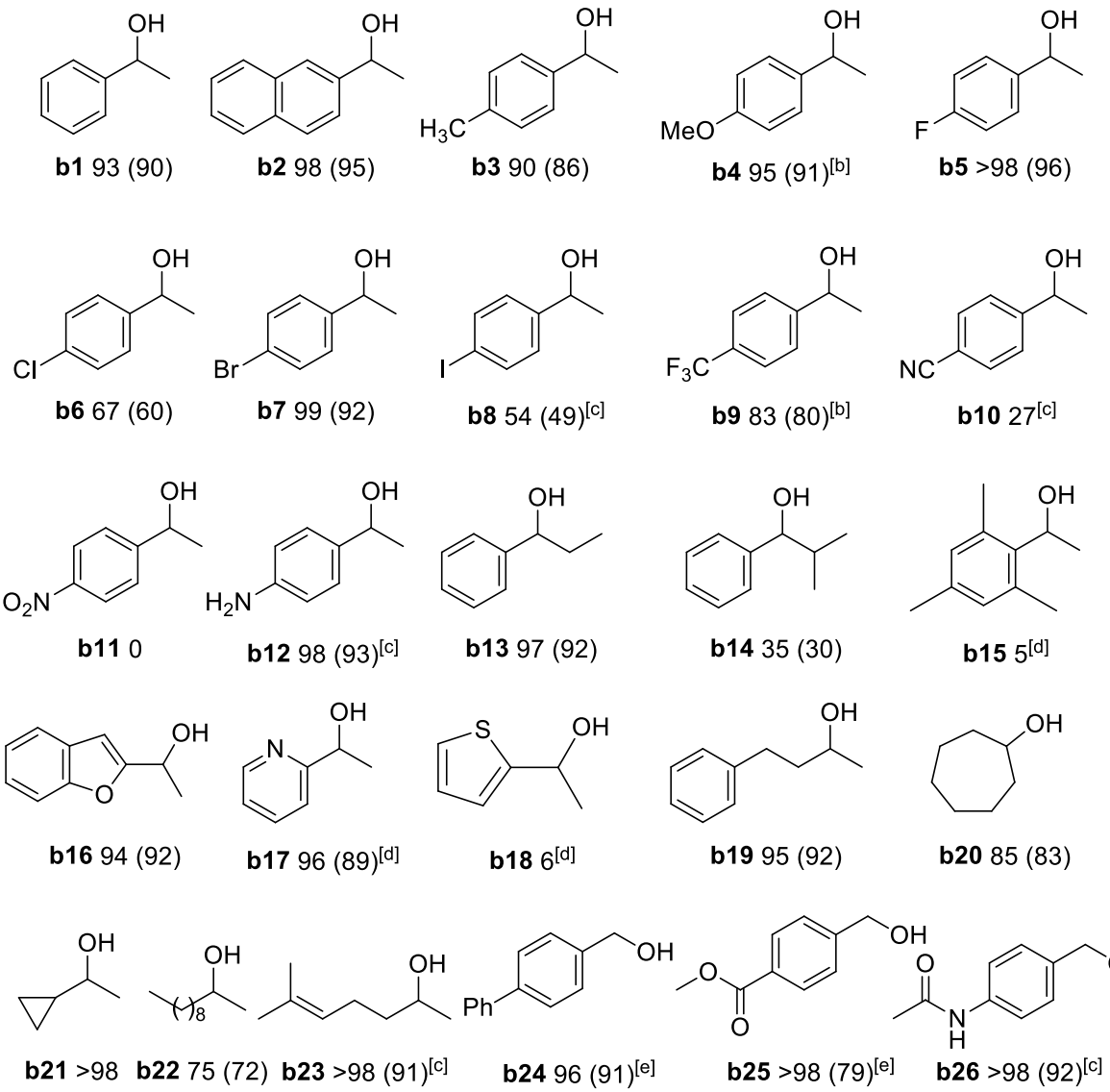

b1 93 (90) **b2** 98 (95) **b3** 90 (86) **b4** 95 (91)[b] **b5** >98 (96)

b6 67 (60) **b7** 99 (92) **b8** 54 (49)[c] **b9** 83 (80)[b] **b10** 27[c]

b11 0 **b12** 98 (93)[c] **b13** 97 (92) **b14** 35 (30) **b15** 5[d]

b16 94 (92) **b17** 96 (89)[d] **b18** 6[d] **b19** 95 (92) **b20** 85 (83)

b21 >98 **b22** 75 (72) **b23** >98 (91)[c] **b24** 96 (91)[e] **b25** >98 (79)[e] **b26** >98 (92)[c]

[a] General conditions: ketone (2 mmol), H_2 (50 bar), **C[3A].2** (0.5 mol%), KHMDS (2 mol%), toluene (4 mL, 0.5 mol.L^{-1}), 50 °C, 20 h. Conversion determined by ^{1}H NMR, isolated yield in parentheses. [b] **C[3A].2** (0.5 mol%), KHMDS (2 mol%), 80 °C. [c] **C[3A].2** (1 mol%), *t*BuOK (2 mol%), 80 °C. [d] **C[3A].2** (5 mol%), *t*BuOK (10 mol%), 80 °C. [e] **C[3A].2** (1 mol%), *t*BuOK (2 mol%), 50 °C.

In the case of α,β-unsaturated 4-phenylbut-3-en-2-one **a27**, under the standard conditions, a 13:87 mixture of fully reduced product **b19** and ketone **a19** was

obtained. Interestingly, under milder conditions, at 30 °C, the saturated ketone **a29** was accessed selectively, while under hasher ones, at 80 °C, the saturated alcohol **b19** was obtained quantitatively (**Scheme A^{3l}.2**, i and ii). Similarly, chalcone **a28** could be reduced selectively to 1,3-diphenylpropan-1-one **a29** or to 1,3(diphenylpropan-1-ol **b28** (Scheme **A^{3l}.2**, iii and iv). The reduction of (*R*)-carvone **a30**, bearing both a conjugated and a non-conjugated C=C bond, under mild conditions, led to the formation of a mixture of isomer of dihydrocarvone[11] **a31** and **a32**. Under harsher conditions, dihydrocarveol[18] **b30** was obtained in high yield (87%). In both cases, the non-conjugated C=C bond remained intact.

Scheme A^{3l}.2 Selective reduction of conjugated enones.

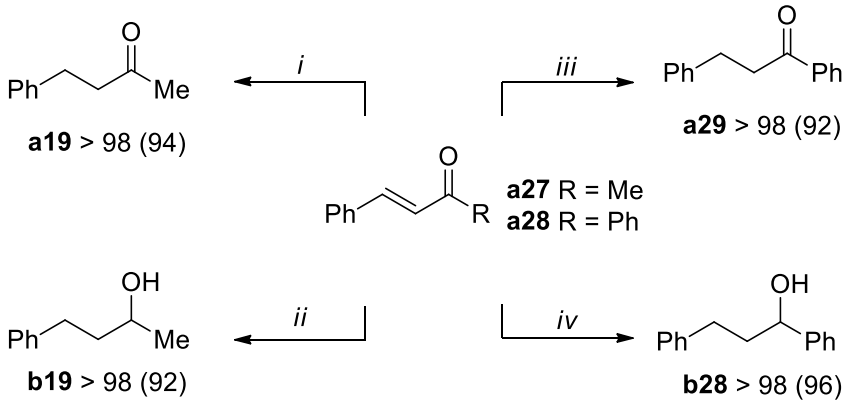

i) **C^{3A}.2** (0.5 mol%), KHMDS (2 mol%), 30 °C, H_2 (50 bar), toluene, 18 h
ii) **C^{3A}.2** (5 mol%), *t*BuOK (10 mol%), 80 °C, H_2 (50 bar), toluene, 18 h
iii) **C^{3A}.2** (2 mol%), *t*BuOK (5 mol%), 80 °C, H_2 (50 bar), toluene, 18 h
iv) **C^{3A}.2** (5 mol%), *t*BuOK (10 mol%), 100 °C, H_2 (50 bar), toluene, 22 h

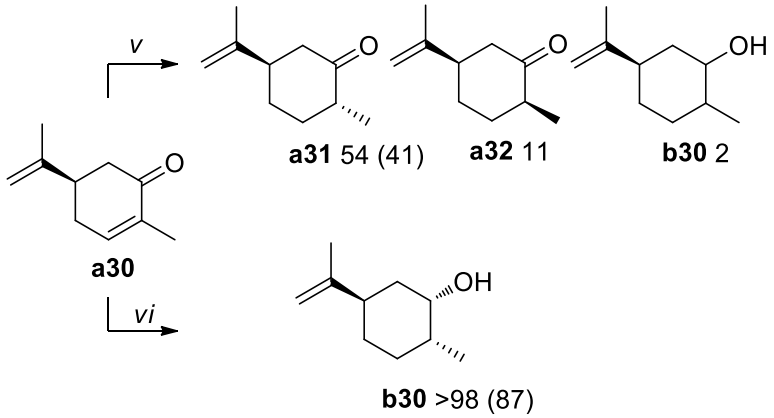

v) **C^{3A}.2** (1 mol%), *t*BuOK (2 mol%), 80 °C, H_2 (50 bar), toluene, 18 h
vi) **C^{3A}.2** (5 mol%), *t*BuOK (10 mol%), 100 °C, H_2 (50 bar), toluene, 18 h

Compared to the reduction of α,β-unsaturated aldehydes by aliphatic PNP manganese catalysts **Mn-1**,[12] where the unsaturated alcohols were produced

selectively, and to the reduction of α,β-unsaturated esters,[13] where solely saturated alcohols were obtained, the present catalytic system allows to reduce exclusively the conjugated C=C double bond, supplementing the previously described ones.

Under the optimized conditions, isomerization of allylic alcohol did not occur meaning that the reduction probably proceeded through a 1-4 addition mechanism.

d) Mechanistic insights

Experiments in Young type NMR tubes were carried out to gain more insight about the nature of the active species in this catalytic system (**Scheme A^{3I}.3**). First, the complex **C^{3A}.2** was mixed with 3 equiv. of *t*BuOK in C_6D_6 then heated at 50 °C giving a single $^{31}P\{^1H\}$ NMR signal at 90.4 ppm. By analogy with our previous work, we assigned this signal to the deprotonated complex **C^{3A}.2b**. However, this complex was difficult to characterize fully. Only one crystal suitable for X-Ray diffraction analysis was obtained in a saturated solution of **C^{3A}.2b** in MeOH.

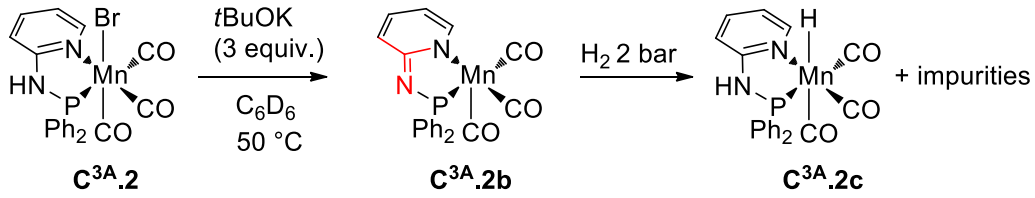

Scheme A^{3I}.3. Mechanistic experiment to deprotonate **C^{3A}.2** with *t*BuOK followed by addition of dihydrogen, realized in C_6D_6 in a Young NMR tube.

Surprisingly, the complex **C^{3A}.2b'**, probably resulting from a partial decomposition, beared two PN ligands. As in the case of PN^{3}P Mn **C^{2A}.1**, one of the PN ligands was deprotonated, de-aromatized and stabilized by hydrogen bonding with one molecule of methanol. The de-aromatization could be verified by measuring the bond lengths from the DRX analysis (**Figure A^{3I}.4**): the bond between the pyridinyl group and the nitrogen from the amino-phosphine moiety was shorter in the de-aromatized ligand than in the aromatized one (C_{36}-N_{37} *vs* C_{16}-N_{17}). In the pyridinyl scaffold, the bonds around the carbon linked to the aminophosphine group were longer in the de-aromatized ligand than in the aromatized one (C_{36}-N_{31} and C_{36}-C_{35} *vs* C_{16}-N_{11} and

C_{16}-C_{15}), which is in agreement with the de-aromatization of one of the ligands. Unfortunately, no NMR spectra of the crystals could be recorded.

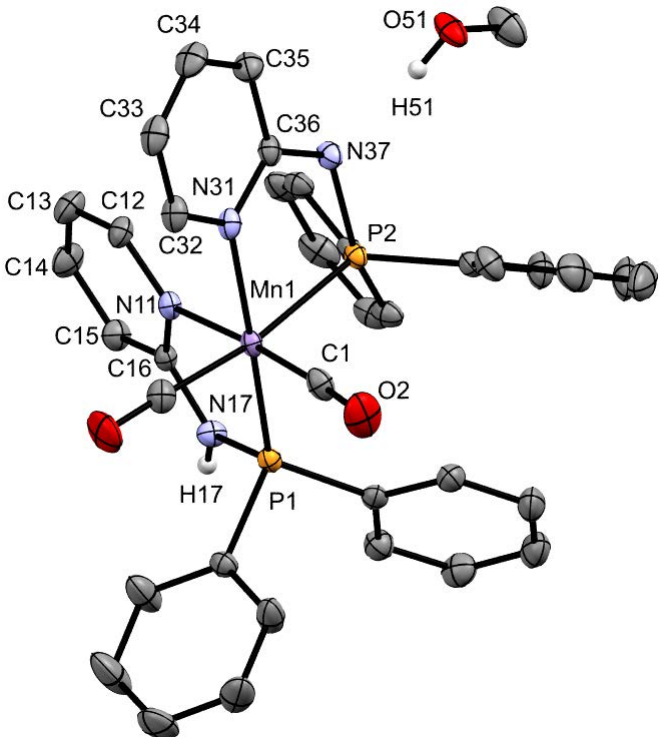

Comparison of the principal bond lengths of the two ligands (Å)

De-aromatized		Aromatized	
C_{36}-N_{37}	1.348(2)	C_{16}-N_{17}	1.367(2)
C_{36}-N_{31}	1.378(2)	C_{16}-N_{11}	1.365(2)
C_{36}-C_{35}	1.426(2)	C_{16}-C_{15}	1.402(2)
C_{35}-C_{34}	1.367(2)	C_{15}-C_{14}	1.369(2)
C_{34}-C_{33}	1.398(3)	C_{14}-C_{13}	1.394(3)
C_{33}-C_{32}	1.387(2)	C_{13}-C_{12}	1.371(2)
C_{32}-N_{31}	1.361(2)	C_{12}-N_{11}	1.357(2)
P_2-N_{37}	1.6686 (14)	P_1-N_{17}	1.6944 (14)
P_2-Mn_1	2.3429 (5)	P_1-Mn_1	2.2043 (5)

Figure A^{3I}.4 Perspective view of the complex **C^{3A}.2b'** with thermal ellipsoids drawn at the 50% probability level. Hydrogen atoms, except on heteroatoms, were omitted for clarity.

Then, a solution of the deprotonated species **C^{3A}.2b** in C_6D_6, generated *in situ*, was submitted to a pressure of hydrogen (2 bar): a typical doublet at - 4.4 ppm in the ^{1}H NMR ($^2J_{HP}$= 60 Hz) appeared, demonstrating that manganese hydride was formed and that only one ligand was present on the hydride complex in solution (**Figure A^{3I}.5**). Several minor signals were present in $^{31}P\{^1H\}$ NMR, along with a major one at 126.6 ppm in C_6D_6, showing that the hydride species is not the sole one in solution.

When the same methodology was employed using one equivalent of KHMDS in toluene-d_8 (**Scheme A^{3I}.4**), the reaction was much clean, and a single peak at 132.0 ppm in $^{31}P\{^1H\}$ NMR was present corresponding to hydride complex **C^{3A}.2c**.

This hydride complex **C^{3A}.2c** can be synthesized on larger scale by reacting **C^{3A}.2** and 1 equiv. of KHMDS in toluene under 2 bar of H_2 in a Schlenk tube (**Figures A^{3I}.5-6**).

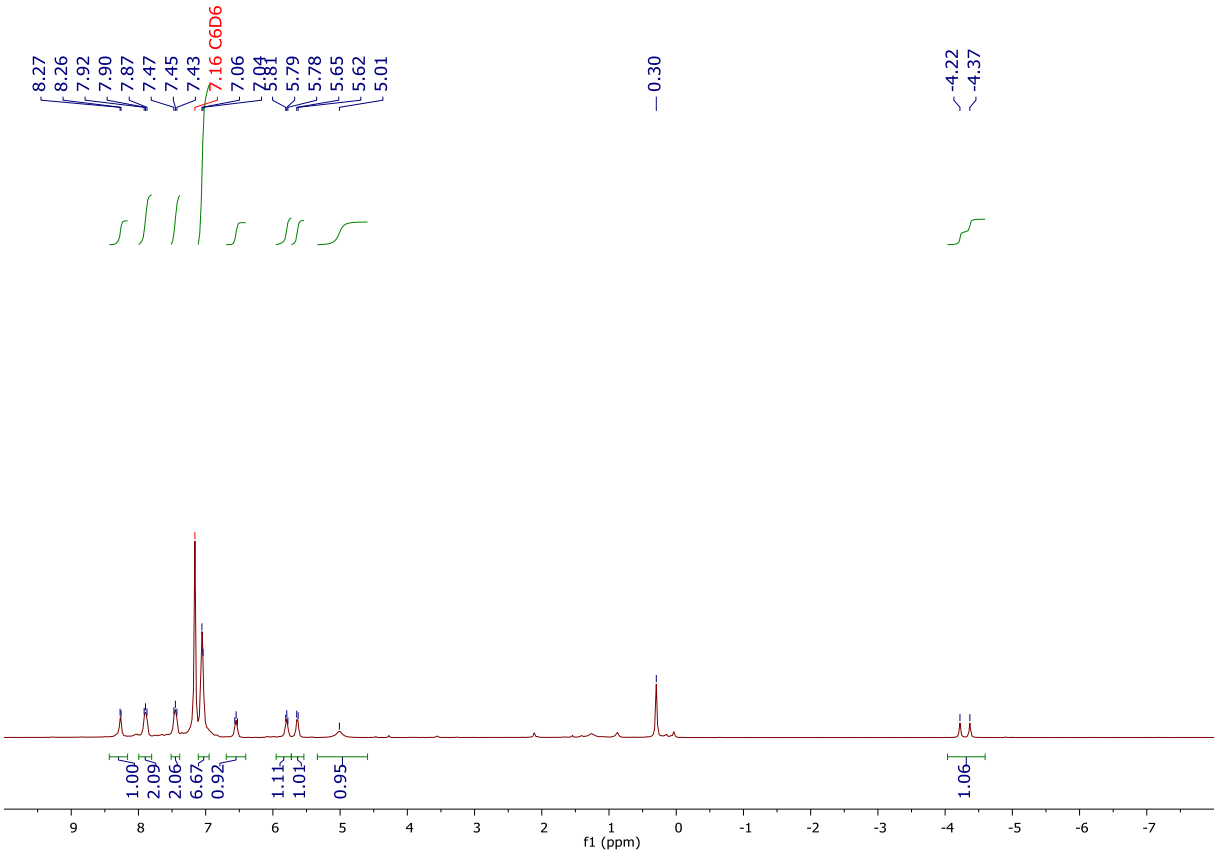

Figure A^{3l}.5 ^{1}H NMR spectrum of the complex **C^{3A}.2c** (C_6D_6, 400 MHz, 298K).

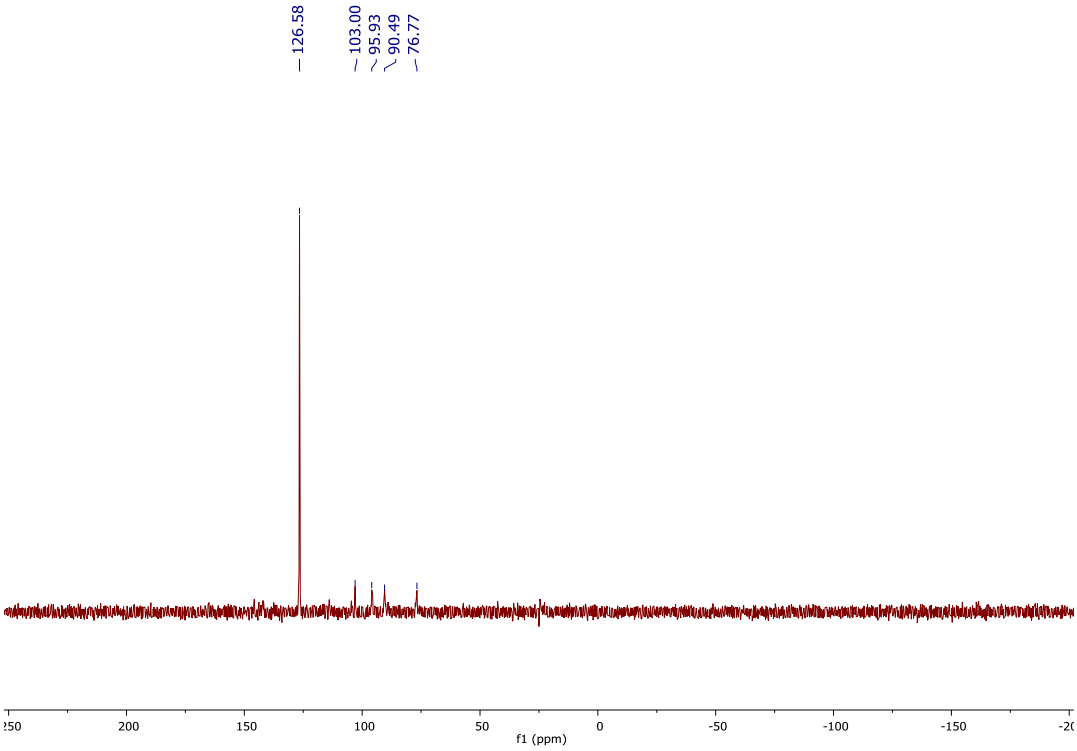

Figure A^{3l}.6 ^{31}P{^{1}H} NMR spectrum of the complex **C^{3A}.2c** (C_6D_6, 162 MHz, 298K).

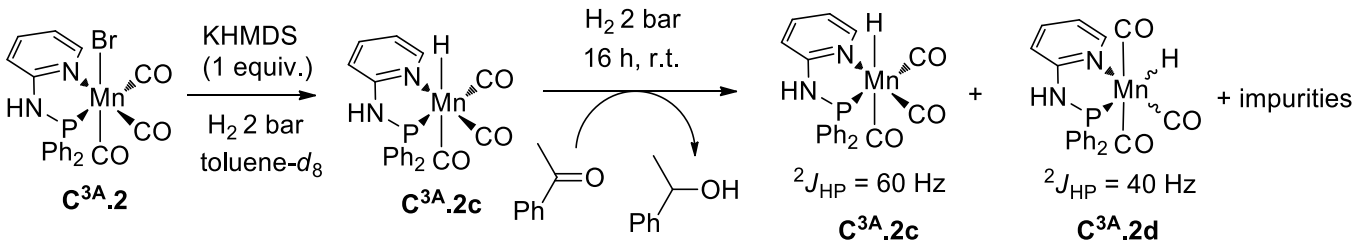

C^{3A}.2 **C^{3A}.2c** **C^{3A}.2c** **C^{3A}.2d**

$^{31}P\{^{1}H\}$ NMR (ppm):	132.0	132.0	151.1	108.2, 101.1

Scheme A^{3I}.4 Mechanistic experiment to deprotonated **C^{3A}.2** with KHMDS followed by addition of dihydrogen then acetophenone, realized in toluene-d_8 in a Young NMR tube

Next, the hydrogenation of acetophenone was monitored by NMR spectroscopies. Acetophenone (10 equiv.) was added to the solution of hydride **C^{3A}.2c** in a Young NMR tube. After one night at room temperature, the ^{1}H NMR (**Figure A^{3I}.7**) showed that phenylethanol was formed partially, with the characteristic signals appearing at 1.25 ppm and 4.50 ppm. Interestingly, in addition to the doublet at - 4.44 ppm ($^{2}J_{HP}$= 60 Hz) corresponding to **C^{3A}.2c**, a new doublet at - 6.27 ppm ($^{2}J_{HP}$= 40 Hz) in the hydride field was also present.

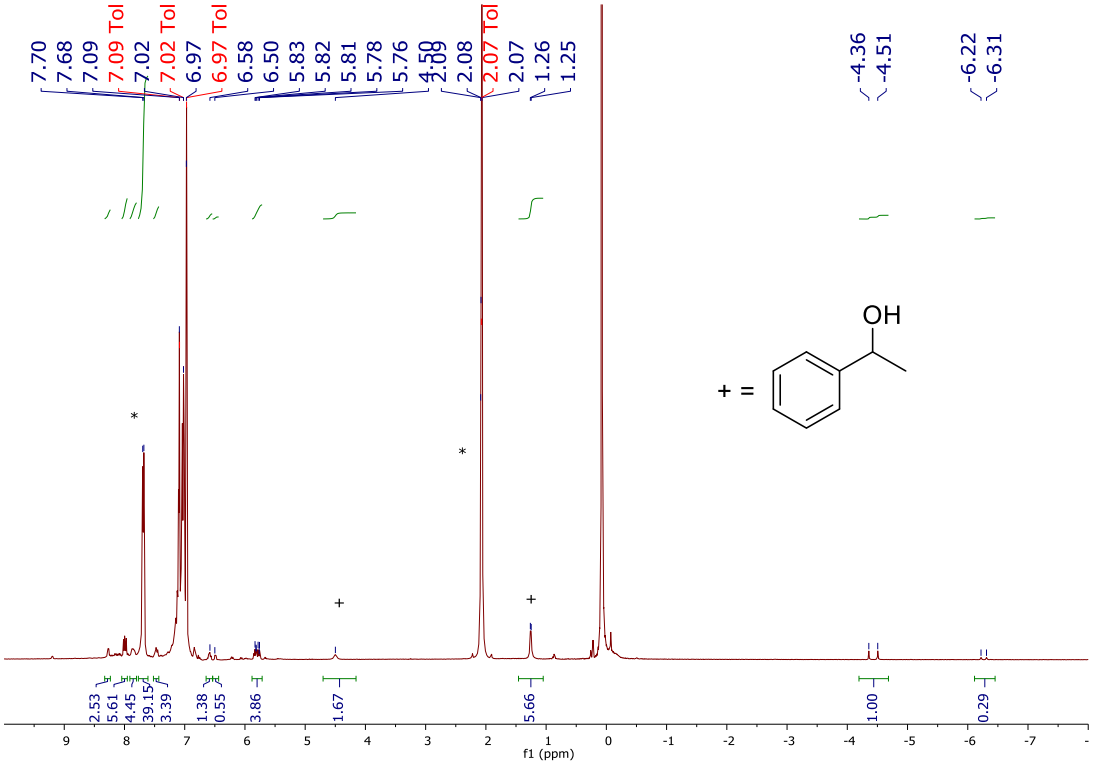

Figure A^{3I}.7 ^{1}H NMR spectrum of the reaction mixture after adding acetophenone (*) (toluene-d_8, 400 MHz, 298K).

A new isomer of the hydride **C^{3A}.2d** could be produced in the presence of the ketone/alcohol mixture characterized by a new doublet and a different $^{2}J_{HP}$ coupling constant (**Scheme A^{3I}.4**). Unfortunately, so far, no single crystals could be obtained. Finally, after a week-end at room temperature, the $^{31}P\{^{1}H\}$ NMR analysis showed that the deprotonated complex **C^{3A}.2b** was reformed as major species in solution, along with disappearance of hydride signals in ^{1}H NMR.

e) Conclusion

In conclusion, a series four new Mn(I) complexes bearing readily available phosphino-pyridinyl PN bidentate ligands have been prepared, fully characterized, and their catalytic activity was evaluated in the hydrogenation of aldehydes and ketones. The complex $Mn(CO)_3Br(\kappa^2P,N\text{-}Ph_2PN(H)Py)$ (**C^{3A}.2**) showed good performances for the hydrogenation of carbonyl derivatives under mild conditions with low catalytic loading and satisfying functional group tolerance, compared to the most active catalytic systems. In terms of catalyst design and taking the PN^{3}P-Mn **C^{2A}.1** complex as reference, it appears that simplifying the ancillary tridentate ligand to a bidentate one by removing one of its wingtip led to a dramatic increase of the activity of the resulting catalytic system (**Scheme A^{3I}.5**). Indeed, the use of the PN-Mn(I) complex **C^{3A}.2** allowed reducing the catalytic loading by a factor of ten, and lowering the temperature from 130 °C to 50 °C, still keeping the same level of activity.

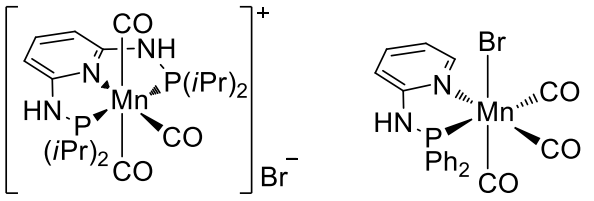

C^{2A}.1 5 mol%, *t*BuOK (10 mol%), toluene, 130 °C.

C^{3A}.2 0.5 mol%, KHMDS (2 mol%), toluene, 50 °C.

Scheme A^{3I}.5 Comparison of tridentate/bidentate catalytic systems for hydrogenation of ketones.

II- Hydrogenation of aldimines, through reductive amination

Contributions in the part: Synthesis of the complexes: D. W., A.B.-V.; Optimization: D. W., Scope: D. W., A.B.-V (minor).

Publication: D. Wei, A. Bruneau-Voisine, D. A. Valyaev, N. Lugan, J.-B. Sortais, *Chem. Commun.* **2018**, *54*, 4302–4305.

With the simple, and yet highly active, pre-catalyst **C^{3A}.2** in hand, we would like to extend the scope of substrates hydrogenated by our catalytic system. Unfortunately esters and nitriles were not reduced with this system but we found that aldimines can be converted into amines efficiently.

a) Optimization of the experimental conditions

We initially focused on the direct hydrogenation of *N*-benzylideneaniline **c1** as model substrate, using catalyst **C^{3A}.2** and a base, under 50 bar of H_2, based on previously optimized conditions for the hydrogenation of ketones.

First, we found that alcohols, and notably ethanol, were suitable solvents for the hydrogenation reaction (**Table A^{3II}.1**) as a green solvent alternative to toluene.

It then appeared that the nature of the base had little influence on the reaction, *t*BuONa, *t*BuOK, KHMDS, or Cs_2CO_3 leading to satisfactory conversions (see **Table A^{3II}.2**).

Table A^{3II}.1 Hydrogenation of benzylideneaniline: influence of the solvent.

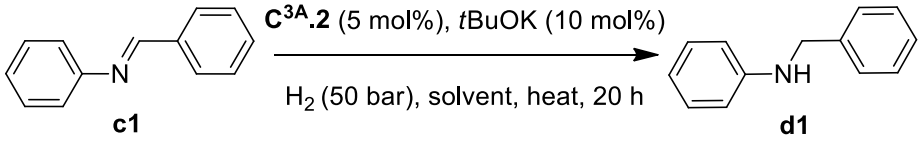

Entry	Temp. (°C)	Solvent	Yield (%)
1	130	Toluene	48
2	130	*t*-amyl alcohol	81
3	130	Dimethyl carbonate	84
4	130	THF	95
5	130	1,4-dioxane	40
6	130	CPME	43
7	100	THF	71
8	100	*t*-amyl alcohol	28
9	100	EtOH	>98
10	100	*n*-BuOH	95
11	100	MeOH	84

Conditions: an autoclave was charged in a glovebox with, in this order, **c1** (45.3 mg, 0.25 mmol), solvent (2.0 mL), **C^{3A}.2** (6.2 mg, 5.0 mol%), *t*BuOK (2.8 mg, 10 mol%), and then pressurized with H_2 (50 bar) and heated at the indicated temperature. Yield determined by GC and ^{1}H NMR spectroscopy.

Table A^{3II}.2 Hydrogenation of benzylideneaniline: influence of the base.

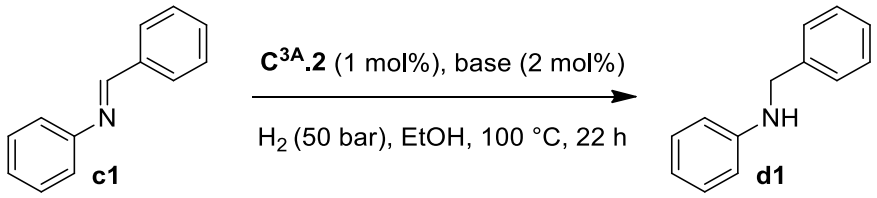

Entry	Base (mol%)	Yield (%)
1	*t*BuOK (2)	64
2	*t*BuONa (2)	50
3	Cs_2CO_3 (2)	57
4	KHMDS (2)	41

Conditions: an autoclave was charged in a glovebox with, in this order, **c1** (90.6 mg, 0.5 mmol), anhydrous ethanol (2.0 mL), **C^{3A}.2** (2.5 mg, 1.0 mol%), base (2 mol%), and then pressurized with H_2 (50 bar) and heated at 100 °C. Yield determined by GC and ^{1}H NMR spectroscopy.

The activity of complexes **C^{3A}.1-4** was compared at 80 °C with 1 mol% catalyst and 2 mol% of *t*BuOK (**Table A^{3II}.3**, entries 1-4) and complex **C^{3A}.2** appeared to be the most active one like in the previous hydrogenation of ketones and aldehydes. Increasing the catalytic loading to 2 mol% led to a full conversion (entry 5). Interestingly, the temperature could be decreased to 50 °C without any detrimental effect on activity (entry 6), and even to 30 °C where a decent conversion still occurred (76%, entry 7).

Table A^{3II}.3 Optimization of the reaction conditions of the hydrogenation of benzylideneaniline **c1** with manganese catalysts **C^{3A}.1-4**.

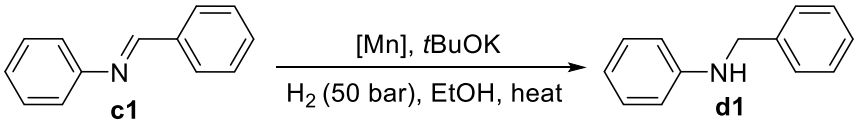

Entry	Catalyst (mol%)	Temperature (°C)	Time (h)	Yield (%)[c]
1[a]	**C^{3A}.1** (1)	80	19	40
2[a]	**C^{3A}.2** (1)	80	24	74
3[a]	**C^{3A}.3** (1)	80	19	17
4[a]	**C^{3A}.4** (1)	80	19	1
5[b]	**C^{3A}.2** (2)	80	17	> 98
6[b]	**C^{3A}.2** (2)	50	17	> 98
7[b]	**C^{3A}.2** (2)	30	24	76

[a] Conditions: an autoclave was charged in a glovebox with, in this order, **c1** (181 mg, 1.0 mmol), EtOH (4.0 mL), Mn-complex (1 mol%), *t*BuOK (2.2 mg, 2 mol%), and then pressurized with H_2 (50 bar) and heated. [b] **c1** (91 mg, 0.5 mmol), EtOH (2.0 mL), **C^{3A}.2** (5.0 mg, 2 mol%), *t*BuOK (2.8 mg, 5 mol%). [c] Yields were determined by ^{1}H NMR spectroscopy and GC on the crude mixture.

In terms of practical and economical synthesis of amines, the direct reductive amination of aldehydes is more desirable than hydrogenation of corresponding isolated imines. Hence, we turned our attention towards the direct synthesis of benzylaniline **d1** from benzaldehyde **f1** and aniline **g1**. In a first attempt, all the components, *i.e.* **C^{3A}.2**, **f1**, **g1**, *t*BuOK, and H_2, were introduced in an autoclave which was heated at 80 °C overnight (**Scheme A^{3II}.1**, conditions A). Disappointingly, a mixture of benzylalcohol **e1** (44%), imine **c1** (38%), and the desired amine **d1** (18%) was obtained, showing that the hydrogenation of benzaldehyde occurred faster than

the condensation with aniline. In a second strategy, the condensation step was carried out in the presence of the catalyst and the base at 80 °C for 5 h, then the reaction mixture was pressurized under H_2 and stirred at 80 °C overnight (conditions B). Unfortunately, the main products were again alcohol **e1** (61%) and imine **c1** (29%). Finally, we decided to perform first the condensation of the aldehyde with the amine in EtOH, imine **c1** being formed in 90% yield after 24 h at 100 °C, and then to add the pre-catalyst, the base, and H_2 to the crude imine before heating under stirring at 80 °C overnight (Conditions C). Under these conditions, the desired *N*-benzylaniline **d1** was obtained in high yield (87%). Here after, 1.2 equivalent of amines **g** were used to ensure the full conversion of the aldehyde **f** into the imines **c** before the hydrogenation step.

Scheme A^{3II}.1 Optimization of the procedure for reductive amination of benzaldehyde with aniline in the presence of manganese pre-catalyst complex **C^{3A}.2**.

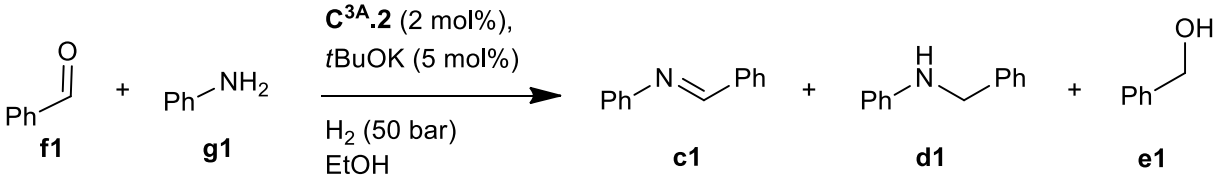

f1 + **g1** → **c1** + **d1** + **e1**

	c1	**d1**	**e1**
Conditions A:	38	18	44
Conditions B:	29	7	61
Conditions C:	2	87	11

Conditions A: an autoclave was charged with **C^{3A}.2** (5.0 mg, 2 mol%), anhydrous ethanol (2.0 mL), aniline (46 µL, 0.5 mmol), benzaldehyde (51.0 µL, 0.5 mmol), *t*BuOK (2.8 mg, 5 mol%) and H_2 (50 bar) and heated at 80 °C for 20 h.

Conditions B: an autoclave was charged with **C^{3A}.2** (5.0 mg, 2 mol%), anhydrous ethanol (2.0 mL), aniline (46 µL, 0.5 mmol), benzaldehyde (51.0 µL, 0.5 mmol) and *t*BuOK (2.8 mg, 5 mol%). After heating at 80 °C for 5 h, H_2 (50 bar) was charged and the mixture heated at 80 °C for 20 h.

Conditions C: in a 20 mL Schlenk tube aniline (46 µL, 0.5 mmol) and benzaldehyde (51.0 µL, 0.5 mmol) in anhydrous ethanol (2.0 mL) were heated at 100 °C for 24 h. The reaction mixture was transferred into an autoclave followed by **C^{3A}.2** (5.0 mg, 2 mol%), *t*BuOK (2.8 mg, 5 mol%) and H_2 (50 bar), then heated at 80 °C for 20 h.

b) Scope of the reaction

We next probe the scope of this first manganese catalyzed reductive amination system thus defined.

In general, as far as the formation of the imines is not a limiting step (for benzaldehyde derivatives with anilines, the condensation may be carried out at r.t. in 1 h, (**Scheme A^{3II}.2**, entry 4), the subsequent hydrogenation proceeded well for a wide variety of aldehydes and amines (**Scheme A^{3II}.2**). First, benzaldehydes derivatives bearing either electron donating or electron withdrawing groups both reacted with anilines to afford *in fine* the corresponding amines in good yield (entries 1-16). Noticeably, halogen substituents (**d6**-**d10**), including iodo substituent, were well tolerated with less than 10% de-iodination in the cases of **d9** and **d10**. Esters and amides moieties were not reduced under these conditions (**d12**-**d13**). Interestingly, starting from 4-formylacetophenone **f14** in the presence of 2 equivalents of aniline **g1**, only the aldimine moiety was reduced in the transient di-imine intermediate **c14** affording the corresponding amino-ketimine **d14,** while in the presence of 1 equivalent of **g1**, amino-ketone **d15** was obtained in good yield. In the same vein, the reductive amination of benzaldehyde **a1** with 4-acetyl-aniline **g16** led selectively to the corresponding 4-acetylamine **d16** leaving the ketone functionality untouched. Organometalllic ferrocenylaldehyde **f17** was also suitable for this protocol. Several heterocycles, including pyrrole, furane, pyridine, thiophene, and thiazole were well tolerated by the catalytic system (entries 18-23). It is noteworthy that this reductive amination protocol is not limited to aniline derivatives, as sulfonylamide **g24** as well as aliphatic primary **g25-g27** and secondary amines **g28-g30** were also successfully coupled. Ethylenediamine **g31** afforded the *N*,*N'*-dibenzylethylenediamine **d31,** without formation of imidazolines.[14] Remarkably, the amino-alcohols **g32**-**g34** were alkylated to afford selectively the corresponding hydroxyamines, the pending hydroxy group not entering into a potentially competitive *N*-alkylation process.[15]

To complete the series of amines amenable for this transformation, α-amino-esters **g35**-**g36** were alkylated with success. A series of aliphatic aldehydes (**f37**-**f40**), including butanal (**f37**), readily available by hydroformylation or bio-sourced aldehydes such cinnamaldehyde (**f40**), were also successfully engaged in the

present reductive amination protocol. Non-conjugated C=C were typically not reduced in the course of the reaction (entries 38-39), while conjugated C=C bonds were reduced under harsher conditions, which is in line with the selectivity observed for the reduction of α,β-unsatured ketones (entry 40).

Finally, it has to be noted that a few functional groups such as terminal alkyne, nitro group, or unprotected pyrrole were not tolerated.

Scheme A^{3II}.2 Scope of the reductive amination of aldehydes with amines in presence of **C^{3A}.2** as pre-catalyst.[a]

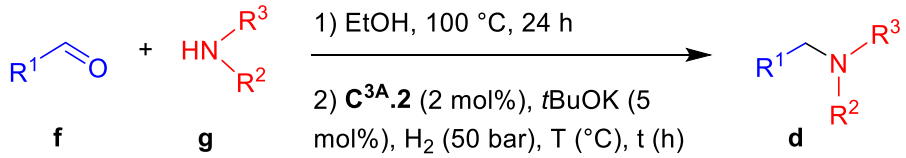

f **g** **d**

Entry	Product		Temp. (°C)	time (h)	Yield (%)[b]
1	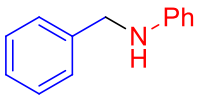	**d1**	50	18	93
2	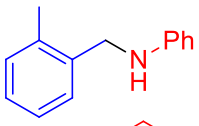	**d2**	100	36	94
3	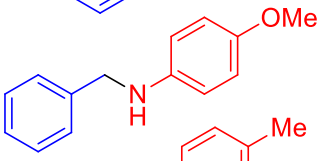	**d3**	100	48	72
4	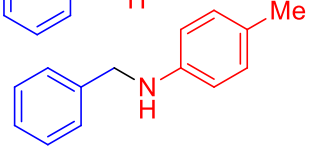	**d4**	100	24	78[c]
5	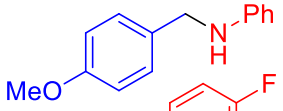	**d5**	50	48	87
6	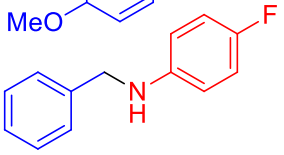	**d6**	100	48	28
7	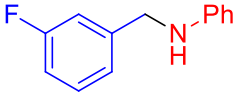	**d7**	80	36	90
8	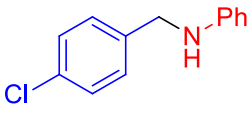	**d8**	50	48	80

Entry	Product		Temp. (°C)	time (h)	Yield (%)[b]
9	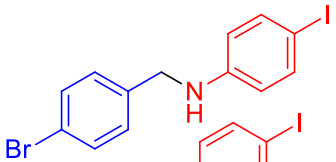	**d9**	100	36	98[d]
10	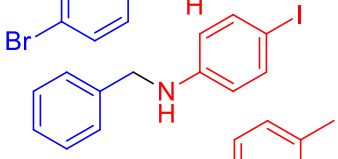	**d10**	100	36	98[d]
11	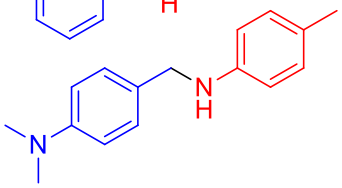	**d11**	80	36	97
12	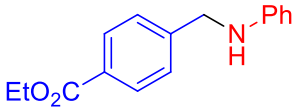	**d12**	80	48	92
13	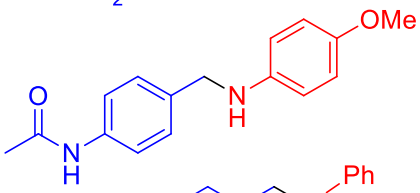	**d13**	100	48	95
14[e]	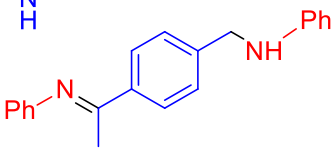	**d14**	80	36	88
15	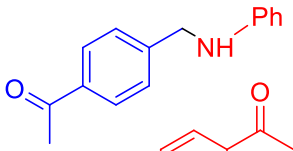	**d15**	50	18	73
16	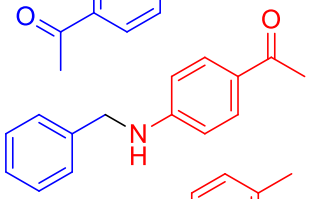	**d16**	50	18	96
17	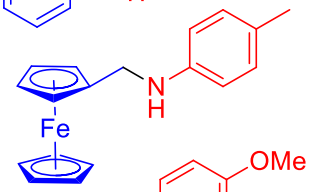	**d17**	80	48	98
18	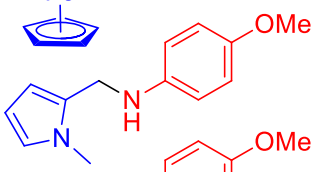	**d18**	100	48	97
19	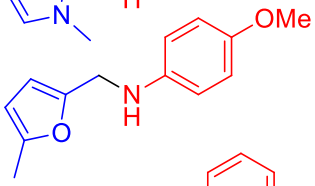	**d19**	100	48	90
20	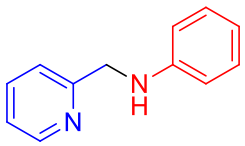	**d20**	80	36	68

Entry	Product		Temp. (°C)	time (h)	Yield (%)
21	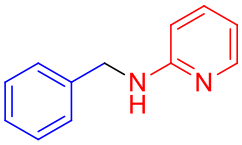	**d21**	80	48	55
22	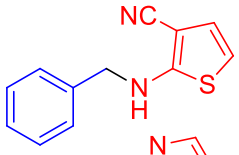	**d22**	80	48	90
23	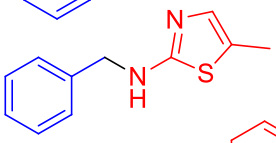	**d23**	80	48	92
24	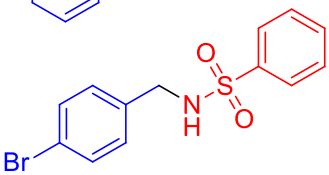	**d24**	80	48	93
25	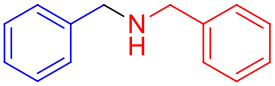	**d25**	100	48	90
26	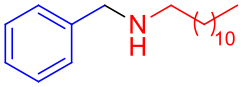	**d26**	80	18	95
27	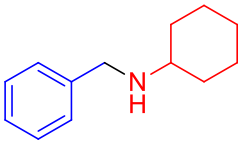	**d27**	80	48	94
28	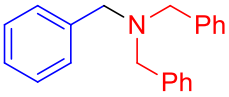	**d28**	80	36	96
29	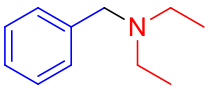	**d29**	80	36	94
30	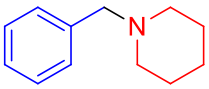	**d30**	80	36	93
31[f]	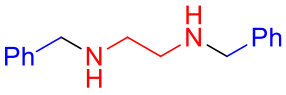	**d31**	100	48	95
32	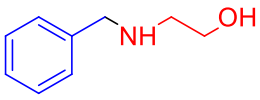	**d32**	100	24	86

Entry	Product		Temp. (°C)	time (h)	Yield (%)
33	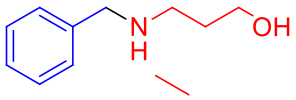	**d33**	100	24	83
34	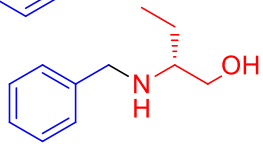	**d34**	100	18	97
35[g]	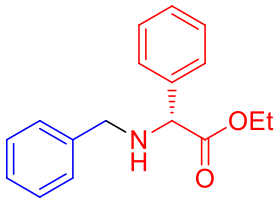	**d35**	100	18	90
36[g]	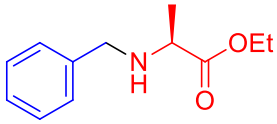	**d36**	100	36	91
37	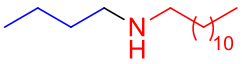	**d37**	50	48	96
38	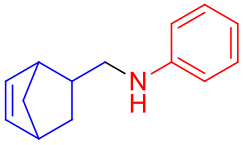	**d38**	50	48	95
39	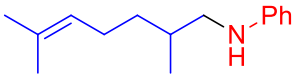	**d39**	50	36	96
40[g]	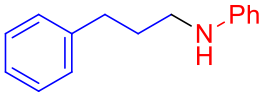	**d40**	100	48	93

[a] Typical reaction conditions: a solution of aldehyde f (0.5 mmol), amine **g** (0.6 mmol) and anhydrous EtOH (2.0 mL) was stirred at 100 °C for 24 h, then transferred to a 20 mL autoclave followed by **C^{3A}.2** (5.0 mg, 2 mol%) and *t*BuOK (2.8 mg, 5 mol%). The autoclave was subsequently charged with H_2 (50 bar) and heated. [b] Isolated yield after purification. [c] a1 (4.3 mmol), condensation: 2 h, r.t. [d] c.a. 10% of deiodination product. [e] **g1** (100 µL, 1.1 mmol). [f] **f1** (122 µL, 1.2 mmol). [g] **C^{3A}.2** (5 %mol), *t*BuOK (10 mol%).

In conclusion, we have shown that a well-defined manganese pre-catalyst featuring a readily available bidendate diphenyl-(2-aminopyridinyl)-phosphine ligand catalyzes efficiently the reductive amination of aldehydes using H_2 as reductant with a wide functional group tolerance. This amine synthesis protocol significantly enlarges the scope of reactions catalyzed by manganese complexes and nicely complements a previous approach based on alkylation of amines with alcohols.[15]

III- Conclusion, Part A

The development of highly active bidentate manganese(I) catalysts such as **C^{3A}.2** is surprising because, usually, removing of one arm on the ligand should bring to easier ligand dissociation. However, **C^{3A}.2** was more active that it tridentate analogue for hydrogenation of ketones. The catalytic performance of this catalyst (0.5 mol%, 50 °C, 50 bar) were close to one of the best systems developed by Kempe (0.1-1 mol%, 60 °C, 20 bar)[16] and Clarke (1 mol%, 50 °C, 50 bar).[17] Moreover, this complex could also catalyze the hydrogenation of aldimines leading to the development of the first manganese catalyzed reductive amination protocol. In addition of being complementary to the hydrogen borrowing strategy to produce alkylated amines, the reductive amination, starting from aldehyde instead of alcohol, could operate under mild conditions as the reaction could be run at 50 °C. Notably, the scope of the reductive amination was not limited to anilines derivatives.

Regarding the price of the ligand, simplifying the ligand was a benefice. However, the presence of a phosphorus atom makes these ligands still relatively expensive. In the next chapter, we will go one step further using inexpensive commercially available ligands in association with manganese to promote hydrogen transfer reactions.

IV- References

[1] D. A. Valyaev, G. Lavigne, N. Lugan, *Coord. Chem. Rev.* **2016**, *308*, 191–235.
[2] R. Langer, F. Bönisch, L. Maser, C. Pietzonka, L. Vondung, T. P. Zimmermann, *Eur. J. Inorg. Chem.* **2015**, 141–148.
[3] M. Stanbury, J.-D. Compain, S. Chardon-Noblat, *Coord. Chem. Rev.* **2018**, *361*, 120–137.
[4] A. Nerush, M. Vogt, U. Gellrich, G. Leitus, Y. Ben-David, D. Milstein, *J. Am. Chem. Soc.* **2016**, *138*, 6985–6997.
[5] A. Bruneau-Voisine, D. Wang, T. Roisnel, C. Darcel, J.-B. Sortais, *Catal. Commun.* **2017**, *92*, 1–4.
[6] S. M. Aucott, A. M. Z. Slawin, J. D. Woollins, *J. Chem. Soc., Dalton Trans.* **2000**, 2559–2575.
[7] D. Benito-Garagorri, K. Mereiter, K. Kirchner, *Collect. Czech. Chem. Commun.* **2007**, *72*, 527–540.
[8] M. Alvarez, N. Lugan, R. Mathieu, *J. Chem. Soc., Dalton Trans.* **1994**, 2755–2760.
[9] E. Mothes, S. Sentets, M. A. Luquin, R. Mathieu, N. Lugan, G. Lavigne, *Organometallics* **2008**, *27*, 1193–1206.
[10] R. K. Henderson, C. Jimenez-Gonzalez, D. J. C. Constable, S. R. Alston, G. G. A. Inglis, G. Fisher, J. Sherwood, S. P. Binks, A. D. Curzons, *Green Chem.* **2011**, *13*, 854–862.
[11] T. Hirata, A. Matsushima, Y. Sato, T. Iwasaki, H. Nomura, T. Watanabe, S. Toyoda, S. Izumi, *J. Mol. Catal. B: Enzym.* **2009**, *59*, 158–162.
[12] S. Elangovan, C. Topf, S. Fischer, H. Jiao, A. Spannenberg, W. Baumann, R. Ludwig, K. Junge, M. Beller, *J. Am. Chem. Soc.* **2016**, *138*, 8809–8814.
[13] S. Elangovan, M. Garbe, H. Jiao, A. Spannenberg, K. Junge, M. Beller, *Angew. Chem. Int. Ed.* **2016**, *55*, 15364–15368.
[14] M. Ishihara, H. Togo, *Tetrahedron* **2007**, *63*, 1474–1480.
[15] S. Elangovan, J. Neumann, J.-B. Sortais, K. Junge, C. Darcel, M. Beller, *Nat. Commun.* **2016**, *7*, 12641.
[16] F. Kallmeier, T. Irrgang, T. Dietel, R. Kempe, *Angew. Chem. Int. Ed.* **2016**, *55*, 11806–9.
[17] M. B. Widegren, G. J. Harkness, A. M. Z. Slawin, D. B. Cordes, M. L. Clarke, *Angew. Chem. Int. Ed.* **2017**, *56*, 5825–5828.

B - Transfer Hydrogenation using isopropanol as proton source

I- Well-defined aminomethylpyridine manganese complexes

Contributions in the part: Synthesis of the complexes: A.B.-V.; Optimization, Mechanistic studies: A.B.-V.; Scope: A.B.-V., D. W.

Publication: A. Bruneau-Voisine, D. Wang, V. Dorcet, T. Roisnel, C. Darcel, J.-B. Sortais, *Org. Lett.* **2017**, *19*, 3656-3659.

In the quest for simple and inexpensive catalytic systems, we were looking for alternative ligands, suitable to promote bi-functional catalysts.[1–3] We were inspired by ruthenium catalysis, and in particular the work of Baratta who demonstrated that simple bidendate aminomethylpyridine ligand (ampy) could significantly improve the activity and the robustness of phosphino-ruthenium **Ru-16/17** hydrogen transfer catalysts, reaching very high TON and TOF.[4]

a) Synthesis of the complexes

We have first prepared a series of four manganese complexes, bearing as ligand 2-hydroxymethylpyridine, 2-aminomethylpyridine, 2-(*N*-methyl-aminomethyl)-pyridine and 2-(*N*,*N*-dimethyl-aminomethyl)pyridine (**Scheme B^{3I}.1**). The synthesis of the complexes is straightforward: for aminomethylpyridine derivatives, complexes **C^{3B}.1-3** were obtained as yellow solids with good yields (93-95%) by reaction of one equivalent of the ligand with one equivalent of $Mn(CO)_5Br$ in toluene at 110 °C for 4 h. Complex **C^{3B}.4** was prepared in hexane at 70 °C as described by Miguel.[5] Complexes **C^{3B}.1-3** were fully characterized by NMR spectroscopies, IR and

elemental analysis. The molecular structures were confirmed by X-Ray diffraction studies on single crystals (**Figure B^{3I}.1**).

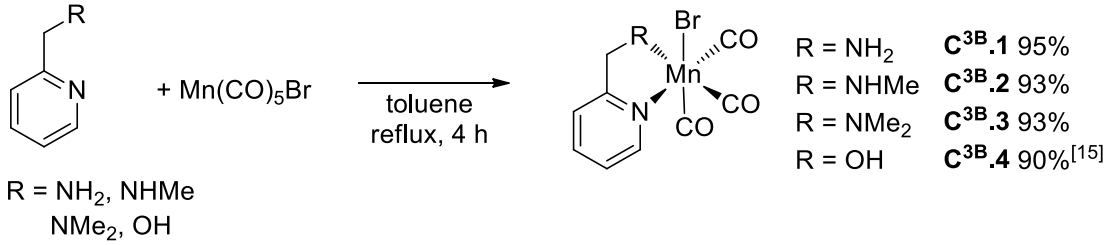

Scheme B^{3I}.1 Synthesis of well-defined Manganese complexes used in this study.

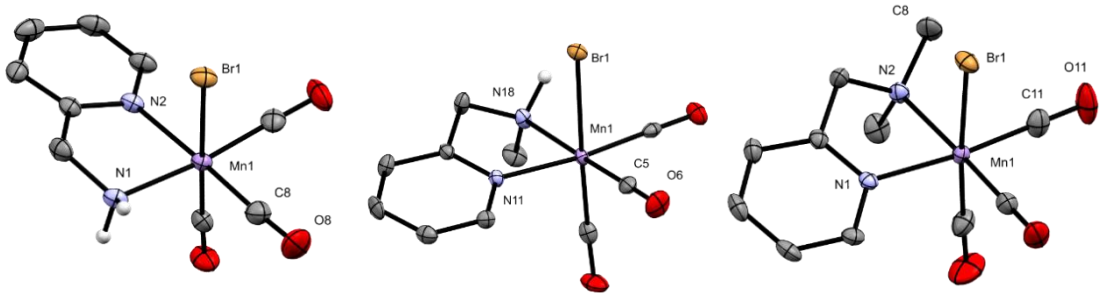

C^{3B}.1 **C^{3B}.2** **C^{3B}.3**

Figure B^{3I}.1 ORTEP views of the molecular structures of complexes **C^{3B}.1-3**, with thermal ellipsoids drawn at 50% probability. Hydrogens, except the NH, were omitted for clarity.

In addition, when two equivalents of 2-aminomethylpyridine reacted with one equivalent of $Mn(CO)_5Br$ in the same conditions, a mixture of the complex **C^{3B}.1** and the cationic complex bearing two ligands **C^{3B}.1e** was obtained (See S.I. Part A-I Figure S42). A single crystal suitable for X-ray diffraction grown in a saturated solution of methanol, revealing that the second ligand in linked by the primary amine to the manganese center (See S.I. Part A-I Figure S32).

b) Optimisation of the transfer hydrogenation of ketones

Then, we explored the catalytic activities of the complex **C^{3B}.1** for the reduction of acetophenone in the presence of isopropanol as the hydrogen source. To our delight, with 1 mol% of **C^{3B}.1**, 2 mol% of *t*BuOK as the base, at 80 °C, within 5 min, we observed a full reduction of the ketone to the corresponding 1-phenylethanol (**Table B^{3I}.1**, entry 1).

Table B^{3I}.1 Optimization of the parameters of the reaction.

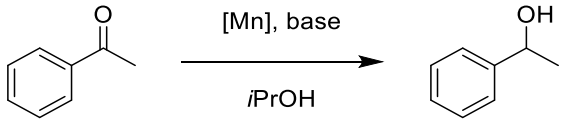

Entry	Catalyst (mol%)	*t*BuOK (mol%)	Temp. (°C)	Time	Conv. (%)
1	**C^{3B}.1** (1)	2	80	5 min	> 97
2	**C^{3B}.1** (0.5)	1	80	15 min	> 97
3	**C^{3B}.1** (0.1)	0.2	80	5 min	31
				10 min	58
				2 h	> 97
4	**C^{3B}.1** (0.05)	0.1	80	2 h 30	80
5	**C^{3B}.1** (0.01)	0.02	80	16 h	20
6	**C^{3B}.1** (0.5)	1	60	1 h	96
7	**C^{3B}.1** (0.5)	1	30	3 h	50
				16 h	97
8	**C^{3B}.1** (0.1)	0.2	30	19 h	90
9	**C^{3B}.1** (1)	-	80	1 h	0
10	-	10	80	1 h	5
11	Ampy (1)	2	80	1 h	0
12	$Mn(CO)_5Br$ (1)	2	80	1 h	< 1
13	**C^{3B}.2** (0.5)	0.1	80	15 min	97
14	**C^{3B}.3** (0.5)	0.1	80	30 min	8
15	**C^{3B}.4** (0.5)	0.1	80	20 min	6

Typical conditions: to a Schlenk tube, under argon, were added in this order: acetophenone (0.5 mmol), *i*PrOH (2 mL), catalyst precursor, and *t*BuOK. The conversion was determined by GC and ^{1}H NMR.

The catalytic loading was then decreased to 0.1 mol%, leading to a conversion of 31% and 58%, after 5 and 10 min respectively (TOF = 3720 and 3480 h^{-1}, respectively). An average TOF of 3600 h^{-1} was obtained, demonstrating the high activity of complex **C^{3B}.1**. With a very low catalytic loading of 0.01 mol%, a TON of 2000 was achieved after 16 h (entry 5). Encouraged by these results, the temperature was then decreased to room temperature. With 0.5 mol% of catalyst,

after 3 h, 50% of the ketone was reduced and a full conversion was obtained after 16 h (entry 7). Even with a ratio substrate: catalyst of 1000, the reduction of acetophenone was still achieved in 90% conversion (entry 8). Control experiments (entries 9-12) demonstrated that all the components of the catalytic system were crucial to obtain high activities.[6] Compared to catalyst **C^{3B}.1**, the catalyst **C^{3B}.2**, bearing one methyl substituent on the amine moiety, was found slightly less active (**Figure B^{3I}.2**) and catalysts **C^{3B}.3** and **C^{3B}.4** showed very low activities (entries 14, 15). These results show that the presence of NH moieties on the ligand is crucial for the hydrogen transfer to occur.

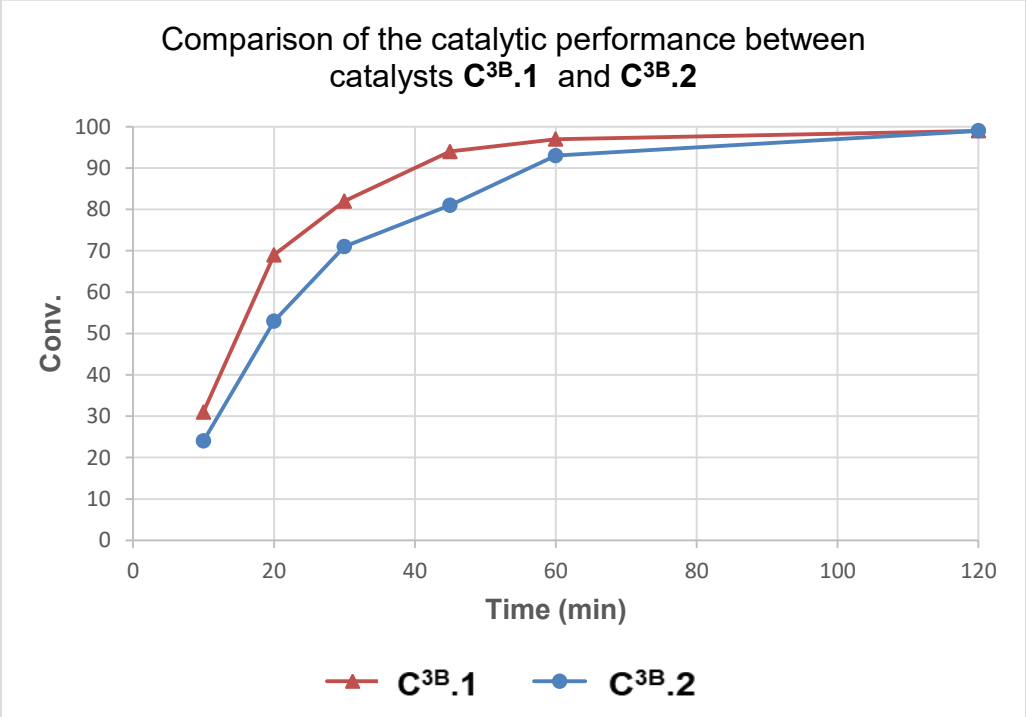

Figure B^{3I}.2 Kinetic of reduction of acetophenone performed at 60 °C by **C^{3B}.1** and **C^{3B}.2** (0.5 mmol acetophenone, 0.5 mol% catalyst, 1 mol% *t*BuOK, *i*PrOH (2 mL)).

A comparison of the activity with different bases has been realized, using 0.5 mol% of **C^{3B}.1**, 1 mol% base in *i*PrOH (0.25 mol.L^{-1}) at 60 °C in 30 min. While the use of *t*BuOK gave the best result (95% conv.), it has to be noted that cheaper bases such as KOH (92% conv.) and NaOH (89 % conv.) were also good alternatives (**Table B^{3I}.2**). Other bases, based on potassium, such as K_2CO_3 and KOAc were inefficient. Triethylamine could not be used as base either.

Table B^{3I}.2: Screening of several bases.

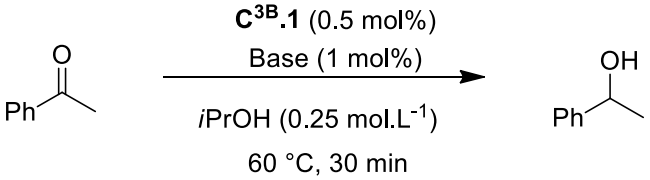

Entry	Base	Conv.
1	*t*BuOK	95
2	KOH	92
3	NaOH	89
4	K_2CO_3	0
5	KOAc	0
6	Et_3N	0

Typical conditions: To a Schlenk tube, under argon, were added in this order: acetophenone (0.5 mmol), *i*PrOH (2 mL), catalyst **C^{3B}.1b** (0.5 mol%), and base (1 mol%). The conversion was determined by GC and ^{1}H NMR.

c) Scope of the transfer hydrogenation of carbonyl derivatives

The generality of the reaction was then probed using two optimal conditions: 80 °C, 20 min or 30 °C, 16 h, 0.5 mol% of **C^{3B}.1** and 1 mol% of *t*BuOK (**Scheme B^{3I}.2**). In general, the reaction proceeded well with a large range of substrates. Steric hindrance was well tolerated as from acetophenone to pivalophenone or 2-methylacetophenone, high yields of the corresponding alcohols were obtained (entries 1-6). Aromatic ketones bearing electron donating groups (entries 6-9) were reduced with high yields. Interestingly, aromatic aldehydes were also converted nicely to the corresponding benzylalcohols (entries 10-11), with almost no side reactions[7] (in the case of 4-phenylbenzaldehyde, less than 5% of the product of the aldol condensation of the aldehyde with acetone was detected in the crude NMR). Halogen-containing substrates are also suitable for this reduction without formation of dehalogenated products (entries 12-17). Functional group tolerance was then evaluated: cyano, nitro, amino, amido and ester were tolerated (entries 18-24). In the

case of ethyl levunilate (entry 24, 98% conversion), a mixture of cyclic γ-valerolactone (84%) and linear isopropyl-4-hydroxy-pentanoate (16 %), resulting from trans-esterification, was obtained. Aliphatic and cyclic ketones were fully converted to the corresponding alcohols (entries 25-29). In contrast to part A with **C^{3A}.2** where saturated ketones were obtained, conjugated α,β-unsaturated ketones were reduced to the corresponding unsaturated alcohols with high selectivity, as the sole reduction of the carbonyl moieties was observed in the case of β-ionone (entry 31), and only 5% of the saturated alcohol was detected in the case of cinnamyl-ketone (entry 30). For very challenging cinnamaldehyde (entry 32), the chemoselectivity was perfect towards the allylic alcohol and less than 7% of aldol consendation by-products were detected after 2 h at 80 °C. Finally, heteroaromatic ketones were tested: thiophenyl derivative was fully reduced to the corresponding alcohol (entry 33), while 4-acetyl pyridine led to moderate conversion at 80 °C and almost no conversion at 30 °C (entry 34). The bidentate 2-acetyl-pyridine poisoned the catalyst, and little conversion was observed under both conditions (entry 35). The same limitation was observed in the case of 2-acetylfurane and several 1,3-diketones.

Methylbenzoate was not reduced with this catalytic system, even with harsh reaction conditions (up to 110 °C), the product of the reaction being isopropylbenzoate.

Scheme B[3l].2: Scope of the hydrogen transfer of ketones giving alcohols under the catalysis of **C[3B].1**.[a]

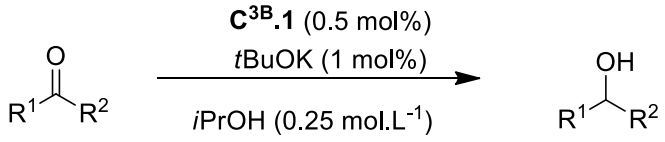

Entry	Substrate	Product		Conv. (Yield) at 80 °C, 20 min	Conv. (Yield) at 30 °C, 16 h
1			X = H, Y = Me	> 99 (93)	> 99
2	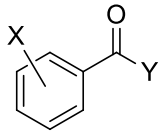	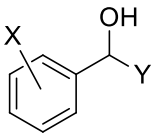	X = H, Y = Et	99	99 (84)
3			X = H, Y = iPr	> 99 (95)	> 99
4			X = H, Y = tBu	92	99 (99)
5			X = H, Y = cyclopropyl	77 (62)	50
6			X = 2-Me, Y = Me	94 (88)	75
7			X = 4-Me, Y = Me	95 (87)	87
8	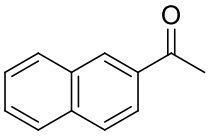	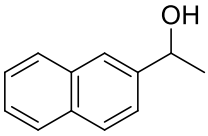		97	94 (89)
9			X = 4-OMe Y = Me	83	66
10			X = 3,4,5-$(OMe)_3$ Y = H	> 99 (99)	62[b]
11			X = 4-Ph, Y = H	> 99[c] (92)	99
12			X = 4-I, Y = Me	26	> 99 (99)[d]
13			X = 4-Br, Y = Me	98	98 (87)
14			X = 2-Cl, Y = Me	> 99	> 99 (99)
15	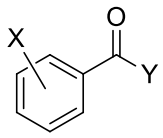	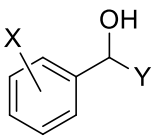	X = 4-F, Y = Me	96(85)	91
16			X = 4-CF_3, Y = Me	> 99	> 99 (96)
17			X = H, Y = CF_3	> 99 (58)	20
18			X = 4-CN, Y = Me	> 99	89 (78)
19			X = 4-NO_2, Y = Me	97	> 99 (99)
20			X = 4-  Y = Me	73	30
21			X = NEt_2, Y = H	97 (83)	74
22			X = NH_2, Y = Me	82	58[e]
23			X = NHC(O)CH_3, Y = H	95 > 99 (90)[c, f]	26

Entry	Substrate	Product		Conv. (Yield) at 80 °C, 20 min	Conv. (Yield) at 30 °C, 16 h
24	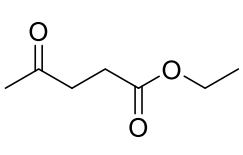	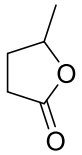		98[g]	41[g]
25	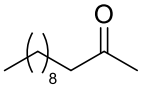	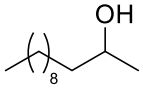		95 (93)	80
26	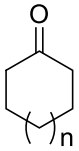	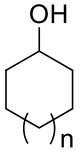	n = 1	> 99 (99)	> 99
27			n = 2	96	94 (94)
28	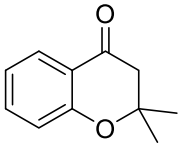	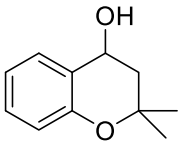		73 > 99 (99)[h]	25
29	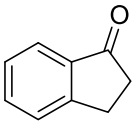	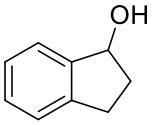		67	50
30	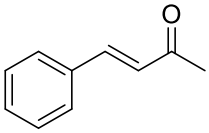	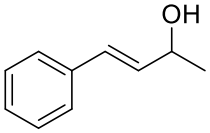		90[i]	92 (87)
31	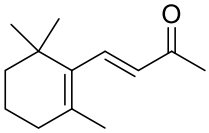	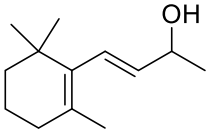		81 100 (90)[f]	87
32	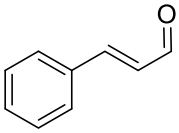	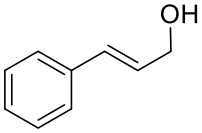		92 (80) [j]	5
33	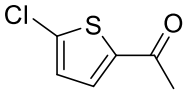	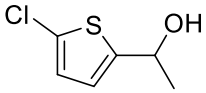		94 96 (96)[f]	80
34	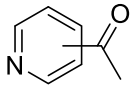	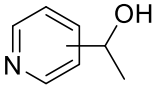	2-acetyl	56	11
35			3-acetyl	13	10

[a] Typical conditions: To a Schlenk tube, under argon, were added in this order: catalyst **C^{3B}.1**, *i*PrOH (0.25 molL^{-1}), ketone or aldehyde (0.5 or 2 mmol) and *t*BuOK. The conversion was determined by ^{1}H NMR on the crude mixture. Isolated yield in parentheses; [b] selectivity alcohol: aldol by-products of 67:33. [c] 5% of aldol condensation by-product were detected in the crude mixture; [d] one week, due to low solubility of the starting material; [e] 72 h; [f] 1 h; [g] selectivity γ-valerolactone/Isopropyl-4-hydroxypentanoate 84/16 at 80 °C and 77/23 at 30 °C; [h] 2 h, *i*PrOH 4 mL; [i] enol 95%, 4-phenylbutan-2-ol 5%; [j] 2 h, 7 % aldol condensation by-products were detected in the crude mixture.

d) Mechanistic insights

Then, to gain insight into the nature of the catalytic active species, we performed stoichiometric reactions between complex **C^{3B}.1** and the base. After 24 h at room temperature, the dimeric manganese complex **C^{3B}.1b,** resulting from the deprotonation of the NH moieties, could be isolated in 42% yield (**Scheme B^{3I}.3**).[8] The similar complex **C^{3B}.2b** has been obtained starting from **C^{3B}.2**, unfortunately not in a pure form. A similar dimer was obtained by Miguel starting from 2-pyridinemethanol.[5] The molecular structure of **C^{3B}.1b** was confirmed by X-Ray diffraction studies (**Figure B^{3I}.3**). Attempts to trap monomeric species after deprotonation in the presence of pyridine or PPh_3 failed, as the formed complexes could not be identified. In the same vein, further reactions of **C^{3B}.1b** with isopropanol or **C^{3B}.1** with $NaBH_4$, did not allow the isolation of any manganese hydride intermediate.

Scheme B^{3I}.3 Synthesis of the manganese dimers **C^{3B}.1b-2b**.

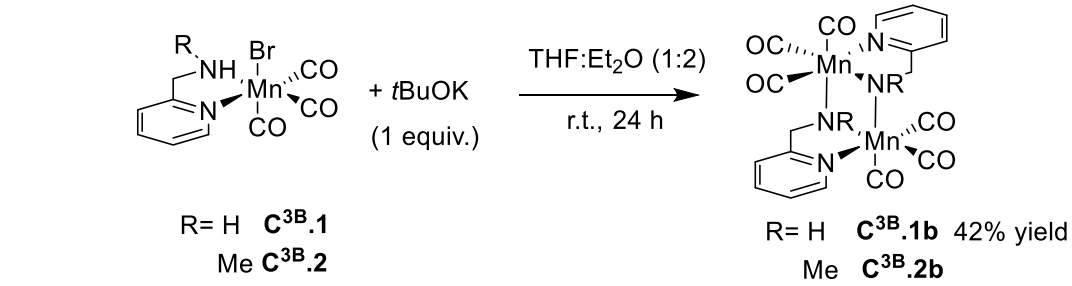

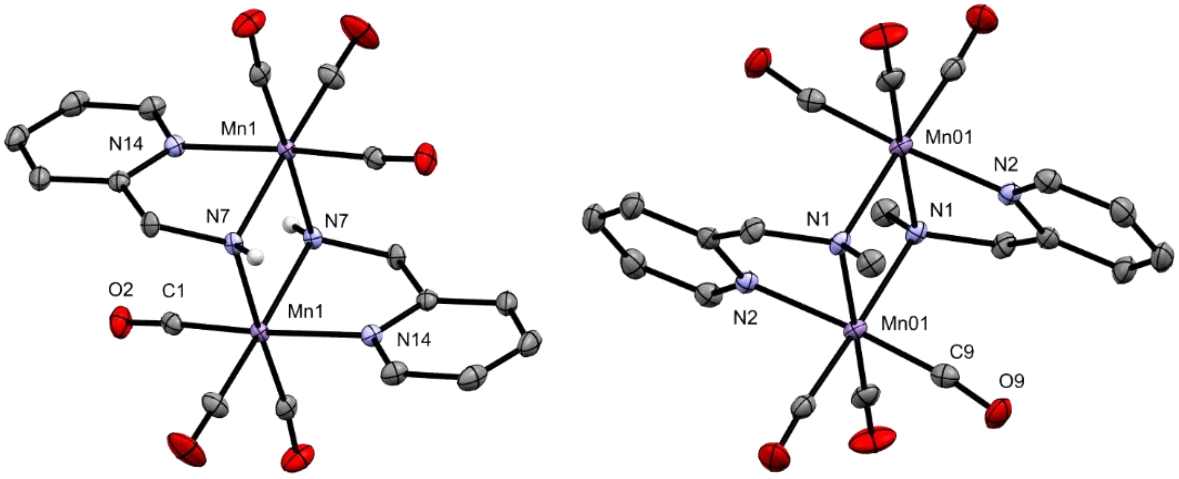

Figure B^{3I}.3 ORTEP view of the molecular structure of complex **C^{3b}5** and **C^{3b}6**, with thermal ellipsoids drawn at 50% probability. Hydrogens, except the NH, were omitted for clarity.

In addition, complex **C^{3B}.1b** was tested as catalyst without addition of external base under standard conditions: with 0.5 mol% of **C^{3B}.1b**, at 80 °C after 90 min, acetophenone was fully reduced to 1-phenylethanol. At 100 °C, the reaction was complete after 1 h. The corresponding deprotonated monomer, formed by the dissociation of the dimer, is likely one intermediate of the catalytic cycle, which is in line with mechanism of ligand-assisted hydrogen transfer reactions. The same kind of experiment gave the same results using **C^{3B}.2b** as catalyst.

Recently, the “classical” bi-functional mechanism proposed by Noyori has been revisited by Hartman or Dub and Gordon.[9–11] In particular, the role of the base, and of the excess of base compared to the catalyst, might not be limited to the deprotonation of the “NH” moieties, but the cation (K^+) could play a crucial role in the proton transfer from *i*PrOH to the substrate (**Scheme B^{3I}.4**).

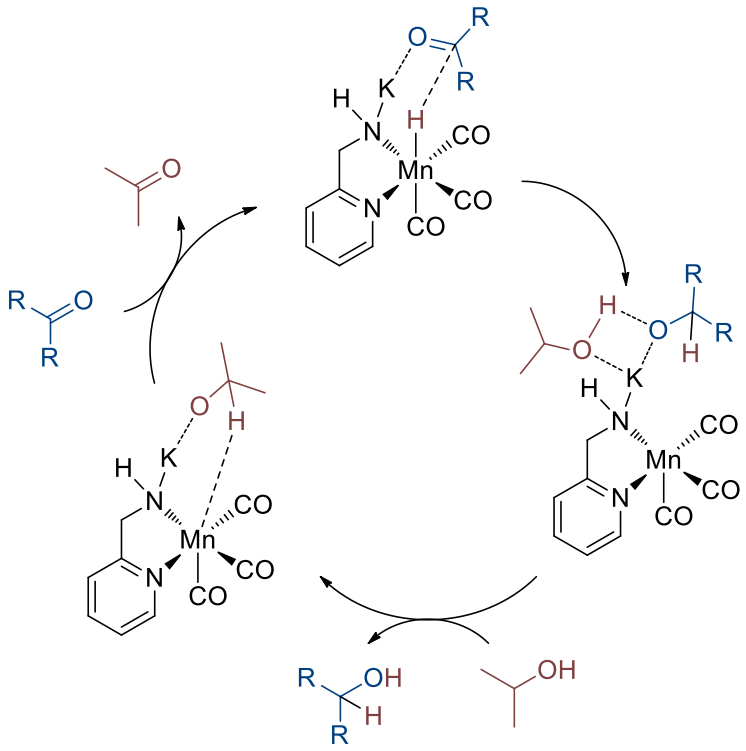

Scheme B^{3I}.4 Plausible mechanism of the reaction adapted from the mechanism described by Dub and Gordon.[10,11]

Therefore, to study the influence of K^+, the kinetic of the reaction has been followed using standard conditions (0.5 mol% **C^{3B}.1**, 1 mol% *t*BuOK, 80 °C) in the presence or in the absence of 18-crown-6-ether. In fact, we observed that in the presence of crown-ether, the rate of the reaction was slower than in its absence (**Figure B^{3I}.4**). At this stage, these preliminary results seemed to indicate that the alkali cation K^+ might

play a role in the mechanism although the presence of oxygen atom of ether moieties could simply slow down the reaction by coordination/decoordination on the vacancy site of the metal.

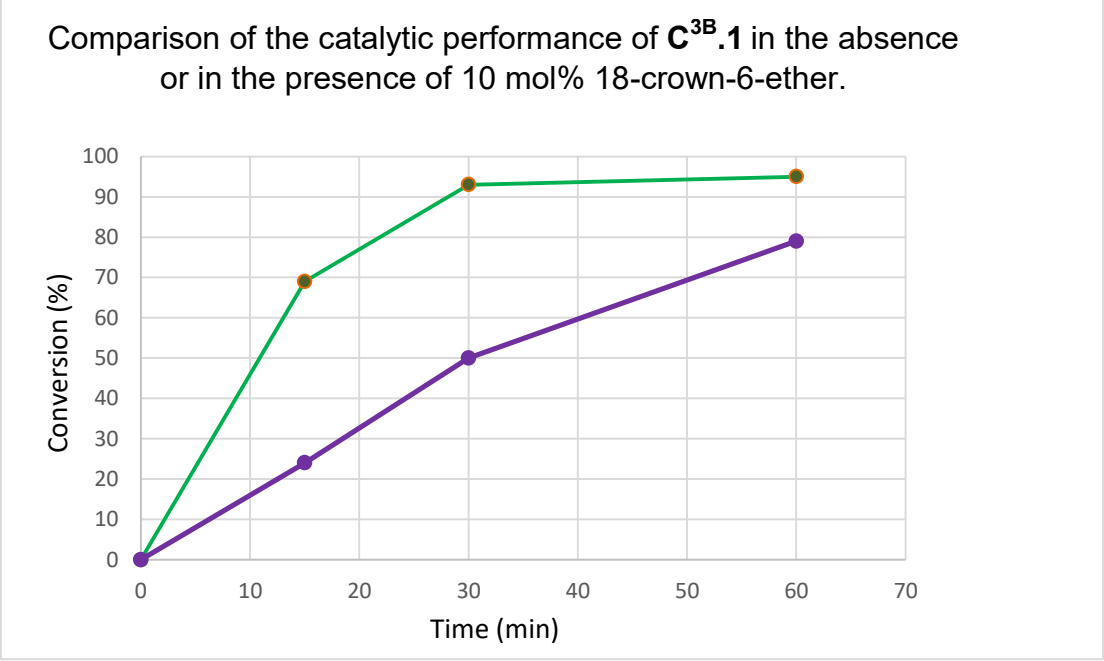

Figure B^{3l}.4 Kinetic of reduction of acetophenone performed at 80 °C by **C^{3B}.1** (1 mmol, 0.5 mol% **C^{3B}.1**, 1 mol% *t*BuOK, *i*PrOH (4 mL)) in the absence (green) or in the presence (purple) of 10 mol% 18-crown-6-ether.

In addition, having in mind the structures of Noyori's and Baratta's catalysts, *i.e.* ruthenium complexes bearing both NN and PP ligand, we tried to react **C^{3B}.1** with a bisphosphine ligand, namely 1,2-bis(diphenylphosphino)ethane (DPPE). Unfortunately, the formed complex could not be identified. In addition the reduction of acetophenone was carried out with **C^{3B}.1** (0.5 mol%) and *t*BuOK (1 mol%) in the presence of DPPE: after 4 h at 100 °C the activity dropped drastically (12% conv.) showing that free phosphine inhibited the reaction.

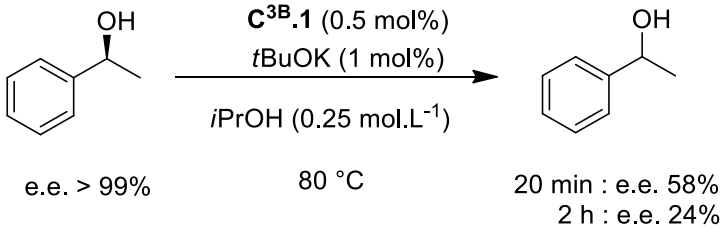

Scheme B^{3l}.5 Racemization of (*S*)-phenylethanol with our catalytic system.

Furthermore, (*S*)-phenylethanol was submitted to our optimized experimental conditions and the enantiomeric excess was monitored by chiral GC (**Scheme B^{3l}.5**): a racemization occurred rapidly as 58% e.e. after 20 min and 24% e.e. after 2 h were measured. It means that the alcohol could be dehydrogenated and re-hydrogenated by the catalyst and that reactions were reversible. This crucial information must be taken into account for the development of an asymmetric version of this catalytic system (*vide infra*).

e) Proposed mechanism

With all of our experiments in mind, we can postulate a mechanism for this reaction (**Scheme B^{3l}.6**). First, the pre-catalyst **C^{3B}.1** is deprotonated by the base to give the 16 electrons amido-complex **C^{3B}.1c**. Then, **C^{3B}.1c** dehydrogenates isopropanol to produce acetone and the hydride complex **C^{3B}.1d**. This hydride **C^{3B}.1d** reduces the desired ketone to alcohol. In the absence of substrate, the amido-complex **C^{3B}.1c** with a vacancy site on the metal reacts with itself to give the dimeric complex **C^{3B}.1b**, which can be seen as an off-cycle dormant species.

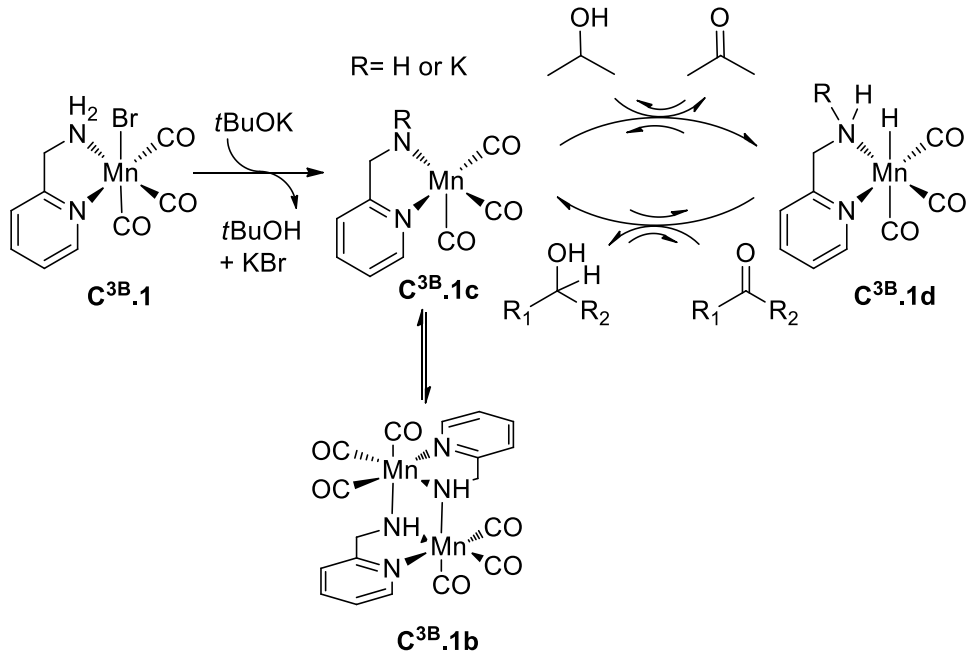

Scheme B^{3l}.6 Proposed mechanism for the transfer hydrogenation of carbonyl derivatives catalyzed by **C^{3B}.1**.

The presence of potassium cation on the nitrogen may accelerate the mechanism as it has been previously described in the literature[11] although the low catalytic loading of base needed and the comparable activities of **C^{3B}.1** and **C^{3B}.2** suggest that in our catalytic system this pathway is maybe not definitely decisive.

In conclusion, we have developed an highly efficient and simple catalytic system for the reduction by hydrogen transfer of ketones and aldehydes, including α,β-unsaturated aldehydes, at room temperature, based on phosphine-free bidentate aminomethyl-pyridine ligand. High TON (2000) and TOF (3600 h^{-1}) were achieved with this catalytic system.

f) Transfer hydrogenation of aldimines

Contributions in the part: Synthesis of the complexes: A.B.-V.; Optimization: A.B.-V., Maxime Dubois; Scope: Maxime Dubois.

Following our previous work on reductive amination with molecular hydrogen, the complex **C^{3B}.1** has been studied for the transfer hydrogenation of aldimines using *i*PrOH as the hydrogen source.

Benzylidene(4-tolyl)amine **c4** was chosen as the model substrate for the optimization of reaction conditions. A full conversion was obtained for the corresponding *N*-(4-tolyl)benzylamine **d4** using 2 mol% of **C^{3B}.1**, 4 mol% of *t*BuOK in *i*PrOH (2 mL) at 80 °C in 3 h (**Table B^{3l}.3**, entry 1). Dividing the catalyst and base loadings by two in 1.5 h gave a lower yield (68%, entry 2). Under the previous conditions, adding toluene as co-solvent did not change the yield (65%, entry 3). Then the quantity of *i*PrOH has been increased (entries 4-6): the best result was obtained with 5 mL of *i*PrOH (82% yield). When the temperature was lowered to 50 °C, after 3 h, the yield dropped to 29% (entry 7). Different bases (*t*BuONa, KHMDS, KOH, K_3PO_4, Na_2CO_3) were compared using 1 mol% of **C^{3B}.1** and 2 mol% of base with 3 mL of *i*PrOH (entries 8-12). KHMDS gave the same result than *t*BuOK (77%, entries 4 and 9). In addition, cheaper base such as KOH can be applied without a significant decline of the activity (65%, entry 10). Interestingly this catalytic system was submitted to the reductive

amination protocol, starting from benzaldehyde and aniline, the corresponding *N*-benzylaniline was obtained with 92% yield (entry 13).

Compared to the reduction of ketones, reduction of aldimines needed a higher dilution and higher catalytic loading.

Table B^{3I}.3: Optimization of the reaction parameters.[a]

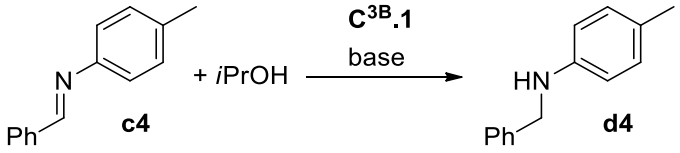

Entry	**C^{3B}.1** (mol%)	Base (mol%)	*i*PrOH (mL)	Temp. (°C)	Time (h)	Yield (%)
1	2	*t*BuOK (4)	2	80	3	99
2	1	*t*BuOK (2)	2	80	1.5	68
3	1	*t*BuOK (2)	1.3 / toluene (1)	80	1.5	65
4	1	*t*BuOK (2)	3	80	1.5	77
5	1	*t*BuOK (2)	5	80	1.5	82
6	1	*t*BuOK (2)	10	80	1.5	83
7	1	*t*BuOK (2)	5	50	3	29
8	1	*t*BuONa (2)	3	80	1.5	63
9	1	KHMDS (2)	3	80	1.5	77
10	1	KOH (2)	3	80	1.5	65
11	1	K_3PO_4 (2)	3	80	1.5	12
12	1	Na_2CO_3 (2)	3	80	1.5	15
13[b]	1	*t*BuOK (2)	2	80	3	92

[a] Typical conditions: To a Schlenk tube, under argon, were added in this order: **C^{3B}.1**, *i*PrOH (and the co-solvent), benzylidene(4-tolyl)amine **c4** (0.5 mmol, 97 mg) and base. The yield was determined by GC and ^{1}H NMR. [b] Reductive amination conditions: To a Schlenk tube, under argon, were added in this order: benzaldehyde (0.5 mmol), aniline (0.6 mmol) and anhydrous *i*PrOH (2 mL). After stirring the reaction mixture at r.t. during 3h, **C^{3B}.1** (1mol %) was added to the Schlenk tube followed by *t*BuOK (2 mol %). Then the mixture was stirred at 80 °C during 3 h. The yield was determined by GC and ^{1}H NMR.

The beginning of the scope of this reaction has been realized with 2 mol% of **C^{3B}.1**, 4 mol% of *t*BuOK at 80°C during 3 h in 5 mL of *i*PrOH (**Scheme B^{3I}.7**). *N*-(4-tolyl)benzylamine **d4** and *N*-(4-methylbenzyl)-4-methylaniline **d41** were obtained in very high yields (93% and 92%). The presence of electron withdrawing group (F, Cl, Br) was well tolerated by the catalyst and led to full conversions for **d42** and **d44**. On the contrary, the conversion fell to respectively 18% and 14% in the presence of methoxy **d45** and phenoxy **d46** groups in the molecule. The generality of this reaction will be thoroughly studied in the near future.

Scheme B^{3I}.7 Scope of the hydrogen transfer of aldimines to give amines under the catalysis of **C^{3B}.1**.

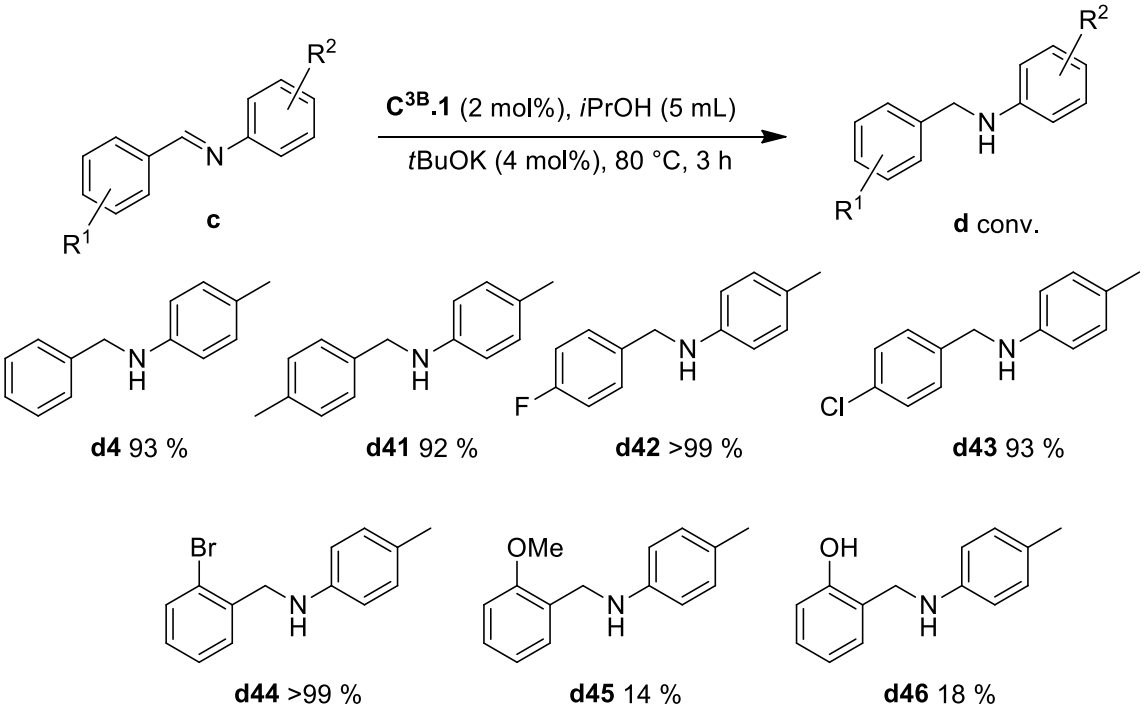

Typical conditions: To a Schlenk tube, under argon, were added in this order: catalyst **C^{3B}.1** (2 mol%), *i*PrOH (5 mL), aldimine (0.5 mmol) and *t*BuOK (4 mol%). The conversion was determined by ^{1}H NMR on the crude mixture.

II- *In situ* formation of the complexes

In the quest of further simplified procedure, we have considered generating *in situ* the pre-catalyst from the commercially available manganese precursor and ligands.

a) (Asymmetric) transfer hydrogenation of ketones with (chiral) diamine ligands

Contributions in the part: Screening: D. W., A. B.-V., Scope: A. B.-V., D. W.; Calculations: Noël Lugan.

Publication: D. Wang*, A. Bruneau-Voisine*, J.-B. Sortais, *Catal. Commun.* **2018**, *105*, 31-36. *equal contributions

Inspired by the breakthrough of Noyori, introducing chiral diamines as ligands in ruthenium catalyzed asymmetric reduction of ketones,[1,12] we envisioned that simple diamines could be suitable for manganese-catalyzed reduction of ketones using isopropanol as the hydrogen donor, and that eventually asymmetric reduction of ketones could be achieved with chiral diamines.

To start our investigation, based on our optimized conditions for well-defined picolylamine manganese complexes, we have screened a series of diamines as ligands (0.5 mol%), using $Mn(CO)_5Br$ as metal precursor (0.5 mol%) and *t*BuOK as base (1 mol%) for the reduction of acetophenone at 80 °C for 1 h. The results are summarized in **Scheme B^{3II}.1**. First, several amines were found inactive for this transformation, demonstrating that the base-catalyzed reaction was limited under these conditions.[6] Second, the reduction of acetophenone proceeded well with *in situ* generated catalysts based on aminomethylpyridine ligand **L^{3B}.1**, as a full conversion of acetophenone into 1-phenylethanol was observed after 1 h. *N*-methylaminomethylpyridine ligand **L^{3B}.2,** featuring one NH moieties, led also to a full conversion in 1 h but *N,N*-dimethylaminomethylpyridine **L^{3B}.3** was almost inactive. These results are in line with those obtained previously with well-defined complexes based on picolylamine ligands.

Scheme B^{3II}.1 Screening of bidentate nitrogen based ligands for the reduction of acetophenone in the presence of $Mn(CO)_5Br$ and *t*BuOK in *i*PrOH.

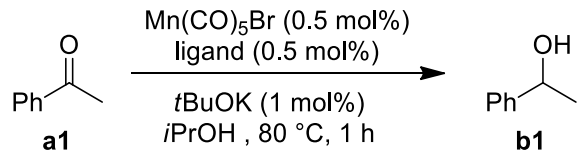

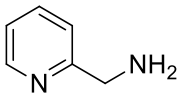

L^{3B}.1 97%

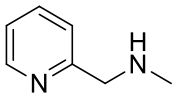

L^{3B}.2 96%

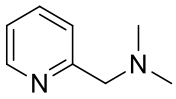

L^{3B}.3 6%

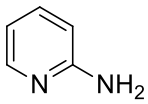

L^{3B}.4 0%

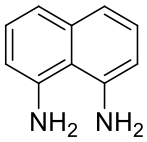

L^{3B}.5 3%

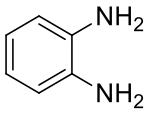

L^{3B}.6 0%

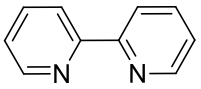

L^{3B}.7 0%

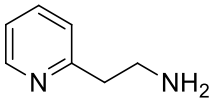

L^{3B}.8 7%

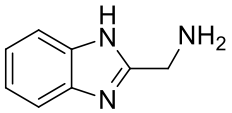

L^{3B}.9 76%

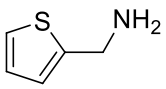

L^{3B}.10 0%

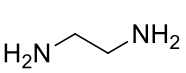

L^{3B}.11 65%

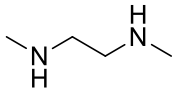

L^{3B}.12 45%

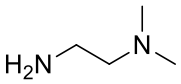

L^{3B}.13 6%

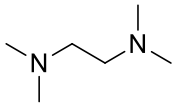

L^{3B}.14 0%

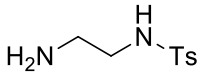

L^{3B}.15 0%

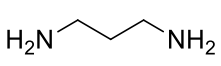

L^{3B}.16 25%

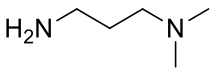

L^{3B}.17 17%

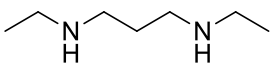

L^{3B}.18 2%

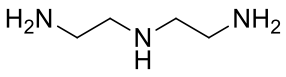

L^{3B}.19 1%

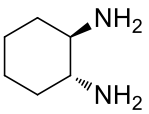

L^{3B}.20-*rac* 22%

Typical conditions: to a Schlenk tube, under argon, were added in this order: acetophenone **a1** (2 mmol), *i*PrOH (8 mL), $Mn(CO)_5Br$ (0.5 mol%), ligand (0.5 mol%) and *t*BuOK (1 mol%), 80 °C, 1 h. Conversions were determined by ^{1}H NMR.

Due to the simplicity of the system, we then explored different parameters to optimize the design of the ligand. Aromatic amines, such as 2-amino-pyridine **L^{3B}.4**, 1,8-

diaminonaphtalene **L^{3B}.5** and 1,2-diaminobenzene **L^{3B}.6,** did not promote the hydrogen transfer. 2,2'-Bipyidine **L^{3B}.7** was completely inactive.[13] The length of the linker in between the pyridinyl unit and the amine moieties was also found to be crucial as 2-pyridin-2-ylethanamine **L^{3B}.8** was inactive, as **L^{3B}.4**. Interestingly, benzimidazolyl analogue of **L^{3B}.1**, namely 1*H*-benzimidazole-2-methanamine **L^{3B}.9**, gave a good conversion (76%), but 2-aminomethylthiophene **L^{3B}.10** was inactive. In order to develop the simplest and the less expensive catalytic system as possible, we tested the simplest diamine, namely, ethylenediamine **L^{3B}.11**: to our delight, a very encouraging conversion was obtained under standard conditions (65%). Several diamines were also tested: the presence of at least two NH moieties was found to be crucial to detect some activity (**L^{3B}.11**, **L^{3B}.12** *versus* **L^{3B}.13**, **L^{3B}.14**). The presence of a tosyl group on one nitrogen atom inhibited the reduction, probably due to a slow coordination of the ligand to the manganese precursor. An ethylene bridge, leading to a five-membered metallacycle, was more favorable than a propylene one (**L^{3B}.16**, **L^{3B}.17**, **L^{3B}.18**) (65 % conversion with **L^{3B}.11** versus 25% with **L^{3B}.16**). Finally, racemic ligand **L^{3B}.20-rac,** (±)-*trans*-1,2-diaminocyclohexane, gave moderate (22%) conversion, opening the gate to asymmetric reduction of acetophenone (*vide infra*).

Taking into account both the simplicity and the low cost of ethylenediamine **L^{3B}.11** compared to 2-aminomethylpyridine **L^{3B}.1**, the scope of the reaction was then explored using **L^{3B}.11** as ligand (0.5 mol%), $Mn(CO)_5Br$ (0.5 mol%) and *t*BuOK as base (1 mol%) in isopropanol at 80 °C for 3 h (**Scheme B^{3II}.2**). In most cases, ketones were fully reduced, and the corresponding alcohols were isolated in high yields. Increasing the length and the branching of the alkyl chains from methyl (**a1)** to *tert*-butyl (**a5**) had little influence on the reaction. On the opposite, for *ortho*-substituted acetophenones (**b6**-**b9** and **b15**), a higher catalytic loading (1 mol%) was required to afford the alcohols in quantitative yields.

Scheme B^{3II}.2: Generality of the reduction of ketones with the *in situ* prepared manganese-ethylenediamine catalytic system.[a]

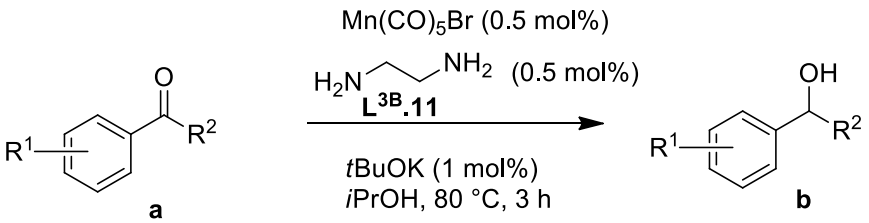

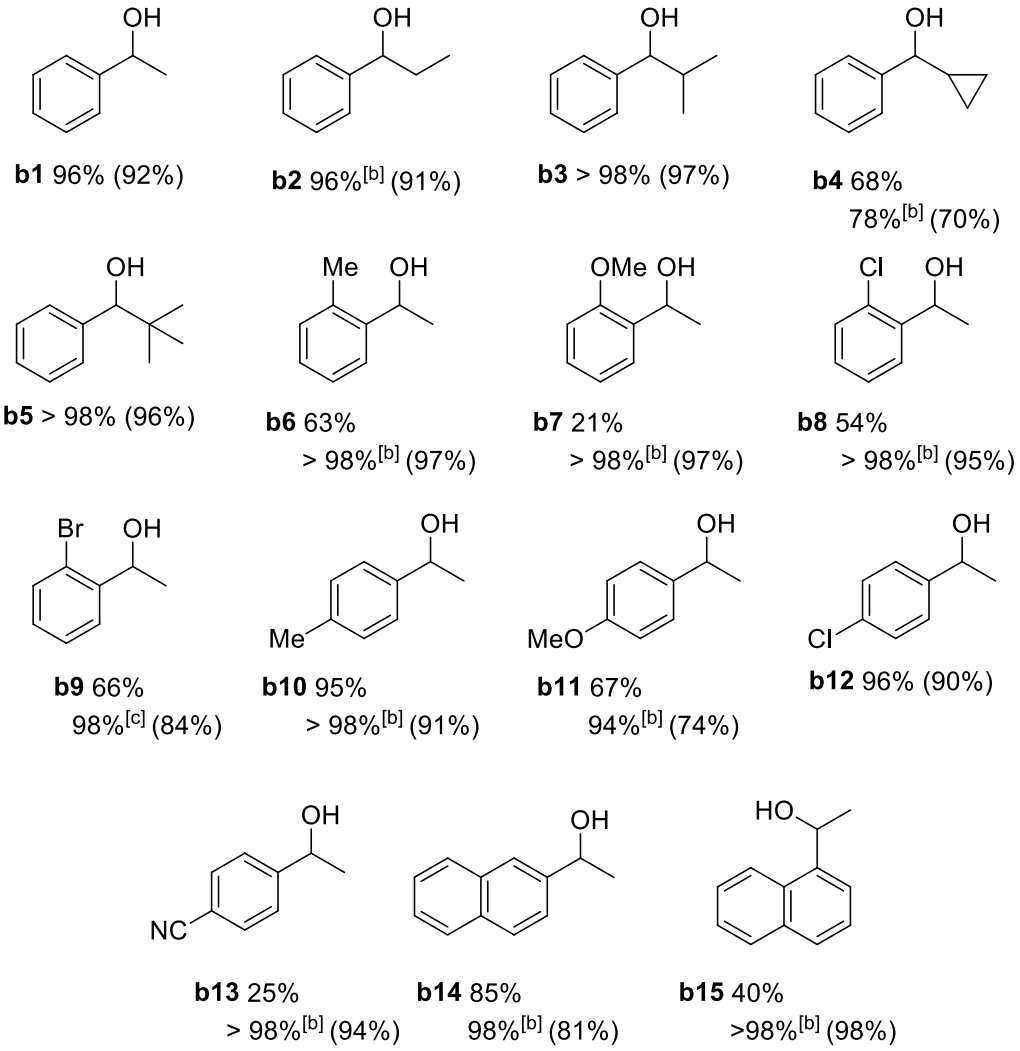

b1 96% (92%) **b2** 96%[b] (91%) **b3** > 98% (97%) **b4** 68% 78%[b] (70%)

b5 > 98% (96%) **b6** 63% > 98%[b] (97%) **b7** 21% > 98%[b] (97%) **b8** 54% > 98%[b] (95%)

b9 66% 98%[c] (84%) **b10** 95% > 98%[b] (91%) **b11** 67% 94%[b] (74%) **b12** 96% (90%)

b13 25% > 98%[b] (94%) **b14** 85% 98%[b] (81%) **b15** 40% >98%[b] (98%)

[a] Typical conditions: Ketone (0.5 mmol), *i*PrOH (2 mL) $Mn(CO)_5Br$ (0.5 mol%), ethylenediamine (0.5 mol%), *t*BuOK (1 mol%), 80 °C, 3 h. Conversion determined by ^{1}H NMR, isolated yield given in parentheses. [b] $Mn(CO)_5Br$ (1 mol%), ethylenediamine (1 mol%), *t*BuOK (2 mol%). [c] $Mn(CO)_5Br$ (1 mol%), ethylenediamine **L^{3B}.11** (1 mol%), *t*BuOK (2 mol%), 6 h. Conversions were determined by ^{1}H NMR, and isolation of the alcohols.

Encouraged by these results, especially by the activity of **L^{3B}.20**-*rac*, we submitted a series of commercial chiral diamines featuring an ethylenediamine motif for the reduction of acetophenone (**Scheme B^{3II}.3**, **Table B^{3II}.1**) using one equivalent of

ligand (1 mol%) per $Mn(CO)_5Br$ (1 mol%) and two equivalents of *t*BuOK (2 mol%) at 80 °C for 3 h.

Scheme B^{3II}.3: Chiral diamines screened for the asymmetric reduction of ketones.

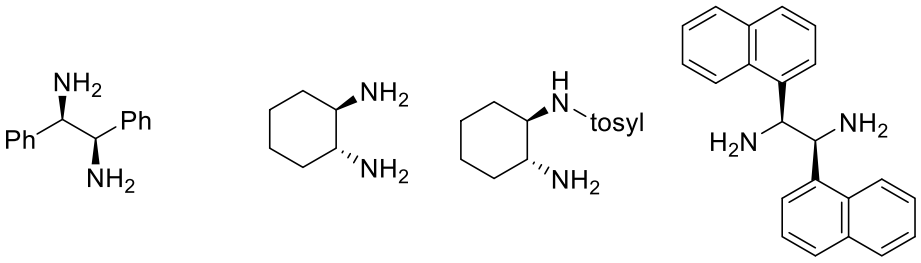

(1*R*, 2*R*) **L^{3B}.21**

(1*R*, 2*R*) **L^{3B}.22**

(1*R*, 2*R*) **L^{3B}.23**

(1*S*, 2*S*) **L^{3B}.24**

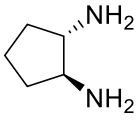

(1*S*, 2*S*) **L^{3B}.25**

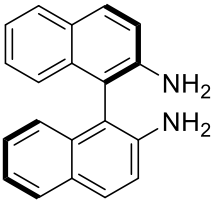

(*R*) **L^{3B}.26**

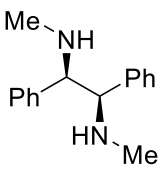

(1*R*, 2*R*) **L^{3B}.27**

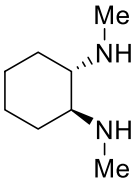

(1*S*, 2*S*) **L^{3B}.28**

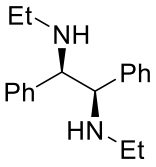

(1*R*, 2*R*) **L^{3B}.29**

With (1*R*,2*R*)-(+)-1,2-diphenyl-1,2-ethanediamine (DPEN) **L^{3B}.21**, a promising enantiomeric excess of 36 % was obtained (entry 1). Using (1*R*,2*R*)-(-)-1,2-diaminocyclohexane **L^{3B}.22**, under the same conditions, the selectivity increased to 43% e.e. (entry 2). The enantiomeric excess of the product dropped to 38% after 24 h of reaction (entry 3), probably due to racemization of the product under hydrogen transfer conditions. The activity dramatically decreased if the reaction was performed at 30 °C (entry 4). *N*-tosyl substituted ligand **L^{3B}.23** displayed no activity, as **L^{3B}.15**, even if a preactivation step at 100 °C in toluene was accomplished (entries 5-6). Disappointingly, more sterically demanding diamine **L^{3B}.24** or less bulky (1*S*,2*S*)-*trans*-1,2-cyclopentanediamine **L^{3B}.25** gave both a lower activity and selectivity (entries 7-8). (1*S*,2*S*)-1,2-di-1-naphthyl-ethylenediamine **L^{3B}.26**, as the achiral aniline derivatives **L^{3B}.4**- **L^{3B}.6**, gave almost no conversion and no enantiomeric excess (entry 9). Gratifyingly, *N*,*N*'-dimethylated ligands **L^{3B}.27** and **L^{3B}.28** displayed a significant higher selectivity than their analogues **L^{3B}.21** and **L^{3B}.22** (64% and 52% e.e. respectively, entries 10-11), (1*R*,2*R*)-(+)-*N*,*N*'-dimethyl-1,2-diphenyl-1,2-ethane

diamine **L^{3B}.27** giving the highest e.e. Further increasing of the steric hindrance on the nitrogen to an ethyl group **L^{3B}.29** resulted in a decrease of the enantiomeric excess (52%, entry 12).

Table B^{3II}.1. Asymmetric reduction of acetophenone with chiral diamines ligands and $Mn(CO)_5Br$.[a]

Entry	Ligand	Temp. (°C)	Time (h)	e.e.[b] (%)	Conv.[c] (%)
1	**L^{3B}.21**	80	3	36 (*S*)	> 97
2	**L^{3B}.22**	80	3	43 (*S*)	87
3	**L^{3B}.22**	80	24	38 (*S*)	> 97
4	**L^{3B}.22**	30	24	42 (*S*)	8
5	**L^{3B}.23**	80	3	0	0
6	**L^{3B}.23**[d]	80	3	46 (*S*)	4
7	**L^{3B}.24**[e]	80	3	16 (*R*)	7
8	**L^{3B}.25**[e]	80	3	0	16
9	**L^{3B}.26**	80	3	6 (*S*)	13
10	**L^{3B}.27**	80	3	64 (*S*)	95
11	**L^{3B}.28**	80	3	52 (*R*)	94
12	**L^{3B}.29**	80	3	52 (S)	96

[a] Typical conditions : To a solution of acetophenone in *i*PrOH were added in this order the diamine (1 mol%), $Mn(CO)_5Br$ (1 mol%) and finally *t*BuOK (2 mol%). [b] Enantiomeric excess values were determined by chiral GC. [c] Conversions were determined by ^{1}H NMR. [d] Preactivation step was operated: $Mn(CO)_5Br$ (0.02 mmol) and **L^{3B}.23** (0.02 mmol) were stirred in refluxing toluene (1 mL) for 1 h, then *i*PrOH (8 mL), acetophenone (2 mmol) and base (0.04 mmol) were added. [e] Commercial **L^{3B}.24**. 2HCl and **L^{3B}.25**. 2HCl were first neutralized with *t*BuOK (5 mol%) in *i*PrOH for 30 min prior to reaction.

For a better understanding of the role of the methyl group on the nitrogen in the enantiodifferenciation, preliminary DFT calculations on the transition states were made by Noël Lugan. In these transition states, both nitrogen atoms (N_1 and N_2) are chiral, the transfer of the hydride can occur either on the *Re* face or on the *Si* face, the N-H—O hydrogen bonding can take place either from N_1 or from N_2, and the methyl group on the other nitrogen atom can point either up (in the direction of the ketone) or down. The four more stable transition states are represented in **Scheme B^{3II}.4**.

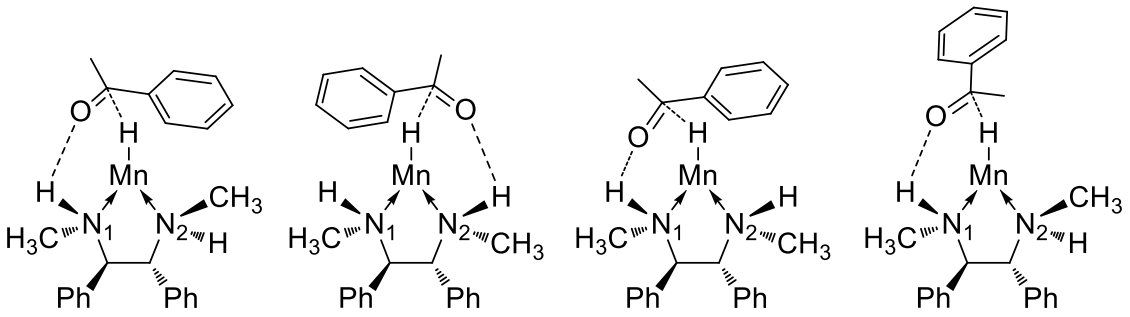

Energy (kcal/mol)	0	+1.6	+2.0	+2.4

Scheme B^{3II}.4 Energy values (kcal/mol) of the four more stable presumed transition states for the hydride complex bearing **L^{3B}.27**.

The most favorable transition state with the lowest energy, taken as reference for the energy data, possesses the *S* configuration on the two nitrogen atoms and the attack of the hydride occurs on the *Re* face of the acetophenone with the oxygen atom orientated towards the nitrogen N_1. The methyl group on the other nitrogen N_2 points up, in the direction of the phenyl ring of the acetophenone. The alcohol resulting from this hydride/proton transfer is the (*S*)-1-phenylethanol, as we mostly obtained during the experiment.

The second transition state is 1.6 kcal/mol less stable and contains the *S* configuration on the nitrogen N_1 and the *R* configuration on the nitrogen N_2, the *Si* face of the ketone is attacked by the hydride and the oxygen is orientated towards the nitrogen N_2 with the methyl group from the other nitrogen N_2 orientated down, giving the (*R*)-1-phenylethanol. The third transition state is 2.0 kcal/mol less stable and contains the same configuration on the ligand than the second one but the attack of the hydride happened on the *Re* face and the oxygen is orientated towards the nitrogen N_1 with the methyl group from the other nitrogen N_2 orientated down, giving the (*S*)-1-phenylethanol. The fourth transition state is 2.4 kcal/mol less stable and contains the same configuration on the ligand than the first one but the attack of the hydride happened on the *Si* face with the oxygen pointed towards the nitrogen N_1 with the methyl group from the other nitrogen N_2 orientated up, giving the (*R*)-1-phenylethanol.

The stabilization of transition state (S_{N1},S_{N2}) Re_{N1} can be explained by the presence of non-covalent interactions[14] between the methyl from the nitrogen N_2 and the phenyl

group from the substrate (C-H···π interactions) in association with the hydrogen N_1-*H* orientated in the direction of the oxygen atom from the ketone (**Figure B^{3II}.1**).

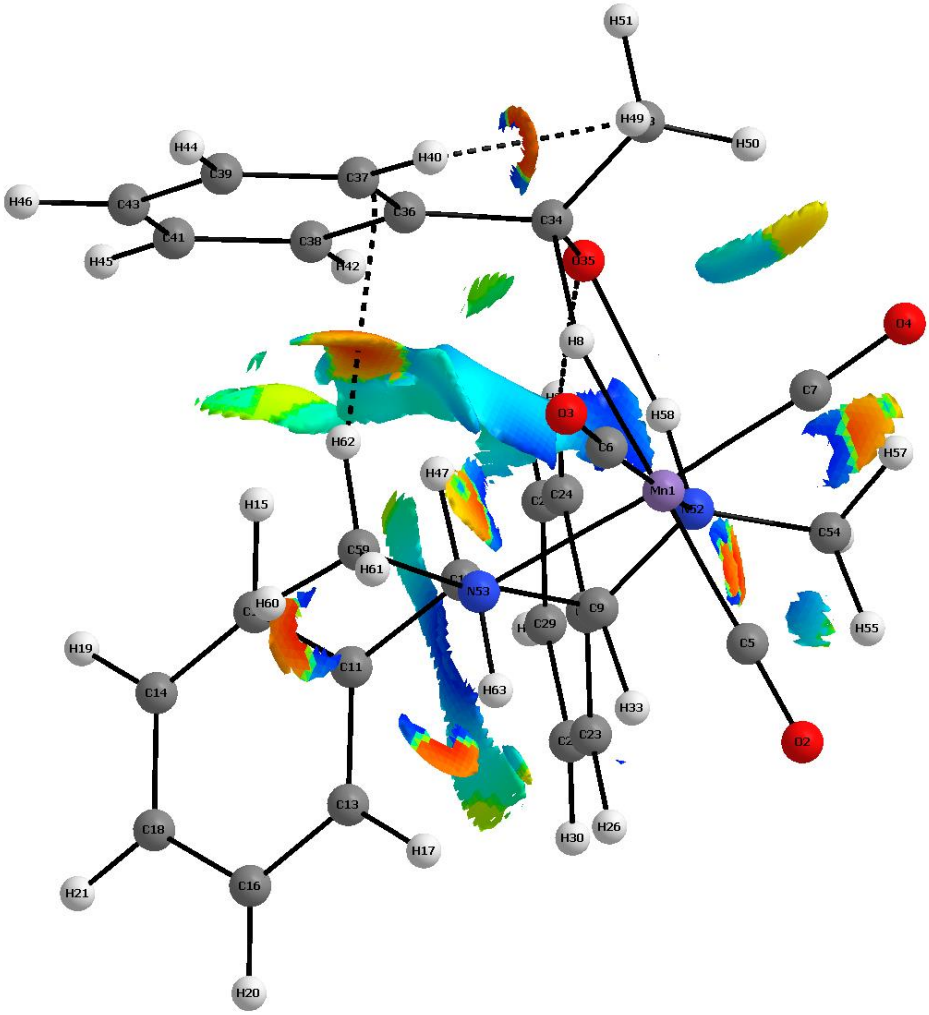

Figure B^{3II}.1 Non-covalent interactions in the most stable transition state (S_{N1},S_{N2}) Re_{N1}.

Based on the promising enantioselectivity obtained with **L^{3B}.27** for the reduction of acetophenone, we probed the scope of the reaction with several aromatic ketones (**Scheme B^{3II}.5**), under the optimized conditions. In most cases, good to excellent conversions were obtained in 3 h. Increasing the substitution on the methyl group of the acetophenone has a beneficial impact on the enantioselectivity, as 2,2-dimethyl-1-phenyl-1-propanol **b'5** was obtained with 86% e.e. from pivalophenone **a5**. The selectivity could even be improved further to 90% e.e. by lowering the temperature to 50 °C. On the other hand, in the case of *ortho*-substituted acetophenone, the substitution on the aromatic ring has also a positive effect on the enantioselectivity, leading to moderate to good e.e. up to 80% for **b'6** and 84 % for **b'15**. In the case of

both electron donating (**a10**, **a11**) and electron withdrawing (**a12**, **a13**) substituents at the *para*-position, the selectivity was lower than for the reduction of acetophenone **a1**, with e.e. ranging from 30% to 46%.

Scheme B^{3II}.5: Scope of the asymmetric reduction of ketones catalyzed by (1*R*,2*R*)-(+)-*N*,*N*'-dimethyl-1,2-diphenyl-1,2-ethane diamine **L^{3B}.27** and $Mn(CO)_5Br$.[a]

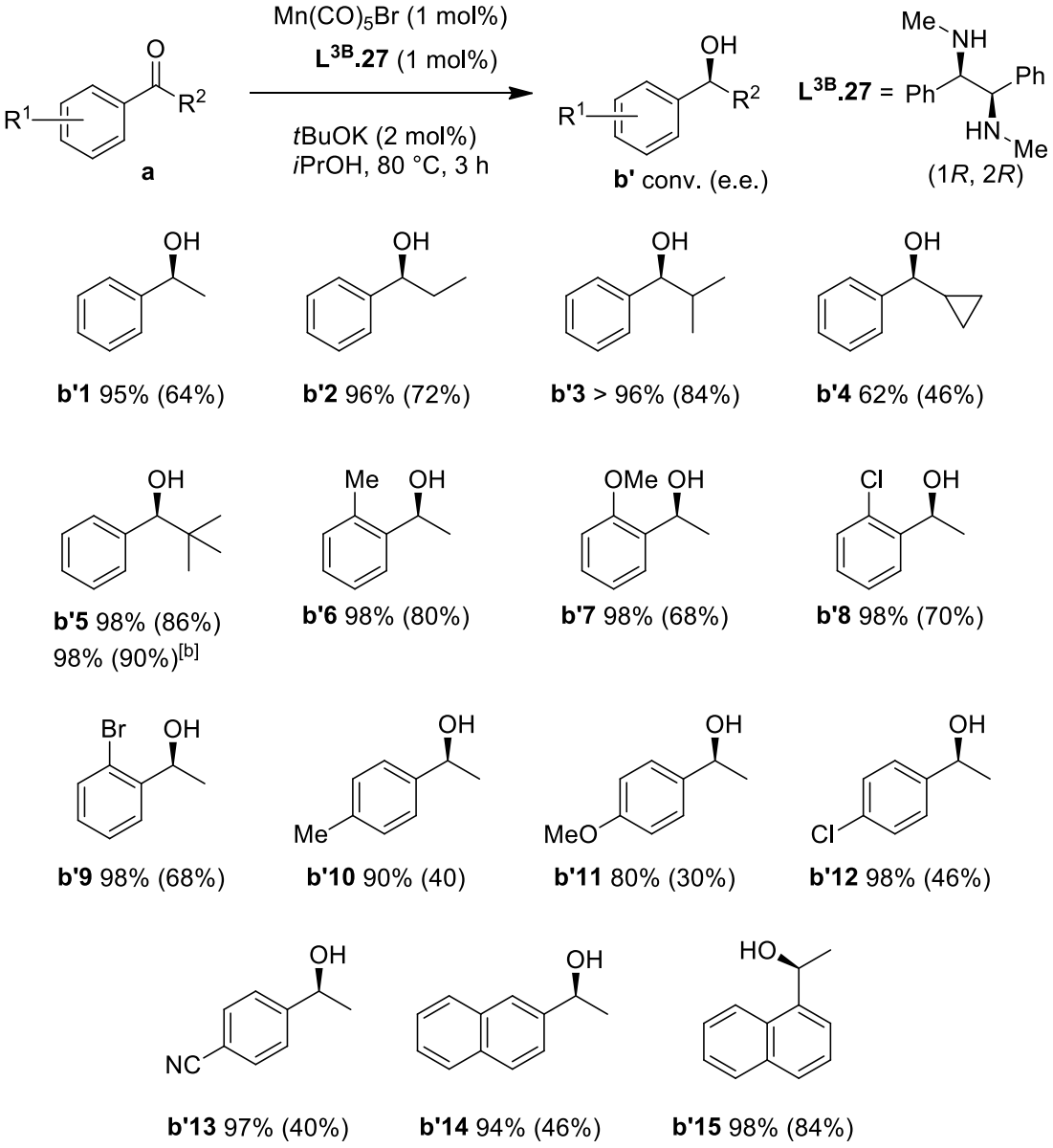

[a] Typical conditions: To a solution of ketone (2 mmol) in *i*PrOH (8 mL) were added in this order the diamine (1 mol%), $Mn(CO)_5Br$ (1 mol%) and finally *t*BuOK (2 mol%). Conversion determined by ^1H NMR, e.e. determined by chiral GC given in parentheses. Each reaction was repeated at least twice. [b] 50 °C, 24 h.

Finally, the synthesis of the well-defined complexes **C^{3B}.21** and **C^{3B}.27** was realized by using the same conditions than our previous studies: toluene at reflux for 3 h (**Scheme B^{3II}.6**). According to the ^1H NMR, they were obtained in good purity (See

S.I. PartB-II Figures S47-51). Unfortunately, no single crystals could be obtained yet, whatever the solvents used for crystallization.

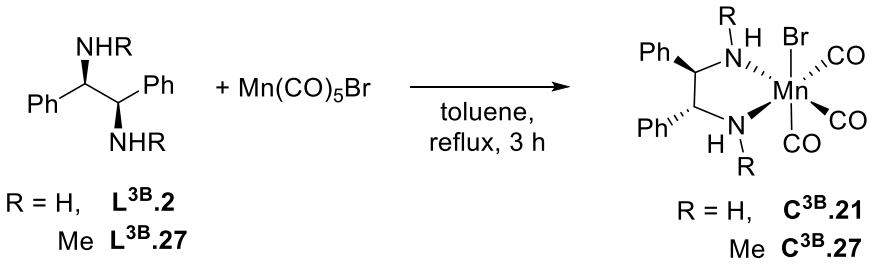

Scheme B^{3II}.6 Synthesis of complexes **C^{3B}.21** and **C^{3B}.27**.

The reduction of acetophenone was then performed with these complexes under similar conditions than those used with the *in situ* generated systems (**Scheme B^{3II}.7**). In the case of the complex based on (1*R*,2*R*)-(+)-1,2-diphenyl-1,2-ethanediamine **L^{3B}.21**, the activity and enantioselectivity was identical between *in situ* (97% conv., 36% e.e. after 3 h) and *ex situ* systems (82% conv., 34% e.e. after 1 h).

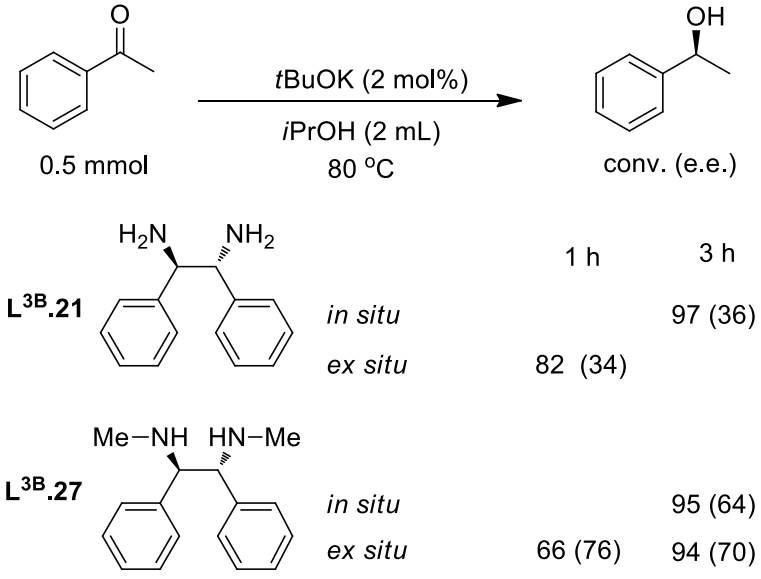

Scheme B^{3II}.7 Comparison between *ex situ* and *in situ* generated catalytic systems for the transfer hydrogenation of acetophenone.

For the complex based on (1*R*,2*R*)-(+)-*N*,*N*'-dimethyl-1,2-diphenyl-1,2-ethane diamine **L^{3B}.27**, the well-defined system **C^{3B}.27** exhibited a slightly better enantioselectivity as 70% e.e. were obtained after 3 h (64 % e.e. for the *in situ* system) and the e.e. was even 76 % after 1 h showing a racemization during the process. In conclusion, we have developed a very simple and efficient catalytic system based on manganese pentacarbonyl bromide and ethylenediamine for the reduction of ketones by hydrogen transfer using isopropanol as the donor. The low

cost of both metal precursor and ligand, associated with the *in situ* generation of the catalytic active species, make this system economically attractive as a simple sustainable alternative to sodium borohydride for the reduction of ketones. More importantly, the reactivity was extended to asymmetric reaction of sterically hindered ketones with e.e. up to 90% using (1*R*,2*R*)-*N*,*N*'-dimethyl-1,2-diphenylethane-1,2-diamine as chiral ligand. This first approach demonstrated that simple bidendate, phosphine-free ligand, can be used with manganese to promote enantioselective reactions with a good selectivity.

b) Asymmetric transfer hydrogenation of ketones with chiral phosphine-amine ligands

Inspired the work of Saudan[15] with ruthenium catalysts and more recently the work of Pidko[16] with manganese catalysts, we decided to explore a new family of commercially available chiral phosphine-amine ligands (**Scheme B^{3II}.8**, **Table B^{3II}.2**) for asymmetric transfer hydrogenation. The presence of a phosphine moiety should increase the electron density on the metal and make the hydride more reactive.

Under the same conditions than for the diamine screening (0.5 mol% $Mn(CO)_5Br$, 0.5 mol% ligand, 80 °C), the first phosphine-amine tested was (1*S*,2*S*)-2-(diphenylphosphino)-1,2-diphenylethanamine **L^{3B}.31**. A conversion of 85% was reached in a shorter time, 45 min. instead of 3 h for diamine ligands, but the racemic 1-phenylethanol was formed. Replacement of the phenyl group close to the amine by a methyl on the ligand (**L^{3B}.32**) had a good impact on the activity as 80% conversion was attained in 15 min. with an e.e. of 36%. Racemization occurred as, after 45 min., the e.e. was 34% (conv. 91%) and, after overnight reaction, the e.e. fell to 5%. As previously noticed, the use of (1*S*,2*S*)-1-(diphenylphosphino)-*N*-methyl-1-phenylpropan-2-amine **L^{3B}.33**, similar ligand than **L^{3B}.32** with a single methyl group on the nitrogen, increased the e.e. to 56% with a sluggish conversion of 69 % after 45 min.

Scheme B^{3II}.8: Chiral phosphine-amines screened for the asymmetric reduction of ketones.

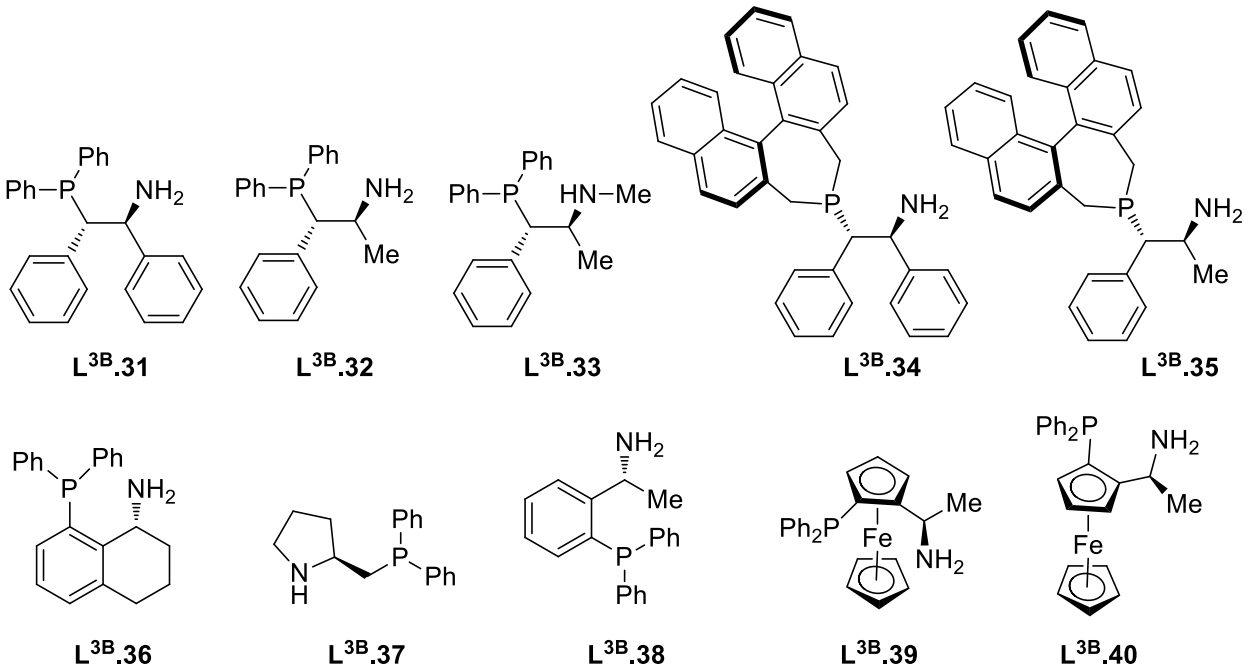

L^{3B}.31 **L^{3B}.32** **L^{3B}.33** **L^{3B}.34** **L^{3B}.35**

L^{3B}.36 **L^{3B}.37** **L^{3B}.38** **L^{3B}.39** **L^{3B}.40**

The e.e. could be further increased to 66% by incorporation a chiral group, *i.e.* a binepine unit ((4*R*,11b*S*)-3*H*-dinaphtho[2,1-*c*:1′,2′-*e*]phosphepin-4(*5H*)-yl), on the phosphorus atom **L^{3B}.34** with a moderate conversion of 60 % after 15 min. accompanied again by a slow racemization. The best conversion of 95 % in 15 min. was reached with **L^{3B}.35**, analogue to **L^{3B}.32** bearing a binepine group on the phosphorus moiety, with 64% e.e. This very active catalytic system was also quickly racemizing the alcohol product as the e.e. dropped to 42 % after only 45 min. (*R*)-8-(Diphenylphosphino)-1,2,3,4-tetrahydronaphthalen-1-amine **L^{3B}.36** and (*R*)-1-(2-(diphenylphosphino)phenyl)ethanamine **L^{3B}.38** gave good conversions (70 and 83%, respectively after 15 min.) and moderate e.e. (26%) for **L^{3B}.36** or racemic for **L^{3B}.38**. Similarly, (*S*)-2-((diphenylphosphino)methyl)pyrrolidine **L^{3B}.37** gave a fast conversion (94% in 15 min.) but a poor e.e. (5%). Ferrocenyl-based PN ligands **L^{3B}.39** and **L^{3B}.40** were not active in terms of conversion and enantioselectivity compared to other PN ligands.

Table B^{3II}.2. Asymmetric reduction of acetophenone with chiral phosphine-amine ligands and $Mn(CO)_5Br$.[a]

Entry	Ligand	Time (min.)	e.e.[b] (%)	Conv.[c] (%)
1	**L^{3B}.31**	45	1 (*R*)	85
2	**L^{3B}.32**	15	36 (*R*)	80
3		45	34 (*R*)	91
4		overnight	5 (*R*)	97
5	**L^{3B}.33**	45	56 (*R*)	69
6	**L^{3B}.34**	15	66 (*R*)	60
7		45	62 (*R*)	92
8		overnight	0	97
9	**L^{3B}.35**	15	64 (*R*)	95
10		45	42 (*R*)	96
11	**L^{3B}.36**	15	26 (*S*)	70
12	**L^{3B}.37**	15	5 (*S*)	94
13	**L^{3B}.38**	15	1 (*R*)	83
14	**L^{3B}.39**	45	12 (*S*)	5
15	**L^{3B}.40**	45	8 (*R*)	5

[a] Typical conditions : To a solution of acetophenone (2 mmol) in *i*PrOH (8 mL) were added in this order the phosphine-amine (0.5 mol%), $Mn(CO)_5Br$ (0.5 mol%) and finally *t*BuOK (1 mol%), 80 °C. [b] Enantiomeric excess values were determined by chiral GC. [c] Conversions were determined by ^{1}H NMR.

Finally, a comparison between the *in situ* generated and the well-defined systems was realized for the reduction of 2,2-dimethylpropiophenone with (1*R*,2*R*)-2-(diphenylphosphino)cyclohexylamine **L^{3B}.30**. The synthesis of the corresponding chiral complex **C^{3B}.30*** was realized at 50 °C in toluene for 4 h. The crude ^{31}P NMR revealed that two species were present in solution (^{31}P NMR (162 MHz, CD_2Cl_2) δ (ppm) 67.8 (major), 57.8), which could be due to the presence of two isomers according to the position of the bromide atom. A single crystal has grown in dichloromethane showing retention of configuration (*R,R*) of the ligand after coordination to the manganese (the quantity was not enough to analyzed it by NMR) (**Figure B^{3II}.2**).

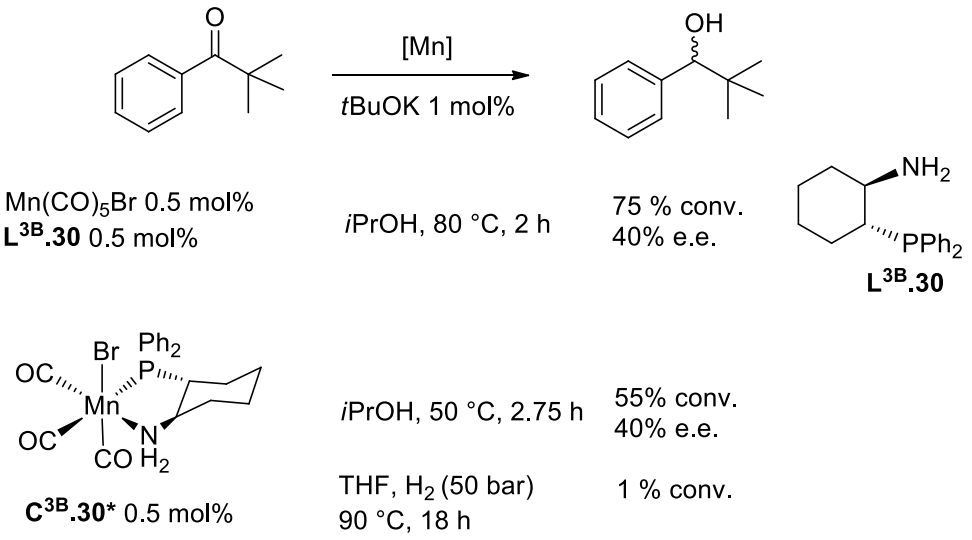

Scheme B^{3II}.9 Comparison of the activity for reduction of 2,2-dimethylpropiophenone with (1*R*,2*R*)-2-(diphenylphosphino)cyclohexylamine **L^{3B}.30**.

The same enantiomeric excess of 40% was achieved when the *in situ* and the well-defined systems (0.5 mol%, *t*BuOK 1 mol%) were used (**Scheme B^{3II}.9**). The complex **C^{3B}.30***, having a purity of *c.a.* 90%, was also considered as pre-catalyst for the hydrogenation of the same substrate with molecular dihydrogen in THF at 90 °C but was found to be inactive.[16]

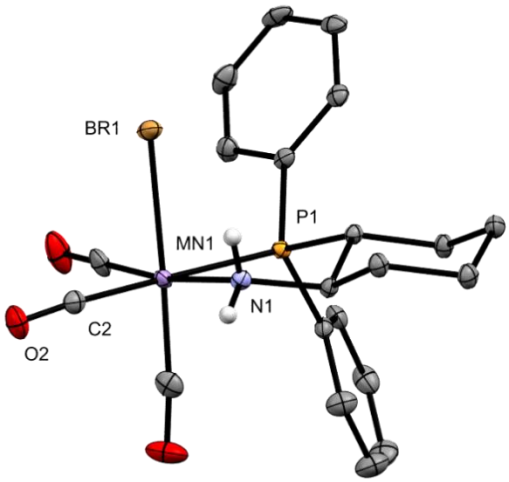

Figure B^{3II}.2 ORTEP views of the molecular structures of complex **C^{3B}.30***, with thermal ellipsoids drawn at 50% probability. Hydrogens, except the N*H*, were omitted for clarity.

According to this preliminary studies, PN ligands are good candidates as ligand for Mn(I) complexes for transfer hydrogenation of ketones. The best PN ligands are **L^{3B}.34** and **L^{3B}.35**. They showed a better activity than NN ligands while the

enantioselectivity was comparable with the use of the best NN ligand **L^{3B}.27**. Surprisingly first hydrogenation attempts failed with **C^{3B}.30***.

III- Conclusion, Part B

The results in this part show that simple, commercially available diamine bidentate ligands on manganese(I) can give rise to high activities for transfer hydrogenation of ketones and aldehydes.

In comparison with the other catalytic system based on dipicolylamine developed by Beller,[17] the removal of one part of the ligand resulted in an impressive increase in activity. Indeed, Beller's catalytic system (TON: 48, TOF: 2 h^{-1}) needed 70 °C during 24 h to be efficient while 20 min at 80 °C, or 24 h at 30 °C, were sufficient in our case, associated with a TON (2000) multiplied by 40 and a TOF (3600 h^{-1}) multiplied by 1800 (**Figure B^{3II}.3**).

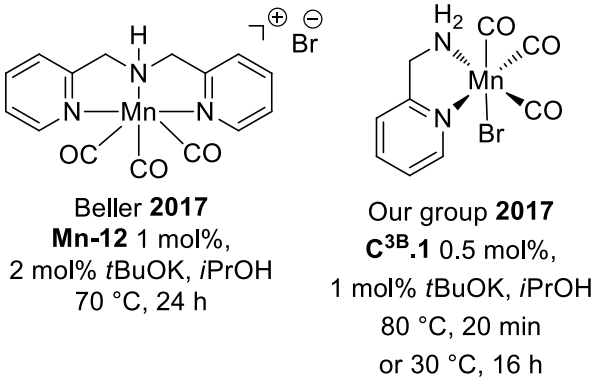

Beller **2017**
Mn-12 1 mol%,
2 mol% *t*BuOK, *i*PrOH
70 °C, 24 h

Our group **2017**
C^{3B}.1 0.5 mol%,
1 mol% *t*BuOK, *i*PrOH
80 °C, 20 min
or 30 °C, 16 h

Figure B^{3II}.3 Comparison of the experimental conditions for the transfer hydrogenation with manganese pre-catalysts.

Preliminary tests have demonstrated that aldimines can be also reduced with manganese catalysts supported with aminomethylpyridine ligand.

We also succeeded to simplify the procedure, by generating *in situ* the catalyst from commercial precursors. This easily accessible procedure encouraged us to study a screening of ligands. Among them, ethylene diamine showed good activity, pushing the simplicity of the catalytic system to it limits. Simple commercial chiral ligands were also submitted to this procedure and e.e. up to 90% was reached. Further investigations in the architecture of the ligand will be done.

IV- Reference

[1] H. Doucet, T. Ohkuma, K. Murata, T. Yokozawa, M. Kozawa, E. Katayama, A. F. England, T. Ikariya, R. Noyori, *Angew. Chem. Int. Ed.* **1998**, *37*, 1703–1707.

[2] R. Noyori, M. Yamakawa, S. Hashiguchi, *J. Org. Chem.* **2001**, *66*, 7931–7944.

[3] B. Zhao, Z. Han, K. Ding, *Angew. Chem. Int. Ed.* **2013**, *52*, 4744–4788.

[4] W. Baratta, E. Herdtweck, K. Siega, M. Toniutti, P. Rigo, *Organometallics* **2005**, *24*, 1660–1669.

[5] C. M. Alvarez, R. Carrillo, R. Garcia-Rodriguez, D. Miguel, *Chem. Commun.* **2012**, *48*, 7705–7707.

[6] A. Ouali, J.-P. Majoral, A.-M. Caminade, M. Taillefer, *ChemCatChem* **2009**, *1*, 504–509.

[7] S. Baldino, S. Facchetti, A. Zanotti-Gerosa, H. G. Nedden, W. Baratta, *ChemCatchem* **2016**, *8*, 2279–2288.

[8] T. K. Mukhopadhyay, C. L. Rock, M. Hong, D. C. Ashley, T. L. Groy, M.-H. Baik, R. J. Trovitch, *J. Am. Chem. Soc.* **2017**, *139*, 4901–4915.

[9] R. Hartmann, P. Chen, *Angew. Chem. Int. Ed.* **2001**, *40*, 3581–3585.

[10] P. A. Dub, B. L. Scott, J. C. Gordon, *J. Am. Chem. Soc.* **2017**, *139*, 1245–1260.

[11] P. A. Dub, N. J. Henson, R. L. Martin, J. C. Gordon, *J. Am. Chem. Soc.* **2014**, *136*, 3505–3521.

[12] T. Ohkuma, H. Ooka, S. Hashiguchi, T. Ikariya, R. Noyori, *J. Am. Chem. Soc.* **1995**, *117*, 2675–2676.

[13] A. Dubey, L. Nencini, R. R. Fayzullin, C. Nervi, J. R. Khusnutdinova, *ACS Catal.* **2017**, *7*, 3864–3868.

[14] E. Pastorczak, C. Corminboeuf, *J. Chem. Phys.* **2017**, *146*, 120901.

[15] L. A. Saudan, C. Saudan, C. Debieux, P. Wyss, *Angew. Chem. Int. Ed.* **2007**, *46*, 7473–7476.

[16] R. van Putten, E. A. Uslamin, M. Garbe, C. Liu, A. Gonzalez-de-Castro, M. Lutz, K. Junge, E. J. M. Hensen, M. Beller, L. Lefort, E. Pidko, *Angew. Chem. Int. Ed.* **2017**, *56*, 7531–7534.

[17] M. Perez, S. Elangovan, A. Spannenberg, K. Junge, M. Beller, *ChemSusChem* **2017**, *10*, 83–86.

Supporting Information Chapter 3

General informations

All reactions were carried out with oven-dried glassware using standard Schlenk techniques under an inert atmosphere of dry argon or in an argon-filled glove-box. Toluene, THF, diethyl ether (Et_2O), and dichloromethane were dried over Braun MB-SPS-800 solvent purification system and degassed by thaw-freeze cycles. Ethanol (EtOH absolute anhydrous, Pure, Carlo Erba) was degassed and stored on molecular sieves 4 Å. Technical grade petroleum ether and ethyl acetate were used for chromatography column. Analytical TLC was performed on Merck $60F_{254}$ silica gel plates (0.25 mm thickness). Column chromatography was performed on Acros Organics Ultrapure silica gel (mesh size 40-60 µm, 60 Å). All reagents were obtained from commercial sources and liquid reagents were dried on 4 Å molecular sieves and degassed prior to use. Manganese pentacarbonyl bromide, min. 98%, were purchased from Strem Chemicals.

^{1}H, ^{13}C, ^{19}F and ^{31}P NMR spectra were recorded in $CDCl_3$, acetone-d_6, or CD_3OD at 298 K, on Bruker, AVANCE 400 and AVANCE 300 spectrometers at 400.1, 100.6, 376.5 and 162.2 MHz, respectively. ^{1}H and ^{13}C NMR spectra were calibrated using the residual solvent signal at the corresponding central peak (^{1}H: $CDCl_3$ 7.26 ppm, acetone-d_6 2.05 ppm, CD_3OD 3.31 ppm; ^{13}C: $CDCl_3$ 77.16 ppm, acetone-d_6 29.84 ppm, CD_3OD 49.0 ppm). ^{19}F and ^{31}P NMR spectra calibrated against $CFCl_3$ and 85% H_3PO_4 internal standard, respectively. Chemical shift (δ) and coupling constants (*J*) are given in ppm and in Hz, respectively. The peak patterns are indicated as follows: (s, singlet; d, doublet; t, triplet; q, quartet; quin, quintet; ; sex, sextuplet; sept, septuplet; oct, octuplet; m, multiplet, and br. for broad).

A – I – Hydrogenation of ketones

Non-stirred Parr autoclaves (22 mL) were used for the hydrogenation.

IR spectra were measured in CH_2Cl_2 solution with a Shimadzu IR-Affinity 1 instrument and given in cm^{-1} with a relative intensity in the parenthesis (vs, very strong; s, strong; m, medium). HR–MS spectra (ESI positive mode) and microanalysis were carried out by the corresponding facilities at the CRMPO (Centre Régional de Mesures Physiques de l'Ouest), University of Rennes 1.

GC analyses were performed with GC-2014 (Shimadzu) 2010 equipped with a 30 m capillary column (Supelco, SPBTM-20, fused silica capillary column, 30 m × 0.25 mm × 0.25 mm film thickness).

Low Resolution mass spectra were obtained on a QP2010 GC/MS apparatus from Shimadzu equipped with a 30 m capillary column (Supelco, SLBTM-5ms, fused silica capillary column, 30 M × 0.25 mm × 0.25 mm film thickness).

Synthesis of ligands L^{3A}.1-4

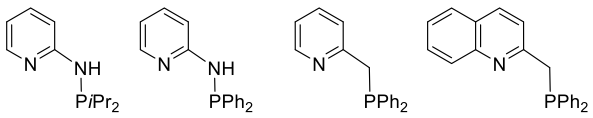

L1 L2 L3 L4

The ligands L^{3A}.1,[1] L^{3A}.2,[2] L^{3A}.3[3] and L^{3A}.4[4] were synthesized according to the literature procedures.[1-4]

Synthesis of complexes C^{3A}.1-4

Complex C^{3A}.1

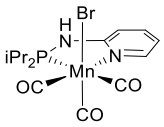

$Mn(CO)_3Br(L1)$ (C^{3A}.1). **L^{3A}.1** (210 mg, 0.365 mmol) was added to a solution of $Mn(CO)_5Br$ (100 mg, 0.365 mmol, 1.0 equiv.) in anhydrous toluene (6 mL). The mixture was stirred at 100 °C overnight, then cooled to r.t. and toluene was evaporated under vacuum. The crude residue was dissolved in dichloromethane (1 mL) and then pentane (5 mL) was added to afford yellow needle crystals. The supernatant was removed and the crystals were washed with pentane (3×2 mL) and dried under vacuum to afford pure compound **C^{3A}.1** (136 mg, 87%). Single crystals suitable for X-Ray diffraction studies were grown by slow diffusion of pentane into a CH_2Cl_2 solution at r.t.

^{1}H NMR (400.1 MHz, acetone-d_6) δ 8.68 – 8.44 (m, 1H, Py), 7.77 (br. d, J_{HH} = 5.0 Hz, 1H, N*H*), 7.63 (t, J_{HH} = 7.7 Hz, 1H, Py), 7.02 (d, J_{HH} = 8.4 Hz, 1H, Py), 6.81 (t, J_{HH} = 6.5 Hz, 1H), 3.57 – 3.24 (m, 1H, C*H*$(CH_3)_2$, 2.98 – 2.66 (m, 1H, C*H*$(CH_3)_2$), 1.58 – 1.33 (m, 9H, CH(C*H*$_3)_2$), 1.27 (dd, J_{PH} = 15.0, J_{HH} = 7.2 Hz, 3H, CH(C*H*$_3)_2$).

^{13}C{^{1}H} NMR (100.6 MHz, acetone-d_6) δ 224.1 (br. s, CO), 216.6 (br. s, CO), 162.9 (d, $^2J_{PC}$ = 12.6 Hz, C_{Py}), 154.0 (d, J = 4.4 Hz, CH_{Py}), 140.2 (s, CH_{Py}), 116.6 (s, CH_{Py}), 111.9 (d, J_{PC} = 6.9 Hz, CH_{Py}), 28.7 (d, $^1J_{PC}$ = 24.3 Hz, *C*H$(CH_3)_2$), 27.6 (d, $^1J_{PC}$ = 22.6 Hz, *C*H$(CH_3)_2$), 19.4 (d, $^3J_{PC}$ = 7.7 Hz, CH(*C*H$_3)_2$), 19.0 (d, $^3J_{PC}$ = 6.2 Hz, CH(*C*H$_3)_2$), 18.4 (s, CH(*C*H$_3)_2$), 17.3 (d, $^3J_{PC}$ = 4.6 Hz, CH(*C*H$_3)_2$).

^{31}P{^{1}H} NMR (162.0 MHz, acetone-d_6) δ 125.5.

IR (CH_2Cl_2): ν_{CO} 2021 (s), 1936 (m), 1911 (s), 1884 (vs) cm^{-1}.

Anal. Calcd. (%) for $C_{14}H_{19}BrMnN_2O_3P$: C, 39.18; H, 4.46; N, 6.53. Found: C, 39.12; H, 4.44; N, 6.40.

HR MS (ESI): m/z calcd for $C_{14}H_{19}{}^{79}BrMnN_2NaO_3P$ ($M + Na^+$) 450.9589, found 450.9587 (0 ppm).

Complex **C^{3A}.2**

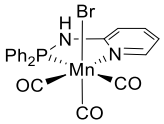

Mn(CO)$_3$Br(L2) (C^{3A}.2): Following the general procedure employed for the synthesis of **C^{3A}.1**, starting from **L2** (101 mg, 0.365 mmol) and Mn(CO)$_5$Br (100 mg, 0.365 mmol) the product **C^{3A}.2** (161 mg, 89%) was obtained as yellow crystals.

^{1}H NMR (400.1 MHz, acetone-d_6) δ 8.86 (d, J_{HH} = 5.3 Hz, 1H, N*H*), 8.63 (d, J_{HH} = 5.6 Hz, 1H, Py), 7.97 – 7.81 (m, 2H, Ph), 7.78 – 7.70 (m, 3H, Ph), 7.63 – 7.38 (m, 6H, Ph + Py), 7.27 (br d, J_{HH} = 6.5 Hz, 1H, Py), 6.92 (t, J_{HH} = 6.4 Hz, 1H, Py).
^{13}C{^{1}H} NMR (100.6 MHz, acetone-d_6) δ 224.1 (br. s, CO), 221.9 (br. s, CO), 217.0 (br. s, CO), 162.1 (d, $^2J_{PC}$ = 15.9 Hz, C_{Py}), 154.1 (d, J_{PC} = 4.5 Hz, CH_{Py}), 140.6 (s, CH_{Py}), 138.0 (d, $^1J_{PC}$ = 47.4 Hz, $C_{ipso\ Ph}$), 133.5 (d, $^1J_{PC}$ = 48.9 Hz, $C_{ipso\ Ph}$), 133.2 (d, J_{PC} = 11.2 Hz, CH_{Ph}), 131.5 (d, J_{PC} = 4.7 Hz, CH_{Ph}), 131.45 (d, J_{PC} = 4.2 Hz, CH_{Ph}), 130.8 (d, J_{PC} = 12.3 Hz, CH_{Ph}), 129.6 (d, J_{PC} = 9.9 Hz, CH_{Ph}), 128.8 (d, J_{PC} = 10.6 Hz, CH_{Ph}), 117.4 (s, CH_{Py}), 112.6 (d, J_{PC} = 8.1 Hz, CH_{Py}).

^{31}P{^{1}H} NMR (162.0 MHz, acetone-d_6) δ 101.9.

IR (CH_2Cl_2): ν_{CO} 2023 (s), 1948 (s), 1917 (s) cm^{-1}.

Anal. Calcd. (%) for $C_{20}H_{15}BrMnN_2O_3P$: C, 48.32; H, 3.04; N, 5.63. Found: C, 47.98; H, 3.10; N, 5.61.

HR MS (ESI): m/z calcd for $C_{17}H_{15}MnN_2P$ (M^+–3CO–Br) 333.03478, found 333.0345 (1 ppm).

Complex **C^{3A}.**3

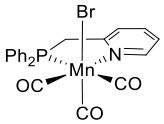

Mn(CO)$_3$Br(L3) (C^{3A}.3): Following the general procedure employed for the synthesis of **C^{3A}.1**, starting from **L3** (101 mg, 0.365 mmol) and Mn(CO)$_5$Br (100 mg, 0.364 mmol), the product **C^{3A}.3** (164.5 mg, 91%) was obtained as yellow crystals.

^{1}H NMR (400.1 MHz, acetone-d_6) δ 9.11 (d, J_{HH} = 5.0 Hz, 1H, Py), 8.14 – 7.95 (m, 3H, Ph), 7.90 (d, J = 7.1 Hz, 1H, Py), 7.63 – 7.49 (m, 3H, Ph), 7.48 – 7.40 (m, 6H, Ph +Py), 4.79 – 4.53 (m, 2H, PCH_2).

^{13}C{^{1}H} NMR (100.6 MHz, acetone-d_6) δ 225.1 (br. s, CO), 223.1 (br. s, CO), 217.4 (br. s, CO), 162.8 (d, $^2J_{PC}$ = 7.6 Hz, C_{Py}), 156.2 (d, J_{PC} = 3.8 Hz, CH_{Py}), 140.3 (s, CH_{Py}), 135.7 (d, $^1J_{PC}$ = 39.2 Hz, $C_{ipso\ Ph}$), 134.9 (d, J_{PC} = 9.7 Hz, CH_{Ph}), 132.0 (d, J_{PC} = 2.5 Hz, CH_{Ph}), 131.6 (d, J_{PC} = 10.0 Hz, CH_{Ph}), 131.1 (d, J_{PC} = 2.1 Hz, CH_{Ph}), 131.1 (d, J_{PC} = 44.1 Hz, $C_{ipso\ Ph}$), 129.8 (d, J_{PC} = 9.2 Hz, CH_{Ph}), 129.5 (d, J_{PC} = 10.0 Hz, CH_{Ph}), 125.8 (d, J_{PC} = 9.6 Hz, CH_{Py}), 124.4 (s, CH_{Py}) , 41.1 (d, $^1J_{PC}$ = 25.4 Hz, PCH_2).

^{31}P{^{1}H} NMR (162.0 MHz, acetone-d_6) δ 57.3.

IR (CH_2Cl_2): ν_{CO} 2021 (s), 1939 (m), 1915 (vs) cm^{-1}.

Anal. Calcd (%). for $C_{21}H_{16}BrNO_3PMn$: C, 50.83; H, 3.25; N, 2.82. Found: C, 50.64; H, 3.23; N, 2.78.

HR MS (ESI): m/z calcd for $C_{18}H_{16}MnNP$ (M^+–3CO–Br) 332.03953, found 332.0404 (3 ppm).

Complex **C^{3A}.4**

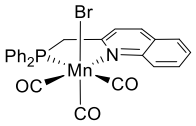

Mn(CO)$_3$Br(L4) (C^{3A}.4): Following the general procedure employed for the synthesis of **C^{3A}.1**, starting from **L4** (119 mg, 0.365 mmol) and Mn(CO)$_5$Br (100 mg, 0.365 mmol), the product **C^{3A}.4** (179 mg, 90%) was obtained as yellow crystals.

^{1}H NMR (400.1 MHz, acetone-d_6) δ 9.00 (d, J_{HH} = 8.8 Hz, 1H, Py), 8.56 (s, 1H, Ar), 8.20 – 7.84 (m, 5H, Ph + Ar), 7.74 (t, J_{HH} = 6.3 Hz, 1H, Ar), 7.68 – 7.50 (m, 3H, Ph + Ar), 7.46 – 7.33 (m, 5H, Ph + Ar), 5.30 (dd, $^{2}J_{HH}$ = 16.5 Hz, $^{2}J_{PH}$ = 6.7 Hz, 1H, PCH_2), 4.90 (t, $^{2}J_{PH}$ = $^{2}J_{HH}$ = 16.0 Hz, 1H, PCH_2).

^{13}C{^{1}H} NMR (100.6 MHz, acetone-d_6) δ 225.9 (br. s, CO), 223.9 (br. s, CO), 217.7 (br. s, CO), 166.8 (d, J_{PC} = 6.9 Hz, C_{Py}), 150.3 (d, J_{PC} = 1.9 Hz, CH_{Py}), 141.1 (d, J_{PC} = 1.7 Hz, CH_{Ph}), 134.9 (d, J_{PC} = 9.8 Hz, CH_{Ph}), 134.8 (d, $^{1}J_{PC}$ = 39.7 Hz, $C_{ipso\ Ph}$), 134.0 (s, C_{Ar}), 132.2 (d, J_{PC} = 2.4 Hz, CH_{Ph}), 132.0 (s, CH_{Ar}), 131.7 (d, J_{PC} = 10.0 Hz, CH_{Ph}), 131.1 (d, J_{PC} = 2.2 Hz, CH_{Ph}), 130.6 (d, J_{PC} = 46.1 Hz, $C_{ipso\ Ph}$), 130.3 (s, CH_{Ar}), 130.25 (s, CH_{Ar}), 129.8 (d, J_{PC} = 9.2 Hz, CH_{Ph}), 129.6 (d, J_{PC} = 10.1 Hz, CH_{Ph}), 129.2 (s, C_{Ar}), 128.7 (s, CH_{Ar}), 127.9 (s, CH_{Ph}), 123.3 (d, J_{PC} = 9.7 Hz, CH_{Py}), 44.7 (d, $^{1}J_{PC}$ = 26.8 Hz, PCH_2).

^{31}P{^{1}H} NMR (162.0 MHz, acetone-d_6) δ 55.4.

IR (CH_2Cl_2): ν_{CO} 2015 (s), 1934 (m), 1915 (vs) cm^{-1}.

Anal. Calc (%). for ($C_{25}H_{18}BrMnNO_3P$).(CH_2Cl_2): C, 49.48; H, 3.19; N, 2.22. Found: C, 49.43; H, 3.30; N, 2.44.

HR MS (ESI): m/z calcd for $C_{22}H_{18}MnNP$ (M^+–3CO–Br) 382.05518, found 382.0545 (2 ppm).

Complex hydride **C^{3A}.2c**

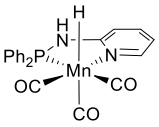

In a Schlenk tube under inert atmosphere, KHMDS (20 mg, 0.1 mmol, 1 equiv.) was added to a solution of **C^{3A}.2** (50 mg, 0.1 mmol) in toluene (8 mL). The reaction mixture was then cooled down to -78 °C, the schlenk tube was pressurized with 2 bar of H_2 (do not pressurized over 2 bar in a schlenk tube). The solution was stirred overnight at r.t. After filtration, the solvent was removed under reduced pressure and the solid was washed with pentane (2 x 5mL). Attempts to crystallize this complex failed. And the ^{31}P{^{1}H} NMR analysis show that the complex is not highly pure.

^{1}H NMR (400 MHz, C_6D_6) δ 8.27 (m, 1H), 7.88 (m, 2H), 7.46 (m, 2H), 7.05 (m, 6H), 6.55 (m, 1H), 5.79 (m, 1H), 5.64 (m, 1H), 5.01 (br s, 1H), -4.29 (d, J = 59.0 Hz, 1H).

^{31}P NMR (162 MHz, C_6D_6) δ 126.6.

General procedure for hydrogenation reactions

In an argon filled glove box, an autoclave was charged with complex **C^{3A}.2** (5.0 mg, 0.5 mol%) and anhydrous toluene (4.0 mL), followed by ketone (2.0 mmol) and potassium bis(trimethylsilyl)amide (KHMDS, 8.0 mg, 2 mol%), in this order. The autoclave is then charged H_2 (50 bar). The mixture was stirred for 20 hours at 50 °C in an oil bath. The solution was then diluted with ethyl acetate (2.0 mL) and filtered through a small pad of silica (2 cm in a Pasteur pipette). The silica was washed with ethyl acetate. The filtrate was evaporated and the crude residue was purified by column chromatography (SiO_2, mixture of petroleum ether/ethyl acetate as eluent).

Mercury test

In an argon filled glove box, an autoclave was charged with complex **C^{3A}.2** (0.5 mol%, 5.0 mg), KHMDS (2 mol%, 8.0 mg) and anhydrous toluene (4.0 mL), followed by Hg (1.5 mmol, 602 mg) and acetophenone (234 µL, 2.0 mmol) in this order. The autoclave is then charged H_2 (50 bar). The mixture was stirred for 18 hours at 80 °C in an oil bath. The solution was then diluted with ethyl acetate (2.0 mL) and filtered through a small pad of silica (2 cm in a Pasteur pipette). The silica was washed with ethyl acetate (2.0 mL × 2). The filtrate was evaporated to provide the crude NMR in $CDCl_3$ (93 % conversion).

Mechanistic insights

Young NMR tube experiments

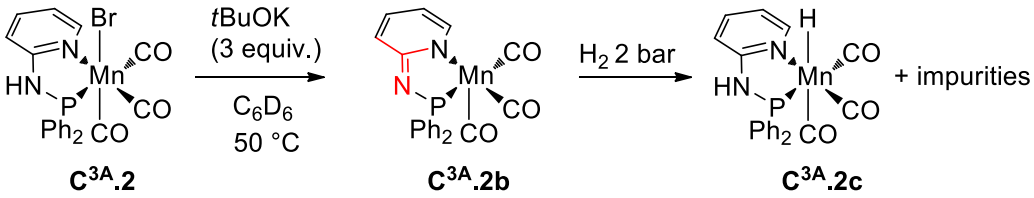

C^{3A}.2 **C^{3A}.2b** **C^{3A}.2c**

Procedure: In the glovebox, *t*BuOK (5 mg, 3 equiv.) was added to a solution of manganese complex **C^{3A}.2** (7.5 mg, 0.015 mmol) in C_6D_6 in a Young tube. Due to the low solubility of the complex in C_6D_6 and the presence of salts in the brown solution, the reaction mixture was sonicated and a precipitate fell down in the bottom of the NMR tube. After NMR analysis, the reaction mixture was cooled down to -78 °C to freeze the solvent and the tube was pressurized with 2 bar of H_2, the solution turn yellow within few minutes and the solution was heated at 80 °C during 3 days.

Signals **C^{3A}.2**: $^{31}P\{^1H\}$ NMR (162 MHz, C_6D_6) δ 103.8.

After adding *t*BuOK: $^{31}P\{^1H\}$ NMR (162 MHz, C_6D_6) δ 90.4.

After adding H_2: $^{31}P\{^1H\}$ NMR (162 MHz, C_6D_6) δ 126.6, 96.2, 90.5, 49.0.

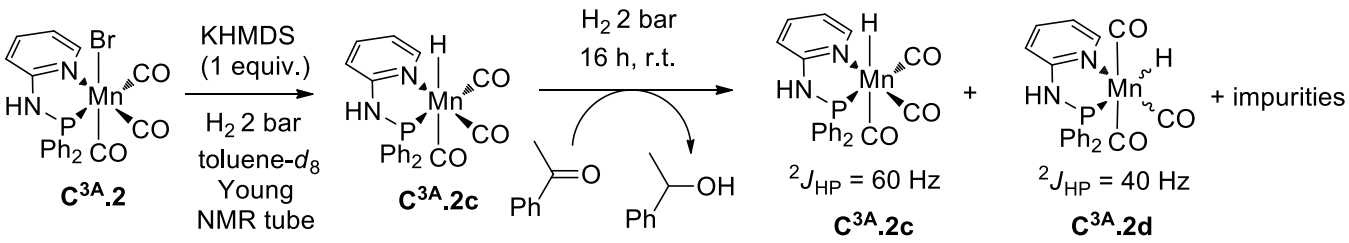

C^{3A}.2 **C^{3A}.2c** **C^{3A}.2c** **C^{3A}.2d**

Procedure: In the glovebox, KHMDS (3 mg, 1.05 equiv.) was added to a solution of manganese complex **C^{3A}.2** (7 mg, 0.014 mmol) in toluene-d_8 in a Young NMR tube. Outside of the glovebox, the reaction mixture was then cooled down to -78 °C to freeze the solvent and the tube was pressurized with 2 bar of H_2. After 2 h at r.t., acetophenone (8 µL, 10 equiv.) was added to the NMR tube in the glovebox. NMR analyses were done after 16 h at r.t. then after 3 days.

Typical signals after adding hydrogen:

$^{31}P\{^1H\}$ NMR (162 MHz, Toluene-d_8) δ 132.0, 95. 1.

^1H NMR (400 MHz, Toluene-d_8) δ -4.46 (d, J = 60 Hz, 1H).

Typical signals after adding acetophenone:

$^{31}P\{^1H\}$ NMR (162 MHz, Toluene-d_8) δ 151.1, 131.9, 108.2, 101.1, 95.3.

^1H NMR (400 MHz, Toluene-d_8) δ -4.44 (d,Mn-H **C^{3A}.2c** ,J = 60 Hz), -6.27 (d, Mn-H **C^{3A}.2d**, J = 40 Hz).

Characterization of the products of the catalysis

1-Phenylethanol[5] (b1)

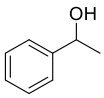

According to general procedure, acetophenone **a1** (234 µL, 2.0 mmol) gave the title compound **b1** as a colorless oil (220 mg, 90%).

^1H NMR (400.1 MHz, $CDCl_3$): δ 7.38 – 7.25 (m, 5H), 4.88 (q, J_{HH} = 6.5 Hz, 1H), 1.95 (s, br, 1H), 1.49 (d, J_{HH} = 6.5 Hz, 3H).
$^{13}C\{^1H\}$ NMR (100.6 MHz, $CDCl_3$): δ 145.9, 128.6, 127.6, 125.5, 70.5, 25.3.

1-(Naphthalen-2-yl)ethanol[5] (b2)

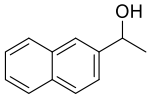

According to general procedure, 1-(naphthalen-2-yl)ethan-1-one **a2** (340 mg, 2.0 mmol) gave the title compound **b2** as a white solid (330.5 mg, 95%).
^1H NMR (400.1 MHz, $CDCl_3$): δ 7.85 – 7.81 (m, 4H), 7.52 – 7.45 (m, 3H), 5.07 (q, J_{HH} = 6.5 Hz, 1H), 1.91 (br. s, 1H), 1.59 (d, J_{HH} = 6.5 Hz, 3H).
$^{13}C\{^1H\}$ NMR (100.6 MHz, $CDCl_3$): δ 143.3, 133.5, 133.1, 128.4, 128.1, 127.8, 126.3, 125.9, 123.95, 123.93, 70.7, 25.3.

1-(4-Tolyl)ethanol[5] (b3)

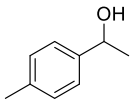

According to general procedure, 4'-methylacetophenone **a3** (267 µL, 2.0 mmol) gave the title compound **b3** as a colorless oil (234 mg, 86%).
^{1}H NMR (400.1 MHz, $CDCl_3$): δ 7.27 (d, J_{HH} = 8.0 Hz, 2H), 7.16 (d, J_{HH} = 8.0 Hz, 2H), 4.87 (q, J_{HH} = 6.5 Hz, 1H), 2.35 (s, 3H), 1.49 (br. s, 1H), 1.47 (d, J_{HH} = 6.5 Hz, 3H).
$^{13}C\{^{1}H\}$ NMR (100.6 MHz, $CDCl_3$): δ 143.0, 137.3, 129.3, 125.5, 70.4, 25.2, 21.2.

1-(4-Methoxyphenyl)ethanol[5] (b4)

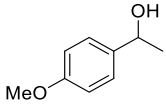

According to general procedure, 4'-methoxyacetophenone **a4** (300 mg, 2.0 mmol) gave the title compound **b4** as a colorless oil (277 mg, 91%).
^{1}H NMR (400.1 MHz, $CDCl_3$): δ 7.30 (d, J_{HH} = 8.7 Hz, 2H), 6.88 (d, J_{HH} = 8.7 Hz, 2H), 4.85 (q, J_{HH} = 6.5 Hz, 1H), 3.80 (s, 3H), 1.79 (br. s, 3H), 1.48 (d, J_{HH} = 6.5 Hz, 3H).
$^{13}C\{^{1}H\}$ NMR (100.6 MHz, $CDCl_3$): δ 159.1, 138.1, 126.8, 114.0, 70.1, 55.4, 25.1.

1-(4-Fluorophenyl)ethanol[5] (b5)

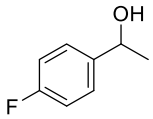

According to general procedure, 4'-fluoroacetophenone **a5** (244 µL, 2.0 mmol) gave the title compound **b5** as a pale yellow oil (269 mg, 96%).

^{1}H NMR (400.1 MHz, $CDCl_3$): δ 7.35 – 7.32 (m, 2H), 7.05 – 7.00 (m, 2H), 4.88 (q, J_{HH} = 6.5 Hz, 1H), 1.84 (br. s, 1H), 1.48 (d, J_{HH} = 6.5 Hz, 3H).

$^{13}C\{^{1}H\}$ NMR (100.6 MHz, $CDCl_3$): δ 162.2 (d, J_{CF} = 245 Hz), 141.6 (d, J_{CF} = 3 Hz), 127.2 (d, J_{CF} = 8 Hz), 115.4 (d, J_{CF} = 21 Hz), 69.9, 25.4.

$^{19}F\{^{1}H\}$ NMR (376.5 MHz, $CDCl_3$): δ –115.37.

1-(4-Chlorophenyl)ethanol[5] (b6)

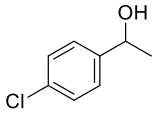

According to general procedure, 4'-chloroacetophenone **a6** (259.5 µL, 2.0 mmol) gave the title compound **b6** as a pale yellow oil (188 mg, 60%).
^{1}H NMR (400.1 MHz, $CDCl_3$): δ 7.37 – 7.24 (m, 4H), 4.88 (q, J_{HH} = 6.5 Hz, 1H), 1.90 (br. s, 1H), 1.47 (d, J_{HH} = 6.5 Hz, 3H).
$^{13}C\{^{1}H\}$ NMR (100.6 MHz, $CDCl_3$): δ 144.4, 133.2, 128.7, 126.9, 69.9, 25.4.

1-(4-Bromophenyl)ethanol (b7)

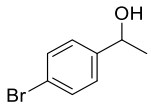

According to general procedure, 4'-bromoacetophenone **a7** (398 mg, 2.0 mmol) gave the title compound **b7** as a pale yellow oil (370 mg, 92%).
^{1}H NMR (400.1 MHz, $CDCl_3$): δ 7.49 (d, *J* = 8.4 Hz, 2H), 7.27 (d, J_{HH} = 8.4 Hz, 2H), 4.89 (q, J_{HH} = 6.5 Hz, 1H), 1.89 (br. s, 1H), 1.49 (d, J_{HH} = 6.5 Hz, 3H).
^{13}C{^{1}H} NMR (100.6 MHz, $CDCl_3$): δ 144.7, 131.4, 127.1, 121.0, 69.5, 25.1.

1-(4-Iodophenyl)ethanol[5] (b8)

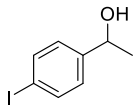

According to general procedure, 4'-iodoacetophenone **a8** (246 mg, 1.0 mmol) gave the title compound **b8** as a brown oil (122 mg, 49%).
^{1}H NMR (400.1 MHz, $CDCl_3$): δ 7.66 (d, J_{HH} = 8.3 Hz, 1H), 7.10 (d, J_{HH} = 8.2 Hz, 1H), 4.82 (q, J_{HH} = 6.2 Hz, 1H), 2.12 (br. s, 1H), 1.45 (d, J_{HH} = 6.2 Hz, 3H).
^{13}C{^{1}H} NMR (100.6 MHz, $CDCl_3$): δ 145.6, 137.6, 127.5, 92.8, 69.9, 25.3.

1-(4-Trifluoromethylphenyl)ethanol[5] (b9)

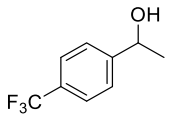

According to general procedure, 4'-trifluoromethylacetophenone **a9** (376 mg, 2.0 mmol) gave the title compound **b9** as a colorless oil (304 mg, 80%).
^{1}H NMR (400.1 MHz, $CDCl_3$): δ 7.61 (d, J_{HH} = 8.1 Hz, 2H), 7.49 (d, J_{HH} = 8.1 Hz, 2H), 4.97 (q, J_{HH} = 6.5 Hz, 1H), 1.90 (s, br, 1H), 1.51 (d, J_{HH} = 6.5 Hz, 3H).
^{13}C{^{1}H} NMR (100.6 MHz, $CDCl_3$): δ 149.8, 129.8 (q, J_{CF} = 33 Hz), 125.8, 125.6 (q, J_{CF} = 4 Hz), 124.3 (q, J_{CF} = 270 Hz), 70.0, 25.5.
^{19}F {^{1}H} NMR (376.5 MHz, $CDCl_3$): δ –62.5.

1-(4-Aminophenyl)ethanol[5] (b12)

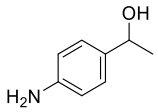

According to general procedure, 4'-aminoacetophenone **a12** (135 mg, 1.0 mmol) gave the title compound **b12** as a yellowish brown solid (128 mg, 93%).
^{1}H NMR (400.1 MHz, $CDCl_3$): δ 7.14 (d, J_{HH} = 8.4 Hz, 2H), 6.63 (d, J_{HH} = 8.4 Hz, 2H), 4.75 (q, J_{HH} = 6.5 Hz, 1H), 3.65 (s, 2H), 2.27 (s, 1H), 1.44 (d, J_{HH} = 6.5 Hz, 3H).
^{13}C{^{1}H} NMR (100.6 MHz, $CDCl_3$): δ 145.7, 136.1, 126.7, 115.2, 70.0, 24.9.

1-Phenylpropanol[5] (b13)

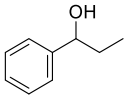

According to general procedure, propiophenone **a13** (266 µL, 2.0 mmol) gave the title compound **b13** as a colorless oil (251 mg, 92%).
^{1}H NMR (400.1 MHz, $CDCl_3$): δ 7.40 – 7.28 (m, 5H), 4.62 (t, J_{HH} = 6.8 Hz, 1H), 1.89 – 1.74 (m, 3H, CH_2+OH), 0.95 (t, J_{HH} = 7.5 Hz, 3H).
$^{13}C\{^{1}H\}$ NMR (100.6 MHz, $CDCl_3$): δ 144.7, 128.5, 127.6, 126.1, 76.2, 32.0, 10.3.

2-Methyl-1-phenylpropanol[5] (b14)

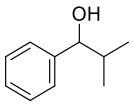

According to general procedure, 2-methyl-1-phenylpropanone **a14** (300 µL, 2.0 mmol) gave the title compound **b14** as a colorless oil (90 mg, 30%).
^{1}H NMR (400.1 MHz, $CDCl_3$): δ 7.39 – 7.27 (m, 5H), 4.38 (d, J_{HH} = 6.9 Hz, 1H), 2.05 – 1.93 (m, 2H, CH+OH), 1.03 (d, J_{HH} = 6.7 Hz, 3H), 0.83 (d, J_{HH} = 6.7 Hz, 3H).
$^{13}C\{^{1}H\}$ NMR (100.6 MHz, $CDCl_3$): δ 143.8, 128.3, 127.5, 126.7, 80.2, 35.4, 19.1, 18.4.

1-(Benzofuran-2-yl)ethan-1-ol[5] (b16)

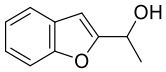

According to general procedure, 1-(benzofuran-2-yl)ethan-1-one **a16** (321 mg, 2.0 mmol) gave the title compound **b16** as a brown oil (299 mg, 92%).
^{1}H NMR (400.1 MHz, $CDCl_3$): δ 7.57 (d, J_{HH} = 7.7 Hz, 1H), 7.48 (d, J_{HH} = 7.8 Hz, 1H), 7.31 – 7.22 (m, 2H), 6.63 (s, 1H), 5.05 (q, J_{HH} = 6.5 Hz, 1H), 2.19 (br. s, 1H), 1.67 (d, J_{HH} = 6.5 Hz, 3H).
$^{13}C\{^{1}H\}$ NMR (100.6 MHz, $CDCl_3$): δ 160.3, 154.9, 128.3, 124.3, 122.9, 121.2, 111.3, 101.9, 64.3, 21.6.

1-(Pyridin-2-yl)ethan-1-ol[5] (b17)

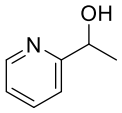

According to general procedure, 1-(pyridin-2-yl)ethan-1-one **a17** (28 µL, 0.25 mmol) gave the title compound **b17** as a dark-red oil (28 mg, 89%).
^{1}H NMR (400.1 MHz, $CDCl_3$): δ 8.54 (br. s, 1H), 7.70 (t, J_{HH} = 7.6 Hz, 1H), 7.29 (d, J_{HH} = 8.3 Hz, 1H), 7.22 – 7.19 (m, 1H), 4.91 – 4.89 (br. m, 1H), 1.51 (d, J_{HH} = 6.6 Hz, 3H).
$^{13}C\{^{1}H\}$ NMR (100.6 MHz, $CDCl_3$): δ 163.1, 148.3, 137.0, 122.4, 120.0, 68.9, 24.4.

4-Phenylbutan-2-ol[6] (b19)

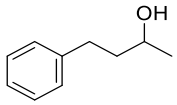

According to general procedure, 4-phenyl-2-butanone **a19** (293 µL, 2.0 mmol) gave the title compound **b19** as a pale yellow oil (277 mg, 92%).

In an argon filled glove box, an autoclave was charged with complex **C^{3A}.2** (6.25 mg, 5 mol%) and anhydrous toluene (1 mL), followed by 4-phenyl-3-buten-2-one **a27** (35 µL,0.25 mmol) and *t*BuOK (2.8 mg, 10 mol%), in this order. The autoclave is then charged H_2 (50 bar). The mixture was stirred for 18 hours at 80 °C in an oil bath. The solution was then diluted with ethyl acetate (2.0 mL) and filtered through a small pad of silica (2 cm in a Pasteur pipette). The silica was washed with ethyl acetate. The filtrate was evaporated and the crude residue was purified by column chromatography (SiO2, mixture of petroleum ether/ethyl acetate as eluent). The title compound **b19** is obtained as a pale yellow oil (35 mg, 92%).

^{1}H NMR (400.1 MHz, $CDCl_3$): δ 7.33 – 7.28 (m, 2H), 7.24 – 7.19 (m, 3H), 3.89 – 3.83 (m, 1H), 2.83 – 2.66 (m, 2H), 1.84 – 1.77 (m, 2H), 1.34 (br. s, 1H), 1.26 (d, J_{HH} = 6.1 Hz, 3H).
^{13}C{^{1}H} NMR (100.6 MHz, $CDCl_3$): δ 142.2, 128.5, 125.9, 67.7, 41.0, 32.3, 23.8.

Cycloheptanol[5] (b20)

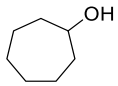

According to general procedure, cycloheptanone **a20** (256 µL, 2.0 mmol) gave the title compound **b20** as a pale yellow oil (190 mg, 83%).
^{1}H NMR (400.1 MHz, $CDCl_3$): δ 3.86 – 3.80 (m, 1H), 1.94 – 1.87 (m, 2H), 1.67 – 1.50 (m, 8H), 1.43 – 1.33 (m, 3H).
^{13}C{^{1}H} NMR (100.6 MHz, $CDCl_3$) δ 72.9, 37.7, 28.2, 22.8.

Cyclopropylethan-1-ol[5] (b21)

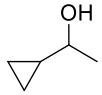

According to general procedure, cyclopropylethan-1-one **a21** (186 µL, 2.0 mmol) gave the title compound **b21** as a pale yellow oil (98% NMR yield).
^{1}H NMR (400.1 MHz, $CDCl_3$): δ 3.10 – 3.02 (m, 1H), 1.73 (s, 1H), 1.27 (d, J_{HH} = 6.2 Hz, 3H), 0.94 – 0.85 (m, 1H), 0.52 – 0.44 (m, 2H), 0.31 – 0.12 (m, 2H).
^{13}C{^{1}H} NMR (100.6 MHz, $CDCl_3$): δ 73.1, 22.6, 19.4, 3.1, 2.4.

Undecan-2-ol[5] (b22)

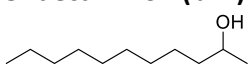

According to general procedure, 2-undecanone **a22** (413 µL, 2.0 mmol) gave the title compound **b22** as a pale yellow oil (248 mg, 72%).
^{1}H NMR (400.1 MHz, $CDCl_3$): δ 3.83 – 3.75 (m, 1H), 1.48 – 1.23 (m, 17H), 1.11 (d, J_{HH} = 6.1 Hz, 3H), 0.88 (t, J_{HH} = 6.8 Hz, 3H).
^{13}C{^{1}H} NMR (100.6 MHz, $CDCl_3$): δ 68.4, 39.5, 32.0, 29.79, 29.78, 29.71, 29.5, 25.9, 23.6, 22.8, 14.3.

6-Methylhept-5-en-2-ol[5] (b23)

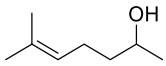

According to general procedure, 6-methylhept-5-en-2-one **a23** (148 µL, 1.0 mmol) gave the title compound **b23** as a pale yellow oil (117 mg, 91%).

^{1}H NMR (400.1 MHz, $CDCl_3$): δ 5.12 (t, J_{HH} = 7.2 Hz, 1H), 3.83 – 3.76 (m, 1H), 2.12 – 1.99 (m, 2H), 1.68 (s, 3H), 1.61 (s, 3H), 1.51 – 1.44 (m, 3H), 1.18 (d, J_{HH} = 6.2 Hz, 3H).

$^{13}C\{^{1}H\}$ NMR (100.6 MHz, $CDCl_3$): δ 132.2, 124.2, 68.1, 39.3, 25.8, 24.6, 23.6, 17.8.

4-Biphenylmethanol[5] (b24)

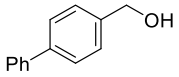

According to general procedure, 4-biphenylmethanal **a24** (182 mg, 1.0 mmol) gave the title compound **b24** as a white solid (168 mg, 91%).

^{1}H NMR (400.1 MHz, $CDCl_3$): δ 7.63 – 7.59 (m, 4H), 7.48 – 7.43 (m, 4H), 7.40 – 7.36 (m, 1H), 4.73 (s, 2H), 2.08 (br. s, 1H).

$^{13}C\{^{1}H\}$ NMR (100.6 MHz, $CDCl_3$): δ 140.9, 140.7, 140.0, 128.9, 127.56, 127.42 127.39, 127.2, 65.1.

Methyl-4-(hydroxymethyl)benzoate[7] (b25)

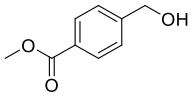

According to general procedure, methyl-4-formylbenzoate **a25** (164 mg, 1.0 mmol) gave the title compound **b25** as a white solid (131 mg, 79%).

^{1}H NMR (400.1 MHz, $CDCl_3$): δ 7.97 (d, J_{HH} = 8.2 Hz, 2H), 7.38 (d, J_{HH} = 8.2 Hz, 2H), 4.71 (s, 2H), 3.88 (s, 3H), 2.56 (br. s, 1H).

$^{13}C\{^{1}H\}$ NMR (100.6 MHz, $CDCl_3$): δ 167.2, 146.3, 129.8, 129.2, 126.5, 64.5, 52.2.

***N*-[4-(hydroxymethyl)phenyl]-acetamide[5,8] (b26)**

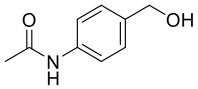

According to general procedure, 4-acetamido-benzaldehyde **a26** (163 mg, 1.0 mmol) gave the title compound **b26** as a pale yellow solid (152 mg, 92%).

^{1}H NMR (400.1 MHz, CD_3OD): δ 7.51 (d, J_{HH} = 8.5 Hz, 2H), 7.28 (d, J_{HH} = 8.5 Hz, 2H), 4.86 (br. s, 2H), 4.55 (s, 2H), 2.10 (s, 3H).

$^{13}C\{^{1}H\}$ NMR (100.6 MHz, CD_3OD): δ 171.7, 138.9, 138.4, 128.5, 121.1, 64.8, 23.8.

4-Phenyl-2-butanone[9] (a19)

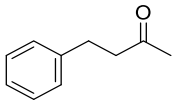

According to general procedure but performing the reaction at 30 °C for 18 h, 4-phenyl-3-buten-2-one **a27** (293 µL, 2.0 mmol) gave the title compound **a19** as a colorless oil (279 mg, 94%).

^{1}H NMR (400.1 MHz, $CDCl_3$): δ 7.33 – 7.28 (m, 2H), 7.24 – 7.20 (m, 3H), 2.93 (t, J_{HH} = 7.6 Hz, 2H), 2.79 (t, J_{HH} = 7.5 Hz, 2H), 2.17 (s, 3H).

$^{13}C\{^{1}H\}$ NMR (100.6 MHz, $CDCl_3$): δ 207.9, 141.1, 128.6, 128.4, 126.2, 45.2, 30.1, 29.8.

1,3-Diphenylpropan-1-one (a29)

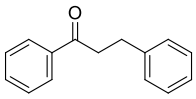

In an argon filled glove box, an autoclave was charged with complex **C^{3A}.2** (10 mg, 2 mol%) and anhydrous toluene (2 mL), followed by (*E*)-chalcone **a28** (104 mg, 1 mmol) and *t*BuOK (5.6 mg, 5 mol%), in this order. The autoclave is then charged H_2 (50 bar). The mixture was stirred for 18 hours at 80 °C in an oil bath. The solution was then diluted with ethyl acetate (2.0 mL) and filtered through a small pad of silica (2 cm in a Pasteur pipette). The silica was washed with ethyl acetate. The filtrate was evaporated and the crude residue was purified by column chromatography (SiO2, mixture of petroleum ether/ethyl acetate as eluent). The title compound a29 is obtained as a white solid (97 mg, 92%).

^{1}H NMR (400.1 MHz, $CDCl_3$): δ 8.01 (d, J_{HH} = 7.4 Hz, 2H), 7.60 (t, J_{HH} = 7.4 Hz, 1H), 7.50 (t, J_{HH} = 7.6 Hz, 2H), 7.41 – 7.20 (m, 5H), 3.35 (t, J_{HH} = 7.7 Hz, 2H), 3.13 (t, J_{HH} = 7.7 Hz, 2H).
^{13}C{^{1}H} NMR (100.6 MHz, $CDCl_3$): δ 199.2, 141.3, 136.9, 133.1, 128.6, 128.6, 128.5, 128.1, 126.2, 40.5, 30.2.

1,3-diphenylpropan-1-ol (b28)

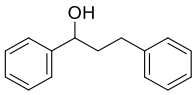

In an argon filled glove box, an autoclave was charged with complex **C^{3A}.2** (6.3 mg, 5 mol%) and anhydrous toluene (1 mL), followed by (*E*)-chalcone **a28** (52 mg, 0.25 mmol) and *t*BuOK (2.8 mg, 10 mol%), in this order. The autoclave is then charged H_2 (50 bar). The mixture was stirred for 22 hours at 100 °C in an oil bath. The solution was then diluted with ethyl acetate (2.0 mL) and filtered through a small pad of silica (2 cm in a Pasteur pipette). The silica was washed with ethyl acetate. The filtrate was evaporated and the crude residue was purified by column chromatography (SiO2, mixture of petroleum ether/ethyl acetate as eluent). The title compound **b28** is obtained as a pale yellow liquid (51 mg, 96%).

^{1}H NMR (400.1 MHz, $CDCl_3$): δ 7.36 (d, J_{HH} = 4.4 Hz, 4H), 7.32 – 7.24 (m, 3H), 7.20 (d, J_{HH} = 7.4 Hz, 3H), 4.70 (m, 1H), 2.84 – 2.62 (m, 2H), 2.22 – 1.98 (m, 2H), 1.85 (s, 1H).
^{13}C{^{1}H} NMR (100.6 MHz, $CDCl_3$): δ 144.7, 141.9, 128.7, 128.6, 128.5, 127.8, 126.1, 126.0, 74.0, 40.6, 32.2.

(1*R*,4*R*)-Dihydrocarvone[10] (a31)

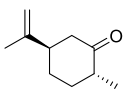

In an argon filled glove box, an autoclave was charged with complex **C^{3A}.2** (10 mg, 1 mol%) and anhydrous toluene (2 mL), followed (*R*)-(−)-Carvone **a30** (157 µL, 1 mmol) and *t*BuOK (2.2 mg, 2 mol%), in this order. The autoclave is then charged H_2 (50 bar). The mixture was stirred for 18 hours at 80 °C in an oil bath. The solution was then diluted with ethyl acetate (2.0 mL) and filtered through a small pad of silica (2 cm in a Pasteur pipette). The silica was washed with ethyl acetate. The filtrate was evaporated and the crude residue was purified by column chromatography (SiO2, mixture of petroleum ether/ethyl acetate as eluent). The title compound **a31** is obtained as a colorless oil (63 mg, 41%).

^{1}H NMR (400.1 MHz, $CDCl_3$): δ 4.74 (d, J_{HH} = 10.6 Hz, 2H), 2.55 – 2.20 (m, 4H), 2.13 (ddt, J_{HH} = 12.9, 6.3, 3.3 Hz, 1H), 2.01 – 1.88 (m, 1H), 1.74 (s, 3H), 1.70 – 1.55 (m, 1H), 1.49 – 1.31 (m, 1H), 1.03 (d, J_{HH} = 6.5 Hz, 3H).
^{13}C{^{1}H} NMR (100.6 MHz, $CDCl_3$): δ 212.8, 147.8, 109.7, 47.2, 47.0, 44.9, 35.1, 30.9, 20.6, 14.5.

(1*S*,2*R*,5*R*)-Dihydrocarveol[11] (b30)

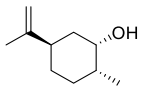

In an argon filled glove box, an autoclave was charged with complex **C^{3A}.2** (6.3 mg, 5 mol%) and anhydrous toluene (1 mL), followed ((*R*)-(−)-Carvone **a30** (39.2 µL, 0.25 mmol) and *t*BuOK (2.8 mg, 10 mol%), in this order. The autoclave is then charged H_2 (50 bar). The mixture was stirred for 18 hours at 100 °C in an oil bath. The solution was then diluted with ethyl acetate (2.0 mL) and filtered through a small pad of silica (2 cm in a Pasteur pipette). The silica was washed with ethyl acetate. The filtrate was evaporated and the crude residue was purified by column chromatography (SiO2, mixture of petroleum ether/ethyl acetate as eluent). The title compound **b30** is obtained as a colorless oil (33 mg, 87%).

^{1}H NMR (400.1 MHz, $CDCl_3$): δ 4.69 (s, 2H), 3.89 (q, *J* = 2.8 Hz, 1H), 2.37 – 2.17 (m, 1H), 1.98 – 1.86 (m, 1H), 1.82 – 1.67 (m, 4H), 1.66 – 1.27 (m, 5H), 1.27 – 1.10 (m, 1H), 0.97 (d, *J* = 6.7 Hz, 3H).
^{13}C{^{1}H} NMR (100.6 MHz, $CDCl_3$): δ 150.4, 108.5, 71.1, 38.8, 37.9, 36.2, 31.5, 28.3, 21.1, 18.4.

NMR data for the complexes

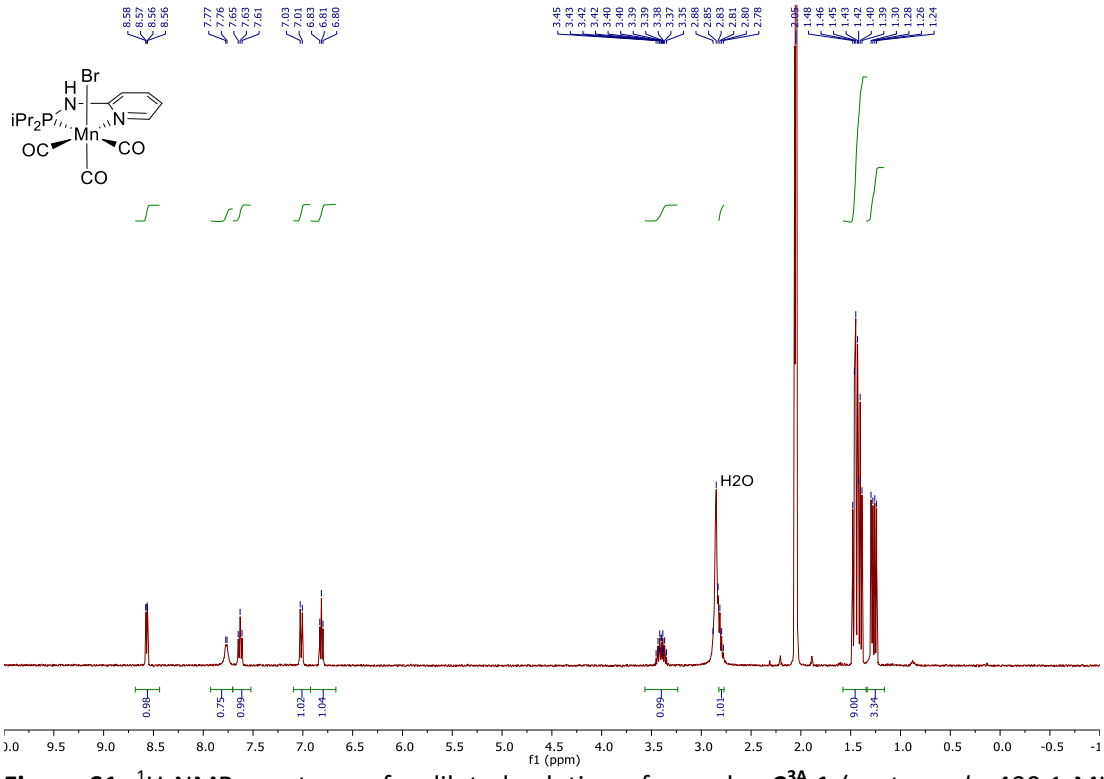

Figure S1: ^{1}H NMR spectrum of a diluted solution of complex **C^{3A}.1** (acetone-d_6, 400.1 MHz, 298K) showing a good resolution, but with the signal of H_2O overlapping with signals of the complex.

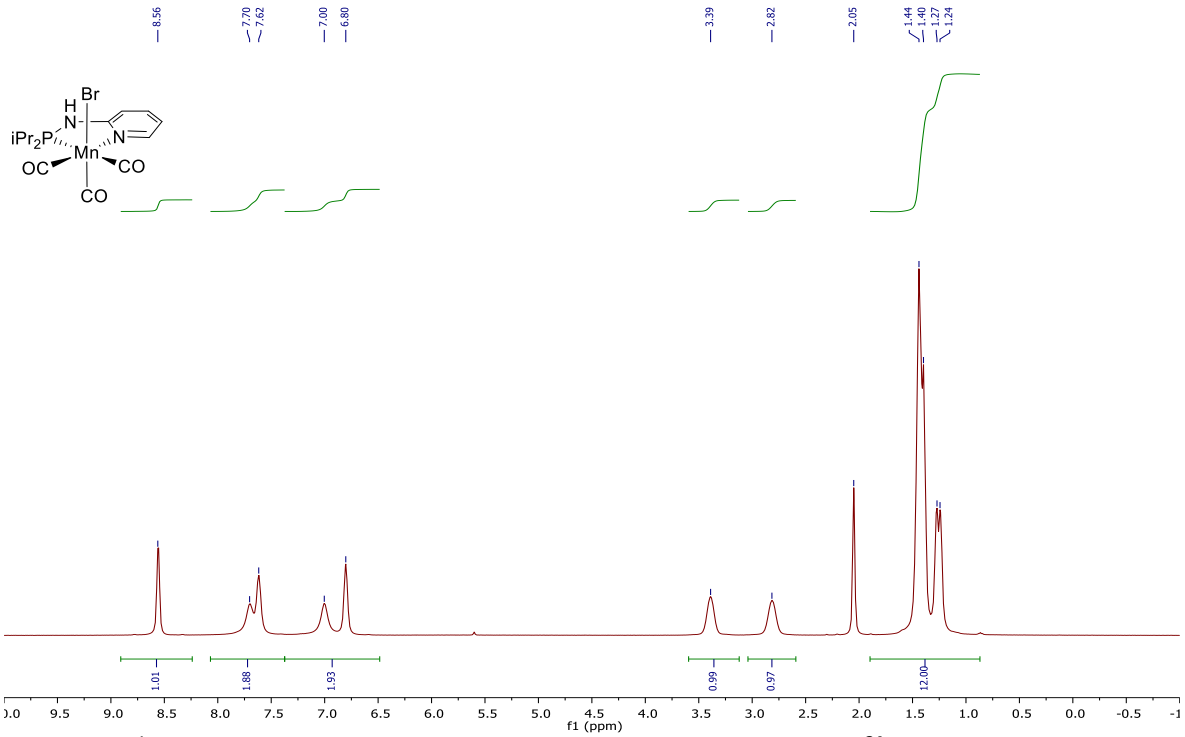

Figure S2: ^{1}H NMR spectrum of a concentrated solution of complex **C^{3A}.1** (acetone-d_6, 400.1 MHz, 298K) showing that the integration of the signal are in good agreement with the proposed structure at the expense of the resolution.

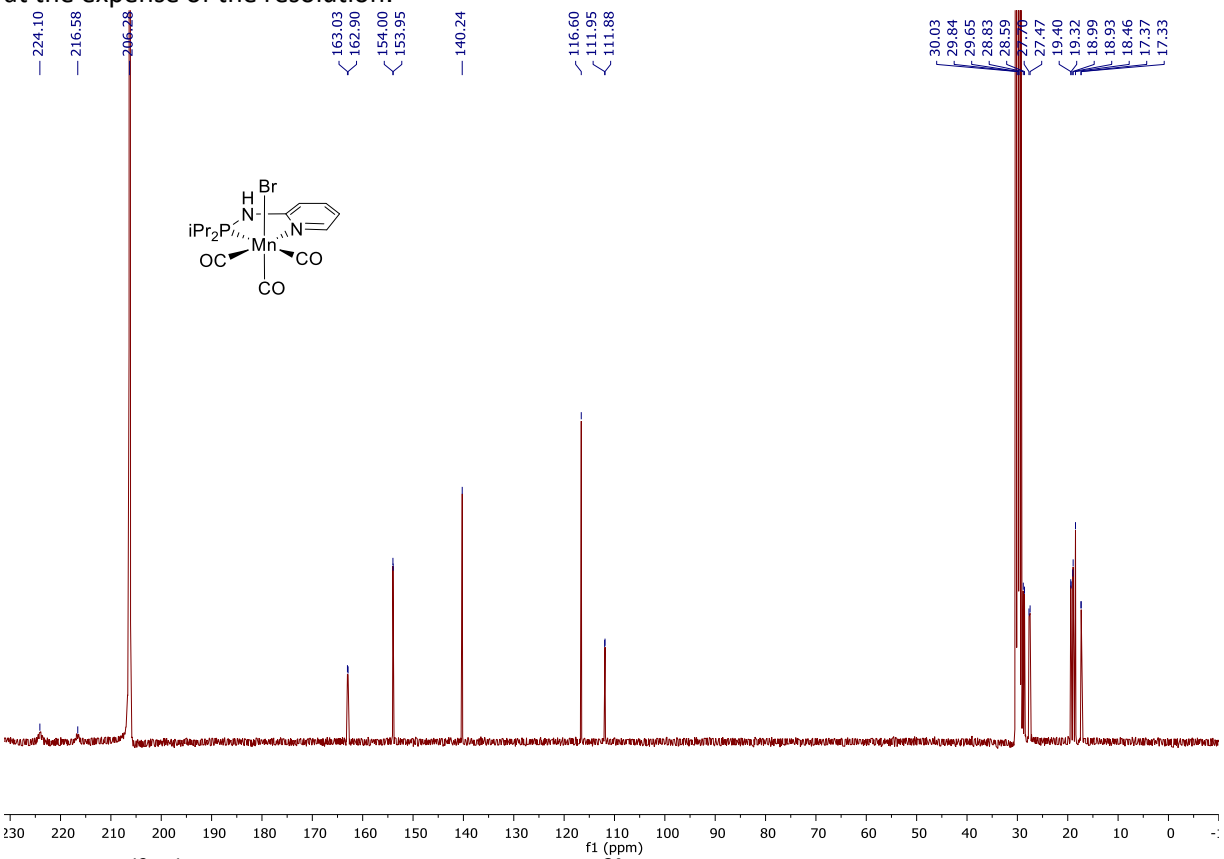

Figure S3: ^{13}C{^{1}H} NMR spectrum of the complex **C^{3A}.1** (acetone-d_6, 100.6 MHz, 298K).

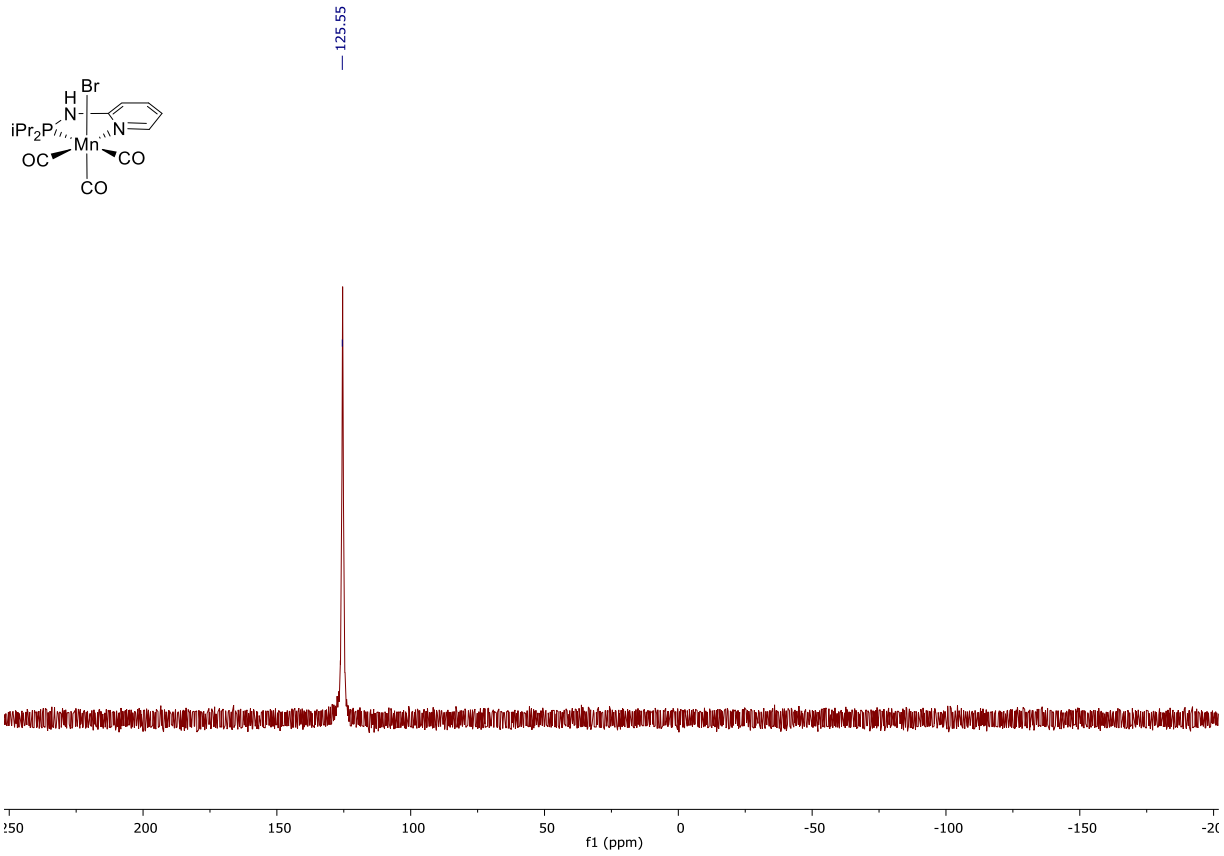

Figure S4: $^{31}P\{^{1}H\}$ NMR spectrum of the complex **C^{3A}.1** (acetone-d_6, 162.0 MHz, 298K).

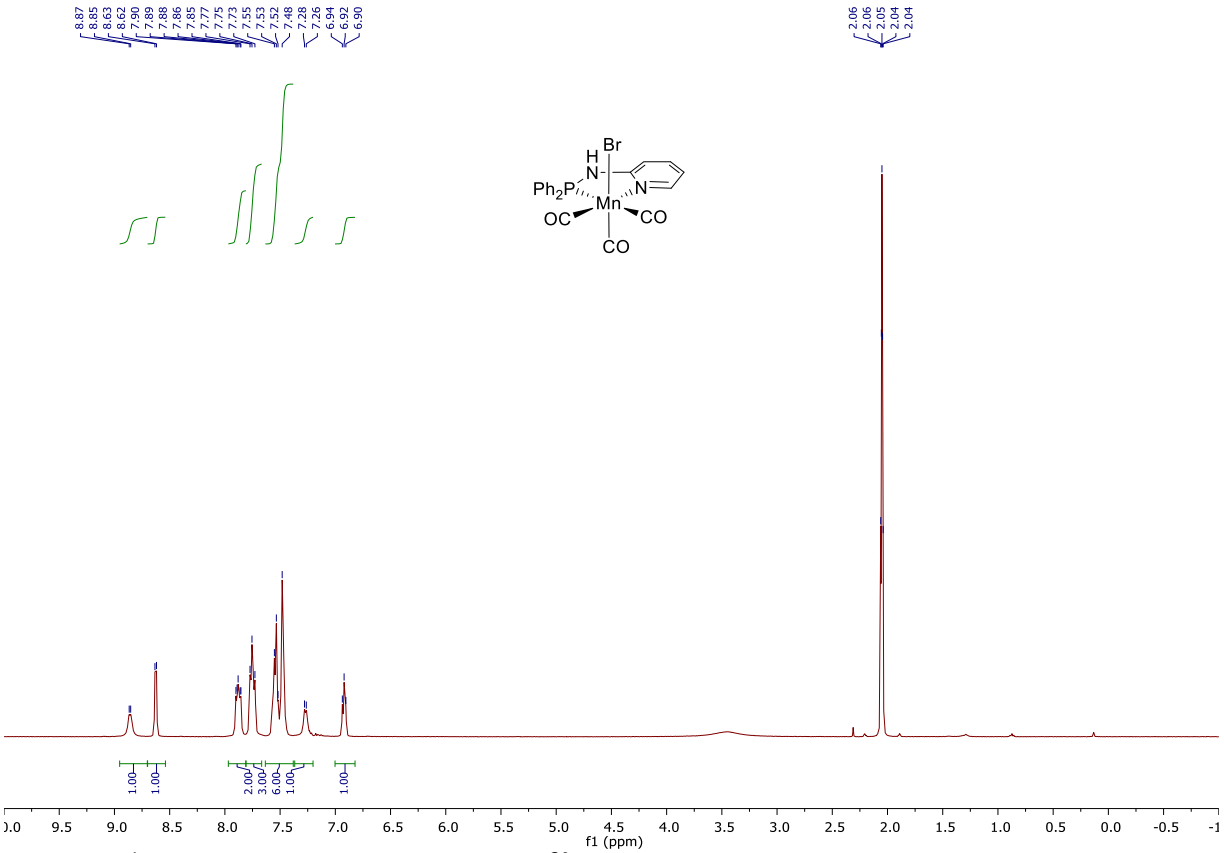

Figure S5: ^{1}H NMR spectrum of the complex **C^{3A}.2** (acetone-d_6, 400.1 MHz, 298K).

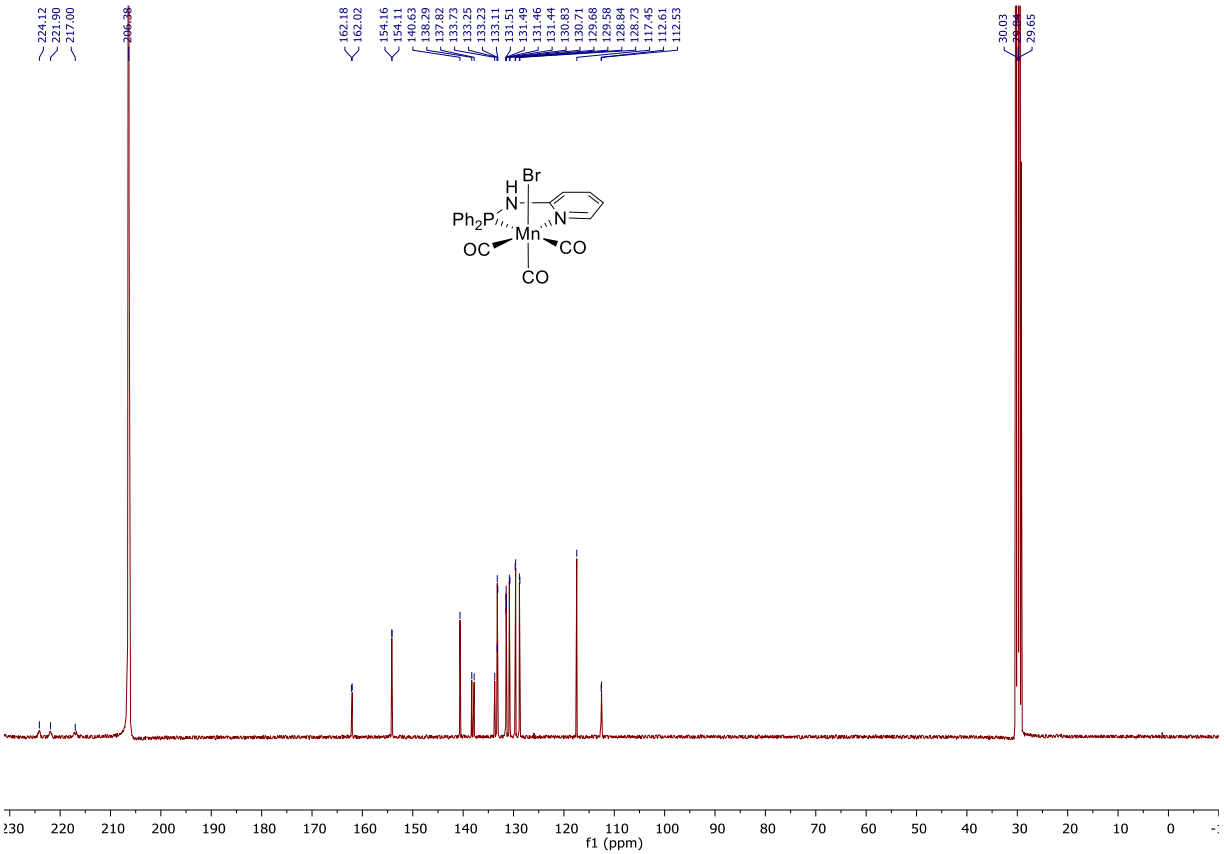

Figure S6: $^{13}C\{^{1}H\}$ NMR spectrum of the complex **C^{3A}.2** (acetone-d_6, 100.6 MHz, 298K).

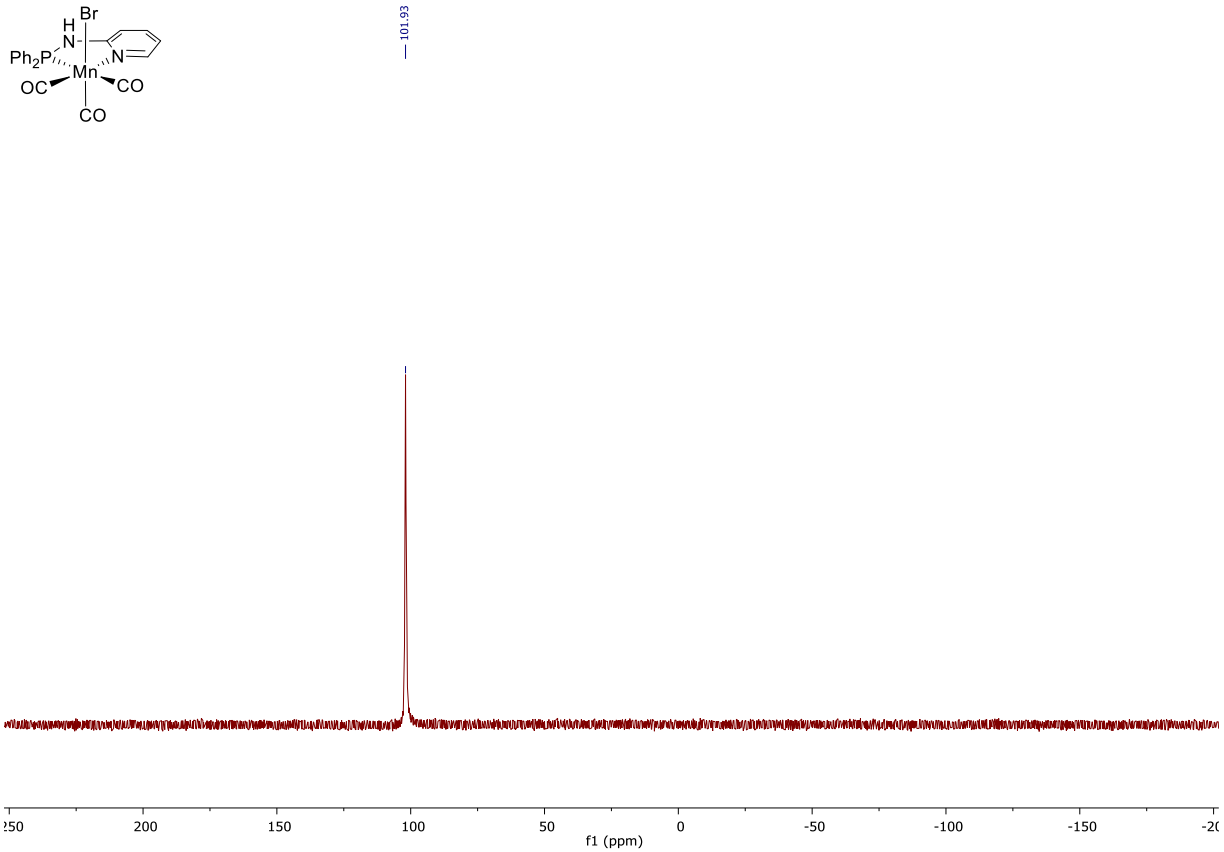

Figure S7: $^{31}P\{^{1}H\}$ NMR spectrum of the complex **C^{3A}.2** (acetone-d_6, 162.0 MHz, 298K).

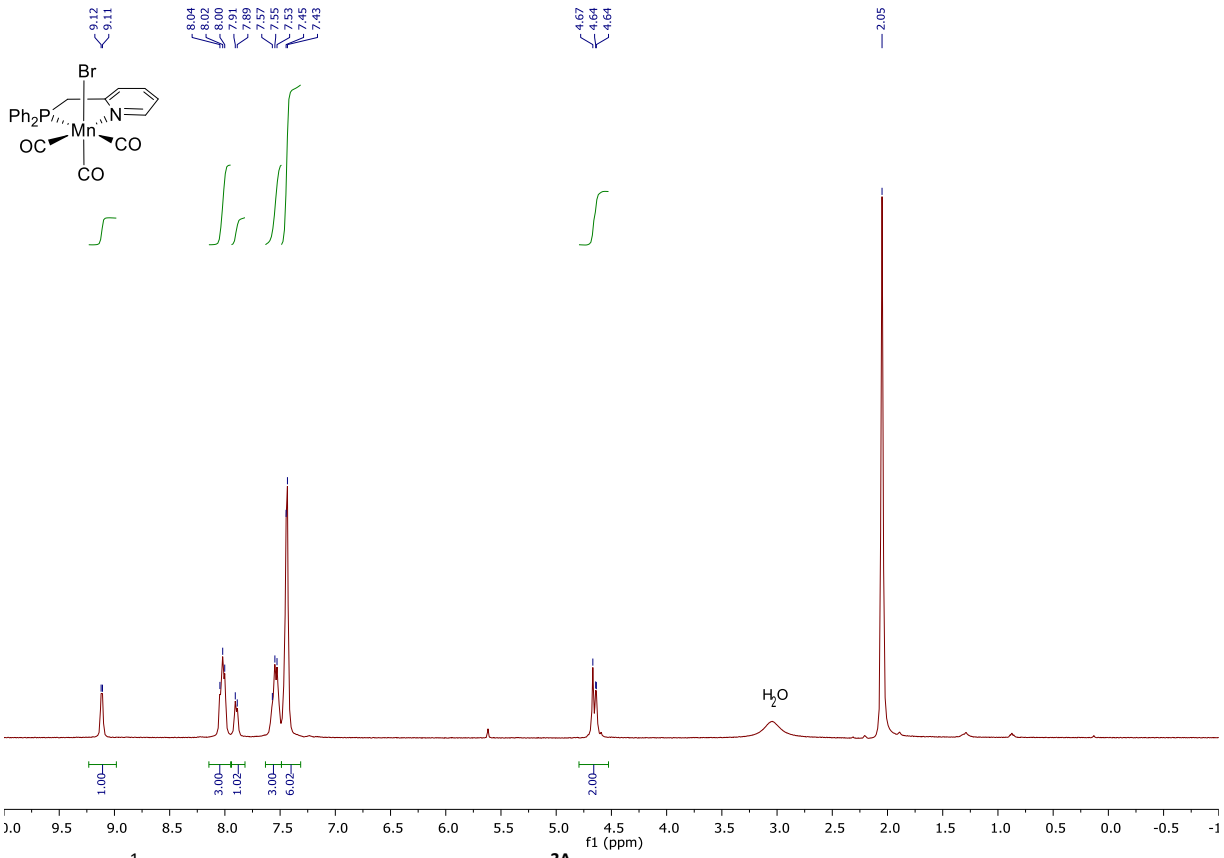

Figure S8: ^{1}H NMR spectrum of the complex **C^{3A}.3** (acetone-d_6, 400.1 MHz, 298K).

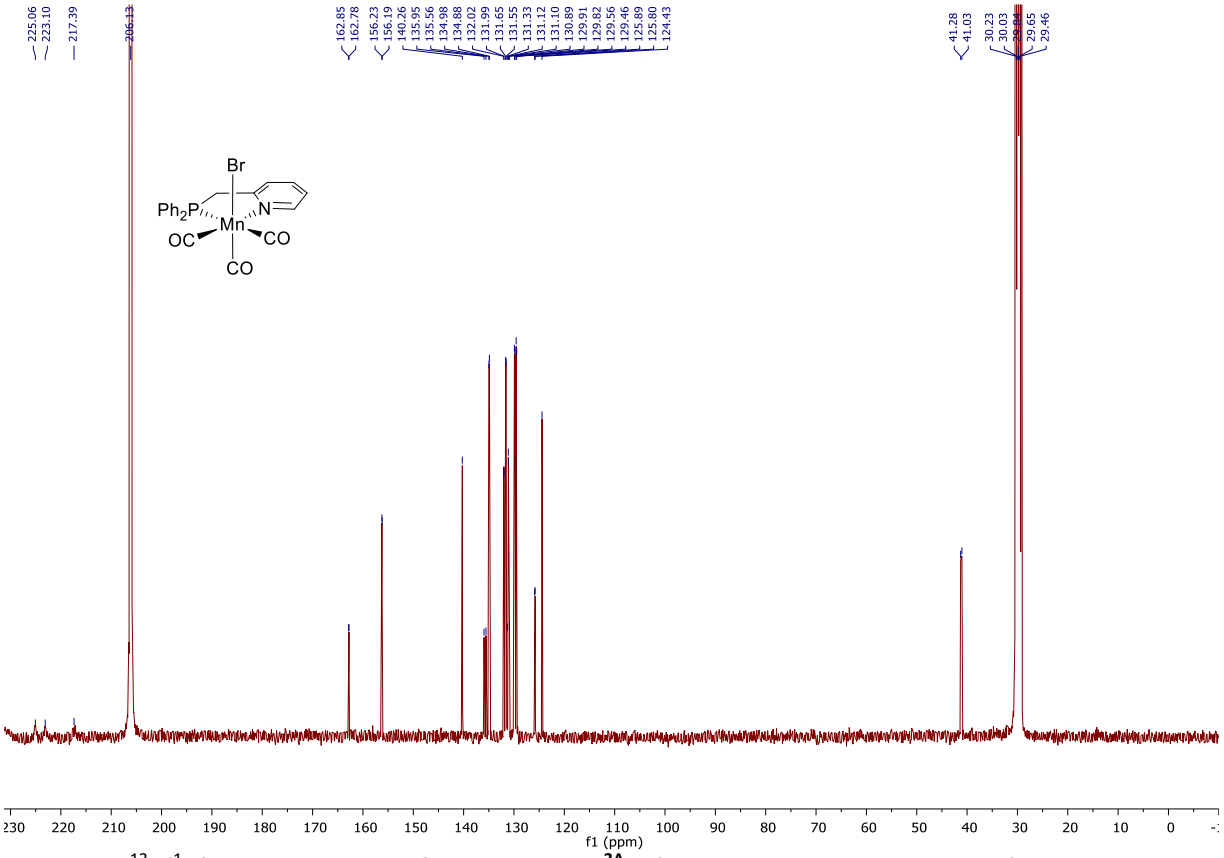

Figure S9: ^{13}C{^{1}H} NMR spectrum of the complex **C^{3A}.3** (acetone-d_6, 100.6 MHz, 298K).

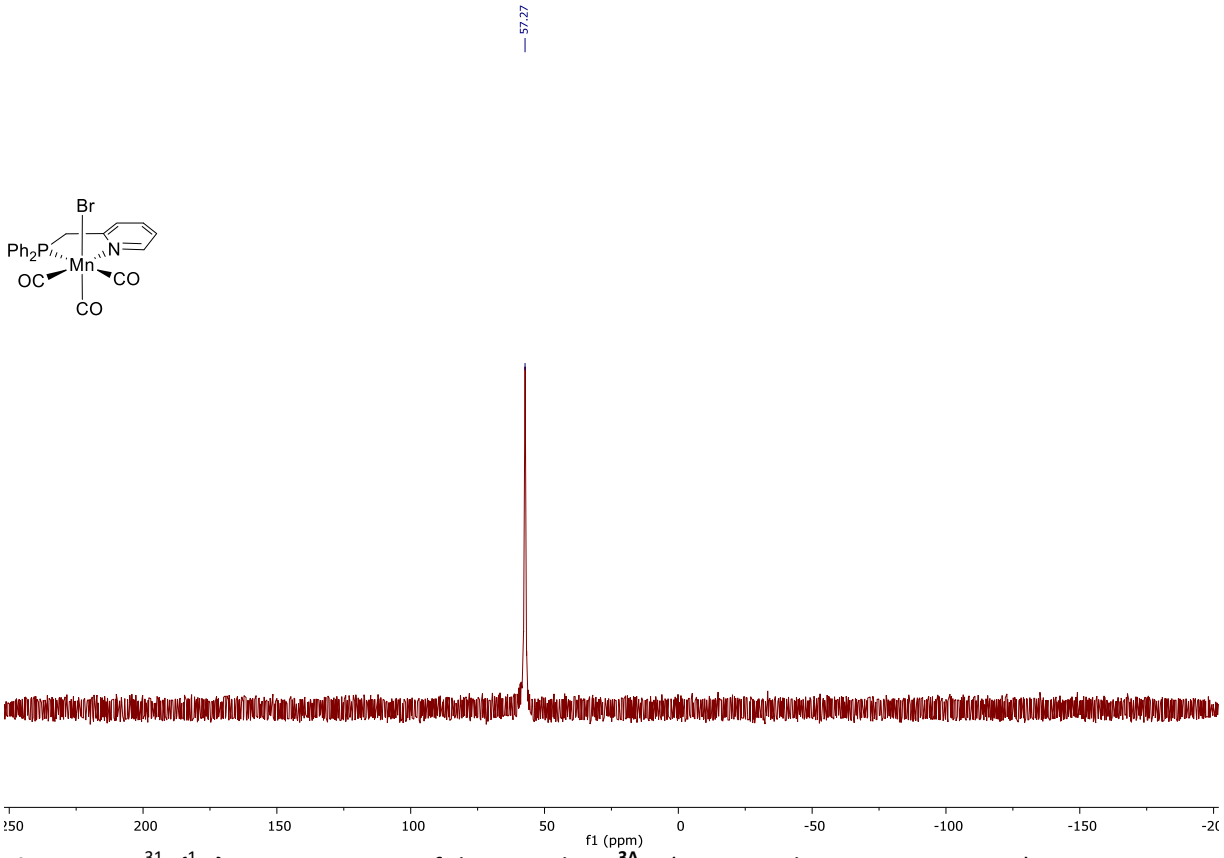

Figure S10: $^{31}P\{^{1}H\}$ NMR spectrum of the complex **C^{3A}.3** (acetone-d_6, 162.0 MHz, 298K).

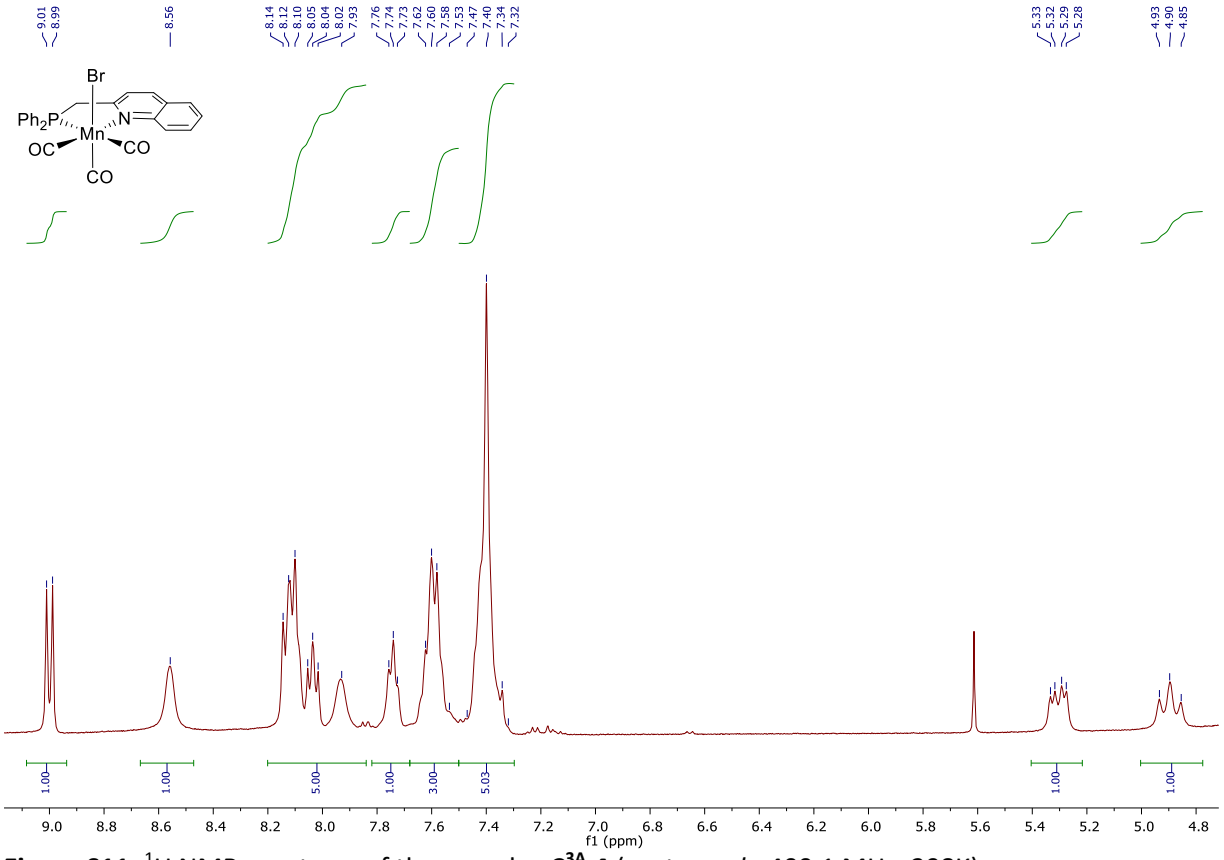

Figure S11: ^{1}H NMR spectrum of the complex **C^{3A}.4** (acetone-d_6, 400.1 MHz, 298K).

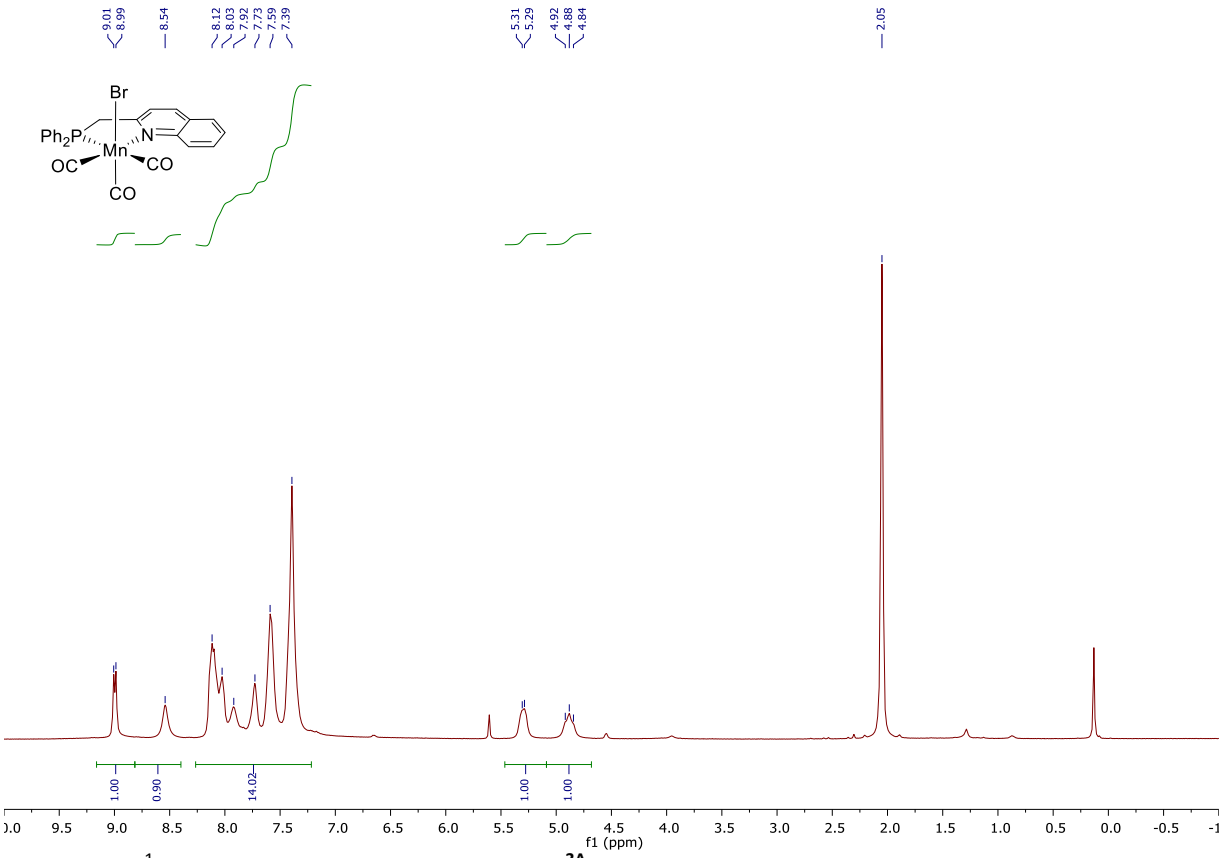

Figure S12: ^{1}H NMR spectrum of the complex **C^{3A}.4** (acetone-d_6, 400.1 MHz, 298K).

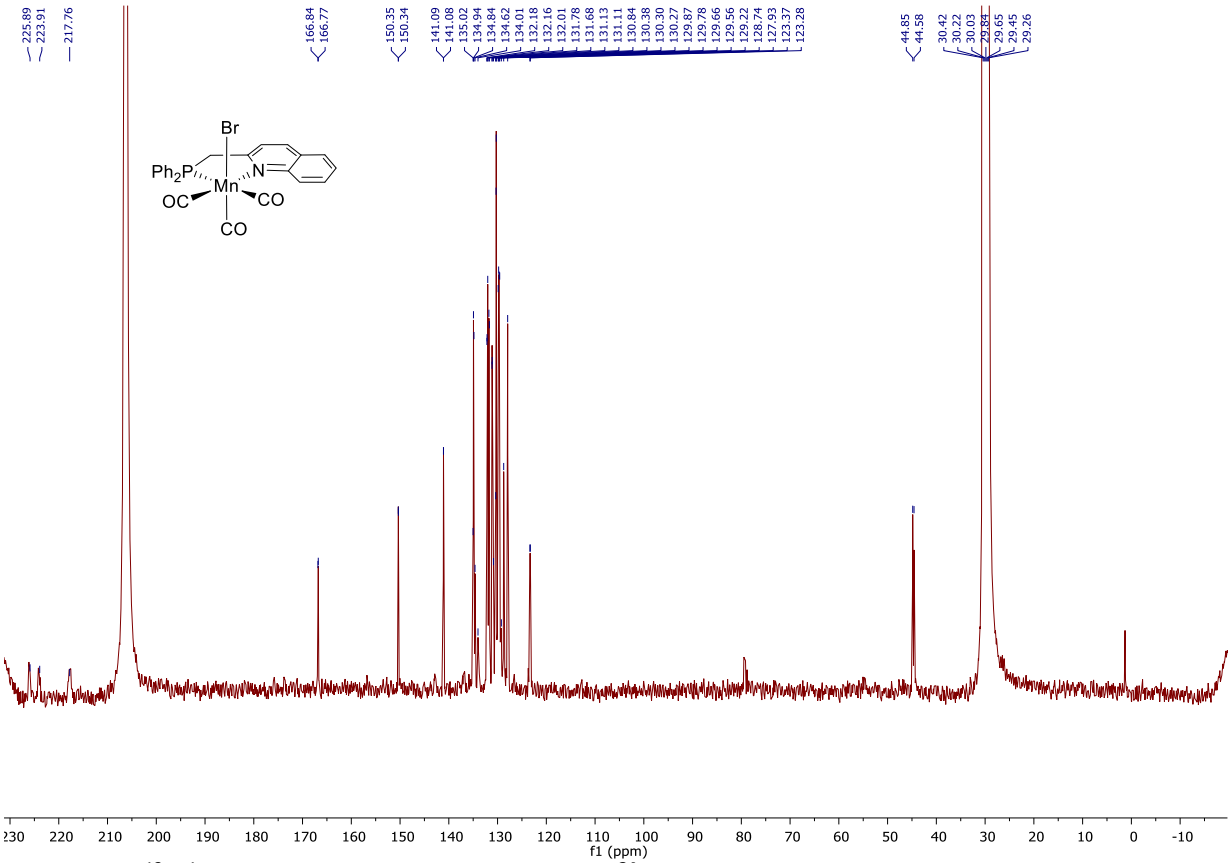

Figure S13: ^{13}C{^{1}H} NMR spectrum of the complex **C^{3A}.4** (acetone-d_6, 100.6 MHz, 298K).

.

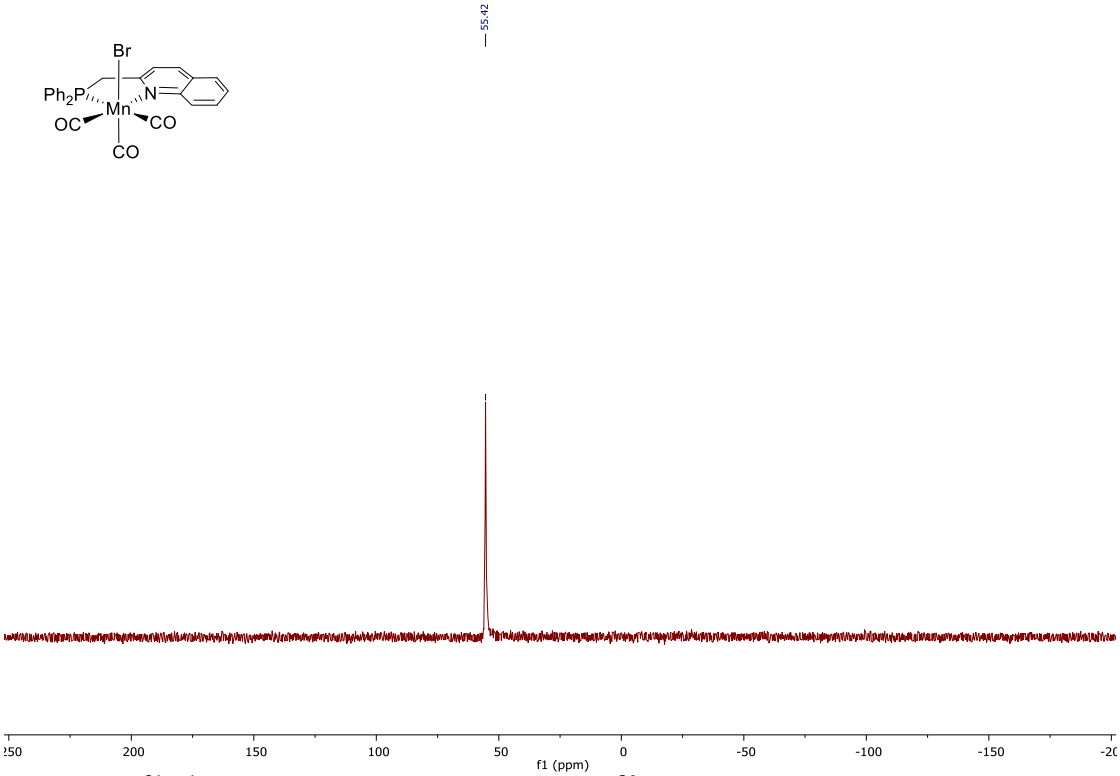

Figure S14: $^{31}P\{^{1}H\}$ NMR spectrum of the complex **C^{3A}.4** (acetone-d_6, 162.0 MHz, 298K).

NMR data for mechanistic experiments

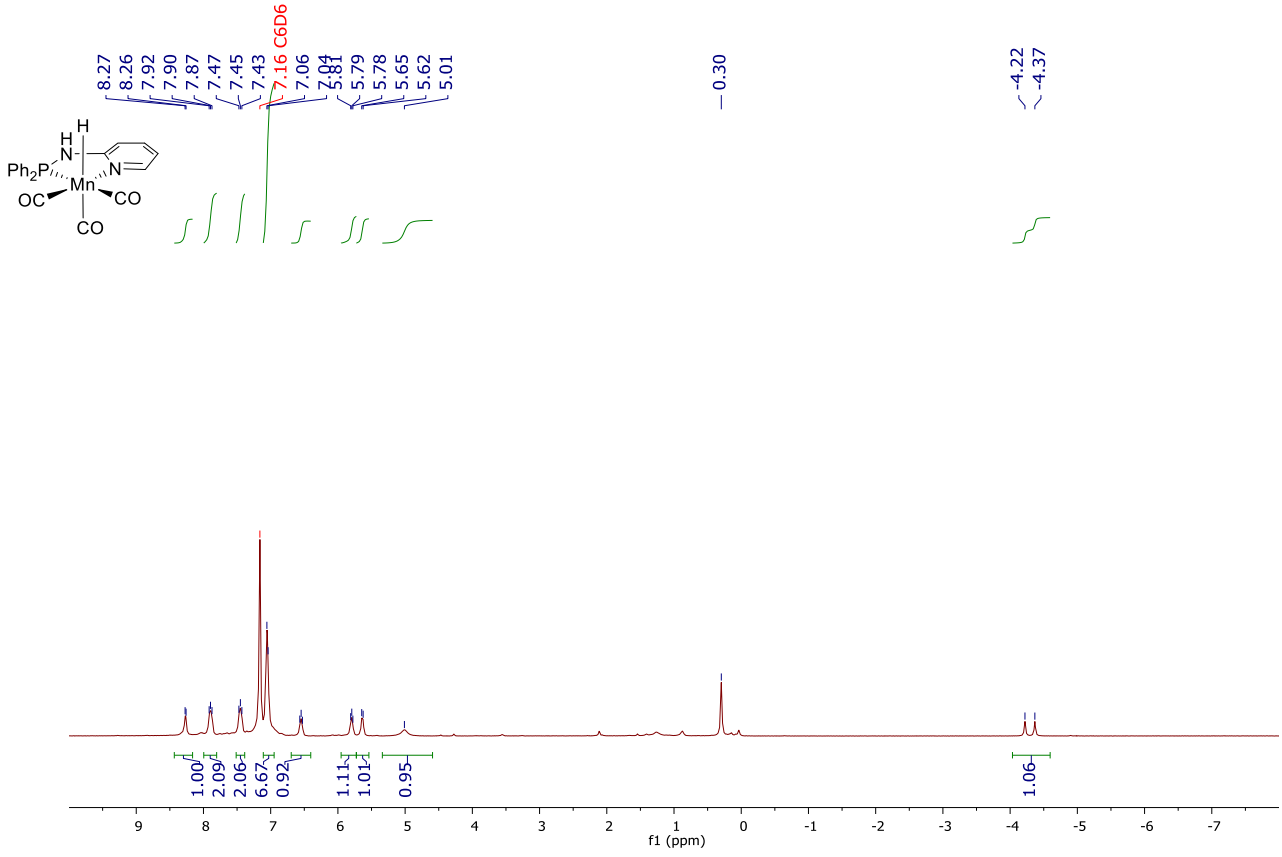

Figure S15: ^{1}H NMR spectrum of the complex **C^{3A}.2c** (C_6D_6, 400.1 MHz, 298K).

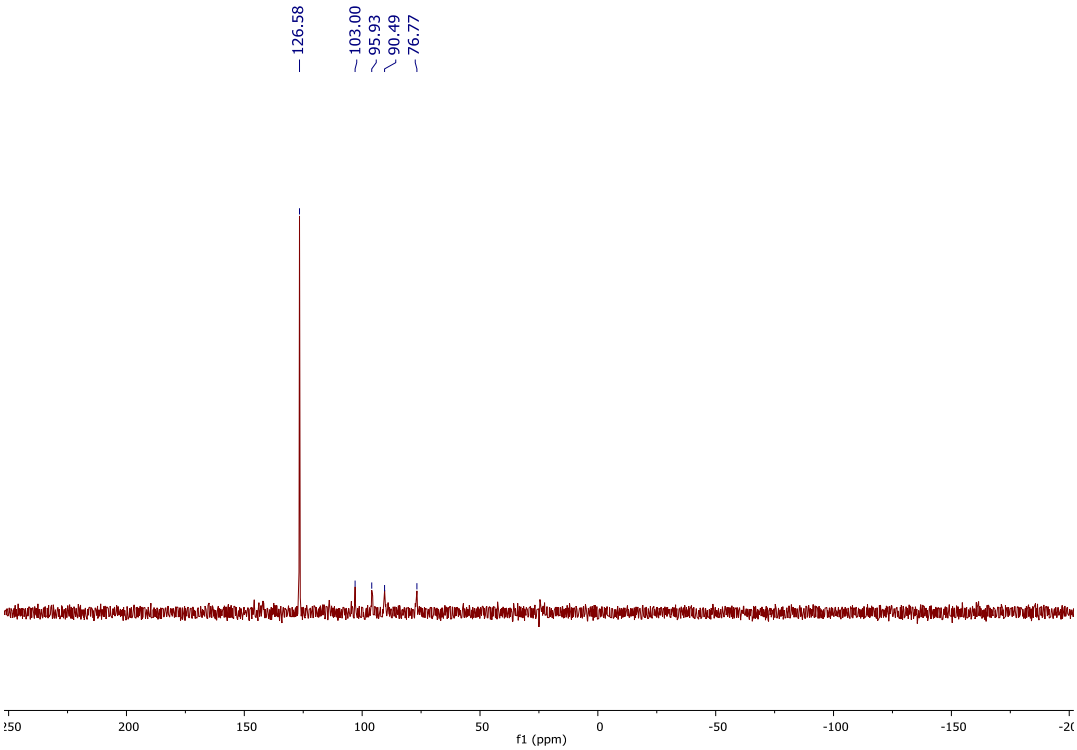

Figure S16: $^{31}P\{^{1}H\}$ NMR spectrum of the complex **C^{3A}.2c** (C_6D_6, 162.0 MHz, 298K).

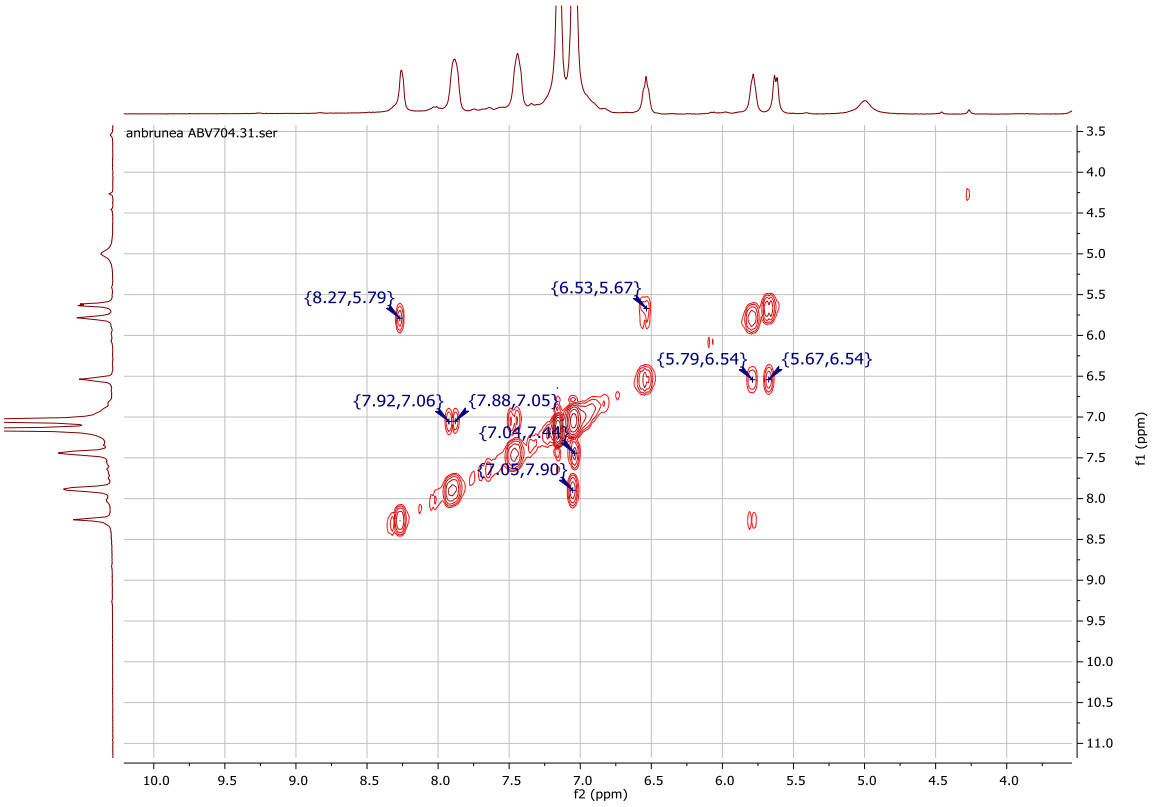

Figure S17: ^{1}H COSY NMR spectrum of complex **C^{3A}.2c** in C_6D_6 recorded at 400 MHz

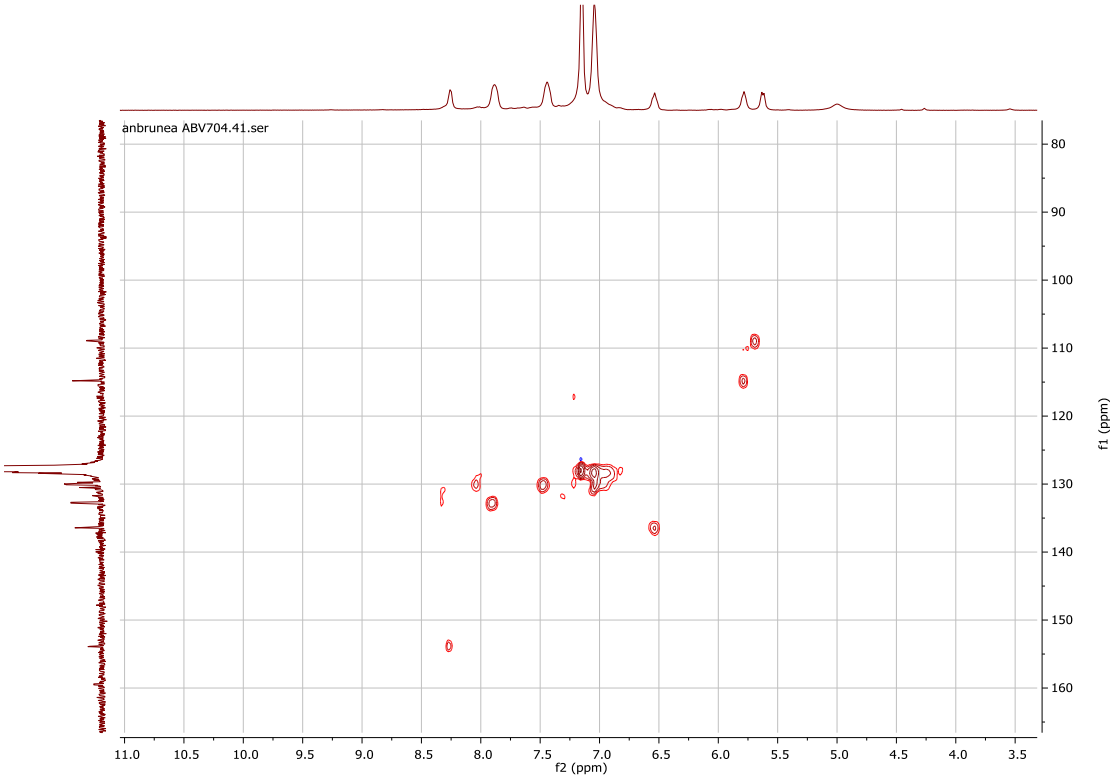

Figure S18: HSQC Edited NMR spectrum of complex **C^{3A}.2c** in C_6D_6 recorded at 400/101 MHz.

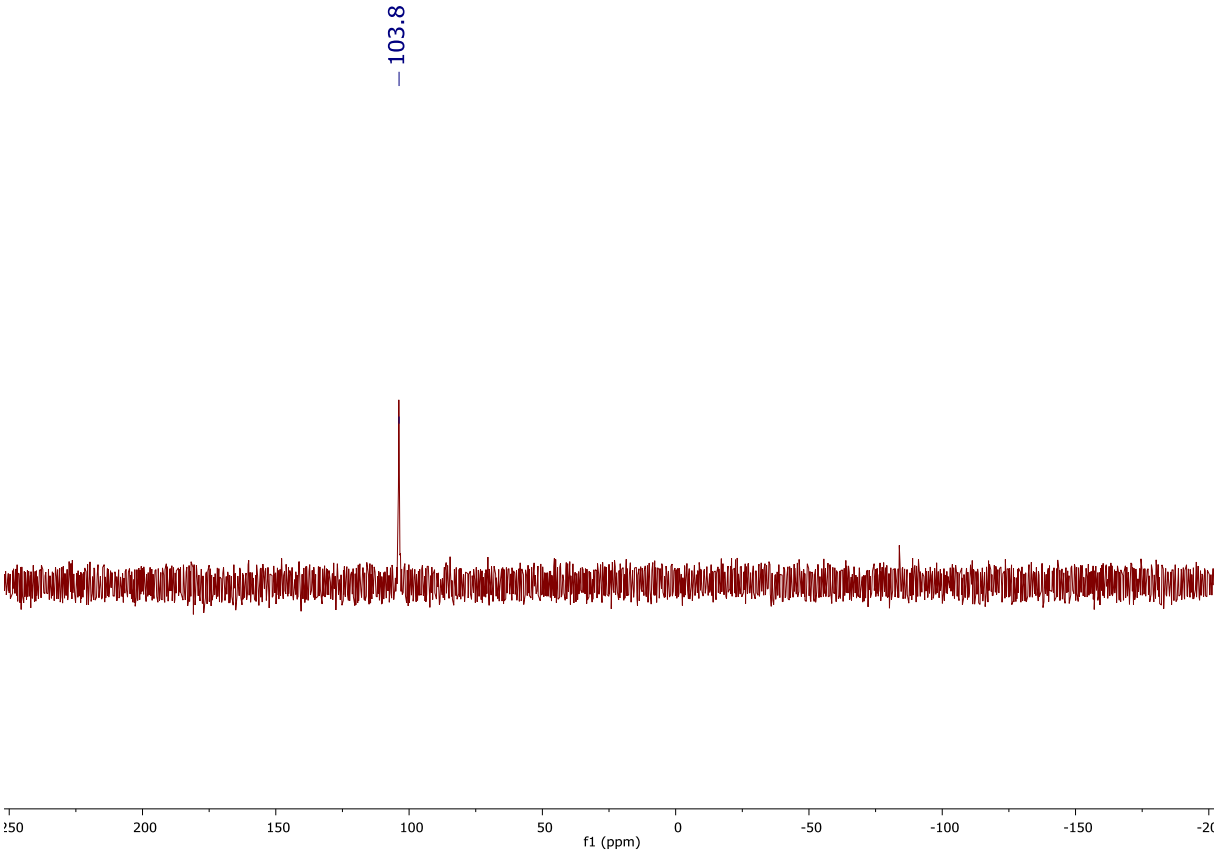

Figure S19: $^{31}P\{^{1}H\}$ NMR spectrum of the complex **C^{3A}.2** (C_6D_6, 162.0 MHz, 298K).

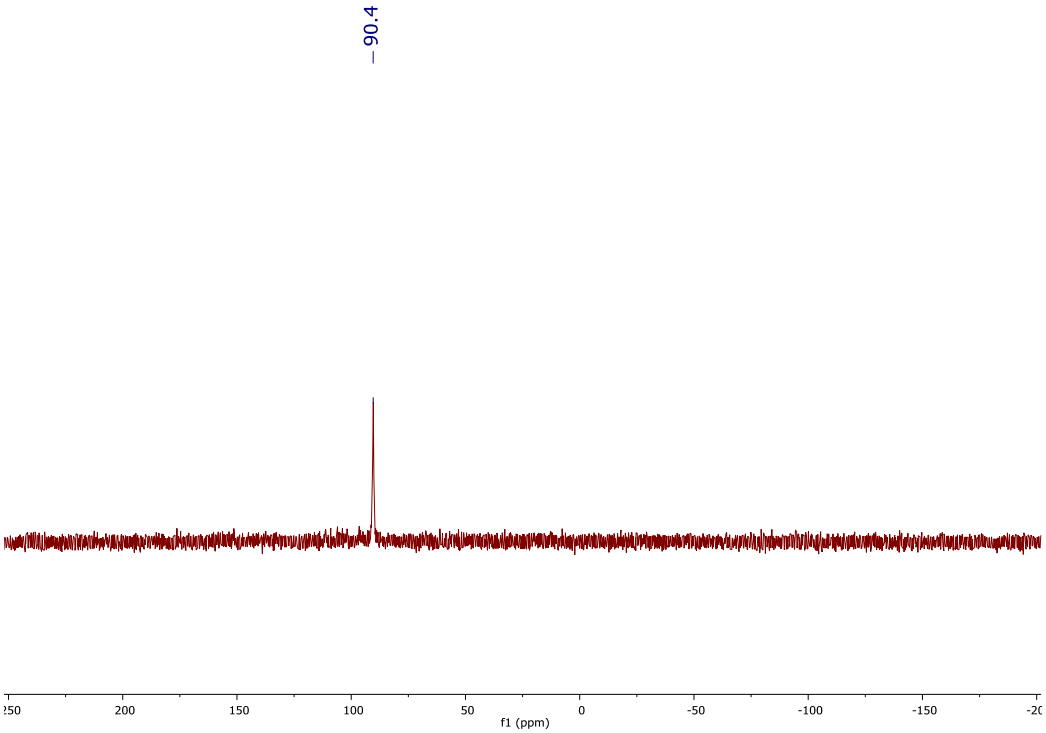

Figure S20: $^{31}P\{^{1}H\}$ NMR spectrum of the complex **C^{3A}.2** + *t*BuOK (C_6D_6, 162.0 MHz, 298K).

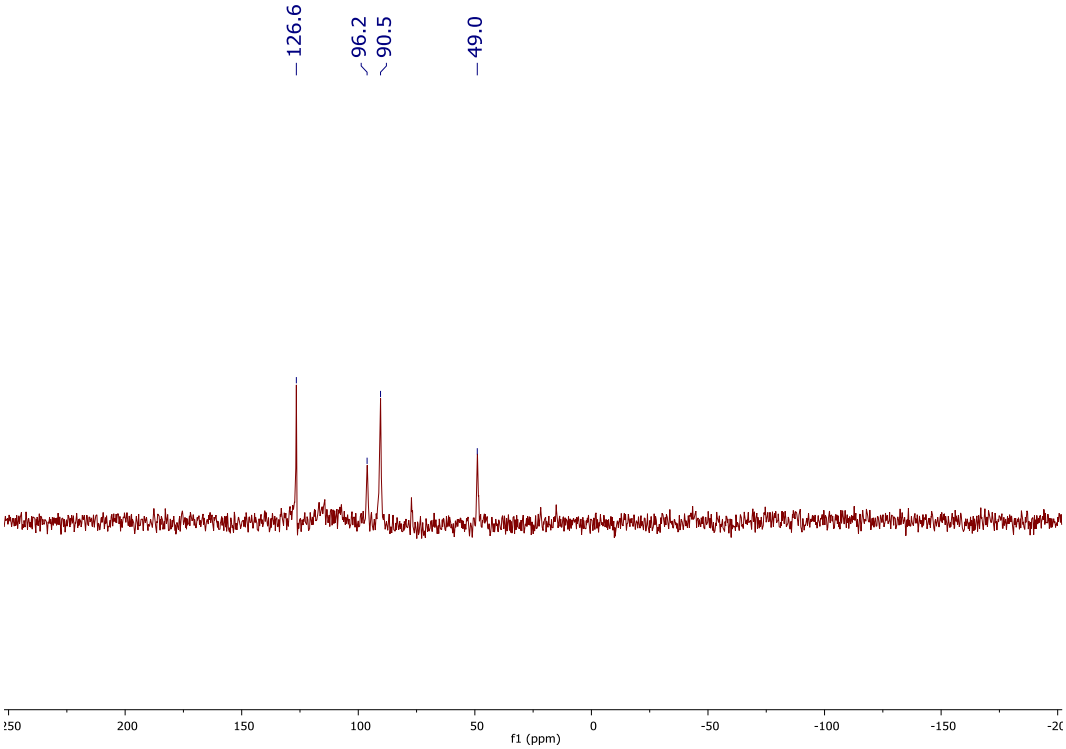

Figure S21: $^{31}P\{^{1}H\}$ NMR spectrum of the complex **C^{3A}.2** + *t*BuOK + H_2 : mixture of complexes including hydride and deprotonated ones (C_6D_6, 162.0 MHz, 298K).

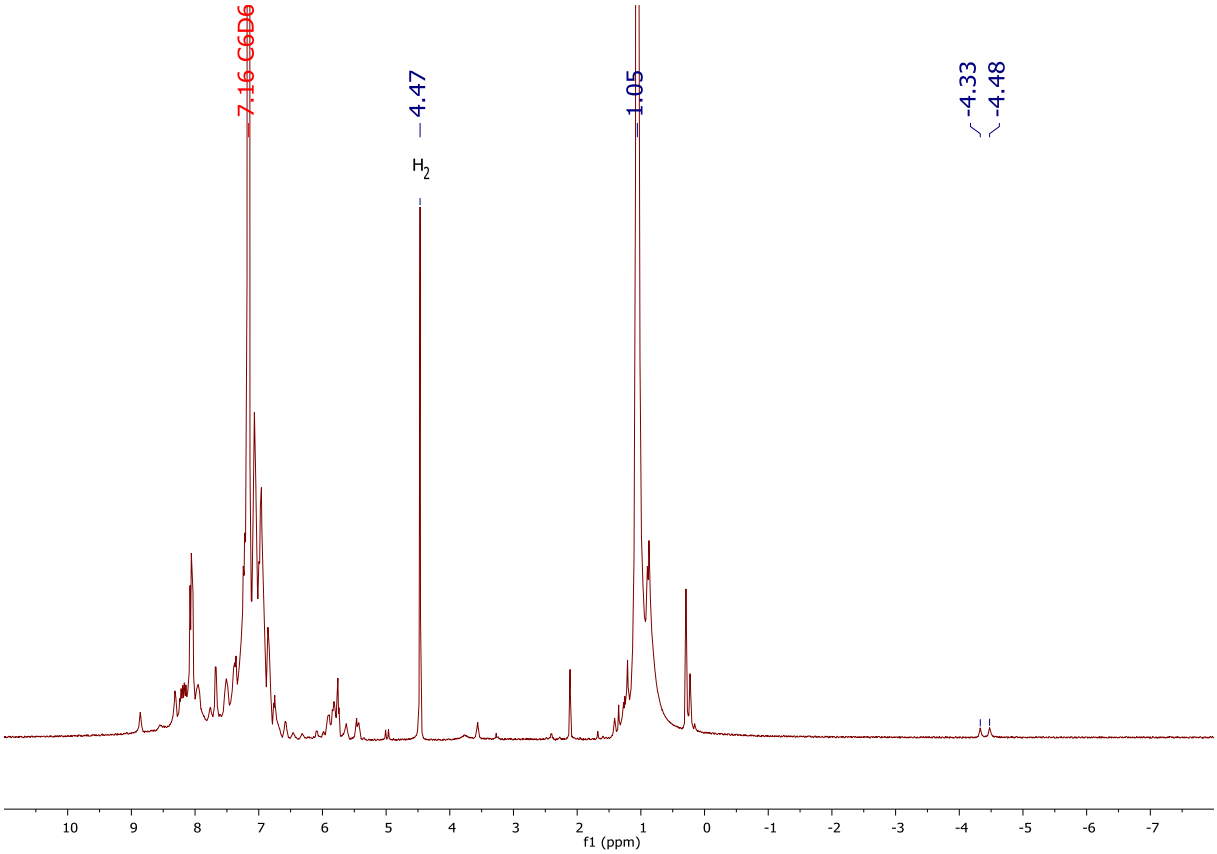

Figure S22: ^{1}H NMR spectrum of the complex **C^{3A}.2** + *t*BuOK + H_2 : mixture of complexes including hydride (C_6D_6, 400.1 MHz, 298K).

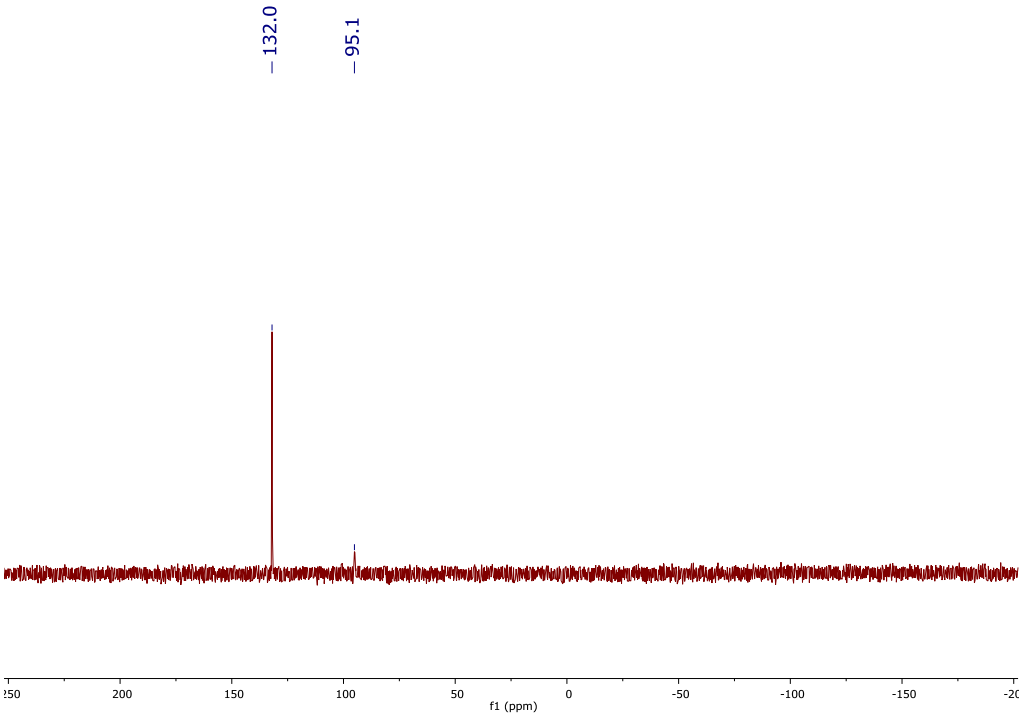

Figure S23: $^{31}P\{^{1}H\}$ NMR spectrum of the complex **C^{3A}.2** + KHMDS + H_2: mixture of hydride (132.0 ppm) and deprotonated (95.1 ppm) complexes (toluene-d_8, 162.0 MHz, 298K).

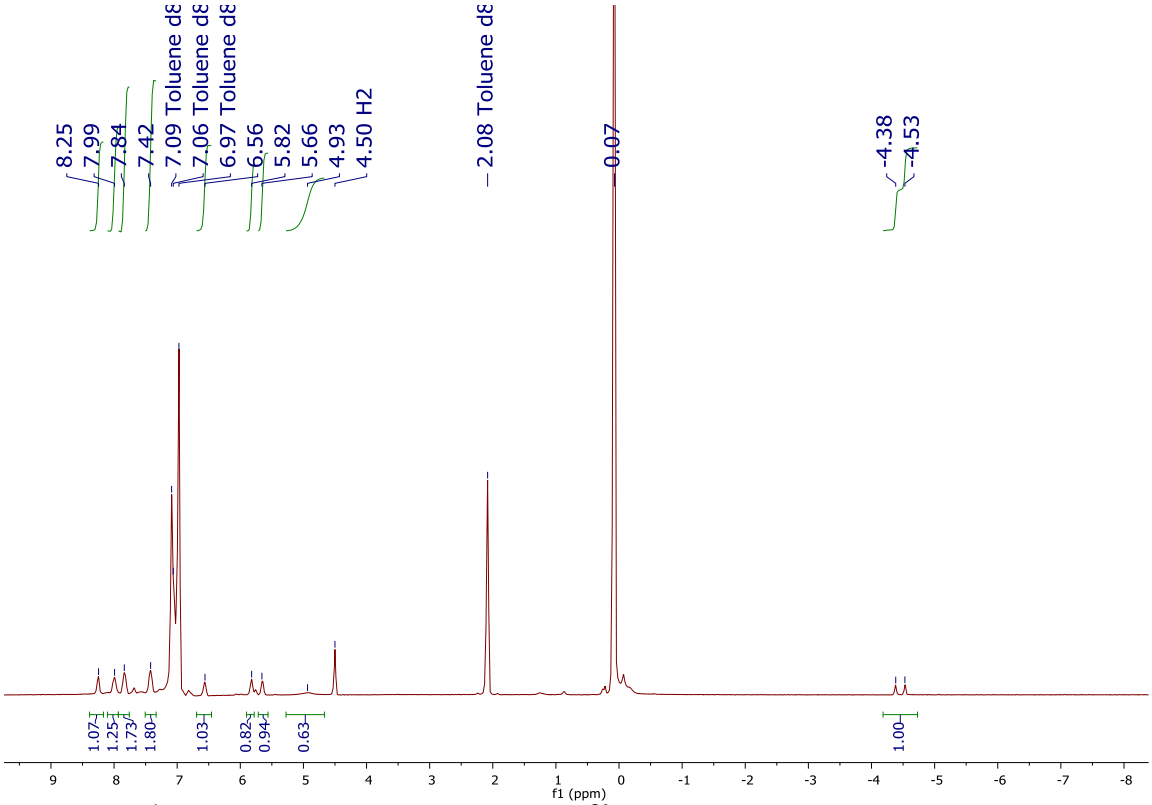

Figure S24: ^{1}H NMR spectrum of the complex **C^{3A}.2** + *t*BuOK + H_2: mixture of hydride (major) and deprotonated complexes (toluene-d_8, 400 MHz, 298K).

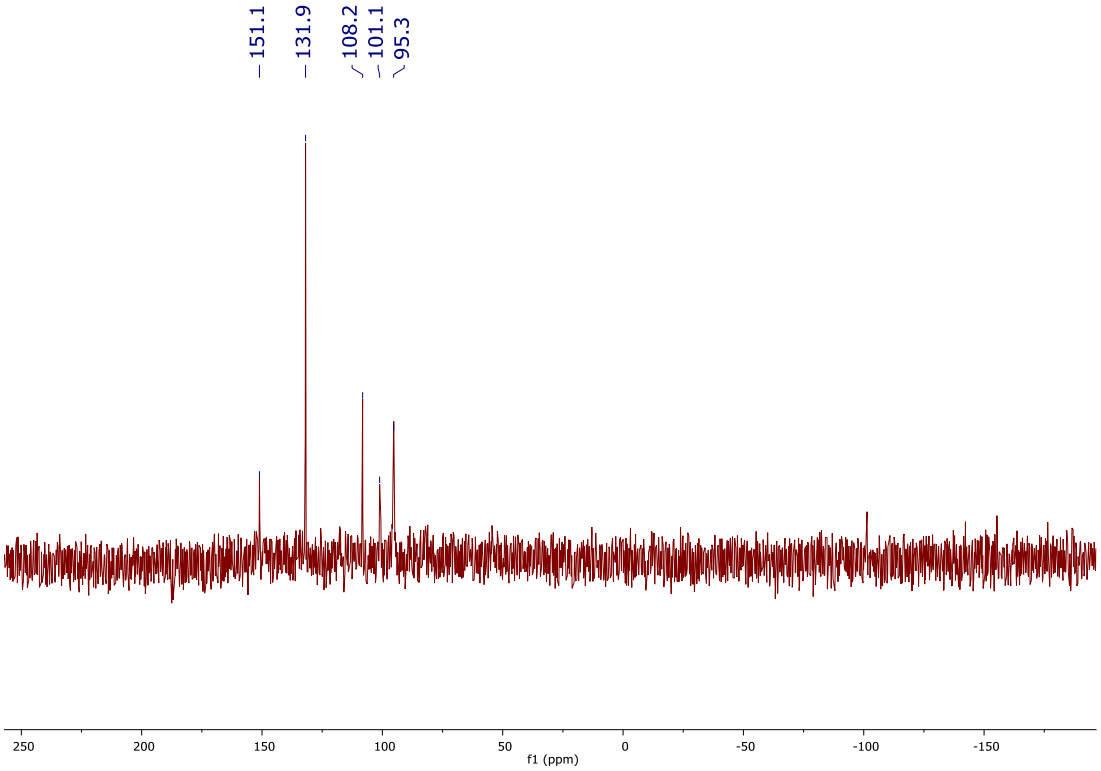

Figure S25: ^{31}P{^{1}H} NMR spectrum of the reaction mixture after adding acetophenone (toluene-d_8, 162.0 MHz, 298K).

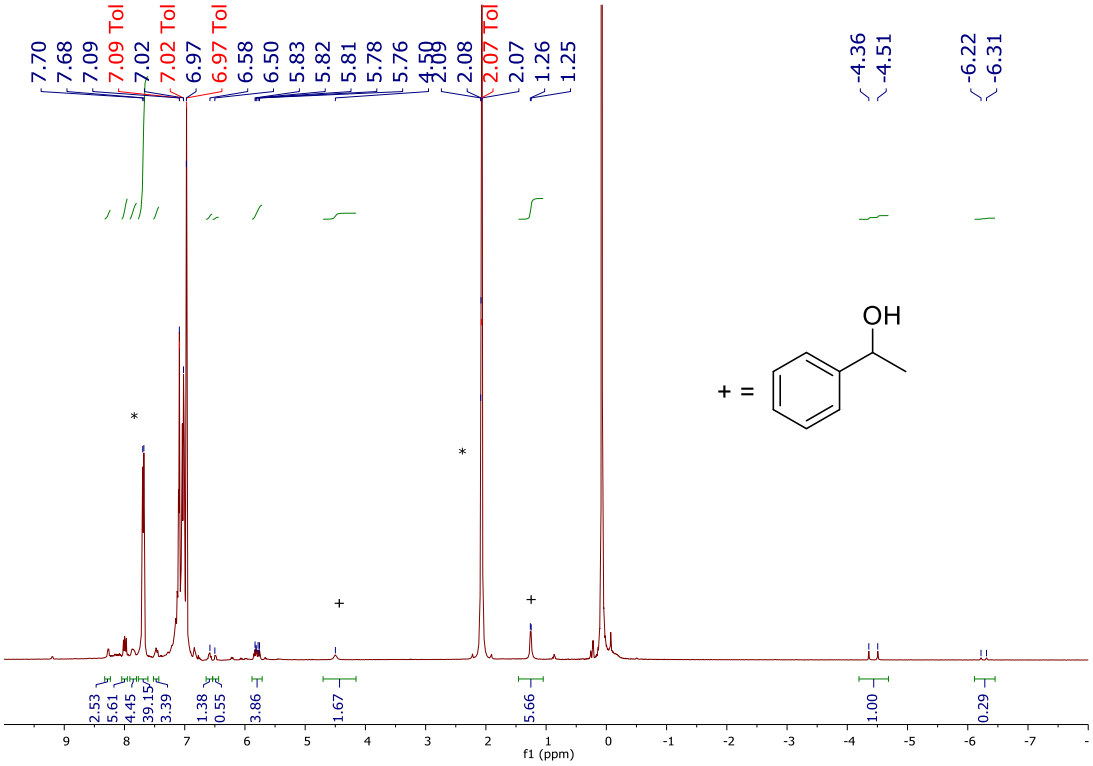

Figure S26: ^{1}H NMR spectrum of the reaction mixture after adding acetophenone (*) (toluene-d_8, 400 MHz, 298K).

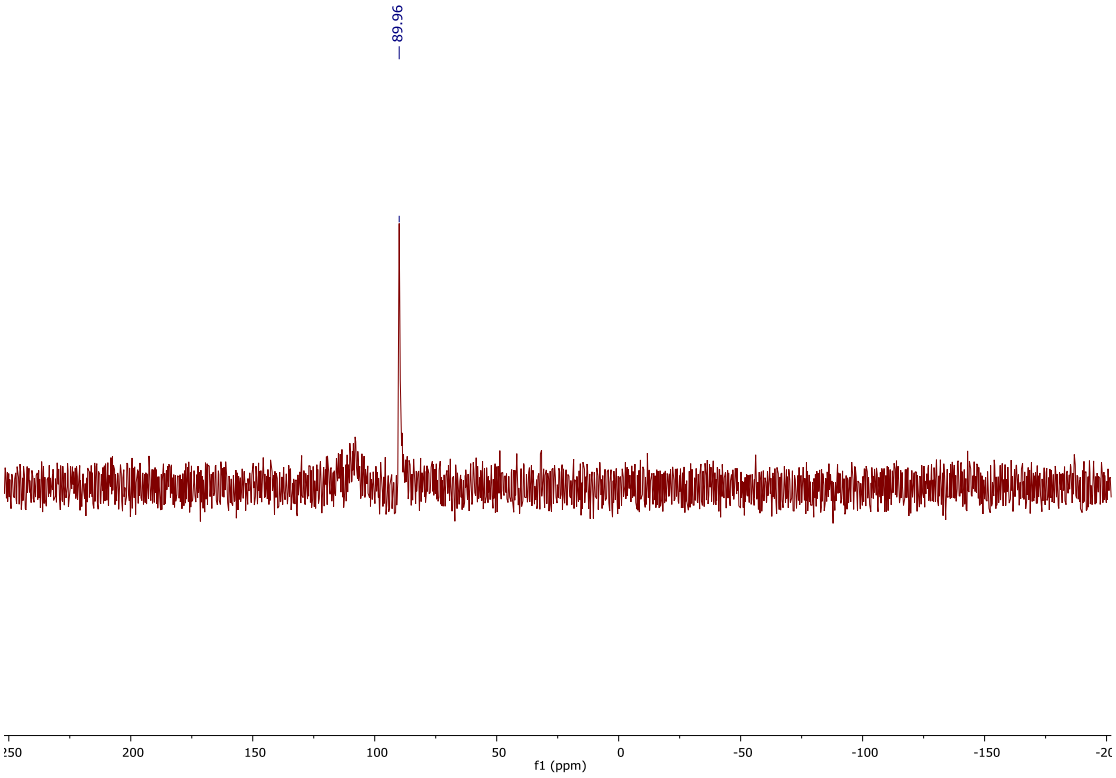

Figure S27: ^{31}P{^{1}H} NMR spectrum of the reaction mixture after 3 days (toluene-d_8, 162.0 MHz, 298K).

^{1}H NMR spectra of crude mixtures

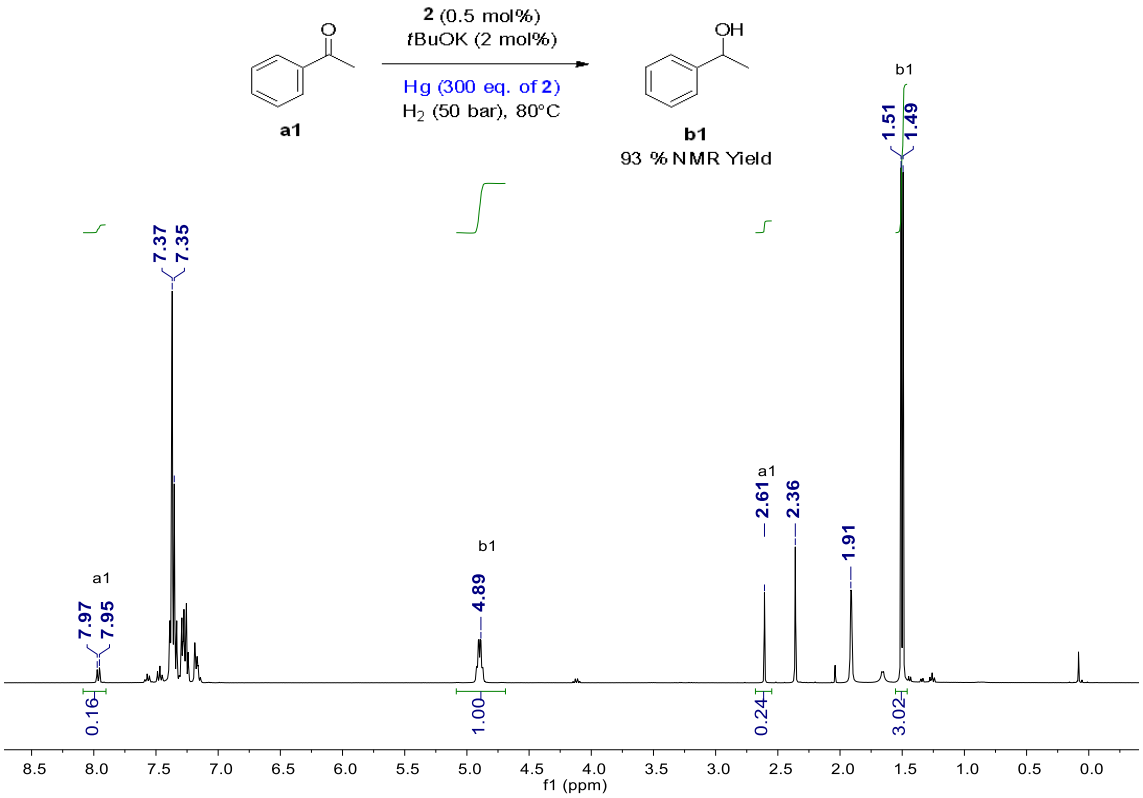

Figure S28: ^{1}H NMR spectrum of the crude hydrogenation mixture of acetophenone in the presence of Hg ($CDCl_3$, 400.1 MHz, 298K)

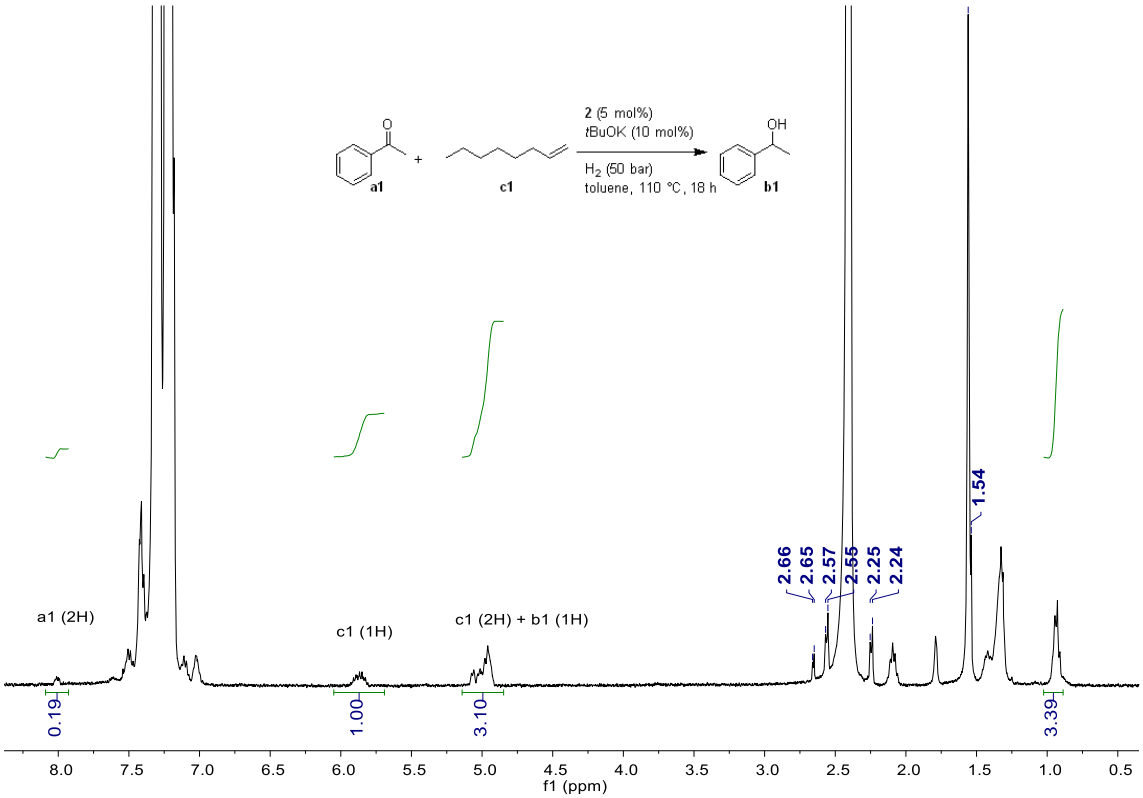

Figure S29: ^{1}H NMR spectrum of the crude hydrogenation mixture of acetophenone in the presence of 1-octene ($CDCl_3$, 400.1 MHz, 298K)

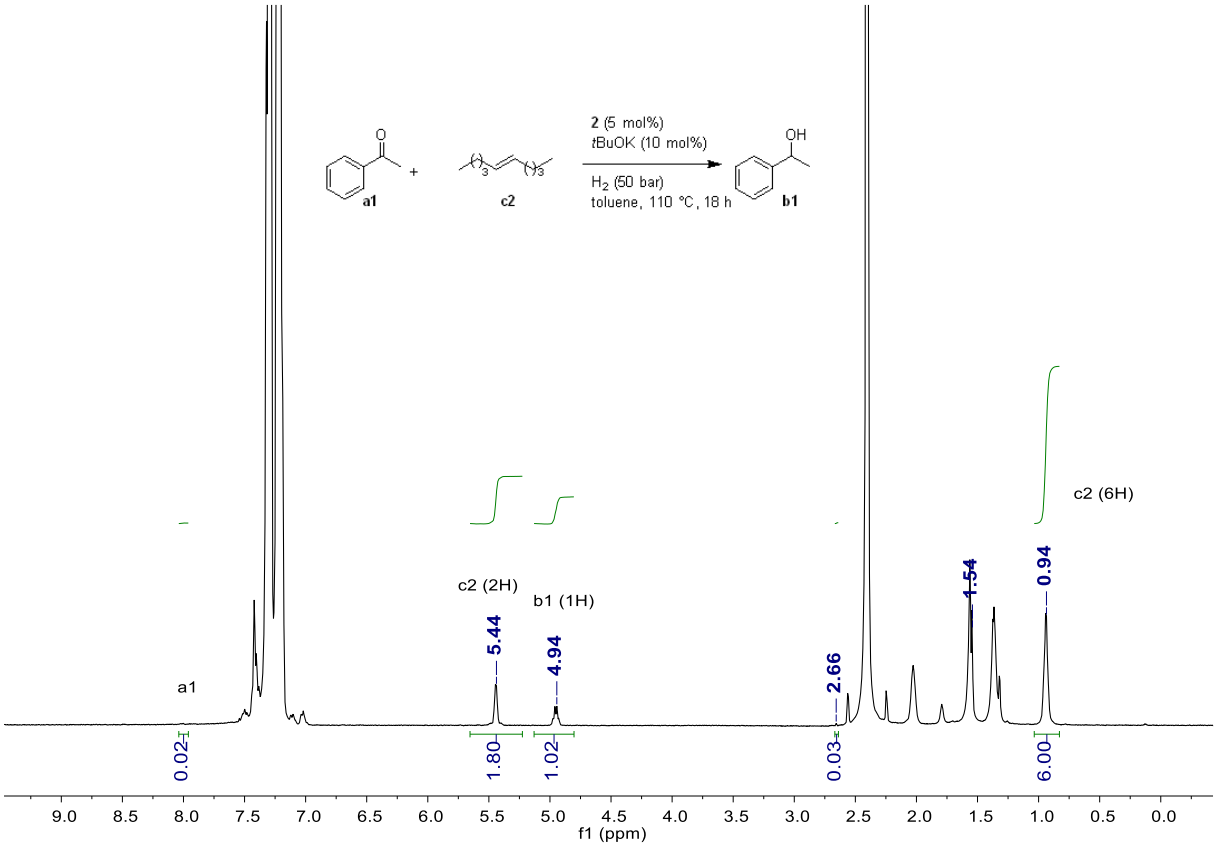

Figure S30: ^{1}H NMR spectrum of the crude hydrogenation mixture of acetophenone in the presence of 5-decene ($CDCl_3$, 400.1 MHz, 298K)

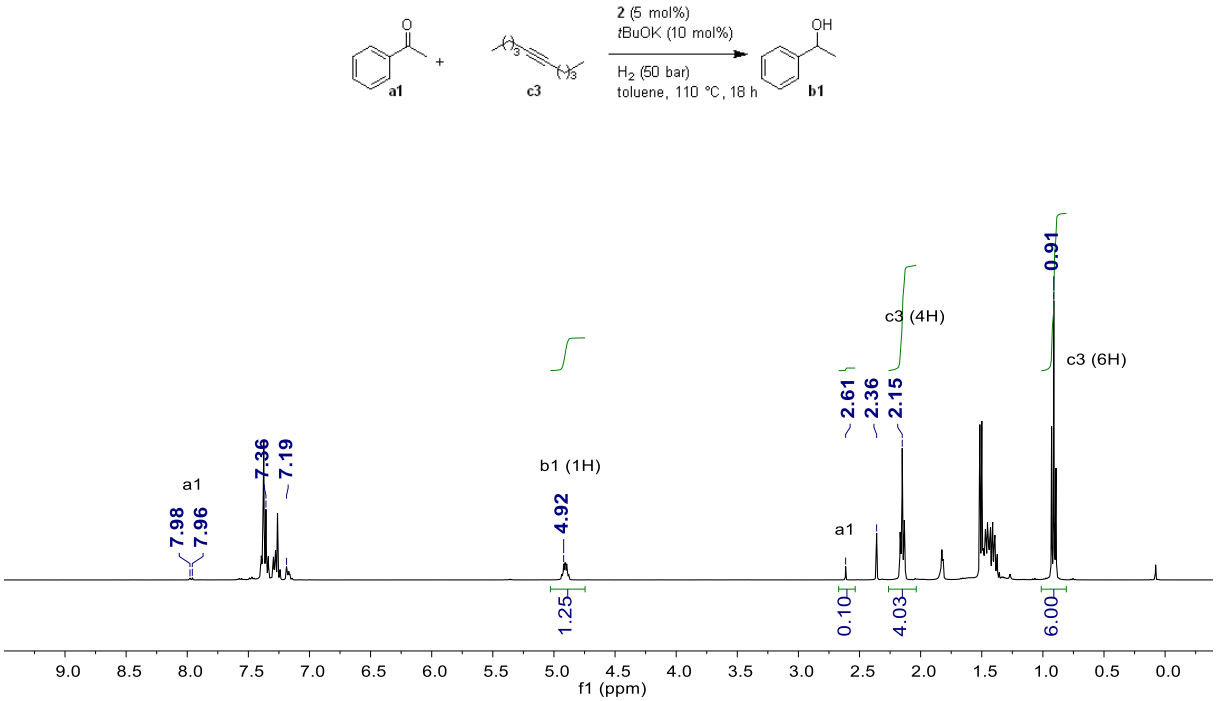

Figure S31: ^{1}H NMR spectrum of the crude hydrogenation mixture of acetophenone in the presence of 5-decyne ($CDCl_3$, 400.1 MHz, 298K)

X-ray data

CCDC-1565260-1565263 contains the supplementary crystallographic data for complexes **C^{3A}.1**, **C^{3A}.2**, **C^{3A}.3** and **C^{3A}.4**.

Complex **C^{3A}.1**

X-ray diffraction data were collected on a D8 VENTURE Bruker AXS diffractometer equipped with a PHOTON 100 CMOS detector, using multilayers monochromated Mo-Kα radiation (λ = 0.71073 Å) at T = 150(2) K. The structure was solved by dual-space algorithm using the *SHELXT* program,[12] and then refined with full-matrix least-square methods based on F^2 (*SHELXL-2014*).[13] All non-hydrogen atoms were refined with anisotropic atomic displacement parameters. H atoms were finally included in their calculated positions. A final refinement on F^2 with 4024 unique intensities and 203 parameters converged at $\omega R(F^2)$ = 0.0805 ($R(F)$ = 0.0408) for 3315 observed reflections with $I > 2\sigma(I)$.

Table S1. Crystal data and structure refinement for complex **C^{3A}.1**.

Empirical formula	C_{14} H_{19} Br Mn N_2 O_3 P
Formula weight	429.13
Temperature	150(2) *K*
Wavelength	0.71073 Å
Crystal system, space group	orthorhombic, *P b c n*
Unit cell dimensions	a = 29.2332(11) Å, α = 90 ° b = 9.9889(4) Å, β = 90 ° c = 12.0827(4) Å, γ = 90 °
Volume	3528.2(2) $Å^3$
Z, Calculated density	8, 1.616 ($g.cm^{-3}$)
Absorption coefficient	3.115 mm^{-1}
F(000)	1728
Crystal size	0.600 x 0.100 x 0.060 mm
Crystal color	yellow
Theta range for data collection	2.920 to 27.473 °
h_min, h_max	-37, 37
k_min, k_max	-12, 12
l_min, l_max	-15, 13
Reflections collected / unique	20407 / 4024 [R(int)[a] = 0.0477]
Reflections [I>2σ]	3315
Completeness to theta_max	0.997
Absorption correction type	multi-scan
Max. and min. transmission	0.830 , 0.608
Refinement method	Full-matrix least-squares on F^2
Data / restraints / parameters	4024 / 0 / 203
[b]Goodness-of-fit	1.099
Final *R* indices [I>2σ]	$R1^c$ = 0.0408, $wR2^d$ = 0.0805
R indices (all data)	$R1^c$ = 0.0539, $wR2^d$ = 0.0847
Largest diff. peak and hole	0.605 and -0.881 $e^-.Å^{-3}$

[a] $R_{int} = \sum |F_o^2 - < F_o^2 >| / \sum [F_o^2]$
[b] $S = \{\sum [w(F_o^2 - F_c^2)^2] / (n - p)\}^{1/2}$
[c] $R1 = \sum | |F_o| - |F_c| | / \sum |F_o|$
[d] $wR2 = \{\sum [w(F_o^2 - F_c^2)^2] / \sum [w(F_o^2)^2]\}^{1/2}$
$w = 1 / [\sigma(F_o^2) + aP^2 + bP]$ where $P = [2F_c^2 + MAX(F_o^2, 0)] /3$

Complex **C^{3A}.2**

X-ray diffraction data were collected on a APEXII Bruker AXS diffractometer equipped with a CCD detector, using graphite-monochromated Mo-Kα radiation (λ = 0.71073 Å) at T = 150 (2) K. The structure was solved by dual-space algorithm using the *SHELXT* program,[12] and then refined with full-matrix least-square methods based on F^2 (*SHELXL-2014*).[13] All non-hydrogen atoms were refined with anisotropic atomic displacement parameters. H atoms were finally included in their calculated positions. A final refinement on F^2 with 4664 unique intensities and 253 parameters converged at $\omega R(F^2)$ = 0.0966 ($R(F)$ = 0.0729) for 2438 observed reflections with $I > 2\sigma(I)$.

Table S2. Crystal data and structure refinement for complex **C^{3A}.2**.

Empirical formula	C_{20} H_{15} Br Mn N_2 O_3 P
Formula weight	497.16
Temperature	150(2) *K*
Wavelength	0.71073 Å
Crystal system, space group	monoclinic, *P* $2_1/c$
Unit cell dimensions	a = 10.298(2) Å, α = 90 °
	b = 12.401(2) Å, β = 105.890(7) °
	c = 16.675(4) Å, γ = 90 °
Volume	2048.0(8) $Å^3$
Z, Calculated density	4, 1.612 ($g.cm^{-3}$)
Absorption coefficient	2.696 mm^{-1}
F(000)	992
Crystal size	0.250 x 0.200 x 0.110 mm
Crystal color	colourless
Theta range for data collection	3.025 to 27.482 °
h_min, h_max	-13, 13
k_min, k_max	-15, 15
l_min, l_max	-21, 21
Reflections collected / unique	13584 / 4664 [R(int)[a] = 0.1067]
Reflections [I>2σ]	2438
Completeness to theta_max	0.994
Absorption correction type	multi-scan
Max. and min. transmission	0.743 , 0.633
Refinement method	Full-matrix least-squares on F^2
Data / restraints / parameters	4664 / 0 / 253
[b]Goodness-of-fit	0.989
Final *R* indices [I>2σ]	$R1^c$ = 0.0729, $wR2^d$ = 0.0966
R indices (all data)	$R1^c$ = 0.1610, $wR2^d$ = 0.1225
Largest diff. peak and hole	0.750 and -0.616 $e^-.Å^{-3}$

[a] $R_{int} = \sum |F_o^2 - < F_o^2 >| / \sum [F_o^2]$

[b] $S = \{\sum [w(F_o^2 - F_c^2)^2] / (n - p)\}^{1/2}$

[c] $R1 = \sum | |F_o| - |F_c| | / \sum |F_o|$

[d] $wR2 = \{\sum [w(F_o^2 - F_c^2)^2] / \sum [w(F_o^2)^2]\}^{1/2}$

$w = 1 / [\sigma(F_o^2) + aP^2 + bP]$ where $P = [2F_c^2 + MAX(F_o^2, 0)] /3$

Complex **C^{3A}.3**

X-ray diffraction data were collected on a D8 VENTURE Bruker AXS diffractometer equipped with a PHOTON 100 CMOS detector, using multilayers monochromated Mo-Kα radiation (λ = 0.71073 Å) at T = 150(2) K. The structure was solved by dual-space algorithm using the *SHELXT* program,[12] and then refined with full-matrix least-square methods based on F^2 (*SHELXL*).[13] All non-hydrogen atoms were refined with anisotropic atomic displacement parameters. H atoms were finally included in their calculated positions. A final refinement on F^2 with 4688 unique intensities and 253 parameters converged at $\omega R(F^2)$ = 0.0508 ($R(F)$ = 0.0214) for 4340 observed reflections with $I > 2\sigma(I)$.

Table S3. Crystal data and structure refinement for complex **C^{3A}.3**.

Empirical formula	C_{21} H_{16} Br Mn N O_3 P
Formula weight	496.17
Temperature	150 *K*
Wavelength	0.71073 Å
Crystal system, space group	monoclinic, *P* $2_1/c$
Unit cell dimensions	a = 9.2456(5) Å, α = 90 °
	b = 8.5879(3) Å, β = 90.599(3) °
	c = 25.8035(10) Å, γ = 90 °
Volume	2048.69(15) $Å^3$
Z, Calculated density	4, 1.609 ($g.cm^{-3}$)
Absorption coefficient	2.694 mm^{-1}
F(000)	992
Crystal size	0.280 x 0.180 x 0.150 mm
Crystal color	yellow
Theta range for data collection	3.158 to 27.482 °
h_min, h_max	-12, 12
k_min, k_max	-11, 11
l_min, l_max	-33, 33
Reflections collected / unique	22344 / 4688 [R(int)[a] = 0.0259]
Reflections [I>2σ]	4340
Completeness to theta_max	0.999
Absorption correction type	multi-scan
Max. and min. transmission	0.668 , 0.584
Refinement method	Full-matrix least-squares on F^2
Data / restraints / parameters	4688 / 0 / 253
[b]S (Goodness-of-fit)	1.071
Final *R* indices [I>2σ]	$R1^c$ = 0.0214, $wR2^d$ = 0.0508
R indices (all data)	$R1^c$ = 0.0244, $wR2^d$ = 0.0520
Largest diff. peak and hole	0.314 and -0.516 $e^-.Å^{-3}$

[a] $R_{int} = \sum |F_o^2 - \langle F_o^2 \rangle| / \sum [F_o^2]$
[b] $S = \{\sum [w(F_o^2 - F_c^2)^2] / (n - p)\}^{1/2}$
[c] $R1 = \sum | |F_o| - |F_c| | / \sum |F_o|$
[d] $wR2 = \{\sum [w(F_o^2 - F_c^2)^2] / \sum [w(F_o^2)^2]\}^{1/2}$
$w = 1 / [\sigma(F_o^2) + aP^2 + bP]$ where $P = [2F_c^2 + MAX(F_o^2, 0)] /3$

Complex **C^{3A}.4**

X-ray diffraction data were collected on a APEXII Bruker AXS diffractometer equipped with a CCD detector, using graphite-monochromated Mo-Kα radiation (λ = 0.71073 Å) at T = 295 K. The structure was solved by dual-space algorithm using the *SHELXT* program,[12] and then refined with full-matrix least-square methods based on F^2 (*SHELXL*).[13] The contribution of the disordered solvents to the structure factors was calculated by the *PLATON* SQUEEZE procedure[14] and then taken into account in the final *SHELXL-2014* least-square refinement. All non-hydrogen atoms were refined with anisotropic atomic displacement parameters. H atoms were finally included in their calculated positions. A final refinement on F^2 with 6433 unique intensities and 217 parameters converged at $\omega R(F^2)$ = 0.1417 ($R(F)$ = 0.0601) for 4884 observed reflections with $I > 2\sigma(I)$.

Table S4. Crystal data and structure refinement for complex **C^{3A}.4**.

Empirical formula	C_{25} H_{18} Br Mn N O_3 P
Formula weight	546.22
Temperature	295 *K*
Wavelength	0.71073 Å
Crystal system, space group	triclinic, *P* -1
Unit cell dimensions	a = 10.966(4) Å, α = 72.966(11) °
	b = 11.067(4) Å, β = 81.251(11) °
	c = 13.178(4) Å, γ = 67.615(11) °
Volume	1412.4(8) $Å^3$
Z, Calculated density	2, 1.284 ($g.cm^{-3}$)
Absorption coefficient	1.961 mm^{-1}
F(000)	548
Crystal size	0.580 x 0.360 x 0.140 mm
Crystal color	yellow
Theta range for data collection	2.929 to 27.484 °
h_min, h_max	-14, 14
k_min, k_max	-13, 14
l_min, l_max	-17, 16
Reflections collected / unique	35439 / 6433 [R(int)[a] = 0.0281]
Reflections [I>2σ]	4884
Completeness to theta_max	0.993
Absorption correction type	multi-scan
Max. and min. transmission	0.760 , 0.573
Refinement method	Full-matrix least-squares on F^2
Data / restraints / parameters	6433 / 0 / 217
[b]S (Goodness-of-fit)	1.022
Final *R* indices [I>2σ]	$R1^c$ = 0.0601, $wR2^d$ = 0.1417
R indices (all data)	$R1^c$ = 0.0840, $wR2^d$ = 0.1617
Largest diff. peak and hole	2.149 and -1.171 $e^-.Å^{-3}$

[a] $R_{int} = \sum |F_o^2 - < F_o^2 >| / \sum [F_o^2]$

[b] $S = \{\sum [w(F_o^2 - F_c^2)^2] / (n - p)\}^{1/2}$

[c] $R1 = \sum | |F_o| - |F_c| | / \sum |F_o|$

[d] $wR2 = \{\sum [w(F_o^2 - F_c^2)^2] / \sum [w(F_o^2)^2]\}^{1/2}$

$w = 1 / [\sigma(F_o^2) + aP^2 + bP]$ where $P = [2F_c^2 + MAX(F_o^2, 0)] /3$

Complex C^{3A}.2b'

X-ray diffraction data were collected on a D8 VENTURE Bruker AXS diffractometer equipped with a PHOTON 100 CMOS detector, using multilayers monochromated Mo-Kα radiation (λ = 0.71073 Å) at T = 150(2) K. The structure was solved by dual-space algorithm using the *SHELXT* program, and then refined with full-matrix least-square methods based on F^2 (*SHELXL-2014*). All non-hydrogen atoms were refined with anisotropic atomic displacement parameters. H atoms were finally included in their calculated positions.

Table S5. Crystal data and structure refinement for complex **C^{3A}.2b'**.

Empirical formula	$C_{37}\ H_{33}\ Mn\ N_4\ O_3\ P_2$
Formula weight	698.55 g/mol
Temperature	150 K
Wavelength	0.71073 Å
Crystal system, space group	monoclinic, P 21/c
Unit cell dimensions	a = 20.1007(15) Å, alpha = 90°
	b = 9.8322(7) Å, beta = 116.713(3) °
	c = 19.0628(15) Å, gamma = 90°
Volume	3365.4(4) $Å^3$
Z, Calculated density	4, 1.379 $g.cm^{-3}$
Absorption coefficient	0.530 mm^{-1}
F(000)	1448
Crystal size	0.360 x 0.100 x 0.045 mm
Crystal color	yellow
Theta range for data collection	3.073 to 27.485 °
h_min, h_max	-26, 26
k_min, k_max	-12, 12
l_min, l_max	-24, 24
Reflections collected / unique	63665 / 7719 [R(int)[a] = 0.0571]
Reflections [I>2σ]	6458
Completeness to theta_max	0.999
Absorption correction type	multi-scan
Max. and min. transmission	0.974 , 0.811
Refinement method	Full-matrix least-squares on F^2
Data / restraints / parameters	7719 / 0 / 431
[b]S (Goodness-of-fit)	1.049
Final R indices [I>2σ]	R1[c] = 0.0311, wR2[d] = 0.0760
R indices (all data)	R1[c] = 0.0428, wR2[d] = 0.0834
Largest diff. peak and hole	0.295 and -0.465 $e^-.Å^{-3}$

[a] $R_{int} = \sum |F_o^2 - < F_o^2 >| / \sum [F_o^2]$

[b] $S = \{\sum [w(F_o^2 - F_c^2)^2] / (n - p)\}^{1/2}$

[c] $R1 = \sum | |F_o| - |F_c| | / \sum |F_o|$

[d] $wR2 = \{\sum [w(F_o^2 - F_c^2)^2] / \sum [w(F_o^2)^2]\}^{1/2}$

$w = 1 / [\sigma(F_o^2) + aP^2 + bP]$ where $P = [2F_c^2 + MAX(F_o^2, 0)] /3$

References

[1] D. Benito-Garagorri, K. Mereiter, K. Kirchner, Collect. *Czech. Chem. Commun*. **2007**, *72*, 527-540.
[2] S. M. Aucott, A. M. Z. Slawin, J. D. Woollins*, J. Chem. Soc., Dalton Trans.* **2000**, 2559-2575.
[3] M. Alvarez, N. Lugan, R. Mathieu, *J. Chem. Soc., Dalton Trans*. **1994**, 2755-2760.
[4] E. Mothes, S. Sentets, M. A. Luquin, R. Mathieu, N. Lugan, G. Lavigne, *Organometallics* **2008**, *27*, 1193-1206.
[5] D. Wei, T. Roisnel, C. Darcel, E. Clot, J.-B. Sortais, *ChemCatChem* **2017**, *9*, 80-83.
[6] L. Shi, Y.-Q. Tu, M. Wang, F.-M. Zhang, C.-A. Fan, Y.-M. Zhao, W.-J. Xia, *J. Am. Chem. Soc*. **2005**, *127*, 10836-10837.
[7] K. Miyamoto, N. Tada, M. Ochiai, *J. Am. Chem. Soc.* **2007**, *129*, 2772-2773.
[8] B. T. Cho, S. K. Kang, M. S. Kim, S. R. Ryu, D. K. An, *Tetrahedron* **2006**, *62*, 8164-8168.
[9] D. J. Fox, D. S. Pedersen, S. Warren, *Org. Biomol. Chem.* **2006**, *4*, 3102-3107.
[10] T. Hirata, A. Matsushima, Y. Sato, T. Iwasaki, H. Nomura, T. Watanabe, S. Toyoda, S. Izumi, *J. Mol. Catal. B: Enzym.* **2009**, *59*, 158-162.
[11] X. Chen, X. Gao, Q. Wu, D. Zhu, *Tetrahedron: Asymmetry* **2012**, *23*, 734-738.
[12] G. M. Sheldrick, *Acta Cryst.* **2015**, *A71*, 3-8.
[13] G. M. Sheldrick, *Acta Cryst.* **2015**, *C71*, 3-8.
[14] A. Spek, *Acta Cryst.* **2015**, *C71*, 9-18.

A – II – Reductive amination

Manganese complexes **1**-**4** were synthesized according to our procedure.[1]

Low Resolution mass spectra were obtained on a QP2010 GC/MS apparatus from Shimadzu equipped with a 30 m capillary column (Supelco, SLBTM-5ms, fused silica capillary column, 30 M × 0.25 mm × 0.25 mm film thickness).

Specific rotations (in deg cm^2 g^{-1}) were measured in a 1 dm thermostated quartz cell on a Jasco-P1010 polarimeter.

General procedure for reductive amination reaction.

In an argon filled glove box, a 20 mL Schlenk tube was charged with aldehyde (0.5 mmol), amine (0.6 mmol) and anhydrous ethanol (2.0 mL). The reaction mixture was stirred at 100 °C (or at room temperature for aldehyde containing α-protons) for 24 h. After cooling to room temperature, the mixture was transferred to a 20 mL autoclave followed by manganese complex $\mathbf{C^{3a}2}$ (5.0 mg, 2 mol%) and *t*BuOK (2.8 mg, 5 mol%). The autoclave was charged with H_2 (50 bar) and the mixture was stirred at indicated temperature in an oil bath. After cooling to room temperature, the solution was diluted with ethyl acetate (2.0 mL) and filtered through a small pad of celite (2 cm in a Pasteur pipette). The celite was washed with ethyl acetate (2×2.0 mL). The filtrate was evaporated and the crude residue was purified by column chromatography (SiO_2, mixture of petroleum ether/ethyl acetate as eluent).

Specific procedure for reductive amination reaction on large scale

(Scheme **A^{3II}.2**, entry 4).

A 50 mL Maximator autoclave ("Réacteur à ouverture rapide") was purged with N_2 and then charged with a solution of benzaldehyde (475 µL, 4.3 mmol) and *p*-toluidine (500.0 mg, 4.6 mmol, 1.08 equiv.) in EtOH (10 mL). After stirring for 2 h at r.t., a solution of complex **C^{3A}.2** (43 mg, 2 mol%) in EtOH (4 mL) and a solution of *t*BuOK (28 mg, 5 mol%) in EtOH (4 mL) were added under N_2 flow. The autoclave was charged with H_2 (50 bar) and the mixture was stirred at 100 °C for 24 h. The solution was concentrated under reduced pressure, and the crude residue was purified by column chromatography (SiO_2, mixture of petroleum ether/ethyl acetate as eluent). *N*-benzyl-4-methylaniline **d4** was obtained as pale yellow oil (663 mg, 78%).

Characterization of the products of the catalysis

_N_-benzylaniline[2] (d1)

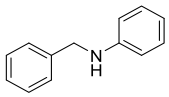

Following the general procedure at 50 °C for 18 h, benzaldehyde (51.0 µL, 0.5 mmol) and aniline (54.8 µL, 0.6 mmol) gave the title compound **d1** as a brown liquid (85.2 mg, 93% yield).

^{1}H NMR (400.1 MHz, $CDCl_3$) δ 7.43 – 7.36 (m, 4H), 7.34 – 7.28 (m, 1H), 7.23 – 7.19 (m, 2H), 6.76 (td, *J* = 7.3, 1.1 Hz, 1H), 6.68 (d, *J* = 7.7 Hz, 2H), 4.36 (s, 2H), 4.08 (br, 1H).

^{13}C{^{1}H} NMR (100.6 MHz, $CDCl_3$) δ 148.2, 139.5, 129.4, 128.7, 127.6, 127.3, 117.7, 113.0, 48.5.

_N_-(2-methylbenzyl)aniline[3] (d2)

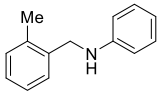

Following the general procedure at 100 °C for 36 h, 2-methylbenzaldehyde (57.8 µL, 0.5 mmol) and aniline (54.8 µL, 0.6 mmol) gave the title compound **d2** as a dark brown liquid (52.7 mg, 94% yield).

^{1}H NMR (400.1 MHz, $CDCl_3$) δ 7.35 (d, *J* = 6.7 Hz, 1H), 7.26 – 7.17 (m, 5H), 6.74 (tt, *J* = 7.3, 1.1 Hz, 1H), 6.67 – 6.64 (m, 2H), 4.29 (s, 2H), 3.84 (s, 1H), 2.39 (s, 3H).

^{13}C{^{1}H} NMR (100.6 MHz, $CDCl_3$) δ 148.4, 137.1, 136.5, 130.5, 129.4, 128.4, 127.6, 126.3, 117.6, 112.8, 46.5, 19.1.

_N_-benzyl-4-methoxyaniline[2] (d3)

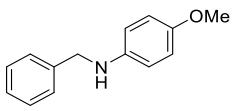

Following the general procedure at 100 °C for 48 h, benzaldehyde (51.0 µL, 0.5 mmol) and 4-methoxyaniline (73.9 mg, 0.6 mmol) gave the title compound **d3** as a brown solid (76.8 mg, 72% yield).

^{1}H NMR (400.1 MHz, $CDCl_3$) δ 7.40 – 7.33 (m, 4H), 7.29 (d, *J* = 7.1 Hz, 1H), 6.81 – 6.77 (m, 2H), 6.64 – 6.60 (m, 2H), 4.30 (s, 2H), 3.75 (s, 3H).

^{13}C{^{1}H} NMR (100.6 MHz, $CDCl_3$) δ 152.4, 142.5, 139.8, 128.7, 127.7, 127.3, 115.0, 114.3, 55.9, 49.4.

***N*-benzyl-4-methylaniline[2] (d4)**

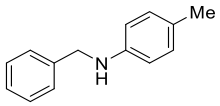

Following the specific procedure at 100 °C for 24 h, benzaldehyde (475.0 µL, 4.3 mmol) and 4-methylaniline (500.0 mg, 4.6 mmol) gave the title compound **d4** as a pale yellow oil (663 mg, 78% yield).

^{1}H NMR (400.1 MHz, $CDCl_3$) δ 7.50 – 7.21 (m, 5H), 7.14 – 6.96 (m, 2H), 6.68 – 6.57 (m, 2H), 4.36 (s, 2H), 3.94 (s, 1H), 2.31 (s, 3H).

^{13}C{^{1}H} NMR (100.6 MHz, $CDCl_3$) δ 146.0, 139.8, 129.9, 128.7, 127.6, 127.2, 126.8, 113.1, 48.7, 20.5.

***N*-(4-methoxybenzyl)aniline[2] (d5)**

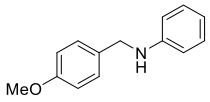

Following the general procedure at 50 °C for 48 h, 4-methoxybenzaldehyde (60.8 µL, 0.5 mmol) and aniline (54.8 µL, 0.6 mmol) gave the title compound **d5** as a yellow liquid (92.8 mg, 87% yield).

^{1}H NMR (400.1 MHz, $CDCl_3$) δ 7.30 (d, *J* = 8.6, 2H), 7.21 – 7.16 (m, 2H), 6.89 (d, *J* = 8.6 Hz, 2H), 6.73 (t, *J* = 7.3 Hz, 1H), 6.66 (dd, *J* = 7.7, 1.1 Hz, 2H), 4.27 (s, 2H), 3.81 (s, 3H).

^{13}C{^{1}H} NMR (100.6 MHz, $CDCl_3$) δ = 159.0, 148.2, 131.4, 129.4, 129.0, 117.8, 114.2, 113.1, 55.4, 48.0.

***N*-benzyl-4-fluoroaniline[2] (d6)**

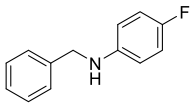

Following the general procedure at 100 °C for 48 h, benzaldehyde (51.0 µL, 0.5 mmol) and 4-fluoroaniline (57.6 µL, 0.6 mmol) gave the title compound **d6** as a brown solid (28.2 mg, 28% yield).

^{1}H NMR (400.1 MHz, $CDCl_3$) δ 7.39 – 7.26 (m, 5H), 6.89 (t, *J* = 8.7, 2H), 6.60 – 6.55 (m, 2H), 4.30 (s, 2H), 3.94 (br, 1H).

^{19}F NMR (376.5 MHz, $CDCl_3$) δ -127.91.

^{13}C{^{1}H} NMR (100.6 MHz, $CDCl_3$) δ 156.0 (d, $^{1}J_{CF}$ = 235.0), 144.6 (d, J_{CF} = 1.5 Hz), 139.4, 128.8, 127.6, 127.4, 115.8 (d, J_{CF} = 22.3 Hz), 113.8 (d, J_{CF} = 7.4 Hz), 49.1.

***N*-(3-fluorobenzyl)aniline[4] (d7)**

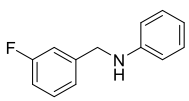

Following the general procedure at 80 °C for 36 h, 3-fluorobenzaldehyde (53.0 µL, 0.5 mmol) and aniline (54.8 µL, 0.6 mmol) gave the title compound **d7** as a pale yellow solid (90.6 mg, 90% yield).

^{1}H NMR (400.1 MHz, $CDCl_3$) δ 7.30 (td, *J* = 7.9, 7.3 Hz, 1H), 7.20-7.14 (m, 3H), 7.09 (dt, *J* = 9.8, 2.0 Hz, 1H), 6.96 (td, *J* = 8.4, 2.6 Hz, 1H), 6.74 (t, *J* = 7.3 Hz, 1H), 6.62 (d, *J* = 7.9 Hz, 2H), 4.35 (s, 2H), 4.09 (br, 1H).

^{19}F NMR (376 MHz, $CDCl_3$) δ -113.00.

^{13}C{^{1}H} NMR (75 MHz, $CDCl_3$) δ 163.2 (d, $^{1}J_{CF}$ = 246.2 Hz), 147.9, 142.4 (d, J_{CF} = 6.8 Hz), 130.2 (d, J_{CF} = 8.2 Hz), 129.4, 122.9 (d, J_{CF} = 2.8 Hz), 117.9, 114.4 (d, J_{CF} = 8.3 Hz), 114.1 (d, J_{CF} = 7.9 Hz), 113.0, 47.9.

GC-MS, m/z (%) = 201 ([M]+, 100), 109 (100), 77 (57), 65 (18), 51 (20).

***N*-(4-chlorobenzyl)aniline[5] (d8)**

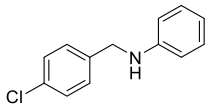

Following the general procedure at 50 °C for 48 h, 4-chlorobenzaldehyde (70.3 mg, 0.5 mmol) and aniline (54.8 µL, 0.6 mmol) gave the title compound **d8** as a pale yellow liquid (87.1 mg, 80% yield).

^{1}H NMR (400.1 MHz, $CDCl_3$) δ 7.31 (s, 4H), 7.18 (t, *J* = 7.9 Hz, 2H), 6.74 (t, *J* = 7.3 Hz, 1H), 6.62 (d, *J* = 7.8 Hz, 2H), 4.32 (s, 2H), 4.06 (br, 1H).

^{13}C{^{1}H} NMR (100.6 MHz, $CDCl_3$) δ 147.9, 138.1, 133.0, 129.4, 128.9, 128.8, 117.9, 113.0, 47.8.

***N*-(4-bromobenzyl)-4-iodoaniline (d9)**

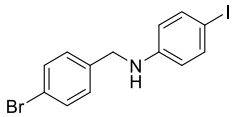

Following the general procedure at 100 °C for 36 h, 4-bromobenzaldehyde (92.5 mg, 0.5 mmol) and 4-iodoaniline (131.4 mg, 0.6 mmol) gave the title compound **d9** as a white solid (190.1 mg, 98% yield). The isolated product contains about 13% of 4-bromobenzylaniline[4] resulting from deiodination.

^{1}H NMR (400.1 MHz, $CDCl_3$) δ = 7.46 (d, *J* = 7.9, 2H), 7.41 (d, *J* = 8.1, 2H), 7.21 (d, *J* = 8.1, 2H), 6.38 (d, *J* = 8.2, 2H), 4.26 (s, 2H), 4.12 (br, 1H).

^{13}C{^{1}H} NMR (100.6 MHz, $CDCl_3$) δ = 147.4, 138.03, 137.99, 131.9, 129.1, 121.3, 115.2, 78.6, 47.6.

GC-MS, m/z (%) = 389 ([M]+, 67), 308 (8), 169 (100), 90 (53), 76 (18), 63 (11), 50 (10).

***N*-benzyl-4-iodoaniline[6] (d10)**

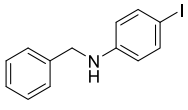

Following the general procedure at 100 °C for 36 h, benzaldehyde (51.0 µL, 0.5 mmol) and 4-iodoaniline (131.4 mg, 0.6 mmol) gave the title compound **d10** as a brown liquid (149.9 mg, 97% yield). The isolated product contains about 10% of benzylaniline resulting from deiodination.

^{1}H NMR (400.1 MHz, $CDCl_3$) δ 7.41 (d, *J* = 8.6 Hz, 2H), 7.37 – 7.34 (m, 5H), 6.42 (d, *J* = 8.6 Hz, 2H), 4.30 (d, *J* = 3.9 Hz, 2H), 4.10 (br, 1H).

^{13}C{^{1}H} NMR (100.6 MHz, $CDCl_3$) δ 147.8, 139.0, 137.9, 128.8, 127.6, 127.5, 115.2, 78.3, 48.2.

***N*,*N*-dimethyl-4-((*p*-tolylamino)methyl)aniline[7] (d11)**

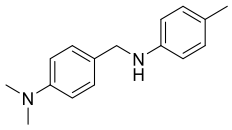

Following the general procedure at 80 °C for 36 h, 4-(dimethylamino)benzaldehyde (74.6 mg, 0.5 mmol) and *p*-toluidine (64.3 mg, 0.6 mmol) gave the title compound **d11** as a colorless solid (117.8 mg, 97% yield).

^{1}H NMR (400.1 MHz, $CDCl_3$) δ 7.25 (d, *J* = 8.8 Hz, 2H), 6.99 (d, *J* = 7.9 Hz, 2H), 6.73 (d, *J* = 8.2 Hz, 2H), 6.58 (d, *J* = 8.0 Hz, 2H), 4.19 (s, 2H), 3.76 (br, 1H), 2.94 (s, 6H), 2.25 (s, 3H).

^{13}C{^{1}H} NMR (100.6 MHz, $CDCl_3$) δ 150.1, 146.4, 129.8, 128.8, 127.5, 126.6, 113.1, 112.9, 48.4, 40.9, 20.5.

Ethyl 4-((phenylamino)methyl)benzoate (d12)

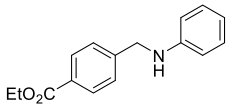

Following the general procedure at 80 °C for 48 h, methyl 4-formylbenzoate (82.1 mg, 0.5 mmol) and aniline (54.8 µL, 0.6 mmol) gave the title compound **d12** as a pale yellow liquid (117.4 mg, 92% yield).

^{1}H NMR (400.1 MHz, $CDCl_3$) δ 8.02 (d, *J* = 8.2 Hz, 1H), 7.44 (d, *J* = 8.1 Hz, 2H), 7.17 (t, *J* = 7.9 Hz, 2H), 6.73 (t, *J* = 7.3 Hz, 1H), 6.61 (d, *J* = 8.1 Hz, 2H), 4.41 – 4.34 (m, 5H, *N*-CH_2+CH_2+NH), 1.39 (t, *J* = 7.1 Hz, 3H).

^{13}C{^{1}H} NMR (100.6 MHz, $CDCl_3$) δ 166.6, 147.9, 145.0, 130.0, 129.4, 127.2, 118.0, 113.0, 61.1, 48.1, 14.5.

GC-MS, m/z(%) = 255 ([M]+, 100), 226(24), 210(28), 182(49), 163(100), 135(60), 106(51), 89(34), 77(40), 65(10), 51(8).

***N*-(4-(((4-methoxyphenyl)amino)methyl)phenyl)acetamide[2] (d13)**

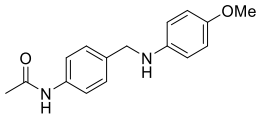

Following the general procedure at 100 °C for 48 h, *N*-(4-formylphenyl)acetamide (81.6 mg, 0.5 mmol) and 4-methoxyaniline (73.9, 0.6 mmol) gave the title compound **d13** as a pale yellow solid (128.4 mg, 95% yield).

^{1}H NMR (400.1 MHz, $CDCl_3$) δ 7.45 (d, *J* = 8.3 Hz, 2H), 7.31 (d, *J* = 8.2 Hz, 2H), 6.77 (d, *J* = 8.9 Hz, 2H), 6.59 (d, *J* = 8.9 Hz, 2H), 4.24 (s, 2H), 3.74 (s, 3H), 2.16 (s, 3H), 1.67 (br, 1H).

^{13}C{^{1}H} NMR (100.6 MHz, $CDCl_3$) δ 168.4, 152.3, 142.5, 137.0, 135.8, 128.3, 120.3, 115.0, 114.3, 56.0, 48.9, 24.7.

***N*-(4-(1-(phenylimino)ethyl)benzyl)aniline (d14)**

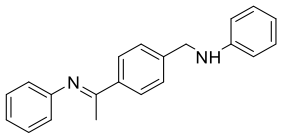

Following the general procedure at 80 °C for 36 h, 4-acetylbenzaldehyde (74.1 mg, 0.5 mmol) and aniline (100.4 µL, 1.1 mmol) gave the title compound **d14** as a dark brown liquid (132.2 mg, 88% yield, 95% purity).

^{1}H NMR (400.1 MHz, $CDCl_3$) δ 7.96 (d, *J* = 8.3 Hz, 2H), 7.45 (d, *J* = 8.1 Hz, 2H), 7.36 (t, *J* = 7.8 Hz, 2H), 7.18 (t, *J* = 7.3 Hz, 2H), 7.09 (t, *J* = 7.3 Hz, 1H), 6.80 (d, *J* = 7.3 Hz, 2H), 6.74 (t, *J* = 7.3 Hz, 1H), 6.64 (d, *J* = 7.8 Hz, 2H), 4.41 (s, 2H), 4.12 (br, 1H), 2.23 (s, 3H).

^{13}C{^{1}H} NMR (100.6 MHz, $CDCl_3$) δ 165.3, 151.8, 148.1, 142.3, 138.7, 129.4, 129.1, 127.7, 127.4, 123.3, 119.5, 117.9, 113.1, 48.1, 17.5.

GC-MS, m/z(%) = 300 ([M]+, 100), 285(23), 208(68), 193(33), 143(17), 116(15), 105(88), 90(30), 77(55), 51(14)

1-(4-((Phenylamino)methyl)phenyl)ethan-1-one[8] (d15)

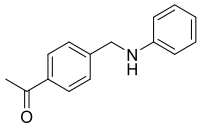

Following the general procedure at 50 °C for 18 h, 4-acetylbenzaldehyde (74.1 mg, 0.5 mmol) and aniline (54.8 µL, 0.6 mmol) gave the title compound **d15** as a pale yellow solid (82.2 mg, 73% yield).

^{1}H NMR (400.1 MHz, $CDCl_3$) δ 7.93 (d, *J* = 8.2 Hz, 2H), 7.47 (d, *J* = 8.2 Hz, 2H), 7.17 (dd, *J* = 8.6, 7.2 Hz, 2H), 6.73 (t, *J* = 7.3 Hz, 1H), 6.61 (d, *J* = 7.7 Hz, 2H), 4.42 (s, 2H), 4.19 (s, br, 1H), 2.59 (s, 3H).

^{13}C{^{1}H} NMR (100.6 MHz, $CDCl_3$) δ 197.9, 147.8, 145.3, 136.3, 129.4, 128.9, 127.4, 118.0, 113.1, 48.1, 26.7.

1-(4-(Benzylamino)phenyl)ethan-1-one[9] (d16)

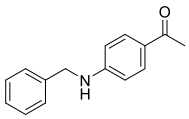

Following the general procedure at 50 °C for 18 h, benzaldehyde (51.0 µL, 0.5 mmol) and 4-amino acetophenone (67.6 mg, 0.5 mmol) gave the title compound **d16** as a pale yellow solid (108.1 mg, 96% yield).

^{1}H NMR (400.1 MHz, $CDCl_3$) δ 7.82 (d, *J* = 8.6 Hz, 2H), 7.38 – 7.30 (m, 5H), 6.60 (d, *J* = 8.6 Hz, 2H), 4.58 (br, 1H), 4.41 (d, *J* = 5.5 Hz, 2H), 2.49 (s, 3H).

^{13}C{^{1}H} NMR (100.6 MHz, $CDCl_3$) δ 196.5, 152.1, 138.4, 130.9, 128.9, 127.6, 127.4, 127.0, 111.7, 47.6, 26.1.

_N_-(ferrocenylmethyl)-4-methylaniline[7] (d17)

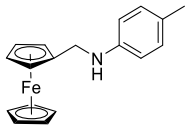

Following the general procedure at 80 °C for 48 h, ferrocenecarboxaldehyde (107.0 mg, 0.5 mmol) and *p*-toluidine (64.3 mg, 0.6 mmol) gave the title compound **d17** as a dark brown liquid (149.5 mg, 98% yield).

^{1}H NMR (400.1 MHz, $CDCl_3$) δ 7.02 (d, *J* = 8.1 Hz, 2H), 6.60 (d, *J* = 8.3 Hz, 2H), 4.24 (t, *J* = 1.9 Hz, 2H), 4.18 (s, 5H), 4.14 (t, *J* = 1.8 Hz, 2H), 3.94 (s, 2H), 3.75 (br, 1H), 2.26 (s, 3H).

^{13}C{^{1}H} NMR (100.6 MHz, $CDCl_3$) δ 146.3, 129.9, 126.9, 113.2, 86.9, 68.6, 68.2, 68.0, 43.9, 20.6.

4-Methoxy-_N_-((1-methyl-1H-pyrrol-2-yl)methyl)aniline[7] (d18)

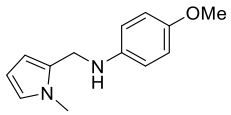

Following the general procedure at 100 °C for 48 h, 1-methyl-1*H*-pyrrole-2-carbaldehyde (53.7 µL, 0.5 mmol) and 4-methoxyaniline (73.9 mg, 0.6 mmol) gave the title compound **d18** as a dark brown liquid (104.9 mg, 97% yield).

^{1}H NMR (400.1 MHz, $CDCl_3$) δ 6.84 – 6.79 (m, 2H), 6.67 – 6.66 (m, 2H), 6.63 – 6.62 (m, 1H), 6.12 – 6.11 (m, 1H), 6.08 (t, *J* = 3.1 Hz, 1H), 4.17 (s, 2H), 3.76 (s, 3H), 3.64 (s, 3H), 3.41 (br, 1H).

^{13}C{^{1}H} NMR (100.6 MHz, $CDCl_3$) δ 152.5, 142.6, 130.1, 122.9, 115.1, 114.4, 108.5, 106.9, 56.0, 41.5, 33.9.

4-Methoxy-_N_-((5-methylfuran-2-yl)methyl)aniline[7] (d19)

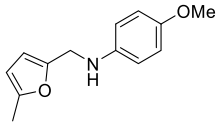

Following the general procedure at 100 °C for 48 h, 5-methylfuran-2-carbaldehyde (50.1 µL, 0.5 mmol) and 4-methoxyaniline (73.9 mg, 0.6 mmol) gave the title compound **d19** as a brown solid (97.8 mg, 90% yield).

^{1}H NMR (400.1 MHz, $CDCl_3$) δ 6.79 (d, *J* = 8.9 Hz, 2H), 6.65 (d, *J* = 8.8 Hz, 2H), 6.09 (d, *J* = 3.0 Hz, 1H), 5.98 (d, *J* = 2.5 Hz, 1H), 4.21 (s, 2H), 3.75 (s, 4H, OCH_3+NH), 2.28 (s, 3H).

^{13}C{^{1}H} NMR (100.6 MHz, $CDCl_3$) δ 152.7, 151.7, 151.2, 142.1, 115.0, 114.8, 107.9, 106.2, 55.9, 42.7, 13.7.

***N*-(pyridin-2-ylmethyl)aniline[3] (d20)**

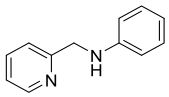

Following the general procedure at 80 °C for 36 h, pyridine-2-carboxaldehyde (47.6 µL, 0.5 mmol) and aniline (54.8 µL, 0.6 mmol) gave the title compound **d20** as a brown liquid (62.6 mg, 68% yield, 90% purity by ^{1}H NMR).

^{1}H NMR (400.1 MHz, $CDCl_3$) δ 8.59 (d, *J* = 4.8 Hz, 1H), 7.63 (td, *J* = 7.7, 1.8 Hz, 1H), 7.34 (d, *J* = 7.8 Hz, 1H), 7.21 – 7.16 (m, 3H), 6.73 (tt, *J* = 7.4, 1.1 Hz, 1H), 6.69 – 6.66 (m, 2H), 4.84 (br, 1H), 4.47 (s, 2H).

^{13}C{^{1}H} NMR (100.6 MHz, $CDCl_3$) δ 158.6, 149.2, 147.9, 136.7, 129.3, 122.2, 121.7, 117.6, 113.1, 49.3.

***N*-benzylpyridin-2-amine[5] (d21)**

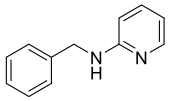

Following the general procedure at 80 °C for 48 h, benzaldehyde (51.0 µL, 0.5 mmol) and 2-aninopyridine (56.5 mg, 0.6 mmol) gave the title compound **d21** as a colorless solid (50.7 mg, 55% yield).

^{1}H NMR (400.1 MHz, $CDCl_3$) δ 8.12 (ddd, *J* = 5.0, 2.0, 0.9 Hz, 1H), 7.44 – 7.34 (m, 5H), 7.32-7.28 (m, 1H), 6.61 (ddd, *J* = 7.1, 5.0, 0.9 Hz, 1H), 6.39 (dt, *J* = 8.3, 1.0 Hz, 1H), 5.05 (s, 1H), 4.53 (d, *J* = 5.8 Hz, 2H).

^{13}C{^{1}H} NMR (100.6 MHz, $CDCl_3$) δ 158.8, 148.3, 139.3, 137.6, 128.7, 127.5, 127.3, 113.2, 106.9, 46.4.

2-(Benzylamino)thiophene-3-carbonitrile (d22)

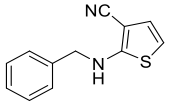

Following the general procedure at 80 °C for 48 h, benzaldehyde (51.0 µL, 0.5 mmol) and 2-aminothiophene-3-carbonitrile (74.5 mg, 0.6 mmol) gave the title compound **d22** as a dark green solid (96.4 mg, 90% yield).

^{1}H NMR (400.1 MHz, $CDCl_3$) δ 7.41 – 7.30 (m, 5H), 6.78 (d, *J* = 5.7 Hz, 1H), 6.29 (d, *J* = 5.7 Hz, 1H), 5.57 (br, 1H), 4.41 (s, 2H).

^{13}C{^{1}H} NMR (100.6 MHz, $CDCl_3$) δ 165.3, 136.6, 128.9, 128.2, 127.8, 126.1, 116.4, 108.7, 84.5, 51.8.

GC-MS, m/z(%) = 214 ([M]+, 19), 91(100), 65(15).

***N*-benzyl-5-methylthiazol-2-amine[10] (d23)**

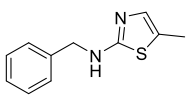

Following the general procedure at 80 °C for 48 h, benzaldehyde (51.0 µL, 0.5 mmol) and 5-methylthiazol-2-amine (68.5 mg, 0.6 mmol) gave the title compound **d23** as a colorless solid (94.0 mg, 92% yield, 95% purity).

^{1}H NMR (400.1 MHz, $CDCl_3$) δ 7.38 – 7.26 (m, 5H), 6.65 (s, 1H), 6.28 (br, 1H), 4.42 (s, 2H), 2.26 (s, 3H).

$^{13}C\{^{1}H\}$ NMR (100.6 MHz, $CDCl_3$) δ 169.2, 138.0, 135.3, 128.7, 127.74, 127.66, 121.0, 49.9, 12.1.

_N_-(4-bromobenzyl)benzenesulfonamide (d24)

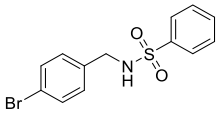

Following the general procedure at 80 °C for 48 h, 4-bromobenzaldehyde (92.5 mg, 0.5 mmol) and benzenesulfonamide (94.3 mg, 0.6 mmol) gave the title compound **d24** as a white solid (151.7 mg, 93% yield, 90% purity).

^{1}H NMR (400.1 MHz, $CDCl_3$) δ 7.81 (d, *J* = 7.6 Hz, 2H), 7.57 (t, *J* = 7.4 Hz, 1H), 7.47 (t, *J* = 7.7 Hz, 2H), 7.34 (d, *J* = 8.3 Hz, 2H), 7.04 (d, *J* = 8.2 Hz, 2H), 5.43 (t, *J* = 6.4 Hz, 1H), 4.06 (d, *J* = 5.8 Hz, 2H).

$^{13}C\{^{1}H\}$ NMR (100.6 MHz, $CDCl_3$) δ 139.9, 135.5, 132.9, 131.9, 129.6, 129.3, 127.2, 121.9, 46.7.

GC-MS, m/z(%) = 325 ([M]+, 0.5), 246(0.5), 184(100), 157(10), 143(20), 125(11), 104(10), 90(13), 77(91), 51(31).

Dibenzylamine[2] (d25)

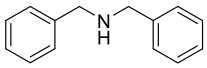

Following the general procedure at 100 °C for 48 h, benzaldehyde (51.0 µL, 0.5 mmol) and benzylamine (65.5 µL, 0.6 mmol) gave the title compound **d25** as a pale yellow liquid (88.8 mg, 90% yield).

^{1}H NMR (400.1 MHz, $CDCl_3$) δ 7.38 – 7.26 (m, 10H), 3.84 (s, 4H), 1.91 (br, 1H).

$^{13}C\{^{1}H\}$ NMR (100.6 MHz, $CDCl_3$) δ 140.4, 128.5, 128.3, 127.1, 53.3.

_N_-benzyldodecan-1-amine[11] (d26)

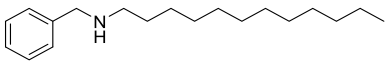

Following the general procedure at 80 °C for 18 h, benzaldehyde (51.0 µL, 0.5 mmol) and dodecylamine (111.2 mg, 0.6 mmol) gave the title compound **d26** as a pale yellow liquid (130.9 mg, 95% yield).

^{1}H NMR (400.1 MHz, $CDCl_3$) δ 7.37 – 7.22 (m, 5H), 3.79 (s, 2H), 2.63 (t, *J* = 7.0 Hz, 2H), 1.58 -1.47 (m, 2H), 1.35 –1.26 (m, 20H), 0.88 (t, *J* = 6.8 Hz, 3H).

$^{13}C\{^{1}H\}$ NMR (100.6 MHz, $CDCl_3$) δ 140.7, 128.5, 128.3, 127.0, 54.2, 49.7, 32.1, 30.3, 29.81, 29.79, 29.76, 29.72, 29.5, 27.5, 22.8, 14.3.

***N*-benzylcyclohexanamine[12] (d27)**

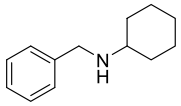

Following the general procedure at 80 °C for 48 h, benzaldehyde (51.0 µL, 0.5 mmol) and cyclohexanamine (68.8 µL, 0.6 mmol) gave the title compound **d27** as a pale yellow liquid (89.0 mg, 94% yield).

^{1}H NMR (400.1 MHz, $CDCl_3$) δ 7.35 – 7.22 (m, 5H), 3.82 (s, 2H), 2.52 – 2.47 (m, 1H), 1.93 – 1.91 (m, 2H), 1.76 – 1.71 (m, 2H), 1.64 – 1.59 (m, 1H), 1.42 (br, 1H), 1.31 – 1.08 (m, 5H).

^{13}C{^{1}H} NMR (100.6 MHz, $CDCl_3$) δ 141.1, 128.5, 128.2, 126.9, 56.3, 51.2, 33.7, 26.3, 25.2.

Tribenzylamine[13] (d28)

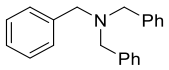

Following the general procedure at 80 °C for 36 h, benzaldehyde (51.0 µL, 0.5 mmol) and dibenzylamine (116.1 µL, 0.6 mmol) gave the title compound **d28** as a pale yellow solid (138.0 mg, 96% yield).

^{1}H NMR (400.1 MHz, $CDCl_3$) δ 7.47 (d, *J* = 7.5 Hz, 6H), 7.37 (t, *J* = 7.4 Hz, 6H), 7.29 (d, *J* = 7.2 Hz, 3H), 3.62 (s, 6H).

^{13}C{^{1}H} NMR (100.6 MHz, $CDCl_3$) δ 139.8, 128.9, 128.3, 127.0, 58.1.

***N*-benzyl-*N*-ethylethanamine[14] (d29)**

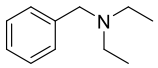

Following the general procedure at 80 °C for 36 h, benzaldehyde (51.0 µL, 0.5 mmol) and diethylamine (61.8 µL, 0.6 mmol) gave the title compound **d29** as a pale yellow liquid (76.7 mg, 94% yield).

^{1}H NMR (400.1 MHz, $CDCl_3$) δ 7.38 – 7.21 (m, 5H), 3.57 (s, 2H), 2.52 (q, *J* = 7.1 Hz, 4H), 1.04 (t, *J* = 7.1 Hz, 6H).

^{13}C{^{1}H} NMR (100.6 MHz, $CDCl_3$) δ 138.8, 129.3, 128.3, 127.1, 57.2, 46.5, 11.4.

1-Benzylpiperidine[13] (d30)

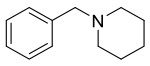

Following the general procedure at 80 °C for 36 h, benzaldehyde (51.0 µL, 0.5 mmol) and piperidine (59.3 µL, 0.6 mmol) gave the title compound **d30** as a pale yellow liquid (81.5 mg, 93% yield).

^{1}H NMR (400.1 MHz, $CDCl_3$) δ 7.39 – 7.28 (m, 5H), 3.53 (s, 2H), 2.50 – 2.41 (m, 4H), 1.63 – 1.57 (m, 4H), 1.45 – 1.43 (m, 2H).

^{13}C{^{1}H} NMR (100.6 MHz, $CDCl_3$) δ 138.0, 129.6, 128.3, 127.2, 63.7, 54.4, 25.9, 24.4.

_N_,_N_'-dibenzylethane-1,2-diamine[15] (d31)

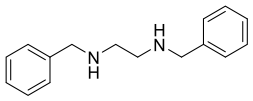

Following the general procedure at 100 °C for 48 h, benzaldehyde (122.4 µL, 1.2 mmol) and ethane-1,2-diamine (33.5 µL, 0.5 mmol) gave the title compound **d31** as a pale yellow solid (114.2 mg, 95% yield).

^{1}H NMR (400.1 MHz, $CDCl_3$) δ 7.37-7.25 (m, 10H), 3.81 (s, 4H), 2.79 (s, 4H), 1.86 (s, 2H, NH).

^{13}C{^{1}H} NMR (100.6 MHz, $CDCl_3$) δ 140.5, 128.5, 128.2, 127.0, 54.0, 48.8.

2-(Benzylamino)ethan-1-ol[16] (d32)

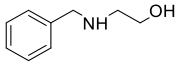

Following the general procedure at 100 °C for 24 h, benzaldehyde (51.0 µL, 0.5 mmol) and 2-aminoethan-1-ol (30.0 µL, 0.5 mmol) gave the title compound **d32** as a pale yellow liquid (65.0 mg, 86% yield).

^{1}H NMR (400.1 MHz, $CDCl_3$) δ 7.35 – 7.23 (m, 5H), 3.81 (s, 2H), 3.65 (t, *J* = 5.2 Hz, 2H), 2.80 (t, *J* = 5.2 Hz, 2H), 2.07 (br, 2H, NH + OH + H_2O).

^{13}C{^{1}H} NMR (100.6 MHz, $CDCl_3$) δ 140.1, 128.6, 128.3, 127.2, 61.1, 53.6, 50.7.

3-(Benzylamino)propan-1-ol (d33)

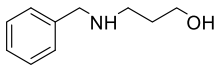

Following the general procedure at 100 °C for 24 h, benzaldehyde (51.0 µL, 0.5 mmol) and 3-aminopropan-1-ol (38.2 µL, 0.5 mmol) gave the title compound **d33** as a colorless liquid (68.6 mg, 83% yield).

^{1}H NMR (400.1 MHz, $CDCl_3$) δ = 7.35 – 7.23 (m, 5H), 3.81 (t, *J* = 5.2, 2H), 3.79 (s, 2H), 2.89 (t, *J* = 5.8 Hz, 2H), 2.81 (br, 2H), 1.72 (quint., *J* = 5.5 Hz, 2H).

^{13}C{^{1}H} NMR (100.6 MHz, $CDCl_3$) δ = 139.7, 128.6, 128.3, 127.3, 64.4, 54.1, 49.5, 30.9.

GC-MS, m/z(%) = 165([M]+, 2), 120(50), 106(19), 91(100), 77(3), 65(9).

(*R*)-2-(Benzylamino)butan-1-ol[17] (d34)

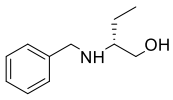

Following the general procedure at 100 °C for 18 h, benzaldehyde (51.0 µL, 0.5 mmol) and (*R*)-2-amino-1-butanol (CAS: 5856-63-3, 47.5 µL, 0.5 mmol) gave the title compound **d34** as a white solid (86.9 mg, 97% yield).

^{1}H NMR (400.1 MHz, $CDCl_3$) δ 7.37 – 7.24 (m, 5H), 3.91 – 3.79 (m, 2H), 3.67 – 3.65 (m, 1H), 3.34 (br, 1H), 2.64 (br, 1H), 1.56 – 1.42 (m, 2H), 0.93 (t, *J* = 6.8, 3H).

^{13}C{^{1}H} NMR (100.6 MHz, $CDCl_3$) δ 140.5, 128.6, 128.2, 127.2, 62.7, 59.8, 51.2, 24.5, 10.5.

$[\alpha]_D^{20}$= -30.61 (*C* 0.5, CH_2Cl_2).

Ethyl (*R*)-2-(benzylamino)-2-phenylacetate[18] (d35)

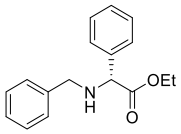

(*R*)-2-Phenylglycinemethyl ester hydrochloride (CAS: 19883-41-1, 121.0 mg, 0.6 mmol) was added into an Et_3N (111.5 µL, 0.8 mmol) solution in THF (5.0 mL) and stirred for 2 h. The solution was filtered through celite then washed with ethyl acetate (3×2.0 mL). The filtrate was evaporated to dryness to afford (*R*)-2-phenylglycinemethyl ester, which was used for the following step without further purification.

Following the general procedure with **C^{3A}.2** (5 mol%) and *t*BuOK (10 mol%) at 100 °C for 18 h, benzaldehyde (51.0 µL, 0.5 mmol) and the freshly prepared (*R*)-2-phenylglycinemethyl gave the title compound **d35** as a pale yellow liquid (121.2 mg, 90% yield).

^{1}H NMR (400.1 MHz, $CDCl_3$) δ 7.41 – 7.24 (m, 10H), 4.39 (s, 1H), 4.24 – 4.09 (m, 2H), 3.75 (s, 2H), 1.21 (t, *J* = 7.0 Hz, 3H).

^{13}C{^{1}H} NMR (100.6 MHz, $CDCl_3$) δ 173.1, 139.6, 138.3, 128.7, 128.5, 128.4, 128.1, 127.6, 127.2, 64.5, 61.2, 51.5, 14.2.

$[\alpha]_D^{20}$= -4.98 (*C* 1.2, CH_2Cl_2)

Ethyl benzyl-L-alaninate[19] (d36)

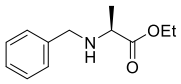

L-Alanine ethyl ester hydrochloride (CAS: 1115-59-9, 92.2 mg, 0.6 mmol) was added into an Et_3N (111.5 µL, 0.8 mmol) solution in THF (5.0 mL) and stirred for 2 h. The solution was filtered through celite then washed with ethyl acetate (3×2.0 mL mL). The filtrate was evaporated to dryness to afford L-alanine ethyl ester, which was used for the following step without further purification.

Following the general procedure with **C^{3A}.2** (5 mol%) and *t*BuOK (10 mol%) at 100 °C for 36 h, benzaldehyde (51.0 µL, 0.5 mmol) and the freshly prepared L-alanine ethyl ester gave the title compound **d36** as a pale yellow liquid (94.3 mg, 91% yield).

^{1}H NMR (400.1 MHz, $CDCl_3$) δ = 7.34– 7.22 (m, 5H), 4.19 (q, *J* = 7.1, 2H), 3.83 – 3.66 (m, 2H), 3.40 – 3.38 (m, 1H), 2.10 (br, 1H), 1.32 (d, *J* = 6.3, 3H), 1.29 (t, *J* = 7.0, 4H).

^{13}C{^{1}H} NMR (100.6 MHz, $CDCl_3$) δ = 175.9, 139.7, 128.5, 128.4, 127.2, 60.8, 56.0, 52.2, 19.2, 14.4.

$[\alpha]_D^{20}$= + 3.17 (*C* 0.9, CH_2Cl_2)

***N*-butyldodecan-1-amine (d37)**

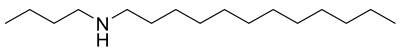

Following the general procedure at 50 °C for 48 h, butyraldehyde (45.1 µL, 0.5 mmol) and dodecylamine (111.2 mg, 0.6 mmol) gave the title compound **d37** as a yellow-green liquid (115.9 mg, 96% yield). This compound was further purified by bulb to bulb distillation.

^{1}H NMR (400.1 MHz, $CDCl_3$) δ 2.59 (m, 4H), 1.70 – 1.12 (m, 25H), 0.93 – 0.86 (m, 6H).

$^{13}C\{^{1}H\}$ NMR (100.6 MHz, $CDCl_3$) δ 50.3, 49.9, 32.4, 32.1, 30.2, 29.82, 29.79, 29.77, 29.74, 29.5, 27.6, 22.8, 20.7, 14.27, 14.18.

GC-MS, m/z(%) = 241 ([M]+, 25), 198(100), 184(9), 142(9), 87(100), 70(11), 57(27).

***N*-(Bicyclo[2.2.1]hept-5-en-2-ylmethyl)aniline (d38)**

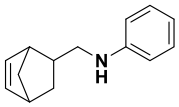

Following the general procedure at 50 °C for 48 h, 5-norbornene-2-carboxaldehyde (52.6 µL, 0.5 mmol) and aniline (54.8 µL, 0.6 mmol) gave the title compound **d38** as mixture of *endo*/*exo* isomers as a brown liquid (94.7mg, 95% yield).

M = Major isomer *endo*, *m* = minor isomer *exo*, ratio *M*:*m* = 60:40

^{1}H NMR (400.1 MHz, $CDCl_3$) δ 7.20-7.16 (m, 2H, *M* + *m*, C*H*$_{Ar}$), 6.75 – 6.66 (m, 1H, *M* + *m*, C*H*$_{Ar}$), 6.64 – 6.58 (m, 2H, C*H*$_{Ar}$), 6.19 (dd, *J* = 5.7, 3.0 Hz, 1H, *M*, C*H*=CH), 6.15 – 6.02 (m, 2H, *m*, C*H*=CH), 5.97 (dd, *J* = 5.8, 2.9 Hz, 1H, *M*, C*H*=CH), 3.18 (dd, *J* = 11.9, 6.9 Hz, 1H, *m*, C*H*$_2$N), 3.09 (dd, *J* = 11.9, 8.3 Hz, 1H, *m*, C*H*$_2$N), 2.92 (br s, 1H, *M*, CH), 2.90 – 2.76 (m, 4H, *M*, C*H*$_2$N +C*H*, m, C*H*), 2.73 (br s, 1H, *m*, C*H*), 2.36 (m, 1H, *M*, C*H*), 1.92 (ddd, *J* = 11.5, 9.1, 3.9 Hz, 1H, *M*, C*H*$_2$), 1.76 – 1.64 (m, 1H, *m*, C*H*), 1.47 (dd, *J* = 8.2, 2.2 Hz, 1H, *M*, C*H*$_2$), 1.44 – 1.33 (m, 3H, *m*, C*H*$_2$), 1.28 (dt, *J* = 8.3, 1.6 Hz, 1H, *M*, C*H*$_2$), 1.23 (dt, *J* = 11.6, 3.8 Hz, 1H, *m*, C*H*$_2$), 0.64 (ddd, *J* = 11.5, 4.4, 2.6 Hz, 1H, *M*, C*H*$_2$).

$^{13}C\{^{1}H\}$ NMR (100.6 MHz, $CDCl_3$) δ 148.69 (C$_{qAr}$, *M*), 148.63 (C$_{qAr}$, *m*), 137.76 (*M*, *C*H=CH), 136.91 (*m*, *C*H=CH), 136.56 (*m*, *C*H=CH), 132.19 (*M*, *C*H=CH), 129.37 (*m*, *C*H$_{Ar}$), 129.34 (*M*, *C*H$_{Ar}$), 117.24 (*m*, *CHAr*), 117.20 (*M*, *C*H$_{Ar}$), 112.83 (*M*, *C*H$_{Ar}$), 112.78 (*m*, *C*H$_{Ar}$), 49.72 (*m*, *C*H$_2$), 49.70 (*M*, *C*H$_2$), 48.33 (*M*, *C*H$_2$), 45.39 (*m*, *C*H$_2$), 44.63 (*m*, *C*H), 44.38 (*M*, *C*H), 42.53 (*M*, *C*H), 41.83 (*m*, *C*H), 39.14 (*m*, *C*H), 38.87 (*M*, *C*H), 31.41 (*m*, *C*H$_2$), 30.59 (*M*, *C*H$_2$).

GC-MS, m/z(%) = 199([M]+, 47), 158(12), 132(88), 106(100), 91(13), 77(42), 65(13), 51(13)

***N*-(2,6-Dimethylhept-5-en-1-yl)aniline (d39)**

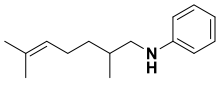

Following the general procedure at 50 °C for 36 h, 2,6-dimethyl-5-heptenal (84.2 µL, 0.5 mmol) and aniline (54.8 µL, 0.6 mmol) gave the title compound **d39** as a brown liquid (104.3 mg, 96% yield).

^{1}H NMR (400.1 MHz, $CDCl_3$) δ 7.17 (td, *J* = 7.4, 1.8 Hz, 2H), 6.68 (tt, *J* = 7.3, 1.1 Hz, 1H), 6.60 (dd, *J* = 8.6, 1.1 Hz, 2H), 5.11 (m , 1H), 3.70 (br, 1H), 3.06 (dd, *J* = 12.2, 5.9 Hz, 1H), 2.89 (dd, *J* = 12.2, 7.3 Hz, 1H), 2.14 – 1.94 (m, 2H), 1.82 – 1.72 (m, 1H), 1.69 (s, 3H), 1.62 (s, 3H), 1.54 – 1.42 (m, 1H), 1.32 – 1.08 (m, 1H), 0.99 (d, *J* = 6.7, 3H).

$^{13}C\{^{1}H\}$ NMR (100.6 MHz, $CDCl_3$) δ 148.77, 131.71, 129.35, 124.64, 117.07, 112.77, 50.40, 35.02, 32.70, 25.87, 25.59, 18.17, 17.85.

GC-MS, m/z(%) = 217([M]+, 60), 146(100), 133(10), 106(95), 93(20), 77(35), 69(9), 51(9).

***N*-(3-phenylpropyl)aniline[20] (d40)**

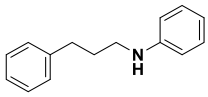

Following the general procedure with **C^{3A}.2** (5 mol%) and *t*BuOK (10 mol%) at 100 °C for 48 h, cinnamaldehyde (62.9 µL, 0.5 mmol) and aniline (54.8 µL, 0.6 mmol) gave the title compound **d40** as pale yellow liquid (98.3 mg, 93% yield).

^{1}H NMR (400.1 MHz, $CDCl_3$) δ 7.36 – 7.11 (m, 7H), 6.70 (t, *J* = 7.3 Hz, 1H), 6.59 (d, *J* = 7.9 Hz, 2H), 3.62 (s, 1H), 3.16 (t, *J* = 7.0 Hz, 2H), 2.75 (t, *J* = 7.5 Hz, 2H), 1.97 (p, *J* = 7.2 Hz, 2H).

$^{13}C\{^{1}H\}$ NMR (100.6 MHz, $CDCl_3$) δ 148.5, 141.8, 129.4, 128.6, 128.5, 126.1, 117.3, 112.9, 43.6, 33.5, 31.2.

Supplementary tables

Table S6. Hydrogenation of benzylideneaniline: control experiments.[a]

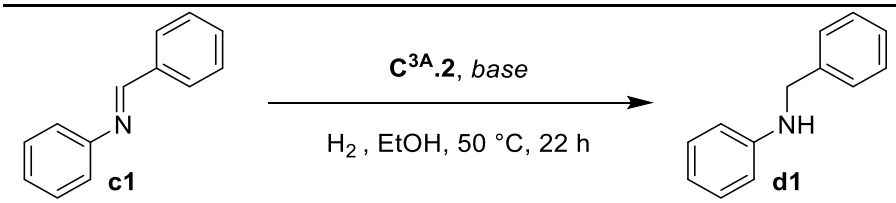

Entry	Catalyst (mol%)	Base (mol%)	H_2 (bar)	Yield (%)
1	-	*t*BuOK (5)	50	< 1
2	2 (2)	-	50	3
3	2 (2)	*t*BuOK (5)	25	87

[a] Conditions: An autoclave was charged in a glovebox with, in this order, **c1** (90.6 mg, 0.5 mmol), anhydrous ethanol (2.0 mL), **C^{3A}.2** (5.0 mg, 2.0 mol%), *t*BuOK (2.8 mg, 5 mol%), and then pressurized with H_2 (50 or 25 bar) and heated at 50 °C. Yield determined by GC and 1H NMR spectroscopy.

Table S7. Hydrogenation of ketimine.

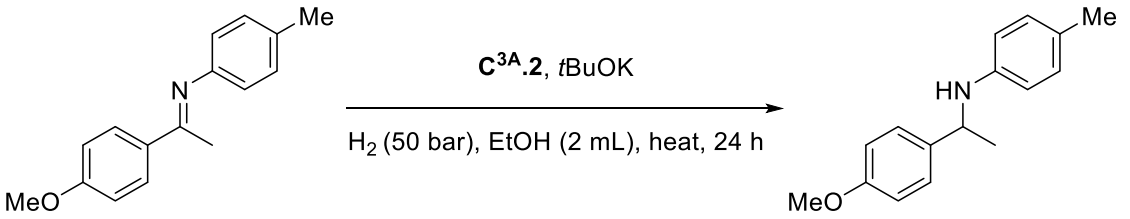

Entry[a]	2 (mol%)	*t*BuOK (mol%)	Temp. (°C)	Yield (%)
1	2	5	50	<1
2	5	10	100	<1

[a] Conditions: an autoclave was charged in a glovebox with, in this order, ketimine (119.7 mg, 0.5 mmol), anhydrous ethanol (2.0 mL), **C^{3A}.2** (2.0 or 5.0 mol%), *t*BuOK (5 or 10 mol%), pressurized with H_2 (50 bar), then heated at the indicated temperature.

References

[1] D. Wei, A. Bruneau-Voisine, T. Chauvin, V. Dorcet, T. Roisnel, D. Valyaev, N. Lugan and J.-B. Sortais, *Adv. Synth. Catal.*, **2018**, *360*, 676-681.

[2] J. Zheng, T. Roisnel, C. Darcel and J. B. Sortais, *ChemCatChem*, **2013**, *5*, 2861-2864.

[3] M. Zhang, H. Yang, Y. Zhang, C. Zhu, W. Li, Y. Cheng and H. Hu, *Chem. Commun.*, **2011**, *47*, 6605-6607.

[4] P. Liu, R. Liang, L. Lu, Z. Yu and F. Li, *J. Org. Chem.*, **2017**, *82*, 1943-1950.

[5] D. B. Bagal, R. A. Watile, M. V. Khedkar, K. P. Dhake and B. M. Bhanage, *Catal. Sci. Technol.*, **2012**, *2*, 354-358.

[6] M. Yang and F. Liu, *J. Org. Chem.*, **2007**, *72*, 8969-8971.

[7] L. P. Bheeter, M. Henrion, M. J. Chetcuti, C. Darcel, V. Ritleng and J.-B. Sortais, *Catal. Sci. Technol.*, **2013**, *3*, 3111-3116.

[8] R. Cano, M. Yus and D. J. Ramón, *Tetrahedron*, **2011**, *67*, 8079-8085.

[9] C. T. Yang, Y. Fu, Y. B. Huang, J. Yi, Q. X. Guo and L. Liu, *Angew. Chem.*, **2009**, *121*, 7534-7537.

[10] R. Cano, D. J. Ramon and M. Yus, *J. Org. Chem.*, **2011**, *76*, 5547-5557.

[11] P. R. Likhar, R. Arundhathi, M. L. Kantam and P. S. Prathima, *Eur. J. Org. Chem.*, **2009**, 5383-5389.

[12] L. C. M. Castro, J.-B. Sortais and C. Darcel, *Chem. Commun.*, **2012**, *48*, 151-153.

[13] T. Dombray, C. Helleu, C. Darcel and J. B. Sortais, *Adv. Synth. Catal.*, **2013**, *355*, 3358-3362.

[14] L. Blackburn and R. J. K. Taylor, *Org. Lett.*, **2001**, *3*, 1637-1639.

[15] S. Lateef, S. Reddy Krishna Mohan and S. Reddy Jayarama Reddy, *Tetrahedron Lett.*, **2007**, *48*, 77-80.

[16] M. Largeron and M.-B. Fleury, *Org. Lett.*, **2009**, *11*, 883-886.

[17] (a) Y. Turgut, N. Demirel and H. Hoşgören, *J. Incl. Phenom. Macrocycl. Chem.*, **2006**, *1*, 29-33; (b) H. Bräuner-Osborne, L. Bunch, N. Chopin, F. Couty, G. Evano, A. A. Jensen, M. Kusk, B. Nielsen and N. Rabasso, *Org. Biomol. Chem.*, **2005**, *3*, 3926-3936.

[18] Q.-H. Deng, H.-W. Xu, A. W.-H. Yuen, Z.-J. Xu and C.-M. Che, *Org. Lett.*, **2008**, *10*, 1529-1532.

[19] B. T. Cho and S. K. Kang, *Tetrahedron*, **2005**, *61*, 5725-5734.

[20] R. Kubiak, I. Prochnow and S. Doye, *Angew. Chem. Int. Ed.*, **2010**, *49*, 2626-2629.

B- I- Well-defined aminomethylpyridine manganese complexes

IR spectra were measured with a Shimadzu IR-Affinity 1 instrument.HR–MS spectra and microanalysis were carried out by the corresponding facilities at the CRMPO (Centre Régional de Mesures Physiques de l'Ouest), University of Rennes 1.

2-[(dimethylamino)methyl]pyridine[1] and complex **C^{3B}.4**[2] were prepared according to reported procedures.

Synthesis of manganese complexes

Complex **C^{3B}.1**

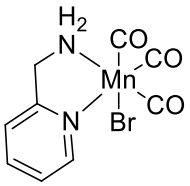

To a solution of 2-(aminomethyl)pyridine (0.73 mmol, 79 mg, 75 µL) in toluene (15 mL) was added 1 equivalent of manganese pentacarbonyl bromide (0.73 mmol, 200 mg). After stirring at 110 °C during 4 h, the toluene was evaporated under reduced pressure to afford a yellow solid. This solid was washed two times with pentane to give complex **C^{3B}.1**, as a yellow powder (227 mg, 95% yield). Suitable single crystals for X-Ray diffraction studies were obtained by evaporation of a saturated solution of the complex in diethyl ether.

^{1}H NMR (400 MHz, Acetone-d_6) δ 9.00 (br. d, *J* = 5.0 Hz, 1H), 7.92 (br. t, *J* = 6.1 Hz, 1H), 7.56 (br. d, *J* = 5.5 Hz, 1H), 7.49 (br. t, *J* = 5.5 Hz, 1H), 5.06 (br. s, 1H, NH), 4.67 (d, *J* = 14 Hz, 1H, CH_2), 4.37 (d, *J* = 14 Hz, 1H, CH_2), 3.59 (br. s, 1H, NH).

^{13}C{^{1}H}c NMR (101 MHz, Acetone-d_6) δ223.2 (br., CO), 162.3 (C_q), 153.7(CH_{py}), 139.0(CH_{py}), 124.9(CH_{py}), 121.9(CH_{py}), 51.5 (CH_2).

Anal.Calc (%). for ($C_9H_8BrMnN_2O_3$): C, 33.06; H, 2.47; N, 8.57. Found: C, 32.67; H, 2.62; N, 8.60.

IR (ν, cm^{-1}, CH_2Cl_2): 2029, 1936, 1911.

Complex **C^{3B}.2**

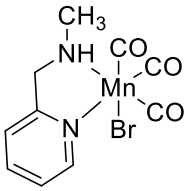

According to the same procedure, starting for 2-[(methylamino)methyl]pyridine(0.73 mmol, 89 mg, 90 µL), complex **C^{3B}.2** was obtained as a yellow solid (231 mg, 93% yield).

^{1}H NMR (400 MHz, Acetone-d_6) δ 8.96 (d, *J* = 5.0 Hz, 1H), 7.97 (t, *J* = 7.0 Hz, 1H), 7.60 (d, *J* = 7.4 Hz, 1H), 7.56 – 7.42 (t, *J* = 5.5 Hz, 1H), 4.67 (d, *J* = 12.0 Hz, 1H, CH_2), 4.24 – 4.13 (m, 1H, CH_2), 4.10 (br. s, 1H, NH), 3.03 (d, *J* = 4.4 Hz, 3H, CH_3).

^{13}C{^{1}H} NMR (101 MHz, Acetone-d_6) δ 161.0 (C_q), 154.4 (CH_{py}), 139.4 (CH_{py}), 125.5 (CH_{py}), 122.3 (CH_{py}), 61.9 (CH_2), 43.9 (CH_3). (CO signals were not detected)

Anal.Calc (%). for ($C_{10}H_{10}BrMnN_2O_3$): C, 35.22; H, 2.96; N, 8.21; Found: C, 35.49; H, 3.08; N,8.32.

IR (ν, cm^{-1}, CH_2Cl_2): 2029, 1936, 1911.

Complex **C^{3B}.3**

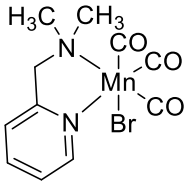

According to the same procedure, starting for 2-[(dimethylamino)methyl]pyridine (0.37 mmol, 50 mg), complex **C^{3B}.3** was obtained as an yellow solid (120 mg, 93% yield).

^{1}H NMR (400 MHz, Acetone-d_6) δ 9.01 (s, 1H), 7.97 (s, 1H), 7.55 (s, 2H), 4.77 (s, 1H), 3.69 (s, 1H), 3.03 (s, 3H), 2.85 (s, 3H).

^{13}C{^{1}H} NMR (101 MHz, Acetone-d_6) δ 223.1 (br.,CO), 161.4 (Cq), 153.6 (CH_{py}), 139.8 (CH_{py}), 125.1 (CH_{py}), 123.9 (CH_{py}), 69.0 (CH_2), 56.0 (CH_3), 52.5 (CH_3).

Anal.Calc (%). for ($C_{11}H_{12}BrMnN_2O_3$): C, 37.21; H, 3.41; N, 7.89; Found: C, 36.42; H, 3.85; N ,7.53.

HR MS (ESI): m/z $[M^+Na]^+$ calcd for $C_{11}H_{12}N_2O_3{}^{79}BrNaMn$, 376.93039 found 376.9306 (0 ppm); m/z $[M^+K]^+$ calcd for $C_{11}H_{12}N_2O_3{}^{79}BrKMn$, 392.90433 found 392.9041 (1 ppm)

IR (ν, cm^{-1}, CH_2Cl_2): 2027, 1936, 1909.

Complex **C^{3B}.1b**

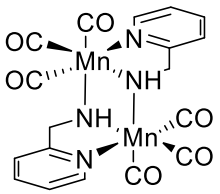

To a solution of **C^{3B}.1** (0.3 mmol, 100 mg) in a mixture of THF (3.4 mL) : Et_2O (6.7 mL) was added *t*BuOK (0.3 mmol, 34 mg). After stirring at room temperature overnight, solvents were removed and the brown solid was washed with pentane (2 x 5 mL) and then with cold acetone (2 x 7 mL) to give pure **5** (31 mg, 0.063 mmol, 42% yield). **C^{3B}.1b** has a low solubility is most common organic solvent (methanol, acetone, toluene, dichloromethane and DMSO) which hampers the acquisition of ^{13}C{^{1}H} NMR spectrum.

^{1}H NMR (400 MHz, Toluene-d_8) δ 8.63 (d, *J* = 4.9 Hz, 1H), 6.73 (d, *J* = 7.7 Hz, 1H), 6.61 (t, *J* = 6.2 Hz, 1H), 4.19 (d, *J* = 16.3 Hz, 1H), 3.89 (dd, *J* = 16.3, 5.2 Hz, 1H), -1.02 (s, 1H). Note : one aromatic CH is overlapping with toluene-d_8 signal
^{1}H NMR (400 MHz, Acetone-d_6) δ 9.26 (d, *J* = 5.2 Hz, 1H), 8.00 (t, *J* = 7.6 Hz, 1H), 7.77 (d, *J* = 7.8 Hz, 1H), 7.62 (t, *J* = 6.4 Hz, 1H), 4.62 (d, *J* = 16.6 Hz, 1H), 4.37 (dd, *J* = 16.6, 5.3 Hz, 1H), 0.18 (d, *J* = 2.8 Hz 1H).
^{13}C{^{1}H} NMR (101 MHz, Acetone-d_6) δ 168.6, 153.5, 138.8, 124.7, 123.2, 67.3.
IR (ν, cm^{-1}, CH_2Cl_2): 1990, 1892.

Complex **C^{3B}.2b**

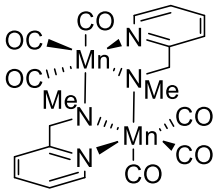

To a solution of **C^{3B}.2** (0.087 mmol, 30 mg) in a mixture of THF (4 mL) : Et_2O (2 mL) was added *t*BuOK (0.087 mmol, 10 mg). After stirring at r.t. overnight, solvents were removed and the brown solid was washed with pentane (2 x 5 mL) and then with cold acetone (2 x 7 mL) to give **C^{3B}.2b** not completely pure. **C^{3B}.2b** has a low solubility is most common organic solvent (methanol, acetone, toluene, dichloromethane and DMSO) which hampers the acquisition of ^{13}C{^{1}H} NMR spectrum.

^{1}H NMR (400 MHz, Acetone-d_6) δ 9.22 (d, *J* = 5.6 Hz, 1H), 8.08 (t, *J* = 7.8 Hz, 1H), 7.85 (d, *J* = 7.9 Hz, 1H), 7.66 (t, *J* = 6.6 Hz, 1H), 4.72 (d, *J* = 17.1 Hz, 1H), 4.02 (d, *J* = 17.1 Hz, 1H), 2.69 (s, 3H).

Complex **C^{3B}.1e**

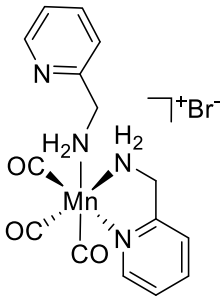

To a solution of 2-(aminomethyl)pyridine (0.397 mmol, 2.2 equiv., 41 µL) in hexane was added 1 equivalent of manganese pentacarbonyl bromide (0.181 mmol, 49.6 mg). After stirring at r.t. during 4 h, the solid precipitated. After filtration, this solid was washed two times with pentane to give complex **C^{3B}.1e** in a mixture with **C^{3B}.1** and other unidentified products, as a yellow powder. Suitable single crystals for X-Ray diffraction studies were obtained by evaporation of a saturated solution of the complex in acetone. The purpose of this experiment was to identify typical signals of this complex **C^{3B}.1e** in ^{1}H NMR.

^{1}H NMR (400 MHz, Acetone-d_6) δ 8.98 (m, 1H), 8.50 (m, 1H), 8.03 (s, 1H), 7.80 - 7.40 (m, 4H), 7.26 (m, 1H), 6.14 (s, 1H), 5.14 (s, 2H), 4.67 (s, 1H), 4.39 (s, 1H), 4.19 (s, 1H), 4.00 (s, 1H), 3.64 (s, 1H).

General procedure for transfer hydrogenation reactions

Stock solutions of manganese precatalyst **C^{3B}.1** (0.005 mol.L^{-1}) and base (0.005 mol.L^{-1}) in degassed *i*PrOH were first prepared in two Schlenk tubes. Then to a solution of ketone (0.5 mmol or 2 mmol) in *i*PrOH (final concentration 0.25 mol.L^{-1}) was added the stock solution of pre-catalyst, followed, in this order, by the stock solution of base. The reaction mixture was stirred for 20 minutes at 80 °C or 16 hours at 30 °C in an oil bath. The solution was then filtered through a small pad of silica (2 cm in a Pasteur pipette). The silica was washed with ethyl acetate. The filtrate was evaporated and the conversion was determined by ^{1}H NMR. The crude residue was then purified by column chromatography (SiO_2, mixture of petroleum ether/ethyl acetate or dietyl ether as eluent).

Representative procedure for transfer hydrogenation reaction of acetophenone **a1** (0.5 mmol scale)

To a solution of acetophenone **a1** (58 µL, 0.5 mmol) in *i*PrOH (2 mL) was added the stock solution of pre-catalyst **C^{3B}.1** (0.5 mL, 0.005 mol.L-1) followed, in this order, by the stock solution of *t*BuOK (0.5 mL, 0.005 mol.L-1).The reaction mixture was stirred for 20 minutes at 80 °C in an oil bath. The solution was then filtered through a small pad of silica (2 cm in a Pasteur pipette). The silica was washed with ethyl acetate. The filtrate was evaporated and the conversion was determined by ^{1}H NMR. The crude residue was then purified by column chromatography (SiO_2, mixture of petroleum ether/ethyl acetate or dietyl ether as eluent), giving the corresponding alcohol **b1** as a colorless oil (57 mg, 93%).

Representative procedure for transfer hydrogenation reaction of propiophenone **a2** (2 mmol scale)

To a solution of propiophenone **a2** (266 µL, 2 mmol) in *i*PrOH (8 mL, 0.25 mol L-1) was added pre-catalyst **C^{3B}.1** (3.3 mg, 0.01 mmol, 0.5 mol %), followed, in this order, by *t*BuOK (2.2 mg, 0.02 mmol, 1 mol %). The reaction mixture was stirred for 16 hours at 30 °C in an oil bath. The solution was then filtered through a small pad of silica (2 cm in a Pasteur pipette). The silica was washed with ethyl acetate. The filtrate was evaporated and the conversion was determined by ^{1}H NMR. The crude residue was then purified by column chromatography (SiO_2, mixture of petroleum ether/ethyl acetate or dietyl ether as eluent), giving the corresponding alcohol **b2** as a colorless oil (229 mg, 84 %).

Mechanistic studies:

Base-free experiments

To a solution of acetophenone **a1** (116 µL, 1 mmol) in *i*PrOH (4 mL) was added complex **C^{3B}.1b** as solid (2.5 mg, 0.5 mol%). The reaction mixture was stirred for 90 min at 80 °C or 1 h at 100 °C in an oil bath. The solution was then filtered through a small pad of silica (2 cm in a Pasteur pipette). The silica was washed with ethyl acetate. The filtrate was evaporated and the conversion was determined by ^{1}H NMR to give a 97 % conversion.

Characterization of the hydrogenated products

1-Phenylethanol (b1)[3]

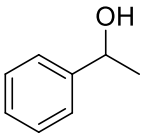

According to general procedure, acetophenone **a1** (58 µL, 0.5 mmol) gave the title compound as a colorless oil (57 mg, 93%).

^{1}H NMR (400 MHz, $CDCl_3$) δ 7.41 – 7.28 (m, 5H), 4.89 (q, *J*=6.4, 1H), 2.35 (s, 1H), 1.51 (d, *J*=6.5, 3H).

$^{13}C\{^{1}H\}$ NMR (101 MHz, $CDCl_3$) δ 145.9, 128.5, 127.5, 125.5, 70.4, 25.2.

1-Phenylpropan-1-ol (b2)[4]

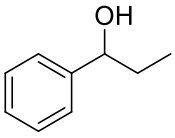

According to general procedure, propiophenone **a2** (266 µL, 2 mmol) gave the title compound as a colorless oil (229 mg, 84%).

^{1}H NMR (400 MHz, $CDCl_3$) δ 7.40-7.34 (m, 4H), 7.33 – 7.26 (m, 1H), 4.61 (t, *J* = 6.6 Hz, 1H), 2.08 (s, 1H), 1.96 – 1.55 (m, 2H), 0.94 (t, *J* = 7.4 Hz, 3H).

$^{13}C\{^{1}H\}$ NMR (101 MHz, $CDCl_3$) δ 144.7, 128.5, 127.6, 126.1, 76.1, 32.0, 10.2.

2-Methyl-1-phenylpropan-1-ol (b3)[3]

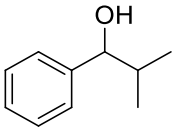

According to general procedure, isobutyrophenone **a3** (75 µL, 0.5 mmol) gave the title compound as a light yellow oil (71 mg, 95%).

^{1}H NMR (300 MHz, $CDCl_3$) δ 7.31 (m, 5H), 4.36 (d, *J* = 6.4 Hz, 1H), 1.97 (oct., *J* = 6.8 Hz, 1H), 1.87 (s, 1H), 1.01 (d, *J* = 6.8 Hz, 3H), 0.81 (d, *J* = 6.8 Hz, 3H).

$^{13}C\{^{1}H\}$ NMR (101 MHz, $CDCl_3$) δ 143.8, 128.3, 127.5, 126.7, 80.2, 35.4, 19.1, 18.4.

2,2-Dimethyl-1-phenylpropan-1-ol (b4)[5]

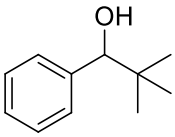

According to general procedure, 2,2-dimethyl-1-phenylpropan-1-one **a4** (336 µL, 2 mmol) gave the title compound as a colorless oil (326 mg, 99%).

^{1}H NMR (400 MHz, $CDCl_3$) δ 7.67-7.03 (m, 5H), 4.42 (s, 1H), 2.04 (s, 1H), 0.96 (s, 9H).

$^{13}C\{^{1}H\}$ NMR (101 MHz, $CDCl_3$) δ 142.3, 127.7, 127.6, 127.3, 82.5, 35.7, 26.0.

Cyclopropylphenylmethanol (b5)

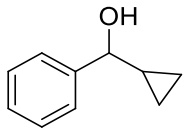

According to general procedure, cyclopropyl phenyl ketone **a5** (69 µL, 0.5 mmol) gave the title compound as a colorless oil (45 mg, 62%).

^{1}H NMR (400 MHz, $CDCl_3$) δ 7.49 – 7.43 (m, 2H), 7.42 – 7.35 (m, 2H), 7.35 – 7.29 (m, 1H), 4.05 (d, *J* = 8.3 Hz, 1H), 2.00 (s, 1H), 1.29-1.21 (m, 1H), 0.70-0.64 (m, 1H), 0.63 – 0.55 (m, 1H), 0.54 – 0.47 (m, 1H), 0.45 – 0.36 (m, 1H).

$^{13}C\{^{1}H\}$ NMR (101 MHz, $CDCl_3$) δ 143.9, 128.5, 127.7, 126.1, 78.7, 19.3, 3.7, 2.9.

1-(2-Methylphenyl)ethanol (b6)[6]

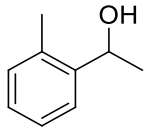

According to general procedure, 2-methylacetophenone **a6** (66 µL, 0.5 mmol) gave the title compound as a yellow oil (60 mg, 88%).

^{1}H NMR (400 MHz, $CDCl_3$) δ 7.52 (d, *J* = 7.4 Hz, 1H), 7.30-7.13 (m, 3H), 5.11 (q, *J* = 5.7 Hz, 1H), 2.36 (s, 3H), 2.21 (s, 1H), 1.47 (d, *J* = 6.2 Hz, 3H).

$^{13}C\{^{1}H\}$ NMR (101 MHz, $CDCl_3$) δ 143.9, 134.3, 130.4, 127.2, 126.4, 124.6, 66.8, 24.0, 19.0.

1-(4-Methylphenyl)ethanol (b7)[3]

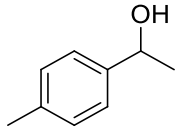

According to general procedure, 4-methylacetophenone **a7** (67 µL, 0.5 mmol) gave the title compound as a colorless oil (59 mg, 87%).

^{1}H NMR (400 MHz, $CDCl_3$) δ 7.29 (d, *J* = 8.0 Hz, 2H), 7.19 (d, *J* = 7.9 Hz, 2H), 4.88 (q, *J* = 6.5 Hz, 1H), 2.38 (s, 3H), 2.07 (s, 1H), 1.51 (d, *J* = 6.5 Hz, 3H).

$^{13}C\{^{1}H\}$ NMR (101 MHz, $CDCl_3$) δ = 143.0, 137.2, 129.2, 125.5, 70.3, 25.2, 21.2.

1-(2-Naphthyl)ethanol (b8)[7]

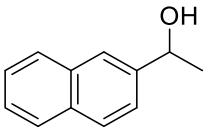

According to general procedure, 1-(naphthalen-2-yl)ethanone **a8** (340 mg, 2 mmol) gave the title compound as a white solid (307 mg, 89%).

^{1}H NMR (400 MHz, $CDCl_3$) δ 8.27-7.71 (m, 4H), 7.55-7.45 (m, 3H), 5.01 (q, *J* = 6.4 Hz, 1H), 2.70 (s, 1H), 1.58 (d, *J* = 6.5 Hz, 3H).

^{13}C{^{1}H} NMR (101 MHz, $CDCl_3$) δ 143.3, 133.3, 132.9, 128.3, 128.0, 127.7, 126.1, 125.8, 123.9, 123.8, 70.4, 25.1.

(3,4,5-Trimethoxyphenyl)-methanol (b10)[6]

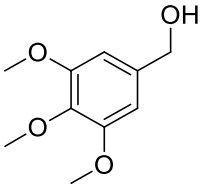

According to general procedure, 3,4,5-trimethoxybenzaldehyde **a10** (98 mg, 0.5 mmol) gave the title compound as a brown oil (97 mg, 99 %).

^{1}H NMR (400 MHz, $CDCl_3$) δ 6.57 (s, 2H), 4.60 (s, 2H), 3.83 (s, 9H), 2.14 (s, 1H).

^{13}C{^{1}H} NMR (101 MHz, $CDCl_3$) δ 153.4, 137.3, 136.8, 103.9, 65.5, 60.9, 56.2.

[1,1'-Biphenyl]-4-yl-methanol (b11)[8]

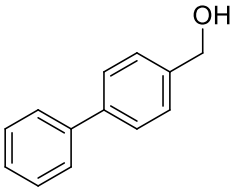

According to general procedure, 1,1'-biphenyl-4-carboxaldehyde **a11** (91 mg, 0.5 mmol) gave the title compound as a white solid (85 mg, 92 %). Note: the alcohol is contaminated with c.a. 5% of (*E*)-4-([1,1'-biphenyl]-4-yl)but-3-en-2-one resulting from the aldol condensation of the aldehyde with acetone.

^{1}H NMR (400 MHz, $CDCl_3$) δ 7.60 (d, *J* = 7.7 Hz, 4H), 7.50 – 7.37 (m, 4H), 7.36 (t, *J* = 7.1 Hz, 1H), 4.75 (s, 2H), 1.77 (s, 1H).

^{13}C{^{1}H} NMR (101 MHz, $CDCl_3$) δ = 140.9, 140.8, 140.0, 128.9, 127.6, 127.4, 127.2, 65.3.

1-(4-Iodophenyl)ethanol (b12)[4]

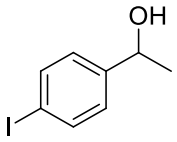

According to general procedure, 4-iodoacetophenone **a12** (246 mg, 1 mmol) gave the title compound as a brown oil after one week at 30 °C (244 mg, 99 %).

^{1}H NMR (400 MHz, $CDCl_3$) δ 7.67 (d, *J* = 7.8 Hz, 2H), 7.11 (d, *J* = 7.9 Hz, 2H), 4.84 (q, *J* = 6.6 Hz, 1H), 1.96 (s, 1H), 1.46 (d, *J* = 6.2 Hz, 3H).

^{13}C{^{1}H} NMR (101 MHz, $CDCl_3$) δ 145.6, 137.6, 127.5, 92.8, 70.0, 25.3.

1-(4-Bromophenyl)ethanol (b13)[6]

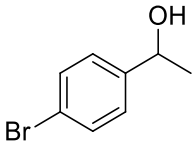

According to general procedure for 30 °C, 4-bromoacetophenone **a13** (398 mg, 2 mmol) gave the title compound as a colorless oil (352 mg, 87%).

^{1}H NMR (400 MHz, $CDCl_3$) δ7.45 (d, *J* = 8.4 Hz, 2H), 7.23 (d, *J* = 8.3 Hz, 2H), 4.85 (q, *J* = 6.4 Hz, 1H), 1.74 (s, 1H), 1.45 (d, *J* = 6.4 Hz, 3H).

^{13}C{^{1}H} NMR (101 MHz, $CDCl_3$) δ144.8, 131.5, 127.2, 121.1, 69.7, 25.2.

1-(2-Chlorophenyl)ethanol (b14)[9]

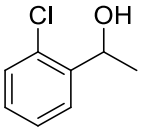

According to general procedure, 2-chloroacetophenone **a14** (260 µL, 2 mmol) gave the title compound as a colorless oil (341 mg, 99 %).

^{1}H NMR (400 MHz, $CDCl_3$) δ7.57 (d, *J* = 7.6 Hz, 1H), 7.34-7.25 (m, 2H), 7.18 (t, *J* = 8.2 Hz, 1H), 5.27 (q, *J* = 6.4 Hz, 1H), 2.26 (s, 1H), 1.47 (d, *J* = 6.4 Hz, 3H).

^{13}C{^{1}H} NMR (101 MHz, $CDCl_3$) δ143.2, 131.7, 129.5, 128.5, 127.3, 126.5, 67.0, 23.6.

1-(4-Fluorophenyl)ethanol (b15)[3]

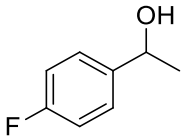

According to general procedure, 4-fluoroacetophenone **a15** (61 µL, 0.5 mmol) gave the title compound as a light-rose oil (70 mg, 85 %).

^{1}H NMR (400 MHz, $CDCl_3$) δ 7.32-7.27 (m, 2H), 7.03-6.97 (m, 2H), 4.82 (q, *J* = 6.4 Hz, 1H), 2.51 (s, 1H), 1.43 (d, *J* = 6.5 Hz, 3H).

^{19}F NMR (376 MHz, $CDCl_3$) δ -115.44.

$^{13}C\{^1H\}$, NMR (101 MHz, $CDCl_3$) δ 162.1 (d, *J* = 245 Hz), 141.6 (d, *J* = 3.1 Hz), 127.1 (d, *J* = 8.1 Hz), 115.3 (d, *J* = 21.4 Hz), 69.7, 25.3.

1-(4-Trifluoromethylphenyl)ethanol (b16)[10]

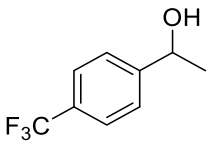

According to general procedure, 4-trifluoromethylacetophenone **a16** (412 µL, 2 mmol) gave the title compound as a colorless oil (365 mg, 96 %).

^{1}H NMR (400 MHz, $CDCl_3$) δ 7.61 (d, *J* = 8.0 Hz, 2H), 7.49 (d, *J* = 8.0 Hz, 2H), 4.97 (q, *J* = 6.5 Hz, 1H), 1.94 (s, 1H), 1.51 (d, *J* = 6.5 Hz, 3H).

^{19}F NMR (376 MHz, $CDCl_3$) δ -62.48.

$^{13}C\{^1H\}$ NMR (101 MHz, $CDCl_3$) δ 149.8, 129.7 (q, *J* = 32.3 Hz), 125.7, 125.5 (q, *J* = 3.7 Hz), 124.3 (q, *J* = 271.9 Hz), 69.9, 25.4.

2,2,2-Trifluoro-1-phenylethanol (b17)[4]

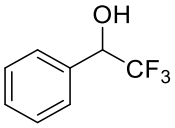

According to general procedure, 2,2,2-trifluoroacetophenone **a17** (70 µL, 0.5 mmol) gave the title compound as a colorless oil (51 mg, 58 %).

^{1}H NMR (400 MHz, $CDCl_3$) δ 7.57 – 7.36 (m, 5H), 5.03 (qd, *J* = 6.6, 2.9 Hz, 1H), 2.60 (d, *J* = 3.3 Hz, 1H).

$^{13}C\{^1H\}$ NMR (101 MHz, $CDCl_3$)δ 129.7, 128.8, 127.6, 123.0, δ 73.0 (q, *J* = 32.0 Hz).Note: the quartet for carbon of CF_3 was not observed due to low intensity.

^{19}F NMR (376 MHz, $CDCl_3$) δ -78.37 (d, *J* = 6.7 Hz).

4-(1-Hydroxyethyl)benzonitrile (b18)[11]

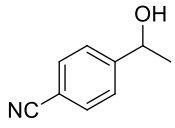

According to general procedure, 4-acetylbenzonitrile **a18** (290 mg, 2 mmol) gave the title compound as a brown oil (230 mg, 78 %).

^{1}H NMR (400 MHz, $CDCl_3$) δ 7.62 (d, *J* = 8.3 Hz, 2H), 7.47 (d, *J* = 8.3 Hz, 2H), 4.95 (q, *J* = 6.5 Hz, 1H), 2.23 (s, 1H), 1.48 (d, *J* = 6.5 Hz, 3H).

$^{13}C\{^1H\}$ NMR (101 MHz, $CDCl_3$) δ151.3, 132.4, 126.2, 119.0, 111.1, 69.7, 25.5.

1-(4-Nitrophenyl)ethanol (b19)[12]

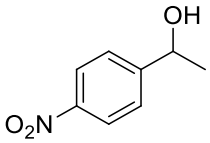

According to general procedure, 4-nitroacetophenone **a19** (330 mg, 2 mmol) gave the title compound as a white solid (333 mg, 99%).

^{1}H NMR (400 MHz, $CDCl_3$) 8.16 (d, *J* = 8.3 Hz, 2H), 7.52 (d, *J* = 8.3 Hz, 2H), 5.00 (q, *J* = 6.6 Hz, 1H), 2.38 (s, 1H), 1.50 (d, *J* = 6.4 Hz, 4H).

^{13}C{^{1}H} NMR (101 MHz, $CDCl_3$) δ = 153.3, 147.2, 126.2, 123.8, 69.6, 25.6.

(4-(Diethylamino)phenyl)methanol (b21)[12]

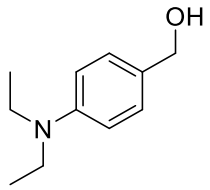

According to general procedure, 4-(diethylamino)benzaldehyde **a21** (89 mg, 0.5 mmol) gave the title compound as a yellow oil (74 mg , 83 %).

^{1}H NMR (400 MHz, $CDCl_3$) δ 7.22 (d, *J* = 8.7 Hz, 2H), 6.68 (d, *J* = 8.7 Hz, 2H), 4.55 (s, 2H), 3.36 (q, *J* = 7.0 Hz, 4H), 1.66 (s, 1H), 1.17 (t, *J* = 7.1 Hz, 6H).

^{13}C {^{1}H} NMR (101 MHz, $CDCl_3$) δ 147.6, 129.1, 127.8, 111.9, 65.5, 44.5, 12.6.

***N*-(4-(Hydroxymethyl)phenyl)acetamide (b23)[13]**

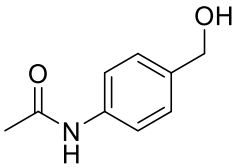

According to general procedure, *N*-(4-formylphenyl)acetamide **a23** (81 mg, 0.5 mmol) gave the title compound as a white solid (73 mg, 90%).

^{1}H NMR (400 MHz, $CDCN_3$) δ 8.33 (s, 1H), 7.52 (d, *J* = 8.4 Hz, 2H), 7.29 (d, *J* = 8.4 Hz, 2H), 4.54 (d, *J* = 5.8 Hz, 2H), 3.15 (t, *J* = 5.9 Hz, 1H), 2.07 (s, 3H). Note: c.a. 5% of the product of aldol condensation with acetone is present in the product.
^{13}C{^{1}H} NMR (101 MHz, Acetone-d_6) δ 168.9, 139.2, 138.1, 127.9, 119.8, 64.4, 24.2.

Undecan-2-ol (b25)[3]

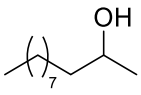

According to general procedure, undecan-2-one **a25** (103 µL, 0.5 mmol) gave the title compound as a colorless oil (80 mg, 93 %).

^{1}H NMR (400 MHz, $CDCl_3$) δ 3.77 (m, 1H), 1.51 – 1.2 (m, 20H), 0.87 (t, *J* = 6.7 Hz, 3H).

^{13}C{^{1}H} NMR (101 MHz, $CDCl_3$) δ 68.3, 39.5, 32.0, 29.79, 29.77, 29.70, 29.5, 25.9, 23.6, 22.8, 14.2.

Cyclohexanol (b26)

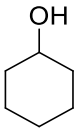

According to general procedure, cyclohexanone **a26** (52 µL, 0.5 mmol) gave the title compound as a colorless oil (49 mg, 99 %).

^{1}H NMR (400 MHz, $CDCl_3$) δ 3.60-3.57 (m, 1H), 1.92-1.66 (m, 5H), 1.54-1.51 (m, 1H), 1.31 – 1.06 (m, 5H).

^{13}C{^{1}H} NMR (101 MHz, $CDCl_3$) δ 70.4, 35.6, 25.6, 24.3.

Cycloheptanol (b27)[3]

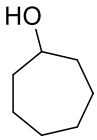

According to general procedure, cycloheptanone **a27** (236 µL, 2 mmol) gave the title compound as a colorless oil (215 mg, 94 %).

^{1}H NMR (400 MHz, $CDCl_3$) δ 3.85-3.79 (m, 1H), 1.92-1.86 (m, 2H), 1.69-1.47 (m, 9H), 1.43 – 1.28 (m, 2H).

^{13}C{^{1}H} NMR (101 MHz, $CDCl_3$) δ 72.9, 37.7, 28.2, 22.7.

2,2-Dimethylchroman-4-ol (b28)

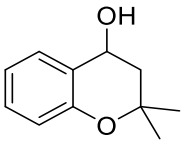

According to general procedure, 2,2-dimethylchroman-4-one **a28** (88 mg, 0.5 mmol) gave the title compound as a colorless oil (88 mg, 99%).

^{1}H NMR (400 MHz, $CDCl_3$) δ 7.45 (d, *J* = 7.5 Hz, 1H), 7.22 – 7.13 (m, 1H), 6.93 (td, *J* = 7.4, 1.2 Hz, 1H), 6.79 (dd, *J* = 8.2, 1.2 Hz, 1H), 4.85 (q, *J* = 7.3 Hz, 1H), 2.18 (dd, *J* = 13.4, 6.1 Hz, 1H), 1.87 (dd, *J* = 13.4, 8.7 Hz, 1H), 1.74 (d, *J* = 7.4 Hz, 1H), 1.45 (s, 3H), 1.32 (s, 3H).

^{13}C{^{1}H} NMR (101 MHz, $CDCl_3$) δ 153.3, 129.4, 127.7, 124.5, 120.4, 117.4, 75.4, 63.9, 42.9, 29.0, 26.1.

4-Phenylbut-3-en-2-ol (b30)[10]

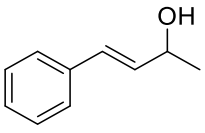

According to general procedure, 4-phenylbut-3-en-2-one **a30** (412 µL, 2 mmol) gave the title compound as a yellow oil (258 mg, 87 %).

^{1}H NMR (400 MHz, $CDCl_3$) δ 7.42 (d, *J* = 7.4 Hz, 2H), 7.36 (t, *J* = 7.5 Hz, 2H), 7.29 (d, *J* = 7.9 Hz, 1H), 6.61 (d, *J* = 15.9 Hz, 1H), 6.31 (dd, *J* = 15.9, 6.4 Hz, 1H), 4.54 (quint., *J* = 6.3 Hz, 1H), 1.62 (s, 1H), 1.42 (d, *J* = 6.4 Hz, 3H).

^{13}C{^{1}H} NMR (101 MHz, $CDCl_3$) δ = 136.8, 133.7, 129.5, 128.7, 127.8, 126.6, 69.1, 23.6.

4-(2,6,6-Trimethylcyclohex-1-en-1-yl)but-3-en-2-ol (β-ionol) (b31)[10]

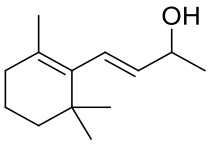

According to general procedure, β-ionone **a31** (103 µL, 2 mmol) gave the title compound as a colorless oil (88 mg, 90 %).

^{1}H NMR (400 MHz, $CDCl_3$) δ 6.03 (d, *J* = 15.9 Hz, 1H), 5.47 (dd, *J* = 15.9, 6.7 Hz, 1H), 4.34 (quint., *J* = 6.4, 1H), 1.96 (t, *J* = 6.0 Hz, 2H), 1.71 (br. s, 1H), 1.65 (s, 3H), 1.62 – 1.51 (m, 2H), 1.48 – 1.38 (m, 2H), 1.30 (d, *J* = 6.3 Hz, 3H), 0.97 (s, 6H).

^{13}C{^{1}H} NMR (101 MHz, $CDCl_3$) δ 137.8, 136.78, 128.9, 127.6, 69.6, 39.5, 34.0, 32.8, 28.8, 28.8, 23.7, 21.4, 19.3.

Cinnamylalcohol (b32)[10]

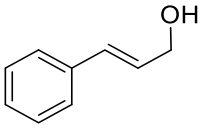

According to general procedure, cinnamyl ketone **a32** (63 µL, 0.5 mmol) gave the title compound as a colorless oil (54 mg, 80 %).

^{1}H NMR (400 MHz, $CDCl_3$) δ 7.41-7.39 (m, 2H), 7.35 (t, *J* = 7.4 Hz, 1H), 7.28-7.24 (m, 1H), 6.63 (d, *J* = 15.9 Hz, 1H), 6.38 (dt, *J* = 15.9, 5.7 Hz, 1H), 4.33 (dd, *J* = 5.7, 1.5 Hz, 1H), 2.06 (br. s, 1H).

^{13}C{^{1}H} NMR (101 MHz, $CDCl_3$) δ 136.8, 131.2, 128.7, 128.6, 127.8, 126.6, 63.8.

1-(5-Chlorothiophen-2-yl)ethanol (b33)[4]

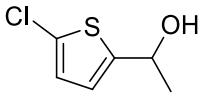

According to general procedure, 1-(5-chlorothiophen-2-yl)ethanone **a33** (80 mg, 0.5 mmol) gave the title compound as a brown oil (78 mg, 96 %).

^{1}H NMR (400 MHz, $CDCl_3$) δ 6.75 (d, *J* = 3.8 Hz, 1H), 6.71 (d, *J* = 3.8 Hz, 1H), 4.99 (q, *J* = 6.4 Hz, 1H), 2.24 (s, 1H), 1.55 (d, *J* = 6.4 Hz, 3H).

^{13}C{^{1}H} NMR (101 MHz, $CDCl_3$) δ148.7, 129.1, 125.7, 122.5, 66.5, 25.1.

X-ray data

CCDC 1545746-1545749 contain the supplementary crystallographic data for complexes **C^{3B}.1**- **3** and **C^{3B}.1b**. These data can be obtained free of charge from The Cambridge Crystallographic Data Centre.

Complex **C^{3B}.1**

X-ray diffraction data were collected on a D8 VENTURE Bruker AXS diffractometer equipped with a PHOTON 100 CMOS detector, using multilayers monochromated Mo-Kα radiation (λ = 0.71073 Å) at T = 150 (2) K. The structure was solved by dual-space algorithm using the *SHELXT* program,[14] and then refined with full-matrix least-square methods based on F^2 (*SHELXL-2014*).[15] All non-hydrogen atoms were refined with anisotropic atomic displacement parameters. H atoms were finally included in their calculated positions. A final refinement on F^2 with 3811 unique intensities and 192 parameters converged at $\omega R(F^2)$ = 0.0733 ($R(F)$ = 0.0353) for 3004 observed reflections with $I > 2\sigma(I)$.

Table S8. Crystal data and structure refinement for complex **C^{3B}.1**.

Empirical formula	C_{13} H_{18} Br Mn N_2 O_4
Formula weight	401.14
Temperature	150(2) K
Wavelength	0.71073 Å
Crystal system, space group	monoclinic, P $2_1/c$
Unit cell dimensions	a = 9.8700(9) Å, alpha = 90 °
	b = 10.2436(10) Å, beta = 95.410(4) °
	c = 16.5179(15) Å, gamma = 90 °
Volume	1662.6(3) $Å^3$
Z, Calculated density	4, 1.603 ($g.cm^{-3}$)
Absorption coefficient	3.212 mm^{-1}
F(000)	808
Crystal size	0.550 x 0.450 x 0.090 mm
Crystal color	orange
Theta range for data collection	3.050 to 27.484 °
h_min, h_max	-12, 12
k_min, k_max	-13, 13
l_min, l_max	-21, 21
Reflections collected / unique	19509 / 3811 [R(int) = 0.0827]
Reflections [I>2sigma(I)]	3004
Completeness to theta_max	0.998
Absorption correction type	multi-scan
Max. and min. transmission	0.749 , 0.412
Refinement method	Full-matrix least-squares on F^2
Data / restraints / parameters	3811 / 0 / 192
Goodness-of-fit	1.042
Final R indices [I>2sigma(I)]	$R1^a$ = 0.0353, $wR2^b$ = 0.0733
R indices (all data)	$R1^a$ = 0.0539, $wR2^b$ = 0.0790
Largest diff. peak and hole	0.624 and -0.433 $e.Å^{-3}$

Complex **C^{3B}.2**

X-ray diffraction data were collected on a D8 VENTURE Bruker AXS diffractometer equipped with a PHOTON 100 CMOS detector, using multilayers monochromated Mo-Kα radiation (λ = 0.71073 Å) at T = 150 K. The structure was solved by dual-space algorithm using the *SHELXT* program,[14] and then refined with full-matrix least-square methods based on F^2 (*SHELXL-2014*).[15] All non-hydrogen atoms were refined with anisotropic atomic displacement parameters. Except nitrogen linked hydrogen atom that was introduced in the structural model through Fourier difference maps analysis, H atoms were finally included in their calculated positions. A final refinement on F^2 with 2522 unique intensities and 159 parameters converged at $\omega R(F^2)$ = 0.1038 ($R(F)$ = 0.0398) for 2400 observed reflections with $I > 2\sigma(I)$.

Table S9. Crystal data and structure refinement for complex **C^{3B}.2**.

Empirical formula	C_{10} H_{10} Br Mn N_2 O_3
Formula weight	341.05
Temperature	150 K
Wavelength	0.71073 Å
Crystal system, space group	triclinic, P -1
Unit cell dimensions	a = 6.7610(15) Å, alpha = 78.215(8) °
	b = 7.2814(16) Å, beta = 85.488(8) °
	c = 13.336(3) Å, gamma = 72.757(7) °
Volume	613.7(2) $Å^3$
Z, Calculated density	2, 1.846 ($g.cm^{-3}$)
Absorption coefficient	4.327 mm^{-1}
F(000)	336
Crystal size	0.330 x 0.250 x 0.160 mm
Crystal color	yellow
Theta range for data collection	2.984 to 27.523 °
h_min, h_max	-8, 8
k_min, k_max	-9, 9
l_min, l_max	0, 17
Reflections collected / unique	2522 / 2522
Reflections [I>2sigma(I)]	2400
Completeness to theta_max	0.917
Absorption correction type	multi-scan
Max. and min. transmission	0.500 , 0.371
Refinement method	Full-matrix least-squares on F^2
Data / restraints / parameters	2522 / 0 / 159
Goodness-of-fit	1.059
Final R indices [I>2sigma(I)]	R1 = 0.0398, wR2 = 0.1038
R indices (all data)	R1 = 0.0449, wR2 = 0.1066
Largest diff. peak and hole	0.769 and -0.957 $e.Å^{-3}$

Complex **C^{3B}.3**

(X-ray diffraction data were collected on a D8 VENTURE Bruker AXS diffractometer equipped with a PHOTON 100 CMOS detector, using multilayers monochromated Mo-Ka radiation (λ = 0.71073 Å) at T = 150 (2) K. The structure was solved by dual-space algorithm using the *SHELXT* program,[14] and then refined with full-matrix least-square methods based on F^2 (*SHELXL-2014*).[15] All non-hydrogen atoms were refined with anisotropic atomic displacement parameters. H atoms were finally included in their calculated positions. A final refinement on F^2 with 3113 unique intensities and 165 parameters converged at ω$R(F^2)$ = 0.0589 ($R(F)$ = 0.0230) for 2805 observed reflections with $I > 2\sigma(I)$.

Table S10. Crystal data and structure refinement for complex **C^{3B}.3**.

Empirical formula	C_{11} H_{12} Br Mn N_2 O_3
Formula weight	355.08
Temperature	150(2) K
Wavelength	0.71073 Å
Crystal system, space group	monoclinic, P $2_1/c$
Unit cell dimensions	a = 13.6291(7) Å, alpha = 90 °
	b = 7.5001(3) Å, beta = 113.980(2) °
	c = 14.5567(7) Å, gamma = 90 °
Volume	1359.55(11) $Å^3$
Z, Calculated density	4, 1.735 ($g.cm^{-3}$)
Absorption coefficient	3.910 mm^{-1}
F(000)	704
Crystal size	0.350 x 0.110 x 0.070 mm
Crystal color	yellow
Theta range for data collection	3.063 to 27.482 °
h_min, h_max	-17, 17
k_min, k_max	-8, 9
l_min, l_max	-18, 18
Reflections collected / unique	19651 / 3113 [R(int) = 0.0352]
Reflections [I>2sigma(I)]	2805
Completeness to theta_max	0.999
Absorption correction type	multi-scan
Max. and min. transmission	0.761 , 0.577
Refinement method	Full-matrix least-squares on F^2
Data / restraints / parameters	3113 / 0 / 165
Goodness-of-fit	0.711
Final R indices [I>2sigma(I)]	$R1^a$ = 0.0230, $wR2^b$ = 0.0589
R indices (all data)	$R1^a$ = 0.0279, $wR2^b$ = 0.0642
Largest diff. peak and hole	0.449 and -0.508

Complex $\mathbf{C^{3B}.1b}$

X-ray diffraction data were collected on a D8 VENTURE Bruker AXS diffractometer equipped with a PHOTON 100 CMOS detector, using multilayers monochromated Mo-Ka radiation (λ = 0.71073 Å) at T = 150 (2) K. The structure was solved by dual-space algorithm using the *SHELXT* program,[14] and then refined with full-matrix least-square methods based on F^2 (*SHELXL-2014*).[15] All non-hydrogen atoms were refined with anisotropic atomic displacement parameters. Except nitrogen linked hydrogen atoms that were introduced in the structural model through Fourier difference maps analysis, H atoms were finally included in their calculated positions. A final refinement on F^2 with 2189 unique intensities and 139 parameters converged at $\omega R(F^2)$ = 0.0982 ($R(F)$ = 0.0262) for 2132 observed reflections with $I > 2\sigma(I)$.

Table S11. Crystal data and structure refinement for complex $\mathbf{C^{3B}.1b}$.

Empirical formula	$C_{18}\ H_{14}\ Mn_2\ N_4\ O_6$
Formula weight	492.21
Temperature	150 K
Wavelength	0.71073 Å
Crystal system, space group	triclinic, P -1
Unit cell dimensions	a = 7.2912(9) Å, alpha = 106.422(3)°
	b = 8.1947(10) Å, beta = 100.106(4)°
	c = 9.5912(11) Å, gamma = 113.184(3)°
Volume	477.83(10) $Å^3$
Z, Calculated density	1, 1.711 ($g.cm^{-3}$)
Absorption coefficient	1.366 mm^{-1}
F(000)	248
Crystal size	0.590 x 0.260 x 0.210 mm
Crystal color	yellow
Theta range for data collection	2.935 to 27.484°
h_min, h_max	-9, 9
k_min, k_max	-10, 10
l_min, l_max	-12, 12
Reflections collected / unique	9005 / 2189 [R(int) = 0.0265]
Reflections [I>2sigma(I)]	2132
Completeness to theta_max	0.998
Absorption correction type	multi-scan
Max. and min. transmission	0.751 , 0.621
Refinement method	Full-matrix least-squares on F^2
Data / restraints / parameters	2189 / 0 / 139
Goodness-of-fit	1.373
Final R indices [I>2sigma(I)]	R1 = 0.0262, wR2 = 0.0982
R indices (all data)	R1 = 0.0280, wR2 = 0.1075
Largest diff. peak and hole	0.648 and -0.696 $e.Å^{-3}$

Complex **C^{3B}.2b**

X-ray diffraction data were collected on a APEXII Bruker AXS diffractometer equipped with a CCD detector, using graphite-monochromated Mo-Kα radiation (λ = 0.71073 Å) at T = 150 (2) K. The structure was solved by dual-space algorithm using the *SHELXT* program,[14] and then refined with full-matrix least-square methods based on F^2 (*SHELXL-2014*).[15] All non-hydrogen atoms were refined with anisotropic atomic displacement parameters. H atoms were finally included in their calculated positions.

Table S12. Crystal data and structure refinement for complex **C^{3B}.2b**.

Empirical formula	$C_{20}\ H_{18}\ Mn_2\ N_4\ O_6$
Formula weight	520.26
Temperature	150(2) K
Wavelength	0.71073 Å
Crystal system, space group	monoclinic, P 21/n
Unit cell dimensions	a = 9.2389(11) Å, alpha = 90 °
	b = 12.7300(12) Å, beta = 115.771(4) °
	c = 9.8277(10) Å, gamma = 90 °
Volume	1040.89(19) $Å^3$
Z, Calculated density	2, 1.660 ($g.cm^{-3}$)
Absorption coefficient	1.259 mm^{-1}
F(000)	528
Crystal size	0.370 x 0.330 x 0.150 mm
Crystal color	yellow
Theta range for data collectio	n 2.925 to 27.483 °
h_min, h_max	-11, 11
k_min, k_max	-16, 14
l_min, l_max	-12, 8
Reflections collected / unique	6967 / 2375 [R(int) = 0.0316]
Reflections [I>2σ(*I*)]	1911
Completeness to theta_max	0.997
Absorption correction type	multi-scan
Max. and min. transmission	0.828 , 0.749
Refinement method	Full-matrix least-squares on F^2
Data / restraints / parameters	2375 / 0 / 146
Goodness-of-fit	1.027
Final R indices [I>2σ(*I*)]	$R1^a$ = 0.0315, $wR2^b$ = 0.0660
R indices (all data)	$R1^a$ = 0.0456, $wR2^b$ = 0.0720
Largest diff. peak and hole	0.358 and -0.358 $e^-.Å^{-3}$

$R_{int} = \sum |F_o^2 - \langle F_o^2 \rangle| / \sum [F_o^2]$

$S = \{\sum [w(F_o^2 - F_c^2)^2] / (n - p)\}^{1/2}$

$R1 = \sum ||F_o| - |F_c|| / \sum |F_o|$

$wR2 = \{\sum [w(F_o^2 - F_c^2)^2] / \sum [w(F_o^2)^2]\}^{1/2}$

$w = 1 / [\sigma(F_o^2) + aP^2 + bP]$ where $P = [2F_c^2 + MAX(F_o^2, 0)] /3$

Complex **C^{3B}.1e**

X-ray diffraction data were collected on a D8 VENTURE Bruker AXS diffractometer equipped with a PHOTON 100 CMOS detector, using multilayers monochromated Mo-Ka radiation (λ = 0.71073 Å) at T = 150 (2) K. The structure was solved by dual-space algorithm using the *SHELXT* program,[14] and then refined with full-matrix least-square methods based on F^2 (*SHELXL-2014*).[15] All non-hydrogen atoms were refined with anisotropic atomic displacement parameters. Except nitrogen linked hydrogen atoms that were introduced in the structural model through Fourier difference maps analysis, H atoms were finally included in their calculated positions.

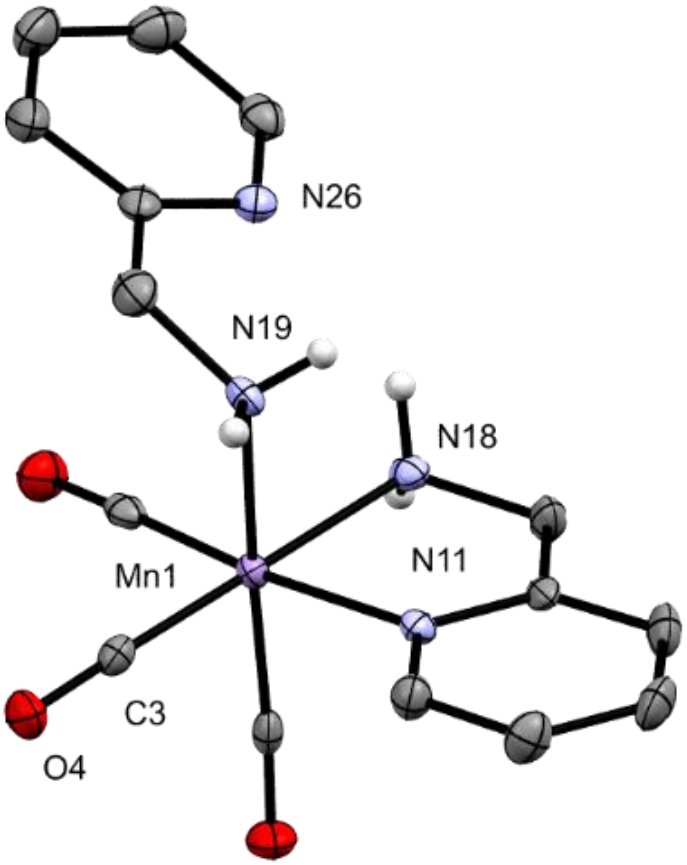

Figure S32: Perspective view of the molecular structure of complex **C^{3B}.1e** with thermal ellipsoids drawn at 50% probability. Hydrogen atoms, except N*H*, were omitted for clarity.

Table S13. Crystal data and structure refinement for complex **C^{3B}.1e**.

Empirical formula	C_{15} H_{16} Br Mn N_4 O_3
Formula weight	435.17
Temperature	150 K
Wavelength	0.71073 Å
Crystal system, space group	monoclinic, P 21/c
Unit cell dimensions	a = 9.0554(4) Å, alpha = 90 °
	b = 14.5940(10) Å, beta = 103.409(2) °
	c = 13.1181(8) Å, gamma = 90 °
Volume	1686.36(17) $Å^3$
Z, Calculated density	4, 1.714 ($g.cm^{-3}$)
Absorption coefficient	3.173 mm^{-1}
F(000)	872
Crystal size	0.100 x 0.070 x 0.065 mm
Crystal color	colourless
Theta range for data collection	3.193 to 27.480 °
h_min, h_max	-11, 11
k_min, k_max	-16, 18
l_min, l_max	-17, 17
Reflections collected / unique	14039 / 3845 [R(int) = 0.0703]
Reflections [I>2σ(*I*)]	2824
Completeness to theta_max	0.995
Absorption correction type	multi-scan
Max. and min. transmission	0.814 , 0.709
Refinement method	Full-matrix least-squares on F^2
Data / restraints / parameters	3845 / 0 / 229
Goodness-of-fit	1.034
Final R indices [I>2σ(*I*)]	R1 = 0.0371, wR2 = 0.0626
R indices (all data)	R1 = 0.0661, wR2 = 0.0736
Largest diff. peak and hole	0.471 and -0.466 $e^-.Å^{-3}$

$R_{int} = \sum |F_o^2 - \langle F_o^2 \rangle| / \sum [F_o^2]$

$S = \{\sum [w(F_o^2 - F_c^2)^2] / (n - p)\}^{1/2}$

$R1 = \sum ||F_o| - |F_c|| / \sum |F_o|$

$wR2 = \{\sum [w(F_o^2 - F_c^2)^2] / \sum [w(F_o^2)^2]\}^{1/2}$

$w = 1 / [\sigma(F_o^2) + aP^2 + bP]$ where $P = [2F_c^2 + MAX(F_o^2, 0)] / 3$

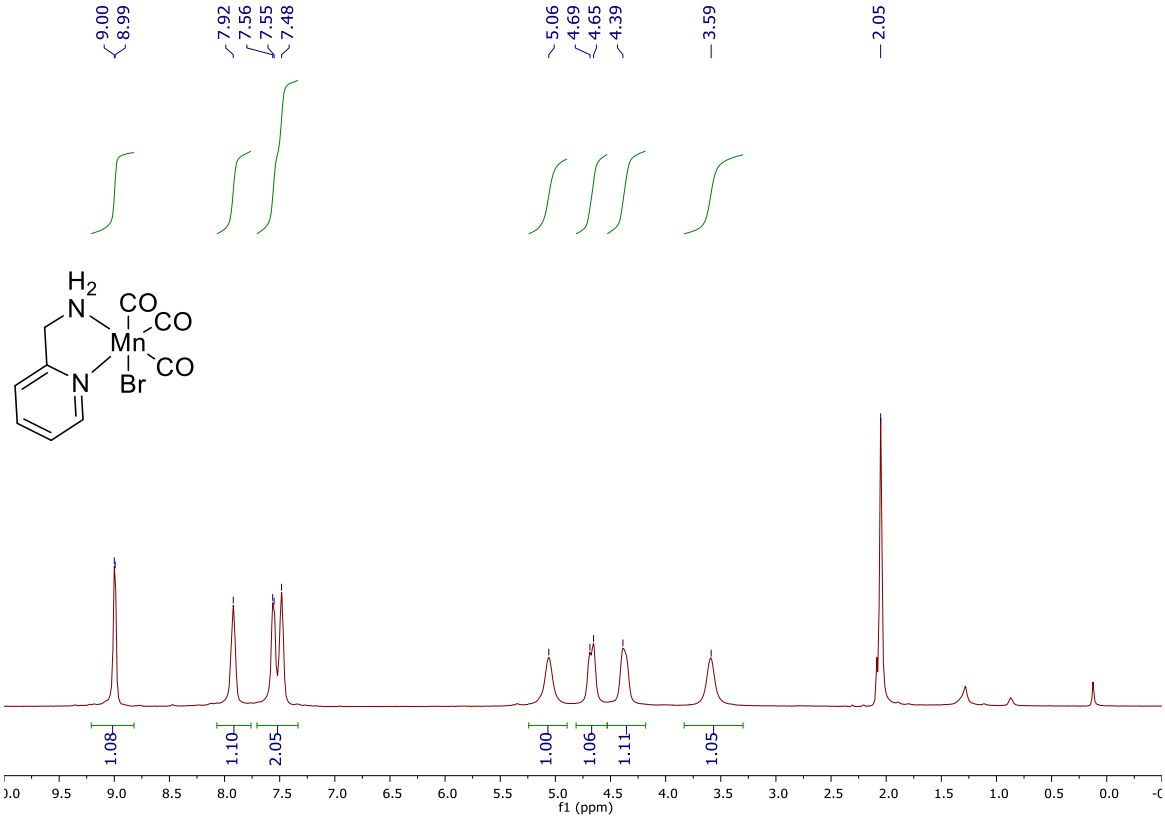

Figure S33: ^{1}H NMR spectrum of manganese complex **C^{3B}.1** in $(CD_3)_2CO$ (400 MHz).

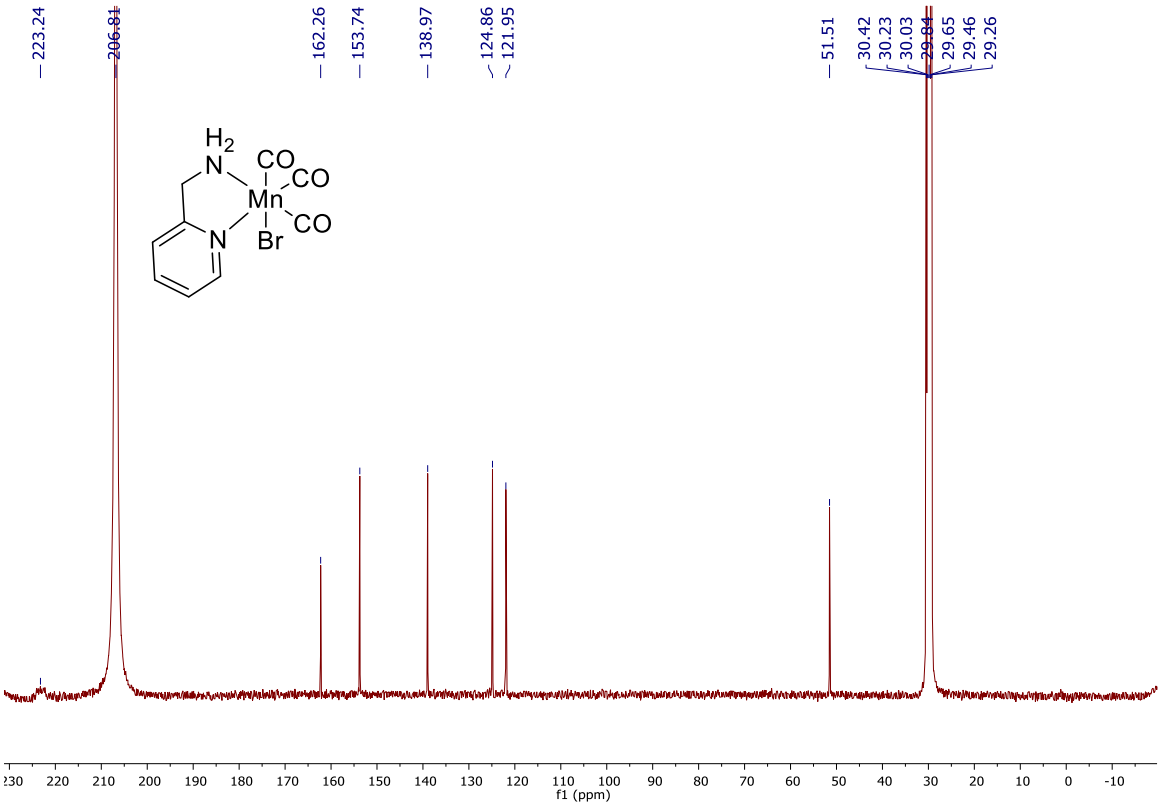

Figure S34: ^{13}C{^{1}H} NMR spectrum of manganese complex **C^{3B}.1** in $(CD_3)_2CO$ (101 MHz).

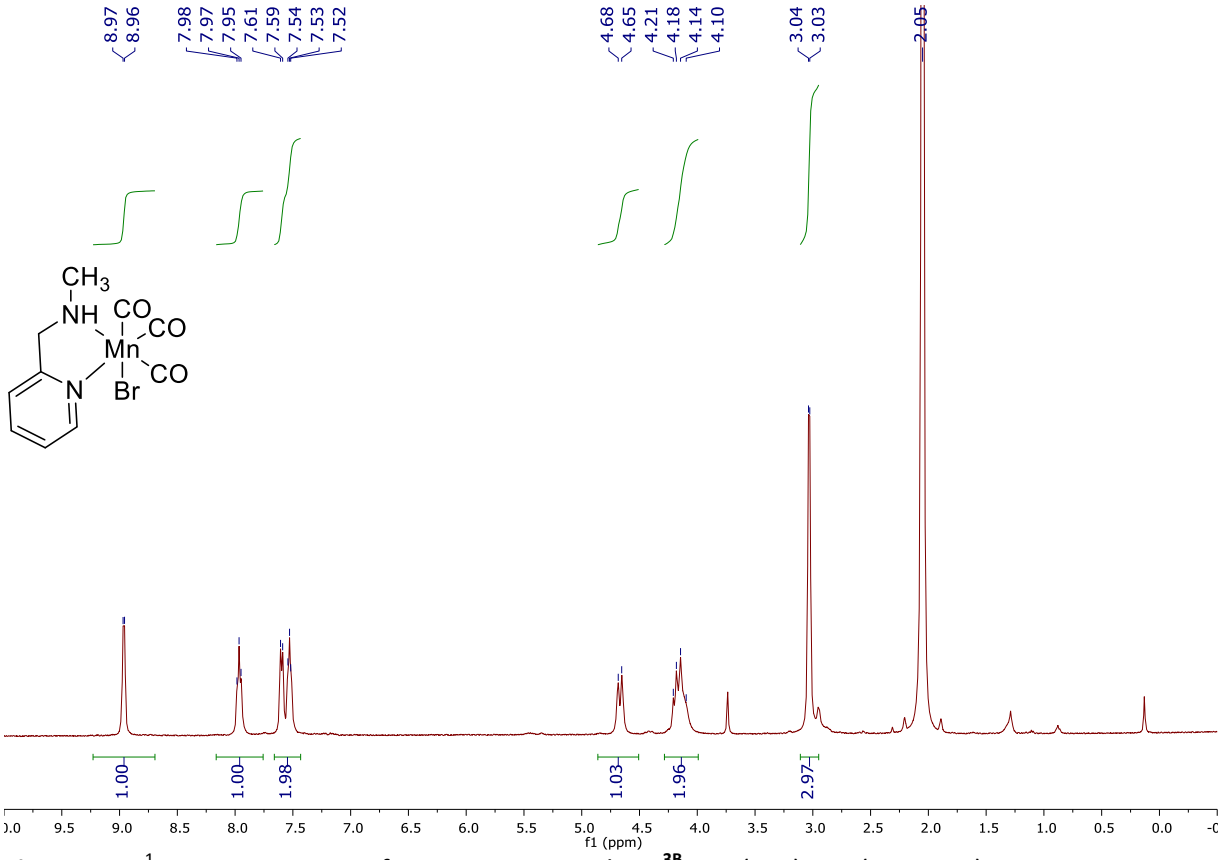

Figure S35: ^{1}H NMR spectrum of manganese complex **C^{3B}.2** in $(CD_3)_2CO$ (400 MHz).

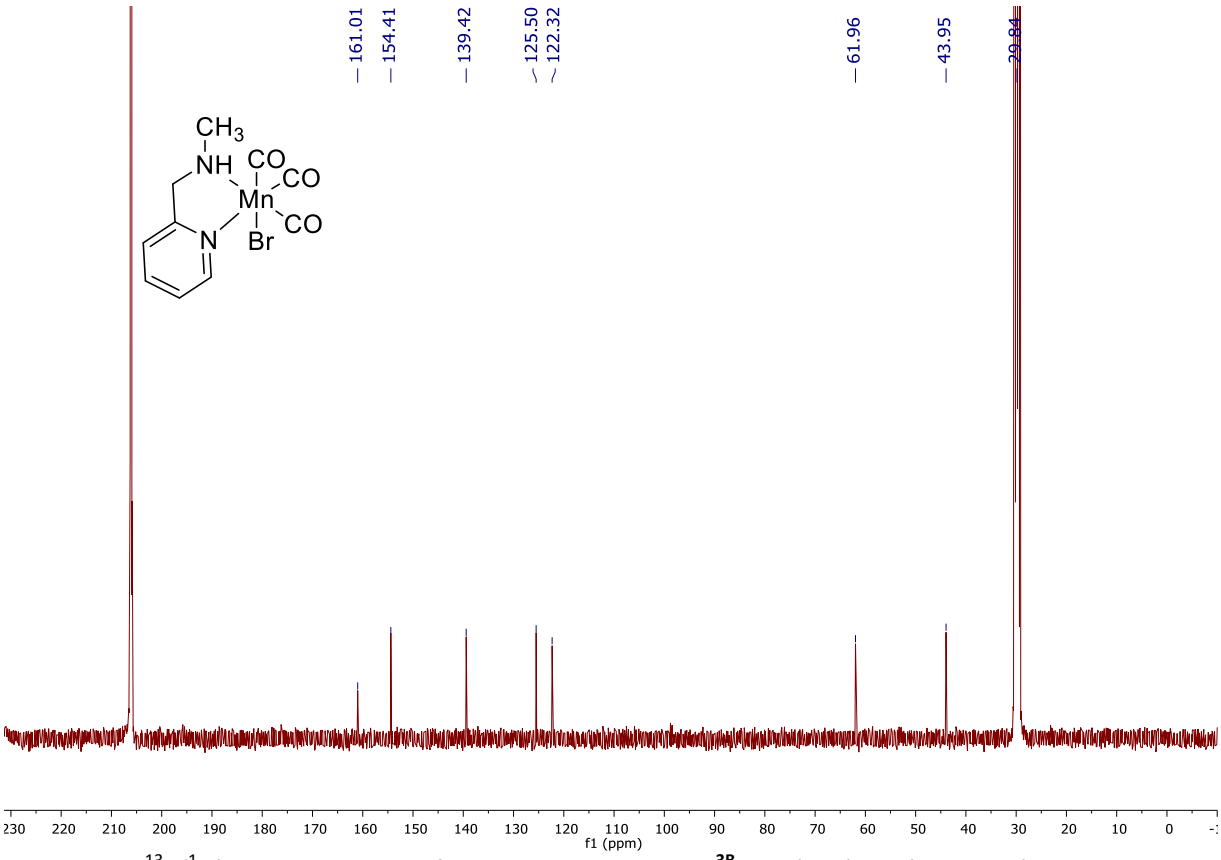

Figure S36: $^{13}C\{^{1}H\}$ NMR spectrum of manganese complex **C^{3B}.2** in $(CD_3)_2CO$ (101 MHz).

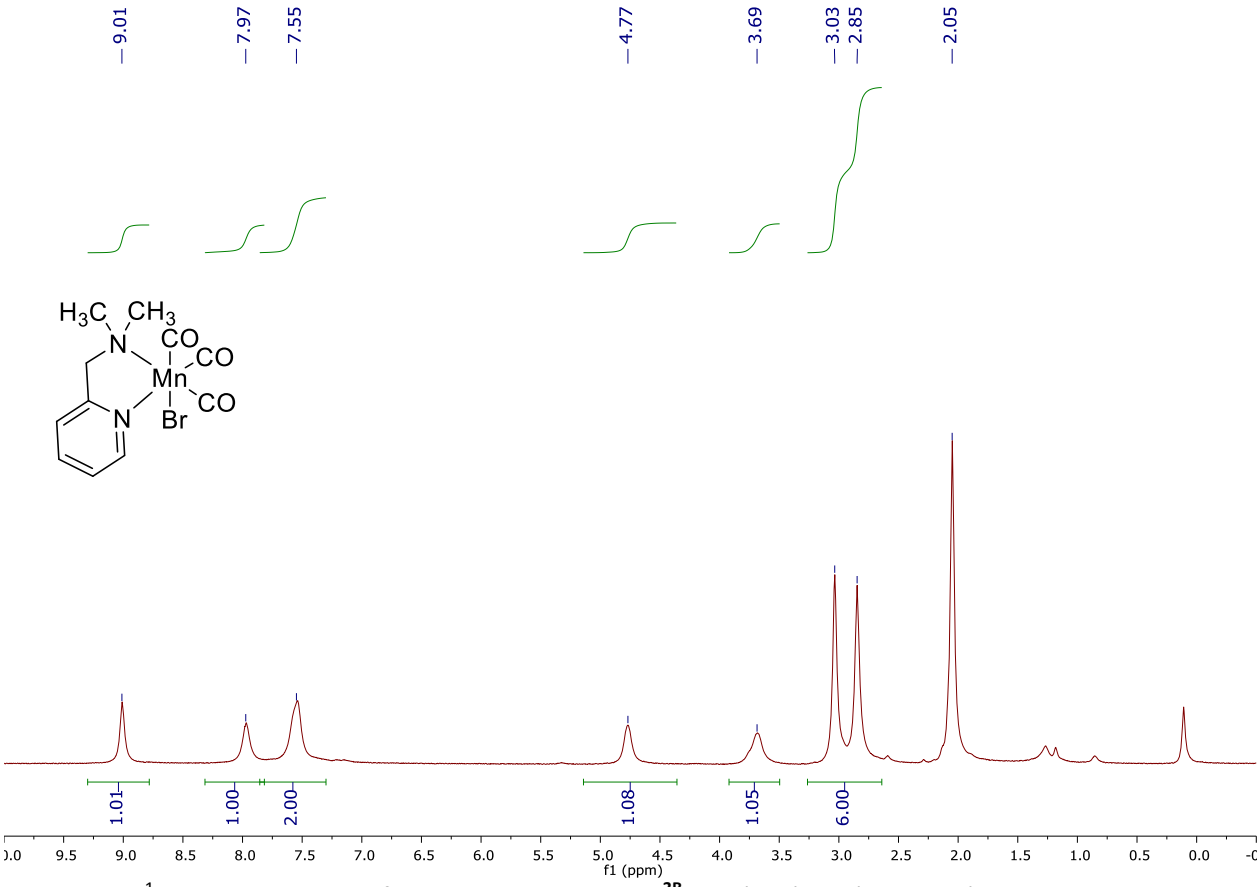

Figure S37: ^{1}H NMR spectrum of manganese complex **C^{3B}.3** in $(CD_3)_2CO$ (400 MHz).

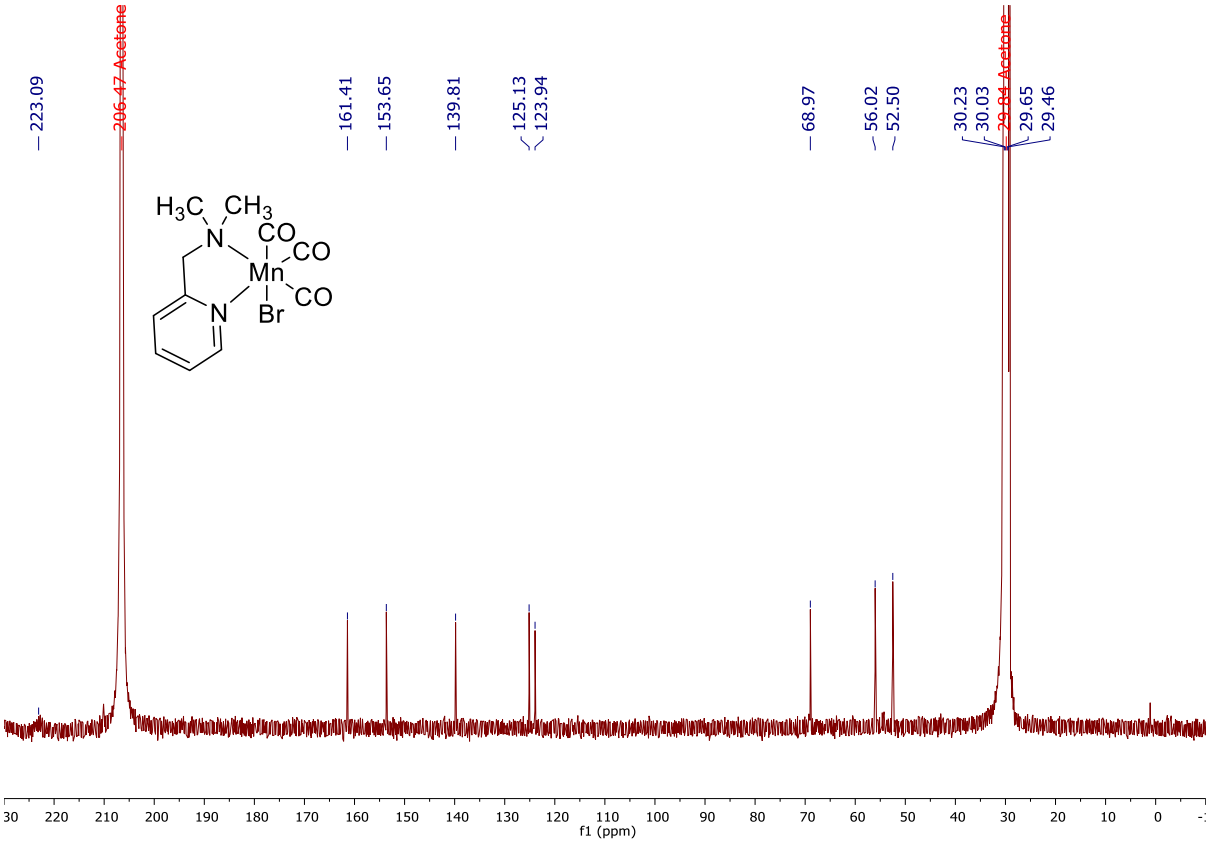

Figure S38: $^{13}C\{^{1}H\}$ NMR spectrum of manganese complex **C^{3B}.3** in $(CD_3)_2CO$ (101 MHz).

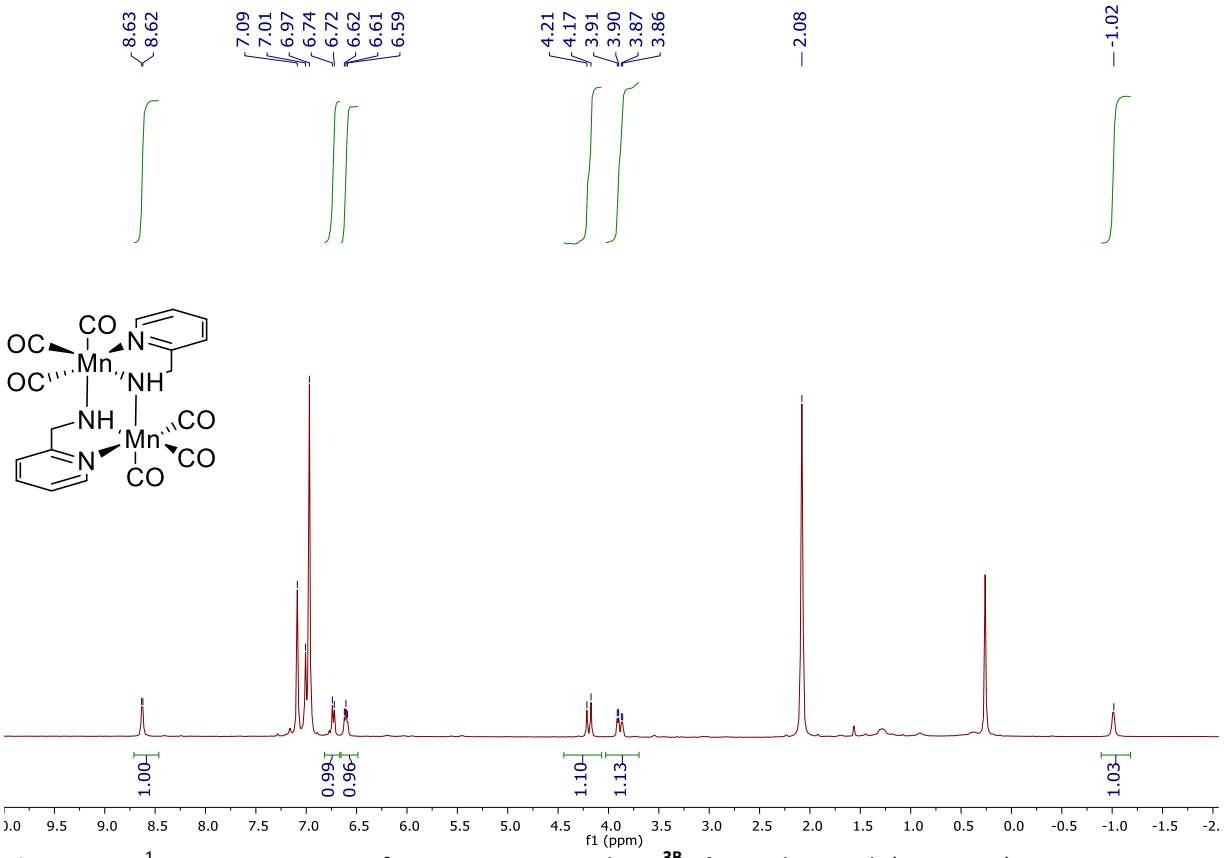

Figure S39: ^{1}H NMR spectrum of manganese complex **C^{3B}.1b** in toluene-d_8 (400 MHz).

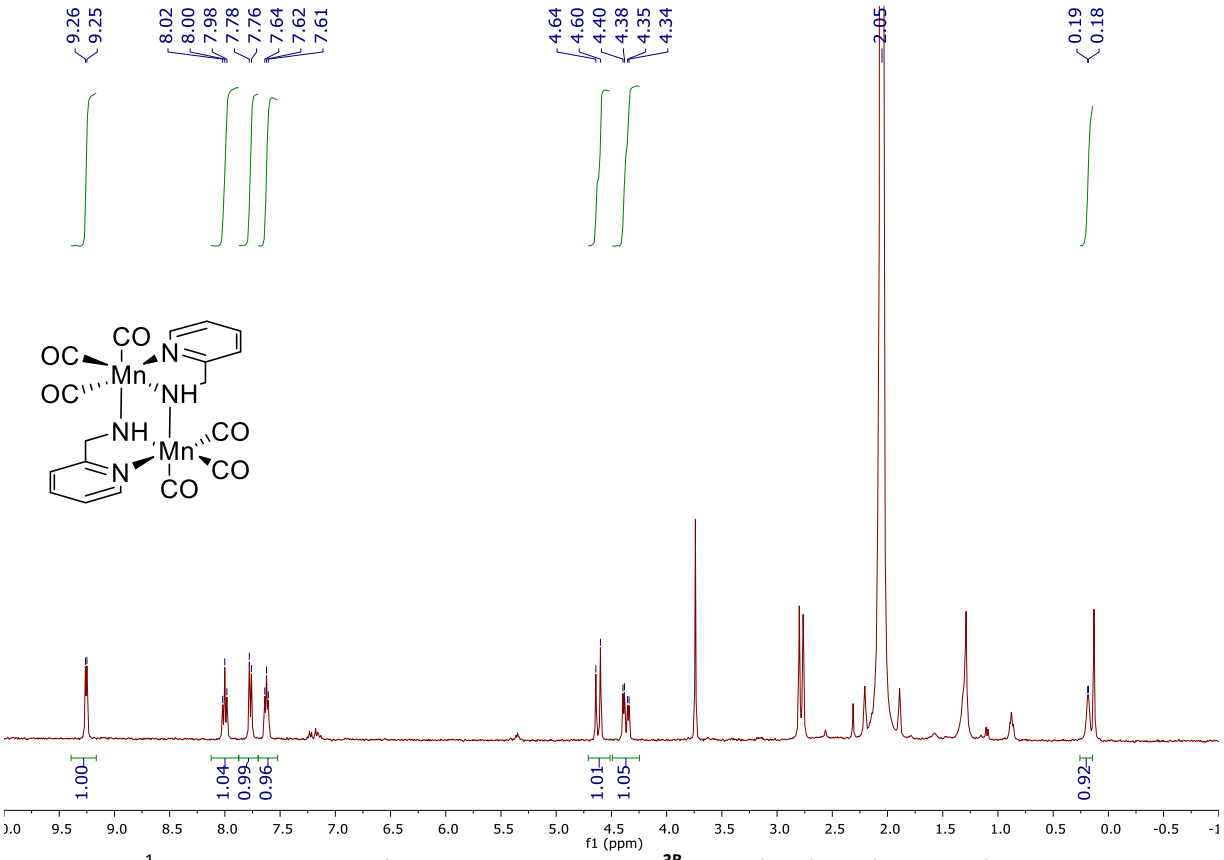

Figure S40: ^{1}H NMR spectrum of manganese complex **C^{3B}.1b** in $(CD_3)_2CO$ (400 MHz).

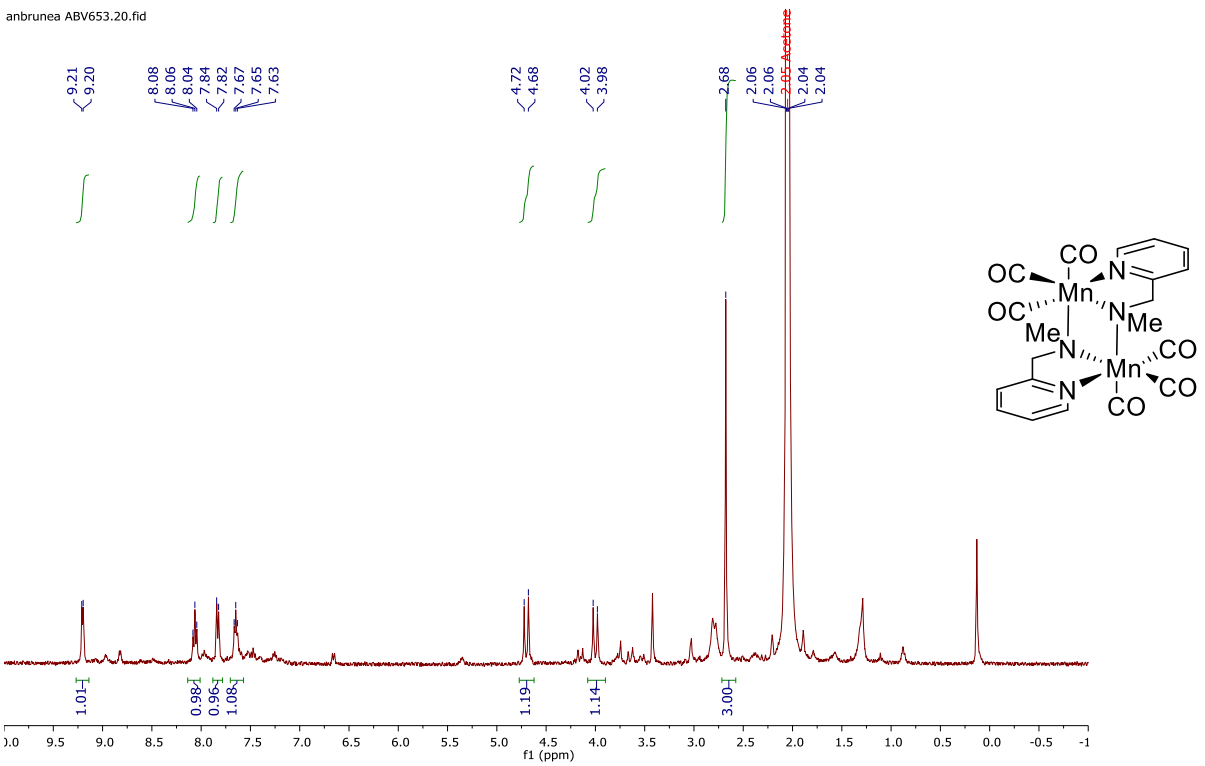

Figure S41: ^{1}H NMR spectrum of manganese complex **C^{3B}.2b** in $(CD_3)_2CO$ (400 MHz).

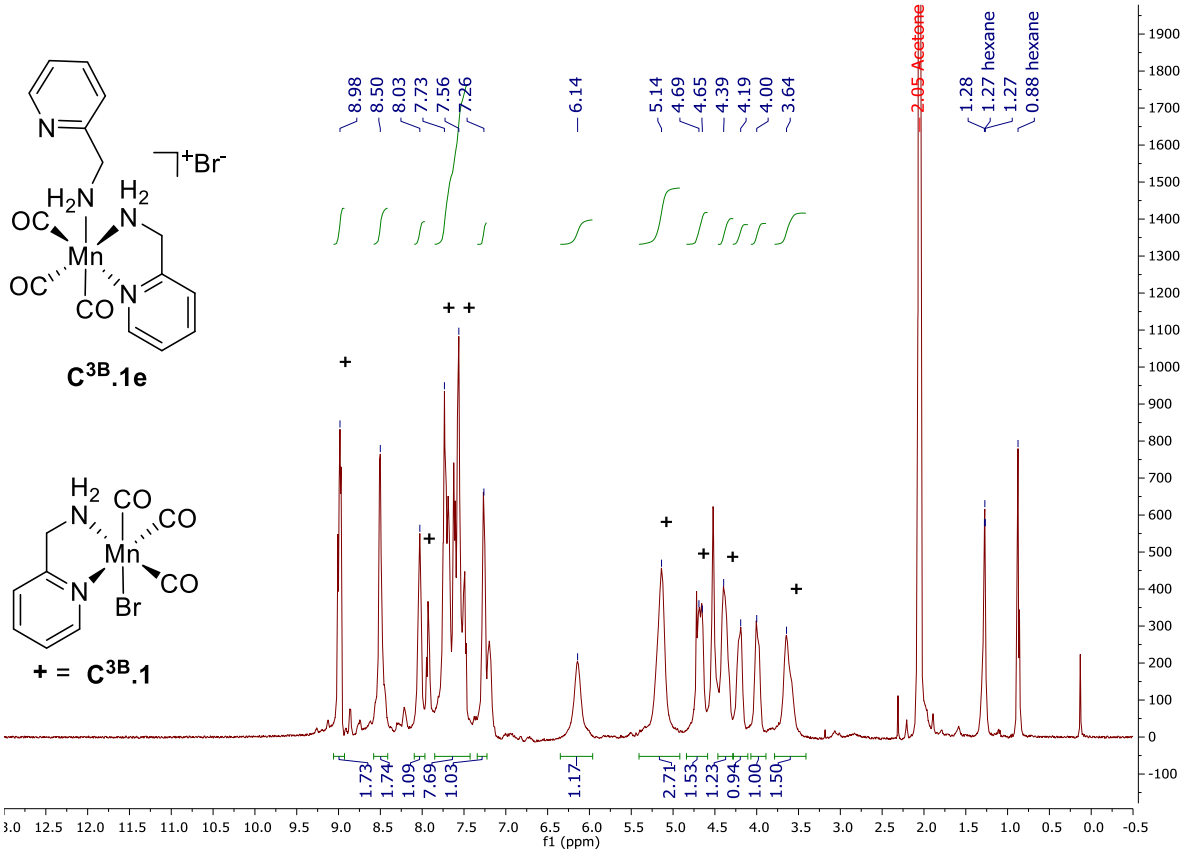

Figure S42: ^{1}H NMR spectrum of manganese complex **C^{3B}.1e** (with **C^{3B}.1**) in $(CD_3)_2CO$ (400 MHz).

Typical ^{1}H NMR of crude mixture after reaction

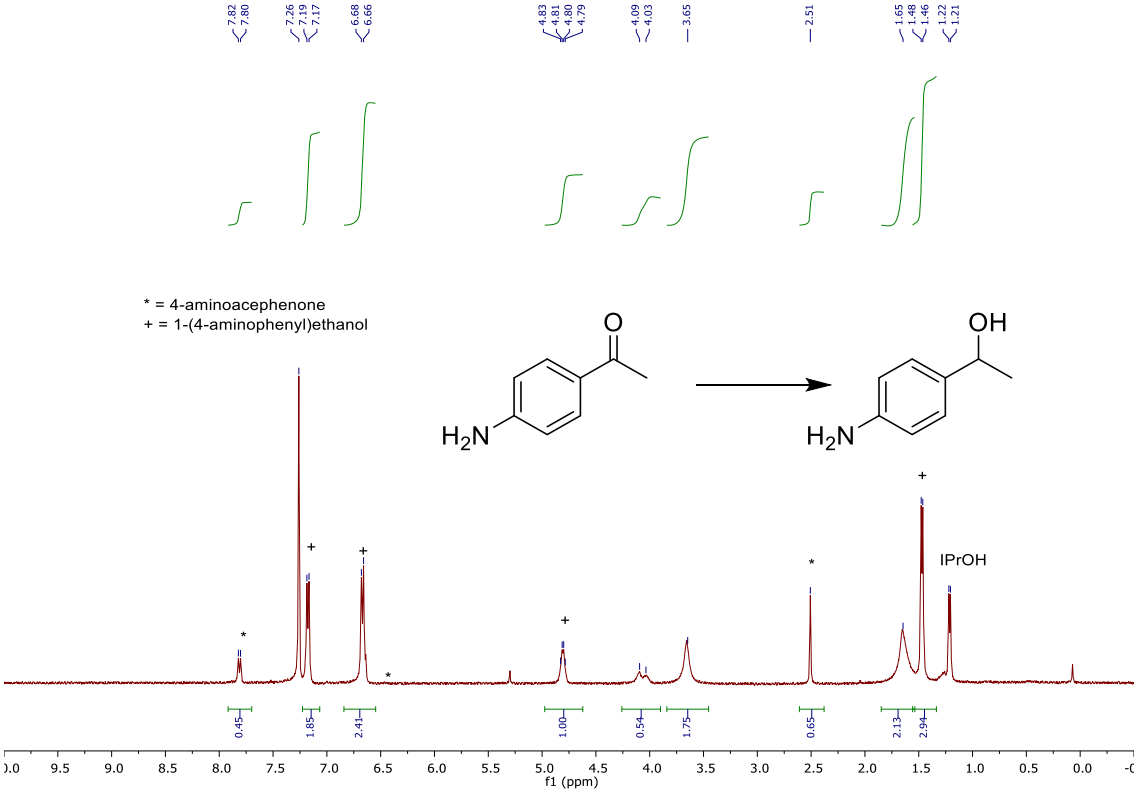

Figure S43: ^{1}H NMR spectrum of the crude mixture for the reduction of 4-aminoacetophenone recorded after 20 min at 80 °C at 300 MHz (82 % conversion).

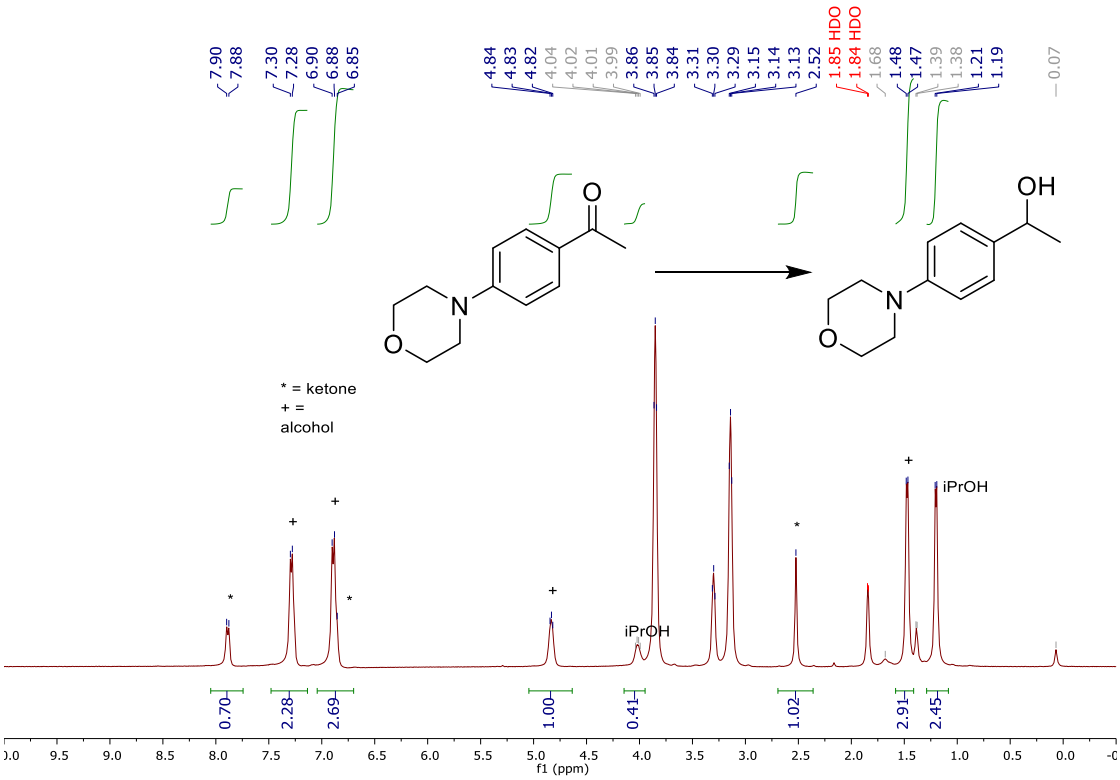

Figure S44: ^{1}H NMR spectrum of the crude mixture for the reduction of 4-morpholino-acetophenone recorded after 20 min at 80 °C at 300 MHz (74 % conversion).

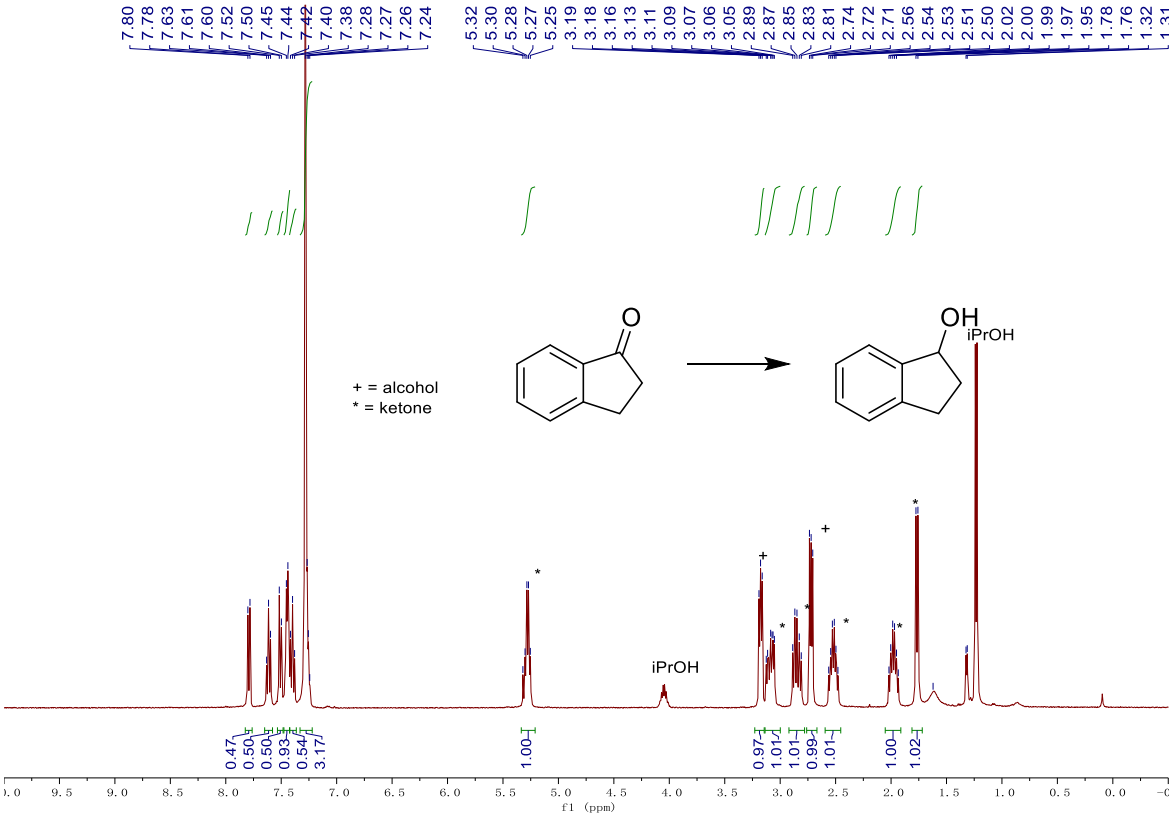

Figure S45: ^{1}H NMR spectrum of the crude mixture for the reduction of indanone recorded after 20 min at 80 °C at 300 MHz (67 % conversion).

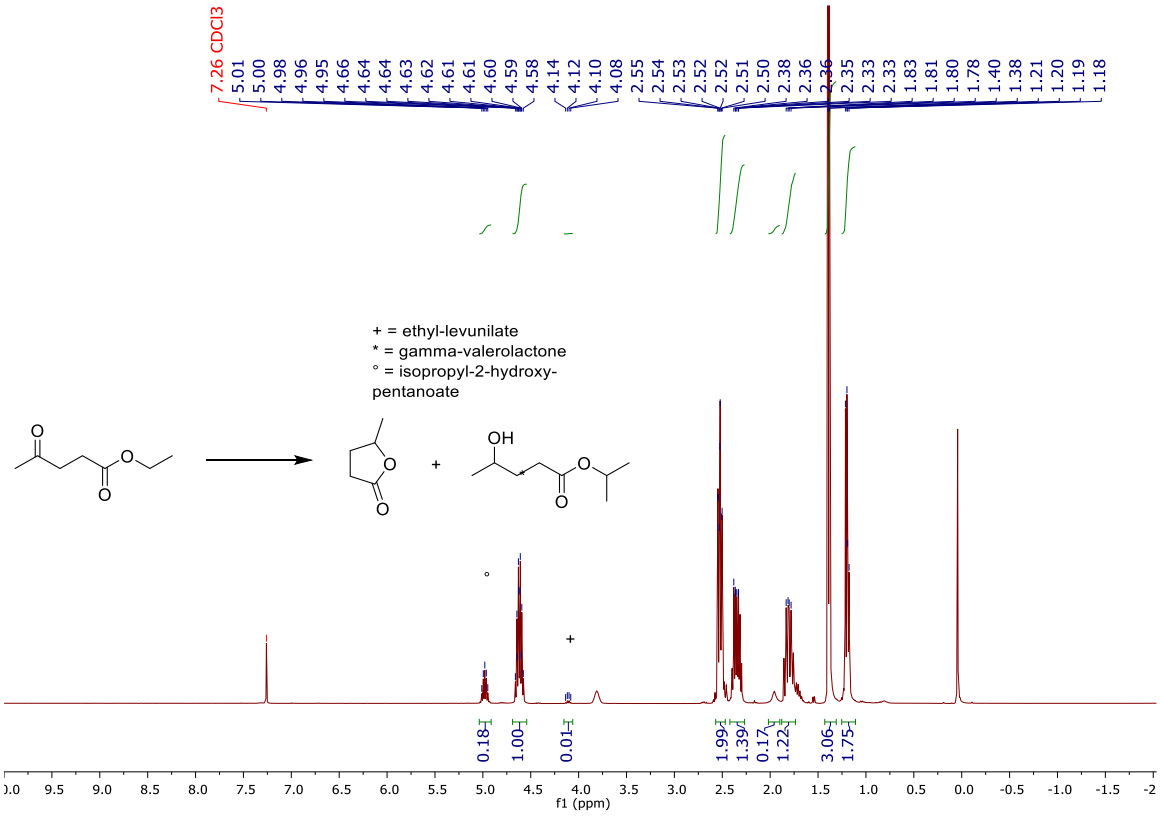

Figure S46: ^{1}H NMR spectrum of the crude mixture for the reduction of ethyl-levunilate recorded after 20 min at 80 °C at 300 MHz (67 % conversion).

References

[1] N. D. Schley, G. E. Dobereiner, R. H. Crabtree, *Organometallics* **2011**, *30*, 4174-4179.
[2] C. M. Alvarez, R. Carrillo, R. Garcia-Rodriguez, D. Miguel, *Chem. Commun.* **2012**, *48*, 7705-7707.
[3] J. Zheng, C. Darcel, J.-B. Sortais, *Catal. Sci. Technol.* **2013**, *3*, 81-84.
[4] D. Wei, T. Roisnel, C. Darcel, E. Clot, J.-B. Sortais, *ChemCatChem* **2017**, *9*, 80-83.
[5] A. Ouali, J.-P. Majoral, A.-M. Caminade, M. Taillefer,, *ChemCatChem* **2009**, *1*, 504-509.
[6] L. C. Misal Castro, D. Bézier, J.-B . Sortais, C. Darcel, *Adv. Synth. Catal.* **2011**, *353*, 1279-1284.
[7] J. Zheng, S. Elangovan, D. A. Valyaev, R. Brousses, V. César, J.-B. Sortais, C. Darcel, N. Lugan, G. Lavigne, *Adv. Synth. Catal.* **2014**, *356*, 1093-1097.
[8] L. Ford, F. Atefi, R. D. Singer, P. J. Scammells, *Eur. J. Org. Chem.* **2011**, 942-950.
[9] C. Azerraf, D. Gelman,, *Organometallics* **2009**, *28*, 6578-6584.
[10] F. Jiang, D. Bézier, J.-B. Sortais, C. Darcel, *Adv. Synth. Catal.* **2011**, *353*, 239-244.
[11] A. Bruneau-Voisine, D. Wang, T. Roisnel, C. Darcel, J.-B. Sortais, *Catal. Commun.* **2017**, *92*, 1-4.
[12] L. P. Bheeter, M. Henrion, L. Brelot, C. Darcel, M. J. Chetcuti, J.-B. Sortais, V. Ritleng, *Adv. Synth. Catal.* **2012**, *354*, 2619-2624.
[13] (a) D. Das, S. Roy, P. K. Das, *Org. Lett.* **2004**, *6*, 4133-4136; (b) B. T. Cho, S. K. Kang, M. S. Kim, S. R. Ryu, D. K. An, *Tetrahedron* **2006**, *62*, 8164-8168.
[14] G. M. Sheldrick, *Acta Cryst.* **2015**, *A71*, 3-8.
[15] G. M. Sheldrick, *Acta Cryst.* **2015**, *C71*, 3-8.

B- II- *In situ* formation of complexes

(1*R*, 2*R*)-(-)-1,2-diaminocyclohexane, (*R*)-(+)-2,2'-diamino-1,1'-binaphthalene and (1*R*,2*R*)-(+)-N,N'-Dimethyl-1,2-diphenyl-1,2-ethane diamine were purchased from Acros Organics, (1*R*,2*R*)-(-)-N-p-tosyl-1,2-cyclohexanediamine, (1*S*,2*S*)-trans-1,2-cyclopentanediamine dihydrochloride and (1*S*, 2*S*)-1,2-di-1-naphthyl-ethylenediamine dihydrochloride from Aldrich, and (1*R*,2*R*)-(+)-1,2-diphenyl-1,2-ethanediamine, (1*S*,2*S*)-(+)-trans-1,2-Bis(methylamino)cyclohexane from Alfa Aesar.

Enantiomeric excess were determined by GC analyses performed on GC-2014 (Shimadzu) 2010 apparatus equipped with Supelco betaDEX 120 column (30 m x 0.25 mm) (method 1: 120 °C for 20 min, than 20 °C/min to 200 °C, 200 °C for 5 min; method 2: 80°C, than 1.5 °C/min to 140 °C, than 15 °C/min to 170 °C, 170 °C for 10 min; method 3: 140 °C for 20 min, than 20 °C/min to 200 °C, 200 °C for 10 min; method 4: 90°C, than 1.5 °C/min to 140 °C, than 5 °C/min to 220 °C, 220 °C for 10 min; method 5: 120 °C for 90 min, than 10 °C/min to 200 °C, 200 °C for 5 min; method 6: 150 °C for 45 min, than 5 °C/min to 200 °C, 200 °C for 10 min; method 7: 170 °C for 15 min, than 2 °C/min to 200 °C, 200 °C for 5 min).

The determination of the absolute configuration was done by comparison with (S)-alcohol obtained by kinetic resolution of racemic alcohol with Novozym 435 (Candida Antarctica Lipase B) and by comparison of the retention time with the literature.[1-3]

General procedure for in situ transfer hydrogenation reactions

Representative procedure for transfer hydrogenation reaction of acetophenone.

To a solution of acetophenone (58 µL, 0.5 mmol) in *i*PrOH (0.5 mL) was added a stock solution of manganese pentacarbonyl bromide (0.5 mL, 0.005 mol.L^{-1}; 2.7 mg, 0.010 mmol, in 2 mL *i*PrOH) followed, in this order, by a stock solution of ethylenediame (0.5 mL, 0.005 mol.L^{-1}; 1.0 µL, 0.0125 mmol, in 2.5 mL *i*PrOH) and *t*BuOK (0.5 mL, 0.010 mol.L^{-1}; 2.4 mg, 0.020 mmol, in 2 mL *i*PrOH). The reaction mixture was stirred for 3 h at 80 °C in an oil bath. The solution was then filtered through a small pad of silica (2 cm in a Pasteur pipette). The silica was washed with ethyl acetate. The filtrate was evaporated and the conversion was determined by ^{1}H NMR. The crude residue was then purified by column chromatography (SiO_2, mixture of petroleum ether/ethyl acetate or dietyl ether as eluent), giving the corresponding alcohol as a colorless oil (55 mg, 92%).

Representative procedure for asymmetric transfer hydrogenation reaction of acetophenone with diamine ligand.

To a solution of acetophenone (58 µL, 0.5 mmol) in *i*PrOH (0.5 mL) was added a stock solution of manganese pentacarbonyl bromide (0.5 mL, 0.010 mol.L^{-1}) followed, in this order, by a stock solution of *(1R,2R)-(-)-1,2-diaminocyclohexane* (0.5 mL, 0.010 mol.L^{-1}; 1.2 mg, 0.010 mmol, in 1.0 mL *i*PrOH) and *t*BuOK (0.5 mL, 0.020 mol.L^{-1}). The mixture was stirred for 3 h at 80 °C in a pre-heated oil bath. The solution was then filtered through a small pad of silica (2 cm in a Pasteur pipette). The filtrate was then fulfilled with pre-dried ethyl acetate in a GC test bottle. The crude reaction mixture was then analyzed by chiral GC chromatography, giving 43% *e.e.* value. Conversion was determined by ^{1}H NMR.

Representative procedure for asymmetric transfer hydrogenation reaction of acetophenone.

Procedure: In glovebox, to a schlenk tube containing the chiral ligand (0.5mol%)) was added a solution of acetophenone (232 µL, 2 mmol) in *i*PrOH (8 mL a stock manganese pentacarbonyl bromide (0.5 mol%, 2.7 mg) followed, in this order, *t*BuOK (1 mol%, 1.1 mg). The mixture was stirred for 15 min. at 80 °C in a pre-heated oil bath. Aliquot of the solution was then filtered through a small pad of silica (2 cm in a Pasteur pipette). The filtrate was then fulfilled with pre-dried ethyl acetate in a GC test bottle. The crude reaction mixture was then analyzed by chiral GC chromatography. Conversion was determined by ^{1}H NMR.

Synthesis of well-defined complexes

Complex **C^{3B}.21**

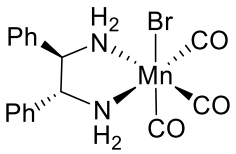

To a solution of (1*R*,2*R*)-(+)-1,2-diphenyl-1,2-ethanediamine **L^{3B}.21** (0.71 mmol, 150 mg) in toluene was added 1 equivalent of manganese pentacarbonyl bromide (0.71 mmol, 194 mg). After stirring at 110 °C during 3 h, the toluene was evaporated under reduced pressure to afford a dark-yellow solid.

This solid was washed two times with pentane and Et_2O to give complex **C^{3B}.21**, as a yellow powder (274 mg, 89% yield).

^{1}H NMR (400 MHz, Acetone-d_6) δ 7.70 – 6.76 (m, 10H), 5.52 (d, *J* = 8 Hz, 1H), 4.62 (t, *J* = 12 Hz, 1H), 4.37 (td, *J* = 12, 4 Hz, 1H), 4.20 (td, *J* = 12, 4 Hz, 1H), 4.11 (dd, *J* = 8, 4 Hz, 1H), 3.31 (t, *J* = 12 Hz, 1H).

IR (ν, cm^{-1}, CH_2Cl_2): 2020, 1924, 1895.

Complex **C^{3B}.27**

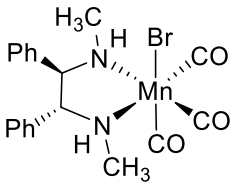

To a solution of (1*R*,2*R*)-(+)-*N*,*N*'-dimethyl-1,2-diphenyl-1,2-ethane diamine **L^{3B}.27** (0.42 mmol, 100 mg) in toluene was added 1 equivalent of manganese pentacarbonyl bromide (0.42 mmol, 115 mg). After stirring at 110 °C during 3 h, the toluene was evaporated under reduced pressure to afford a yellow oily-solid. This oily-solid was dissolved in dichloromethane and pentane was added to precipitate it. After filtration the solid was washed two times with pentane to give complex **C^{3B}.27**, as a yellow powder (152 mg, 79% yield) (not highly pure according to NMR analysis).

^{1}H NMR (400 MHz, Acetone-d_6) δ 7.22 (m, 10H), 5.24 (br s, 1H), 4.19 (t, *J* = 12 Hz, 1H), 4.04 (br s + t, 1 + 1H), 2.73 (d, *J* = 4 Hz, 3H), 2.60 (d, *J* = 4 Hz, 3H).

^{13}C NMR (101 MHz, Acetone-d_6) δ 223.0 (br CO), 222.3 (br CO), 138.0, 137.4, 129.6, 129.3, 129.2, 129.1, 75.1, 71.6, 42.2, 38.82.

IR (ν, cm^{-1}, CH_2Cl_2): 2022, 1927, 1897.

Complex **C^{3B}.30**

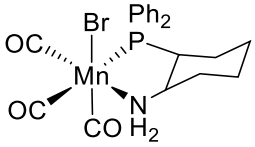

To a solution of (1*R*,2*R*)-2-(diphenylphosphino)cyclohexylamine **L^{3B}.30** (0.39 mmol, 110 mg) in toluene was added 1 equivalent of manganese pentacarbonyl bromide (0.39 mmol, 107 mg). After stirring at 110 °C during 3 h, the toluene was evaporated under reduced pressure to afford a yellow solid. This solid was washed two times with pentane and Et_2O to give complex **C^{3B}.21**, as a yellow powder (184 mg, 94% yield) (not highly pure according to NMR analysis).

^{31}P NMR (162 MHz, CD_2Cl_2) δ 67.8, 57.8.

^{1}H NMR (400 MHz, CD_2Cl_2) δ 7.68 (m, 2H), 7.60 – 7.34 (m, 8H), 3.67 (s, 1H), 2.52 (m, 2H), 2.42 – 2.21 (m, 2H), 1.99 (d, J = 14.0 Hz, 1H), 1.78 (d, J = 14.0 Hz, 1H), 1.67 (d, J = 14.0 Hz, 1H), 1.45 – 1.17 (m, 2H), 1.10 (q, J = 13 Hz, 1H), 0.69 (m, 1H).

NMR data for manganese complexes

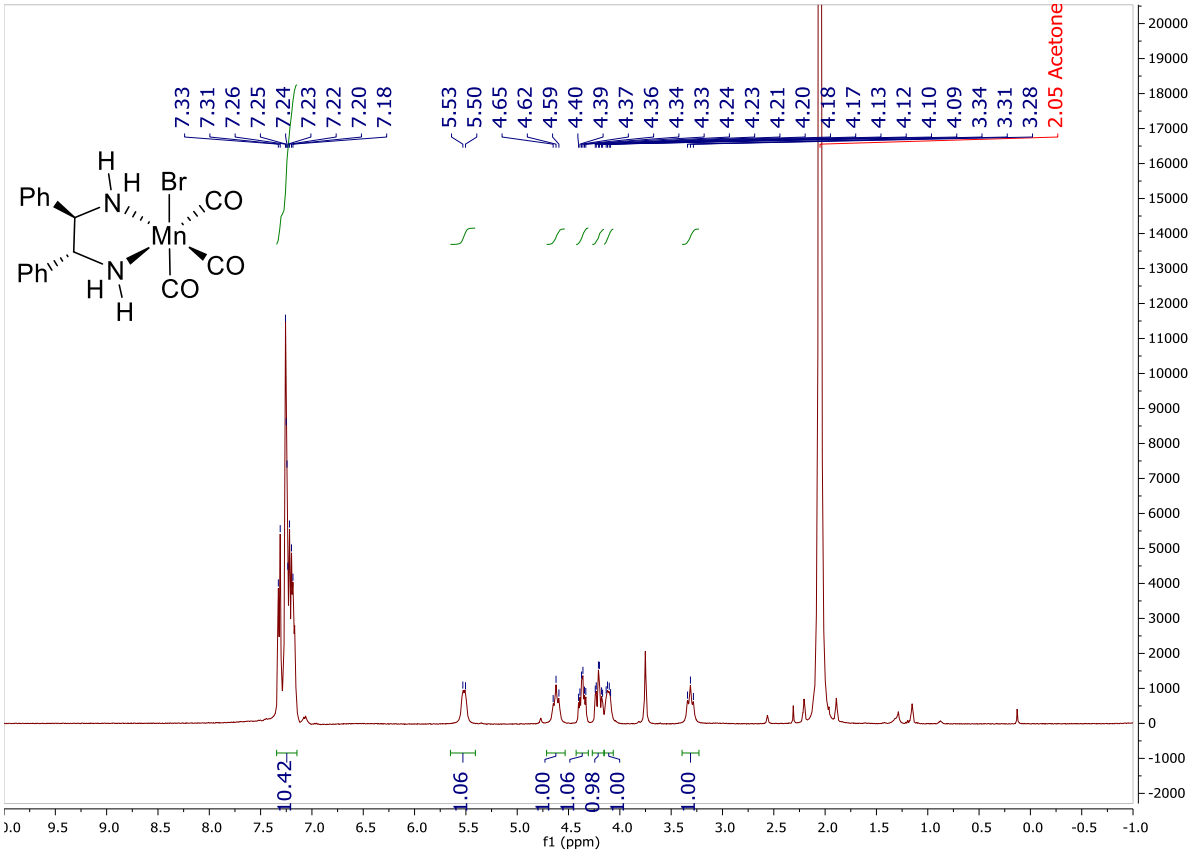

Figure S47: ^{1}H NMR spectrum of manganese complex **C^{3B}.21** in $(CD_3)_2CO$ recorded at 400 MHz.

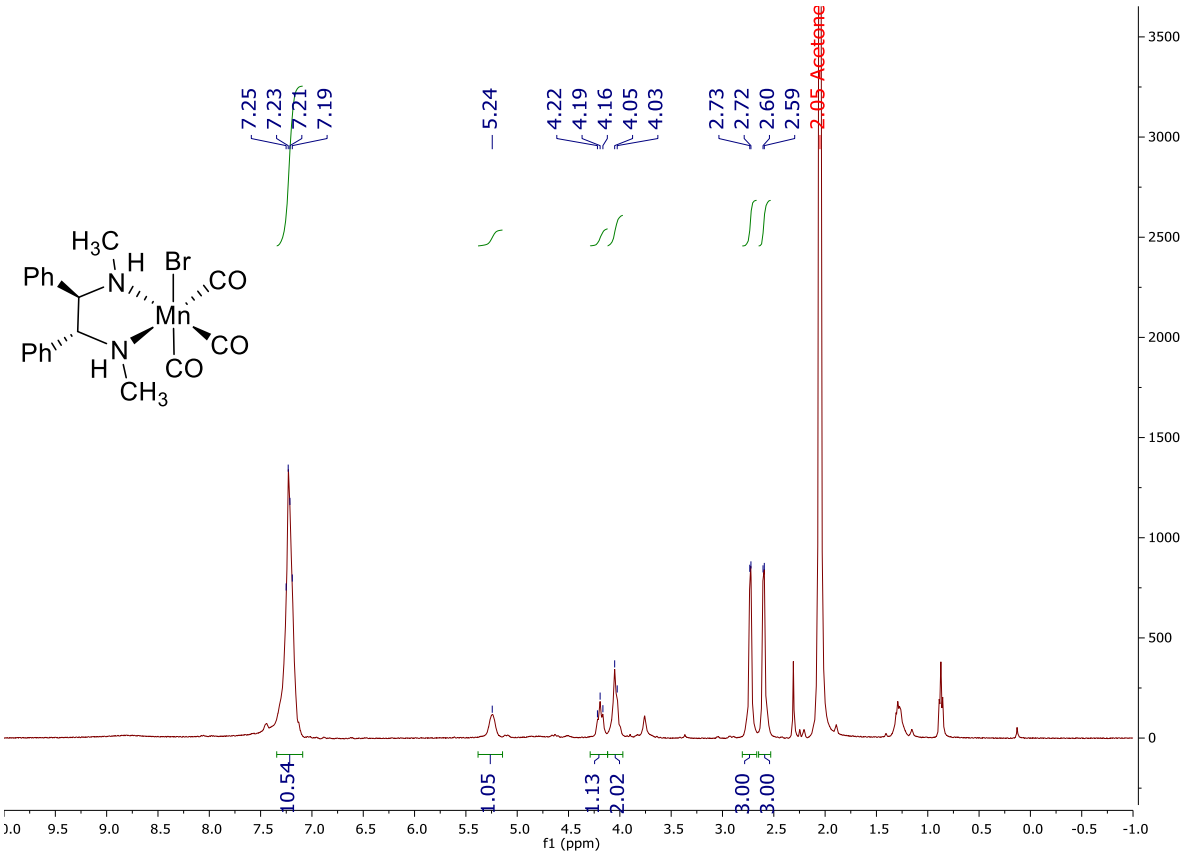

Figure S48: ^{1}H NMR spectrum of manganese complex **C^{3B}.27** in $(CD_3)_2CO$ recorded at 400 MHz.

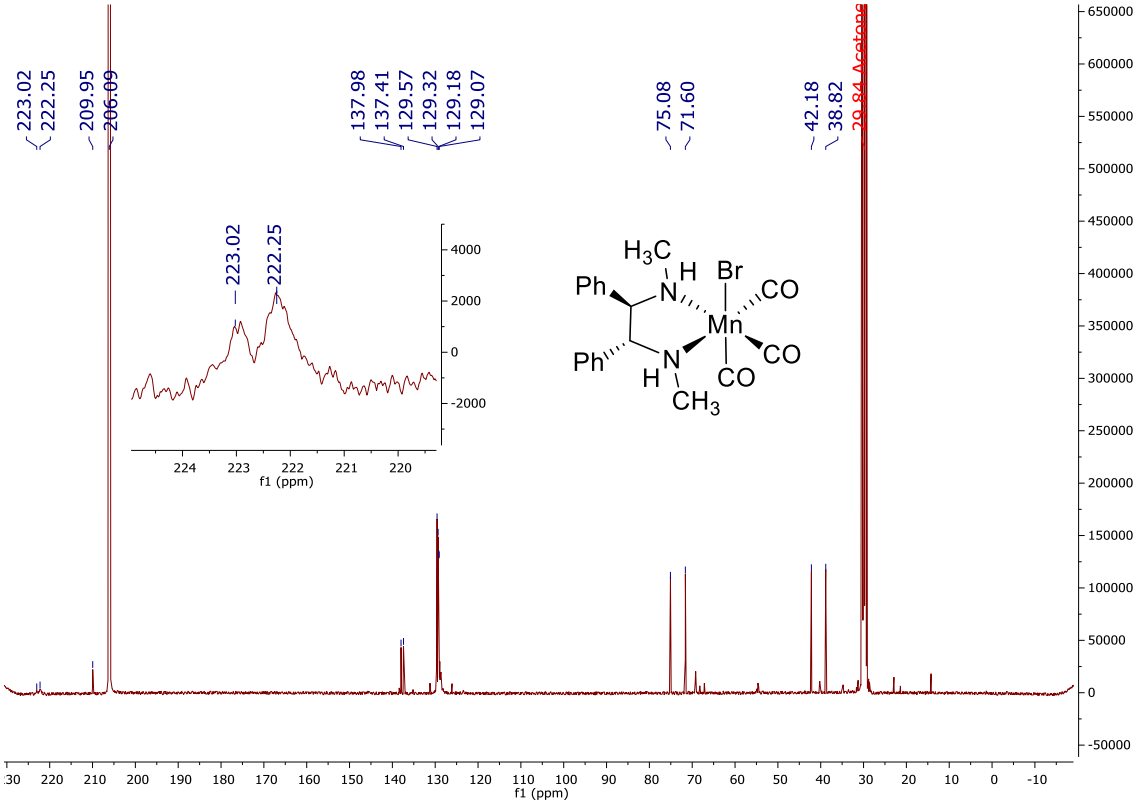

Figure S49: $^{13}C\{^{1}H\}$ NMR spectrum of manganese complex **C^{3B}.27** in $(CD_3)_2CO$ recorded at 101 MHz.

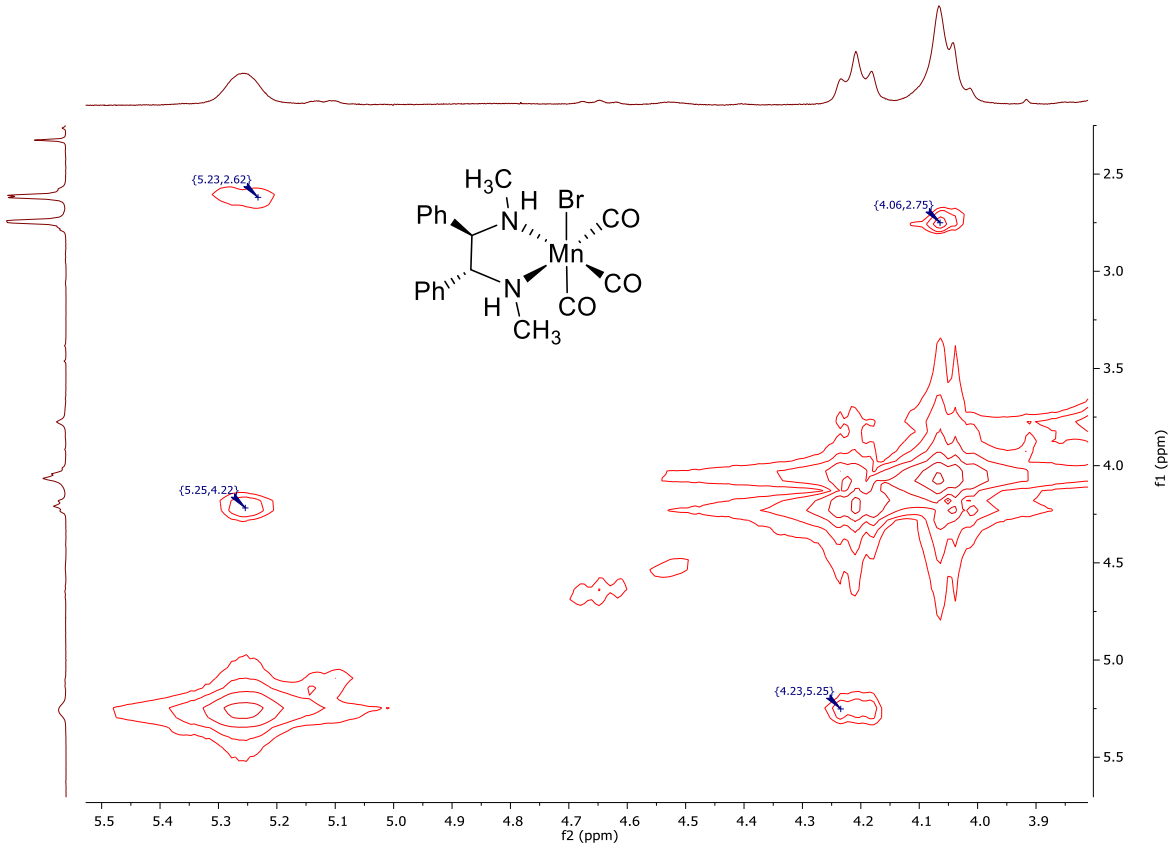

Figure S50: ^{1}H COSY NMR spectrum of complex **C^{3B}.27** in $(CD_3)_2CO$ recorded at 400 MHz.

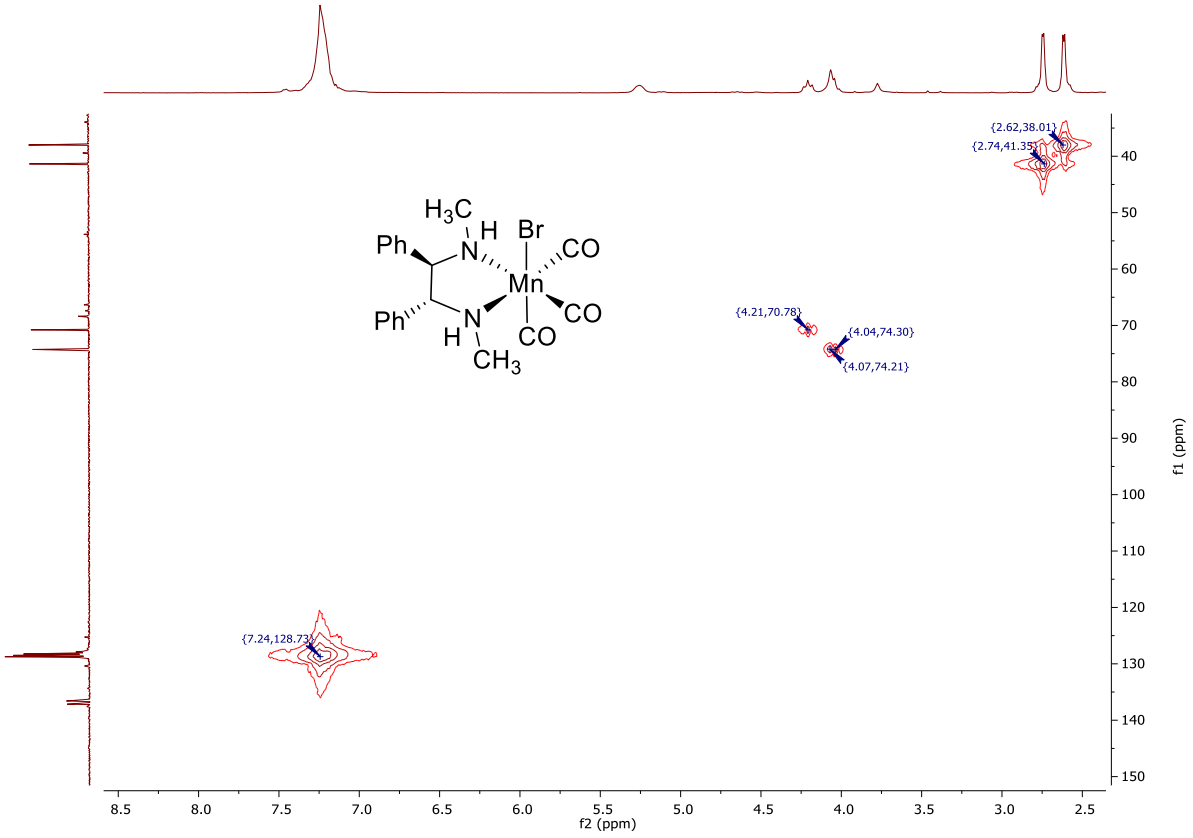

Figure S51: HSQC Edited NMR spectrum of complex **C^{3B}.27** in $(CD_3)_2CO$ recorded at 400/101 MHz.

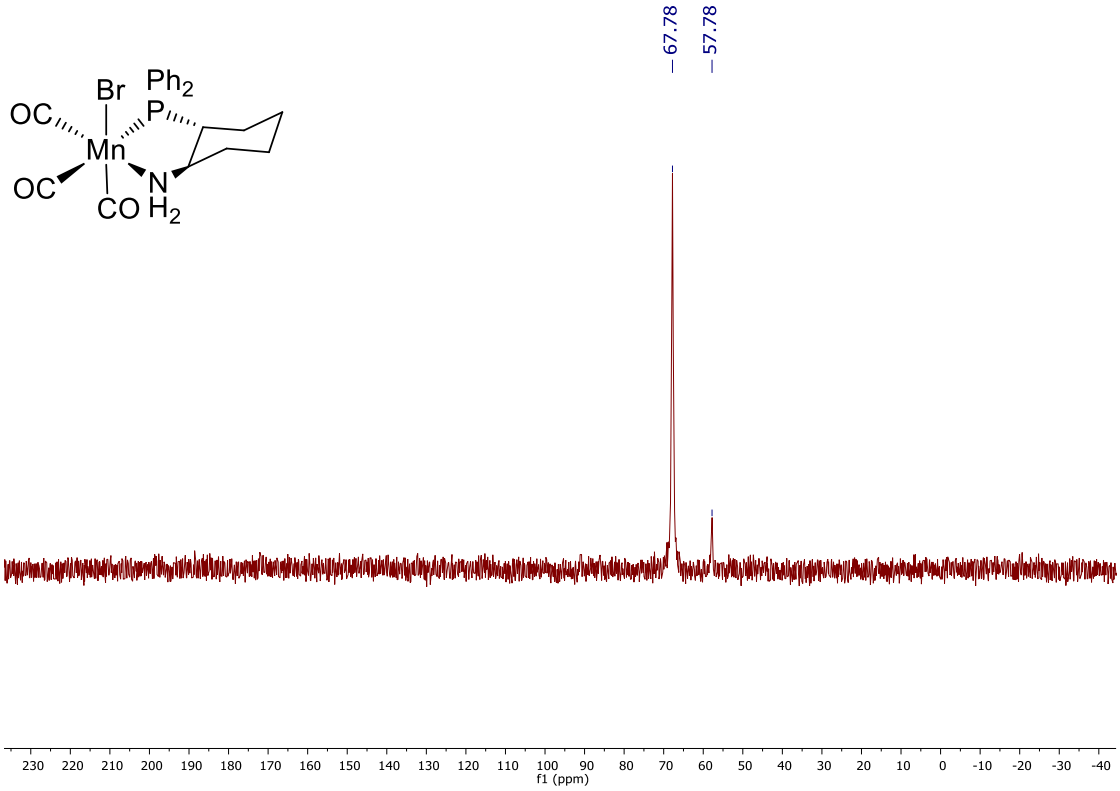

Figure S52: $^{31}P\{^1H\}$ NMR spectrum of the synthesis of complex **C^{3B}.30** in CD_2Cl_2 recorded at 162 MHz.

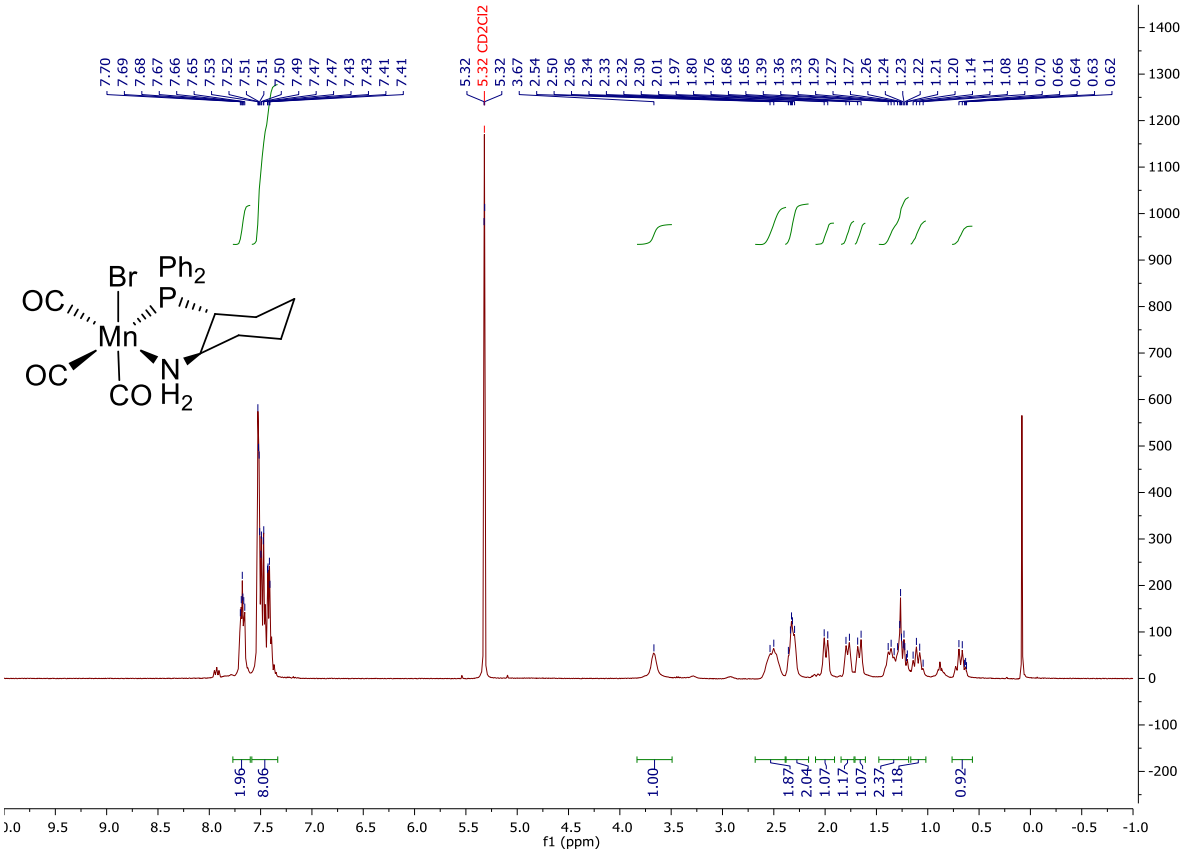

Figure S53: ^{1}H NMR spectrum of manganese complex **C^{3B}.30** in CD_2Cl_2 recorded at 400 MHz.

Characterization of the products of the catalysis

1-Phenylethanol (b1)

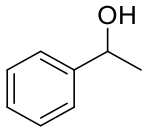

According to general procedure, acetophenone **a1** (58µL, 0.5 mmol) gave the title compound **b1** as a colorless oil (55 mg, 92%)

^{1}H NMR (400 MHz, $CDCl_3$) δ 7.44 – 7.30 (m, 5H), 4.90 (q, *J* = 6.5 Hz, 1H), 2.51 (s, 1H), 1.53 (d, *J* = 6.5 Hz, 3H).

$^{13}C\{^{1}H\}$ NMR (101 MHz, $CDCl_3$) δ 145.9, 128.5, 127.4, 125.4, 70.3, 25.2.

1-Phenylpropanol (b2)

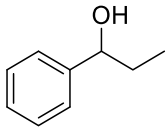

According to general procedure, propiophenone **a2** (66 µL, 0.5 mmol) gave the title compound **b2** as a colorless oil (62 mg, 91%).

^{1}H NMR (300 MHz, $CDCl_3$) δ 7.43 – 7.21 (m, 5H), 4.58 (t, *J* = 6.5 Hz, 1H), 2.48 (s, 1H), 1.94 – 1.64 (m, 2H), 0.93 (t, *J* = 7.4 Hz, 3H).

$^{13}C\{^{1}H\}$ NMR (101 MHz, $CDCl_3$) δ 144.7, 128.4, 127.4, 126.0, 76.0, 31.9, 10.2.

1-Phenyl-2-methylpropanol (b3)

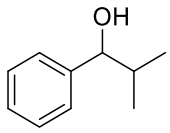

According to general procedure, isobutyrophenone **a3** (75µL, 0.5 mmol) gave the title compound **b3** as a colorless oil (73 mg, 97%).

^{1}H NMR (300 MHz, $CDCl_3$) δ 7.54 – 7.21 (m, 5H), 4.39 (d, *J* = 6.8 Hz, 1H), 2.29 (s, 1H), 2.01 (oct, *J* = 6.8 Hz, 1H), 1.07 (d, *J* = 6.8 Hz, 3H), 0.86 (d, *J* = 6.8 Hz, 3H).

$^{13}C\{^{1}H\}$ NMR (75 MHz, $CDCl_3$) δ 143.7, 128.2, 127.4, 126.7, 80.0, 35.3, 19.0, 18.4.

Cyclopropylphenylmethanol (b4)

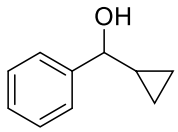

According to general procedure cyclopropyl phenyl ketone **a4** (69 µL, 0.5mmol) gave the title compound **b4** as a colorless oil (52 mg, 70 %).

^{1}H NMR (400 MHz, $CDCl_3$) δ 7.45-7.41 (m, 2H), 7.39 – 7.33 (m, 2H), 7.32 – 7.26 (m, 1H), 4.02 (d, *J* = 8.3 Hz, 1H), 1.94 (s, 1H), 1.26 – 1.20 (m, 1H), 0.67-0.61 (m, 1H), 0.60 – 0.52 (m, 1H), 0.51-0.45 (m, 1H), 0.43 – 0.32 (m, 1H).

$^{13}C\{^{1}H\}$ NMR (101 MHz, $CDCl_3$) δ 143.9, 128.5, 127.7, 126.2, 78.7, 19.4, 3.7, 3.0.

2,2-Dimethyl-1-phenylpropanol (b5)

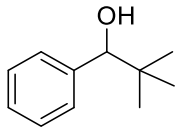

According to general procedure, pivalophenone **a5** (84 µL, 0. 5 mmol) gave the title compound **b5** as a colorless oil (79 mg, 96%).

^{1}H NMR (300 MHz, $CDCl_3$) δ 7.41 – 7.22 (m, 5H), 4.39 (s, 1H), 2.21 (s, 1H), 0.96 (s, 9H).

$^{13}C\{^{1}H\}$ NMR (101 MHz, $CDCl_3$) δ 142.3, 127.7, 127.6, 127.3, 82.4, 35.6, 26.0.

1-(2-Methylphenyl)ethanol (b6)

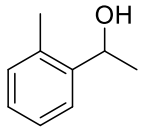

According to general procedure, 2'-methylacetophenone **a6** (65 µL, 0.5 mmol) gave the title compound **b6** as a yellow oil (66 mg, 97%).

^{1}H NMR (300 MHz, $CDCl_3$) δ 7.55 (d, *J* = 7.4 Hz, 1H), 7.33 – 7.15 (m, 3H), 5.12 (q, *J* = 6.4 Hz, 1H), 2.67 (s, 1H), 2.38 (s, 3H), 1.49 (d, *J* = 6.4 Hz, 3H).

$^{13}C\{^{1}H\}$ NMR (75 MHz, $CDCl_3$) δ 144.0, 134.2, 130.3, 127.1, 126.4, 124.6, 66.7, 23.9, 18.9.

1-(2-Methoxyphenyl)ethanol (b7)

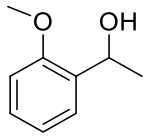

According to general procedure, 2′-methoxyacetophenone **a7** (69 µL, 0.5 mmol) gave the title compound **b7** as a yellow oil (74 mg, 97%).
^{1}H NMR (300 MHz, $CDCl_3$) δ 7.40 (d, *J* = 7.4 Hz, 1H), 7.28 (t, *J* = 7.7 Hz, 1H), 7.00 (t, *J* = 7.4 Hz, 1H), 6.91 (d, *J* = 8.2 Hz, 1H), 5.15 (q, *J* = 6.4 Hz, 1H), 3.88 (s, 3H), 2.98 (s, 1H), 1.53 (d, *J* = 6.2 Hz, 3H).
^{13}C{^{1}H} NMR (101 MHz, $CDCl_3$) δ 156.5, 133.7, 128.2, 126.1, 120.8, 110.4, 66.4, 55.3, 23.1.

1-(2-Chlorophenyl)ethanol (b8)

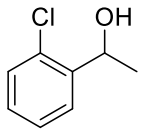

According to general procedure, 2′-chloroacetophenone **a8** (65 µL, 0.5 mmol) gave the title compound **b8** as a yellow oil (74 mg, 95%).
^{1}H NMR (300 MHz, $CDCl_3$) δ 7.62 – 7.54 (m, 1H), 7.35-7.27 (m, 2H), 7.20 (td, *J* = 7.6, 1.5 Hz, 1H), 5.27 (qd, *J* = 6.4, 2.9 Hz, 1H), 3.35 (s, 1H), 1.47 (d, *J* = 6.5 Hz, 3H).
^{13}C{^{1}H} NMR (75 MHz, $CDCl_3$) δ 143.2, 131.5, 129.3, 128.3, 127.2, 126.5, 66.7, 23.6.

1-(2-Bromophenyl)ethanol (b9)

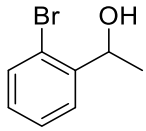

According to general procedure, 2′-bromoacetophenone **a9** (68 µL, 0.5 mmol) gave the title compound **b9** as a colorless oil (84 mg, 84%).
^{1}H NMR (400 MHz, $CDCl_3$) δ 7.60 (dd, *J* = 7.8, 1.8 Hz, 1H), 7.52 (dd, *J* = 8.0, 1.3 Hz, 1H), 7.34 (tdd, *J* = 7.8, 1.3, 0.5 Hz, 1H), 7.13 (td, *J* = 7.7, 1.8 Hz, 1H), 5.25 (qd, *J* = 6.4, 3.5 Hz, 1H), 1.96 (d, *J* = 3.5 Hz, 1H), 1.49 (d, *J* = 6.4 Hz, 3H).

^{13}C{^{1}H} NMR (101 MHz, $CDCl_3$) δ 144.7, 132.8, 128.9, 128.0, 126.8, 121.9, 69.4, 23.7.

1-(4-Methylphenyl)ethanol (b10)

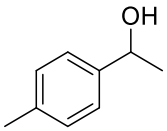

According to general procedure, 4′-methylacetophenone **a10** (67 µL, 0.5 mmol) gave the title compound **b10** as a colorless oil (62 mg, 91%).
^{1}H NMR (400 MHz, $CDCl_3$) δ 7.28 (d, *J* = 8.0 Hz, 2H), 7.18 (d, *J* = 7.9 Hz, 2H), 4.86 (q, *J* = 6.5 Hz, 1H), 2.37 (s, 3H), 2.06 (s, 1H), 1.49 (d, *J* = 6.5 Hz, 3H).
^{13}C{^{1}H} NMR (101 MHz, $CDCl_3$) δ 142.9, 137.1, 129.2, 125.4, 70.2, 25.1, 21.1.

1-(4-Methoxyphenyl)ethanol (b11)

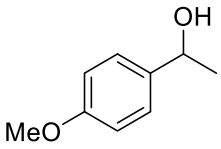

According to general procedure, 4-methoxyacetophenone **a11** (75 mg, 0.5 mmol) gave the title compound **b11** as a colourless oil (56 mg, 74 %).
^{1}H NMR (400 MHz, $CDCl_3$) δ 7.33 – 7.29 (m, 2H), 6.91-6.86 (m, 2H), 4.86 (q, *J* = 6.4 Hz, 1H), 3.80 (s, 3H), 1.79 (s, 1H), 1.48 (d, *J* = 6.4 Hz, 3H).
$^{13}C\{^{1}H\}$ NMR (101 MHz, $CDCl_3$) δ 159.1, 138.1, 126.8, 114.0, 70.1, 55.4, 25.2.

1-(4-Chlorophenyl)ethanol (b12)

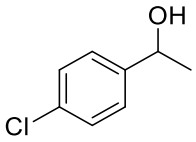

According to general procedure, 4'-chloroacetophenone **a12** (65 µL, 0.5 mmol) gave the title compound **b12** as a yellow oil (70 mg, 90%).
^{1}H NMR (300 MHz, $CDCl_3$) δ 7.35 – 7.21 (m, 4H), 4.81 (q, *J* = 6.5 Hz, 1H), 2.85 (s, 1H), 1.44 (d, *J* = 6.5 Hz, 3H).
$^{13}C\{^{1}H\}$ NMR (101 MHz, $CDCl_3$) δ 144.3, 132.9, 128.5, 126.8, 69.6, 25.2.

4-(1-Hydroxyethyl)benzonitrile (b13)

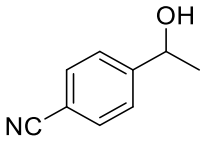

According to general procedure, 4-acetylbenzonitrile **a13** (72 mg, 0.5 mmol) gave the title compound **b13** as an orange-yellow oil (69 mg, 94 %).
^{1}H NMR (400 MHz, $CDCl_3$) δ 7.53 (d, *J* = 7.8 Hz, 3H), 7.42 (d, *J* = 7.8 Hz, 2H), 4.87 (q, *J* = 6.1 Hz, 1H), 3.20 (s, 1H), 1.41 (d, *J* = 6.1 Hz, 3H).
$^{13}C\{^{1}H\}$ NMR (101 MHz, $CDCl_3$) δ 151.5, 132.2, 126.1, 118.9, 110.6, 69.4, 25.3.

1-(2-Naphthyl)ethanol (b14)

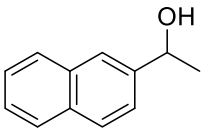

According to general procedure, 1-(naphthalen-2-yl)ethanone **a14** (85 mg, 0.5 mmol) gave the title compound **b14** as a colorless oil (70 mg, 81 %).
^{1}H NMR (400 MHz, $CDCl_3$) δ 8.10 – 7.80 (m, 4H), 7.52-7.47 (m, 3H), 5.05 (q, *J* = 6.5 Hz, 1H), 2.14 (s, 1H), 1.58 (d, *J* = 6.5 Hz, 3H).

$^{13}C\{^{1}H\}$ NMR (101 MHz, $CDCl_3$) δ 143.3, 133.4, 133.0, 128.4, 128.0, 127.8, 126.2, 125.9, 123.93, 123.90, 70.6, 25.2.

1-(1-Naphthyl)ethanol (b15)

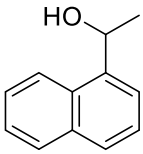

According to general procedure 1-(naphthalen-1-yl)ethanone **a15** (76 µL, 0.5 mmol) gave the title compound **b15** as a colorless oil (85 mg, 98%)

^{1}H NMR (400 MHz, $CDCl_3$) δ 8.14 – 8.10 (m, 1H), 7.90 – 7.86 (m, 1H), 7.82 – 7.77 (m, 1H), 7.68-7.66 (m, 1H), 7.54 – 7.40 (m, 3H), 5.65 (q, *J* = 6.5 Hz, 1H), 2.08 (s, 1H), 1.67 (d, *J* = 6.5 Hz, 3H).

^{13}C{^{1}H} NMR (101 MHz, $CDCl_3$) δ 141.5, 133.9, 130.4, 129.0, 128.0, 126.1, 125.6, 123.3, 122.1, 67.2, 24.5.

X-ray data

Complex **C^{3B}.30***

X-ray diffraction data were collected on a Bruker Kappa APEX II using a graphite-monochromated Mo-Kα radiation (λ= 0.71073 Å), and equipped with an Oxford Cryosystems Cryostream Cooler Device.

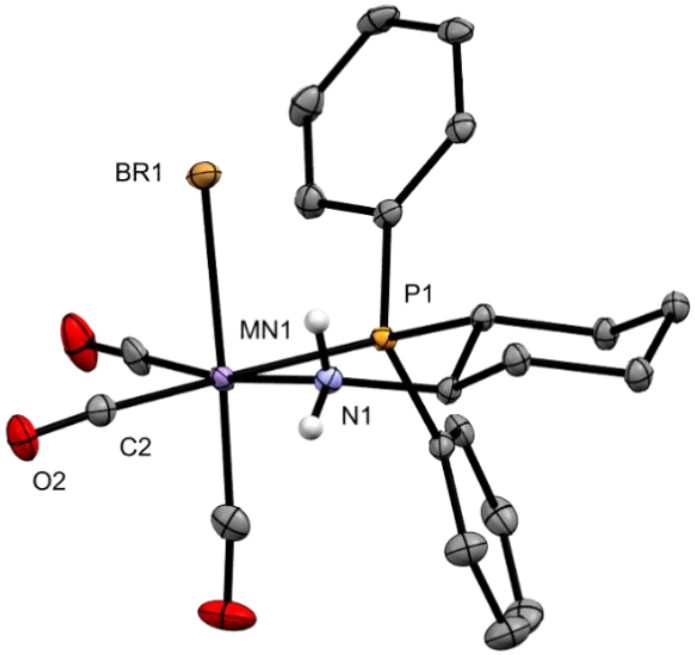

Figure S54: ORTEP view of molecular structure of complex **C^{2A}.30*** drawn at 50%. H atoms, except on the NH, were omitted for clarity.

Table S14. Crystal data and structure refinement for complex **C^{3B}.30***.

Empirical formula	$C_{21}H_{22}BrMnNO_3P$
Formula weight	502.21
Temperature	100 K
Wavelength	0.71073 Å
Crystal system, space group	Orthorhombic, $P2_12_12_1$
Unit cell dimensions	a = 10.6929 (5) Å, alpha = 90 °
	b = 11.4939 (5) Å, beta = 90°
	c = 17.5674(9) Å, gamma = 90 °
Volume	2159.09 (18) $Å^3$
Z, Calculated density	4, 1.545 ($g.cm^{-3}$)
Absorption coefficient	2.557 mm^{-1}
F(000)	1016
Crystal size	0.2x 0.12x 0.08mm
Crystal color	yellow
Theta range for data collection	2.6 to 27.2 °
h_min, h_max	-13, 13
k_min, k_max	-14, 14
l_min, l_max	-22, 22
Reflections collected / unique	57059 / 4780 [R(int) = 0.025]
Reflections [I>2σ(*I*)]	4579
Completeness to theta_max	0.999
Absorption correction type	multi-scan
Max. and min. transmission	0.746, 0.639
Refinement method	Full-matrix least-squares on F^2
Data / restraints / parameters	4780 / 3 / 259
Goodness-of-fit	1.19
Final R indices [I>2σ(*I*)]	$R1^a$ = 0.0152, $wR2^b$ = 0.0376
R indices (all data)	$R1^a$ = 0.0168, $wR2^b$ = 0.0442
Largest diff. peak and hole	0.33 and −0.22 $e^-.Å^{-3}$
Flack parameter	0.0062 (16)

GC chromatograms

a) Scope with L^{3B}.27

Representative chromatograms taken from the publication.[4]

1-Phenylethanol (method 1)

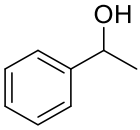

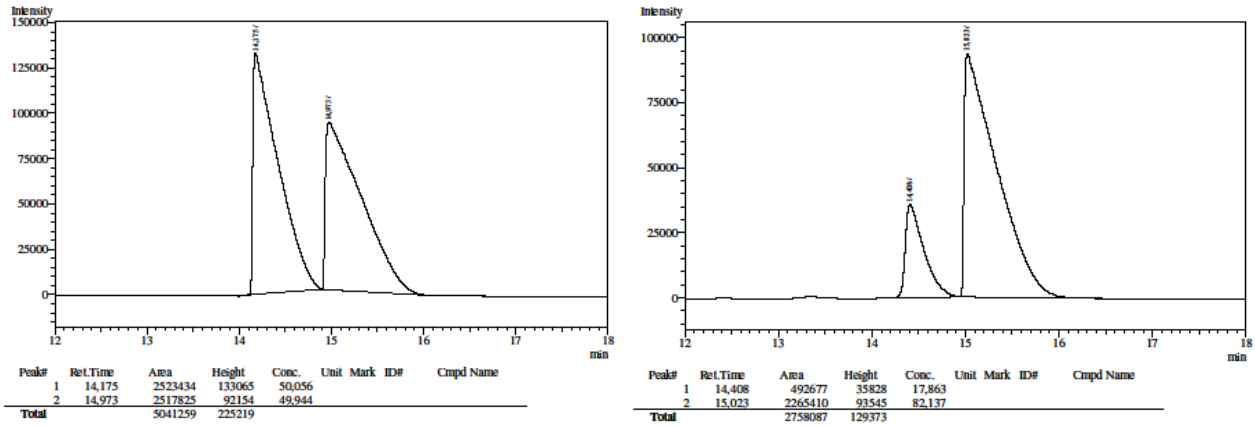

Figure S55: Chromatogram of *rac*-1-phenylethanol **b1** and enantio-enriched 1-phenylethanol **b'1**

2,2-Dimethyl-1-phenylpropanol (method 5)

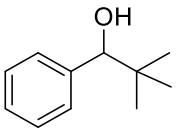

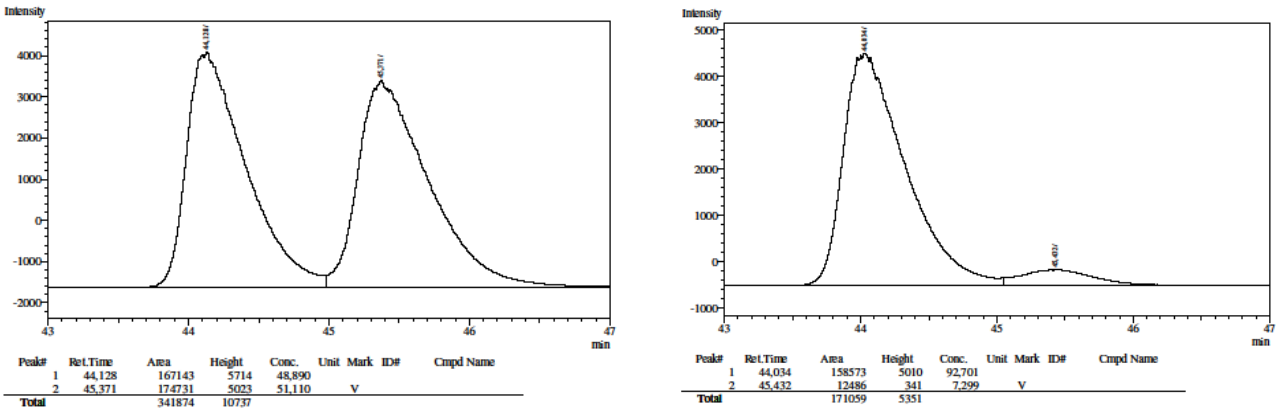

Figure S56: Chromatogram of *rac*- **2,2-Dimethyl-1-phenylpropanol b5** and enantio-enriched **2,2-Dimethyl-1-phenylpropanol b'5**

b) Screening with chiral phosphino-amine ligands (method 1)

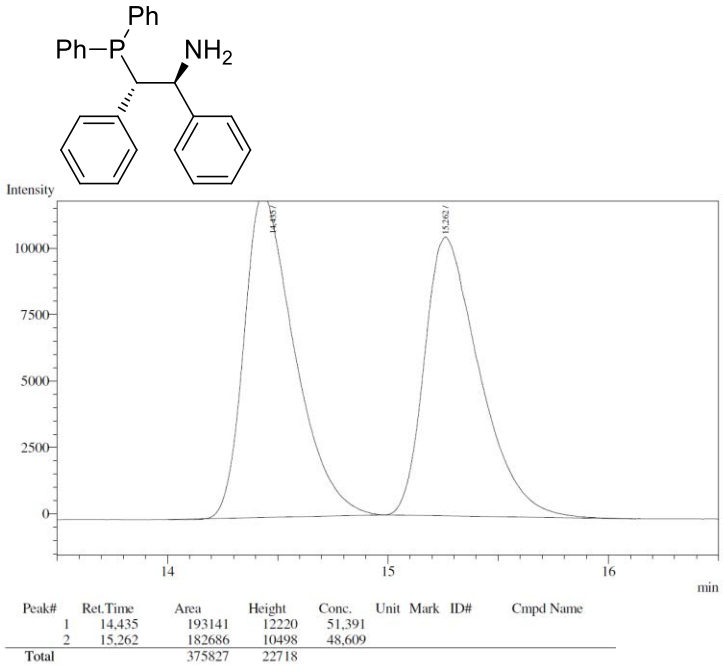

Peak#	Ret.Time	Area	Height	Conc.	Unit	Mark	ID#	Cmpd Name
1	14,435	193141	12220	51,391				
2	15,262	182686	10498	48,609				
Total		375827	22718					

Figure S57: Chromatogram of enantio-enriched 1-phenylethanol **b'1** with **L^{3B}.31**

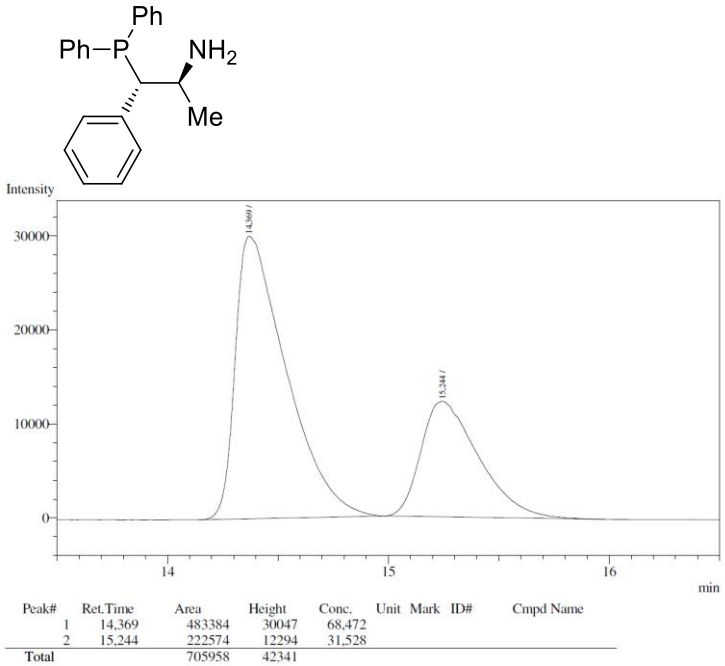

Peak#	Ret.Time	Area	Height	Conc.	Unit	Mark	ID#	Cmpd Name
1	14,369	483384	30047	68,472				
2	15,244	222574	12294	31,528				
Total		705958	42341					

Figure S58: Chromatogram of enantio-enriched 1-phenylethanol **b'1** with **L^{3B}.32**

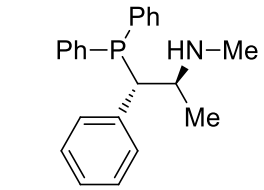

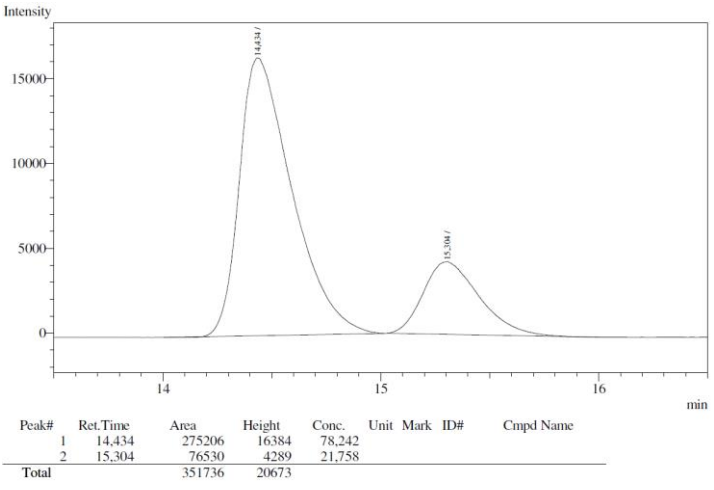

Peak#	Ret.Time	Area	Height	Conc.	Unit	Mark	ID#	Cmpd Name
1	14,434	275206	16384	78,242				
2	15,304	76530	4289	21,758				
Total		351736	20673					

Figure S59: Chromatogram of enantio-enriched 1-phenylethanol **b'1** with **L^{3B}.33**

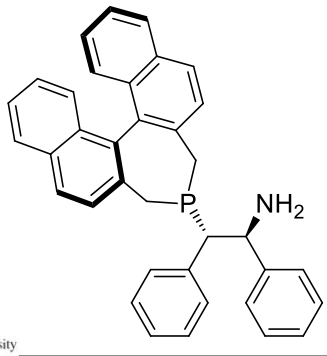

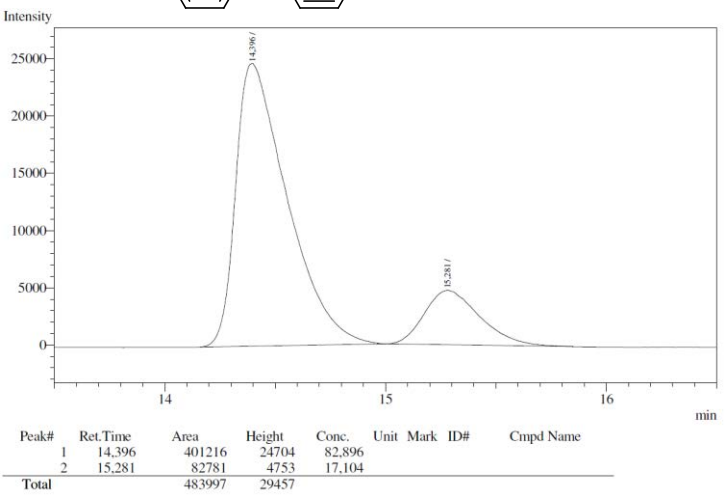

Peak#	Ret.Time	Area	Height	Conc.	Unit	Mark	ID#	Cmpd Name
1	14,396	401216	24704	82,896				
2	15,281	82781	4753	17,104				
Total		483997	29457					

Figure S60: Chromatogram of enantio-enriched 1-phenylethanol **b'1** with **L^{3B}.34**

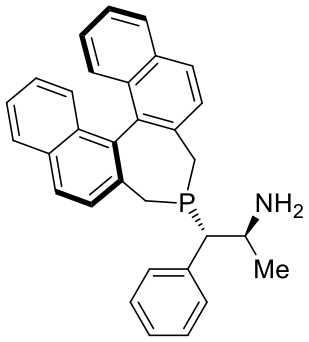

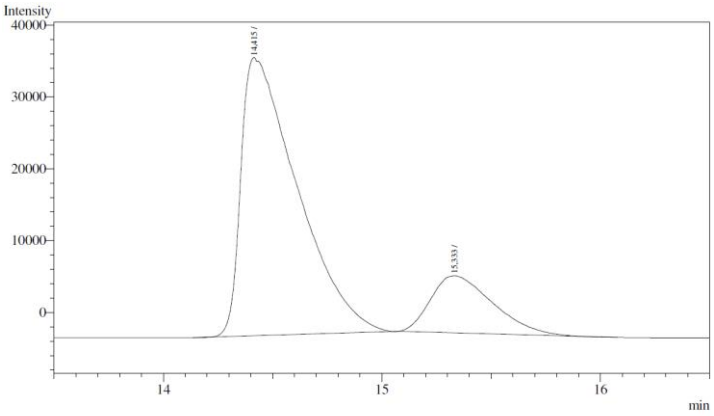

Peak#	Ret.Time	Area	Height	Conc.	Unit	Mark	ID#	Cmpd Name
1	14,415	693811	38714	81,567				
2	15,333	156793	7961	18,433				
Total		850604	46675					

Figure S61: Chromatogram of enantio-enriched 1-phenylethanol **b'1** with **L^{3B}.35**

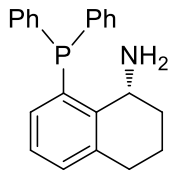

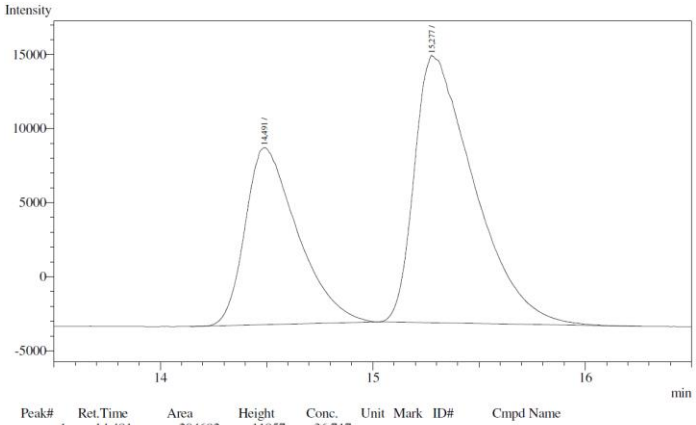

Peak#	Ret.Time	Area	Height	Conc.	Unit	Mark	ID#	Cmpd Name
1	14,491	204682	11957	36,717				
2	15,277	352773	18038	63,283				
Total		557455	29995					

Figure S62: Chromatogram of enantio-enriched 1-phenylethanol **b'1** with **L^{3B}.36**

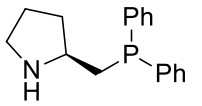

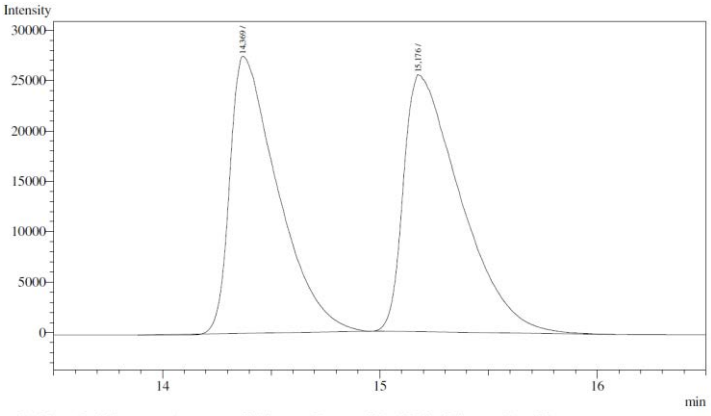

Peak#	Ret.Time	Area	Height	Conc.	Unit	Mark	ID#	Cmpd Name
1	14,369	421239	27478	47,513				
2	15,176	465328	25495	52,487				
Total		886567	52973					

Figure S63: Chromatogram of enantio-enriched 1-phenylethanol **b'1** with **L^{3B}.37**

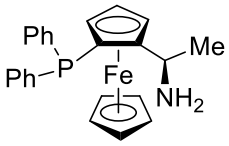

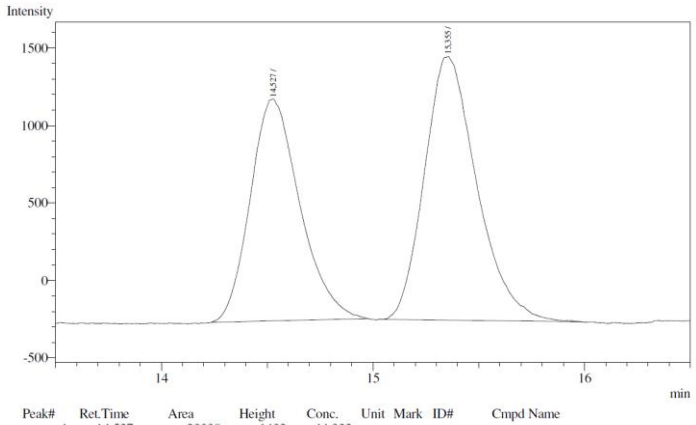

Peak#	Ret.Time	Area	Height	Conc.	Unit	Mark	ID#	Cmpd Name
1	14,527	23330	1432	44,322				
2	15,355	29307	1702	55,678				
Total		52637	3134					

Figure S64: Chromatogram of enantio-enriched 1-phenylethanol **b'1** with **L^{3B}.39**

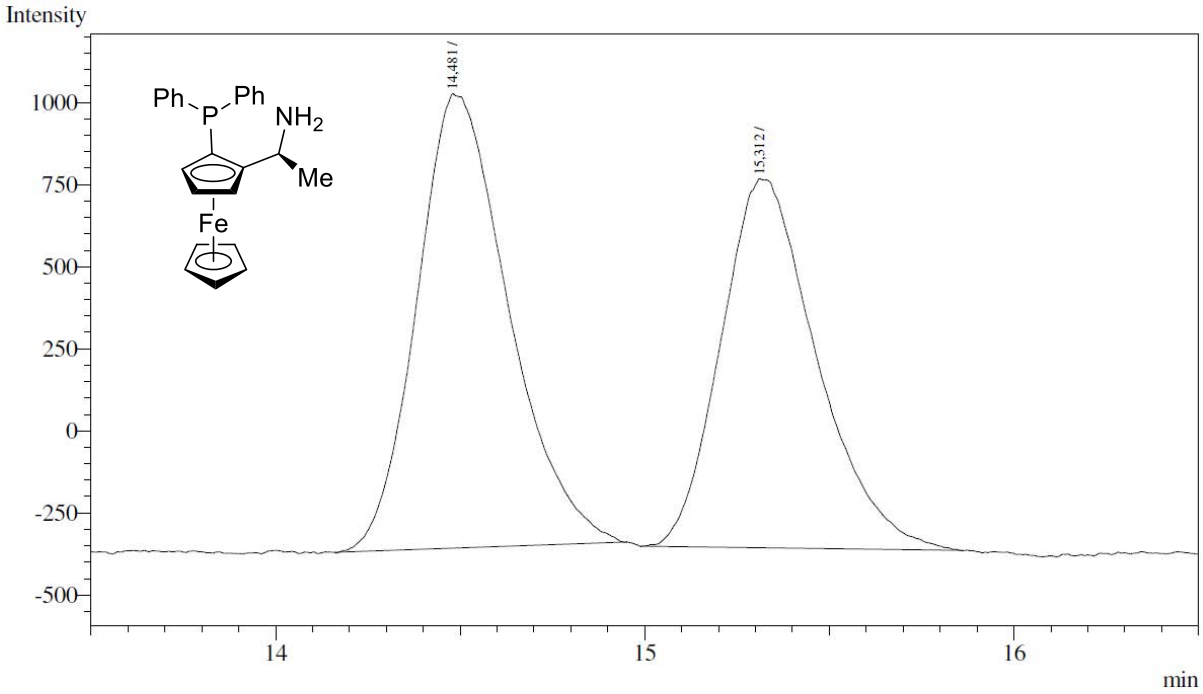

Peak#	Ret.Time	Area	Height	Conc.	Unit	Mark	ID#	Cmpd Name
1	14,481	23840	1383	54,021				
2	15,312	20291	1123	45,979				
Total		44131	2506					

Figure S65: Chromatogram of enantio-enriched 1-phenylethanol **b'1** with **L^{3B}.40**

References

[1] F. Jiang, K. Yuan, M. Achard, C. Bruneau, *Chem. Eur. J.* **2013**, *19*, 10343-10352.

[2] C. Bornschein, K. P. J. Gustafson, O. Verho, M. Beller, J. E. Bäckvall, *Chem. Eur. J.* **2016**, 22, 11583-11586.

[3] I. Cano, M. J. L. Tschan, L. M. Martinez-Prieto, K. Philippot, B. Chaudret, P. W. N. M. van Leeuwen, *Catal. Sci. Technol.* **2016**, *6*, 3758-3766.

[4] D. Wang, A. Bruneau-Voisine, J.-B. Sortais, *Catal. Commun.* **2018**, *105*, 31-36.

Chapter 4 - Conclusion

A - Summary of recent advances in (de)hydrogenation reactions catalyzed by manganese complexes

As mentioned in the introduction, a survey of the advances made by our group and others in the field of hydrogenation, transfer hydrogenation and hydrogen borrowing reactions catalyzed by homogeneous manganese complexes will be summarized (up to the beginning of July 2018). Several reviews about applications of manganese in this field appeared in 2 years.[1–5] The area of hydrosilylation and hydroboration will not be discussed.[6–8]

I- Hydrogenation

Since the first reports on hydrogenation of ketones published by Beller, Kempe and us briefly mentionned in the last chapters, the field has rapidly grown.

The achiral hydrogenation of ketones, aldehydes and nitriles was initiated by Beller in 2016 catalyzed by 1 mol% of MACHO-Mn complex **Mn-1** in the presence of 3 mol% of *t*BuONa at 100 °C in toluene during 24 h.[9] The group of Kempe succeeded to increase the activity of catalysts for the hydrogenation of ketones: using PN^6P manganese complex **Mn-2** (0.1 to 2 mol%) the temperature could be lowered to 80 °C in toluene with short reaction time (4 h).[10] In parallel, our group also proved that parent PN^3P Mn $\mathbf{C^{2A}.1}$ can catalyze this reaction, albeit with lower activity.[11]

Interestingly Kirchner published later a related catalytic system that could hydrogenate selectively aldehydes in the presence of ketones in very mild conditions: 0.1 mol% of **C^{2A}.1d** at 25 °C in EtOH during 18 h without additives.[12] With a surprising catalyst design, *i.e.* removing one wingtip of the complex **C^{2A}.1**, the activity of the complex **C^{3A}.2** was superior as the catalytic system could produce alcohols with very high yield at only 0.5 mol% catalytic loading, 2 mol% KHMDS in toluene at 50 °C during 20 h.[13] In addition, with **C^{3A}.2**, the hydrogenation of α-β unsaturated ketones yielded to saturated ketones, while with **Mn-1** the unsaturated alcohol was obtained.

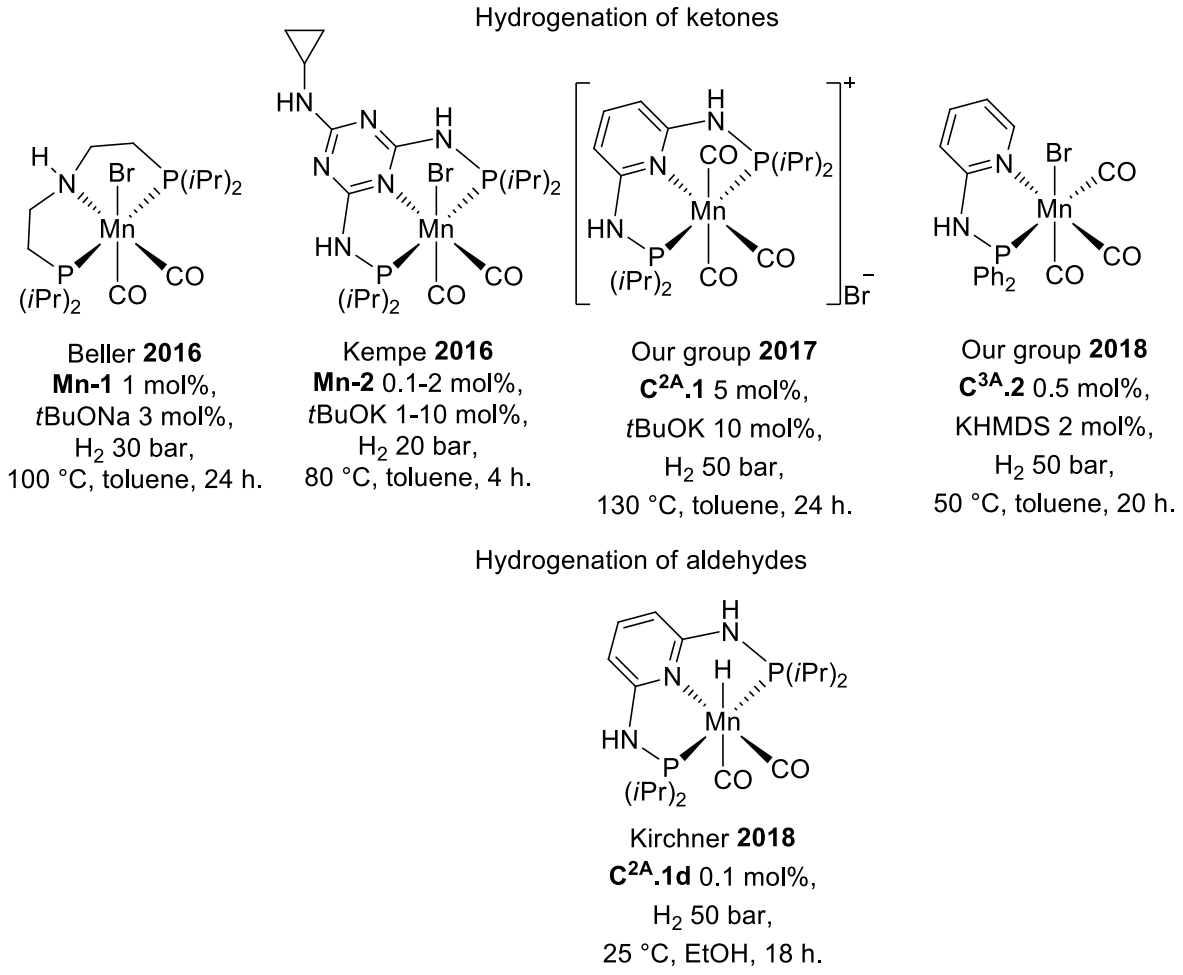

Figure A^{4l}.1 Manganese complexes used to catalyze hydrogenation of ketones and aldehydes.

The asymmetric hydrogenation of ketones was taken up by Clarke using 1 mol% of ^{py}NNP-Mn **Mn-5** and 10 mol% of *t*BuOK in EtOH at 50 °C during 16 h. High to very high enantiomeric excess (between 61 and 91%) were obtained for sterically hindered ketones while a moderate e.e. of 20% was reached for acetophenone.[14]

Beller reported that a chiral derivative of **Mn-1**, **Mn-4** (1 mol%), bearing a chiral phospholane, could also reduce prochiral ketones at 30 °C in 1,4-dioxane during 4 h with very good e.e. especially for aliphatic ketones (e.e. up to 84%). In contrast, lower e.e. was obtained for acetophenone (18%) and its derivatives.[15]

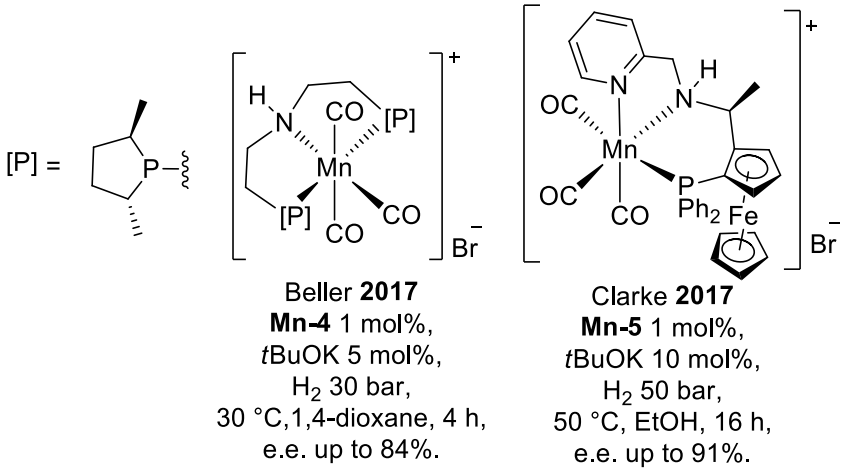

Beller **2017**
Mn-4 1 mol%,
*t*BuOK 5 mol%,
H_2 30 bar,
30 °C,1,4-dioxane, 4 h,
e.e. up to 84%.

Clarke **2017**
Mn-5 1 mol%,
*t*BuOK 10 mol%,
H_2 50 bar,
50 °C, EtOH, 16 h,
e.e. up to 91%.

Figure A[4l].2. Manganese complexes used to catalyze asymmetric hydrogenation of ketones.

The challenging field of hydrogenation of esters was approached by Beller in 2016. They pointed out that replacing *i*Pr group by Et group on the phosphorus atom of MACHO **Mn-1**, as in **Mn-6**, made a huge impact on the catalytic activity, as previously reported in the case of iron catalysts.[16] Their catalytic system operated at 110 °C in dioxane with 10 mol% of *t*BuOK.[17] The same year, Milstein succeeded to reduce esters under similar conditions: 1 mol% of $PN^{py}N$ Mn **Mn-7** and 2 mol% of KH at 100 °C in toluene.[18] While strong bases are often needed to run the reactions, Clarke proved that K_2CO_3 (1-10 mol%) could be a suitable base for hydrogenation of enantiomerically pure esters, such as (*R*)-ethyl 3-phenylbutyrate, with retention of configuration in the presence of their catalyst **Mn-5** (0.1-1 mol%) at lower temperatures (50-110 °C) in *i*PrOH.[19] A breakthrough was made by a collaborative work between the groups of Pidko and Beller: the use of bidentate PN ligand allowed to perform this reaction at 100 °C with a low catalytic loading (**Mn-8**, 0.2 mol%) even if 75 mol% of *t*BuOK was needed.[20]

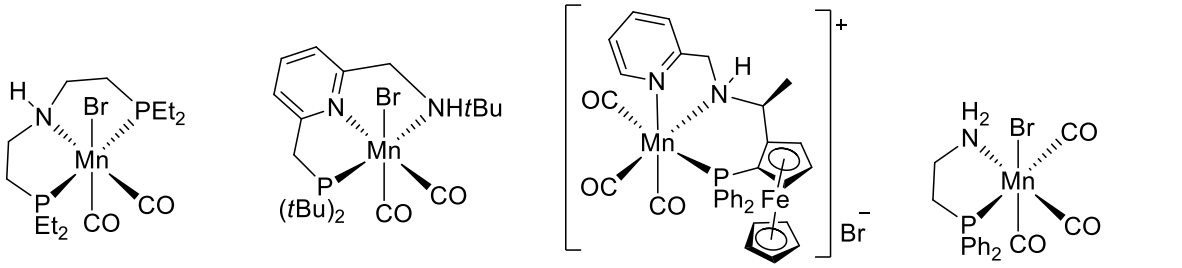

Beller **2016**
Mn-6 2 mol%,
*t*BuOK 10 mol%,
H_2 30 bar,
110 °C,1,4-dioxane, 24 h.

Milstein **2017**
Mn-7 1 mol%,
KH 2 mol%,
H_2 20 bar,
100 °C, toluene, 21 h.

Clarke **2018**
Mn-5 0.1-1 mol%,
K_2CO_3 1-10 mol%,
H_2 50 bar,
50-110 °C, *i*PrOH, 16 h.

Pidko **2017**
Mn-8 0.2 mol%,
*t*BuOK 75 mol%,
H_2 50 bar,
100 °C,1,4-dioxane, 16 h.

Figure A[4l].3. Manganese complexes used to catalyze hydrogenation of esters.

The hydrogenolysis of amides to alcohols and amines was achiveved with the complex supported by imidazolylaminophosphino ligand (**Mn-9**). Relatively mild conditions were needed: 100 °C in cyclohexane with 2 mol% of catalyst and 10 mol% of base. It is important to note that challenging primary amides were also reduced at 140 °C.[21]

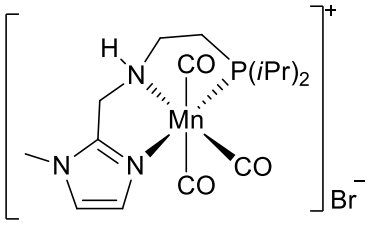

Beller **2017**
Mn-9 2 mol%,
*t*BuOK 10 mol%,
H_2 30 bar,
100 °C, cyclohexane, 16 h.

Figure A[4l].4. Manganese complex used to catalyze hydrogenolysis of amides.

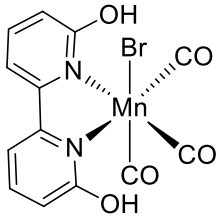

Nervi, Kushnutdinova **2017**
Mn-10
30 bar CO_2, 30 bar H_2, DBU,
65 °C, MeCN,
TON max= 6250 (formate)
= 588 (formamide)

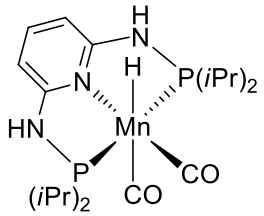

Kirchner, Gonsalvi **2017**
C^{2A}.1d
40 bar CO_2, 40 bar H_2, DBU,
100 °C,THF/H_2O, LiOTf,
TON max= 31600 (formate)

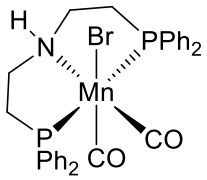

Prakash **2017**
Mn-11
60 bar CO_2/H_2, amines,
then 80 bar H_2,
110 °C then 150 °C,THF,
TON max= 36
(MeOH *via* formamide)

Figure A^{4I}.5. Manganese complexes used to catalyze hydrogenation of carbon dioxide.

The reduction of CO_2 could also be catalyzed by manganese complexes. Electro- and photoreduction of CO_2 by manganese carbonyl complexes have been popular since 2010 but will not be discussed herein.[22] Nervi and Kushnutdinova employed a **Mn-10** complex based on bipyridine ligand to hydrogenate carbon dioxide with a TON recorded at 65 °C in acetonitrile of 6250 for the production of formate.[23] For the same reaction, at 100 °C in a mixture THF/water, Kirchner and Gonsalvi could obtain a TON of 31600 in the presence of LiOTf with **C^{2A}.1d**.[24] Prakash and co-workers could produce methanol starting from CO_2 in two step *via* a formamide intermediate with a TON of 36 with **Mn-11**.[25]

II- Transfer hydrogenation

Manganese was studied for the first time in transfer hydrogenation of ketones by the group of Beller in 2017 using **Mn-12** bearing tridentate dipicolylamine ligand (1mol%) at 70 °C in *i*PrOH for 24 h in the presence of 2 mol% *t*BuOK (**Figure A^{4II}.1**).[26] Surprisingly, the similar complex bearing a methyl group on the nitrogen **Mn-13** was also active in the same conditions without any drop of the conversion, suggesting that cooperation of the NH moiety with the metal center was not mandatory for this reaction. On our side, we highlighted that simplifying the pre-catalyst **C^{3B}.1**, by using bidentate aminomethylpyridine ligand, led to higher activity than **Mn-12**. Various alcohols were produced in very high yields with 0.5 mol% load, 1 mol% of *t*BuOK in

*i*PrOH at 80 °C for only 20 min.[27] To go further in the simplicity, we succeeded to generate the catalytic system *in situ* using $Mn(CO)_5Br$ and the most simple diamine ligand: ethylene diamine **L^{3B}.11**.

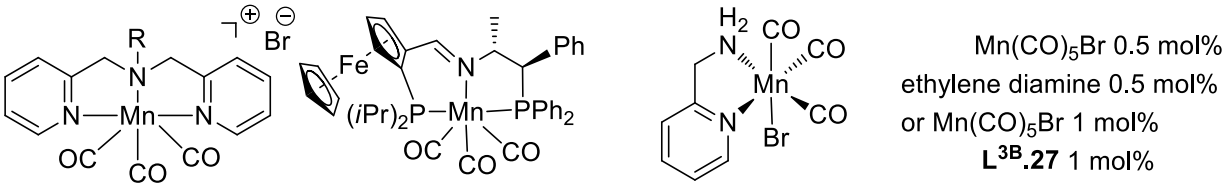

Figure A^{4II}.1 Manganese complexes used to catalyze transfer hydrogenation of polar double bonds

The same year, Kirchner took advantage of the chiral PNP ligand, inspired by the work of Clarke with chiral ferrocene, to perform asymmetric transfer hydrogenation with **Mn-14** (1 mol%) at 25 °C in *i*PrOH for 5 h with 4 mol% of *t*BuOK (e.e. values between 20 and 85 %).[28] Following our strategy to develop readily available catalytic systems, we proved that commercial chiral diamines such as (1*R*,2*R*)-(+)-1,2-diphenyl-1,2-ethanediamine **L^{3B}.27** could be employed which allowed to reach high levels of enantioselectivity (up to 90%).[29]

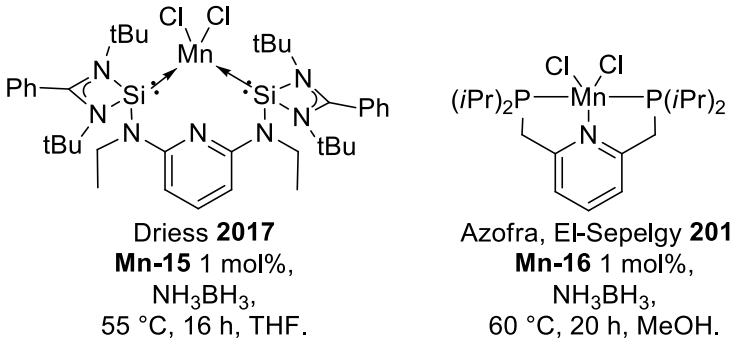

Figure A^{4II}.2 Manganese complexes used to catalyze transfer hydrogenation of alkynes

Finally, the transfer semi-hydrogenation of alkynes with ammonia-borane as hydrogen source was first reported by Driess:[30] they obtained selectively the *E*-alkenes with **Mn-15** (**Figure A^{4II}.2**) while Azofra and El Sepelgy obtained selectively the opposite *Z*-isomers with **Mn-16**.[31]

III- Hydrogen borrowing

a) For C-N bond formation

The first manganese catalyzed alkylation of amines and sulfonamides with alcohols was described in 2011 by Xu (**Scheme A^{4III}.1**, a. and b.), using high load (10-20 mol%) of ligand-free MnO_2 in combination with the same amount of CsOH or K_2CO_3 at 135 °C under solvent-free condition. It is noteworthy that working under air was a key parameter for this reaction.[32]

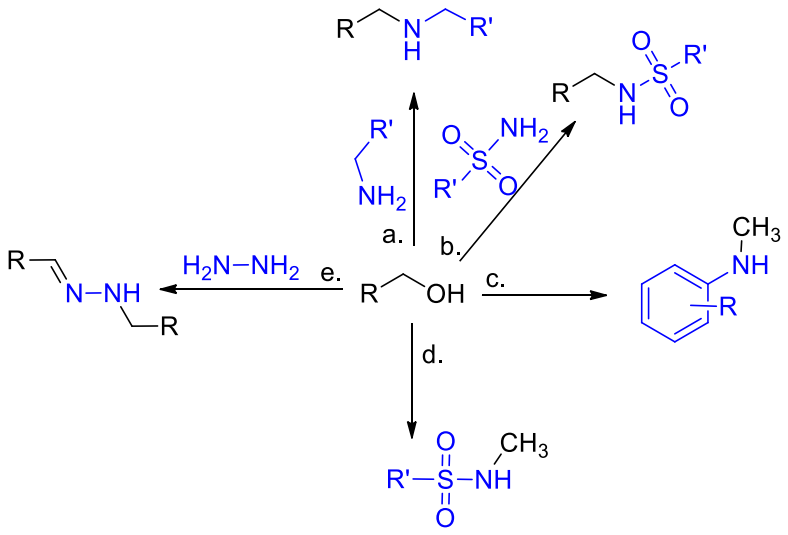

Scheme A^{4III}.1 Alkylation of amines with alcohols catalyzed with manganese.

The use of well-defined pincer manganese(I) complexes was introduced by Beller in collaboration with our group in 2016 (**Figure A^{4III}.1**). **Mn-1** (3 mol%) was associated with 0.75 equiv. of *t*BuOK to alkylate various amines in toluene at 80 °C with a large diversity of alcohols (**Scheme A^{4III}.1**, a.). Importantly, methanol could be activated to formaldehyde with this system by increasing the loading of the base to 1 equivalent and the temperature to 100 °C (**Scheme A^{4III}.1**, c.).[33] One year later, in a parallel study based on PNP ligands, Beller succeeded to divide by two the amount of base needed for the *N*-methylation of anilines with methanol using **Mn-17**,[34] and we lowered the base loading to 20 mol% using **C^{2A}.1** (5 mol%) in toluene at 120 °C (**Scheme A^{4III}.1**, c.).[35] Our procedure was extended to the mono-*N*-methylation of sulfonamides using 1.2 equivalent of *t*BuOK (**Scheme A^{4III}.1**, d.). More recently

Milstein employed PNN complex **Mn-18** (3 mol%) to couple alcohols with hydrazine to give *N*-substituted hydrazones at 110 °C with low catalytic amount of base (5 mol% of *t*BuOK) (**Scheme A^{4III}.1**, e.).[36]

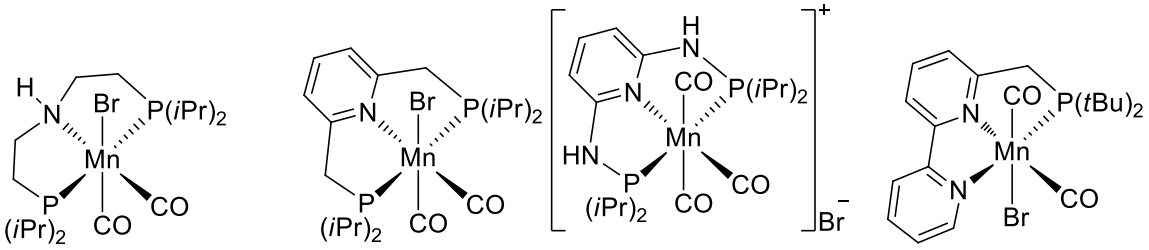

Figure A^{4III}.1 Manganese complexes used to catalyze hydrogen borrowing reactions for C-N bond formation

b) For C-C bond formation

In 2016, the group of Beller reported the α-alkylation of ketones and 2-oxindole with 2 mol% of **Mn-1** and 5 mol% of $CsCO_3$ at 140 °C (**Scheme A^{4III}.2**, a. and b., **Figure A^{4III}.2**).[37] Very recently the group of Maji, produced *in situ* a pre-catalyst starting from $Mn(CO)_5Br$ and phosphorus-free tridentate NNN ligand to perform the same reaction (**Figure A^{4III}.2**).[38] With the catalyst **Mn-1**, Liu performed the selective conversion of ethanol into 1-butanol at 160 °C (**Scheme A^{4III}.1**, c.).[39] Very recently the group of Yu mentioned that phosphine-free bidentate NN complex **Mn-19** could efficiently catalyze the formal β-alkylation of secondary alcohols with primary alcohols in toluene at 110 °C with 30 mol% of *t*BuOK (**Scheme A^{4III}.1**, d.).[40] They mentioned that without catalyst, the base-promoted reaction afforded the alkylated ketones, instead of the reduced alcohols, which led to questions about the exact role of manganese in this case. Multicomponent synthesis of pyrimidines from alcohols and amidines, published by Kempe, could also be seen as alkylation of alcohols in the first step of the reaction (**Scheme A^{4III}.1**, d'.).[41] Finally the α-methylation of ketones and esters was achieved by us, using **C^{2A}.1** (3 mol%) with *t*BuOK (respectively 50 mol% and 100 mol%) at 120 °C (**Scheme A^{4III}.1**, e. and f.).

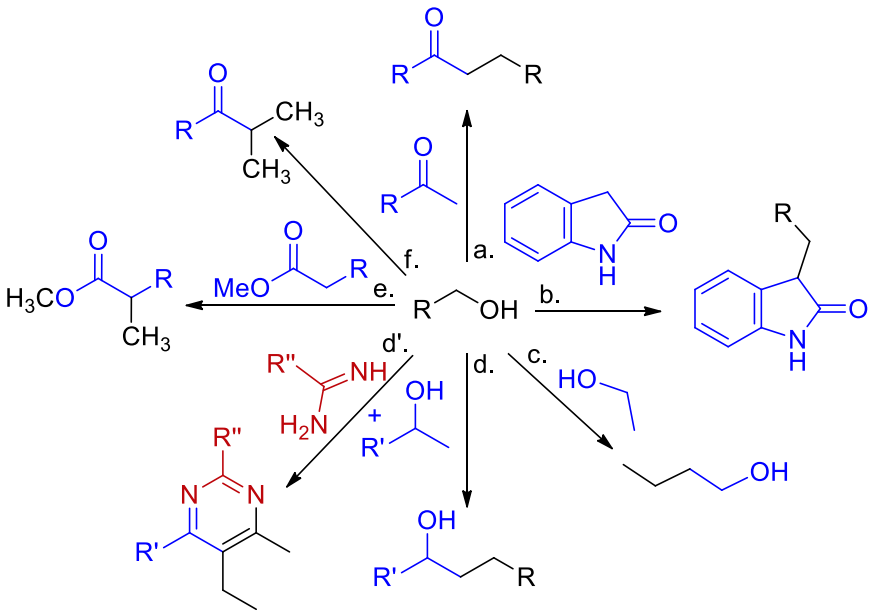

Scheme A^{4III}.2 Alkylation of other substrates with alcohols catalyzed with manganese.

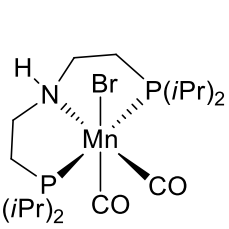

Beller **2016**
Mn-1 2 mol%,
$CsCO_3$ 5 mol%,
140 °C, *t*AmOH.

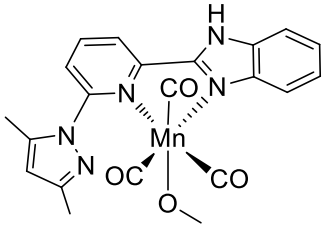

Yu **2018**
Mn-19 2.1 mol%,
*t*BuOK 30 mol%,
110 °C, toluene.

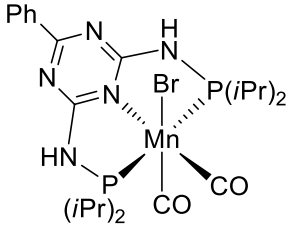

Kempe **2017**
Mn-3 2.5 mol%,
*t*BuOK 100 mol%,
120 °C, toluene.

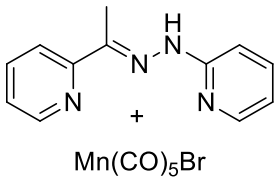

Maji **2018**
2 mol%,
*t*BuOK 10 mol%,
140 °C, *t*AmOH.

Figure A^{4III}.2 Manganese complexes used to catalyze hydrogen borrowing reactions for C-C bond formation

c) <u>Acceptorless dehydrogenative coupling</u>

Several catalytic systems were developed for the semi-hydrogen borrowing reaction, *i.e.* reactions in which the products resulting from the reaction are not reduced *in situ*. Only selected examples will be discussed in the following paragraph.

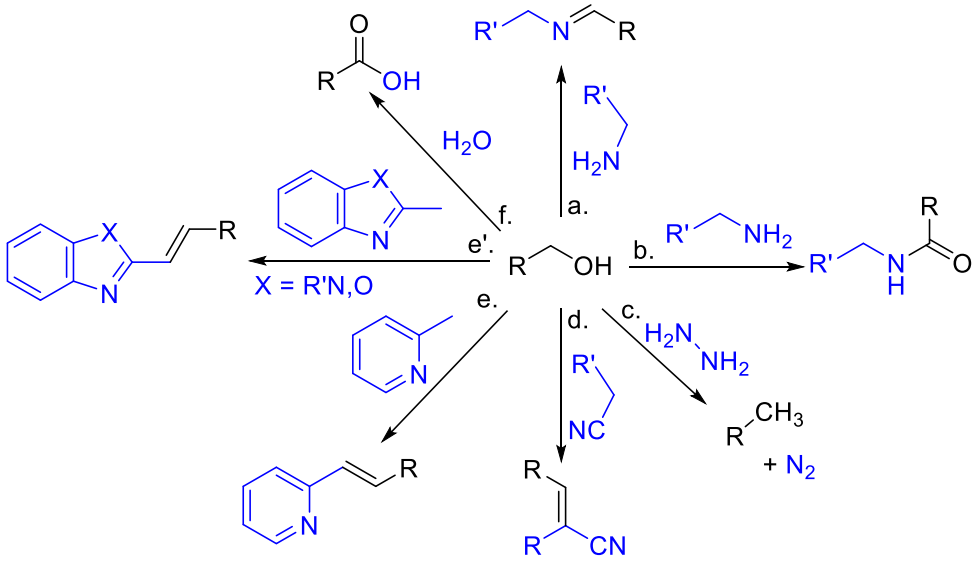

Scheme A^{4III}.3 Semi-hydrogen borrowing with alcohols catalyzed with manganese.

The dehydrogenative coupling of alcohols and amines to form imines was first published by Milstein using complex **Mn-20** in 2016 (135 °C in benzene, generation of H_2) (**Figure A^{4III}.3**, **Scheme A^{4III}.3**, a.). Interestingly **Mn-20** (3 mol%), a deprotonated 16 electron complex, is the active catalyst and the reaction proceeded without any additive or activator.[42] The same year, Kirchner can perform the same reaction under the catalysis of **C^{2A}.1d** (3 mol%), at 140 °C in toluene. Interestingly, in the same publication they showed that, in the same reaction conditions using related Fe(II) catalyst, the product was the amine.[50] Later **Mn-21** induced the dehydrogenation of MeOH in the presence of amines to produce formamides[43] or various amides starting from alcohols or esters (**Scheme A^{4III}.3**, b.).[44,45] Interestingly, using **Mn-22**, primary alcohols could be deoxygenated leading to the methylene derivatives, *via* a sequence oxidative dehydrogenation/Wolff–Kishner reduction, with concomitant liberation of H_2, N_2 and H_2O (**Scheme A^{4III}.3**, c.).[46] With this **Mn-22** catalyst, the same group developed the α-olefination of nitriles (**Scheme A^{4III}.3** d.).[47] The α-olefination was a new reaction and has been extended to alkyl-substituted *N*-heteroarenes (**Scheme A^{4III}.3**, e.).[48,49]

Multicomponent reactions involving alcohols and amines were studied by the group of Kempe (**Mn-3**, pyrroles[41]) and Kirchner (**C^{2A}.1d**, quinolines and pyrimidines[50]). In this case, the formation of *N*-heterocyclic products showed that the aromatization could be a driving force to perform the reaction. A mild temperature of 78 °C was applied by Kempe with **Mn-3** (0.5 mol%) for the synthesis of pyrroles using

stoichiometric amount of base.[51] In addition, related iron and cobalt complexes were totally inactive for this reaction.

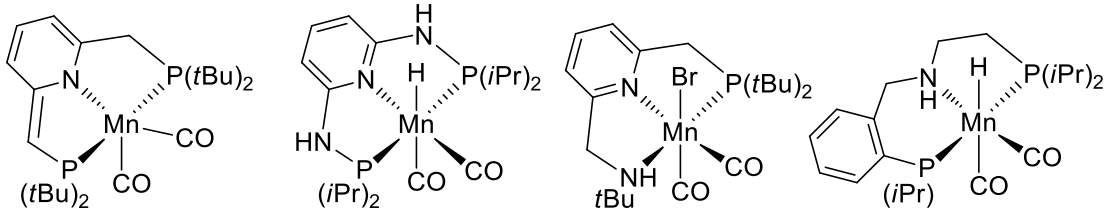

Figure A^{4III}.3 Manganese complexes used to catalyze semi-hydrogen borrowing reactions

In 2017, Boncella showed that **Mn-1** could activate a molecule of water to produce the corresponding hydroxyl complex, which can further react with an aldehyde to produce a carboxylic acid.[52] Inspired by this work, the group of Liu developed a catalyzed acceptorless dehydrogenative transformation of primary alcohols to carboxylic acids using water as oxidant, with the same **Mn-1** pre-catalyst (**Scheme A^{4III}.1**, f.).[53]

IV- Global conclusion about manganese catalyzed (de)hydrogenation reactions

Since the first reports by the groups of Milstein and Beller, the use of manganese(I) complexes for (de)hydrogenation reactions is on the rise. As described in the last part, within just two years, the number of catalytic systems employing manganese has increased very rapidly. This topic, still in its infancy, has shown promising results. It is worth noting that the design or the choice of the ligands (mostly tridentate) to support manganese complexes was strongly influenced by previous works on iron or cobalt (or noble metal) complexes.[5] It is also important to note that metal-ligand cooperativity is always involved, to date, in active catalytic systems based on manganese for (de)hydrogenation reactions.

For (transfer) hydrogenation reactions, tridentate phosphorus-containing ligands were first applied proving that this class of complexes can be very active. However, the price and the synthetic complexity of such ligands is a severe drawback for large-scale applications. Efforts have been made to replace the phosphine moieties on the ligands by more easily accessible and cheaper scaffolds such as pyridines, imidazoles, pyrazoles. We can anticipate that furthers developments will be make in that direction using other donating groups (carbenes or thioethers). In addition, the development of complexes supported by bidentate ligands to give highly efficient catalysts is in contrast with the chemistry of iron catalysts that requires tridentate ligands to be stable pre-catalyts and efficient catalysts.

A comparison can be made between similar tridentate or bidentate based catalysts. For the hydrogenation of ketones: **C^{3A}.2** is more active than **C^{2A}.1** (5 mol%, 130 °C *vs* 0.5 mol%, 50 °C). For the reduction of esters: the catalytic loading is ten times lower with **Mn-8** than **Mn-6**. For transfer hydrogenation of ketones: **C^{3B}.1** is much more active than **Mn-12** (20 min instead of 24 h, TOF up to 3600 *vs* 2 h^{-1}). Therefore simplifying the ligands seems to have a beneficial effect in these cases although tridentate ligands are still useful to achieve more challenging reactions like the reduction of amides.

In the case of hydrogen borrowing reactions, only one bidentate complex **Mn-19** is described even if the presence of non-coordinated pyrazole moiety on the ligand is not clear so far. All the other complexes are based on tridentate type ligands containing a chelating phosphorus atom. Manganese catalysts seem to be especially efficient for dehydrogenative part of the coupling reactions. Yet being developed more recently, they disclosed a high activity competing with the one of other first raw metals. The activity of the best noble metal catalysts can even be reached for methylation with methanol for example. In addition, new reactions have been described such as α-olefination with alcohols.

To conclude this part, the fast growing use of manganese complexes for (de)hydrogenation reactions led to impressive results within two years. Up to now, this field was largely dominated by late transition metals. The development of manganese catalysts shows that middle transition metals are also suitable to promote (de)hydrogenation reactions, and are not limited to oxidation reactions.

Probably, new organometallic approaches should also be envisioned to get access of manganese catalysts starting from the inexpensive precursors such as $MnCl_2$, cymanthrene or methylcyclopentadienyl manganese tricarbonyl (MMT). In fact, $Mn(CO)_5Br$ is a quite expensive precursor which is a drawback when using an abundant metal. One has to keep in mind that carbonyl ligands seem to be crucial to get highly active manganese catalysts.

B- General conclusion

The goal of this PhD thesis was to develop and study new families of complexes based on manganese, with the idea of developing a sustainable catalysis.

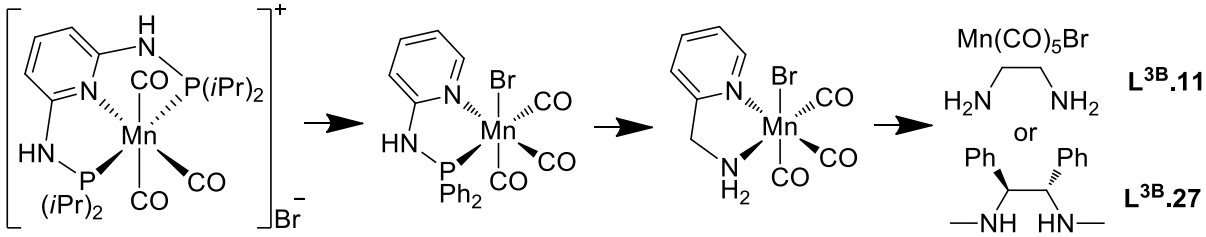

C^{2A}.1 **C^{3A}.2** **C^{3B}.1**

Figure B^4.1 Manganese complexes developed during this thesis

As starting point, we focused our attention on the synthesis and valorization of manganese complex **C^{2A}.1** bearing a pincer PN^{3}P ligand (**Figure B^4.1**). We proved that this complex could efficiently catalyze on one side the challenging mono-*N*-methylation of anilines and sulfonamides, and on the other side, the α-alkylation of ketones and esters with methanol, as a sustainable C1 source. The activity of this base metal complex is similar to the best catalysts based on noble metals (Ru, Ir).

Guided by the concept of micro-reversibility, we then turned our attention to hydrogenation reactions. Indeed, we proved that the same complex **C^{2A}.1** could catalyze the hydrogenation of ketones, albeit with modest performances compared to other catalysts based on manganese.

By modifying the design of the ligand, we succeeded to improve significantly the efficiency of the catalysts by removing one wingtip of the ligand. With this new catalyst **C^{3A}.2**, we could hydrogenate ketones, aldehydes and aldimines under mild conditions.

In order to simplify the catalytic system, we demonstrated that using affordable, commercially available, phosphorus-free, 2-aminomethylpyridine as ligand was a powerful strategy to promote the transfer hydrogenation of ketones, aldehydes and aldimines in very mild conditions with the complex **C^{3B}.1**. The catalytic system could eventually be generating *in situ* starting from the ligand and the manganese precursor. Finally, diamine ligand as simple as ethylene diamine **L^{3B}.11** could be employed for the reduction of ketones. We took advantage of the convenience of the protocol to screen a few commercially available chiral diamines to enter the challenging field of asymmetric reduction of ketones. In a short period, we succeeded to achieve high level of enantioselectivity for the reduction of ketones (up to 90%). We revealed the importance of having one methyl group on the nitrogen on the best ligand **L^{3B}.21**, showing the importance of our first work on mono-*N*-methylation.

In conclusion, the way for the development of highly efficient catalysts based on manganese is now open. The possibility in terms of innovative organic transformations is nearly infinite, as long as the right combination of ligand and experimental conditions are discovered.

V- References

[1] M. Garbe, K. Junge, M. Beller, *Eur. J. Org. Chem.* **2017**, 4344–4362.
[2] G. A. Filonenko, R. van Putten, E. J. M. Hensen, E. A. Pidko, *Chem. Soc. Rev.* **2018**, *47*, 1459–1483.
[3] F. Kallmeier, R. Kempe, *Angew. Chem. Int. Ed.* **2018**, *57*, 46–60.
[4] B. Maji, M. K. Barman, *Synthesis* **2017**, 3377–3393.
[5] T. Zell, R. Langer, *ChemCatChem* **2018**, *9*, 1930–1940.
[6] R. J. Trovitch, *Synlett* **2014**, 1638–1642.
[7] X. Yang, C. Wang, *Chem. Asian J.* **2018**, DOI 10.1002/asia.201800618.
[8] V. Vasilenko, C. K. Blasius, H. Wadepohl, L. H. Gade, *Angew. Chem. Int. Ed.* **2017**, *56*, 8393–8397.
[9] S. Elangovan, C. Topf, S. Fischer, H. Jiao, A. Spannenberg, W. Baumann, R. Ludwig, K. Junge, M. Beller, *J. Am. Chem. Soc.* **2016**, *138*, 8809–8814.
[10] F. Kallmeier, T. Irrgang, T. Dietel, R. Kempe, *Angew. Chem. Int. Ed.* **2016**, *55*, 11806–9.
[11] A. Bruneau-Voisine, D. Wang, T. Roisnel, C. Darcel, J.-B. Sortais, *Catal. Commun.* **2017**, *92*, 1–4.
[12] M. Glatz, B. Stöger, D. Himmelbauer, L. F. Veiros, K. Kirchner, *ACS Catal.* **2018**, 4009–4016.
[13] D. Wei, A. Bruneau-Voisine, T. Chauvin, V. Dorcet, T. Roisnel, D. A. Valyaev, N. Lugan, J.-B. Sortais, *Adv. Synth. Catal.* **2018**, *360*, 676–681.
[14] M. B. Widegren, G. J. Harkness, A. M. Z. Slawin, D. B. Cordes, M. L. Clarke, *Angew. Chem. Int. Ed.* **2017**, *56*, 5825–5828.
[15] M. Garbe, K. Junge, S. Walker, Z. Wei, H. Jiao, A. Spannenberg, S. Bachmann, M. Scalone, M. Beller, *Angew. Chem. Int. Ed.* **2017**, *56*, 11237–11241.
[16] S. Elangovan, B. Wendt, C. Topf, S. Bachmann, M. Scalone, A. Spannenberg, H. Jiao, W. Baumann, K. Junge, M. Beller, *Adv. Synth. Catal.* **2016**, *358*, 820–825.
[17] S. Elangovan, M. Garbe, H. Jiao, A. Spannenberg, K. Junge, M. Beller, *Angew. Chem. Int. Ed.* **2016**, *55*, 15364–15368.
[18] N. A. Espinosa Jalapa, A. Nerush, L. J. W. Shimon, G. Leitus, L. Avram, Y. Ben-David, D. Milstein, *Chem. Eur. J.* **2017**, *23*, 5934–5938.
[19] M. B. Widegren, M. L. Clarke, *Org. Lett.* **2018**, *20*, 2654–2658.
[20] R. van Putten, E. A. Uslamin, M. Garbe, C. Liu, A. Gonzalez-de-Castro, M. Lutz, K. Junge, E. J. M. Hensen, M. Beller, L. Lefort, E. Pidko, *Angew. Chem. Int. Ed.* **2017**, *56*, 7531–7534.
[21] V. Papa, J. R. Cabrero-Antonino, E. Alberico, A. Spanneberg, K. Junge, H. Junge, M. Beller, *Chem. Sci.* **2017**, *8*, 3576–3585.
[22] M. Stanbury, J.-D. Compain, S. Chardon-Noblat, *Coord. Chem. Rev.* **2018**, *361*, 120–137.
[23] A. Dubey, L. Nencini, R. R. Fayzullin, C. Nervi, J. R. Khusnutdinova, *ACS Catal.* **2017**, *7*, 3864–3868.
[24] F. Bertini, M. Glatz, N. Gorgas, B. Stoger, M. Peruzzini, L. F. Veiros, K. Kirchner, L. Gonsalvi, *Chem. Sci.* **2017**, *8*, 5024–5029.
[25] S. Kar, A. Goeppert, J. Kothandaraman, G. K. S. Prakash, *ACS Catal.* **2017**, *7*, 6347–6351.
[26] M. Perez, S. Elangovan, A. Spannenberg, K. Junge, M. Beller, *ChemSusChem* **2017**, *10*, 83–86.
[27] A. Bruneau-Voisine, D. Wang, V. Dorcet, T. Roisnel, C. Darcel, J.-B. Sortais, *Org. Lett.* **2017**, *19*, 3656–3659.
[28] A. Zirakzadeh, S. R. M. M. de Aguiar, B. Stöger, M. Widhalm, K. Kirchner, *ChemCatChem* **2017**, *9*, 1744–1748.
[29] D. Wang, A. Bruneau-Voisine, J.-B. Sortais, *Catal. Commun.* **2017**, *105*, 31–36.
[30] Y.-P. Zhou, Z. Mo, M.-P. Luecke, M. Driess, *Chem. Eur. J.* **2018**, *24*, 4780-4784.
[31] A. Brzozowska, L. M. Azofra, V. Zubar, I. Atodiresei, L. Cavallo, M. Rueping, O. El-Sepelgy, *ACS Catal.* **2018**, *8*, 4103–4109.
[32] X. Yu, C. Liu, L. Jiang, Q. Xu, *Org. Lett.* **2011**, *13*, 6184–6187.
[33] S. Elangovan, J. Neumann, J.-B. Sortais, K. Junge, C. Darcel, M. Beller, *Nat. Commun.* **2016**, *7*, 12641.
[34] J. Neumann, S. Elangovan, A. Spannenberg, K. Junge, M. Beller, *Chem. Eur. J.* **2017**, *23*, 5410–5413.

[35] A. Bruneau-Voisine, D. Wang, V. Dorcet, T. Roisnel, C. Darcel, J.-B. Sortais, *J. Catal.* **2017**, *347*, 57–62.
[36] U. K. Das, Y. Ben-David, Y. Diskin-Posner, D. Milstein, *Angew. Chem. Int. Ed.* **2018**, *130*, 2201–2204.
[37] M. Peña-López, P. Piehl, S. Elangovan, H. Neumann, M. Beller, *Angew. Chem. Int. Ed.* **2016**, *55*, 14967–14971.
[38] M. K. Barman, A. Jana, B. Maji, *Adv. Synth. Catal.* **2018**, DOI 10.1002/adsc.201800380.
[39] S. Fu, Z. Shao, Y. Wang, Q. Liu, *J. Am. Chem. Soc.* **2017**, *139*, 11941–11948.
[40] T. Liu, L. Wang, K. Wu, Z. Yu, *ACS Catal.* **2018**, *8*, 7201-7207.
[41] N. Deibl, R. Kempe, *Angew. Chem. Int. Ed.* **2017**, *56*, 1663–1666.
[42] A. Mukherjee, A. Nerush, G. Leitus, L. J. W. Shimon, Y. Ben David, N. A. Espinosa Jalapa, D. Milstein, *J. Am. Chem. Soc.* **2016**, *138*, 4298–4301.
[43] S. Chakraborty, U. Gellrich, Y. Diskin-Posner, G. Leitus, L. Avram, D. Milstein, *Angew. Chem. Int. Ed.* **2017**, *56*, 4229–4233.
[44] A. Kumar, N. A. Espinosa-Jalapa, G. Leitus, Y. Diskin-Posner, L. Avram, D. Milstein, *Angew. Chem. Int. Ed.* **2017**, *56*, 14992–14996.
[45] N. A. Espinosa-Jalapa, A. Kumar, G. Leitus, Y. Diskin-Posner, D. Milstein, *J. Am. Chem. Soc.* **2017**, *139*, 11722–11725.
[46] J. O. Bauer, S. Chakraborty, D. Milstein, *ACS Catal.* **2017**, *7*, 4462–4466.
[47] S. Chakraborty, U. K. Das, Y. Ben-David, D. Milstein, *J. Am. Chem. Soc.* **2017**, *139*, 11710–11713.
[48] M. K. Barman, S. Waiba, B. Maji, *Angew. Chem. Int. Ed.* **2018**, *57*, 9126–9130.
[49] G. Zhang, T. Irrgang, T. Dietel, F. Kallmeier, R. Kempe, *Angew. Chem. Int. Ed.* **2018**, *57*, 9131–9135.
[50] (a) M. Mastalir, M. Glatz, N. Gorgas, B. Stöger, E. Pittenauer, G. Allmaier, L. F. Veiros, K. Kirchner, *Chem. Eur. J.* **2016**, *22*, 12316–12320; (b) M. Mastalir, M. Glatz, E. Pittenauer, G. Allmaier, K. Kirchner, *J. Am. Chem. Soc.* **2016**, *138*, 15543–15546.
[51] F. Kallmeier, B. Dudziec, T. Irrgang, R. Kempe, *Angew. Chem. Int. Ed.* **2017**, *56*, 7261–7265.
[52] A. M. Tondreau, R. Michalczyk, J. M. Boncella, *Organometallics* **2017**, *36*, 4179–4183.
[53] Z. Shao, Y. Wang, Y. Liu, Q. Wang, X. Fu, Q. Liu, *Org. Chem. Front.* **2018**, DOI 10.1039/C8QO00023A.

Glossary of complexes

Manganese complexes related to this work:

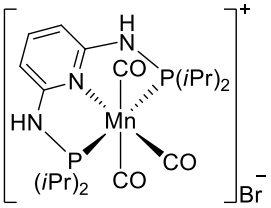

C^{2A}.1

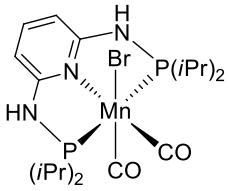

C^{2A}.2

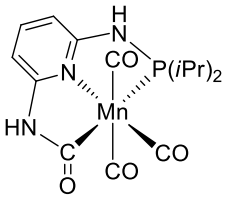

C^{2A}.3

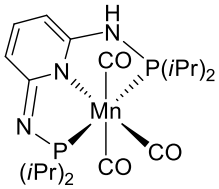

C^{2A}.1b

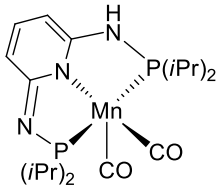

C^{2A}.1c

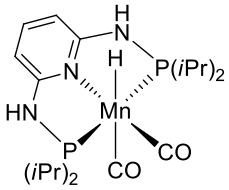

C^{2A}.1d

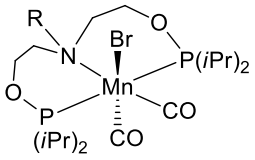

R = H, **C^{2B}.1**
R = CH_3, **C^{2B}.2**

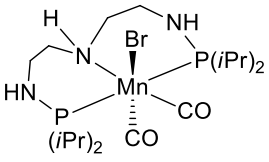

C^{2B}.4

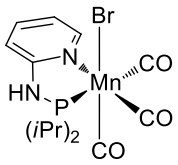

C^{3A}.1

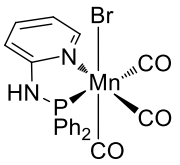

C^{3A}.2

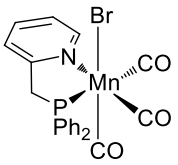

C^{3A}.3

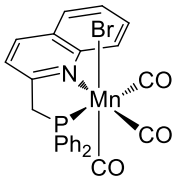

C^{3A}.4

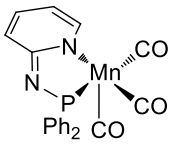

C^{3A}.2b

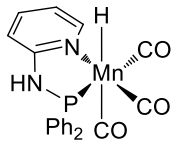

C^{3A}.2c

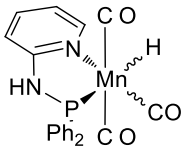

C^{3A}.2d

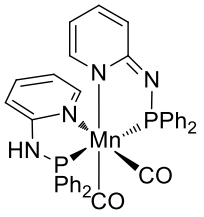

C^{3A}.2b'

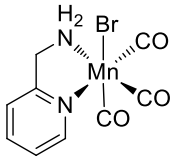

C^{3B}.1

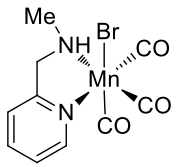

C^{3B}.2

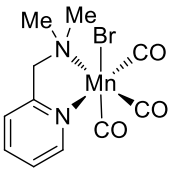

C^{3B}.3

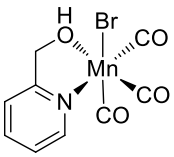

C^{3B}.4

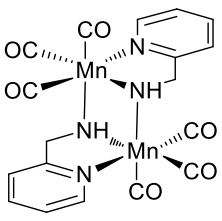

C^{3B}.1b

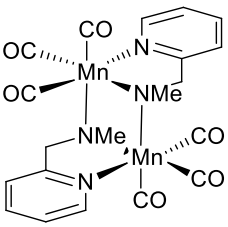

C^{3B}.2b

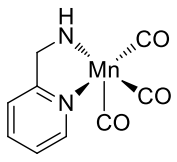

C^{3B}.1c

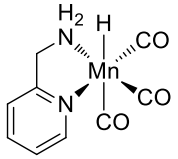

C^{3B}.1d

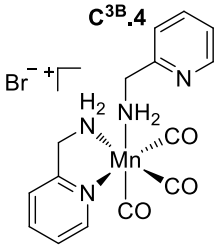

C^{3B}.1e

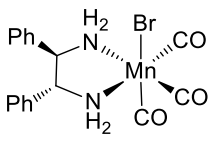

C^{3B}.21

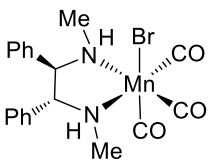

C^{3B}.27

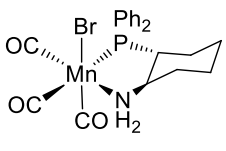

C^{3B}.30*

Manganese complexes taken from the literature:

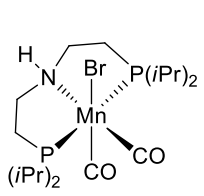

Mn-1

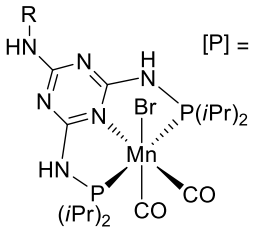

R= cyclopropyl **Mn-2**
= Ph **Mn-3**

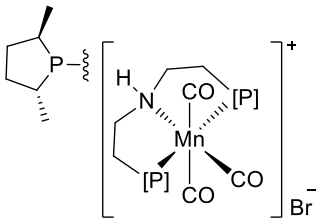

Mn-4

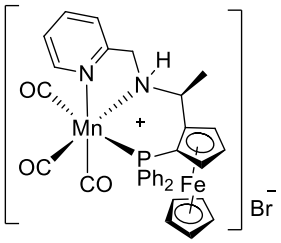

Mn-5

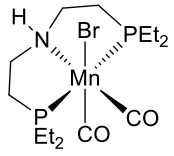

Mn-6

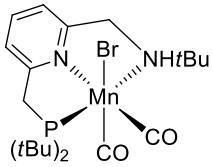

Mn-7

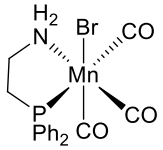

Mn-8

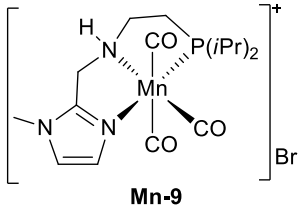

Mn-9

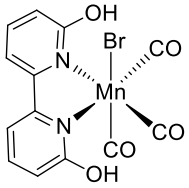

Mn-10

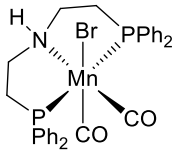

Mn-11

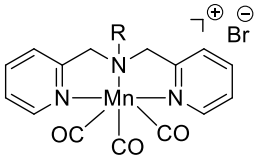

Mn-12 R= H,
Mn-13 R= Me

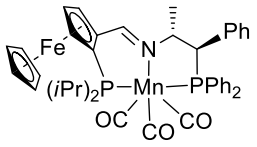

Mn-14

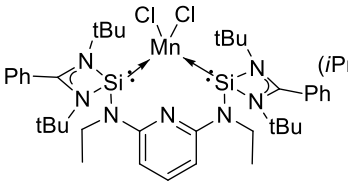

Mn-15

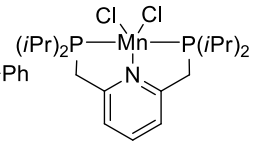

Mn-16

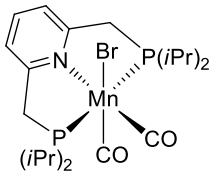

Mn-17

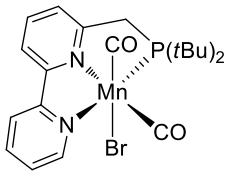

Mn-18

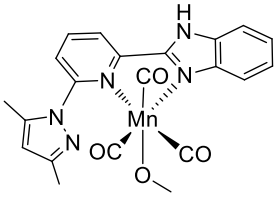

Mn-19

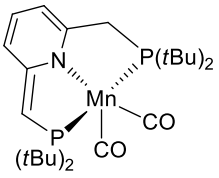

Mn-20

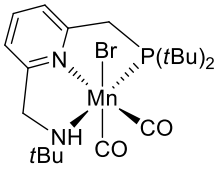

Mn-21

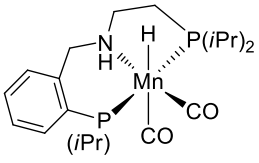

Mn-22

Résumé en français

Chapitre 1 : Introduction

Depuis les accords de Kyoto sur les émissions des gaz à effets de serre, jusqu'à la COP 21 à Paris, le développement durable est au cœur des préoccupations sociétales. En chimie, les grands principes associés au développement d'une chimie durable, ont été regroupés et formalisés par P. Anastas et J. Warner en 1998 avec les « douze principes de la chimie verte ».

Parmi ces douze principes, l'utilisation de matières premières renouvelables est primordiale. Les dérivés de la biomasse, actuellement considérés comme des déchets et brulés, sont bon-marchés et présents en quantités suffisantes pour remplacer les dérivés du pétrole pour l'industrie chimique. La principale difficulté est le changement de paradigme impliqué par le changement de nature des matières premières. Alors que les ressources fossiles, constituées principalement d'hydrocarbures, devaient être oxydées et fonctionnalisées, l'utilisation de la biomasse, hautement oxygénée et fonctionnalisée, requiert le développement d'une chimie de réduction, dépolymérisation et défonctionnalisation. Deux stratégies d'intégration des molécules biosourcées dans la production industrielle sont en compétition : à moyen terme, une approche convergente permet de produire les mêmes molécules plateformes que celles actuellement utilisées, provenant du pétrole, alors qu'à long terme, l'approche émergente, plus en adéquation avec les propriétés intrinsèques des synthons biosourcées, nécessite la découverte de nouvelles molécules plateformes et de nouveaux matériaux.

Un autre principe clef de la chimie verte est l'utilisation de la catalyse qui permet de réduire drastiquement la production de déchets (*via* l'absence de réactifs stœchiométriques et l'amélioration de la sélectivité des transformations) et les consommations énergétiques des réactions. Ce large domaine d'activité a reçu une attention soutenue au XX^{ème} siècle, amenant à l'obtention de plusieurs prix Nobel en catalyse homogène et hétérogène. En catalyse homogène organométallique, grâce à leur forte activité et versatilités, les métaux nobles ont été les métaux de choix

pendant plusieurs décennies. Cependant, leur rareté, leur prix et leur toxicité incitent les chercheurs, depuis une quinzaine d'année, à trouver des alternatives plus durable (voir l'abondance des métaux dans le **schéma 1**). De manière évidente, le fer, qui est le métal le plus abondant de la croûte terrestre, a été fortement étudié depuis une décennie comme centre actif pour les réactions de réduction. De manière surprenante, le manganèse, qui est le troisième métal de transition le plus abondant après le titane, n'était quasiment pas connu comme catalyseur pour les réactions de (dé)hydrogénation au début de cette thèse.

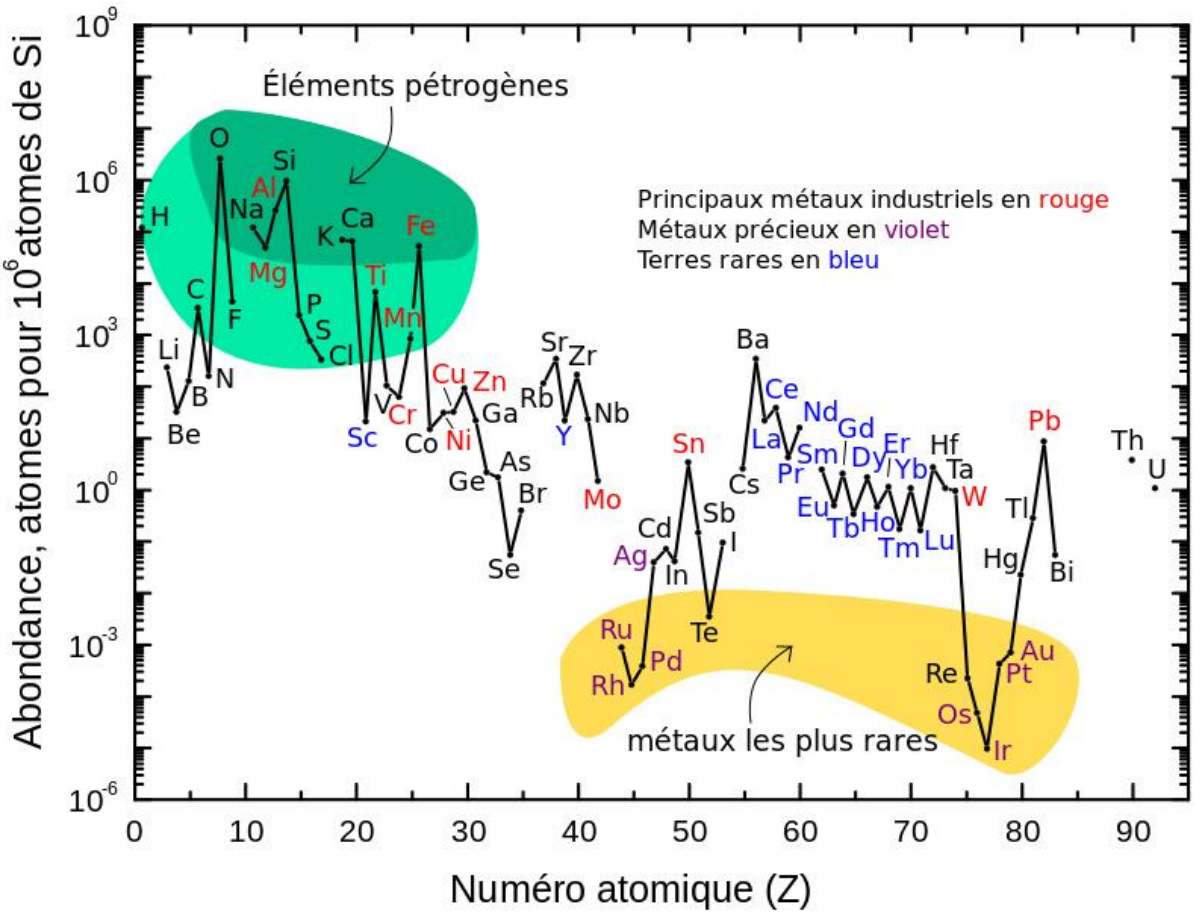

Schéma 1 Abondance d'éléments chimiques dans la croûte terrestre externe en fonction de leur numéro atomique soulignant les éléments les plus rares (en jaune) et les plus abondant (en vert). Source: https://pubs.usgs.gov/fs/2002/fs087-02/.

L'objectif de ce travail de doctoral a donc été de développer des catalyseurs organométalliques à base de manganèse pour promouvoir des réactions de (dé)hydrogénation. Pour ce faire, deux familles de catalyseurs, portant soit des ligands tridentés soit des ligands bidentés, ont été préparées. L'activité de ces complexes a ensuite été démontrée pour les réactions d'alkylation des anilines, des

cétones et des esters à l'aide méthanol, comme source durable de carbone C1, et pour les réactions de réduction (hydrogénation, transfert d'hydrogène) incluant la réduction asymétrique des cétones.

Chapitre 2 : Développement de complexes tridentés de manganèse(I)

A. Pour des réactions de prêt d'hydrogène avec du méthanol

Dans un premier temps, inspiré par l'essor des complexes de fer supportés par des ligands tridentés en hydrogénation et auto-transfert d'hydrogène, nous nous sommes intéressés aux ligands phosphorés dérivant du motif 2,6-diaminopyridine. La synthèse d'un premier complexe de manganèse **C^{2A}.1** (**Schéma 2**) portant un ligand de type 2,6-(diaminopyridinyl)diphosphine ligand (PN^3P), a été réalisée avec un bon rendement (68%).

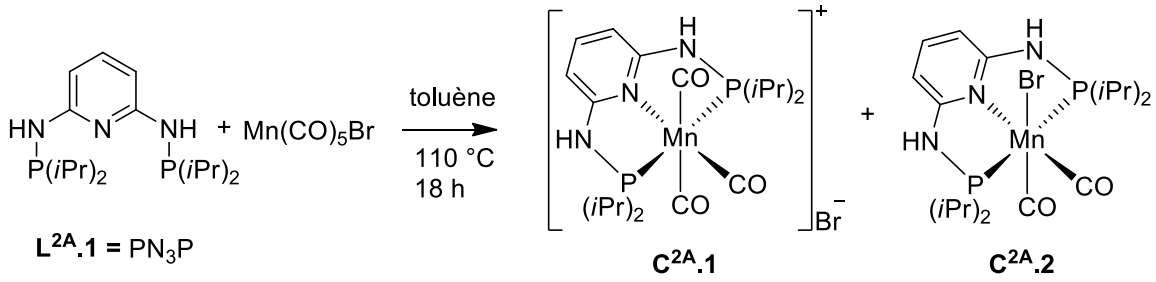

L^{2A}.1 = PN_3P **C^{2A}.1** **C^{2A}.2**

Schéma 2 Synthèse du complexe tridenté PN_3P de manganèse **C^{2A}.1**.

Ce complexe s'est ensuite avéré actif et très sélectif pour catalyser la méthylation d'anilines et de sulfonamides avec du méthanol, comme agent alkylant, avec des conditions optimisées douces (5 %mol du complexe, 20 %mol de tBuOK, dans le toluène à 120 °C pendant 24 h). De bons, voire excellents, rendements ont été obtenus en faveur des anilines mono-*N*-méthylées en présence de groupements réactifs ou réductibles tels que les halogènes, nitro, cyano, acétyl, acétal, ester et amide primaire. L'étude de la généralité de cette réaction a également démontré une tolérance moindre à l'encombrement en position *ortho* des anilines.

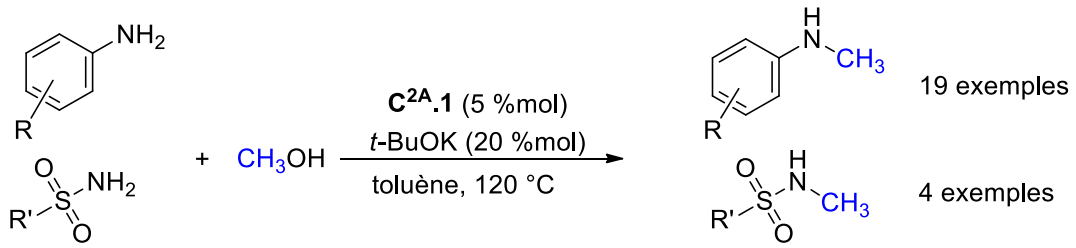

Schéma 3 Mono-*N*-méthylation sélective d'anilines et sulfonamides avec du méthanol catalysée par le complexe **C^{2A}.1**.

L'étude mécanistique de la réaction nous a permis d'isoler et de caractériser un intermédiaire organométallique déprotoné **C^{2A}.1b** (voir analyse DRX **Figure 1**), ainsi qu'un hydrure de manganèse **C^{2A}.1d** (**Schéma 4**).

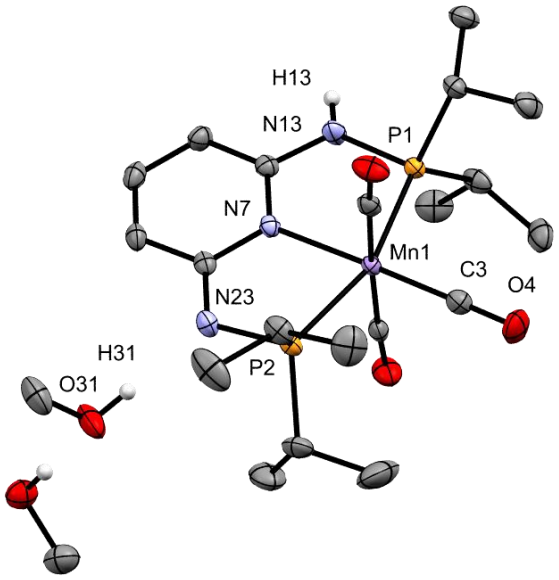

Figure 1 Structure moléculaire du complexe **C^{2A}.1b** (ellipsoïdes dessinés à 50% de probabilité). Pour plus de clarté, les atomes d'hydrogène, exceptés ceux sur des hétéroatomes, ont été omis. Le complexe est stabilisé, *via* des liaisons hydrogènes avec deux molécules de méthanol.

La mise en évidence expérimentale de ces deux complexes de manganèse est cohérente avec un mécanisme coopératif métal-ligand (**Schéma 4**) : en présence de base, le complexe **C^{2A}.1** est déprotoné pour donner **C^{2A}.1b** qui par décarbonylation conduit à l'espèce réactive à 16 électrons **C^{2A}.1c**. Celle-ci déshydrogène le méthanol pour former du formaldéhyde et le complexe **C^{2A}.1d** possédant un hydrure. Cet hydrure de manganèse va ensuite réduire l'imine produite *in situ* pour reformer l'espèce active **C^{2A}.1c** et aboutir à la production de l'amine méthylée.

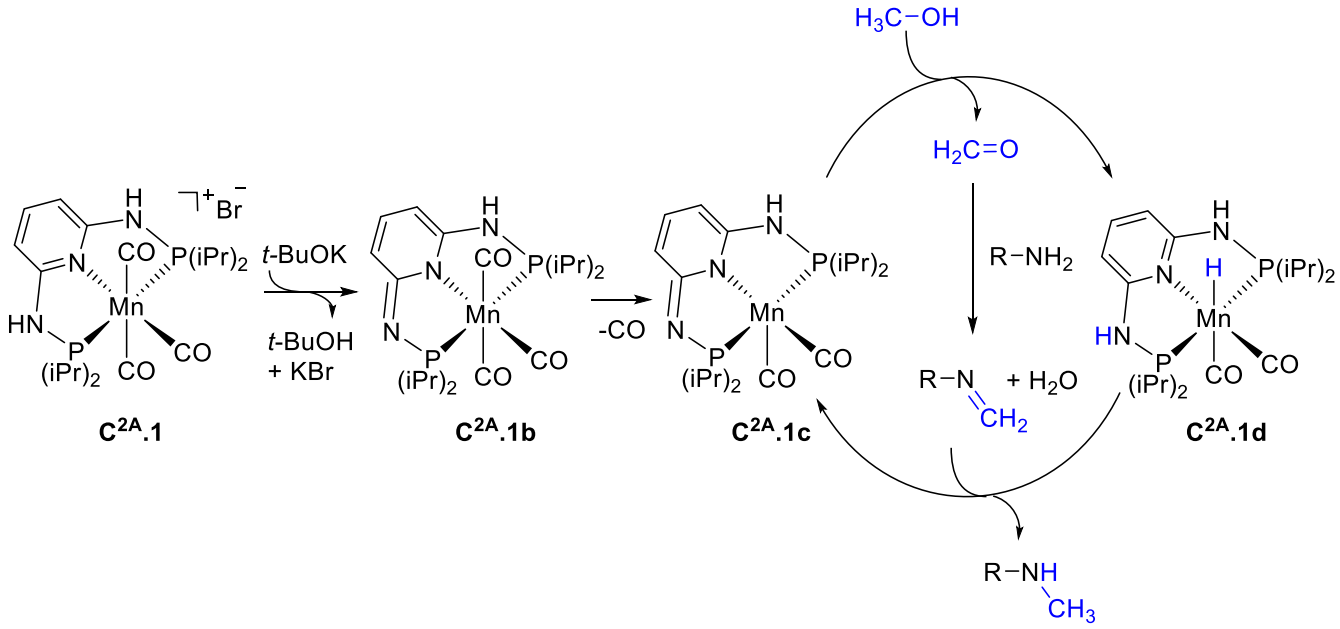

Schéma 4 Mécanisme proposé pour la mono-*N*-méthylation d'aniline avec du méthanol catalysée par le complexe **C^{2A}.1**.

La généralité de la réaction a pu être élargie à l'utilisation de cétones et d'esters, qui sont des substrats plus difficiles compte tenu du nombre plus importants de réactions secondaires pouvant avoir lieu. En ajustant les conditions optimales (**Schéma 5**), avec une charge catalytique abaissée à 3 %mol de nombreuses cétones et esters ont été α-méthylés avec de bons rendements.

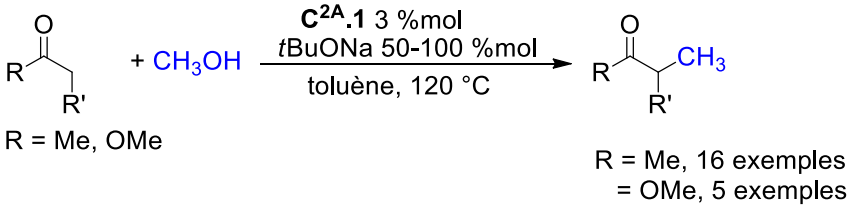

Schéma 5 Méthylation de cétones et d'esters avec du méthanol catalysée par le complexe **C^{2A}.1**.

B. Pour l'hydrogénation de cétones

Dans un deuxième temps, ce même complexe **C^{2A}.1** a pu servir de pré-catalyseur pour la réaction de réduction de cétones avec du dihydrogène en utilisant 5 %mol de complexe, 10 %mol de *t*BuOK, dans le toluène à 130 °C pendant 20 h (**Schéma 6**).

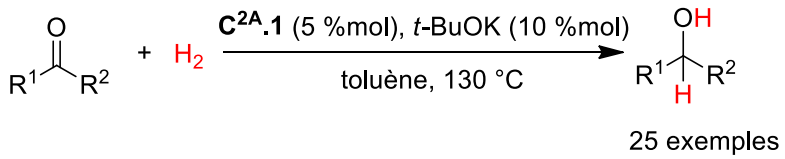

Schéma 6 Hydrogénation de cétones catalysée par le complexe **C^{2A}.1**.

D'autres complexes tridentés, portant des ligands aliphatiques de type PONOP et PNNNP, ont aussi été considérés pour cette même réaction d'hydrogénation.

Ce chapitre a donc démontré que l'utilisation de manganèse, jusqu'ici très rare, était possible pour les réactions de prêt d'hydrogène et d'hydrogénation. Un inconvénient majeur de ce type de système catalytique est la complexité et le prix des ligands utilisés qui contrebalance avec l'utilisation de métal bon-marché. Le prochain chapitre s'est concentré sur la conception de nouveaux catalyseurs permettant d'améliorer l'activité du système catalytique, tout en simplifiant les ligands.

Publications du chapitre 2:

A. Bruneau-Voisine, D. Wang, V. Dorcet, T. Roisnel, C. Darcel, J.-B. Sortais, *J . Catal.* **2017**, *347*, 57-62.

A. Bruneau-Voisine, D. Wang, V. Dorcet, T. Roisnel, C. Darcel, J.-B. Sortais, *Catal. Commun*. **2017**, *92*, 1-4.

H. Li, D. Wei, A. Bruneau-Voisine, M. Ducamp, M. Henrion, T. Roisnel, V. Dorcet, C. Darcel, J.-F. Carpentier, J.-F. Soulé, J.-B. Sortais, *Organometallics* **2018**, *37*, 1271-1279.

A. Bruneau-Voisine, J.-B. Sortais, Submitted

Chapitre 3 : Développement de complexes bidentés de manganèse(I)

A. Complexes PN^{py} et leurs activités en hydrogénation

Dans ce chapitre, nous avons d'abord simplifié le système catalytique en étudiant les ligands bidentés analogues à ceux du premier chapitre. La synthèse quantitative de complexes de manganèse avec des ligands bidentés dérivant de la plateforme 2-

aminopyridine ou 2-methylpyridine (**Schéma 7**) nous a permis de comparer leurs activités pour l'hydrogénation des cétones par rapport à leur pendant tridenté (PN^3P).

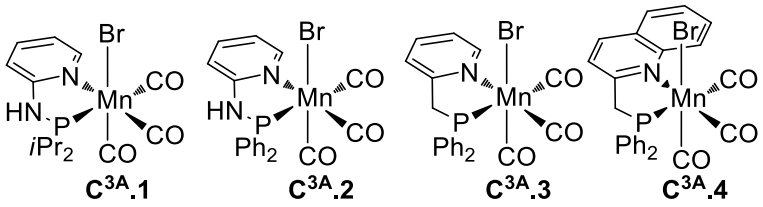

Schéma 7 Complexes bidentés de manganèse **C^{3A}.1-4** étudiés pour des réactions d'hydrogénation.

Le complexe **C^{3A}.2** est le plus actif de ces nouveaux complexes pour l'hydrogénation de l'acétophénone. Son activité est supérieure à celle du complexe **C^{2A}.1** puisque des conditions plus douces (0.5 %mol de **C^{3A}.2**, 2 %mol de KHMDS, dans le toluène à 50 °C pendant 20 h. contre 5 %mol de **C^{2A}.1**, 10 %mol de *t*-BuOK, dans le toluène à 130 °C pendant 20 h.) ont été employées pour hydrogéner des cétones et des aldéhydes (**Schéma 8**). Les TON ont donc été améliorés d'un facteur 16 (27 contre 430).

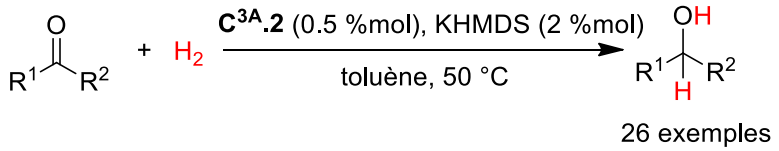

Schéma 8 Hydrogénation de cétones et d'aldéhydes catalysée par le complexe **C^{3A}.2**.

Outre une grande tolérance vis-à-vis de nombreux groupements fonctionnels, l'étude de la généralité de cette réaction a démontré une chimiosélectivité intéressante pour l'hydrogénation de cétones α-β insaturés, car dans des conditions douces, l'obtention de cétones saturées est possible alors que dans des conditions plus poussées les alcools saturés sont produits.

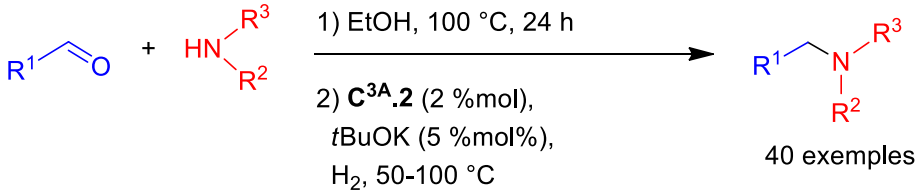

Schéma 9 Hydrogénation d'aldimines, *via* un protocole d'amination réductrice d'aldéhydes, catalysée par le complexe **C^{3A}.2**.

Ce même pré-catalyseur **C^{3A}.2** s'est aussi révélé actif pour l'hydrogénation de aldimines : par exemple, la *N*-benzylideneaniline est réduite quantitativement en présence de complexe **C^{3A}.2**, 5 %mol de *t*BuOK, dans l'éthanol à 50 °C pendant 17 h. L'amination réductrice d'une variété d'aldéhydes a été étudiée *via* une réaction séquentielle (un réacteur, deux étapes), en faisant dans un premier temps la condensation entre les aldéhydes et les amines dans l'éthanol puis, dans un deuxième temps, l'hydrogénation de l'imine en présence de 2 %mol de complexe **C^{3A}.2**, 5 %mol de *t*BuOK dans un autoclave sous 50 bar de dihydrogène (**Schéma 9**).

B. Complexes NN et leurs activités en transfert d'hydrogène

Pour rendre les catalyseurs encore plus accessibles, des ligands de type 2-aminométhylpyridine (NN^{py}) bon-marchés sans atome de phosphore ont été associés au manganèse(I). Les complexes **C^{3B}.1-4** ont été obtenus avec des rendements presque quantitatifs (**Schéma 10**).

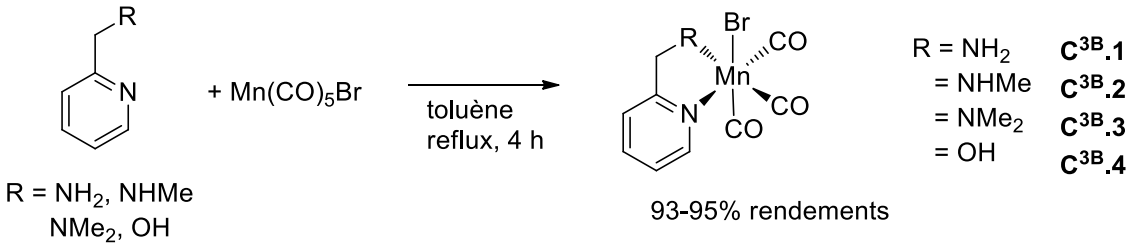

Schéma 10 Complexes bidentés de manganèse **C^{3B}.1-4** étudiés pour des réactions de transfert d'hydrogène.

Les complexes **C^{3B}.1** et **C^{3B}.2** (0.5 %mol) ont été très actifs pour la réduction d'acétophénone dans l'isopropanol à 80 °C pendant 15 minutes en présence de 1 %mol de *t*BuOK. Au contraire, les complexes **C^{3B}.3** et **C^{3B}.4** ne sont pas très actifs dans ces conditions démontrant l'utilité d'avoir une fonction « NH » sur le ligand pour accélérer la réaction.

Le complexe **C^{3B}.1** s'est révélé très actif pour la réduction de cétones, aldéhydes et aldimines par transfert d'hydrogène (**Schéma 11**). Les conditions optimales (0.5 %mol de complexe, 1 %mol de base dans l'isopropanol à 80 °C pendant 20 min ou 30 °C pendant 16 h) ont permis la réduction de 35 cétones démontrant une forte chimiosélectivité et tolérance de ce système. Par exemple, la réduction de cétones et

aldéhydes α-β insaturés a permis d'obtenir des alcools α-β insaturés avec de très bons rendements.

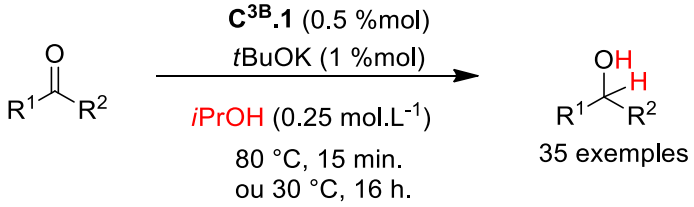

Schéma 11 Transfert d'hydrogène d'isopropanol vers des cétones et aldéhydes catalysé par le complexe **C^{3B}.1**.

Le mécanisme de la réaction a ensuite été étudié : par réaction du complexe bromé **C^{3B}.1** avec un équivalent de base dans des conditions stœchiométriques, le complexe dimérique **C^{3B}.1b** a pu être isolé et cristallisé (**Figure 2**). Ce complexe correspond à la forme stabilisée du complexe déprotoné amido à 16 électrons **C^{3B}.1c** formé en absence de substrats (**Schéma 12**). En présence d'isopropanol, ce complexe **C^{3B}.1c** déshydrogène l'alcool pour former le complexe amino-hydrure **C^{3B}.1d**. Bien que la présence d'hydrure n'est pas pu être mis en évidence expérimentalement, il est fort probable qu'un mécanisme de type Noyori opère pour ces catalyseurs. Cet hydrure est ensuite transféré au substrat (cétone), puis un proton est transféré à l'alcoolate pour donner l'alcool corespondant.

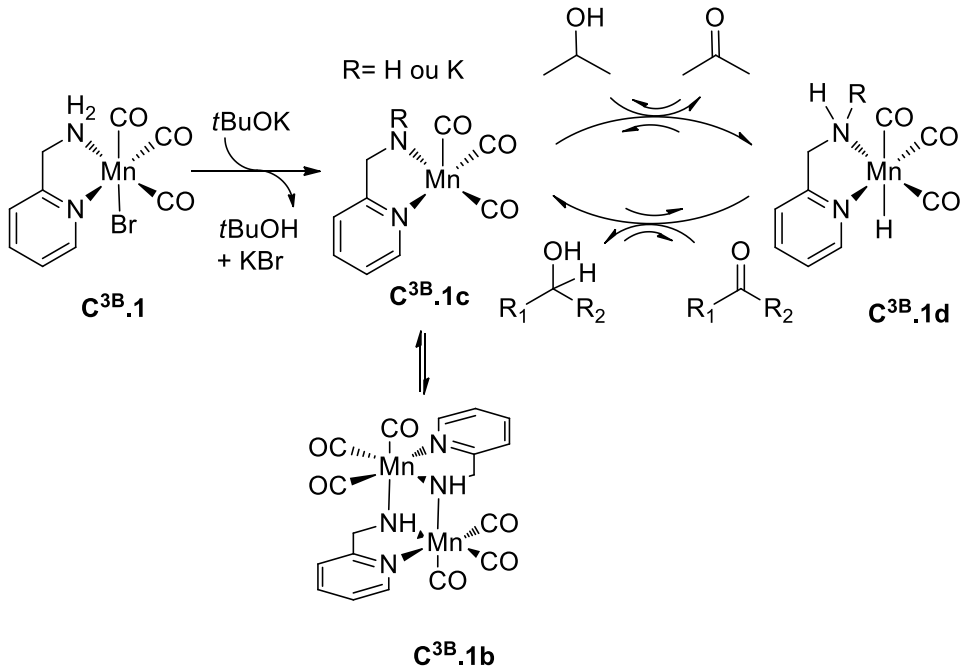

Schéma 12 Mécanisme proposé pour la réduction des dérivés carbonylés par transfert d'hydrogène d'isopropanol catalysé par le complexe **C^{3B}.1**.

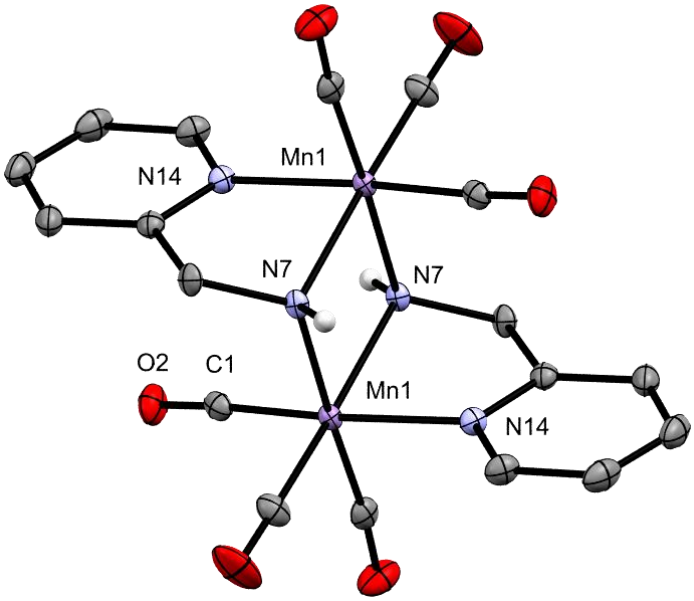

Figure 2 Structure moléculaire du complexe **C^{3B}.1b** (ellipsoïdes dessinés à 50% de probabilité). Pour plus de clarté, les atomes d'hydrogène, exceptés ceux sur les azotes, ont été omis.

La mise en œuvre a été simplifiée également en produisant *in situ* le système catalytique, sans perte de rendement, pour la réduction de l'acétophénone dans l'isopropanol.

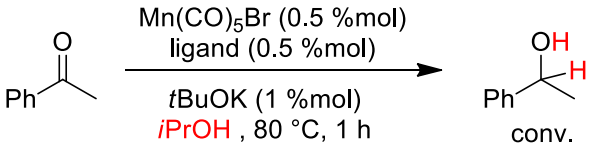

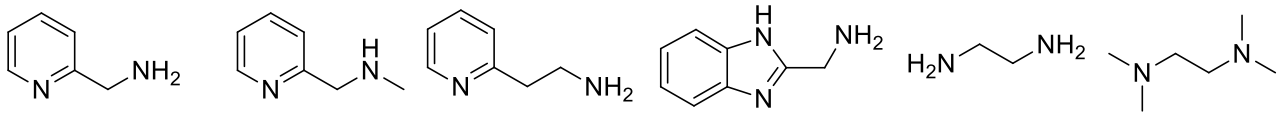

L^{3B}.1 97% **L^{3B}.2** 96% **L^{3B}.8** 7% **L^{3B}.9** 76% **L^{3B}.11** 65% **L^{3B}.14** 0%

Schéma 13 Sélection de diamines testées pour la réduction d'acétophénone avec génération *in situ* du système catalytique.

Compte tenu de la praticité du protocole expérimental, différentes diamines ont ainsi été testées *in situ* comme ligand pour cette même réaction (**Schéma 13**), afin d'établir les conditions nécessaires et suffisantes pour obtenir un système catalytique actif. La formation d'un métallacycle à 5 chainons et la présence de groupement « NH » sont indispensables pour obtenir de bonnes conversions. La plus simple d'entre-elles, l'éthylène diamine **L^{3B}.11** (NN), a montré une remarquable activité (0.5

%mol d'éthylène diamine, 0.5 %mol de $Mn(CO)_5Br$, 1 %mol de *t*BuOK dans l'isopropanol à 80 °C pendant 3 h) pour diverses cétones (**Schéma 14**)

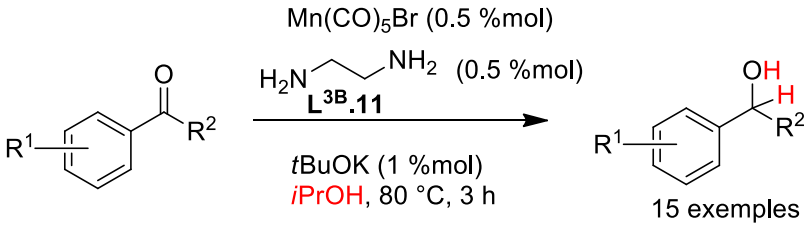

Schéma 14 Transfert d'hydrogène d'isopropanol vers des cétones catalysé par le système catalytique formé *in situ* à partie de $Mn(CO)_5Br$ et **L^{3B}.11**.

Dans une dernière partie, la réduction asymétrique des cétones a été réalisée, en utilisant des ligands diazotés possédant un squelette de type éthylènediamine. Avec la (1*R*,2*R*)-1,2-diphényl-1,2-éthane diamine **L^{3B}.21**, un excès énantiomérique prometteur de 36 % a été obtenu pour la réduction de l'acétophénone (**Schéma 15**). La mono-méthylation des deux fonctions amines (**L^{3B}.27**) a permis d'augmenter l'excès énantiomérique jusqu'à 64%. Cependant, si on augmente l'encombrement avec l'introduction d'un groupement *N*-éthyl (**L^{3B}.29**), l'excès énantiomérique de l'alcool est plus faible (52%) soulignant l'importance de la mono-*N*-méthylation d'amine.

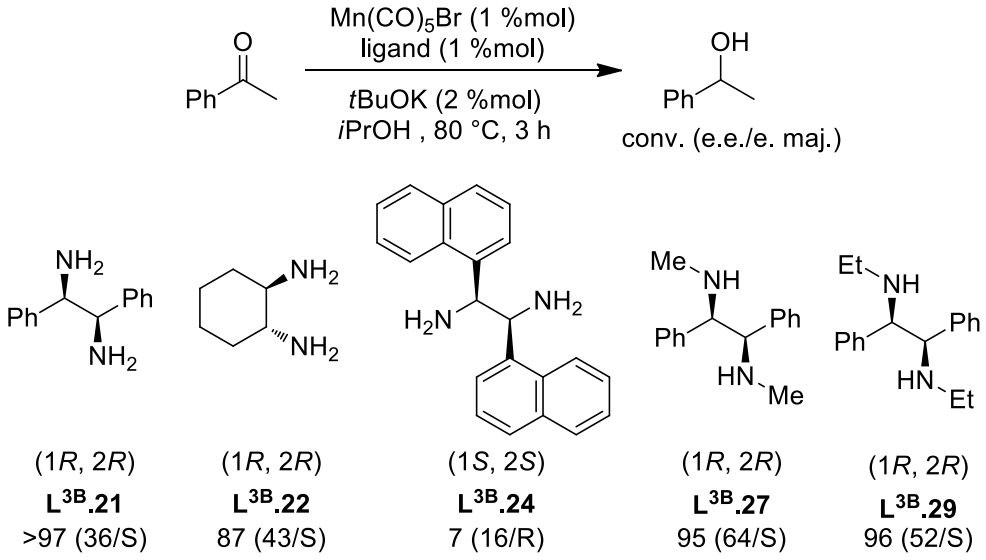

Schéma 15 Sélection de diamines chirales testées pour la réduction asymétrique d'acétophénone avec génération *in situ* du système catalytique.

Le rôle clef du groupement *N*-méthyl dans le processus d'énantio-discrimination des faces de l'acétophénone a été rationalisé à l'aide d'une étude théorique préliminaire

(DFT et NCI) *via* la présence d'interactions non-covalentes CH-π entre les groupements méthyles du ligand et le groupement aryle de la cétone.

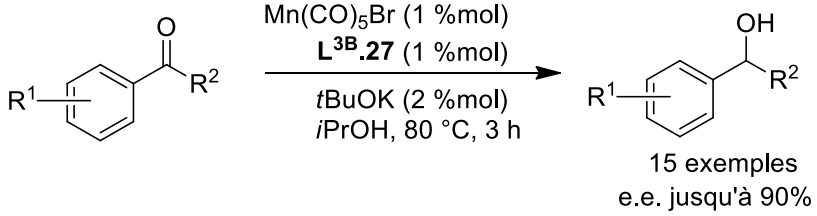

Schéma 16 Transfert d'hydrogène asymétrique d'isopropanol vers des cétones catalysé par le système catalytique formé *in situ* à partie de $Mn(CO)_5Br$ et **L^{3B}.27**.

La généralité de cette réaction a été étudiée avec différentes cétones (**Schéma 16**). Des alcools énantio-enrichis ont été obtenus avec de très bonnes conversions et des excès énantiomérique pouvant atteindre 90% avec comme ligand la (1*R*,2*R*)-(+)-*N,N'*-diméthyl-1,2-diphényl-1,2-éthane diamine **L^{3B}.27** (NN*).

Publications pour ce chapitre:

A. Bruneau-Voisine, D. Wang, V. Dorcet, T. Roisnel, C. Darcel, J.-B. Sortais, *Org. Lett.* **2017**, *19*, 3656-3659.

D. Wang*, A. Bruneau-Voisine*, J.-B. Sortais, *Catal. Commun.* **2018**, *105*, 31-36. *même contribution

D. Wei, A. Bruneau-Voisine, T. Chauvin, V. Dorcet, T. Roisnel, D. A. Valyaev, N. Lugan, J.-B. Sortais, *Adv. Synth. Catal*. **2018**, *360*, 676-681.

D. Wei, A. Bruneau-Voisine, D. A. Valyaev, N. Lugan, J.-B. Sortais, *Chem. Commun.* **2018**, *54*, 4302-4305.

Chapitre 4 : Conclusion

Bien qu'étant le troisième métal de transition, par ordre d'abondance, après le fer et le titane, le manganèse, jusqu'à récemment, était principalement utilisé en oxydation et très peu en réduction. En l'espace de trois années, l'utilisation du manganèse en catalyse homogène pour la réduction a connu un essor impressionnant, comme en témoigne l'évolution entre la revue de Lugan en 2016 et celle de Kempe en 2018.[1,2]

Au cours de cette thèse, nous avons démontré à travers plusieurs exemples que les complexes de manganèse supportés par des ligands bifonctionnels, autant tridentes que bidentes, pouvaient être des catalyseurs efficaces pour les réactions

d’hydrogénation, transfert d’hydrogène et d’auto-transfert d’hydrogène. Nous avons d’abord mis en évidence le potentiel du manganèse pour activer par déshydrogénation le méthanol, ouvrant la voie à de nombreuses réactions de méthylation par auto-transfert d’hydrogène. Ensuite, nous avons démontré dans le cadre des ligands aminophosphine pyridine que les complexes portant des ligands bidentes avaient une activité nettement supérieure à ceux possédant des ligands tridentes en hydrogénation. Enfin, à ce jour, nous avons découvert les systèmes les plus actifs en transfert d’hydrogène et les plus sélectifs pour la réduction asymétrique des cétones à l’aide ligands diazotés très simples.

L’ensemble de ces résultats, associés à ceux décrits par d’autres groupes, tend à prouver que le manganèse, et plus globalement les métaux abondants et bon-marchés peuvent remplacer les métaux nobles dans de plus en plus de domaines.

Références :

[1] D. A. Valyaev, G. Lavigne, N. Lugan, *Coord. Chem. Rev*. **2016**, *308*, 191–235.

[2] F. Kallmeier, R. Kempe, *Angew. Chem. Int. Ed*. **2018**, *57*, 46–60.

Titre : Réactions de (dé)hydrogénation catalysées par des complexes de manganèse(I).

Mots clés : Catalyse, Homogène, Manganèse(I), Reduction, Prêt d'Hydrogène, Hydrogénation.

Résumé : Pour répondre aux enjeux économiques et sociaux modernes, le développement de catalyseurs organométalliques à base de métaux abondants et bon marché, comme alternatives aux catalyseurs historiques basés sur les métaux précieux, connait un essor constant depuis deux décennies. L'objectif du présent travail doctoral a été de développer des catalyseurs à base de manganèse, troisième métal de transition le plus abondant après le fer et le titane, et précédemment principalement utilisé en oxydation, pour les réactions de (dé)-hydrogénation.

La première partie de ce travail doctoral porte sur l'utilisation de complexes bien définis de manganèse(I), portant un ligand tridenté 2,6-(diaminopyridinyl)diphosphine, comme catalyseur pour les réactions de mono-*N*-méthylation d'anilines et d'α-*C*-alkylation des dérivés carbonylés avec du méthanol comme agent méthylant durable. Lors de l'étude mécanistique, des intermédiaires organométalliques tels qu'un complexe déprotoné contenant une dé-aromatisation du groupement pyridinyl et un hydrure de manganèse ont pu être identifiés. Ce même catalyseur s'est aussi révélé actif pour l'hydrogénation des cétones (TON 27).

Dans la deuxième partie de cette thèse l'activité de cette classe de pré-catalyseur a été augmentée pour l'hydrogénation des cétones et des aldéhydes en simplifiant le ligand choisi, dorénavent bidenté 2-(aminopyridinyl)phosphine (TON 430). Ce même système catalytique est également efficace pour la réaction d'amination réductrice. Dans une démarche de sobriété accrue dans le design puis dans la mise en oeuvre du système catalytique, la génération *in situ* de catalyseur possédant de simples ligands diamines, tels que la 2-aminométhylpyridine, pouvant accélérer le transfert d'hydrogène de l'isopropanol vers des cétones, aldéhydes et aldimines a démontré une grande activité (TON 2000 and TOF jusqu'à 3600 h^{-1}). Enfin une version asymétrique de cette réduction de cétones a permis l'obtention d'alcools avec des excès énantiomériques pouvant atteindre 90%.

Title: (De)hydrogenation reactions catalyzed by manganese(I) complexes.

Keywords: Catalysis, Homogeneous, Manganese(I), Reduction, Hydrogen borrowing, Hydrogenation.

Abstract : To meet modern economic and social challenges, the development of inexpensive and abundant metal-based organometallic catalysts, as alternatives to historical catalysts based on precious metals, has been growing steadily for two decades. The aim of this doctoral work was to develop catalysts based on manganese, which is the third most abundant transition metal after iron and titanium, and previously mainly used in oxidation, for (de)-hydrogenation reactions.

The first part of this doctoral work deals with the use of well-defined complexes of manganese (I), bearing a tridentate 2,6-(diaminopyridinyl)diphosphine ligand, as a catalyst for the mono-*N*-methylation reactions of anilines and α-*C*-alkylation of carbonyl derivatives with methanol as a sustainable methylating agent. In the mechanistic study, organometallic intermediates such as a deprotonated complex containing a de-aromatization of the pyridinyl scaffold and a manganese hydride could be identified. This same catalyst was also active for the hydrogenation of ketones (TON 27).

In the second part of this thesis the activity of this kind of pre-catalyst was increased for the hydrogenation of ketones and aldehydes by simplifying the ligand chosen, henceforth bidentate 2-(aminopyridinyl)phosphine, leading to a 16 fold better activity (TON 430). In an approach of increased sobriety in the design and then in the implementation of the catalytic system, the *in situ* generation of catalysts possessing simple diamine ligands, such as 2-aminomethylpyridine or ethylenediamine, has accelerated the transfer hydrogenation of ketones, aldehydes and aldimines with isopropanol (TON up to 2000 and TOF up to 3600 h^{-1}). Finally, an asymmetric version of this reduction of ketones allowed obtaining alcohols with enantiomeric excess up to 90%.